

Aus dem Institut für Epidemiologie
Helmholtz Zentrum München

Direktor: Prof. Dr. Annette Peters

***Multi-omics of Chronic Kidney Disease in Individuals with Pre-
diabetes or Type 2 Diabetes in the Era of Precision Health***

Dissertation

zum Erwerb des Doktorgrades der Humanbiologie
an der Medizinischen Fakultät der
Ludwig-Maximilians-Universität zu München

vorgelegt von
Jialing Huang

aus

Guangdong, China

Jahr

2023

Mit Genehmigung der Medizinischen Fakultät
der Universität München

Berichterstatter: Prof. Dr. Annette Peters

Mitberichterstatter: Prof. Dr. Peter Weyrich
Prof. Dr. Maciej Lech

Mitbetreuung durch den
promovierten Mitarbeiter: Dr. Rui Wang-Sattler

Dekan: Prof. Dr. med. Thomas Gudermann

Tag der mündlichen Prüfung: 08.03.2023

Affidavit



LUDWIG-
MAXIMILIANS-
UNIVERSITÄT
MÜNCHEN

Promotionsbüro
Medizinische Fakultät



Affidavit

Huang, Jialing

Surname, first name

Street

Zip code, town, country

I hereby declare, that the submitted thesis entitled:

Multi-omics of Chronic Kidney Disease in Individuals with Pre-diabetes or Type 2 Diabetes in the Era of Precision Health

.....

is my own work. I have only used the sources indicated and have not made unauthorised use of services of a third party. Where the work of others has been quoted or reproduced, the source is always given.

I further declare that the submitted thesis or parts thereof have not been presented as part of an examination degree to any other university.

Munich, 10.03.2023

place, date

Jialing Huang

Signature doctoral candidate

Table of content

Affidavit	I
Table of content	II
List of abbreviations	IV
List of publications	VI
Contribution to papers	VII
Contribution to paper I.....	VII
Contribution to paper II	VII
Contribution to paper III (Appendix).....	VII
Summary	VIII
Zusammenfassung	X
1. Background	1
1.1 Precision health and multi-omics techniques	1
1.2 The global burden of CKD and the contribution from (pre-) T2D	1
1.3 Complex biological processes of hyperglycemia-related CKD.....	2
1.4 Current omics studies in (hyperglycemia-related) CKD	2
1.5 Inadequate early detection of CKD	4
1.6 Discrepancies of (candidate) biomarkers' effects for kidney disease.....	5
1.7 Paucity of systematic biological understanding of hyperglycemia-related CKD	5
2. Contributing papers	6
3. Rationale	7
4. Methods	7
4.1 Study population	7
4.2 Definition of hyperglycemia	8
4.3 Definitions of kidney traits.....	8
4.4 Multi-omics techniques in study population	9
4.5 Mouse study	9
4.6 Statistical analyses.....	10
5. Results	12
5.1 Paper I ⁶⁹	12
5.2 Paper II ⁷⁰	13
5.3 Paper III.....	13
6. Discussion	15
6.1 Early detection of CKD in hyperglycemia	15
6.2 Interaction and condition-specific effects of (candidate) biomarkers for kidney traits	15

6.3	Improve systematic biological understanding to contribute to precision health.....	16
6.4	Limitation	18
7.	Conclusion.....	18
8.	References	19
Paper I	24
Paper II	47
Appendix A: Paper III	64
Acknowledgements	273

List of abbreviations

2-h glucose	Two hour post load glucose
2SMR	Two-sample MR
ACEIs	Angiotensin-converting enzyme inhibitors
ACs	Acylcarnitines
ADA	American Diabetes Association
AdaBoost	Adaptive boosting
AKI	Acute kidney injury
ANOVA	Analysis of variance
ARBs	Angiotensin receptor blockers
AUC	Receiver operating characteristic curve
CKD	Chronic kidney disease
CKD _{eGFR_{crea}}	eGFR _{crea} -based CKD defined as eGFR _{crea} < 60 ml/min/1.73 m ²
CKD _{eGFR_{crea}-cys}	eGFR-based CKD defined as eGFR < 60 ml/min/1.73 m ² , which was calculated from serum creatinine and cystatin C.
CKD-EPI	Chronic Kidney Disease Epidemiology Collaboration
CKD _{UACR}	UACR-based CKD defined as UACR ≥ 30 mg/g.
CRP	C-reactive protein
db/db	Leptin-receptor deficient mouse model
DKD	Diabetes kidney disease
DMMONs	Directed mediating multi-omics networks
DMOIN	Different levels of multi-omics integration network
ECM	Extracellular matrix protein
EGF	Epidermal growth factor
eGFR	Estimated glomerular filtration rate
eGFR _{crea}	Estimated glomerular filtration rate calculated serum creatinine.
EWAS	Epigenome-wide association studies
FG	Fasting glucose
GGM	Gaussian graphical model
GPS	Genome-wide polygenic score
GWAS	Genome-wide association studies

HbA _{1C}	Glycated haemoglobin
IGFBP2	Insulin-like growth factor binding protein 2
IPW	Inverse probability weighting
IVW	Inverse variance weighted
KIM1	Kidney injury molecule1
MOIN	Multi-omics integration network
MR	Mendelian randomization
MR-PRESSO	MR pleiotropy residual sum and outlier
MWAS	Metabolome wide association studies
NGAL	Neutrophil gelatinaseassociated lipocalin
NGT	Normal glucose tolerance
PC aa	Phosphatidylcholine diacyl
PWAS	Proteome wide association studies
QC	Quality control
QN	Quantile normalization
RAS	Renin-angiotensin system
RF	Random forest
SD	Standard deviation
SM	Sphingomyelin
SVM	Support vector machine
T2D	Type 2 diabetes
T2DCKD	T2D-related CKD
TWAS	Transcriptome wide association studies
UACR	Urinary albumin-creatinine ratio
UKBB	UK biobank cohort
WHO	World Health Organization
WT	Wild type

List of publications

This thesis consists of the following papers:

Huang J, Huth C, Covic M, Troll M, Adam J, Zukunft S, et al. Machine Learning Approaches Reveal Metabolic Signatures of Incident Chronic Kidney Disease in Individuals With Prediabetes and Type 2 Diabetes. *Diabetes*. 2020;69(12):2756-65.

Huang J, Covic M, Huth C, Rommel M, Adam J, Zukunft S, et al. Validation of Candidate Phospholipid Biomarkers of Chronic Kidney Disease in Hyperglycemic Individuals and Their Organ-Specific Exploration in Leptin Receptor-Deficient db/db Mouse. *Metabolites*. 2021;11(2):89.

Huang J, et al. Multi-omics landscape of chronic kidney disease in individuals with prediabetes or type 2 diabetes: from associations towards precision medicine. (manuscript)

Contribution to papers

Contribution to paper I

I was responsible for conceptualization, data analyses, and writing the paper.

Contribution to paper II

I was responsible for conceptualization, data analyses, and writing the paper.

Contribution to paper III (Apendix)

I was responsible for conceptualization, data analyses, and writing the manuscript.

Summary

Precision health entails disease risk assessment for individuals, early detection of preclinical conditions, and the implementation of preventive and therapeutic strategies. Multi-omics techniques enable detailed molecular and physiological profiling, thereby advancing towards the goal of precision health. Globally, chronic kidney disease (CKD) affects approximately 9.1% of the general population. Diabetes mellitus is a leading cause of CKD, and the prevalence and burden of (pre) diabetes-related CKD are increasing worldwide. CKD is a multifactorial disease manifested by an assortment of pathological processes. Although various aspects of CKD have been investigated, currently established risk factors have limited predictive power, the effects of proposed (candidate) biomarkers are inconsistent across studies, and the systematic biological mechanism is still uncertain, especially in individuals with (pre-) T2D, a hyperglycemic population at high risk for CKD.

Based on multi-omics (i.e., genotyping, DNA methylation, gene expression, proteomics, metabolomics) and clinical assessment data of the longitudinal population-based KORA (Cooperative Health Research in the Region of Augsburg) cohort, this thesis aims to contribute to improving precision health of CKD in hyperglycemic individuals by enhancing early detection, illustrating the condition-specific effects of identified candidate biomarkers, and expanding our knowledge of the systematic biology.

This thesis first proposed a concise prediction model demonstrating superior predictive capacity for incident CKD in hyperglycemic individuals, consisting of seven predictors (age, fasting glucose, total cholesterol, estimated glomerular filtration rate (eGFR) values, urinary albumin-creatinine ratio (UACR) values, sphingomyelin (SM) C18:1, and phosphatidylcholine diacyl (PC aa) C38:0). A genome-wide polygenic score (GPS) for eGFR (GPS_{eGFR}) values was constructed using *KORA Follow Up 4* individuals and replicated in the UK biobank cohort, which demonstrated consistent improvement in prediction of incident CKD in hyperglycemia and improved the performance on top of these seven predictors. Moreover, 120 multi-omics molecules of prevalent CKD in hyperglycemia were identified, of which 64 (two CpGs, two RNAs, 46 proteins and 14 metabolites) were successfully replicated. In multi-omics prediction, supplementing current suggested predictor sets with omics levels from GPS_{eGFR} , candidate proteins and metabolites was found to improve the prediction performance of future CKD in hyperglycemia.

To determine if the effects of candidate biomarkers of CKD (prevalent/incident) were specific for hyperglycemia, their interaction effects were investigated. SM C18:1 and PC aa C38:0 of CKD (prevalent and incident), and 58 of 64 multi-omics candidates of prevalent CKD were only significant in the hyperglycemic subgroup, particularly SM C18:1, indicating that these molecules may have an interaction effect on CKD with glycemic status.

To better elucidate the intricate biological processes of hyperglycemia-related CKD, we constructed eight subnetworks for T2D-related CKD (T2DCKD) and categorized our identified multi-omics candidates into them. In hyperglycemia, 18 of 64 replicated candidates with prevalent CKD were associated with GPS_{eGFR} and demonstrated mediation effects with GPS_{eGFR} and eGFR. Bi-directional two-sample Mendelian randomization supported that 19 candidates may have a causal relationship with kidney traits (CKD, eGFR, and UACR). These genetic evidence support

that the revealed candidate biomarkers may be part of the upstream/downstream pathways of CKD, eGFR or UACR. In addition, 64 replicated candidates were classified based on their directions of eGFR/UACR, and their potentially involved pathophysiological T2DCKD processes were displayed within each group. Different groups of candidate biomarkers presented diverse relationships of kidney phenotypes (kidney function or kidney damage) and distinct patterns of underlying pathogenetic processes, which will help to improve insights of identifying personalized therapeutic targets for hyperglycemia-related CKD.

The connections between candidate biomarkers from different omics levels and whether they share the same pathways are still unresolved. To enlarge our knowledge of this topic, this thesis utilized Gaussian graphical modeling and causal mediation analyses to examine how different levels of omics molecules (i.e., CpGs, RNAs, proteins and metabolites) that were associated with CKD in hyperglycemia interacted with one another. Thus, potential new causal links, relevant molecular pathways, and probable key drivers of the pathways were identified. In addition, three distinct subgroups of CKD patients with hyperglycemia were identified using three potential novel proteins (i.e., NBL1, EFNA5 and JAM2), confirming that distinct dominant pathological processes in distinct subgroups of CKD patients could result in distinct theoretical therapeutic targets.

In conclusion, this thesis demonstrates that multi-omics profiles can aid in the early detection of future CKD, the identification of subgroups of susceptible populations, and the advancement of systematic biological understanding of CKD in the hyperglycemic population. This thesis delves into the complex multi-omics landscape of CKD in hyperglycemia and demonstrates how multi-omics profiles can provide important contributions towards precision health.

Zusammenfassung

Präzisionsgesundheit umfasst die Bewertung des Krankheitsrisikos individuell für ein Individuum, die frühzeitige Erkennung präklinischer Zustände, sowie die Umsetzung präventiver und therapeutischer Strategien. Multi-omics-Techniken ermöglichen eine detaillierte molekulare und physiologische Profilerstellung und bringen so das Ziel der Präzisionsgesundheit voran. Weltweit sind etwa 9,1 % der Bevölkerung von chronischen Nierenerkrankungen (CKD) betroffen. Diabetes mellitus ist eine der Hauptursachen für CKD, und die Prävalenz und Belastung durch (prä-)diabetesbedingte CKD nehmen weltweit zu. CKD ist eine multifaktorielle Erkrankung, die sich durch eine Reihe von pathologischen Prozessen manifestiert. Obwohl verschiedene Aspekte der CKD untersucht wurden, haben bedingte etablierte Risikofaktoren nur eine begrenzte Vorhersagekraft, die Auswirkungen der vorgeschlagenen Biomarker (-Kandidaten) sind in verschiedenen Studien uneinheitlich, und der systematische biologische Mechanismus ist immer noch ungewiss, insbesondere bei Personen mit (Prä-) T2D, eine hyperglykämische Bevölkerung mit hohem CKD-Risiko.

Auf der Grundlage von Multi-omics (d.h. Genotypisierung, DNA-Methylierung, Genexpression, Proteomics, Metabolomics) und klinischen Beurteilungsdaten der bevölkerungsbasierten KORA-Kohorte (Kooperative Gesundheitsforschung in der Region Augsburg) soll diese Arbeit einen Beitrag zur Verbesserung der Präzisionsgesundheit von CKD bei hyperglykämischen Personen leisten, indem sie die Früherkennung verbessert, die Bedingungsspezifisch Auswirkungen identifizierter Kandidaten-Biomarker veranschaulicht und unser Wissen über die Systembiologie erweitert.

In der vorliegenden Arbeit wurde zunächst ein prägnantes Modell entwickelt, das bei hyperglykämischen Personen eine überdurchschnittliche Vorhersagekraft für das Auftreten von CKD aufweist und sieben Variablen umfasst (Alter, Nüchternglukosestatus, Gesamtcholesterin, geschätzte glomeruläre Filtrationsrate (eGFR), Urin-Albumin-Kreatinin-Verhältnis (UACR), Sphingomyelin (SM) C18:1 und Phosphatidylcholin-Diacyl (PC aa) C38:0). Dabei wurde ein genomweiter polygener (polygenetischen) Score (GPS) für eGFR-Werte (GPS_{eGFR}) unter Verwendung von *KORA Follow Up 4*-Individuen konstruiert und in der britischen Biobank-Kohorte repliziert, was eine konsistente Verbesserung der Vorhersage von CKD-Inzidenzen bei Hyperglykämie aufzeigte und dies zusätzlich zu diesen sieben Vorhersagevariablen verbesserte. Darüber hinaus wurden 120 Multi-omics-Moleküle, identifiziert, die für prävalente CKD bei Hyperglykämie in Frage kommen, von denen 64 (zwei CpGs, zwei RNAs, 46 Proteine und 14 Metaboliten) erfolgreich repliziert wurden. Bei der Multi-omics-Vorhersage zeigte sich, dass die Ergänzung der derzeit vorgeschlagenen Variablen durch omics-Werte von GPS, Protein- und Metabolitenkandidaten die Vorhersageleistung für zukünftige CKD bei Hyperglykämie noch weiter verbessert.

Um festzustellen, ob die Auswirkungen der Biomarkerkandidaten für CKD (Prävalenz/Inzidenz) spezifisch für Hyperglykämie sind, wurden ihre Interaktionseffekte untersucht. Des Weiteren waren SM C18:1 und PC aa C38:0 für CKD (prävalent und inzident), sowie 58 von 64 Multi-omics-Kandidaten für prävalente CKD nur in der hyperglykämischen Untergruppe signifikant,

insbesondere SM C18:1, was darauf hindeutet, dass diese Moleküle möglicherweise einen Interaktionseffekt auf CKD mit dem glykämischen Status haben.

Um die komplizierten biologischen Prozesse der Hyperglykämie-bedingten CKD besser zu verstehen, konstruierten wir acht Subnetzwerke für T2D-bedingte CKD (T2DCKD) und klassifizierten unsere identifizierten Multi-omics-Kandidaten in diesen. Bei Hyperglykämie, 18 von den 64 replizierten Kandidaten waren mit der GPS_{eGFR} assoziiert und zeigten Mediationseffekte mit GPS_{eGFR} und eGFR. Die bidirektionale Mendelsche Randomisierung mit zwei Stichproben ergab, dass 19 Kandidaten eine kausale Beziehung zu Nierenparametern (CKD, eGFR und UACR) haben könnten. Diese genetischen Beweise sprechen dafür, dass die entdeckten Biomarkerkandidaten Teil der vor- / nachgelagerten Pfade von CKD, eGFR oder UACR sein könnten. Es wurden 64 replizierte Kandidaten auf der Grundlage ihrer Richtung der eGFR/UACR klassifiziert und ihre potenziell beteiligten pathophysiologischen T2DCKD-Prozesse innerhalb jeder Gruppe dargestellt. Verschiedene Gruppen von Biomarker-Kandidaten zeigten unterschiedliche Beziehungen von Nieren-Phänotypen (Nierenfunktion oder Nierenschäden) und unterschiedliche Muster der zugrunde liegenden pathogenetischen Prozesse, die zur Verbesserung der Einblicke in die Identifizierung personalisierter therapeutischer Ziele für Hyperglykämie-bedingte CKD beitragen werden.

Die Zusammenhänge zwischen Biomarkerkandidaten aus verschiedenen Omics-Ebenen und die Frage ob sie dieselben Signalwege nutzen, sind noch nicht geklärt. Um dies besser zu verstehen wurden in dieser Arbeit Gaußsche grafische Modellierung und kausale Mediationsanalysen eingesetzt, um zu untersuchen, wie verschiedene Ebenen von Omics-Molekülen (d. h. CpGs, RNAs, Proteine und Metaboliten), die mit CKD bei Hyperglykämie assoziiert waren, miteinander interagierten. So wurden potenzielle neue kausale Zusammenhänge, relevante molekulare Pfade und mögliche Schlüsselfaktoren dieser Pfade identifiziert. Weiterhin wurden drei verschiedene Untergruppen von CKD-Patienten mit Hyperglykämie anhand von drei potenziellen neuen Proteinen (i.e., NBL1, EFNA5 and JAM2) identifiziert. Dies bestätigt, dass verschiedene dominante pathologische Prozesse in verschiedenen Untergruppen von CKD-Patienten zu verschiedenen theoretischen therapeutischen Zielen führen können.

Zusammenfassend zeigt die vorliegende Dissertation, dass Multi-omics-Profile bei der Früherkennung von Nierenerkrankungen, der Identifizierung von Untergruppen anfälliger Bevölkerungsgruppen, sowie zu einem systematischen und biologischen Verständnis von CKD in der hyperglykämischen Bevölkerung signifikant beitragen können. Diese vorliegende Arbeit befasst sich mit der komplexen Multi-omics Landschaft von CKD bei Hyperglykämie und zeigt weiter, wie Multi-omics-Profile zur Präzisionsgesundheit beitragen können.

1. Background

1.1 Precision health and multi-omics techniques

Large-scale multi-omics profiling together with clinical measurements can provide a more complete understanding of the biological processes underlying disease, allowing for improvement of personalized risk prediction, patient stratification, and assignment of molecularly specific treatments, thereby enabling precision health. Zierer *et al.*¹ identified seven models representing distinct aspects of aging in participants from Twins UK cohort through integration of epigenomics, transcriptomics, glycomics and metabolomics with disease traits. This study demonstrate age-related disease is interconnected and that integrating omics data can reveal novel molecular networks underlying complex phenotypes. Through deep profiling of transcriptomics, metabolomes, cytokines, proteomics and microbiome, Zhou *et al.*² provided essential insights into the pathways and responses that differ between glucose-dysregulated and healthy individuals during health and disease. This study also identified early personal molecular signatures of onset of type 2 diabetes (T2D) in one individual, such as high-sensitivity C-reactive protein (CRP). Another study³ from the same cohort have reported the identification of over 67 clinically actionable health discoveries and multiple molecular pathways relevant to metabolic, cardiovascular, and oncologic pathophysiology through integration of clinical measures, genome, immunome, transcriptome, proteome, metabolome, microbiome and wearable monitoring. This study concluded that deep longitudinal profiling can result in actionable health discoveries that contributed to precision health. Liu *et al.*⁴ identified five subgroups of hepatocellular carcinoma with distinct molecular signatures and each with a different survival rate through integrating data on genomic copy number variations, genomic methylation, transcriptome and small transcriptome. These studies show that multi-omics profiles have capacity to inform precision health of disease.

1.2 The global burden of CKD and the contribution from (pre-) T2D

Chronic kidney disease (CKD) affects approximately 9.1% of the general population worldwide⁵. CKD is also associated with substantial mortality worldwide. According to World Health Organization (WHO) global health estimates, CKD claimed 1.5% of deaths worldwide, 1.1% of disability-adjusted life-years and 1.3% of life years lost in 2012⁶. The burden of CKD has continued to grow as the global all-age mortality rate from CKD increased by 41.5% from 1990 to 2017, totaling 1.2 million deaths in 2017⁵. Moreover, in 2017, 1.4 million additional deaths from cardiovascular disease were attributed to impaired kidney function⁵.

Diabetes mellitus is a leading cause of CKD, which accounts for 30% to 50% of all CKD cases when compared to other established risk factors for CKD⁶. Diabetes also contributed the most disability-adjusted life-years for CKD in absolute terms in 2017. Only in 2017, CKD caused by T2D resulted in 8.1 million disability-adjusted life-years. Moreover, T2D was the only cause of CKD to show a significant increase in the age-standardised disability-adjusted life-years rate, which increased by 9.5% between 1990 and 2017⁵. Additionally, undiagnosed diabetes and pre-

diabetes have been related with a high prevalence of CKD in US, European and Asian populations⁷⁻¹⁰.

1.3 Complex biological processes of hyperglycemia-related CKD

CKD is a multifactorial disease characterized by a variety of pathological processes. A single process can have an effect on multiple phenotypes and/or other processes involved in the pathogenesis of CKD, for instance, the renin-angiotensin system, which regulates blood pressure and causes hypertension, also increases inflammation and renal fibrosis¹¹. Ectopic lipid accumulation and incomplete fatty acid beta-oxidation caused by mitochondrial dysfunction contribute to the development of kidney diseases¹². Adipose tissue and adipokines have been shown to have a direct relationship with kidney disease and contribute more than other biological elements¹³ to the regulation of T2D-related CKD (T2DCKD). Convincing evidence suggested that the formation and accumulation of advanced glycation end products is mediating progressive changes in kidney structure and loss of kidney function¹⁴. The intrarenal renin-angiotensin system (RAS) plays a crucial role in regulating glomerular hemodynamics and hypertrophy and sclerosis of glomeruli¹⁴. Hyperglycemia drives the process of excessive deposition of extracellular matrix protein (ECM) that is a hallmark of diabetes kidney disease (DKD)¹⁵. Increased ECM deposition can lead to thickening of the glomerulus and tubule basement membrane, and increased mesangial matrix eventually results in glomerular sclerosis and tubulointerstitial fibrosis¹⁶. Activation of innate immunity (NLRP3 inflammasome, TLR signaling, and cellular responses (such as macrophage activation)) has been shown to coordinate kidney inflammation in DKD¹⁷. Abnormal angiogenesis is a well-defined complication of DKD¹⁸. Hypoxia and oxidative stress in the kidney are the main inducers of angiogenesis. It promotes angiogenesis to counteract hypoxia¹⁹ by up-regulating VEGF and its receptor KDR²⁰. Patients with CKD or DKD exhibit distinct pathological processes and respond differently to various treatments, requiring the development of targeted theoretical therapeutic strategies for different subgroups of CKD patients.

1.4 Current omics studies in (hyperglycemia-related) CKD

The search for effective prevention strategies and optimal therapeutic targets for CKD is fraught with difficulties due to the disease's molecular complexity and complications. The availability of large-scale omics data sets (e.g., genomics, epigenetics, transcriptomics, proteomics, and metabolomics) has revolutionized biology and resulted in the emergence of systematic approaches for advancing our understanding of the biological processes underlying CKD and related kidney traits in order to benefit prevention, develop biomarkers and drugs.

Genotyping. Genome-wide association studies (GWAS) have identified a multitude of genetic variants associated with CKD and related kidney traits, igniting interest in the use of genetic information to study their biology, causality and improve prediction²¹⁻²⁵. Mendelian randomization (MR)²⁶ is used to estimate the causality of an observed association, which used genetic variants as instruments to overcome the limitations (i.e. confounding and reverse causality) of classical epidemiological studies. Through aggregating genome-wide genetic variants into a single score

that reflects an individual's disease risk, genome-wide polygenic score (GPS)²⁷ captures the polygenic structure of complex diseases, including kidney disease. These two GWAS-based approaches open up new avenues for studying CKD and related kidney traits.

Methylation. Increasing evidence suggests that epigenetic mechanism involving DNA methylation, histone modifications and non-coding RNAs contribute to the regulation of DKD characteristics such as an accumulation of extracellular matrix²⁸. Numerous epigenome-wide association studies (EWAS) in populations with CKD or DKD have advanced our understanding of the epigenetic mechanisms underlying CKD and DKD, revealing that methylation changes were associated with ageing, inflammation, cholesterol²⁹, renal fibrosis³⁰, mitochondrial function³¹ or oxidative stress pathways³², etc. However, many of these early EWAS of kidney disease were constrained by cross-sectional designs with relative small sample sizes and the absence of longitudinal follow-up and replication studies²⁸. A EWAS with a large sample size (N = 4,859) has highlighted epigenetic variation associated with kidney function. It identified and replicated 19 CpG sites associated with estimated glomerular filtration rate (eGFR) or CKD, five of which were also associated with renal fibrosis in biopsies from CKD patients and demonstrated consistent DNA methylation changes in the renal cortex³³. Another study showed that changes of kidney cytosine methylation could improve the estimation of kidney function decline in patients with DKD, and that the methylation probes associated with kidney functional decline and injury were located in regulatory regions of the kidney, which are associated with changes in gene expression³⁴. A 2021 meta-analysis of EWAS for eGFR (N = 33,605) and UACR (N = 15,068) provided causal evidence for the effect of methylation at *PHRF1*, *LDB2*, *CSRNP1* and *IRF5* on kidney function via two-sample MR (2SMR)³⁵.

Gene expression. Gene expression biomarkers of kidney diseases have been identified using a variety of human samples such as kidney biopsies, urine or circulatory blood³⁶. Urinary epidermal growth factor (EGF) protein was an independent risk predictor for CKD progression and was capable of improving the prediction of disease events in populations with CKD on top of standard clinical variables. EGF expression in the tubulointerstitial compartment has been proposed as a predictive biomarker of eGFR³⁷. Another transcriptome study reported 96 genes were upregulated in glomerular gene expression profile of individuals with diabetes-related kidney disease, while over 500 genes such as insulin-like growth factor binding protein 2 (IGFBP2) were downregulated³⁸. Patients with CKD stage 4-5 had higher gene expression levels of *COX6C*, *COX7C*, *ATP5ME*, and *UQCRH* in peripheral blood mononuclear cells compared to those with CKD stage 2-3 or non-CKD³⁹. In all stages of DKD, increased serum levels of VEGF, MCP-1, EGF and FGF-2 were observed⁴⁰.

Proteomics. Numerous novel biomarkers for kidney disease have been published, with the majority of these biomarkers being proteins. It reflects the fact that proteins integrate genomic information and environmental influences, are involved in nearly all biological processes, and represent the targets for the majority of drugs⁴¹. Several proteins have been proposed and validated to be novel biomarkers of kidney disease in varying degrees. For instance, different studies have demonstrated that concentrations of serum cystatin C is superior to serum creatinine for assessment of GFR⁴²⁻⁴⁴. When serum cystatin C was added to serum creatinine and albuminuria, the

predictive accuracy for all-cause mortality and end-stage renal disease was increased⁴⁵. Additionally, higher plasma levels of IL6 were observed in elderly patients with renal insufficiency⁴⁶ and patients with stage 3-5 CKD⁴⁷, but IL6 was not significantly associated with eGFR⁴⁷. Elevated plasma levels of resistin were associated with CKD, reduced eGFR and the presence of inflammatory biomarkers⁴⁸. Moreover, levels of circulatory adiponectin elevated in patients with endothelial dysfunction and stage ≥ 3 CKD⁴⁹. However, adiponectin levels were not associated with renal function in men with T2D⁵⁰. Although circulatory levels of several proteins have shown potential to be used as biomarkers of kidney disease, some candidate markers have not been replicated. A number of biomarkers support the role of (chronic) inflammation in CKD, however, their utility as markers of CKD itself is debatable. It could be a reflection of the complex and multifactorial characteristics of CKD. Moreover, discrepancies between studies of particular biomarkers, such as adiponectin, may reflect the fact that relationships with CKD occur only in very specific situations⁴¹.

Metabolomics. The associations between metabolite profiles and CKD have been widely investigated in general and T2D population⁵¹⁻⁵³. For instance, the kidney plays a role in biosynthesis of carnitine and its excretion into plasma and urine⁵⁴. Acylcarnitines (ACs) concentrations indicate beta-oxidation of fatty acids⁵⁵. The occurrence of ACs in serum, plasma and urine is indicative of mitochondrial dysfunction. Higher plasma concentrations of ACs occurred in individuals with reduced eGFR⁵⁶. Another example is that several lipid classes (sphingolipids, fatty acids, sterols and glycerolipids) show potential as biomarkers for CKD. The most common lipids of sphingolipids are sphingomyelins in humans. Moreover, multiple metabolites such as amino acids and lipid metabolites (choline, lysophosphatidylcholines 18:2 and 18:1) were identified to be significantly associated with incident CKD in Framingham Heart Study⁵⁷.

1.5 Inadequate early detection of CKD

With the global increasing prevalence and burden of (pre)diabetes-related CKD, early detection of CKD predisposition in this high risk population can improve the opportunity to effectively prevent and manage this microvascular complication of diabetes. Currently, elevated urinary albumin-creatinine ratio (UACR) and reduced eGFR are used to diagnose CKD⁵⁸. According to the report, UACR, eGFR, age, and gender were highly predictive of the progression of CKD⁵⁹. Moreover, albuminuria and eGFR are the most important variables for predicting the occurrence and progression of early CKD in individuals with T2D. However, even when combined with age and gender, their predictive power is moderate, with an externally verified c-statistic of 0.68⁶⁰. Due to the incapacity of traditional risk factors for accurately predicting of CKD in individuals with T2D, there is an urgent need for identifying more sensitive and specific biomarkers on top of baseline eGFR and UACR and proposing a suitable combination of predictors to improve early detection of CKD in (pre) diabetes. Moreover, whether multi-omics profiles could improve predictive performance on top of traditional risk factors is required to be explored.

1.6 Discrepancies of (candidate) biomarkers' effects for kidney disease

Some potential markers have been described in a single publication and their association with kidney disease appears to be moderate. It may reflect the complicated and multifactorial nature of CKD. For example, the proposed biomarker may perform well and be appropriate for use in children (who are less likely to have comorbidities) or in individuals with a well-defined cause of kidney injury, but not in conditions such as sepsis, where the onset of kidney injury is difficult to define⁴¹. Furthermore, the overlap in biomarker concentrations observed in different conditions casts doubt on their diagnostic utility⁴¹. IL18 was described as a valuable and sensitive urinary biomarker in the context of acute kidney injury (AKI) in a cohort of 124 children admitted to paediatric intensive care units and mechanically ventilated⁶¹. However, the encouraging correlations between neutrophil gelatinase-associated lipocalin (NGAL), kidney injury molecule-1 (KIM-1), or IL18 and kidney disease have not been replicated in other reports, most notably in the context of AKI⁶²⁻⁶⁵. Differences between studies regarding these biomarkers most likely reflect their associations with kidney disease that occur in very specific circumstances. The heterogeneity indicates that a large number of (candidate) biomarkers for CKD have strong interaction effects, implying that their effects on CKD are subgroup- or condition-specific⁴¹. To benefit from personalized CKD management, it is critical to investigate the interaction effects and condition-specific effects of the identified (candidate) biomarkers.

1.7 Paucity of systematic biological understanding of hyperglycemia-related CKD

Given that not all hyperglycemic individuals develop CKD and that not all patients with CKD follow the same disease trajectory, it is critical to investigate their mechanisms of action in order to improve patient stratification and accelerate targeted screening and treatment programs. Previous studies as described above have examined various aspects of CKD or DKD. However, few studies have systematically integrated various types of data including genome, epigenome, transcriptome, proteome, metabolome, and phenome to study CKD in individuals with pre- or T2D. Using multi-omics techniques to investigate CKD will give a more detailed understanding of its pathophysiology. CKD is a multifactorial disease with multiple pathological processes. Although omics studies have proposed many (candidate) biomarkers of CKD or its related kidney traits, their specific roles in diabetes-related CKD remain uncertain. Due to the complex pathogenesis of CKD, identifying more sensitive and specific biomarkers that target the disease's pathological process can help us better understand the disease and possibly prevent or treat it earlier.

Most proposed (candidate) biomarkers currently use observational data and do not investigate causality. Extending observation estimates to causality will increase the possibility to excavate the “true” relationship and directions between these candidates and kidney traits, which is critical to turning candidates into biomarkers. CKD is polygenic disease and the GPS can capture the major genetic information of phenotypes, which is helpful to identify individuals under high genetic risk and investigate whether the circulatory levels of phenotype-associated-omics molecules

are genetically determined. Moreover, GPS can also support investigating how genetic information flow between omics molecules and phenotypes.

Since most (candidate) biomarkers are discovered in a single omics study, the potential interplay among the molecules from different omics levels has few been discussed, e.g. ACs were found to associate with CKD and DKD, but the potential mediating proteins still need to be discovered. The crosstalk among these molecules can help determine they share a pathway and identify the key driver of the pathway. It not only can improve the biological understanding of the disease processes of CKD, but also can help improve personalized prevention and drug discovery by tackling the key driver of the specific pathway.

Even when eGFR and UACR are normal, there may be pathological molecular changes in the kidneys of individuals at risk of CKD ⁶⁶. Current CKD treatments, such as RAS blockade, focus on delaying disease progression rather than reversing pathological damage ⁶⁷. As a result, it is critical to identify biomarkers capable of identifying early pathological changes, predicting eGFR and/or UACR values, and elucidating relevant pathological processes. A panel of multiple protein biomarkers covering many pathophysiological processes underlying DKD may be more reliable and accurate to predict progression of kidney disease ⁴¹. In light of the multiple pathogenic processes involved, a holistic approach is the only rational strategy for preventing CKD progression ⁶⁸. Therefore, it is important to classify (candidate) biomarkers based on their potential directions with eGFR and UACR, as well as their potential involvement in specific T2DKD pathological processes. Thus, changes in molecular profiles within a subgroup represent potentially distinct changes in eGFR/UACR values (kidney function or kidney damage) and associated pathological processes, which may contribute to the identification of personalized therapeutic targets for hyperglycemia-related CKD. Moreover, CKD patients' medication response heterogeneity varies greatly. CKD patients with hyperglycemia necessitates the development of distinct theoretical therapeutic strategies. Therefore, the ability of multi-omics profiles to classify hyperglycemia-related CKD into subgroups and the unique patterns in each subgroup require to be explored to benefit for targeted therapy.

2. Contributing papers

This cumulative thesis comprises three papers.

Paper I: Machine Learning Approaches Reveal Metabolic Signatures of Incident Chronic Kidney Disease in Individuals With Prediabetes and Type 2 Diabetes ⁶⁹.

Paper II: Validation of Candidate Phospholipid Biomarkers of Chronic Kidney Disease in Hyperglycemic Individuals and Their Organ-Specific Exploration in Leptin Receptor-Deficient db/db Mouse ⁷⁰.

Paper III: Multi-omics landscape of chronic kidney disease in individuals with prediabetes or type 2 diabetes: from associations towards precision medicine (Huang *et al.*).

3. Rationale

The overall objectives of this thesis are to improve early detection, understanding of the condition-specific effects of (candidate) biomarkers and systematic biological understanding of CKD in individuals with pre- or T2D using multi-omics techniques. The ultimate goal is to improve precision health of hyperglycemia-related CKD. Three studies were conducted to pursue the following specific research question.

- (1) Paper I aims to identify circulatory metabolite signatures and the best combination of predictors constructed with metabolites and clinical variables to improve early detection of incident CKD specific for hyperglycemia.
- (2) Paper II aims to gain a better biological understanding of the complex metabolic interactions between different organs for candidate biomarkers proposed by paper I for hyperglycemia-related CKD using animal models, and to investigate if these metabolites are associated with the later stage of hyperglycemia-related CKD characterized by reduced eGFR.
- (3) Paper III aims to advance systematic biological understanding of molecules' alterations and mechanisms underlying hyperglycemia-related CKD by utilizing multi-omics techniques and to contribute to precision health for hyperglycemia-related CKD.

4. Methods

4.1 Study population

KORA is a population-based study that consists of health surveys and subsequent follow-up examinations of individuals living in the Augsburg region of southern Germany ⁷¹. The details of study design, sampling method and data collection have been previously described ⁷¹. An overview of KORA study is summarized in Figure 1. Between 1999 and 2001, KORA S4 examined 4,261 individuals. Between 2006 and 2008, the first follow-up (F4) was conducted on 3,080 individuals. Between 2013 and 2014, 2,269 participants were examined in the second follow-up (FF4). KORA S3 (1994-1995) and its follow-up (F3, 2004-2005) examined 4,856 and 3,006 individuals, respectively. Each baseline and follow-up examination included a self-administered questionnaire, physical examinations, and a collection of various biological samples. All study participants gave written informed consent. The KORA study was approved by the ethics committee of the Bavarian Medical Association, Munich, Germany.

Paper I was a longitudinal study analyzing 1,838 participants from F4 and FF4. The human study section of paper II was a cross-sectional study involving 1,907 FF4 participants. Paper III included a cross-sectional design for analyzing data from F4, and a longitudinal design of analyzing data of S4→F4, and F4→FF4, respectively. Part of the results of paper III were replicated in the F3 study (Figure 1).

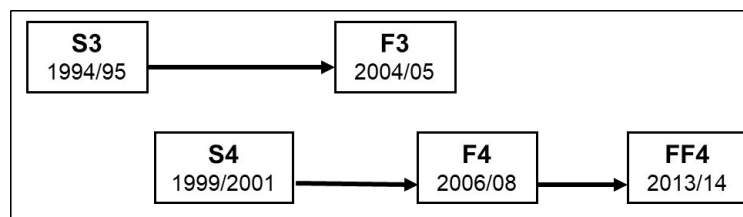


Figure 1. Overview of the baseline surveys and follow-up examinations of KORA study, but does not include the telephone interview-based General Health Follow-up.

4.2 Definition of hyperglycemia

Hyperglycemia was defined using WHO and American Diabetes Association (ADA) criteria, respectively.

Paper I and paper II used the WHO criteria. Individuals with hyperglycemia and normal glucose tolerance (NGT) were classified using the WHO criteria based on their fasting glucose (FG) and two hour post load glucose (2-h glucose) values ⁷². Hyperglycemic group included participants with pre-diabetes and newly diagnosed T2D (i.e., $FG \geq 110$ mg/dl and/or 2-h glucose ≥ 140 mg/dl), as well as known T2D that was diagnosed by physician validated self-reporting and/or current use of anti-diabetes agents ⁷³.

Given the increasing burden of (pre) diabetes-related CKD, paper III extended the WHO hyperglycemic standard to the American Diabetes Association (ADA), which may detect more hyperglycemic-induced CKD signals. Individuals with hyperglycemia and NGT were classified using the ADA diagnostic criteria based on their FG, 2-h glucose and glycated haemoglobin (HbA_{1c}) values ⁷⁴. Hyperglycemic group comprised participants with pre-diabetes and newly diagnosed T2D (i.e., $FG \geq 100$ mg/dl or 2-h-glucose ≥ 140 mg/dl or $HbA_{1c} \geq 5.7\%$), as well as known T2D that was diagnosed by physician validated self-reporting and/or current use of anti-diabetes agents ⁷³.

4.3 Definitions of kidney traits

The eGFR was calculated from serum creatinine (mg/dl) and cystatin C (mg/dl) (IDMS and IFCC standardized values) using the Chronic Kidney Disease Epidemiology Collaboration (CKD-EPI) equation ⁷⁵. CKD was defined as an eGFR < 60 ml/min/1.73 m² or a UACR ≥ 30 mg/g ⁷⁶.

Other definitions of eGFR and CKD were also used in this thesis and were denoted by symbols, including eGFR_{crea} (eGFR was calculated from serum creatinine (mg/dL) (IDMS standardized values) using the CKD-EPI equation ⁷⁵, CKD_{eGFRcrea-cys} (eGFR-based CKD defined as eGFR < 60 ml/min/1.73 m²) ⁷⁶, CKD_{eGFRcrea} (eGFR_{crea}-based CKD defined as eGFR_{crea} < 60 ml/min/1.73 m²) ⁷⁶, and CKD_{UACR} was defined as an UACR ≥ 30 mg/g ⁷⁶.

4.4 Multi-omics techniques in study population

4.4.1 Genotyping

The Affymetrix Axiom Array was used to genotype the KORA S4/F4 individuals. Imputation was performed on 541,422 autosomal SNPs following rigorous quality control (QC). The haplotypes were inferred using Shapeit v2. Minimac3 on the Michigan Imputation Server with the 1000G phase 3 reference panel was used to complete the imputation.

4.4.2 DNA Methylation

The DNA methylation levels of KORA F4 individuals were determined using Illumina HumanMethylation450 BeadChip array as previously described ⁷⁷. The methylation data was pre-processed in accordance with the CPACOR pipeline ⁷⁸ and background correction was performed using R package minfi ⁷⁹. Normalization was accomplished through the use of the quantile normalization (QN) and beta-mixture quantile normalization pipelines. The CpG methylation proportion was reported as a beta-value, a continuous variable ranging from 0 to 1.

4.4.3 Gene expression

The Illumina HumanHT-12 v3 Expression BeadChip was used to determine gene expression levels of KORA F4 individuals ⁸⁰. Expression data were log₂-transformed and QN with the Bioconductor package lumi.

4.4.4 Proteomics

SOMAscan Assay was used to measure the proteomics data of KORA F4 individuals. SOMAscan platform has been described in detail elsewhere ^{81,82}.

4.4.5 Targeted Metabolomics

Absolute*IDQ*TM p150 Kit (BIOCRATES Life Sciences AG, Innsbruck, Austria) ⁸³ were used to measure serum samples from participants in the KORA F4 study. The Absolute*IDQ*TM p180 Kit (BIOCRATES) was used to measure serum samples from participants in the KORA FF4 study.

4.5 Mouse study

Paper II contained multi-tissue data from a mouse study in which male 8-week (± 3 d) old wild type (WT) mice (N = 10) and the leptin-receptor deficient mouse model (db/db) mice (BKS.Cg-*Dock7*^{m+/+} *Lepr*^{db/J}, N = 10) were used. The District Government of Upper Bavaria (Regierung von Oberbayern, Gz.55.2-1-54-2531-70-07, 55.2-1-2532-153-11) approved the animal experiments. Absolute*IDQ*TM p180 Kit (BIOCRATES Life Sciences AG, Innsbruck, Austria) was used to determine metabolite values in plasma, liver, lung, adrenal glands, adipose tissue, cerebellum and testis samples, and Absolute*IDQ*TM p150 Kit (BIOCRATES) was used to determine the metabolite values in urine.

4.6 Statistical analyses

4.6.1 Paper I ⁶⁹

Candidate biomarkers of incident CKD in hyperglycemia were identified from 125 targeted metabolites through three-step feature selection that included multivariable logistic regression adjustment of confounders, priority-lasso ⁸⁴ filtering and stepwise Akaike information criterion selection.

Four sensitivity analyses of candidate biomarkers were conducted: 1) Nearest-neighbor propensity score matching in nested case-control study design. 2) Investigating whether the predictive effects of candidate biomarkers for incident CKD was specific for hyperglycemia. 3) Exploration of interaction effects of candidate biomarker with glucose levels for incident CKD. 4) Examination of associations of candidate biomarkers with incident $\text{CKD}_{\text{eGFRcrea-cys}}$ and CKD_{UACR} separately in hyperglycemic participants with multivariable logistic regression.

The three-step feature selection with 100 random repeats of 10-fold cross-validation was performed to develop the set of metabolite and clinical predictors for incident CKD in hyperglycemia. The receiver operating characteristic curve (AUC) values of developed predictors were compared with the established prediction model. The predictive models of predictors' set were established with three machine learning algorithm (support vector machine (SVM) ⁸⁵, random forest (RF) ⁸⁶ and adaptive boosting (AdaBoost) ⁸⁷) using training data and the AUC values of respective model were computed for the testing data only. In total, 100 repeats of 10-fold cross-validations including 1000 times of three-step feature selection were performed, resulting the best set of predictors for incident CKD in hyperglycemia, which was defined from the most frequently selected set of metabolites and clinical variables.

4.6.2 Paper II ⁷⁰

Inverse probability weighting (IPW) ⁸⁸ for continuous exposures of the generalized propensity score approach was used to provide a more reliable estimate of metabolite-outcome associations in participants of the KORA FF4 study. Multivariable linear regression was used to estimate the generalized propensity score, in which each metabolite was regressed on covariates, respectively ⁸⁹. The corresponding estimated generalized propensity scores were then used to calculate the inverse probability weights of each metabolite ⁸⁸. Weighted multivariable linear and logistic regression with applying corresponding inverse probability weights were performed to analyze metabolite association with $\text{eGFR}_{\text{crea}}$ and $\text{CKD}_{\text{eGFRcrea}}$ in hyperglycemic individuals of KORA FF4, respectively. Weighted multivariable logistic regression after IPW was used to analyze the association between metabolites and $\text{CKD}_{\text{eGFRcrea}}$ in NGT individuals of KORA FF4.

The Mann-Whitney U test was used to assess the statistical differences in clinical and metabolic parameters between db/db and WT mice. Differences in the tissue-specific concentration of creatinine and the two candidate metabolite biomarkers between db/db and WT mice were assessed by the student t -test.

4.6.3 Paper III

Briefly, the discovery CKD - EWAS, transcriptome-, proteome-, and metabolome-wide association studies (TWAS, PWAS, MWAS) were performed with multivariable logistic regression to examine the associations between CpG / RNA / protein / metabolite and prevalent CKD in hyperglycemic individuals of KORA F4. The replication of identified candidates was also used multivariable logistic regression. I examined the associations between omics candidates and kidney traits in hyperglycemia using linear regression for eGFR or UACR values and logistic regression for incident CKD.

I constructed a multi-omics integration network (MOIN) using Gaussian graphical model (GGM)⁹⁰ according to the (extended) Bayesian information criterion and clustered the different levels of MOIN (DMOIN) using Markov Cluster Algorithm. The mediation analyses of multi-omics molecules with three time points of kidney traits were conducted in accordance with the outline of Baron and Kenny⁹¹, and the mediating effect was determined using a non-parametric casual mediation analysis⁹². The *P*-value of mediation effect was calculated by bootstrapping with 1,000 resamples. Using the defined criteria, the best direction for each mediating triangle was determined. I then mapped the best direction(s) of mediation with DMOIN to generate the directed mediating multi-omics networks (DMMONs) to inspect the direction in which nephrogenic effects may potentially pass through each connected edge of our DMOIN.

I constructed GPS of eGFR with KORA F4 individuals using effect size estimates for SNPs on eGFR values derived from 42 European ancestor studies' GWAS meta-analyses²³. GPS was built using an additive model with PRSice-2⁹³ and finally with the effects of 162,818 SNPs. Our GPS_{eGFR} were replicated using the same SNPs in UK biobank cohort (UKBB) and KORA S4 testing individuals. The association between GPS_{eGFR} and eGFR was evaluated with linear regression in three studies. The associations between GPS_{eGFR} and kidney traits in hyperglycemia were examined using linear regression for eGFR values and logistic regression for CKD. The associations between GPS_{eGFR} and replicated candidates were examined with linear regression. I conducted mediation analyses between GPS_{eGFR} , GPS_{eGFR} -associated-candidates and kidney traits following the outline of Baron and Kenny⁹¹ and the mediating effect was evaluated with a non-parametric casual mediation analysis⁹² as well.

I used bi-directional 2SMR to assess the potential causality between replicated proteins/metabolite and kidney traits (CKD, eGFR and UACR values). Our primary MR analysis method was robust adjusted profile score⁹⁴. The heterogeneity of the SNP instruments was determined with Cochran's *Q* statistic of inverse variance weighted (IVW) and MR-Egger, and the horizontal pleiotropic effect of the involved SNPs was tested with the intercept of the MR-Egger and global test of MR pleiotropy residual sum and outlier (MR-PRESSO)⁹⁵. When there was evidence of potential violations of heterogeneity or horizontal pleiotropy ($P < 0.05$), I conducted additional outliers-corrected MR analyses (IVW-radial⁹⁶ and MR-PRESSO) to address the issues.

I investigated the prediction of incident CKD in hyperglycemic individuals of KORA F4 with multi-omics molecules using 100 random repeats of bootstrapping to assess the predictive performance of various combinations of omics levels. Their predictive performance was evaluated using

AUC in testing data. Priority-Lasso was used to select predictors for combinations containing omics candidates. Predictive models were built with RF.

I classified KORA F4 CKD patients with hyperglycemia using various combinations of biomarkers and candidates with Uniform Manifold Approximation and Projection, and identified three distinct groups of CKD patients with three potential novel proteins. The difference among identified groups was determined using the analysis of variance (ANOVA) test for numeric variables with a normal distribution and the Kruskal-Wallis test for those with a skewed distribution. The categorical variables were compared among groups using Pearson chi-squared test or Fisher exact test when any theoretical frequency was less than one. The Cochran–Armitage test was also applied when applicable.

5. Results

5.1 Paper I ⁶⁹

This paper addresses the first aim of this thesis.

Due to the fact that traditional risk factors are insufficient to accurately predict CKD in hyperglycemic individuals, there is an urgent need to identify more sensitive and specific biomarkers in addition to baseline eGFR and UACR and propose a suitable combination of predictors to improve early detection of CKD in (pre) diabetes.

Of 125 analyzed metabolites, this longitudinal study revealed two (sphingomyelin (SM) C18:1 and phosphatidylcholine diacyl (PC aa) C38:0) metabolites presenting significant risk effects of incident CKD in individuals with pre- or T2D after three-step feature selection.

I further illustrated the specificity of the risk effects of two metabolites for hyperglycemia by metabolite-glucose interaction analysis as their risk estimates of incident CKD were significant only in hyperglycemic group and the top tertile of fasting and 2-h glucose, respectively. Notably, SM C18:1 demonstrated strong interaction effects with glucose, as it showed significant multiplicative interaction effects with glycemic status and 2-h glucose, and its effect size estimate of incident CKD has turned to reverse association in other groups compared to the ones in the hyperglycemic subgroup and the top tertile of fasting and 2-h glucose, respectively. It indicated the risk effect of SM C18:1 for future CKD were specific for a subgroup of pre- or T2D individuals with relatively high glucose values, which suggests that a subgroup of susceptible population within pre- or T2D individuals for future CKD may can be represented by molecules like SM C18:1.

The median AUC values of our developed sets of predictors constructed with metabolites and clinical variables outperformed the reference predictors in all three machine learning algorithms (i.e. SVM, RF, Ada) with 100 times of 10-fold cross-validation. The best set of predictors for incident CKD were further identified, consisting of two metabolites (SM C18:1, PC aa C38:0)

and five clinical variables (age, total cholesterol, fasting glucose, eGFR and UACR). The seven variables were the most important ones.

5.2 Paper II ⁷⁰

This paper addresses the second aim of this thesis.

The finding of this animal and cross-sectional human study is that the two metabolites (i.e., SM C18:1 and PC aa C 38:0) discovered by paper I associate with further stages of hyperglycemia-related CKD evolution including i) early changes characterized with glomerular hyperfiltration (8-week-old db/db mice) and ii) later changes characterized with kidney dysfunction (i.e., reduced eGFR_{crea}) (KORA FF4 study).

The organ distribution of the two metabolites was investigated in an 8-week-old db/db mouse model that mimics early human CKD development. The db/db mice exhibited early diabetic nephropathy-associated changes such as glomerular hyperfiltration and hypertrophy. In comparison to WT mice, db/db mice had significantly lower concentrations of both SM C18:1 and PC aa C38:0 in their urine and adipose tissue, but significantly higher concentrations in their lungs. Additionally, SM C18:1 was significantly accumulated in the plasma and liver of db/db mice, whereas PC aa C38:0 was significantly higher in the adrenal glands.

In hyperglycemic individuals, the concentrations of SM C18:1 and PC aa C38:0 were found to be inversely associated with eGFR_{crea} and positively associated with prevalent CKD_{eGFRcrea}, respectively. Moreover, neither SM C18:1 nor PC aa C38:0 were significantly associated with prevalent CKD_{eGFRcrea} in NGT individuals. These findings further supported that the two lipids' risk associations for CKD_{eGFRcrea} characterized by reduced kidney function are hyperglycemia-specific.

5.3 Paper III

This manuscript addresses the third aim of this thesis.

In conjunction with clinical measurements, large-scale multi-omics profiling can provide a more comprehensive understanding of the biological processes underlying disease, thereby contributing to precision medicine.

I reported high throughput EWAS, TWAS, PWAS and MWAS with prevalent CKD in individuals with pre- or T2D of KORA F4, and identified 120 multi-omics candidates. I built GPS of eGFR using KORA F4 individuals and successfully replicated it in UKBB and S4 testing samples.

We constructed eight T2DCKD subnetworks based on literature search and classified the identified candidates or their corresponding genes/proteins into these processes. We successfully replicated 64 of 120 candidates with CKD in Qatar Biobank, Qatar Metabolomics Study on Diabetes, KORA F3 or KORA FF4 studies. Out of 64 replicated candidates, all were associated with eGFR or UACR values (current or follow-up) in KORA F4 hyperglycemic individuals, 11 of which may be novel candidates of CKD, 18 of which were associated with GPS_{eGFR} and demonstrated mediation effects of direction of GPS_{eGFR} → candidate → eGFR and/or GPS_{eGFR} → eGFR → candidate.

Bi-directional 2SMR supported that 19 replicated proteins/metabolites may have a causal relationship with kidney traits (CKD, eGFR and UACR) in one/both direction(s). I further classified 64 replicated candidates into 14 subgroups based on various evidence with eGFR and UACR values, and presented the potentially involved pathophysiological T2DCKD processes for each subgroup. A subgroup of susceptible high-risk individuals may be represented by a subgroup of their molecular profiles, which may provide insight into the identification of personalized therapeutic targets for hyperglycemia-related CKD.

I examined the potential interplay among four-level multi-omics molecules of CKD in hyperglycemia. This section included three main parts of results. I build MOIN with 101 molecules from five omics levels using GGM to uncover potential crosstalk among molecules. The generated DMOIN resulted ten sub-clusters, which confirmed the established link among molecules and revealed potential new ones, such as Tyr negatively linking with protein IGF2BP2. I then performed mediation analyses between different levels of molecules and kidney traits to ascertain the potential best direction(s) of each examining mediating triangle. These exhaustive mediation explorations identified 565 potential best mediation directions, pointing to a complex omic landscape of regulatory interactions between molecules and kidney traits. When the kidney trait was served as an independent variable (X) or outcome (Y), our results showed that our candidate proteins and three known biomarkers were major mediators in connecting other omics candidates to kidney traits in both directions. Furthermore, I mapped our DMOIN with best mediation directions' results from mediation analyses to generate the DMMONs, which contributed to inspect the direction of nephrogenic effects that could be transmitted through each connected edge. Our DMMONs revealed the potential directions of connected molecule pairs and their associated kidney traits, e.g. part of the nephrogenic effects of molecules may operate via an indirect path possibly through their connected molecules. Our DMMONs also showed potential to reveal causal links, e.g. $IL19 \rightarrow RNA\ SLC22A4 \rightarrow CKD$.

Our multi-omics prediction results indicated adding omics levels on top of reference predictors improved prediction performance for future CKD in hyperglycemia, and the omics levels with added predictive values were GPS, candidate proteins, and metabolites instead of candidate RNAs and CpGs. However, except for GPS, this improvement was limited for ref₄ (i.e., seven predictors proposed by paper I), indicating the superior discriminatory ability of this predictor set for future CKD in hyperglycemia that we previously suggested. Moreover, I discovered that GPS_{eGFR}'s predictive effect on future CKD in hyperglycemia, specifically future CKD_{eGFR}, is consistent, stable, and independent of baseline eGFR and UACR values. Furthermore, I used three potential novel proteins to identify three distinct subgroups of CKD patients with hyperglycemia, which presented distinct characteristics and underlying pathological mechanisms.

Overall, along with elucidating biological concepts, our study presents a complex multi-omic landscape of CKD in hyperglycemia and sheds light on how to integrate multi-omics molecular profiles to contribute to precision health of hyperglycemia-related CKD.

6. Discussion

6.1 Early detection of CKD in hyperglycemia

To improve early detection of CKD in hyperglycemia, paper I proposed a parsimonious prediction model for incident CKD specific for hyperglycemic individuals, consisting of seven predictors (age, FG, total cholesterol, eGFR values, UACR values, SM C18:1 and PC aa C38:0). Paper III confirmed the superiority of this combination of predictors and discovered that the GPS_{eGFR} I developed could enhance this combination's performance. Additionally, paper III discovered that adding omics levels from GPS, candidate proteins, and metabolites to current reference predictors that even included baseline eGFR and UACR values could improve prediction performance for future CKD in hyperglycemia. Moreover, our GPS_{eGFR} demonstrated superior improvement of predictive effect on future CKD in hyperglycemia, particularly CKD_{eGFR}. Therefore, this thesis contributes to improve personalized prediction of future CKD in hyperglycemic individuals.

6.2 Interaction and condition-specific effects of (candidate) biomarkers for kidney traits

CKD is a complex and multifactorial disease. Discrepancies between studies on certain biomarkers (such as NGAL, KIM-1, or adiponectin) most likely reflect associations with kidney disease that occur in very specific circumstances⁴¹. For example, adiponectin levels were inversely correlated with eGFR in 406 CKD patients and 88 healthy controls⁴⁹, but were not linked to kidney function in another study of 733 men with T2D⁵⁰. Many (candidate) biomarkers for CKD have strong interaction effects, implying that their effects on CKD are subgroup- or condition-specific⁴¹. This thesis substantiated this claim and investigated the specific effects of proposed candidates. Paper I identified two metabolites with hyperglycemia-specific predictive risk effects for incident CKD as defined by eGFR and UACR. SM C18:1 in particular demonstrated strong interaction effects with glucose levels, and its effect size estimates of incident CKD shifted in the negative direction in other glucose groups when compared to the hyperglycemic subgroup and the top tertile of fasting and 2-h glucose, respectively (Figure 2). Paper III confirmed SM C18:1's strong interaction effects with glycemic status for incident CKD. It indicated that a subgroup of pre- or T2D individuals with high glucose levels was found to be more susceptible to future CKD when presented with high levels of SM C18:1. Moreover, paper III reported 64 replicated candidate biomarkers of prevalent CKD, 58 of which were not FDR significant in NGT individuals, implying that their effects on prevalent CKD were hyperglycemic-specific. This thesis demonstrated that the interaction effects of multi-omics molecules on CKD show potential to contribute to stratify CKD patients or individuals at high risk of developing CKD using their specific markers.

Additionally, the effects of (candidate) biomarkers may be kidney traits specific. Several biomarkers support the involvement of (chronic) inflammation in CKD, but their utility as a marker of CKD is less clear⁴¹. Plasma levels of oxidative stress biomarkers (protein carbonyl groups, free F2 isoprostane, and reduced thiol content of proteins) and inflammatory biomarkers (CRP

and IL6) were significantly increased in 60 patients with CKD (stages 3–5) compared to healthy individuals. However, eGFR was not found to be significantly associated with any of these biomarkers. Although plasma levels of IL6 were found to be significantly higher in elderly patients with renal insufficiency⁴⁶ and in patients with stage 3-5 CKD⁴⁷, IL6 was not found to be significantly associated with eGFR⁴⁷. In this thesis, paper II demonstrated that SM C18:1 and PC aa C38:0 were associated with the later stage of hyperglycemia-associated CKD characterized by reduced kidney function (i.e., reduced eGFR_{crea}) (hyperglycemic individuals in cross-sectional study). In the cross-sectional study, two metabolites were associated with reduced kidney function in which eGFR values were calculated using serum creatinine rather than serum cystatin C or their combination. This could be explained as follows: 1) As demonstrated in paper III, serum creatinine significantly mediated the relationship between SM C18:1 and follow-up eGFR_{crea}; 2) two metabolites were predicting incident CKD in hyperglycemia independently of baseline eGFR (calculated from Cystatin C and creatinine) and UACR.

This thesis demonstrates the critical importance of examining the interaction and condition specific effects of candidate biomarkers of kidney traits in order to aid in the discovery of personalized biomarkers for hyperglycemia-related CKD.

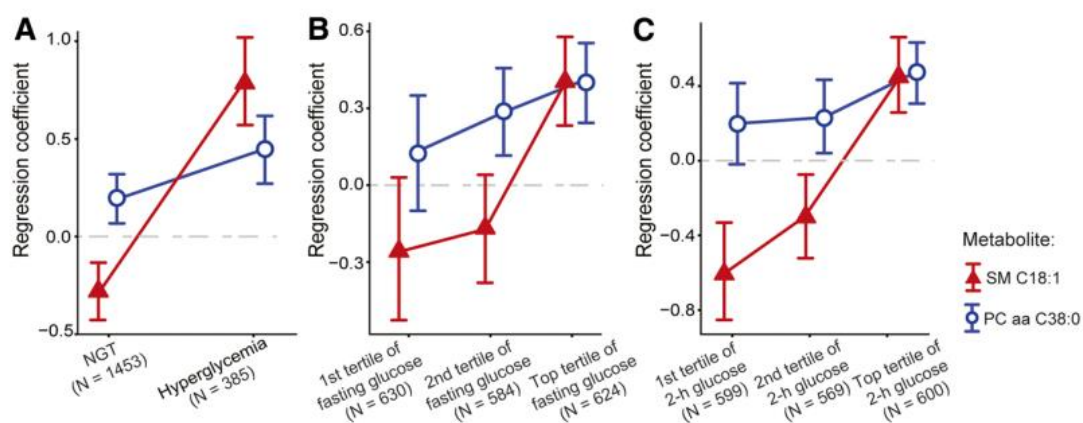


Figure 2. Stratified associations of SM C18:1 and PC aa C38:0 with incident CKD according to glucose status⁶⁹.

6.3 Improve systematic biological understanding to contribute to precision health

Because CKD is a multifactorial disease, a single process can affect multiple phenotypes and/or other processes in CKD pathogenesis. Numerous candidates I identified existed in multiple T2DCKD subnetworks constructed in this thesis, illustrating the intricate network of pathways involved in hyperglycemia-related CKD. RAS blockade is currently the mainstay of CKD therapy, but not all patients respond⁹⁷. CKD patients with hyperglycemia have distinct pathological processes, necessitating the development of distinct theoretical therapeutic strategies. In this thesis, I used omic candidates to stratify CKD patients, which proved to be more effective than eGFR and UACR. This thesis demonstrated that distinct theoretical therapeutic targets may be required for different subgroups of CKD patients, owing to their distinct dominant pathological processes.

The GPS_{eGFR} I constructed identified not only individuals with a high genetic predisposition, but also 11 candidate biomarkers of CKD for the hyperglycemic population's tail, which formed a group strongly suggesting that eGFR has a strong genetic effect on their circulatory levels. Thus, it may help explain why some individuals develop CKD at an early age, given that risk factors for CKD are classified as genetic, behavioral, and environmental, with genetics possibly being the most important factor for those individuals. Our identified omic molecules and GPS demonstrated the ability to identify CKD subgroups of various dominant pathological processes and CKD subgroups of increased genetic risk respectively, enabling more personalized treatment and prevention strategies for CKD in hyperglycemia.

eGFR and UACR are not etiological markers for CKD ⁶⁶. Even if their values remain normal, individuals at risk of CKD may have pathological molecular changes ⁹⁸. Current CKD therapies, such as RAS blockade, aim to slow disease progression rather than reverse pathological damage ⁶⁷. A better understanding of the pathological processes that underpin biomarkers, and their potential effects on processes and eGFR and UACR values, may help improve CKD prevention and treatment. Lesson learned from clinical trials in which drugs targeting a single process, such as transforming growth factor β 1 blockade, failed but drugs targeting the RAS succeeded, owing to the fact that targeting RAS promotes multiple mechanism ⁶⁸. Given the multiple pathogenic processes involved, a holistic approach is the only rational strategy for preventing CKD progression ⁶⁸. Paper III identified and replicated multi-omics candidates of CKD, and extended their observational associations to causality, shedding new light on genetic evidence-based directions via 2SMR. Our 2SMR results also attributed CKD observational signals to specific kidney traits (CKD, eGFR and UACR). Because MR causality does not imply a specific molecular mechanism, our mediation results for 2SMR-supported causal molecules examined the possible mechanism. Aside from corroboration, our GPS_{eGFR} mediation results suggested a potential causal direction not revealed by 2SMR. Early intervention appears to be the most effective way to prevent organ damage manifested by albuminuria and/or decreased eGFR ⁹⁸. A panel of multiple protein biomarkers representing the numerous pathophysiological processes underlying DKD may be more reliable and accurate in predicting kidney disease progression ⁹⁸. In our study, I classified our candidate biomarkers based on their potential directions with eGFR and UACR with and without genetic evidence, and further provided their potential involvement in (several) T2DCKD pathological processes to elucidate biological pathways. Thus, a subgroup of susceptible high-risk individuals may be represented by a subgroup of their molecular profiles, providing critical insight into the identification of personalized therapeutic targets for hyperglycemia-related CKD. Additionally, our subgroups of omic candidates are consistent with a truly translatable biomarker discovery methodology that prioritizes not only clinically evident stages of disease, but also very early disease stages, when therapeutic interventions can still slow or stop disease progression.

This thesis also did intensive exploration of interplay among multi-omics molecules of CKD in hyperglycemia and revealed potential new causal links, relevant molecular pathways, and potential key drivers of the pathways. The crosstalk between molecules can aid in providing insight into whether they share a pathway and identifying the pathway's key driver. For example, paper III demonstrated that well-defined CKD biomarkers (CST3, creatinine, urine albumin, or EGFR) may act as mediators between the eight ACs and their associated kidney traits. Our DMMONs

could deduce potential causal links from multi-omics pairs, e.g., it supported the hypothesis that $IL19 \rightarrow IL1B \rightarrow SLC22A4 \rightarrow \text{ergothioneine} \rightarrow \text{increased risk of proteinuria/ higher blood urea nitrogen levels/ decreased GFR values}$. Numerous molecules, such as cystatin C, creatinine, urine albumin and Tyr, were identified as centers in DMMONs, which connected information between kidney traits and other molecules. Therefore, the crosstalk of multi-omics molecules has the potential to advance not only biological understanding of the disease processes of hyperglycemia-related CKD, but also personalized prevention and drug discovery by addressing the key driver of the specific pathway.

6.4 Limitation

I acknowledge that studies in this thesis are observational-based, limiting our ability to confirm that our findings are indeed true biological signals. Consequently, additional longitudinal cohort studies with a large sample size, as well as interventional studies, are required to confirm our findings.

7. Conclusion

In conclusion, this thesis describes a complex multi-omic landscape of CKD in hyperglycemia and demonstrates how multi-omics profiles can inform precision health by improving early detection of CKD in hyperglycemia, examining the interaction and condition-specific effects of candidate biomarkers, and advancing systematic biological understanding.

8. References

1. Zierer, J., *et al.* Exploring the molecular basis of age-related disease comorbidities using a multi-omics graphical model. *Sci Rep* **6**, 37646 (2016).
2. Zhou, W., *et al.* Longitudinal multi-omics of host-microbe dynamics in prediabetes. *Nature* **569**, 663-671 (2019).
3. Schussler-Fiorenza Rose, S.M., *et al.* A longitudinal big data approach for precision health. *Nat Med* **25**, 792-804 (2019).
4. Liu, G., Dong, C. & Liu, L. Integrated Multiple "-omics" Data Reveal Subtypes of Hepatocellular Carcinoma. *PLoS One* **11**, e0165457 (2016).
5. Bikbov, B., *et al.* Global, regional, and national burden of chronic kidney disease, 1990-2017: a systematic analysis for the Global Burden of Disease Study 2017. *Lancet (London, England)* **395**, 709-733 (2020).
6. Webster, A.C., Nagler, E.V., Morton, R.L. & Masson, P. Chronic Kidney Disease. *Lancet (London, England)* **389**, 1238-1252 (2017).
7. Plantinga, L.C., *et al.* Prevalence of chronic kidney disease in US adults with undiagnosed diabetes or prediabetes. *Clinical journal of the American Society of Nephrology : CJASN* **5**, 673-682 (2010).
8. Melsom, T., *et al.* Prediabetes and Risk of Glomerular Hyperfiltration and Albuminuria in the General Nondiabetic Population: A Prospective Cohort Study. *American journal of kidney diseases : the official journal of the National Kidney Foundation* **67**, 841-850 (2016).
9. Markus, M.R.P., *et al.* Prediabetes is associated with microalbuminuria, reduced kidney function and chronic kidney disease in the general population: The KORA (Cooperative Health Research in the Augsburg Region) F4-Study. *Nutrition, metabolism, and cardiovascular diseases : NMCD* **28**, 234-242 (2018).
10. Li, W., *et al.* Risk of chronic kidney disease defined by decreased estimated glomerular filtration rate in individuals with different prediabetic phenotypes: results from a prospective cohort study in China. *BMJ Open Diabetes Res Care* **8**, 130 (2020).
11. Siragy, H.M. & Carey, R.M. Role of the intrarenal renin-angiotensin-aldosterone system in chronic kidney disease. *Am J Nephrol* **31**, 541-550 (2010).
12. Opazo-Ríos, L., *et al.* Lipotoxicity and Diabetic Nephropathy: Novel Mechanistic Insights and Therapeutic Opportunities. *Int J Mol Sci* **21**(2020).
13. Vahdat, S. The complex effects of adipokines in the patients with kidney disease. *J Res Med Sci* **23**, 60 (2018).
14. Fukami, K., *et al.* AGEs activate mesangial TGF-beta-Smad signaling via an angiotensin II type I receptor interaction. *Kidney Int* **66**, 2137-2147 (2004).
15. Mason, R.M. & Wahab, N.A. Extracellular matrix metabolism in diabetic nephropathy. *J Am Soc Nephrol* **14**, 1358-1373 (2003).
16. Hu, C., *et al.* Insights into the Mechanisms Involved in the Expression and Regulation of Extracellular Matrix Proteins in Diabetic Nephropathy. *Curr Med Chem* **22**, 2858-2870 (2015).
17. Tang, S.C.W. & Yiu, W.H. Innate immunity in diabetic kidney disease. *Nat Rev Nephrol* **16**, 206-222 (2020).
18. Nakagawa, T., Sato, W., Kosugi, T. & Johnson, R.J. Uncoupling of VEGF with endothelial NO as a potential mechanism for abnormal angiogenesis in the diabetic nephropathy. *J Diabetes Res* **2013**, 184539 (2013).
19. Honda, T., Hirakawa, Y. & Nangaku, M. The role of oxidative stress and hypoxia in renal disease. *Kidney Res Clin Pract* **38**, 414-426 (2019).
20. Terman, B.I., *et al.* Identification of the KDR tyrosine kinase as a receptor for vascular endothelial cell growth factor. *Biochem Biophys Res Commun* **187**, 1579-1586 (1992).
21. McDonough, C.W., *et al.* A genome-wide association study for diabetic nephropathy genes in African Americans. *Kidney Int* **79**, 563-572 (2011).
22. Mooyaart, A.L., *et al.* Genetic associations in diabetic nephropathy: a meta-analysis. *Diabetologia* **54**, 544-553 (2011).

23. Wuttke, M., *et al.* A catalog of genetic loci associated with kidney function from analyses of a million individuals. *Nature genetics* **51**, 957-972 (2019).
24. Tin, A., *et al.* Large-scale whole-exome sequencing association studies identify rare functional variants influencing serum urate levels. *Nat Commun* **9**, 4228 (2018).
25. Pattaro, C., *et al.* Genetic associations at 53 loci highlight cell types and biological pathways relevant for kidney function. *Nat Commun* **7**, 10023 (2016).
26. Burgess, S., Scott Ra Fau - Timpson, N.J., Timpson Nj Fau - Davey Smith, G., Davey Smith G Fau - Thompson, S.G. & Thompson, S.G. Using published data in Mendelian randomization: a blueprint for efficient identification of causal risk factors.
27. Khera, A.V., *et al.* Genome-wide polygenic scores for common diseases identify individuals with risk equivalent to monogenic mutations. *Nature genetics* **50**, 1219-1224 (2018).
28. Kato, M. & Natarajan, R. Epigenetics and epigenomics in diabetic kidney disease and metabolic memory. *Nat Rev Nephrol* **15**, 327-345 (2019).
29. Bomotti, S.M., *et al.* Epigenetic markers of renal function in african americans. *Nurs Res Pract* **2013**, 687519 (2013).
30. Ko, Y.A., *et al.* Cytosine methylation changes in enhancer regions of core pro-fibrotic genes characterize kidney fibrosis development. *Genome Biol* **14**, R108 (2013).
31. Swan, E.J., Maxwell, A.P. & McKnight, A.J. Distinct methylation patterns in genes that affect mitochondrial function are associated with kidney disease in blood-derived DNA from individuals with Type 1 diabetes. *Diabet Med* **32**, 1110-1115 (2015).
32. Wing, M.R., *et al.* DNA methylation profile associated with rapid decline in kidney function: findings from the CRIC study. *Nephrol Dial Transplant* **29**, 864-872 (2014).
33. Chu, A.Y., *et al.* Epigenome-wide association studies identify DNA methylation associated with kidney function. *Nat Commun* **8**, 1286 (2017).
34. Gluck, C., *et al.* Kidney cytosine methylation changes improve renal function decline estimation in patients with diabetic kidney disease. *Nat Commun* **10**, 2461 (2019).
35. Schlosser, P., *et al.* Meta-analyses identify DNA methylation associated with kidney function and damage. *Nat Commun* **12**, 7174 (2021).
36. Cañadas-Garre, M., Anderson, K., McGoldrick, J., Maxwell, A.P. & McKnight, A.J. Genomic approaches in the search for molecular biomarkers in chronic kidney disease. *Journal of Translational Medicine* **16**, 292 (2018).
37. Ju, W., *et al.* Tissue transcriptome-driven identification of epidermal growth factor as a chronic kidney disease biomarker. *Sci Transl Med* **7**, 316ra193 (2015).
38. Baelde, H.J., *et al.* Gene expression profiling in glomeruli from human kidneys with diabetic nephropathy. *American journal of kidney diseases : the official journal of the National Kidney Foundation* **43**, 636-650 (2004).
39. Granata, S., *et al.* Mitochondrial dysregulation and oxidative stress in patients with chronic kidney disease. *BMC Genomics* **10**, 388 (2009).
40. Perlman, A.S., *et al.* Serum Inflammatory and Immune Mediators Are Elevated in Early Stage Diabetic Nephropathy. *Ann Clin Lab Sci* **45**, 256-263 (2015).
41. Mischak, H., Delles, C., Vlahou, A. & Vanholder, R. Proteomic biomarkers in kidney disease: issues in development and implementation. *Nat Rev Nephrol* **11**, 221-232 (2015).
42. Hojs, R., Bevc, S., Ekart, R., Gorenjak, M. & Puklavec, L. Serum cystatin C as an endogenous marker of renal function in patients with mild to moderate impairment of kidney function. *Nephrol Dial Transplant* **21**, 1855-1862 (2006).
43. O'Riordan, S.E., *et al.* Cystatin C improves the detection of mild renal dysfunction in older patients. *Ann Clin Biochem* **40**, 648-655 (2003).
44. Grubb, A., *et al.* A cystatin C-based formula without anthropometric variables estimates glomerular filtration rate better than creatinine clearance using the Cockcroft-Gault formula. *Scand J Clin Lab Invest* **65**, 153-162 (2005).
45. Peralta, C.A., *et al.* Detection of chronic kidney disease with creatinine, cystatin C, and urine albumin-to-creatinine ratio and association with progression to end-stage renal disease and mortality. *Jama* **305**, 1545-1552 (2011).
46. Shlipak, M.G., *et al.* Elevations of inflammatory and procoagulant biomarkers in elderly persons with renal insufficiency. *Circulation* **107**, 87-92 (2003).

47. Oberg, B.P., *et al.* Increased prevalence of oxidant stress and inflammation in patients with moderate to severe chronic kidney disease. *Kidney Int* **65**, 1009-1016 (2004).
48. Axelsson, J., *et al.* Elevated resistin levels in chronic kidney disease are associated with decreased glomerular filtration rate and inflammation, but not with insulin resistance. *Kidney Int* **69**, 596-604 (2006).
49. Yilmaz, M.I., *et al.* Serum visfatin concentration and endothelial dysfunction in chronic kidney disease. *Nephrol Dial Transplant* **23**, 959-965 (2008).
50. Lin, J., Hu, F.B. & Curhan, G. Serum adiponectin and renal dysfunction in men with type 2 diabetes. *Diabetes Care* **30**, 239-244 (2007).
51. Hocher, B. & Adamski, J. Metabolomics for clinical use and research in chronic kidney disease. *Nat Rev Nephrol* **13**, 269-284 (2017).
52. Goek, O.N., *et al.* Metabolites associate with kidney function decline and incident chronic kidney disease in the general population. *Nephrol Dial Transplant* **28**, 2131-2138 (2013).
53. Solini, A., *et al.* Prediction of Declining Renal Function and Albuminuria in Patients With Type 2 Diabetes by Metabolomics. *The Journal of clinical endocrinology and metabolism* **101**, 696-704 (2016).
54. Pearson, D.J. & Tubbs, P.K. ACETYL-CARNITINE IN HEART AND LIVER. *Nature* **202**, 91 (1964).
55. Pande, S.V. A mitochondrial carnitine acylcarnitine translocase system. *Proc Natl Acad Sci U S A* **72**, 883-887 (1975).
56. Goek, O.N., *et al.* Serum metabolite concentrations and decreased GFR in the general population. *American journal of kidney diseases : the official journal of the National Kidney Foundation* **60**, 197-206 (2012).
57. Rhee, E.P., *et al.* A combined epidemiologic and metabolomic approach improves CKD prediction. *J Am Soc Nephrol* **24**, 1330-1338 (2013).
58. Levin, A., *et al.* Kidney disease: Improving global outcomes (KDIGO) CKD work group. KDIGO 2012 clinical practice guideline for the evaluation and management of chronic kidney disease. *Kidney International Supplements* **3**, 1--150 (2013).
59. Tangri, N., *et al.* A predictive model for progression of chronic kidney disease to kidney failure. *Jama* **305**, 1553-1559 (2011).
60. Dunkler, D., *et al.* Risk Prediction for Early CKD in Type 2 Diabetes. *Clinical journal of the American Society of Nephrology : CJASN* **10**, 1371-1379 (2015).
61. Washburn, K.K., *et al.* Urinary interleukin-18 is an acute kidney injury biomarker in critically ill children. *Nephrol Dial Transplant* **23**, 566-572 (2008).
62. Wagener, G., *et al.* Urinary neutrophil gelatinase-associated lipocalin and acute kidney injury after cardiac surgery. *American journal of kidney diseases : the official journal of the National Kidney Foundation* **52**, 425-433 (2008).
63. Metzger, J., *et al.* Urinary excretion of twenty peptides forms an early and accurate diagnostic pattern of acute kidney injury. *Kidney Int* **78**, 1252-1262 (2010).
64. Siew, E.D., *et al.* Urine neutrophil gelatinase-associated lipocalin moderately predicts acute kidney injury in critically ill adults. *J Am Soc Nephrol* **20**, 1823-1832 (2009).
65. Haase, M., Bellomo, R., Story, D., Davenport, P. & Haase-Fielitz, A. Urinary interleukin-18 does not predict acute kidney injury after adult cardiac surgery: a prospective observational cohort study. *Crit Care* **12**, R96 (2008).
66. Eddy, S., Mariani, L.H. & Kretzler, M. Integrated multi-omics approaches to improve classification of chronic kidney disease. *Nat Rev Nephrol* **16**, 657-668 (2020).
67. Sanz, A.B., *et al.* Advances in understanding the role of angiotensin-regulated proteins in kidney diseases. *Expert Rev Proteomics* **16**, 77-92 (2019).
68. Ruiz-Ortega, M., Rayego-Mateos, S., Lamas, S., Ortiz, A. & Rodrigues-Diez, R.R. Targeting the progression of chronic kidney disease. *Nat Rev Nephrol* **16**, 269-288 (2020).
69. Huang, J., *et al.* Machine Learning Approaches Reveal Metabolic Signatures of Incident Chronic Kidney Disease in Individuals With Prediabetes and Type 2 Diabetes. *Diabetes* **69**, 2756-2765 (2020).
70. Huang, J., *et al.* Validation of Candidate Phospholipid Biomarkers of Chronic Kidney Disease in Hyperglycemic Individuals and Their Organ-Specific Exploration in Leptin Receptor-Deficient db/db Mouse. *Metabolites* **11**, 89 (2021).

71. Holle, R., Happich, M., Löwel, H. & Wichmann, H.E. KORA--a research platform for population based health research. *Gesundheitswesen* **67 Suppl 1**, S19-25 (2005).
72. World Health, O. & International Diabetes, F. Definition and diagnosis of diabetes mellitus and intermediate hyperglycaemia : report of a WHO/IDF consultation. (World Health Organization, Geneva, 2006).
73. Wang-Sattler, R., *et al.* Novel biomarkers for pre-diabetes identified by metabolomics. *Molecular systems biology* **8**, 615 (2012).
74. Association, A.D. 2. Classification and Diagnosis of Diabetes: Standards of Medical Care in Diabetes—2021. *Diabetes Care* **44**, S15-S33 (2020).
75. Inker, L.A., *et al.* Estimating glomerular filtration rate from serum creatinine and cystatin C. *N Engl J Med* **367**, 20-29 (2012).
76. Stevens, P.E., Levin, A. & Kidney Disease: Improving Global Outcomes Chronic Kidney Disease Guideline Development Work Group, M. Evaluation and management of chronic kidney disease: synopsis of the kidney disease: improving global outcomes 2012 clinical practice guideline. *Ann Intern Med* **158**, 825-830 (2013).
77. Zeilinger, S., *et al.* Tobacco smoking leads to extensive genome-wide changes in DNA methylation. *PLoS One* **8**, e63812 (2013).
78. Lehne, B., *et al.* A coherent approach for analysis of the Illumina HumanMethylation450 BeadChip improves data quality and performance in epigenome-wide association studies. *Genome Biol* **16**, 37 (2015).
79. Aryee, M.J., *et al.* Minfi: a flexible and comprehensive Bioconductor package for the analysis of Infinium DNA methylation microarrays. *Bioinformatics* **30**, 1363-1369 (2014).
80. Schurmann, C., *et al.* Analyzing illumina gene expression microarray data from different tissues: methodological aspects of data analysis in the metaxpress consortium. *PLoS One* **7**, e50938 (2012).
81. Gold, L., *et al.* Aptamer-based multiplexed proteomic technology for biomarker discovery. *PLoS One* **5**, e15004 (2010).
82. Kraemer, S., *et al.* From SOMAmer-based biomarker discovery to diagnostic and clinical applications: a SOMAmer-based, streamlined multiplex proteomic assay. *PLoS One* **6**, e26332 (2011).
83. Römisch-Margl, W., *et al.* Procedure for tissue sample preparation and metabolite extraction for high-throughput targeted metabolomics. *Metabolomics* **8**, 133-142 (2012).
84. Klau, S., Jurinovic, V., Hornung, R., Herold, T. & Boulesteix, A.L. Priority-Lasso: a simple hierarchical approach to the prediction of clinical outcome using multi-omics data. *BMC bioinformatics* **19**, 322 (2018).
85. Chang, C.-C. & Lin, C.-J. LIBSVM: A library for support vector machines. *ACM Trans. Intell. Syst. Technol.* **2**, 1-27 (2011).
86. Liaw, A. & Wiener, M. Classification and Regression by randomForest. *R News* **2**, 18--22 (2002).
87. Culp, M., Johnson, K. & Michailides, G. ada: An R Package for Stochastic Boosting. *Journal of Statistical Software* **017**(2006).
88. Naimi, A.I., Moodie, E.E., Auger, N. & Kaufman, J.S. Constructing inverse probability weights for continuous exposures: a comparison of methods. *Epidemiology* **25**, 292-299 (2014).
89. Robins, J.M., Hernán, M.A. & Brumback, B. Marginal structural models and causal inference in epidemiology. *Epidemiology* **11**, 550-560 (2000).
90. Krumsiek, J., Suhre, K., Illig, T., Adamski, J. & Theis, F.J. Gaussian graphical modeling reconstructs pathway reactions from high-throughput metabolomics data. *BMC Syst Biol* **5**, 21 (2011).
91. Baron, R.M. & Kenny, D.A. The moderator-mediator variable distinction in social psychological research: conceptual, strategic, and statistical considerations. *J Pers Soc Psychol* **51**, 1173-1182 (1986).
92. Tingley, D., *et al.* Mediation: R Package for Causal Mediation Analysis. *Journal of Statistical Software* **59**(2014).

-
93. Euesden, J., Lewis, C.M. & O'Reilly, P.F. PRSice: Polygenic Risk Score software. *Bioinformatics* **31**, 1466-1468 (2015).
 94. Zhao, Q., Wang, J., Bowden, J. & Small, D. Statistical inference in two-sample summary-data Mendelian randomization using robust adjusted profile score. *Annals of Statistics* **48**(2018).
 95. Verbanck, M., Chen, C.Y., Neale, B. & Do, R. Detection of widespread horizontal pleiotropy in causal relationships inferred from Mendelian randomization between complex traits and diseases. *Nature genetics* **50**, 693-698 (2018).
 96. Bowden, J., *et al.* Improving the visualization, interpretation and analysis of two-sample summary data Mendelian randomization via the Radial plot and Radial regression. *Int J Epidemiol* **47**, 1264-1278 (2018).
 97. Perico, N., Benigni, A. & Remuzzi, G. Present and future drug treatments for chronic kidney diseases: evolving targets in renoprotection. *Nat Rev Drug Discov* **7**, 936-953 (2008).
 98. Pena, M.J., Mischak, H. & Heerspink, H.J. Proteomics for prediction of disease progression and response to therapy in diabetic kidney disease. *Diabetologia* **59**, 1819-1831 (2016).

Paper I

Title: Machine Learning Approaches Reveal Metabolic Signatures of Incident Chronic Kidney Disease in Individuals With Prediabetes and Type 2 Diabetes

Authors: Jialing Huang, Cornelia Huth, Marcela Covic, Martina Troll, Jonathan Adam, Sven Zukunft, Cornelia Prehn, Li Wang, Jana Nano, Markus F. Scheerer, Susanne Neschen, Gabi Kastenmüller, Karsten Suhre, Michael Laxy, Freimut Schliess, Christian Gieger, Jerzy Adamski, Martin Hrabe de Angelis, Annette Peters, and Rui Wang-Sattler

Journal: Diabetes

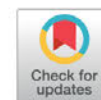
Status: Published

Volume: 69

Page: 2756-2765

Year: 2020

doi: 10.2337/db20-0586



Machine Learning Approaches Reveal Metabolic Signatures of Incident Chronic Kidney Disease in Individuals With Prediabetes and Type 2 Diabetes

Jialing Huang,^{1,2,3} Cornelia Huth,^{2,3} Marcela Covic,^{1,2,3} Martina Troll,^{1,2} Jonathan Adam,^{1,2} Sven Zukunft,⁴ Cornelia Prehn,⁴ Li Wang,^{1,2,5} Jana Nano,^{2,3} Markus F. Scheerer,⁶ Susanne Neschen,⁶ Gabi Kastenmüller,⁷ Karsten Suhre,⁸ Michael Laxy,⁹ Freimut Schliess,¹⁰ Christian Gieger,^{1,2,3} Jerzy Adamski,^{4,11,12} Martin Hrabe de Angelis,^{3,6,12} Annette Peters,^{2,3} and Rui Wang-Sattler^{1,2,3}

Diabetes 2020;69:2756–2765 | <https://doi.org/10.2337/db20-0586>

Early and precise identification of individuals with prediabetes and type 2 diabetes (T2D) at risk for progressing to chronic kidney disease (CKD) is essential to prevent complications of diabetes. Here, we identify and evaluate prospective metabolite biomarkers and the best set of predictors of CKD in the longitudinal, population-based Cooperative Health Research in the Region of Augsburg (KORA) cohort by targeted metabolomics and machine learning approaches. Out of 125 targeted metabolites, sphingomyelin C18:1 and phosphatidylcholine diacyl C38:0 were identified as candidate metabolite biomarkers of incident CKD specifically in hyperglycemic individuals followed during 6.5 years. Sets of predictors for incident CKD developed from 125 metabolites and 14 clinical variables showed highly stable performances in all three machine learning approaches and outperformed the

currently established clinical algorithm for CKD. The two metabolites in combination with five clinical variables were identified as the best set of predictors, and their predictive performance yielded a mean area value under the receiver operating characteristic curve of 0.857. The inclusion of metabolite variables in the clinical prediction of future CKD may thus improve the risk prediction in people with prediabetes and T2D. The metabolite link with hyperglycemia-related early kidney dysfunction warrants further investigation.

Chronic kidney disease (CKD) affects approximately 9.1% of the general population worldwide (1). From 1990 to 2017, the global all-age mortality rate due to CKD increased by 41.5%, resulting in 1.2 million deaths only in 2017 (1).

¹Research Unit of Molecular Epidemiology, Helmholtz Zentrum München – German Research Center for Environmental Health, Neuherberg, Germany

²Institute of Epidemiology, Helmholtz Zentrum München – German Research Center for Environmental Health, Neuherberg, Germany

³German Center for Diabetes Research (DZD), München-Neuherberg, Germany

⁴Research Unit of Molecular Endocrinology and Metabolism, Helmholtz Zentrum München – German Research Center for Environmental Health, Neuherberg, Germany

⁵Department of Scientific Research and Shandong University Postdoctoral Work Station, Liaocheng People's Hospital, Shandong, P. R. China

⁶Institute of Experimental Genetics, Helmholtz Zentrum München – German Research Center for Environmental Health, Neuherberg, Germany

⁷Institute of Bioinformatics and Systems Biology, Helmholtz Zentrum München – German Research Center for Environmental Health, Neuherberg, Germany

⁸Department of Physiology and Biophysics, Weill Cornell Medicine - Qatar, Doha, Qatar

⁹Institute of Health Economics and Health Care Management, Helmholtz Zentrum München – German Research Center for Environmental Health, Neuherberg, Germany

¹⁰Profil Institut für Stoffwechselforschung GmbH, Neuss, Germany

¹¹Department of Biochemistry, Yong Loo Lin School of Medicine, National University of Singapore, Singapore, Singapore

¹²Chair of Experimental Genetics, Center of Life and Food Sciences Weihenstephan, Technische Universität München, Freising, Germany

Corresponding author: Rui Wang-Sattler, ru.wang-sattler@helmholtz-muenchen.de

Received 3 June 2020 and accepted 29 September 2020

This article contains supplementary material online at <https://doi.org/10.2337/figshare.13022624>.

S.Z. is currently affiliated with the Institute for Vascular Signalling, Centre for Molecular Medicine, Goethe University, Frankfurt am Main, Germany.

M.F.S. is currently affiliated with Medical Affairs & Pharmacovigilance, Bayer AG, Berlin, Germany.

S.N. is currently affiliated with Sanofi Aventis Deutschland GmbH, Frankfurt am Main, Germany.

© 2020 by the American Diabetes Association. Readers may use this article as long as the work is properly cited, the use is educational and not for profit, and the work is not altered. More information is available at <https://www.diabetesjournals.org/content/license>.

Among the established risk factors for CKD, diabetes accounts for 30–50% of all CKD cases (2), and its microvascular complication, diabetic nephropathy, is the leading cause of end-stage kidney disease (3). Moreover, undiagnosed diabetes and prediabetes have been related to high prevalence of CKD in U.S., European, and Asian populations (4–7). Early screening of hyperglycemic individuals at risk of developing CKD is therefore crucial for effective prevention and management of incident CKD in the framework of an integrated personalized diabetes management (8).

Increased urinary albumin-to-creatinine ratio (UACR) and reduced estimated glomerular filtration rate (eGFR) are two clinical biomarkers of kidney-related structural damage and functional decline used to diagnose CKD (9). UACR, eGFR, age, and sex were reported to be highly predictive for progression of CKD (10). Albuminuria and eGFR were also found to be the most important variables to predict onset and progression of early CKD in individuals with type 2 diabetes (T2D). However, their predictive ability was modest with an externally validated c-statistic of 0.68 even in combination with age and sex (11). Since the traditional risk factors for CKD are insufficient for reliable prediction of CKD in individuals with T2D, there is an urgent need for more sensitive and specific biomarkers for CKD prognosis in prediabetes and T2D management.

A comprehensive individual profiling by means of metabolomics is a promising approach to discover previously unconsidered associations between metabolic signatures and clinical outcomes such as obesity, prediabetes, and T2D (12–19). Several studies have investigated the metabolite profiles of CKD, both in the general population and populations with T2D (20–22). However, to the best of our knowledge, none of them have explored the metabolites associated with future development of CKD in people with prediabetes or T2D.

In this study, we applied priority-Lasso and multivariate logistic regression (MLR) to identify metabolites associated with incident CKD in the population-based adult cohort KORA (Cooperative Health Research in the Region of Augsburg) (23,24).

Using three machine learning approaches (support vector machine [SVM], random forest [RF], and adaptive boosting [AdaBoost]), we furthermore assessed the predictive power of predictor sets constructed with metabolites and clinical phenotypes and compared their performance with the typically used clinical algorithm for CKD. We finally presented the best set of predictors for incident CKD in individuals with prediabetes or T2D.

RESEARCH DESIGN AND METHODS

Study Design and Participants

We investigated the two follow-ups of the longitudinal cohort KORA survey 4, conducted in the area of Augsburg, Southern Germany. The first follow-up (F4) involved 3,080

individuals (aged 32–81 years) examined between 2006 and 2008. For the second follow-up (FF4), 2,269 participants were examined from 2013 to 2014 (23). Because the metabolomics data and the clinical variables of CKD (eGFR and UACR) were measured in the F4 study, we used F4 as baseline.

Individuals with hyperglycemia and normal glucose tolerance (NGT) were classified according to baseline fasting and 2-h postload glucose (2-h glucose) values with the World Health Organization diagnostic criteria (25). The hyperglycemic group comprised participants with prediabetes and newly diagnosed T2D (i.e., fasting glucose ≥ 110 mg/dL or 2-h-glucose glucose ≥ 140 mg/dL), as well as known T2D that was diagnosed by physician-validated self-reporting and/or current use of antidiabetes agents (13,23).

We examined 2,142 individuals who participated in both KORA F4 and FF4. Exclusion criteria were 1) non-fasting samples ($n = 5$ at F4), 2) missing eGFR and UACR ($n = 16$ at F4, $n = 64$ at FF4) or covariate values ($n = 19$ at F4), and 3) diagnosis for type 1 diabetes ($n = 6$ at F4), unclear type of diabetes ($n = 21$ at F4), or CKD ($n = 173$ at F4). The remaining data set comprised 385 hyperglycemic participants and 1,453 individuals with NGT (Fig. 1 and Table 1). The hyperglycemic participants were used to identify candidate metabolite biomarkers for incident CKD and to develop and evaluate sets of metabolite and clinical predictors. The NGT participants were used for sensitivity analyses of candidate biomarkers.

All study participants gave written informed consent. The KORA study was approved by the ethics committee of the Bavarian Medical Association, Munich, Germany.

Outcome Definition

The eGFR was calculated from serum creatinine (mg/dL) and cystatin C (mg/dL) (isotope dilution mass spectrometry-standardized and International Federation of Clinical Chemistry and Laboratory Medicine-standardized values) using the Chronic Kidney Disease Epidemiology Collaboration (CKD-EPI) equation (26). Non-CKD was defined as an eGFR ≥ 60 mL/min/1.73 m² and an UACR < 30 mg/g at both F4 and FF4 (9). Incident cases of CKD were defined as no CKD at baseline (F4) but reduced kidney function (eGFR < 60 mL/min/1.73 m²) or kidney damage (UACR ≥ 30 mg/g) at follow-up (FF4).

Metabolite Quantification and Normalization

The serum samples from participants in the KORA F4 study were measured with the AbsoluteIDQ p150 kit (biocrates life sciences ag, Innsbruck, Austria) (24,27). In total, 3,061 serum samples of the F4 study were quantified for 163 metabolites in 38 randomly distributed kit plates (Supplementary Table 1). Each plate also contained three quality control (QC) samples (sex-mixed human plasma provided by the manufacturer) and one zero sample (PBS).

Identical QC procedures were used (13). Each metabolite met two criteria: 1) average value of the coefficient of variance in the three QCs $< 25\%$ and 2) 50% of all measured

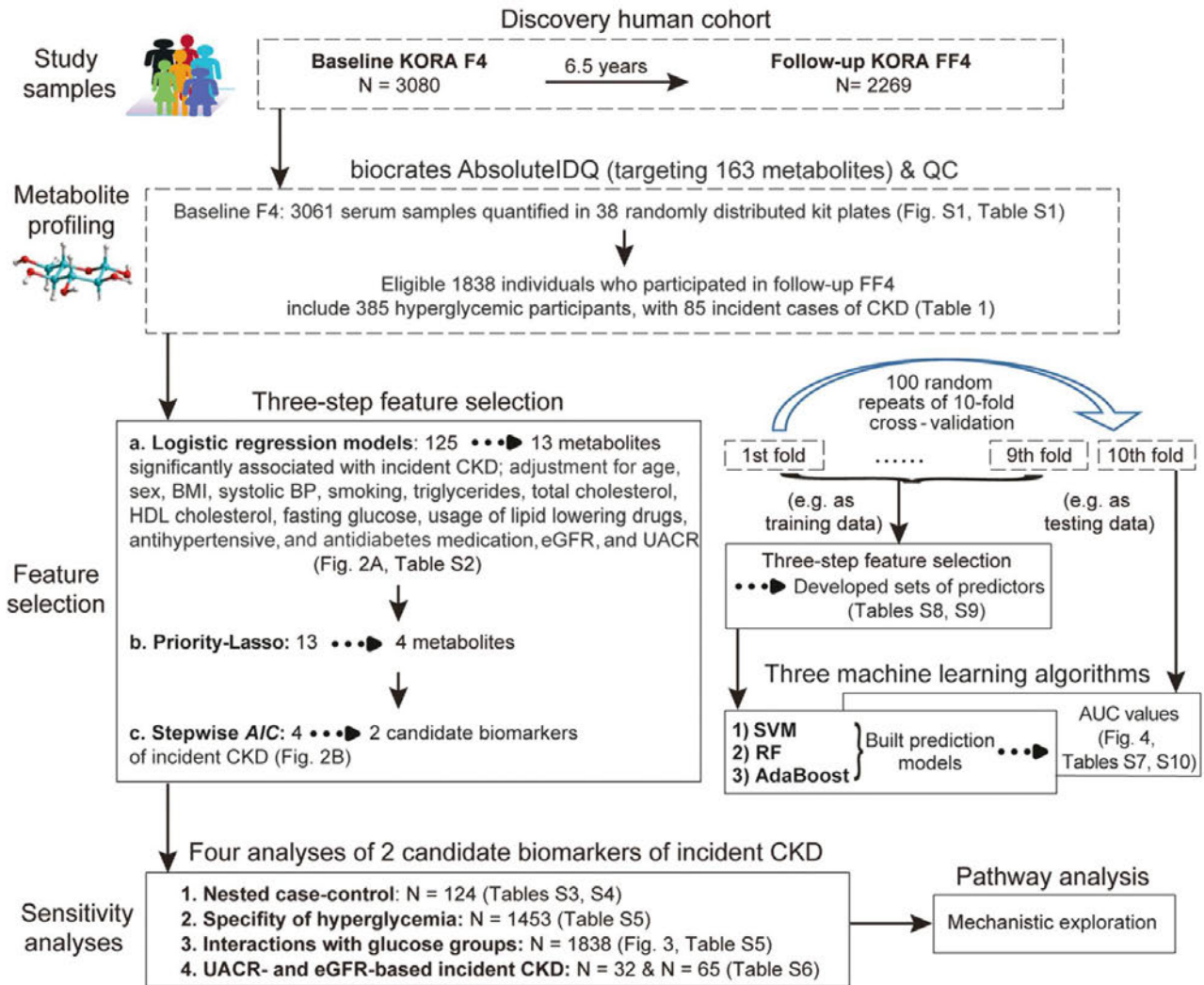


Figure 1—Study design. Fig. S1 and Tables S1–S10 refer to Supplementary Fig. 1 and Supplementary Tables 1–10 and are available in the Supplementary Material.

sample concentrations equal to or above three times the median of the 38 zero samples. In total, 125 metabolites passed the criteria and were used in the subsequent analysis (Supplementary Table 1). For minimization of the plate effect, metabolite concentrations were adjusted for the plate normalization factors. For each metabolite, the plate normalization factors were calculated by division of the mean of QC sample values in each plate with the mean of all QC sample values in 38 plates. As shown in Supplementary Fig. 1, plate normalization efficiently corrected the inter-plate variations in metabolite concentration.

For comparability between different metabolites, their concentrations were natural-log transformed and scaled to a mean value of 0 and SD of 1.

Three-Step Feature Selection

Since feature reduction is an important aspect of predictive modeling, we defined a three-step feature selection procedure.

In order to decrease the false positive rate of the final discovery, we firstly used MLR adjusted for the two sets of covariates based on medical knowledge (11). The basic model was adjusted for age, sex, BMI, systolic blood pressure (BP), smoking status, triglyceride, total cholesterol, HDL cholesterol, and fasting glucose. The full model was additionally adjusted for the use of lipid-lowering, antihypertensive, and antidiabetes medication and for baseline eGFR and UACR (Fig. 1). Metabolites that were significantly associated with incident CKD in the full model ($P < 0.05$) were retained.

Secondly, we applied the machine learning method priority-Lasso to deal with multicollinearity of included variables and to retain metabolite and clinical variables with nonzero coefficients. Priority-Lasso is a Lasso-based intuitive procedure that uses prior knowledge of the study outcome by defining the blocks of different types of predictor variables (28). We defined 14 clinical variables in the full model as block 1, whereas the metabolites retained

Table 1—Characteristics of the KORA study population

Clinical variables	Hyperglycemic participants			NGT participants		
	Incident CKD, N = 85	Non-CKD, N = 300	P	Incident CKD, N = 115	Non-CKD, N = 1,338	P
Age, years	67.78 ± 8.78	59.44 ± 9.39	1.29E−10	60.97 ± 12	50.05 ± 10.82	4.81E−20
Male sex, %	55.29	58.00	0.656	46.09	46.64	0.910
BMI, kg/m ²	30.11 ± 4.58	29.74 ± 4.80	0.522	27.39 ± 4.51	26.29 ± 4.09	0.007
HbA _{1c} (%)	6.06 ± 0.86	5.82 ± 0.57	0.004	5.49 ± 0.29	5.33 ± 0.30	3.71E−08
HbA _{1c} (mmol/mol)	42.81 ± 9.32	40.14 ± 6.24	0.004	36.56 ± 3.24	34.76 ± 3.39	1.03E−07
Fasting glucose, mg/dL	116.02 ± 28.6	110.23 ± 18.82	0.031	93.61 ± 7.42	91.4 ± 7.56	0.003
2-h glucose, mg/dL	173.59 ± 43.17 ^a	159.82 ± 39.87 ^a	0.019	102.7 ± 20.68	96.37 ± 20.53	0.002
Systolic BP, mmHg	132.01 ± 18.72	128.78 ± 17.16	0.135	124.73 ± 18.42	117.69 ± 15.87	9.59E−06
Diastolic BP, mmHg	75.14 ± 9.53	78.25 ± 9.47	0.009	76.36 ± 10.51	74.81 ± 9.3	0.089
Triglyceride, mg/dL	130.0 (93–186)	133.5 (94.8–195.3)	0.859	107 (75–143)	91 (63–130)	0.220
Total cholesterol, mg/dL	212.87 ± 38.32	225.2 ± 39.7	0.012	219.39 ± 40.24	213.45 ± 37.75	0.108
HDL cholesterol, mg/dL	51.87 ± 11.64	51.66 ± 13.66	0.897	57.06 ± 15.27	58.00 ± 14.70	0.514
LDL cholesterol, mg/dL	130.64 ± 35.47	144.77 ± 34.47	0.001	138.45 ± 35.56	134.03 ± 33.84	0.180
Baseline eGFR, mL/min/1.73 m ²	78.42 ± 13.6	90.48 ± 12.48	2.18E−11	83.13 ± 15.85	98.38 ± 12.79	1.39E−25
Follow-up eGFR, mL/min/1.73 m ²	57.5 ± 18.3	81.67 ± 13.12		66.68 ± 19.32	89.5 ± 13.48	
Baseline UACR, mg/g	10.22 (4.8–15.0)	5.45 (3.8–9.1)	2.54E−07	7.16 (4.7–13.8)	4.64 (3.2–7.2)	3.81E−13
Follow-up UACR, mg/g	14.47 (6.02–41.02)	5.54 (3.34–9.47)		18.51 (5.4–54.1)	4.22 (2.9–6.6)	
Smoking, %			0.321			0.699
Nonsmoker	47.06	41.33	Ref.	41.74	42.15	Ref.
Former smoker	47.06	48.00	0.558	41.74	38.57	0.676
Current smoker	5.88	10.67	0.159	16.52	19.28	0.607
Medication usage, %						
Lipid lowering	30.59	11.33	3.20E−05	15.65	6.28	2.78E−04
Antihypertensive	71.76	42.67	4.49E−06	50.43	16.07	8.88E−17
Antidiabetes	16.47	11.33	0.208	0	0	—

Data are means ± SD for quantitative variables or median (25th–75th percentile) unless otherwise indicated. KORA participants were classified according to their hyperglycemic status at baseline (F4) and incident CKD status at follow-up (FF4). Unless indicated, variables show baseline measurements. P values were calculated by univariate logistic regression. P values shown in boldface type represent statistical significance at 0.05 level. ^aIn the hyperglycemic participants, 2-h glucose levels were only available in 61 individuals with incident CKD and 254 individuals without CKD.

after the first-step screen were defined as block 2. The penalization parameters λ in each block were determined as values with maximum area under the receiver operating characteristic curve (AUC) estimated in a 10-fold cross validation.

Thirdly, we used logistic regression with backward stepwise selection according to the Akaike information criterion (AIC) to select for the most strongly associated variables with incident CKD and reduce model complexity (Fig. 1).

After the three-step feature selection, the selected metabolites from the 385 hyperglycemic individuals were regarded as candidate biomarkers.

Sensitivity Analyses of Candidate Biomarkers

We conducted four sensitivity analyses to reduce the possibility of chance findings (Fig. 1): 1) A nearest-neighbor propensity score matching in nested case-control study

design was used to balance case and control subjects on conventional risk factors of CKD. MLR analysis was used to generate propensity scores using incident CKD as outcome and covariates from the full model. The caliper was defined as 0.1. After one-to-one propensity score matching, we investigated the association of candidate biomarkers with incident CKD by conditional logistic regression. 2) We investigated whether the predictive effect of candidate biomarkers for incident CKD was dependent of the hyperglycemic status. We examined the association of the candidate biomarkers with incident CKD in 1,453 normoglycemic participants by MLR. 3) We explored the interaction effects of candidate biomarkers with glucose levels for incident CKD in 1,838 individuals and performed a stratified analysis by MLR. We next examined the multiplicative interaction effects between candidate biomarkers and glucose groups by adding related multiplicative terms in the MLR models. The significance of

interaction terms was tested by ANOVA LRT test. 4) We examined the association of candidate biomarkers with UACR-based ($\text{UACR} \geq 30 \text{ mg/g}$) and eGFR-based ($\text{eGFR} < 60 \text{ mL/min/1.73 m}^2$) incident CKD separately in hyperglycemic participants.

Development and Evaluation of Predictor Sets

We performed the three-step feature selection with 100 random repeats of 10-fold cross validation to develop the sets of metabolite and clinical predictors for incident CKD in hyperglycemia (Fig. 1). Their predictive performances were evaluated using AUC. The AUC values of developed predictors were compared with the established prediction model consisting of age, sex, eGFR, and UACR (10,11). These four clinical variables were used as reference predictors.

In each 10-fold cross validation, the data from 385 hyperglycemic individuals were randomly partitioned into 10 nonoverlapping subsets. Each of these 10 subsets was regarded in turn as testing data, whereas the remaining nine subsets were used as training data (Fig. 1). In each iteration, a set of metabolite and clinical variables for incident CKD was identified with the three-step feature selection procedure using one of the training data sets. The identified predictor set and the reference predictors were used to develop respective prediction models with SVM. In this way, two prediction models were built using one training data set. The AUC values of the respective two models were computed for the testing data only (Fig. 1). The average AUC value over 10 iterations of one 10-fold cross validation was calculated and finally presented. For assessment of the robustness of the predictive results, the predictive models were furthermore built using another two machine learning approaches (i.e., RF and AdaBoost) and the corresponding AUC values were reported.

SVM models were fitted with the R `e1071` package (29). The kernel parameter was defined as radial (i.e., Gaussian radial basis function). RF models were fitted with the R `randomForest` package, which implements Breiman's classic algorithm (30). The two RF parameters, `nTree` (i.e., the number of trees to grow for each forest) and `mTry` (the number of input variables randomly chosen at each split), were set to 600 and the default setting (floor of square root of the number of features), respectively. The R `ada` package was used to fit the AdaBoost models (31). The three AdaBoost parameters loss (i.e., loss function), type (type of boosting algorithm to perform), and iter (number of boosting iterations to perform) were set to `ada` (corresponding to the default boosting under exponential loss), `discrete` (discrete boosting), and 200, respectively.

In total, we performed 100 repeats of 10-fold cross validations including 1,000 times of three-step feature selection. The most frequently selected set of metabolites and clinical variables among these 1,000 selection rounds was subsequently defined as the best set of predictors for incident CKD in hyperglycemia.

All statistical analyses were performed in R (version 3.5.0), and two-sided P value < 0.05 was considered as statistically significant.

Data and Resource Availability

The KORA F4/FF4 data sets are not publicly available because of data protection agreements but can be provided on request through the KORA-PASST (project application self-service tool [www.helmholtz-muenchen.de/kora-gen]).

RESULTS

Baseline Characteristics of Study Participants

Among 1,838 eligible, non-CKD participants of the KORA F4 study, 200 individuals developed CKD during a mean follow-up of 6.5 years (Fig. 1 and Table 1). Incident CKD was diagnosed more frequently in hyperglycemic participants (22.1%) than in individuals with NGT (7.9%) (Table 1). Compared with non-CKD individuals, the incident CKD case subjects in hyperglycemic and NGT groups were significantly older and had significantly higher baseline values of HbA_{1c} , fasting and 2-h glucose, and UACR, whereas their baseline eGFR values were significantly lower. They also self-reported a significantly higher intake of antihypertensive and lipid-lowering medication (Table 1).

Identification of Metabolite Biomarkers for Incident CKD in Hyperglycemia

Of 125 analyzed metabolites in 385 hyperglycemic participants, the baseline values of 13 metabolites were nominally associated ($P < 0.05$) with incident CKD, both in basic and full MLR models (Fig. 2A and Supplementary Table 2). Among the 13 metabolites, nine corresponded to sphingomyelins (SMs) and SM C18:1 remained significant after stringent Bonferroni correction (Fig. 2A and Supplementary Fig. 2). Of the 13 metabolites, 4 metabolites were selected by priority-Lasso and 2 (SM C18:1 and phosphatidylcholine diacyl [PC aa] C38:0) remained significant after stepwise AIC selection (Fig. 1). The relative concentrations of the two metabolites were significantly higher in 85 incident CKD case subjects in comparison with 300 non-CKD individuals (Fig. 2B). For example, a SD increase in the ln-transformed SM C18:1 concentration at baseline was associated with a 122% increased odds of CKD at follow-up (full model $P = 3.315E-04$) (Supplementary Table 2).

The results of the three-step feature selection thus identified two metabolites, SM C18:1 and PC aa C38:0, as candidate biomarkers of incident CKD in hyperglycemic individuals.

Sensitivity Analyses Consolidate the Candidate CKD Biomarkers

Propensity score matching in 385 hyperglycemic individuals resulted in 62 one-to-one matched incident CKD and non-CKD pairs. All covariates from the full model showed similar characteristics between the case and matched

control subjects (Supplementary Table 3), and the two candidate biomarkers showed significant risk associations with incident CKD (Supplementary Table 4).

Both metabolites were not significantly associated with incident CKD in 1,453 normoglycemic individuals, i.e., when 115 incident CKD case subjects were compared with 1,338 non-CKD individuals who were both NGT at baseline (Table 1, Supplementary Table 5, and Fig. 2B). This result indicates that the two candidate biomarkers of incident CKD are specific for hyperglycemia.

Their specificity for hyperglycemia was further confirmed by metabolite-glucose interaction analysis. The risk estimates of SM C18:1 and PC aa C38:0 association with incident CKD were significant only in the hyperglycemic subgroup as well as in the top tertile of fasting and 2-h glucose, respectively (Supplementary Table 5). Moreover, SM C18:1 demonstrated significant multiplicative interaction effects with glycemic status and 2-h glucose (Fig. 3 and Supplementary Table 5).

The fourth sensitivity analysis aimed to address the UACR- and eGFR-based outcomes separately. Among 385 hyperglycemic participants, 32 and 65 developed incident CKD according to UACR and eGFR criteria, respectively. Both metabolites showed consistently significant risk effects for the UACR-based incident CKD in hyperglycemic participants, both in basic and in full MLR

(Supplementary Table 6). Moreover, SM C18:1 was a significant predictor for eGFR-based incident CKD in the basic MLR (Supplementary Table 6).

Superior Discrimination Ability and the Best Set of Predictors of Incident CKD in Hyperglycemia

During 100 times of 10-fold cross-validation, the median AUC values of our developed sets of predictors (i.e., metabolites and clinical variables) were stable in all three machine learning algorithms with corresponding values >0.813 (Fig. 4 and Supplementary Table 7). In comparisons with the reference predictors (age, sex, eGFR, UACR), the median AUC value of our developed sets of predictors increased by 2.5% and reached 0.825 (95% CI 0.801–0.849 [SVM algorithm]) (Supplementary Table 7), thereby outperforming the reference predictors in 97 out of 100 times of 10-fold cross validation (Supplementary Table 7). The improvement remained consistent after application of the other two machine learning approaches, RF (2.9% absolute increase in median AUC value) and AdaBoost (1.6%) (Supplementary Table 7). These results suggest that our developed sets of predictors outperform the established clinical predictors for incident CKD.

We further identified the best set of predictors for incident CKD, which consisted of two metabolites (SM

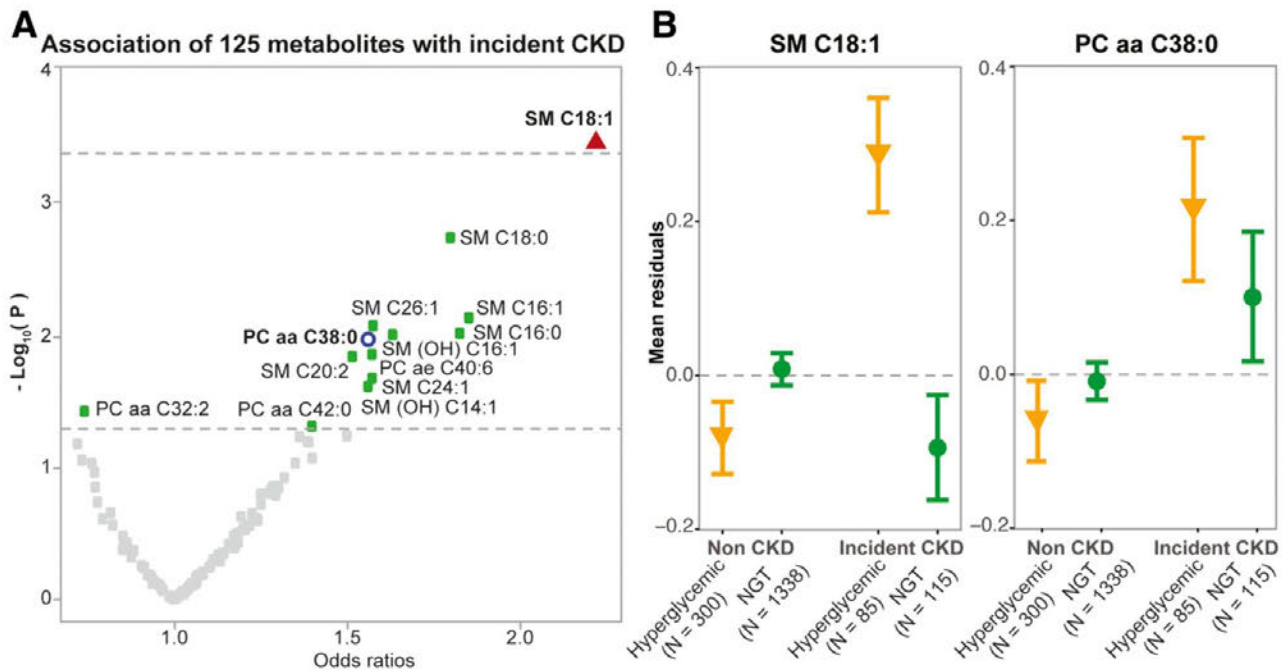


Figure 2—Serum metabolite associations with incident CKD. **A:** Volcano plot of the association results for 125 metabolites with incident CKD in hyperglycemic individuals. Odds ratios and *P* values are from logistic regression analysis adjusted for age, sex, BMI, systolic BP, smoking status, triglyceride, total cholesterol, HDL cholesterol, fasting glucose, use of lipid-lowering drugs, antihypertensive, and antidiabetes medication, and baseline values of eGFR and UACR. The upper and the lower interrupted lines represent Bonferroni-corrected and uncorrected ($P = 0.05$) significance levels, respectively. **B:** Mean residuals (with SEs) of SM C18:1 and PC aa C38:0 for non-CKD and incident CKD in hyperglycemic and NGT individuals, respectively. Metabolite residuals were calculated with linear regression models adjusted for age, sex, BMI, systolic BP, smoking status, triglyceride, total cholesterol, HDL cholesterol, and fasting glucose.

C18:1 and PC aa C38:0) and five clinical variables (age, total cholesterol, fasting glucose, eGFR, and UACR). This set was the most frequently selected set: 113 times over 1,000 selection rounds (Supplementary Table 8). Moreover, these seven variables were the most important ones, and metabolites SM C18:1 and PC aa C38:0 were selected 857 and 593 times over these 1,000 rounds (Supplementary Table 9). The mean AUC value of the best set of predictors for incident CKD was 0.857, which was 4.8% higher than the corresponding AUC value of the full model containing 14 clinical variables including two known CKD biomarkers, eGFR and UACR (Supplementary Table 10).

DISCUSSION

This longitudinal study revealed significant accumulation of sphingo- and glycerophospholipids (SM C18:1 and PC aa C38:0) in individuals with prediabetes and T2D up to 6.5 years before their clinical onset of CKD. These candidate metabolite biomarkers of incident CKD were specific for hyperglycemic state, i.e., individuals with increased fasting and/or 2-h glucose levels. Highly stable performances of the sets of predictors for incident CKD developed from 125 metabolites and 14 clinical variables were furthermore independently confirmed with three machine learning algorithms. The best set of predictors consisted of the two metabolites (SM C18:1 and PC aa C38:0) and five clinical variables (age, total cholesterol, fasting glucose, eGFR, and UACR) and showed the best predictive power for early discrimination of hyperglycemic individuals at high risk of progressing to CKD.

Despite the relatively low coverage of our targeted metabolomics approach, i.e., lack of ceramides and other

sphingolipids, our results support evidence on SM accumulation in glomerular diseases of genetic and nongenetic origin (32). Out of 125 analyzed metabolites comprising amino acids, acylcarnitines, hexoses, and glycerophospho- and sphingolipids (Supplementary Table 1), SMs represented the majority of metabolites associated with incident CKD in hyperglycemic participants ($P < 0.05$) (Fig. 2A). Increased SM levels in relation to CKD were also reported in individuals with type 1 diabetes (33) and T2D (34), except for the nontargeted lipidomic study of type 1 diabetes (35). Isomer annotation of the top significant metabolite, SM C18:1, in our study revealed that it may consist of several sphingoid backbones (d16:1, d18:0, d18:1, d18:2, and d19:1) bound to mainly saturated or monounsaturated fatty acyls with 16–18 carbons (36). A similar preference for saturated fatty acyl chains was found for PC aa C38:0 and PC aa C42:0, two diacyl PCs with positive association trends with incident CKD (Fig. 2A).

Circulatory levels of several other metabolites associated with CKD in our study (SM C16:0, SM C16:1, SM C24:1, and PC aa C38:0) have previously been shown to positively associate with coronary artery disease mortality (37). SM C16:0 and SM C16:1 were also found to be positively associated with myocardial infarction (38). Moreover, higher plasma SMs were found in patients with coronary artery disease and causally related to progression of atherosclerosis lesions in animal models (39,40). The PC aa C32:2 that showed an inverse association with incident CKD in our study was previously found to be protective for coronary artery disease mortality (37). These observations suggest that metabolic alterations associated with incident CKD may also reflect underlying

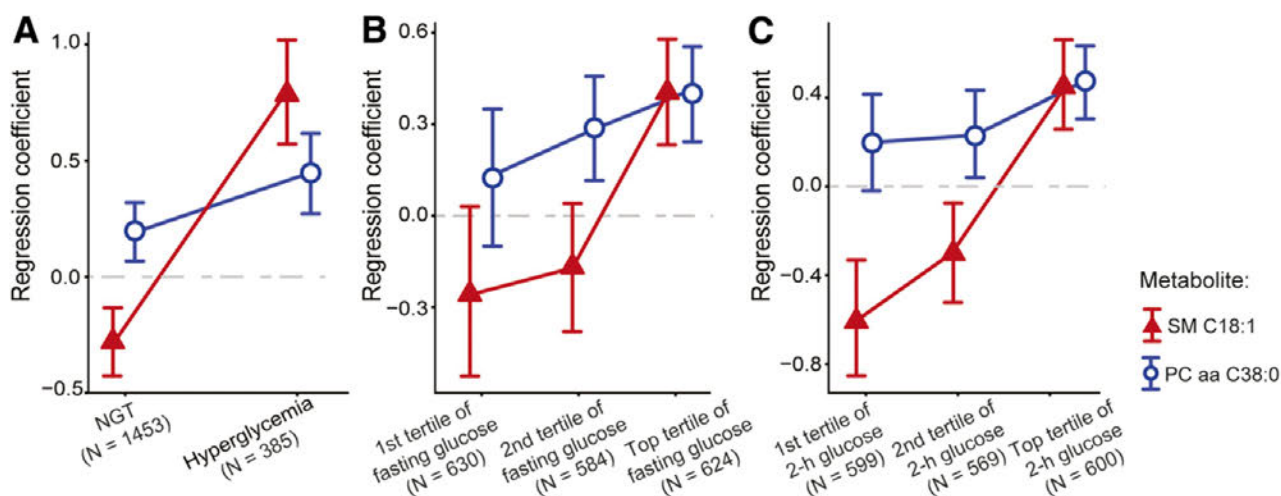


Figure 3—Stratified associations of candidate biomarkers with incident CKD according to glucose status. Associations of SM C18:1 and PC aa C38:0 with incident CKD stratified by hyperglycemic status (A) and each tertile of fasting glucose (B) and 2-h glucose (C) values. Regression coefficients in NGT and first and second tertile of fasting and 2-h glucose were adjusted for age, sex, BMI, systolic BP, smoking status, triglyceride, total cholesterol, HDL cholesterol, fasting glucose, use of lipid-lowering drug and antihypertensive medication, and baseline values of eGFR and UACR. Regression coefficients in the hyperglycemic group and the top tertile of fasting and 2-h glucose were additionally adjusted for antidiabetes medication.

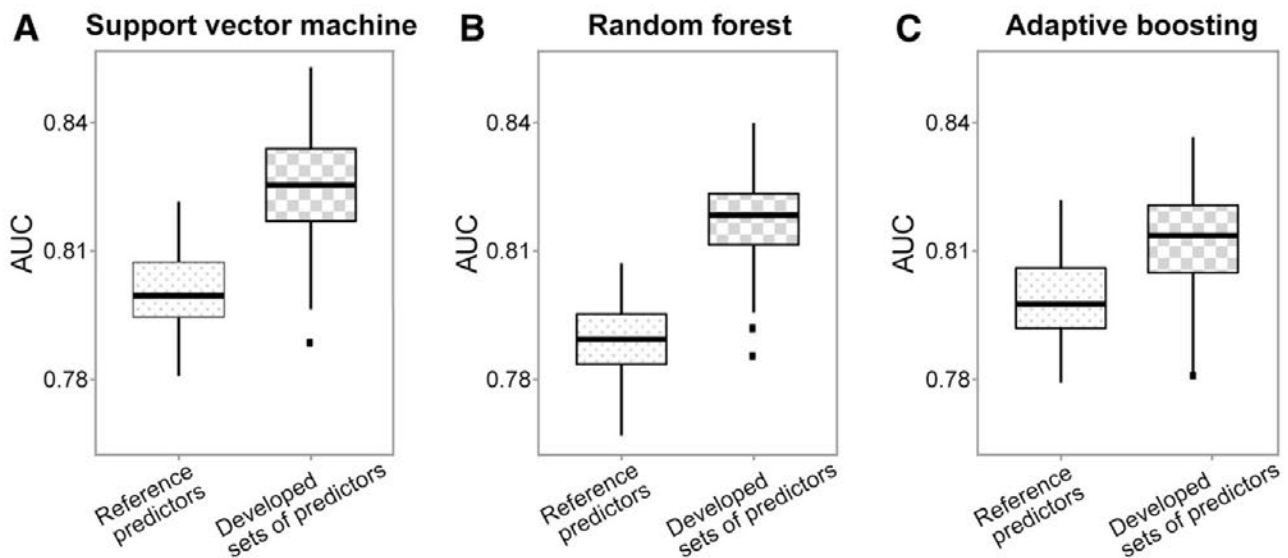


Figure 4—Prediction performance of incident CKD in hyperglycemic individuals in three machine learning approaches. The box plots show the AUC values of two models applying three machine learning approaches over 100 times of 10-fold cross validation. Reference predictors: baseline age, sex, eGFR, and UACR. Developed sets of predictors: combination of metabolites and clinical variables, which were identified by the three-step feature selection in each round. For the resampling rounds, in each iteration of each 10-fold cross validation, the three-step feature selection procedure was conducted and metabolites and clinical variables were selected for the training data. The set of selected metabolites and clinical variables and the reference predictors were used to develop respective prediction models with the three approaches in the training data. The AUC values were computed for the test data only. The 10 AUC values of each model of each approach were averaged to produce a single estimate that was displayed in box plots. The procedure of 10-fold cross validation was randomly repeated 100 times, which generated 100 cross validation AUC values of each prediction model for each approach.

cardiovascular disease, for which CKD is an independent risk factor (41).

Circulatory accumulation in SMs and saturated PCs in individuals with prediabetes and T2D may also reflect early stages of diabetic nephropathy such as mesangial matrix expansion, podocyte injury, and glomerular enlargement (42). The SM (d18:1/16:0) was reported to accumulate in the enlarged glomeruli of diabetic and obese mice and was detected in the glomeruli and vasculature of human kidney (43). The SM (d18:1/16:0) is one of the possible isomers for SM C16:0 that was positively associated with incident CKD in our study (Fig. 2A) and highly correlated with our top hit, SM C18:1 (Pearson correlation coefficient = 0.66, $P < 2.2e-16$) (Supplementary Fig. 2). Renal accumulation in SM (d18:1/16:0) was related to reduced enzyme activity of AMPK in the diabetic kidney glomeruli, mitochondrial dysfunction, and CKD progression (43).

The altered levels of certain SM and PC species in hyperglycemic individuals at increased risk for CKD could be caused by fluctuations in their fatty acid profile, which influences the first rate-limiting step in de novo SM synthesis, due to nutritional oversupply, dyslipidemia (44), or gut microbiome (45). The severity of CKD correlates with increased levels of saturated and monounsaturated fatty acids (46), and enzymes involved in de novo synthesis and the ceramide-SM homeostasis such as SM synthase 2 (SMS2) show fatty acyl chain specificity and may determine the regional expression of SM species in the kidney (47). Reduction of SM levels in the plasma

membranes and lipoproteins improves whole-body insulin sensitivity (48), and SMS2 inhibition was suggested as a potential therapeutic target for controlling inflammatory responses and atherosclerosis (49,50). Whether SMS2 inhibition could prevent the development of CKD in hyperglycemic individuals requires further investigation.

The current predictive models for CKD mainly rely on clinical variables (10,11,51,52). Our study demonstrates that two candidate metabolite biomarkers, in combination with five clinical variables, yield the best performing set of predictors for incident CKD in hyperglycemic individuals. Furthermore, we show the power of appropriate combination of state-of-the-art machine learning and classical statistical approaches to reveal novel biomarkers and improve the performance of classical clinical predictors of CKD. The three-step feature selection, which we define in this study, was able to capture as few predictors as possible but achieve better predictive performance, which fulfills the ideal setting of clinical practice. Many epidemiological studies have used inappropriate ways to evaluate the performance of the identified variables, in which, for example, certain variables were selected from the whole data set and then the predictive performance was only evaluated on those selected variables using resampling approaches on the same data set (53). Consequently, this could have potentially strongly overestimated the predictive performance because the testing data set has been included as part of the whole data set to perform variable selection and it cannot be regarded as the testing

data set anymore (53). In our study, we used cross validation in a combination with three-step feature selection and applied stringent internal validation procedures to evaluate the performance of the identified sets of predictors. In each round, the variable selection was only conducted for the training data and the performance evaluation was only performed for the testing data. In this way, we were able to attain accurate and unbiased internal AUC estimates. Given these advantages as described above, the consistent improvement of our developed sets of predictors on top of four established reference predictors in all three machine learning algorithms can be regarded as significant progress.

Our study has several additional advantages. We used a well-characterized, population-based human cohort that allows for adjustment for the influence of demographic parameters, medication, and other clinical variables. Our stringent QC of metabolite profiles and adjustment for plate effects reduced the noise among all 3,061 measured samples. We performed sensitivity analyses to confirm the candidate metabolite biomarkers and investigate their interaction with glycemia.

A limitation of our study is the missing replication (of 10 international human cohorts, none included at least 50 incident CKD cases in hyperglycemia and metabolites we measured). Discriminatory power of the candidate biomarkers and the best set of predictors cannot be generalized due to lack of external validation. Thus, we are aware that larger prospective studies are needed to validate our discoveries.

In summary, we identified two candidate metabolite biomarkers and the best set of predictors for incident CKD that are specific for individuals with prediabetes and T2D. This study demonstrates the value of metabolomics and appropriate combination of predictors in the improvement of accurate detection of hyperglycemic individuals with enhanced risk for CKD. With rising worldwide prevalence and burden of (pre)diabetes-related CKD, combining metabolite and clinical predictors is a promising approach for effective predictions of future CKD in the framework of an integrated personalized diabetes management.

Acknowledgments. The authors express appreciation to all KORA study participants for donating their blood and time. The authors thank the field staff in Augsburg conducting the KORA studies. The authors are grateful to the staff (J. Scarpa, K. Faschinger, N. Lindemann, A. Ludolph, S. Jelic, and B. Langer) from the Institute of Epidemiology and the Genome Analysis Center Metabolomics Platform, and KORA-PASST Platform at Helmholtz Zentrum München – German Research Center for Environmental Health, who helped in the sample and data logistics, and metabolomics measurements. Additionally, the authors thank Dr. Anne-Laure Boulesteix from the Institute of Medical Information Processing, Biometry and Epidemiology, Ludwig-Maximilians-University of Munich, Germany, for tips on statistical methods.

Funding. The KORA study was initiated and financed by Helmholtz Zentrum München – German Research Center for Environmental Health, which is funded by the German Federal Ministry of Education and Research (BMBF) and by the State of Bavaria. Furthermore, KORA research was supported within the Munich Center

of Health Sciences (MC-Health), Ludwig-Maximilians-Universität, as part of LMUinnovativ. Part of this project was supported by European Union Seventh Framework Programme (EU FP7) grant HEALTH-2013-2.4.2-1/602936 (Project CarTarDis) and the European Institute of Innovation and Technology (EIT) Health-supported 19076 and 20679 iPDM-GO “Integrated Personalized Diabetes Management Goes Europe” innovation project. EIT Health is supported by the EIT, a body of the European Union. K.S. is supported by Biomedical Research Program funds at Weill Cornell Medicine - Qatar, a program funded by the Qatar Foundation.

Duality of Interest. M.F.S. was employed at Helmholtz Center Munich during his PhD thesis and is currently employed in the CardioRenal Medical Department of Bayer AG. No other potential conflicts of interest relevant to this article were reported.

Bayer AG was not involved in work related to data and manuscript generation.

Author Contributions. J.H. conceived the study, analyzed the data, and wrote the manuscript. C.H. researched cohort data and edited the manuscript. M.C. contributed to pathway analysis and wrote the manuscript. M.T. researched data and edited the manuscript. J. Adam edited the manuscript. S.Z. researched data. C.P. researched metabolomics data. L.W. edited the manuscript. J.N. edited the manuscript. M.F.S. researched data and edited the manuscript. S.N. researched data. G.K. researched metabolomics data. K.S. researched metabolomics data. M.L. reviewed the manuscript. F.S. edited the manuscript. C.G. researched cohort data. J.Adam. researched metabolomics data. M.H.d.A. researched data. A.P. researched cohort data. R.W.-S. designed the study, researched metabolomics data, and wrote the manuscript. R.W.-S. is the guarantor of this work and, as such, had full access to all the data in the study and takes responsibility for the integrity of the data and the accuracy of the data analysis.

Prior Presentation. Parts of this study were presented in abstract form at the 15th Annual Conference of the Metabolomics Society The Hague, the Netherlands, 23–27 June 2019, and at the 7th DZD Diabetes Research School, Barcelona, Spain, 14–16 September 2019.

References

1. Bikbov B, Purcell CA, Levey AS, et al.; GBD Chronic Kidney Disease Collaboration. Global, regional, and national burden of chronic kidney disease, 1990–2017: a systematic analysis for the Global Burden of Disease Study 2017. *Lancet* 2020;395:709–733
2. Webster AC, Nagler EV, Morton RL, Masson P. Chronic kidney disease. *Lancet* 2017;389:1238–1252
3. Alicic RZ, Neumiller JJ, Johnson EJ, Dieter B, Tuttle KR. Sodium-glucose cotransporter 2 inhibition and diabetic kidney disease. *Diabetes* 2019;68:248–257
4. Plantinga LC, Crews DC, Coresh J, et al.; CDC CKD Surveillance Team. Prevalence of chronic kidney disease in US adults with undiagnosed diabetes or prediabetes. *Clin J Am Soc Nephrol* 2010;5:673–682
5. Melsom T, Schei J, Stefansson VT, et al. Prediabetes and risk of glomerular hyperfiltration and albuminuria in the general nondiabetic population: a prospective cohort study. *Am J Kidney Dis* 2016;67:841–850
6. Markus MRP, Ittermann T, Baumeister SE, et al. Prediabetes is associated with microalbuminuria, reduced kidney function and chronic kidney disease in the general population: the KORA (Cooperative Health Research in the Augsburg Region) F4-Study. *Nutr Metab Cardiovasc Dis* 2018;28:234–242
7. Li W, Wang A, Jiang J, et al. Risk of chronic kidney disease defined by decreased estimated glomerular filtration rate in individuals with different prediabetic phenotypes: results from a prospective cohort study in China. *BMJ Open Diabetes Res Care* 2020;8:e000955
8. Ceriello A, Barkai L, Christiansen JS, et al. Diabetes as a case study of chronic disease management with a personalized approach: the role of a structured feedback loop. *Diabetes Res Clin Pract* 2012;98:5–10
9. Levin A, Stevens PE, Bilous RW, et al.; Kidney Disease Improving Global Outcomes (KDIGO) CKD Work Group. KDIGO 2012 clinical practice guideline for the evaluation and management of chronic kidney disease. *Kidney Int Suppl* 2013;3:1–150

10. Tangri N, Stevens LA, Griffith J, et al. A predictive model for progression of chronic kidney disease to kidney failure. *JAMA* 2011;305:1553–1559
11. Dunkler D, Gao P, Lee SF, et al.; ONTARGET and ORIGIN Investigators. Risk prediction for early CKD in type 2 diabetes. *Clin J Am Soc Nephrol* 2015;10:1371–1379
12. Floegel A, Stefan N, Yu Z, et al. Identification of serum metabolites associated with risk of type 2 diabetes using a targeted metabolomic approach. *Diabetes* 2013;62:639–648
13. Wang-Sattler R, Yu Z, Herder C, et al. Novel biomarkers for pre-diabetes identified by metabolomics. *Mol Syst Biol* 2012;8:615
14. Wang TJ, Larson MG, Vasan RS, et al. Metabolite profiles and the risk of developing diabetes. *Nat Med* 2011;17:448–453
15. Chen GC, Chai JC, Yu B, et al. Serum sphingolipids and incident diabetes in a US population with high diabetes burden: the Hispanic Community Health Study/Study of Latinos (HCHS/SOL). *Am J Clin Nutr* 2020;112:57–65
16. Carayol M, Leitzmann MF, Ferrari P, et al. Blood metabolic signatures of body mass index: a targeted metabolomics study in the EPIC cohort. *J Proteome Res* 2017;16:3137–3146
17. Leal-Witt MJ, Ramon-Krauel M, Samino S, et al. Untargeted metabolomics identifies a plasma sphingolipid-related signature associated with lifestyle intervention in prepubertal children with obesity. *Int J Obes* 2018;42:72–78
18. Razquin C, Toledo E, Clish CB, et al. Plasma lipidomic profiling and risk of type 2 diabetes in the PREDIMED trial. *Diabetes Care* 2018;41:2617–2624
19. Alderete TL, Jin R, Walker DI, et al. Perfluoroalkyl substances, metabolomic profiling, and alterations in glucose homeostasis among overweight and obese Hispanic children: a proof-of-concept analysis. *Environ Int* 2019;126:445–453
20. Hocher B, Adamski J. Metabolomics for clinical use and research in chronic kidney disease. *Nat Rev Nephrol* 2017;13:269–284
21. Goek ON, Prehn C, Sekula P, et al. Metabolites associate with kidney function decline and incident chronic kidney disease in the general population. *Nephrol Dial Transplant* 2013;28:2131–2138
22. Solini A, Manca ML, Penno G, Pugliese G, Cobb JE, Ferrannini E. Prediction of declining renal function and albuminuria in patients with type 2 diabetes by metabolomics. *J Clin Endocrinol Metab* 2016;101:696–704
23. Herder C, Kannenberg JM, Huth C, et al. Proinflammatory cytokines predict the incidence and progression of distal sensorimotor polyneuropathy: KORA F4/FF4 study. *Diabetes Care* 2017;40:569–576
24. Chak CM, Lacruz ME, Adam J, et al. Ageing investigation using two-time-point metabolomics data from KORA and CARLA studies. *Metabolites* 2019;9:44
25. World Health Organization, International Diabetes Federation. *Definition and Diagnosis of Diabetes Mellitus and Intermediate Hyperglycaemia: Report of a WHO/IDF Consultation*. Geneva, World Health Org., 2006
26. Inker LA, Schmid CH, Tighiouart H, et al.; CKD-EPI Investigators. Estimating glomerular filtration rate from serum creatinine and cystatin C. *N Engl J Med* 2012;367:20–29
27. Römisch-Margl W, Prehn C, Bogumil R, Röhring C, Suhre K, Adamski J. Procedure for tissue sample preparation and metabolite extraction for high-throughput targeted metabolomics. *Metabolomics* 2012;8:133–142
28. Klau S, Jurinovic V, Hornung R, Herold T, Boulesteix AL. Priority-Lasso: a simple hierarchical approach to the prediction of clinical outcome using multi-omics data. *BMC Bioinformatics* 2018;19:322
29. Chang C-C, Lin C-J. LIBSVM: a library for support vector machines. *ACM Trans Intell Syst Technol* 2011;2:1–27
30. Liaw A, Wiener M. Classification and regression by randomForest. *R News* 2002;2:18–22
31. Culp M, Johnson K, Michailides G. ada: an R package for stochastic boosting. *J Stat Softw* 2006;17:1–27
32. Merscher S, Fornoni A. Podocyte pathology and nephropathy - sphingolipids in glomerular diseases. *Front Endocrinol (Lausanne)* 2014;5:127
33. Mäkinen VP, Tynkkynen T, Soininen P, et al. Sphingomyelin is associated with kidney disease in type 1 diabetes (The FinnDiane Study). *Metabolomics* 2012; 8:369–375
34. Liu JJ, Ghosh S, Kovalik JP, et al. Profiling of plasma metabolites suggests altered mitochondrial fuel usage and remodeling of sphingolipid metabolism in individuals with type 2 diabetes and kidney disease. *Kidney Int Rep* 2016;2:470–480
35. Tofte N, Suvitaival T, Ahonen L, et al. Lipidomic analysis reveals sphingomyelin and phosphatidylcholine species associated with renal impairment and all-cause mortality in type 1 diabetes. *Sci Rep* 2019;9:16398
36. Annotation of potential isobaric and isomeric lipid species analyzed using theMxP@Quant 500 Kit. Available from https://www.biocrates.com/wp-content/uploads/2020/02/Biocrates_Q500_isomers_isobars.pdf
37. Sigrüener A, Kleber ME, Heimerl S, Liebisch G, Schmitz G, Maerz W. Glycerophospholipid and sphingolipid species and mortality: the Ludwigshafen Risk and Cardiovascular Health (LURIC) study. *PLoS One* 2014;9:e85724
38. Floegel A, Kühn T, Sookthai D, et al. Serum metabolites and risk of myocardial infarction and ischemic stroke: a targeted metabolomic approach in two German prospective cohorts. *Eur J Epidemiol* 2018;33:55–66
39. Jiang XC, Paultre F, Pearson TA, et al. Plasma sphingomyelin level as a risk factor for coronary artery disease. *Arterioscler Thromb Vasc Biol* 2000;20:2614–2618
40. Li Z, Basterr MJ, Hailemariam TK, et al. The effect of dietary sphingolipids on plasma sphingomyelin metabolism and atherosclerosis. *Biochim Biophys Acta* 2005;1735:130–134
41. Cai Q, Mukku VK, Ahmad M. Coronary artery disease in patients with chronic kidney disease: a clinical update. *Curr Cardiol Rev* 2013;9:331–339
42. Alicic RZ, Rooney MT, Tuttle KR. Diabetic kidney disease: challenges, progress, and possibilities. *Clin J Am Soc Nephrol* 2017;12:2032–2045
43. Miyamoto S, Hsu C-C, Hamm G, et al. Mass spectrometry imaging reveals elevated glomerular ATP/AMP in diabetes/obesity and identifies sphingomyelin as a possible mediator. *EBioMedicine* 2016;7:121–134
44. Torretta E, Barbacini P, Al-Daghri NM, Gelfi C. Sphingolipids in obesity and correlated co-morbidities: the contribution of gender, age and environment. *Int J Mol Sci* 2019;20:5901
45. Johnson EL, Heaver SL, Waters JL, et al. Sphingolipids produced by gut bacteria enter host metabolic pathways impacting ceramide levels. *Nat Commun* 2020;11:2471
46. Czumaj A, Śledziński T, Carrero JJ, et al. Alterations of fatty acid profile may contribute to dyslipidemia in chronic kidney disease by influencing hepatocyte metabolism. *Int J Mol Sci* 2019;20:2470
47. Sugimoto M, Wakabayashi M, Shimizu Y, et al. Imaging mass spectrometry reveals acyl-chain- and region-specific sphingolipid metabolism in the kidneys of sphingomyelin synthase 2-deficient mice. *PLoS One* 2016;11:e0152191
48. Li Z, Zhang H, Liu J, et al. Reducing plasma membrane sphingomyelin increases insulin sensitivity. *Mol Cell Biol* 2011;31:4205–4218
49. Fan Y, Shi F, Liu J, et al. Selective reduction in the sphingomyelin content of atherogenic lipoproteins inhibits their retention in murine aortas and the subsequent development of atherosclerosis. *Arterioscler Thromb Vasc Biol* 2010;30:2114–2120
50. Adachi R, Ogawa K, Matsumoto SI, et al. Discovery and characterization of selective human sphingomyelin synthase 2 inhibitors. *Eur J Med Chem* 2017;136: 283–293
51. Ravizza S, Huschto T, Adamov A, et al. Predicting the early risk of chronic kidney disease in patients with diabetes using real-world data. *Nat Med* 2019;25: 57–59
52. Echouffo-Tcheugui JB, Kengne AP. Risk models to predict chronic kidney disease and its progression: a systematic review. *PLoS Med* 2012;9:e1001344
53. Boulesteix AL, Wright MN, Hoffmann S, König IR. Statistical learning approaches in the genetic epidemiology of complex diseases. *Hum Genet* 2020;139: 73–84

SUPPLEMENTAL MATERIAL

Full Title: Machine learning approaches reveal metabolic signatures of incident chronic kidney disease in individuals with prediabetes and type 2 diabetes

Supplementary Tables

Table S1. Metabolite panel of baseline KORA F4 study

The abbreviations and biochemical names of 163 metabolites are shown in the first and second column, respectively. The third column shows the missing rate of each metabolite among 3,061 KORA F4 individuals. The missing rate was defined as the number of no reported values divided by the number of all measured values. The fourth column presents the arithmetic means of the coefficients of variance (CV) of 114 quality controls samples (i.e. three on each kit plate). The percentage of individuals equal to or above the limit of detection (LOD) among 3,061 KORA F4 participants is shown in the fifth column. The sixth column presents the mean value of metabolite concentration (μM) in 3,061 KORA F4 participants after adjusting for plate effects. The last column shows the status (used/excluded) for each metabolite.

Metabolite	Biochemical name	Missing Rate (%)	CV (%)	Equal to or above LOD (%)	Mean Concentration (μM)	Application
C0	Carnitine	0.0	7.50	99.97	35.89	Used
C10	Decanoylcarnitine	0.0	12.40	98.30	0.36	Used
C10:1	Decenoylcarnitine	0.0	10.45	36.20	0.17	Excluded
C10:2	Decadienylcarnitine	0.0	15.61	58.58	0.04	Used
C12	Dodecanoylcarnitine	0.0	10.63	89.51	0.13	Used
C12:1	Dodecenoylcarnitine	0.0	13.51	2.16	0.15	Excluded
C12-DC	Dodecanedioylcarnitine	0.0	15.71	0.00	0.06	Excluded
C14	Tetradecanoylcarnitine	0.0	11.80	47.60	0.05	Excluded
C14:1	Tetradecenoylcarnitine	0.0	20.10	99.97	0.15	Used
C14:1-OH	Hydroxytetradecenoylcarnitine	0.0	17.88	76.54	0.02	Used
C14:2	Tetradecadienylcarnitine	0.0	11.19	99.44	0.03	Used
C14:2-OH	Hydroxytetradecadienylcarnitine	0.0	24.24	44.10	0.01	Excluded
C16	Hexadecanoylcarnitine	0.0	10.02	99.97	0.12	Used
C16:1	Hexadecenoylcarnitine	0.0	10.39	2.48	0.04	Excluded
C16:1-OH	Hydroxyhexadecenoylcarnitine	0.0	17.20	1.31	0.01	Excluded
C16:2	Hexadecadienylcarnitine	0.0	19.46	77.56	0.01	Used
C16:2-OH	Hydroxyhexadecadienylcarnitine	0.0	20.19	1.08	0.01	Excluded
C16-OH	Hydroxyhexadecanoylcarnitine	0.0	21.99	3.23	0.01	Excluded
C18	Octadecanoylcarnitine	0.0	12.52	99.90	0.05	Used
C18:1	Octadecenoylcarnitine	0.0	13.30	99.93	0.13	Used
C18:1-OH	Hydroxyoctadecenoylcarnitine	0.0	25.50	1.14	0.01	Excluded
C18:2	Octadecadienylcarnitine	0.0	11.00	99.97	0.05	Used
C2	Acetylcarnitine	0.0	9.62	99.97	8.26	Used
C3	Propionylcarnitine	0.0	10.28	99.97	0.40	Used
C3:1	Propenonylcarnitine	0.0	37.84	0.49	0.01	Excluded
C3-OH	Hydroxypropionylcarnitine	0.0	98.90	7.64	0.03	Excluded
C4	Butyrylcarnitine	0.0	11.20	99.97	0.23	Used
C4:1	Butenylcarnitine	0.0	35.99	10.42	0.02	Excluded
C4-OH (C3-DC)	Hydroxybutyrylcarnitine	0.0	34.81	9.64	0.09	Excluded
C5	Valerylcarnitine	0.0	15.83	99.97	0.12	Used
C5:1	Tiglylcarnitine	0.0	26.40	1.83	0.03	Excluded
C5:1-DC	Glutaconylcarnitine	0.0	51.54	13.92	0.02	Excluded
C5-DC (C6-OH)	Glutaryl carnitine (Hydroxyhexa-	0.0	36.29	58.05	0.03	Excluded
C5-M-DC	Methylglutaryl carnitine	0.0	48.62	3.82	0.03	Excluded

C5-OH (C3-DC-	Hydroxyvalerylcarnitine	0.0	24.31	14.05	0.04	Excluded
C6 (C4:1-DC)	Hexanoylcarnitine (Fumaryl-	0.0	14.19	87.62	0.07	Used
C6:1	Hexenoylcarnitine	0.0	36.13	3.50	0.02	Excluded
C7-DC	Pimelylcarnitine	0.0	29.31	73.21	0.05	Excluded
C8	Octanoylcarnitine	0.0	9.73	50.38	0.23	Used
C8:1	Octenoylcarnitine	0.0	8.45	99.22	0.09	Used
C9	Nonanoylcarnitine	0.0	33.00	92.98	0.05	Excluded
Arg	Arginine	0.0	7.58	99.97	115.89	Used
Gln	Glutamine	0.0	14.28	99.97	619.01	Used
Gly	Glycine	0.0	8.35	99.97	307.70	Used
His	Histidine	0.0	10.50	99.97	98.28	Used
Met	Methionine	0.0	14.82	99.97	32.03	Used
Orn	Ornithine	0.0	11.33	99.97	81.47	Used
Phe	Phenylalanine	0.0	8.87	99.97	62.25	Used
Pro	Proline	0.0	10.15	100.00	176.09	Used
Ser	Serine	0.0	9.34	99.97	128.46	Used
Thr	Threonine	0.0	11.20	99.97	106.03	Used
Trp	Tryptophan	0.0	7.45	99.97	82.62	Used
Tyr	Tyrosine	0.0	8.61	99.97	85.47	Used
Val	Valine	0.0	15.51	100.00	277.00	Used
xLeu	Leucine/Isoleucine	0.0	9.48	100.00	213.92	Used
PC aa C24:0	Phosphatidylcholine diacyl C24:0	0.0	24.13	78.93	0.15	Used
PC aa C26:0	Phosphatidylcholine diacyl C26:0	0.0	38.23	11.43	1.08	Excluded
PC aa C28:1	Phosphatidylcholine diacyl C28:1	0.0	9.78	99.97	3.38	Used
PC aa C30:0	Phosphatidylcholine diacyl C30:0	0.0	12.24	99.97	4.74	Used
PC aa C30:2	Phosphatidylcholine diacyl C30:2	95.52	75.42	4.34	0.06	Excluded
PC aa C32:0	Phosphatidylcholine diacyl C32:0	0.0	12.23	99.97	15.21	Used
PC aa C32:1	Phosphatidylcholine diacyl C32:1	0.0	12.32	99.97	21.98	Used
PC aa C32:2	Phosphatidylcholine diacyl C32:2	0.07	20.80	99.90	3.95	Used
PC aa C32:3	Phosphatidylcholine diacyl C32:3	0.0	9.92	99.97	0.48	Used
PC aa C34:1	Phosphatidylcholine diacyl C34:1	0.0	11.63	99.97	240.68	Used
PC aa C34:2	Phosphatidylcholine diacyl C34:2	0.0	16.87	99.97	392.77	Used
PC aa C34:3	Phosphatidylcholine diacyl C34:3	0.0	14.83	99.97	18.07	Used
PC aa C34:4	Phosphatidylcholine diacyl C34:4	0.0	10.15	99.97	2.27	Used
PC aa C36:0	Phosphatidylcholine diacyl C36:0	0.0	19.81	99.97	2.72	Used
PC aa C36:1	Phosphatidylcholine diacyl C36:1	0.0	9.14	99.97	53.89	Used
PC aa C36:2	Phosphatidylcholine diacyl C36:2	0.0	8.32	99.97	232.62	Used
PC aa C36:3	Phosphatidylcholine diacyl C36:3	0.0	10.63	99.97	150.39	Used
PC aa C36:4	Phosphatidylcholine diacyl C36:4	0.0	11.24	100.00	220.61	Used
PC aa C36:5	Phosphatidylcholine diacyl C36:5	0.0	13.45	99.97	29.52	Used
PC aa C36:6	Phosphatidylcholine diacyl C36:6	0.0	15.22	99.97	1.13	Used
PC aa C38:0	Phosphatidylcholine diacyl C38:0	0.0	15.09	99.97	3.29	Used
PC aa C38:1	Phosphatidylcholine diacyl C38:1	0.10	19.94	99.84	0.87	Used
PC aa C38:3	Phosphatidylcholine diacyl C38:3	0.0	7.21	99.97	54.08	Used
PC aa C38:4	Phosphatidylcholine diacyl C38:4	0.0	6.64	99.97	119.83	Used
PC aa C38:5	Phosphatidylcholine diacyl C38:5	0.0	9.96	99.97	62.43	Used
PC aa C38:6	Phosphatidylcholine diacyl C38:6	0.0	10.27	99.97	90.66	Used
PC aa C40:1	Phosphatidylcholine diacyl C40:1	0.0	15.62	9.05	0.47	Excluded
PC aa C40:2	Phosphatidylcholine diacyl C40:2	0.0	13.75	99.97	0.36	Used
PC aa C40:3	Phosphatidylcholine diacyl C40:3	0.0	12.85	99.97	0.66	Used
PC aa C40:4	Phosphatidylcholine diacyl C40:4	0.0	7.60	100.00	4.17	Used
PC aa C40:5	Phosphatidylcholine diacyl C40:5	0.0	6.43	99.97	11.53	Used
PC aa C40:6	Phosphatidylcholine diacyl C40:6	0.03	6.22	99.97	28.76	Used
PC aa C42:0	Phosphatidylcholine diacyl C42:0	0.0	13.59	99.97	0.60	Used
PC aa C42:1	Phosphatidylcholine diacyl C42:1	0.0	15.38	99.97	0.30	Used
PC aa C42:2	Phosphatidylcholine diacyl C42:2	0.0	15.10	99.97	0.21	Used
PC aa C42:4	Phosphatidylcholine diacyl C42:4	0.0	12.77	99.97	0.22	Used
PC aa C42:5	Phosphatidylcholine diacyl C42:5	0.0	10.74	99.97	0.43	Used
PC aa C42:6	Phosphatidylcholine diacyl C42:6	0.0	10.85	62.53	0.63	Used
PC ae C30:0	Phosphatidylcholine acyl-alkyl	0.0	31.78	99.71	0.48	Excluded
PC ae C30:1	Phosphatidylcholine acyl-alkyl	4.57	46.30	94.09	0.24	Excluded
PC ae C30:2	Phosphatidylcholine acyl-alkyl	0.0	17.44	92.22	0.16	Used

PC ae C32:1	Phosphatidylcholine acyl-alkyl	0.0	10.34	99.97	2.85	Used
PC ae C32:2	Phosphatidylcholine acyl-alkyl	0.0	12.20	99.97	0.75	Used
PC ae C34:0	Phosphatidylcholine acyl-alkyl	0.0	11.28	99.97	1.73	Used
PC ae C34:1	Phosphatidylcholine acyl-alkyl	0.0	11.88	99.97	10.56	Used
PC ae C34:2	Phosphatidylcholine acyl-alkyl	0.0	12.38	99.97	12.67	Used
PC ae C34:3	Phosphatidylcholine acyl-alkyl	0.0	9.93	99.97	8.38	Used
PC ae C36:0	Phosphatidylcholine acyl-alkyl	0.0	40.89	99.97	1.10	Excluded
PC ae C36:1	Phosphatidylcholine acyl-alkyl	0.0	12.61	99.97	8.40	Used
PC ae C36:2	Phosphatidylcholine acyl-alkyl	0.0	13.72	99.97	15.19	Used
PC ae C36:3	Phosphatidylcholine acyl-alkyl	0.0	12.59	99.97	8.59	Used
PC ae C36:4	Phosphatidylcholine acyl-alkyl	0.0	11.60	99.97	20.88	Used
PC ae C36:5	Phosphatidylcholine acyl-alkyl	0.0	9.39	99.97	13.85	Used
PC ae C38:0	Phosphatidylcholine acyl-alkyl	0.0	12.57	99.97	2.48	Used
PC ae C38:1	Phosphatidylcholine acyl-alkyl	0.0	14.05	99.97	0.82	Used
PC ae C38:2	Phosphatidylcholine acyl-alkyl	0.0	13.49	99.97	2.15	Used
PC ae C38:3	Phosphatidylcholine acyl-alkyl	0.0	10.85	99.97	4.34	Used
PC ae C38:4	Phosphatidylcholine acyl-alkyl	0.0	12.38	99.97	15.73	Used
PC ae C38:5	Phosphatidylcholine acyl-alkyl	0.0	11.10	100.00	19.96	Used
PC ae C38:6	Phosphatidylcholine acyl-alkyl	0.0	9.18	99.97	8.70	Used
PC ae C40:0	Phosphatidylcholine acyl-alkyl	0.0	8.03	1.14	10.25	Excluded
PC ae C40:1	Phosphatidylcholine acyl-alkyl	0.0	12.62	99.97	1.68	Used
PC ae C40:2	Phosphatidylcholine acyl-alkyl	0.0	11.32	99.97	2.10	Used
PC ae C40:3	Phosphatidylcholine acyl-alkyl	0.0	10.64	99.97	1.14	Used
PC ae C40:4	Phosphatidylcholine acyl-alkyl	0.0	10.30	99.97	2.59	Used
PC ae C40:5	Phosphatidylcholine acyl-alkyl	0.0	8.88	99.97	3.57	Used
PC ae C40:6	Phosphatidylcholine acyl-alkyl	0.0	11.23	99.97	5.06	Used
PC ae C42:0	Phosphatidylcholine acyl-alkyl	0.0	18.33	14.80	0.52	Excluded
PC ae C42:1	Phosphatidylcholine acyl-alkyl	0.0	13.91	99.97	0.38	Used
PC ae C42:2	Phosphatidylcholine acyl-alkyl	0.0	17.58	99.97	0.68	Used
PC ae C42:3	Phosphatidylcholine acyl-alkyl	0.0	11.87	99.97	0.87	Used
PC ae C42:4	Phosphatidylcholine acyl-alkyl	0.03	9.99	99.97	1.01	Used
PC ae C42:5	Phosphatidylcholine acyl-alkyl	0.0	7.27	99.93	2.36	Used
PC ae C44:3	Phosphatidylcholine acyl-alkyl	0.0	13.32	99.97	0.11	Used
PC ae C44:4	Phosphatidylcholine acyl-alkyl	0.0	11.71	99.97	0.43	Used
PC ae C44:5	Phosphatidylcholine acyl-alkyl	0.0	7.15	99.97	2.12	Used
PC ae C44:6	Phosphatidylcholine acyl-alkyl	0.0	7.73	99.97	1.38	Used
lysoPC a C14:0	lysoPhosphatidylcholine acyl C14:0	0.0	26.82	42.21	3.21	Excluded
lysoPC a C16:0	lysoPhosphatidylcholine acyl C16:0	0.0	10.69	99.97	94.07	Used
lysoPC a C16:1	lysoPhosphatidylcholine acyl C16:1	0.0	10.01	99.97	2.90	Used
lysoPC a C17:0	lysoPhosphatidylcholine acyl C17:0	0.0	13.05	99.97	1.72	Used
lysoPC a C18:0	lysoPhosphatidylcholine acyl C18:0	0.0	10.27	99.97	25.96	Used
lysoPC a C18:1	lysoPhosphatidylcholine acyl C18:1	0.0	11.29	99.97	19.22	Used
lysoPC a C18:2	lysoPhosphatidylcholine acyl C18:2	0.0	9.42	99.97	27.22	Used
lysoPC a C20:3	lysoPhosphatidylcholine acyl C20:3	0.0	10.95	99.97	2.38	Used
lysoPC a C20:4	lysoPhosphatidylcholine acyl C20:4	0.0	9.34	99.97	6.77	Used
lysoPC a C24:0	lysoPhosphatidylcholine acyl C24:0	0.0	21.21	8.04	0.36	Excluded
lysoPC a C26:0	lysoPhosphatidylcholine acyl C26:0	0.0	32.22	59.85	0.54	Excluded
lysoPC a C26:1	lysoPhosphatidylcholine acyl C26:1	0.0	10.71	0.00	2.02	Excluded
lysoPC a C28:0	lysoPhosphatidylcholine acyl C28:0	0.0	27.17	46.46	0.48	Excluded
lysoPC a C28:1	lysoPhosphatidylcholine acyl C28:1	0.0	22.50	99.84	0.62	Used
lysoPC a C6:0	lysoPhosphatidylcholine acyl C6:0	0.03	43.89	25.48	0.02	Excluded
SM (OH) C14:1	Hydroxysphingomyeline C14:1	0.03	12.85	99.97	6.18	Used
SM (OH) C16:1	Hydroxysphingomyeline C16:1	0.0	8.72	99.97	3.35	Used
SM (OH) C22:1	Hydroxysphingomyeline C22:1	0.0	14.23	99.97	13.43	Used
SM (OH) C22:2	Hydroxysphingomyeline C22:2	0.0	13.12	99.97	11.40	Used
SM (OH) C24:1	Hydroxysphingomyeline C24:1	0.0	17.05	99.97	1.34	Used
SM C16:0	Sphingomyelin C16:0	0.0	12.92	99.97	105.98	Used
SM C16:1	Sphingomyelin C16:1	0.0	11.64	99.97	15.97	Used
SM C18:0	Sphingomyelin C18:0	0.0	9.29	99.97	23.16	Used
SM C18:1	Sphingomyelin C18:1	0.0	10.86	100.00	11.25	Used
SM C20:2	Sphingomyelin C20:2	0.07	15.99	99.90	0.38	Used
SM C22:3	Sphingomyelin C22:3	43.61	60.99	55.90	0.22	Excluded

SM C24:0	Sphingomyelin C24:0	0.0	14.33	99.97	21.68	Used
SM C24:1	Sphingomyelin C24:1	0.0	15.01	100.00	52.40	Used
SM C26:0	Sphingomyelin C26:0	0.0	57.33	99.97	0.32	Excluded
SM C26:1	Sphingomyelin C26:1	0.0	22.75	99.97	0.42	Used
H1	Sum of Hexoses	0.0	6.33	99.97	5197.44	Used

Table S2. List of 26 metabolites significantly associated with incident chronic kidney disease in either basic or full model in hyperglycemic individuals

Odds ratios (*ORs*) with 95% *CI* and *P*-values of multivariable logistic regression are shown. The basic model was adjusted for age, sex, BMI, systolic blood pressure, smoking status, triglyceride, total cholesterol, HDL cholesterol, and fasting serum glucose. The full model was additionally adjusted for use of lipid lowering drugs, antihypertensive and anti-diabetic medication, baseline estimated glomerular filtration rate and urinary albumin-to-creatinine ratio. *P*-values shown in bold represent statistical significance at 0.05 level. **Abbreviations:** SM, sphingomyelin; PC aa, phosphatidylcholine diacyl; PC ae, phosphatidylcholine acyl-alkyl.

Metabolites	Basic Model		Full Model	
	<i>OR</i> (95% <i>CI</i>)	<i>P</i> -value	<i>OR</i> (95% <i>CI</i>)	<i>P</i> -value
C10	1.42 (1.03 - 1.98)	3.317E-02	1.24 (0.86 - 1.80)	2.495E-01
C12	1.49 (1.09 - 2.05)	1.268E-02	1.35 (0.95 - 1.92)	9.131E-02
C14:1	1.37 (1.04 - 1.83)	2.919E-02	1.36 (0.99 - 1.89)	5.751E-02
C18	1.44 (1.06 - 1.98)	2.331E-02	1.30 (0.92 - 1.84)	1.376E-01
C18:1	1.44 (1.07 - 1.97)	1.892E-02	1.39 (0.99 - 1.96)	6.293E-02
C6 (C4:1-DC)	1.41 (1.05 - 1.89)	2.244E-02	1.25 (0.90 - 1.75)	1.884E-01
C8	1.39 (1.02 - 1.90)	3.948E-02	1.21 (0.85 - 1.71)	2.919E-01
Arginine	1.40 (1.07 - 1.89)	2.154E-02	1.25 (0.93 - 1.73)	1.577E-01
Proline	1.38 (1.01 - 1.89)	4.453E-02	1.39 (0.98 - 1.97)	6.337E-02
PC aa C32:2	0.72 (0.56 - 0.93)	1.275E-02	0.74 (0.56 - 0.99)	3.690E-02
PC aa C38:0	1.51 (1.12 - 2.07)	8.059E-03	1.56 (1.12 - 2.21)	1.043E-02
PC aa C42:0	1.41 (1.04 - 1.92)	2.686E-02	1.40 (1.01 - 1.96)	4.801E-02
PC ae C38:6	1.41 (1.01 - 1.99)	4.573E-02	1.40 (0.96 - 2.06)	8.386E-02
PC ae C40:5	1.42 (1.04 - 1.95)	3.009E-02	1.32 (0.94 - 1.88)	1.181E-01
PC ae C40:6	1.54 (1.12 - 2.14)	9.600E-03	1.57 (1.10 - 2.27)	1.358E-02
PC ae C42:5	1.43 (1.06 - 1.96)	2.234E-02	1.29 (0.92 - 1.81)	1.457E-01
SM (OH) C14:1	1.50 (1.06 - 2.13)	2.277E-02	1.56 (1.07 - 2.32)	2.382E-02
SM (OH) C16:1	1.59 (1.14 - 2.24)	6.923E-03	1.63 (1.14 - 2.39)	9.614E-03
SM (OH) C22:2	1.58 (1.09 - 2.33)	1.880E-02	1.50 (1.00 - 2.30)	5.674E-02
SM C16:0	1.91 (1.29 - 2.91)	1.811E-03	1.82 (1.17 - 2.91)	9.378E-03
SM C16:1	1.91 (1.29 - 2.88)	1.557E-03	1.85 (1.19 - 2.94)	7.145E-03
SM C18:0	1.86 (1.34 - 2.63)	2.839E-04	1.80 (1.26 - 2.63)	1.754E-03
SM C18:1	2.25 (1.54 - 3.39)	4.976E-05	2.22 (1.46 - 3.49)	3.315E-04
SM C20:2	1.40 (1.05 - 1.93)	3.045E-02	1.51 (1.10 - 2.14)	1.411E-02
SM C24:1	1.62 (1.15 - 2.31)	7.066E-03	1.57 (1.08 - 2.33)	2.061E-02
SM C26:1	1.41 (1.05 - 1.93)	2.564E-02	1.57 (1.13 - 2.23)	8.215E-03

Table S3. Baseline characteristics of propensity scores matched case-control hyperglycemic individuals

Clinical variables of incident CKD patients (= cases) matched with non-CKD participants (= controls) are shown. Mean \pm standard deviation is provided when appropriate; *P*-values were calculated by univariate conditional logistic regression. *P*-values shown in bold represent statistical significance at 0.05 level. **Abbreviations:** CKD, chronic kidney disease; eGFR, estimated glomerular filtration rate; UACR, urinary albumin-to-creatinine ratio.

Clinical variables	Incident CKD N = 62	Non-CKD N = 62	<i>P</i> -value
Age, years	65.81 \pm 9.3	65.48 \pm 7.62	0.777
Sex, Male, n (%)	54.84	64.52	0.261
BMI, kg/m ²	30.53 \pm 4.84	29.79 \pm 3.97	0.335
Fasting glucose, mg/dl	112.68 \pm 27.31	114.32 \pm 19.32	0.676
Systolic blood pressure, mmHg	130.03 \pm 19.79	130.83 \pm 16.38	0.819
Triglyceride, mg/dl ^a	136.5 [99.5 - 186]	129 [93.5 - 182.75]	0.784
Total cholesterol, mg/dl	215 \pm 38.05	211 \pm 33.11	0.481
HDL cholesterol, mg/dl	51.81 \pm 11.59	51.66 \pm 14.29	0.951
eGFR, mL/min/1.73 m ²	80.17 \pm 14.79	81.95 \pm 10.92	0.339
UACR, mg/g ^a	8.89 [4.44 - 13.41]	6.8 [4.85 - 14.36]	0.842
Smoking, %			
Non-smoker	43.55	41.94	Reference
Former smoker	50	53.23	0.704
Current smoke	6.45	4.84	0.729
Medication usage, %			
Lipid-lowering	19.35	25.81	0.396
Antihypertensive	62.9	61.29	0.842
Anti-diabetic	14.52	16.13	0.796

^a values are presented as median [25th- 75th percentile].

Table S4. Results of sensitivity analyses - the two metabolites significantly associated with incident chronic kidney disease in the propensity scores matched case-control hyperglycemic individuals

Odds ratios (*ORs*) per standard deviation (*SD*) with 95% *CI* and *P*-values of conditional logistic regression results are shown. *P*-values shown in bold represent statistical significance at 0.05 level. **Abbreviations:** SM, sphingomyelin; PC aa, phosphatidylcholine diacyl.

	SM C18:1	PC aa C38:0
<i>OR</i> (95% <i>CI</i>), per <i>SD</i>	1.77 (1.14 - 2.73)	1.71 (1.12 - 2.62)
<i>P</i> -value	0.011	0.014

Table S5. Results of sensitivity analyses - interaction effects of the two metabolites with different glucose subgroups

Odds ratios (ORs) with 95% CI and *P*-values of multivariate logistic regression results are shown. $P_{\text{interaction}}$ represents *P*-value of multiplicative interaction effects between metabolite and different glucose groups. *P*-values shown in bold represent statistical significance at 0.05 level. **Abbreviations:** SM, sphingomyelin; PC aa, phosphatidylcholine diacyl; NGT, normal glucose tolerance; 2-h glucose, two hour post load glucose.

Group	SM C18:1			PC aa C38:0		
	OR (95% CI)	<i>P</i> - values	$P_{\text{interaction}}$	OR (95% CI)	<i>P</i> - values	$P_{\text{interaction}}$
Glycemic status			1.774E-03^c			0.417 ^c
NGT ^a	0.76 (0.57 - 1.01)	0.057		1.21 (0.95 - 1.55)	0.124	
Hyperglycemia ^b	2.22 (1.46 - 3.49)	3.315E-04		1.56 (1.12 - 2.21)	0.010	
Fasting glucose			0.241 ^d			0.609 ^d
1st tertile ^a	0.78 (0.46 - 1.36)	0.372		1.13 (0.73 - 1.77)	0.579	
2nd tertile ^a	0.84 (0.56 - 1.27)	0.412		1.33 (0.94 - 1.88)	0.106	
Top tertile ^b	1.50 (1.08 - 2.11)	0.019		1.49 (1.10 - 2.03)	0.010	
2-h glucose			0.010^e			0.538 ^e
1st tertile ^a	0.55 (0.33 - 0.92)	0.023		1.22 (0.79 - 1.87)	0.369	
2nd tertile ^a	0.74 (0.48 - 1.14)	0.172		1.27 (0.87 - 1.88)	0.231	
Top tertile ^b	1.58 (1.07 - 2.37)	0.022		1.60 (1.17 - 2.23)	0.004	

^a with adjustments for age, sex, BMI, systolic blood pressure, smoking status, triglyceride, total cholesterol, HDL cholesterol, fasting glucose, use of lipid lowering drugs, antihypertensive medication, baseline estimated glomerular filtration rate and baseline urinary albumin-to-creatinine ratio.

^b with adjustment for the covariates shown in ^a as well as use of anti-diabetic medication.

^c The model setting : $\text{logit}(P) = \beta_0 + \beta_1 * \text{metabolite} + \beta_2 * \text{glycemic status} + \beta_3 * \text{metabolite} * \text{glycemic status} + \beta_4 * \text{covariates} + \epsilon$. The covariates including the covariates shown in ^a as well as use of anti-diabetic medication.

^d The model setting : $\text{logit}(P) = \beta_0 + \beta_1 * \text{metabolite} + \beta_2 * \text{three tertiles group of fasting glucose} + \beta_3 * \text{metabolite} * \text{three tertiles group of fasting glucose} + \beta_4 * \text{covariates} + \epsilon$. The covariates included the covariates shown in ^a as well as use of anti-diabetic medication except fasting glucose.

^e The model setting : $\text{logit}(P) = \beta_0 + \beta_1 * \text{metabolite} + \beta_2 * \text{three tertiles group of 2-h glucose} + \beta_3 * \text{metabolite} * \text{three tertiles group of 2-h glucose} + \beta_4 * \text{covariates} + \epsilon$. The covariates included the covariates shown in ^a except fasting glucose.

Table S6. Results of sensitivity analyses - association of two candidate biomarkers with UACR- and eGFR- based incident CKD in hyperglycemic participants

Odds ratios (*ORs*) with 95% *CI* and *P*-values of each metabolite with UACR-based and eGFR-based incident CKD in basic and full multivariable logistic regression models are shown, respectively. UACR-based incident CKD was defined as UACR \geq 30 mg/g at follow-up (FF4). eGFR-based incident CKD was defined as eGFR $<$ 60 ml/min/1.73 m² at follow-up (FF4). Basic model was adjusted for age, sex, BMI, systolic blood pressure, smoking status, triglyceride, total cholesterol, HDL cholesterol and fasting glucose. Full model was additionally adjusted for use of lipid lowering drugs, antihypertensive and anti-diabetic medication, baseline eGFR and UACR. *P*-values shown in bold represent statistical significance at 0.05 level. **Abbreviations:** CKD, chronic kidney disease; eGFR, estimated glomerular filtration rate; UACR, urinary albumin-to-creatinine ratio; SM, sphingomyelin; PC aa, phosphatidylcholine diacyl.

	SM C18:1		PC aa C38:0	
	Basic model	Full model	Basic model	Full model
UACR- based incident CKD (N = 32) & non-CKD (N = 353)				
<i>P</i> -value	0.024	0.040	0.022	0.004
<i>OR</i> (95 % <i>CI</i>), per SD	1.79 (1.10 - 3.03)	1.80 (1.05 - 3.25)	1.66 (1.08 - 2.58)	2.17 (1.31 - 3.76)
eGFR- based incident CKD (N = 65) & non-CKD (N = 320)				
<i>P</i> -value	0.008	0.107	0.061	0.247
<i>OR</i> (95 % <i>CI</i>), per SD	1.77 (1.17 - 2.75)	1.50 (0.93 - 2.5)	1.38 (0.99 - 1.94)	1.25 (0.86 - 1.85)

Table S7. Comparison of the predictive performances of two sets of predictors of incident chronic kidney disease in hyperglycemic individuals with three machine learning approaches

The median AUC (95% *CI*) of three machine learning approaches over 100 random repeats of 10-fold cross validation are shown. Reference predictors consists of baseline age, sex, estimated glomerular filtration rate and urinary albumin-to-creatinine ratio. Developed sets includes combined metabolites and clinical variables that were selected by the three-step feature selection in each round. **Abbreviation:** AUC, area under the receiver operating characteristic curve.

Algorithms	Models	Median AUC (95% <i>CI</i>)	Absolute increase in median prediction	Outperform times over 100 times
Support Vector Machine	Reference predictors	0.800 (0.783 - 0.816)	2.5%	97
	Developed sets	0.825 (0.801 - 0.849)		
Random Forest	Reference predictors	0.789 (0.771 - 0.807)	2.9%	100
	Developed sets	0.818 (0.794 - 0.836)		
Adaptive Boosting	Reference predictors	0.798 (0.781 - 0.813)	1.6%	87
	Developed sets	0.814 (0.787 - 0.832)		

Table S8. The total selected times for three most frequently selected sets of metabolites and clinical variables over 1000 selection rounds in 100 times of 10-fold cross validation

The three most frequently selected sets of metabolites and clinical variables, as well as their total selected times over 1000 selection rounds are shown. **Abbreviations:** eGFR, estimated glomerular filtration rate; UACR, urinary albumin-to-creatinine ratio; SM, sphingomyelin; PC aa, phosphatidylcholine diacyl.

Sets of metabolites and clinical variables	Selected times
SM C18:1, PC aa C38:0, age, total cholesterol, fasting glucose, eGFR, UACR	113
SM C18:1, age, total cholesterol, fasting glucose, eGFR, UACR	78
SM C18:1, PC aa C38:0, proline, age, total cholesterol, fasting glucose, eGFR, UACR	67

Table S9. The selected times for 15 most important variables over 1000 selection rounds in 100 times of 10-fold cross validation

Out of 125 metabolites and 14 clinical variables, 15 most frequently selected variables and their total selected times over 1000 selection rounds are shown. **Abbreviations:** UACR, urinary albumin-to-creatinine ratio; eGFR, estimated glomerular filtration rate; SM, sphingomyelin; PC aa, phosphatidylcholine diacyl.

Variables	Selected times
UACR	1000
eGFR	1000
Age	999
Total cholesterol	996
Fasting glucose	942
SM C18:1	857
PC aa C38:0	593
Triglyceride	270
Proline	229
PC aa C32:2	156
Tyrosine	129
SM C26:1	109
C18:1	108
PC aa C36:4	92
Use of lipid lowering drugs	81

Table S10. Predictive performance of the best set of predictors and the full model of incident CKD in hyperglycemia

Mean AUC values of the best set of predictors and the full model of incident CKD in hyperglycemia are shown. The mean AUC value of the best set of predictors was the average value of the AUC values of the 113 selected times, in which the models were fitted with support vector machine. The average AUC value of the full model was obtained using logistic regression with 10 times of 10-fold cross validation. **Abbreviations:** CKD, chronic kidney disease; AUC, area under the receiver operating characteristic curve; UACR, urinary albumin-to-creatinine ratio; eGFR, estimated glomerular filtration rate; SM, sphingomyelin; PC aa, phosphatidylcholine diacyl.

Models	Mean AUC	Absolute increase in mean prediction
The best set of predictors (i.e., SM C18:1, PC aa C38: 0, age, total cholesterol, fasting glucose, eGFR and UACR)	0.857	
The full model (i.e., age, sex, BMI, systolic blood pressure, smoking status, triglyceride, total cholesterol, HDL cholesterol, fasting glucose, use of lipid lowering drugs, antihypertensive and anti-diabetic medication, eGFR and UACR)	0.809	4.8%

Supplementary Figures

Figure S1. Technical normalization across the study

Comparison of before and after normalization of plate effect of metabolite data using phosphatidylcholine diacyl (PC aa) C34:2 as an example. Metabolite concentration drifts at 38 plates were independently corrected by conducting plate effect normalization in quality controls samples (QCs, shown in plots A and B) and KORA F4 individual samples (plots C and D).

Fig. S1

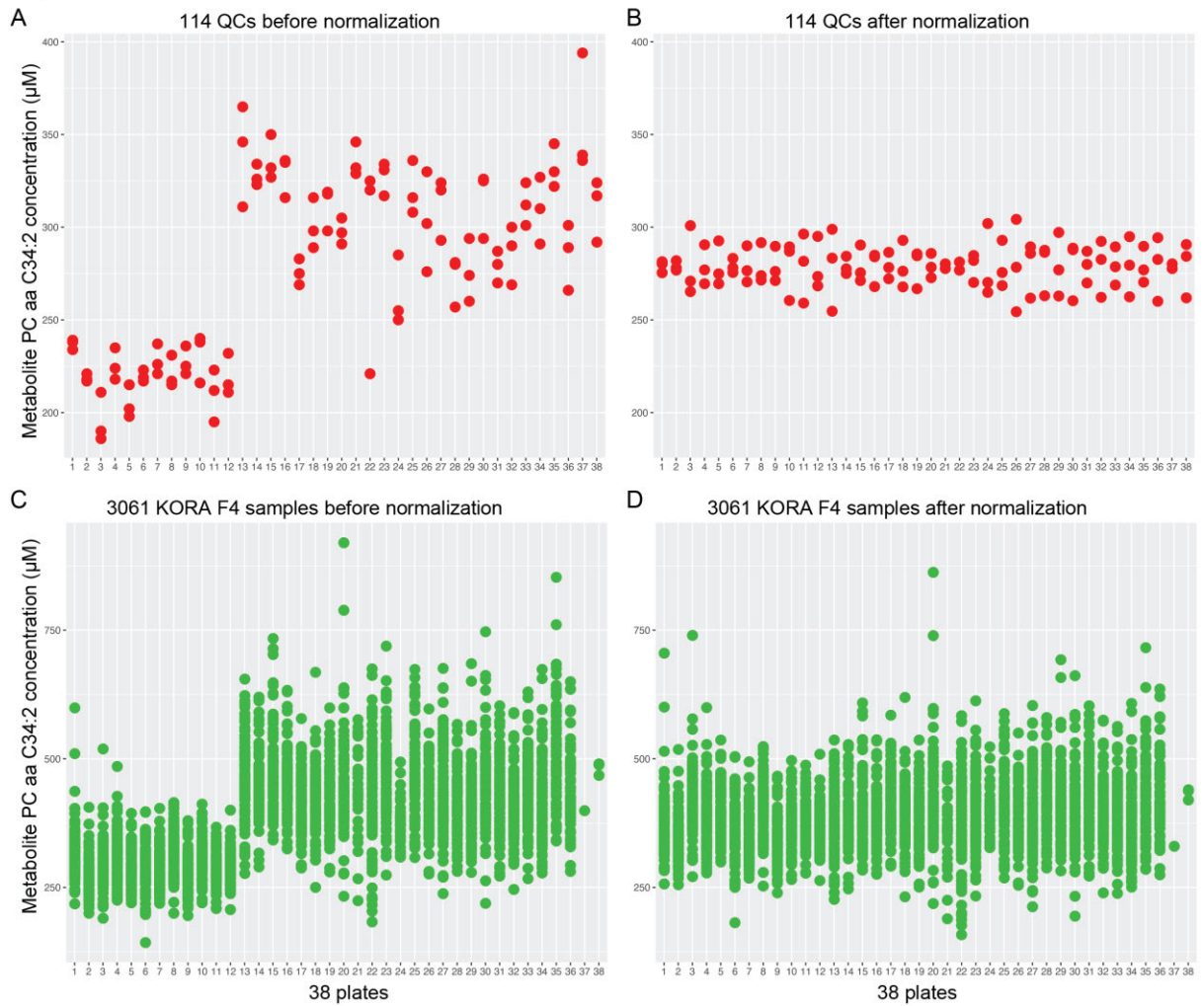
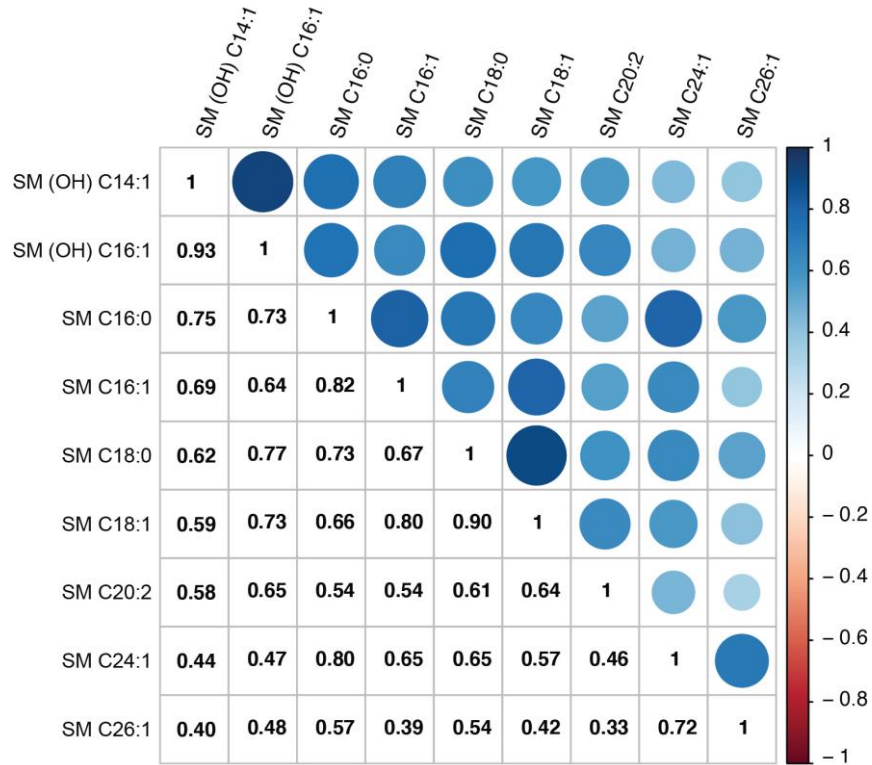


Figure S2. Correlation of nine sphingomyelins in 385 hyperglycemic participants

Pearson's correlation coefficients values of nine sphingomyelins (SMs) in 385 participants with pre-diabetes and T2D are shown. Both the size of the circle and intensity of color indicate the degree of correlation between the metabolites. The numeric values of Pearson's correlation coefficients are shown in the bottom triangle.

Fig. S2



Paper II

Title: Validation of Candidate Phospholipid Biomarkers of Chronic Kidney Disease in Hyperglycemic Individuals and Their Organ-Specific Exploration in Leptin Receptor-Deficient db/db Mouse

Authors: Jialing Huang, Marcela Covic, Cornelia Huth, Martina Rommel, Jonathan Adam, Sven Zukunft, Cornelia Prehn, Li Wang, Jana Nano, Markus F. Scheerer, Susanne Neschen, Gabi Kastenmüller, Christian Gieger, Michael Laxy, Freimut Schliess, Jerzy Adamski, Karsten Suhre, Martin Hrabe de Angelis, Annette Peters, Rui Wang-Sattler

Journal: Metabolites

Status: Published

Volume: 11


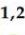
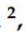
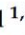
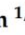


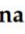

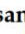


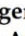
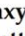
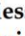
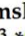


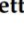
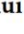
Page: 89

Year: 2021

doi: 10.3390/metabo1102008

Article

Validation of Candidate Phospholipid Biomarkers of Chronic Kidney Disease in Hyperglycemic Individuals and Their Organ-Specific Exploration in Leptin Receptor-Deficient db/db Mouse

Jialing Huang ^{1,2,3} , Marcela Covic ^{1,2,3} , Cornelia Huth ² , Martina Rommel ^{1,2} , Jonathan Adam ^{1,2} , Sven Zukunft ^{4,5} , Cornelia Prehn ⁶ , Li Wang ^{1,2,7} , Jana Nano ^{2,3} , Markus F. Scheerer ^{8,9} , Susanne Neschen ^{8,10} , Gabi Kastenmüller ¹¹ , Christian Gieger ^{1,2,3} , Michael Laxy ¹² , Freimut Schliess ¹³ , Jerzy Adamski ^{4,14,15} , Karsten Suhre ¹⁶ , Martin Hrabe de Angelis ^{3,8,15} , Annette Peters ^{2,3}  and Rui Wang-Sattler ^{1,2,3,*} 



Citation: Huang, J.; Covic, M.; Huth, C.; Rommel, M.; Adam, J.; Zukunft, S.; Prehn, C.; Wang, L.; Nano, J.; Scheerer, M.F.; et al. Validation of Candidate Phospholipid Biomarkers of Chronic Kidney Disease in Hyperglycemic Individuals and Their Organ-Specific Exploration in Leptin Receptor-Deficient db/db Mouse. *Metabolites* **2021**, *11*, 89. <https://doi.org/10.3390/metabo11020089>

Academic Editor: Vladimir V. Tolstikov

Received: 15 December 2020

Accepted: 29 January 2021

Published: 3 February 2021

Publisher's Note: MDPI stays neutral with regard to jurisdictional claims in published maps and institutional affiliations.



Copyright: © 2021 by the authors. Licensee MDPI, Basel, Switzerland. This article is an open access article distributed under the terms and conditions of the Creative Commons Attribution (CC BY) license (<https://creativecommons.org/licenses/by/4.0/>).

- ¹ Research Unit of Molecular Epidemiology, Helmholtz Zentrum München, 85764 Neuherberg, Germany; jialing.huang@helmholtz-muenchen.de (J.H.); marcela.covic@helmholtz-muenchen.de (M.C.); martina.troll@helmholtz-muenchen.de (M.R.); jonathan.adam@helmholtz-muenchen.de (J.A.); wlrst@126.com (L.W.); christian.gieger@helmholtz-muenchen.de (C.G.)
- ² Institute of Epidemiology, Helmholtz Zentrum München, 85764 Neuherberg, Germany; cod.huth@gmail.com (C.H.); jana.nano@helmholtz-muenchen.de (J.N.); peters@helmholtz-muenchen.de (A.P.)
- ³ German Center for Diabetes Research (DZD), 85764 München-Neuherberg, Germany; hrabe@helmholtz-muenchen.de
- ⁴ Research Unit of Molecular Endocrinology and Metabolism, Helmholtz Zentrum München, 85764 Neuherberg, Germany; zukunft@vrc.uni-frankfurt.de (S.Z.); adamski@helmholtz-muenchen.de (J.A.)
- ⁵ Centre for Molecular Medicine, Institute for Vascular Signaling, Goethe University, 60323 Frankfurt am Main, Germany
- ⁶ Metabolomics and Proteomics Core Facility, Helmholtz Zentrum München, 85764 Neuherberg, Germany; prehn@helmholtz-muenchen.de
- ⁷ Liaocheng People's Hospital—Department of Scientific Research, Shandong University Postdoctoral Work Station, Liaocheng 252000, China
- ⁸ Institute of Experimental Genetics, Helmholtz Zentrum München, 85764 Neuherberg, Germany; markus@scheerer-home.de (M.F.S.); susanne.neschen@mail.com (S.N.)
- ⁹ Bayer AG, Medical Affairs & Pharmacovigilance, 13353 Berlin, Germany
- ¹⁰ Sanofi Aventis Deutschland GmbH, Industriepark Hoechst, 65929 Frankfurt am Main, Germany
- ¹¹ Institute of Computational Biology, Helmholtz Zentrum München, 85764 Neuherberg, Germany; g.kastenmueller@helmholtz-muenchen.de
- ¹² Institute of Health Economics and Health Care Management, Helmholtz Zentrum München, 85764 Neuherberg, Germany; michael.laxy@helmholtz-muenchen.de
- ¹³ Profil, 41460 Neuss, Germany; Freimut.Schliess@profil.com
- ¹⁴ Department of Biochemistry, Yong Loo Lin School of Medicine, National University of Singapore, Singapore 117597, Singapore
- ¹⁵ Chair of Experimental Genetics, Center of Life and Food Sciences Weihenstephan, Technische Universität München, 85353 Freising, Germany
- ¹⁶ Department of Physiology and Biophysics, Weill Cornell Medical College in Qatar (WCMC-Q), Education City, Qatar Foundation, Doha P.O. Box 24144, Qatar; karsten@suhre.fr
- * Correspondence: rui.wang-sattler@helmholtz-muenchen.de; Tel.: +49-89-3187-3978; Fax: +49-89-3187-2428

Abstract: Biological exploration of early biomarkers for chronic kidney disease (CKD) in (pre)diabetic individuals is crucial for personalized management of diabetes. Here, we evaluated two candidate biomarkers of incident CKD (sphingomyelin (SM) C18:1 and phosphatidylcholine diacyl (PC aa) C38:0) concerning kidney function in hyperglycemic participants of the Cooperative Health Research in the Region of Augsburg (KORA) cohort, and in two biofluids and six organs of leptin receptor-deficient (db/db) mice and wild type controls. Higher serum concentrations of SM C18:1 and PC aa C38:0 in hyperglycemic individuals were found to be associated with lower estimated glomerular filtration rate (eGFR) and higher odds of CKD. In db/db mice, both metabolites had a significantly lower concentration in urine and adipose tissue, but higher in the lungs. Additionally, db/db mice had significantly higher SM C18:1 levels in plasma and liver, and PC aa C38:0 in adrenal glands.

This cross-sectional human study confirms that SM C18:1 and PC aa C38:0 associate with kidney dysfunction in pre(diabetic) individuals, and the animal study suggests a potential implication of liver, lungs, adrenal glands, and visceral fat in their systemic regulation. Our results support further validation of the two phospholipids as early biomarkers of renal disease in patients with (pre)diabetes.

Keywords: chronic kidney disease; prediabetes and type 2 diabetes; diabetic nephropathy; reduced kidney function; leptin receptor-deficient mouse; high-fat-diet; liver; lungs; metabolomics

1. Introduction

Diabetic nephropathy is the leading cause of chronic kidney disease (CKD) and end-stage kidney disease [1]. Early screening of persons with prediabetes or type 2 diabetes (T2D) for CKD predisposition can increase the opportunity to effectively prevent and manage this microvascular complication of diabetes in the framework of more personalized diabetes management [2]. However, targeted screening is important to assure the efficient allocation of health care resources [3].

Traditional markers for CKD are unable to accurately predict the development of CKD in individuals with T2D. Urinary albumin-to-creatinine ratio (UACR) and estimated glomerular filtration rate (eGFR) were found to be the most important variables to predict the onset and progression of early CKD in individuals with T2D in a large randomized clinical trial with a follow-up period of 5.5 years. However, even when combined with age and sex (i.e., a set of four clinical variables: age, sex, eGFR, and UACR), their predictive ability was found to be modest with an externally validated c-statistic of 0.68 [4].

Metabolomics is still a relatively new approach for studying metabolic changes connected to disease development and progression, as well as for finding predictive biomarkers to enable early interventions [5–8]. Using baseline metabolite profiles of a population-based Cooperative Health Research in the Region of Augsburg (KORA) cohort, we have recently discovered two candidate metabolite biomarkers (sphingomyelin (SM) C18:1 and phosphatidylcholine diacyl (PC aa) C38:0) for incident CKD that were specific for hyperglycemic individuals with prediabetes or T2D [9]. SM C18:1 and PC aa C38:0 were identified from 125 targeted metabolites through three-step feature selection that included multivariate logistic regression adjustment, priority-lasso filtering and stepwise Akaike information criterion selection. These two metabolites were in combination with five clinical variables (age, total cholesterol, fasting glucose, eGFR, and UACR) identified as the best set of predictors for incident CKD. Their predictive performance yielded a mean area value under the receiver operating characteristic curve of 0.857 and outperformed the performance of 14 known risk factors of CKD [9]. However, physiological mechanisms leading to circulatory accumulation of these new candidate biomarkers during the pathogenesis of diabetes-related CKD have not yet been delineated.

Altered serum levels of phospholipids in hyperglycemic individuals under higher risk of developing CKD [9] might indicate early alterations not only in the kidneys [10] but also other organ systems [11]. Insufficient elimination of a large number of potentially toxic organic metabolites from the vascular bed into the urine during CKD affects multiple body systems and organs [12]. Biological exploration of the emerging biomarkers is necessary towards a better understanding of the complex metabolic interactions between the circulatory, musculoskeletal and respiratory systems in CKD and their potential clinical application in diagnostics [12]. Moreover, animal models reflecting the pathogenetic evolution of diabetes-related CKD allow for direct analysis of organ-specific metabolite patterns during aggravation of the disease. The leptin-receptor deficient mouse model (db/db) was shown to exhibit a very consistent and robust increase in albuminuria and mesangial matrix expansion. It is therefore a well-established model for human diabetic nephropathy [13,14].

In this study, we evaluated the associations of SM C18:1 and PC aa C38:0 with eGFR values and risk of CKD with the recently generated targeted metabolites profiles of KORA FF4 study in participants with hyperglycemia. Furthermore, we examined creatinine, SM C18:1, and PC aa C38:0 levels in two biofluids (plasma, urine) and six tissues (liver, lungs, adrenal glands, adipose tissue, cerebellum, and testis) of db/db and wild type (WT) mice under high-fat diet (HFD) to explore organ-specific variations and discuss the potential link to various clinical symptoms. Our findings provide first insights into the potential involvement of several organs in the systemic accumulation of these metabolite biomarkers during CKD pathogenesis.

2. Results

2.1. Associations of the Two Metabolites with eGFR and CKD in Hyperglycemic Individuals

2.1.1. Characteristics of the KORA FF4 Study Participants

Among 1907 eligible KORA FF4 participants, 168 individuals had CKD (8.8%). As expected, hyperglycemic participants were diagnosed more frequently to have CKD (16.3%) than individuals with normal glucose tolerance (NGT) (6.1%) (Table 1). The cases of CKD in hyperglycemic and NGT groups were significantly older and had significantly higher values of creatinine and UACR than non-CKD individuals in each group. The self-reported intake of antihypertensive and lipid-lowering medication was also significantly higher in cases of CKD. Compared to non-CKD individuals, the cases of CKD in the NGT group had also significantly higher values of BMI, triglycerides, glycated hemoglobin (HbA_{1C}), fasting glucose, and 2-h post-load glucose (2-h glucose) (Table 1).

2.1.2. Inverse Associations of the Two Metabolites with eGFR in Hyperglycemic Individuals

The inverse association between eGFR and the concentrations of SM C18:1 and PC aa C38:0 in hyperglycemic individuals was significant in all three weighted regression models (adjusted for imbalanced, basic and full model covariates) after applying inverse probability weighting (IPW). For example, a SD increase in the ln-transformed SM C18:1 concentration was associated with a 1.76 mL/min/1.73 m² decrease in eGFR in the full model ($p = 2.499 \times 10^{-3}$; Table 2).

2.1.3. Associations of the Two Metabolites with CKD Are Specific for Hyperglycemia

The CKD cases with hyperglycemia had higher relative concentrations of the two metabolites (SM C18:1, PC aa C38:0) than non-CKD individuals (Figure 1). The concentrations of SM C18:1 and PC aa C38:0 were significantly positively associated with CKD in hyperglycemic individuals in all three models after IPW (Table 3). One SD increase in the ln-transformed SM C18:1 or PC aa C38:0 concentration was associated with a 99% or 71%, respectively, increased odds of CKD in hyperglycemic participants (full model $p = 4.482 \times 10^{-4}$ and 1.578×10^{-3} , respectively, Table 3).

As a sensitivity analysis, we tested the associations of the two metabolites with CKD in normoglycemic KORA participants. Both SM C18:1 and PC aa C38:0 were not significantly associated with CKD in NGT individuals in all three models after IPW (Table 3). As shown in Figure 1, normoglycemic individuals with diagnosed CKD did not show any significant differences in their relative metabolite concentration when compared to healthy NGTs. These results further confirmed that the risk associations of the two lipids are specific for hyperglycemia.

Table 1. Characteristics of the KORA FF4 participants according to their hyperglycemic status. Mean \pm standard deviation is provided for quantitative variables if not indicated otherwise. *p*-values express the difference between CKD cases and non-CKD controls in hyperglycemic and NGT participants, respectively. *p*-values were calculated by univariate logistic regression if not indicated otherwise. *p*-values shown in bold represent statistical significance at the 0.05 level. Abbreviations: CKD, chronic kidney disease; HbA_{1C}, glycated hemoglobin; HDL, high-density lipoprotein; LDL, low-density lipoprotein; NGT, normal glucose tolerance; 2-h glucose, 2-h post-load glucose; BP, blood pressure; eGFR, estimated glomerular filtration rate; UACR, urinary albumin-to-creatinine ratio.

Clinical Variables	Hyperglycemic Participants			NGT Participants		
	CKD <i>n</i> = 83	Non-CKD <i>n</i> = 427	<i>p</i> -Value	CKD <i>n</i> = 85	Non-CKD <i>n</i> = 1312	<i>p</i> -Value
Age, years	74.36 \pm 7.66	64.32 \pm 10.53	1.003 $\times 10^{-12}$	72.05 \pm 8.23	55.47 \pm 10.53	3.255 $\times 10^{-27}$
Sex, male, %	49.4	57.61	1.686 $\times 10^{-1}$	48.24	43.9	4.361 $\times 10^{-1}$
BMI, kg/m ²	29.25 \pm 4.3	30.16 \pm 5.02	1.228 $\times 10^{-1}$	28.11 \pm 4.94	26.52 \pm 4.37	1.415 $\times 10^{-3}$
HbA _{1C} (%)	5.74 \pm 0.42	5.73 \pm 0.54	7.552 $\times 10^{-1}$	5.56 \pm 0.32	5.3 \pm 0.32	7.958 $\times 10^{-12}$
Fasting glucose, mg/dL	112.55 \pm 20.44	111.3 \pm 16.37 ^b	6.440 $\times 10^{-1}$	96.79 \pm 7.68	94.02 \pm 7.3	1.130 $\times 10^{-3}$
2-h glucose, mg/dL	164.43 \pm 38.98 ^b	160.63 \pm 46.66 ^b	3.724 $\times 10^{-1}$	103.16 \pm 21.18	95.89 \pm 19.9	3.232 $\times 10^{-3}$
Systolic BP, mmHg	120.31 \pm 22.27	124.78 \pm 18.03	4.847 $\times 10^{-2}$	116.65 \pm 18.23	115.85 \pm 16.06	6.617 $\times 10^{-1}$
Diastolic BP, mmHg	68.27 \pm 11.15	74.93 \pm 10.55	5.054 $\times 10^{-7}$	69.41 \pm 10.14	73.06 \pm 8.95	3.048 $\times 10^{-4}$
Triglyceride, mg/dL ^a	121.11 (93.44–157.4)	128 (92.98–178.27)	9.711 $\times 10^{-1}$	109 (78–143.79)	93 (70–127.46)	1.492 $\times 10^{-2}$
Total cholesterol, mg/dL	208.58 \pm 41.45	220.93 \pm 42.16	1.533 $\times 10^{-2}$	211.48 \pm 43.58	218.59 \pm 37.7	9.597 $\times 10^{-2}$
HDL cholesterol, mg/dL	61.12 \pm 18.42	59.78 \pm 17.54	5.303 $\times 10^{-1}$	65.63 \pm 18.42	68.57 \pm 18.75	1.612 $\times 10^{-1}$
LDL cholesterol, mg/dL	126.3 \pm 35.49	140.65 \pm 37.2	1.456 $\times 10^{-3}$	130.94 \pm 37.34	135.83 \pm 34.05	2.025 $\times 10^{-1}$
Creatinine, mg/dL	1.24 \pm 0.21	0.89 \pm 0.15	3.916 $\times 10^{-21}$	1.25 \pm 0.28	0.86 \pm 0.16	6.345 $\times 10^{-31}$
eGFR, mL/min/1.73 m ²	50.5 \pm 7.87	81.33 \pm 11.9	3.645 $\times 10^{-47}$ ^c	50.97 \pm 8.01	86.92 \pm 12.69	5.563 $\times 10^{-54}$ ^c
UACR, mg/g ^a	9.76 (5.73–26.07)	5.43 (3.39–9.86)	1.180 $\times 10^{-7}$	7.33 (4.44–15.38)	4.26 (2.94–7.07)	1.604 $\times 10^{-8}$
Smoking, %			7.394 $\times 10^{-3}$			8.080 $\times 10^{-5}$
Nonsmoker	55.42	43.79	Ref.	40	41.54	Ref.
Former smoker	40.96	42.39	2.789 $\times 10^{-1}$	56.47	40.4	1.086 $\times 10^{-1}$
Current smoker	3.61	13.82	1.028 $\times 10^{-2}$	3.53	18.06	8.628 $\times 10^{-3}$
Medication usage, %						
Lipid-lowering	34.94	22.48	1.684 $\times 10^{-2}$	32.94	7.7	2.377 $\times 10^{-12}$
Antihypertensive	84.34	47.07	1.367 $\times 10^{-8}$	69.41	19.97	2.272 $\times 10^{-19}$

^a Values are presented as median (25th–75th percentile); ^b In the hyperglycemic participants, 2-h glucose values were only available in 68 individuals with CKD and 398 individuals without CKD; one non-CKD individual had no fasting glucose values; ^c *p*-values calculated with Mann–Whitney *U* test.

Table 2. Associations of the two candidate metabolites with eGFR in hyperglycemic individuals. Regression coefficients with 95% CI and *p*-values of weighted multivariable linear regression after inverse probability weighting are shown. The basic model was adjusted for age, sex, BMI, systolic blood pressure, triglyceride, total cholesterol, HDL cholesterol, and HbA_{1C}. The full model was additionally adjusted for smoking status, use of lipid-lowering drugs, and antihypertensive medication, and urinary albumin-to-creatinine ratio. *p*-values shown in bold represent statistical significance at the 0.05 level. Abbreviations: CI, confidence interval; eGFR, estimated glomerular filtration rate; SM, sphingomyelin; PC aa, phosphatidylcholine diacyl.

Models	SM C18:1		PC aa C38:0	
	Effect Estimate (95% CI)	<i>p</i> -Value	Effect Estimate (95% CI)	<i>p</i> -Value
Adjusted imbalanced covariates	−1.51 (−2.92 to −0.1) ^a	3.624 $\times 10^{-2}$	−1.82 (−3.04 to −0.59) ^b	3.757 $\times 10^{-3}$
Basic model	−1.83 (−2.98 to −0.68)	1.879 $\times 10^{-3}$	−1.91 (−3.11 to −0.72)	1.784 $\times 10^{-3}$
Full model	−1.76 (−2.9 to −0.62)	2.499 $\times 10^{-3}$	−1.81 (−2.99 to −0.63)	2.607 $\times 10^{-3}$

^a with adjustments for sex, systolic blood pressure, total cholesterol, smoking status, and use of antihypertensive medication; ^b with adjustments for age, HDL cholesterol, and smoking status.

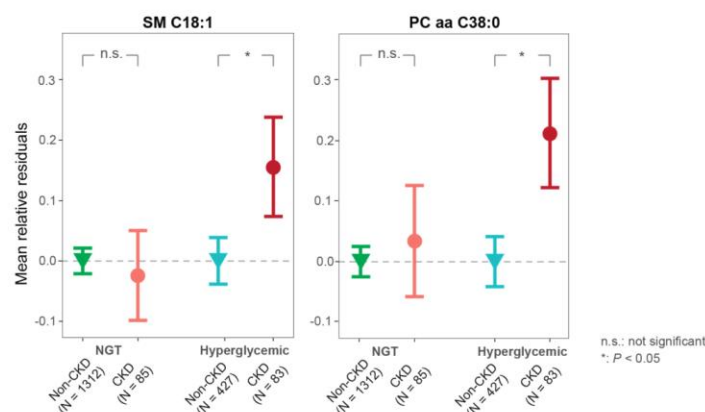


Figure 1. Stratified associations of the two candidate metabolites with CKD according to hyperglycemic and normoglycemic status. Mean relative residuals (with standard errors) of SM C18:1 and PC aa C38:0 for non-CKD and CKD in hyperglycemic and NGT individuals are shown, respectively. Metabolite relative residuals were calculated with linear regression models adjusted for age, sex, BMI, systolic blood pressure, triglyceride, total cholesterol, HDL cholesterol, HbA_{1C}, smoking status, the use of lipid-lowering, antihypertensive medication, and urinary albumin-to-creatinine ratio. *p* values were calculated with multivariable logistic regression using CKD as outcome and adjusting covariates mentioned above. Abbreviations: CKD, chronic kidney disease; SM, sphingomyelin; PC aa, phosphatidylcholine diacyl; NGT, normal glucose tolerance.

Table 3. Associations of the two candidate metabolites with CKD in hyperglycemic and NGT individuals. Odds ratios (ORs) with 95% CI and *p*-values of weighted multivariable logistic regression after inverse probability weighting are shown. The basic model was adjusted for age, sex, BMI, systolic blood pressure, triglyceride, total cholesterol, HDL cholesterol, and HbA_{1C}. The full model was additionally adjusted for smoking status, use of lipid-lowering drugs, and antihypertensive medication, and urinary albumin-to-creatinine ratio. *p*-values shown in bold represent statistical significance at the 0.05 level. Abbreviations: CI, confidence interval; CKD, chronic kidney disease; SM, sphingomyelin; PC aa, phosphatidylcholine diacyl; NGT, normal glucose tolerance.

Metabolites	Models	NGT Participants		Hyperglycemic Participants	
		OR (95% CI)	<i>p</i> -Value	OR (95% CI)	<i>p</i> -Value
SM C18:1	Adjusted imbalance covariates	0.96 (0.77–1.21) ^a	7.233×10^{-1}	1.46 (1.09–1.97) ^b	1.169×10^{-2}
	Basic model	1.05 (0.82–1.35)	6.986×10^{-1}	1.93 (1.38–2.78)	2.251×10^{-4}
	Full model	1.14 (0.86–1.51)	3.733×10^{-1}	1.99 (1.37–2.96)	4.482×10^{-4}
PC aa C38:0	Adjusted imbalance covariates	0.98 (0.78–1.23) ^c	8.438×10^{-1}	1.61 (1.2–2.17) ^d	1.487×10^{-3}
	Basic model	1.12 (0.87–1.46)	3.752×10^{-1}	1.68 (1.24–2.29)	8.723×10^{-4}
	Full model	1.19 (0.91–1.58)	2.142×10^{-1}	1.71 (1.23–2.41)	1.578×10^{-3}

^a with adjustments for BMI, systolic blood pressure, smoking status, and urinary albumin-to-creatinine ratio;

^b with adjustments for sex, systolic blood pressure, total cholesterol, smoking status, and use of antihypertensive medication; ^c no additional adjustment; ^d with adjustments for age, HDL cholesterol, and smoking status.

2.2. Organ-Specific Trends of the Candidate Biomarkers in Diabetic Mice

2.2.1. Characteristics of the Mouse Model

Organ trends of the two phospholipids were explored in the db/db mouse model that mimics the early human CKD development. After 5 weeks of HFD, the 8-week-old db/db mice were obese and had significantly higher heart, kidney and liver weight when compared with WT controls of the same age and diet (Table 4). Furthermore, their blood levels of glucose, insulin, cholesterol, and C-reactive protein were significantly higher confirming that db/db mice developed hyperglycemia, dyslipidemia and inflammation.

Table 4. Phenotypic and metabolic variables in db/db and wild type mice after 5 weeks of a high-fat diet. Values are mean \pm SD. *p*-values were calculated by Mann–Whitney *U* test. *p*-values shown in bold represent statistical significance at the 0.05 level. Abbreviations: db/db, leptin receptor-deficient mouse model; HDL, high-density lipoprotein; LDL, low-density lipoprotein.

Clinical Variables	db/db Mice <i>n</i> = 10	Wild Type Mice <i>n</i> = 10	<i>p</i> -Value
Body weight, g	47.87 \pm 2.37	21.97 \pm 0.58	1.796 $\times 10^{-4}$
Kidney weight, g	0.20 \pm 0.02	0.16 \pm 0.02	2.057 $\times 10^{-4}$
Liver weight, g	2.56 \pm 0.3	1.02 \pm 0.09	1.083 $\times 10^{-5}$
Heart weight, g	0.14 \pm 0.01	0.12 \pm 0.01	4.871 $\times 10^{-4}$
Blood glucose, mg/dL	421.60 \pm 41.24	106.7 \pm 16.88	1.806 $\times 10^{-4}$
Plasma insulin, μ g/L	7.76 \pm 2.33	1.03 \pm 0.4	1.083 $\times 10^{-5}$
Triglyceride, mg/dL	224.78 \pm 106.51	122.24 \pm 24.52	5.869 $\times 10^{-2}$
Total cholesterol, mg/dL	153.24 \pm 16.14	100.58 \pm 12.16	1.817 $\times 10^{-4}$
HDL cholesterol, mg/dL	125.28 \pm 13.12	84.28 \pm 8.65	1.083 $\times 10^{-5}$
LDL cholesterol, mg/dL	18.76 \pm 3.67	14.5 \pm 2.08	8.127 $\times 10^{-3}$
C-reactive protein, mg/L	13.12 \pm 3.27	5.36 \pm 1.12	1.786 $\times 10^{-4}$
Plasma creatinine ^a , mg/dL	0.05 \pm 0.01	0.08 \pm 0.01	2.076 $\times 10^{-4}$
Plasma albumin, g/dL	3.10 \pm 0.34	2.56 \pm 0.13	5.509 $\times 10^{-4}$

^a The clinical chemistry-measured creatinine values are reported here.

Their significantly elevated kidney weight indicated renal hypertrophy, which occurs in the early stage of diabetic nephropathy development [15] and is one of the early markers of morphological changes in renal tissue [16]. It has been shown that 8-week old diabetic mice present glomerular hypertrophy and significantly bigger glomerular tuft surface area compared to nondiabetic mice [17]. Glomerular hyperfiltration and hypertrophy are early features of diabetic nephropathy [15].

2.2.2. Analysis of Creatinine in Eight Murine Tissues

Creatinine concentration in biofluids (plasma, urine) and organs (liver, lungs, adrenal gland, visceral adipose tissue, testis, cerebellum) was determined by targeted metabolomics. In plasma, creatinine was also measured with clinical chemistry. Pearson's correlation coefficient of plasma creatinine concentrations measured with both methods was 0.923 (*p*-value = 6.938 $\times 10^{-9}$), showing a very high correlation between clinical chemistry- and mass spectrometry (MS)-based methods.

In addition to plasma, significantly lower values of creatinine were also detected in the urine, liver and lungs of db/db mice (Table 5). Our observation of approximately 40% lower plasma creatinine (Table 4) and its negative trend in the urine of db/db mice suggests impaired creatine biosynthesis, protein catabolism and glomerular hyperfiltration.

Taken together, our 8-week old db/db mice fed with HFD during 5 weeks reflected characteristic changes of early diabetic nephropathy, such as glomerular hyperfiltration and hypertrophy, as evidenced by significantly lower plasma and urinary creatinine levels and higher kidney weight. Moreover, their phenotypic and metabolic data show obesity, hyperglycemia, dyslipidemia, and inflammation, confirming previous reports about insulin resistance and fatty liver (steatosis) in db/db mice of similar age [13,14,18–20].

2.2.3. Organ-Specific Trends of the Two Metabolites

As compared to WT mice, significantly higher concentrations of both SM C18:1 and PC aa C38:0 were found in the lungs of db/db mice, whereas significantly lower concentrations

were found in urine and adipose tissue (Figure 2, Table 5). Furthermore, SM C18:1 was significantly accumulated in plasma ($p = 3.160 \times 10^{-4}$) and liver ($p = 1.288 \times 10^{-5}$), whereas PC aa C38:0 was significantly higher in adrenal glands ($p = 9.695 \times 10^{-4}$, Table 5) of db/db mice. The concentrations of both metabolites in cerebellum and testis were comparable (Table 5).

Table 5. Biofluid- and tissue-specific trends of creatinine and two candidate CKD metabolites. Results of *t* statistic and *p*-values of two biofluids and six tissues between 10 db/db and 10 WT mice on a high-fat diet are shown. *p*-values shown in bold represent statistical significance at the 0.05 level. Abbreviations: CKD, chronic kidney disease; db/db, leptin receptor-deficient mouse model; WT, wild type mice; SM, sphingomyelin; PC aa, phosphatidylcholine diacyl.

Tissue	Creatinine		SM C18:1		PC aa C38:0	
	<i>t</i> Statistic	<i>p</i> -Value	<i>t</i> Statistic	<i>p</i> -Value	<i>t</i> Statistic	<i>p</i> -Value
Plasma	−5.68	2.284×10^{-5}	4.71	3.160×10^{-4}	0.35	7.327×10^{-1}
Urine ^a	−9.20	9.396×10^{-8}	−2.39	4.193×10^{-2}	−4.56	4.516×10^{-4}
Liver	−9.21	5.298×10^{-8}	6.00	1.288×10^{-5}	0.19	8.499×10^{-1}
Lung	−3.54	2.531×10^{-3}	2.46	2.440×10^{-2}	3.60	2.173×10^{-3}
Adrenal glands ^b	1.33	2.098×10^{-1}	0.16	8.745×10^{-1}	4.11	9.695×10^{-4}
Adipose tissue ^c	−0.49	6.308×10^{-1}	−3.70	1.763×10^{-3}	−2.36	3.856×10^{-2}
Cerebellum	−0.37	7.164×10^{-1}	1.18	2.543×10^{-1}	1.46	1.605×10^{-1}
Testis	2.05	5.560×10^{-2}	−0.52	6.069×10^{-1}	−0.28	7.849×10^{-1}

^a For SM C18:1, $n = 7$ in db/db, $n = 9$ in WT. For PC aa C38:0 and creatinine, $n = 9$ in db/db, $n = 9$ in WT. ^b For creatinine, $n = 9$ in db/db, $n = 9$ in WT. ^c For creatinine, $n = 9$ in db/db, $n = 10$ in WT.

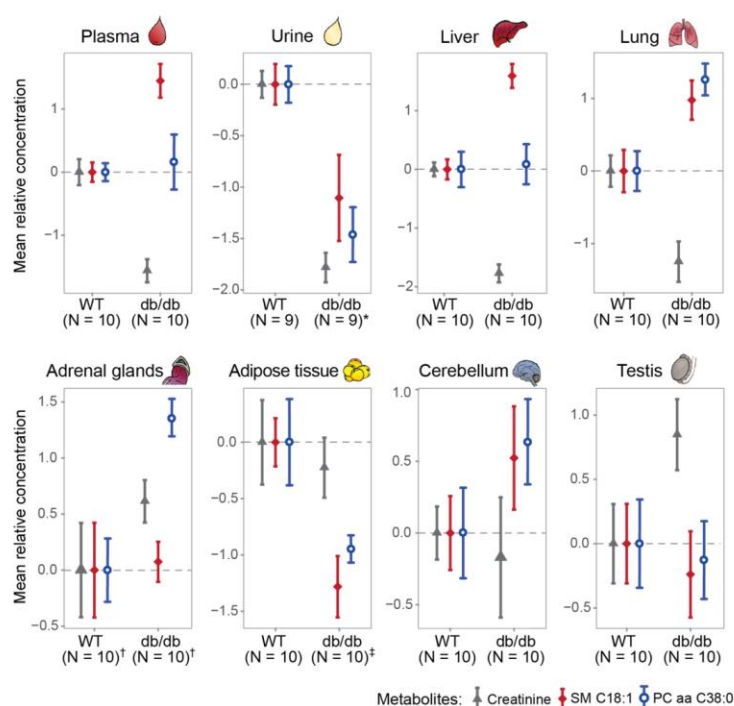


Figure 2. Analysis of creatinine and two candidate metabolites in murine biofluids and tissues. Mean relative concentrations (with standard errors) of the metabolites (creatinine, SM C18:1, and PC aa C38:0) in murine plasma, urine, liver, lung, adrenal tissue, adipose tissue, cerebellum, and testis. * $N = 7$ in db/db for SM C18:1. † For creatinine, $N = 9$ in db/db, $N = 9$ in WT. ‡ $N = 9$ in db/db for creatinine. Abbreviations: db/db, leptin receptor-deficient mouse model; WT, wild type mice; SM, sphingomyelin; PC aa, phosphatidylcholine diacyl.

3. Discussion

According to the natural history of diabetic nephropathy, the early stage displays normal kidney function (normal GFR) and is clinically unsuspecting. It is followed by a transient period of glomerular hyperfiltration (increased GFR) that later normalizes and slowly decreases towards a steep GFR decline at a relatively later stage [21]. Our initial discovery in the longitudinal human cohort showed predictive effects of elevated serum levels of SM C18:1 and PC aa C38:0 for incident CKD in hyperglycemic individuals with normal baseline kidney function [9]. The finding of this animal and cross-sectional human study is that these metabolites associate with further stages of hyperglycemia-related CKD evolution including (i) early changes characterized with glomerular hyperfiltration (8-week-old db/db mice) and (ii) later changes characterized with reduced eGFR (KORA FF4 study).

This cross-sectional KORA FF4 study revealed significant associations between serum levels of SM C18:1 and PC aa C38:0 with decreased eGFR in individuals with prediabetes or T2D. Their associations with kidney function were independent of systolic blood pressure, blood lipids, HbA_{1C}, and UACR suggesting that these two candidate phospholipids biomarkers are independent risk factors for CKD. Both metabolites, SM C18:1 and PC aa C38:0, are phospholipids that are known to regulate inflammation and fibrosis and their alterations in diabetes and metabolic syndrome occur in multiple body systems [11]. Besides hyperglycemia-related CKD [9], metabolomics studies have revealed that plasma PC aa C38:0 was positively associated with coronary artery disease mortality [22] and systemic alterations in SM levels were also predictive of T1D [23], T2D [24], and myocardial infarction [25]. As these outcomes are risk factors or subsequent outcomes for hyperglycemia-related CKD, further studies are necessary to provide insights into the disease-specificity of emerging phospholipid biomarkers before their application in clinical diagnostics. Since not all patients with diabetes develop CKD and not all patients with CKD follow the same disease trajectory, it is also important to explore their mechanisms of actions for better patient stratification and to accelerate targeted screening programs.

Glomerular hyperfiltration is a hallmark of kidney dysfunction in diabetes. The flow-related effects of glomerular and tubular changes caused by glomerular hyperfiltration-related mechanical stress play a major role in the pathogenesis of the glomerular disease, and reduction of hyperfiltration is a crucial therapeutic target in diabetes-induced CKD [26]. In young diabetic mice (6–10 weeks), exert supraphysiological GFR and increased creatinine clearance have been reported [17,27]. As a potential effect of glomerular hyperfiltration in our 8-week-old db/db mice, we observed lower plasma and urinary levels of creatinine. Creatinine is a toxic byproduct of phosphocreatine metabolism and is excreted by glomerular filtration and proximal tubular secretion with little to no reabsorption. Besides the plasma and urine in our db/db mice, lower concentrations of creatinine were also found in the liver and lungs, which could be explained by reduced creatine biosynthesis and/or phosphocreatine energy metabolism in skeletal muscle and other organs. The influence of known factors affecting serum creatinine values (age, sex, ethnicity, muscle mass, protein diet, and intake of drugs [28]) was minimal as these factors were controlled for in our mouse study. Diabetic mice display skeletal mass reduction already at 5 weeks of age and before T2D onset [29] and low serum creatinine in T2D patients indicates muscle loss and predicts T2D independently of glomerular filtration [30,31]. Taken together, creatinine measurements in our 8-week-old db/db mice are suggestive of not only altered kidney function, e.g., glomerular hyperfiltration, but also high-energy phosphate metabolism.

Our db/db mice displayed significantly higher levels of both metabolites, SM C18:1 and PC aa C38:0, in the lungs than WT mice. This could indicate lung dysfunction as PCs and SMs are key components of pulmonary surfactant and their dysregulation was linked with respiratory failure [32]. The db/db mice are prone to pulmonary edema [33] and asthma-related symptoms such as airway hyperresponsiveness [34]. Sphingomyelin synthase 2 (SMS2) deficiency attenuates inflammation and ameliorates recovery after lung injury in mice [35]. Lung dysfunction is common, but clinically less managed, comorbidity

in patients with CKD [36]. Despite some earlier and controversial evidence on better adult respiratory distress syndrome (ARDS) survival in T2D patients, it has been urged to investigate lung dysfunction in T2D patients [37].

The epididymal adipose tissue in db/db mice displayed lower concentrations of SM C18:1 and PC aa C38:0 (Figure 3). In line with our findings, reduced adipose tissue levels of certain SMs and PCs have also been detected in 30-week old db/db mice [38]. The phospholipid metabolism in white adipose tissue and residing macrophages of obese animals is largely perturbed [39]. We speculate that the lower adipose levels of SM C18:1 and PC aa C38:0 could be due to increased efflux of SM- or PC-containing lipoproteins by the ATP-binding cassette transporter ABCG1 [40] that is upregulated in obese mice [41].

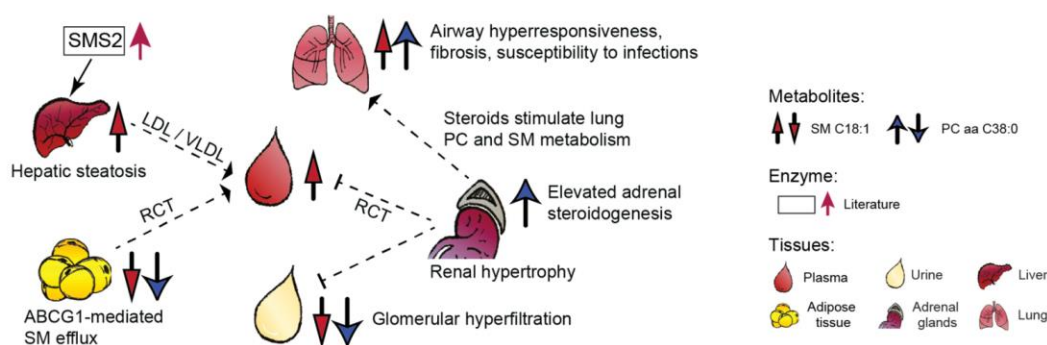


Figure 3. Organ-specific trends of SM C18:1 and PC aa C38:0 in a mouse model of diabetic nephropathy and potential interorgan crosstalk inferred from literature (interrupted lines, references in discussion). Abbreviations: ABCG1, ATP-binding cassette subfamily G member 1; RCT, reverse cholesterol transport; SMS2, sphingomyelin synthase 2; VLDL, very-low-density lipoprotein; LDL, low-density lipoprotein; SM, sphingomyelin; PC, phosphatidylcholine.

Higher hepatic levels of SM C18:1 in db/db mice could be the consequence of fatty liver related upregulation in SMS2 activity [42], which determines hepatic and plasma SM values [43]. SMS2 activity promotes fatty acid uptake and liver steatosis [42], whereas SMS2 deficiency prevents HFD-induced liver steatosis [44] and increases insulin sensitivity [45]. The liver is the central hub of phospholipid synthesis and recycling via lipoprotein particles such as LDL/VLDL (approx. 70% of plasma SMs) and HDL (30%) (Figure 3).

Our observation of higher concentration of PC aa C38:0 in the adrenal glands might be related with reduced biosynthesis of polyunsaturated fatty acids in adrenals of db/db mice [46]. These mice also display an increased synthesis of adrenal steroids [19], which can stimulate PC synthesis in the lungs [47] (Figure 3).

Biofluids such as blood and urine provide insights into interorgan metabolic crosstalk and kidney activity, respectively. Similarly to creatinine, the lower urinary levels of SM C18:1 and PC aa C38:0 in db/db mice may reflect altered glomerular filtration as well as phospholipid accumulation in the kidney tissue as was shown in HFD-fed db/db mice [48]. SMs accumulate in the glomeruli of diabetic and HFD-fed mice might promote CKD [49]. Diabetic kidney disease in db/db mice manifests around 8 weeks of age with albuminuria and increased glomerular surface area, resembling the early stage of human diabetic nephropathy, and is followed by a progressive increase in mesangial matrix and hypertrophy [13,50]. The kidneys modulate HDL metabolism and their early dysfunction could impair reverse cholesterol transport and additionally contribute to lower urinary concentrations of the two phospholipids (Figure 3). In summary, this detailed assessment of two biofluids and six tissues in a well-characterized mouse model of diabetic nephropathy indicates altered levels of SM C18:1 and PC aa C38:0 in the liver, lungs, adrenal gland, adipose tissue, and urine. Of these, the lungs appear especially interesting due to phospholipid implication in various pulmonary diseases and injuries [51]. At the current stage

of knowledge, it is unclear but possible (based on literature) that these organs could also contribute to the circulatory regulation of SM C18:1 and PC aa C38:0.

This study has several limitations and advantages. Limited availability of the mouse data did not allow us to analyze kidney tissue nor validate metabolite profiles by histological analysis. Compared with humans, the difference in the genetic background of db/db mice that causes hyperglycemia and diabetic nephropathy may confound metabolite profiles. Therefore, multiorgan contribution to systemic dysregulation of SM C18:1 and PC aa C38:0 and their potential functional implication in kidney function (by feeding experiments in diabetic mouse models) require further investigations. One of strengths of our study is the validation of two candidate biomarkers of incident CKD not only in a cross-sectional human study, but also in multiorgan mouse models with hyperglycemia and obesity. Our study provides first insights into multistage CKD association, early stage characterized with glomerular hyperfiltration (8-week-old db/db mice), and later stage characterized with reduced eGFR (KORA FF4 study), as well as potential multiorgan contribution to circulatory regulation of the two phospholipid metabolites for CKD.

4. Materials and Methods

4.1. Study Participants, Outcome Definition

The KORA FF4 study was conducted in the area of Augsburg, Southern Germany. All study participants gave written informed consent. The KORA study was approved by the ethics committee of the Bavarian Medical Association, Munich, Germany.

Individuals with hyperglycemia and NGT were classified according to fasting glucose and 2-h glucose values using the World Health Organization diagnostic criteria. Hyperglycemic group comprised participants with prediabetes and newly diagnosed T2D (i.e., fasting glucose ≥ 110 mg/dL and/or 2-h-glucose ≥ 140 mg/dL), as well as known T2D that was diagnosed by physician validated self-reporting and/or current use of antidiabetes agents [8].

We examined 2218 individuals who had metabolite measurements and excluded 311 participants in the analysis including (1) nonfasting samples ($n = 15$); (2) missing eGFR, UACR, or covariate values ($n = 37$); (3) diagnosis for type 1 diabetes ($n = 5$), unclear type of diabetes mellitus ($n = 69$) or age equal to or greater than 85 ($n = 23$) or self-reported use of antidiabetic medication ($n = 162$). The remaining dataset comprised 510 hyperglycemic participants and 1397 individuals with NGT (Table 1). The hyperglycemic individuals were used to study the associations of eGFR and CKD with the two metabolites. The NGT individuals served as a sensitivity analysis of the associations of CKD with the two metabolites.

The eGFR was calculated from serum creatinine (mg/dL) (IDMS standardized values) using the Chronic Kidney Disease Epidemiology Collaboration (CKD-EPI) equation [52]. CKD was defined as an eGFR < 60 mL/min/1.73 m² [53].

4.2. Mouse Study

We used male 8-week (± 3 d) old WT mice ($n = 10$) and db/db mice (BKS.Cg-Dock7^m+/+ *Lepr*^{db}/J, $n = 10$, Figure 4). The animals were bred and housed in a temperature- and humidity-controlled environment in compliance with FELASA (the Federation of Laboratory Animal Science Associations) protocols [54]. Animal experiments were approved by the District Government of Upper Bavaria (Regierung von Oberbayern, Gz.55.2-1-54-2531-70-07, 55.2-1-2532-153-11).

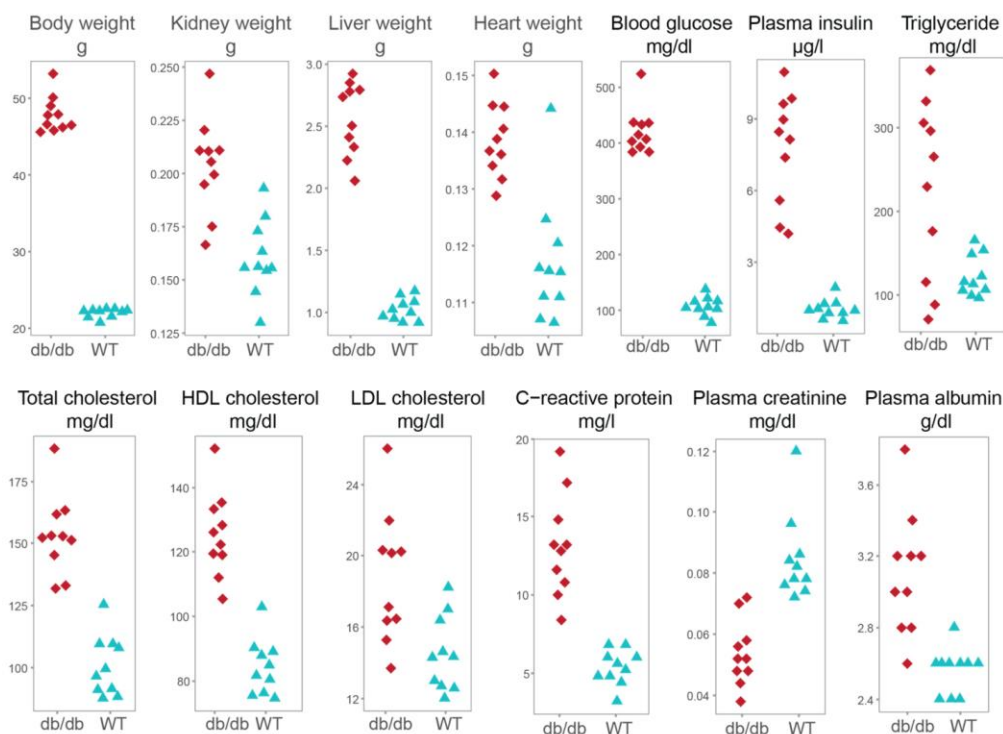


Figure 4. Scatter plots of phenotypic and metabolic variables in db/db and wild type mice fed with a high-fat diet. Abbreviations: HDL, high-density lipoprotein; LDL, low-density lipoprotein; db/db, leptin receptor-deficient mouse model; WT, wild type mice.

From an age of 3 weeks, all mice were fed with HFD (S0372-E010, ssniff Spezialdiäten, Soest, Germany) [54]. After receiving vehicle (5% solutol and 95% hydroxyethylcellulose), all mice were fasted for 4 h before biofluid and organ collection. Urine was collected individually with absorbing tissue pads. Blood samples were collected from lateral tail veins. Liver, epididymal adipose tissue, cerebellum, lung, adrenal, and testis samples were immediately dissected and freeze-clamped after sacrifice with an isoflurane overdose [54]. All samples were stored at -80°C until further analyses.

4.3. Metabolite Quantification and Normalization

Serum samples from participants in the KORA FF4 study were measured with the AbsoluteIDQ™ p180 Kit (BIOCRATES Life Sciences AG, Innsbruck, Austria). Metabolite concentrations were adjusted for plate normalization factors (NFs) to minimize the plate effect. For each metabolite, the plate NFs were calculated by dividing the mean of reference samples in each plate with the mean of all reference samples in all measured plates. Metabolite concentrations were natural-log transformed and scaled to a mean value of zero and standard deviation (SD) of one to ensure comparability between the metabolites.

In the mouse study, creatinine, SM C18:1 and PC aa C38:0 values in plasma, liver, lung, adrenal glands, adipose tissue, cerebellum, and testis samples were determined with the AbsoluteIDQ™ p180 Kit (BIOCRATES Life Sciences AG, Innsbruck, Austria) and in urine with the AbsoluteIDQ™ p150 Kit (BIOCRATES). Tissue homogenization, extraction solvents, assay preparation, and LC-MS/MS measurements have been described elsewhere [55]. Since each tissue sample from db/db and WT mice was measured on the same kit plate, we did not conduct plate correction. Metabolite concentrations were natural-log transformed and then scaled to a mean value of zero and SD of one for each tissue.

4.4. Statistical Analysis

IPW for continuous exposures of the generalized propensity score approach was applied to reduce the confounding effects and provide a more reliable estimate of metabolite–outcome associations in participants of the KORA FF4 study [56]. The IPW-adjusted analysis improved the balance between two metabolites and covariates, e.g., all of the absolute Spearman’s correlation coefficients between PC aa C38:0 and covariates were below 0.1, both in hyperglycemic and NGT individuals (Figure 5).

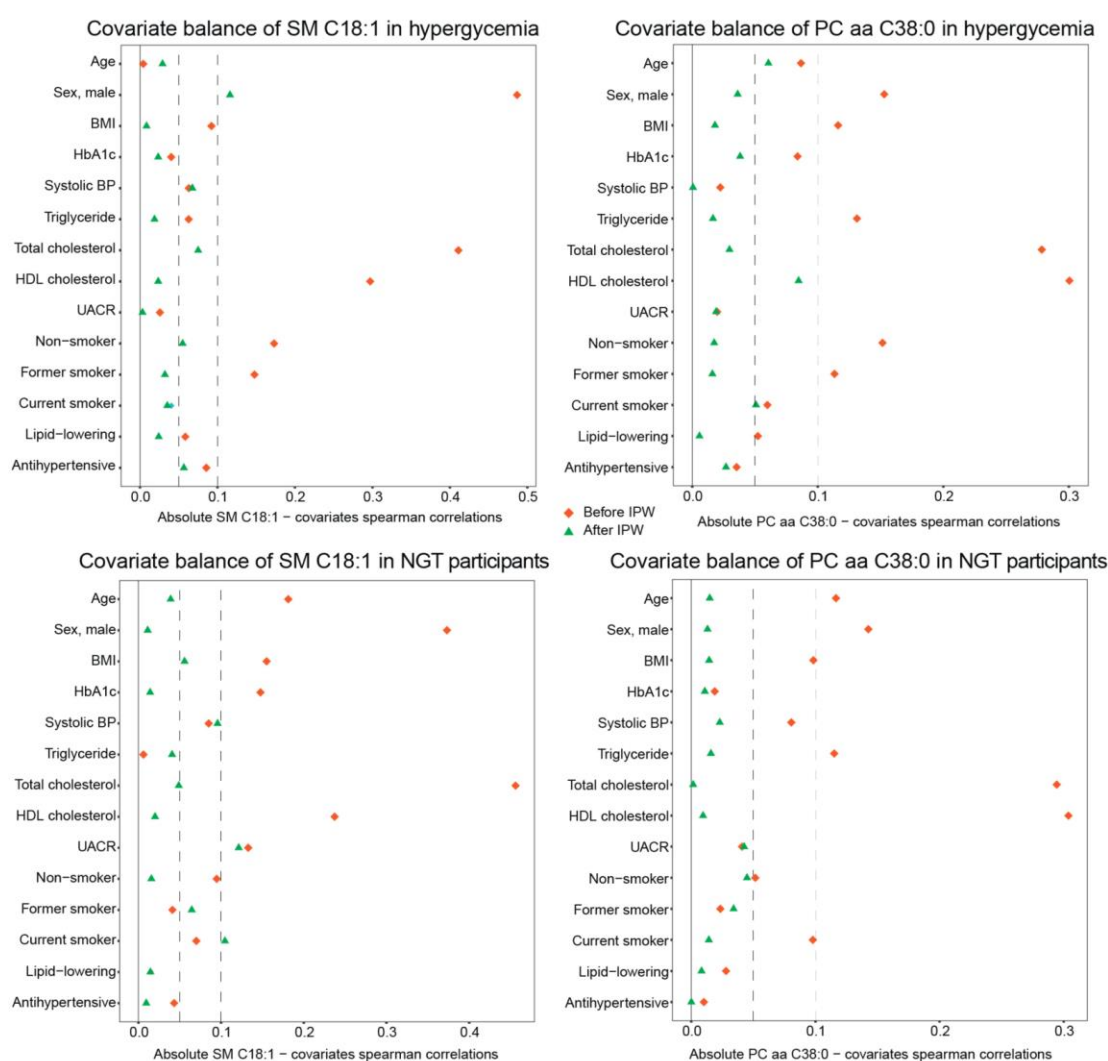


Figure 5. Inverse probability weighting improves metabolite–covariate balance. The absolute values of Spearman’s correlation coefficients for SM C18:1 or PC aa C38:0 with various covariates before and after IPW in hyperglycemic and NGT individuals of KORA FF4 are shown. The interrupted lines represent 0.05 (left) and 0.1 (right) absolute value of Spearman’s correlation coefficients. Abbreviations: IPW, inverse probability weighting; SM, sphingomyelin; PC aa, phosphatidylcholine diacyl; NGT, normal glucose tolerance. HbA_{1c}, glycated hemoglobin; BP, blood pressure; UACR, urinary albumin-to-creatinine ratio.

We defined two sets of covariates. The basic model included age, sex, BMI, systolic blood pressure, triglyceride, total cholesterol, HDL cholesterol, and HbA_{1c}. The full model was additionally adjusted for smoking status, use of lipid-lowering drugs and

antihypertensive medication, and UACR. The values of UACR, HbA_{1C} and triglyceride were natural log-transformed before analysis due to their right-skewed distribution.

Generalized propensity scores were estimated with multivariable linear regression in which each metabolite was regressed on covariates from the full model, respectively [57]. The inverse probability weights for each metabolite were then calculated using the corresponding estimated generalized propensity scores [56]. The balance between each metabolite and covariate before and after IPW was estimated by Spearman's correlation coefficients. Their imbalance was defined using stringent criteria, i.e., with absolute Spearman's correlation coefficient greater than 0.05.

Metabolite association with eGFR and CKD in hyperglycemic individuals of KORA FF4 was analyzed with weighted multivariable linear and logistic regression with applying corresponding inverse probability weights, respectively. As a sensitivity analysis, metabolite association with CKD was analyzed in NGT individuals of KORA FF4 with weighted multivariable logistic regression after IPW.

Statistical differences in clinical and metabolic parameters between db/db and WT mice were assessed with the Mann–Whitney *U* test. Differences in tissue-specific concentration of creatinine and two candidate metabolite biomarkers between db/db and WT mice were assessed with Student's *t*-test.

A two-sided *p*-value < 0.05 was considered statistically significant. All statistical analyses were performed using R version 4.0.3.

5. Conclusions

This study provides biological insights into our recent discovery of SM C18:1 and PC aa C38:0 as predictive metabolites for incident CKD in hyperglycemic individuals [9]. The cross-sectional analysis showed that the inverse association of both phospholipids with glomerular filtration in hyperglycemic individuals was independent of systolic blood pressure, cholesterol, triglycerides, HbA_{1C}, and UACR. Multiorgan analysis in a well-characterized mouse model of early diabetic nephropathy revealed a possible contribution of lungs, liver, adipose tissue, and adrenal glands in their systemic regulation and CKD progression. As a remarkable example of interdisciplinary collaboration, this human and animal study corroborated our initial discovery and provided insights into a relationship with kidney function and the potential implication of other organs. This study contributes to human validation of SM C18:1 and PC aa C38:0 as new biomarkers for early identification of persons with (pre)diabetes with increased risk of CKD and serves as a step ahead towards risk stratification and improved targeted screening programs for CKD. In-depth molecular phenotyping of these novel metabolite predictors of CKD is warranted.

Author Contributions: Conceptualization, J.H. and R.W.-S.; methodology, J.H., M.C., C.H., M.R., J.A. (Jonathan Adam), L.W., J.N., S.Z., C.P., M.F.S., K.S.; formal analysis, J.H.; data curation, S.Z., C.P., M.F.S., S.N., G.K., C.G.; writing—original draft preparation, J.H., M.C., R.W.-S.; writing—review and editing, C.H., M.R., J.A. (Jonathan Adam), J.N., M.F.S., M.L., F.S.; visualization, J.H., M.C., L.W., R.W.-S.; supervision, J.A. (Jerzy Adamski), M.H.d.A., A.P., R.W.-S.; funding acquisition, M.L., F.S., J.A. (Jerzy Adamski), M.H.d.A., A.P., R.W.-S. All authors have read and agreed to the published version of the manuscript.

Funding: Part of this research was supported by the 19076 and 20679 iPDM-GO “Integrated Personalized Diabetes Management goes Europe” innovation project supported by EIT Health. EIT Health is supported by the EIT, a body of the European Union. K.S. is supported by Biomedical Research Program funds at Weill Cornell Medical College in Qatar, a program funded by the Qatar Foundation. The KORA study was initiated and financed by the Helmholtz Zentrum München—German Research Center for Environmental Health, which is funded by the German Federal Ministry of Education and Research (BMBF) and by the State of Bavaria. Furthermore, KORA research was supported within the Munich Center of Health Sciences (MC-Health), Ludwig-Maximilians-Universität, as part of LMUinnovativ.

Institutional Review Board Statement: The study was conducted according to the guidelines of the Declaration of Helsinki, and approved by the Institutional Review Board of KORA-Study Group (PV K119/17g).

Informed Consent Statement: Informed consent was obtained from all subjects involved in the study.

Data Availability Statement: The KORA FF4 data sets are not publicly available because of data protection agreements but can be provided upon request through the KORA-PASST (Project application self-service tool, www.helmholtz-muenchen.de/kora-gen).

Acknowledgments: We express our appreciation to all KORA study participants for donating their blood and time. We thank the field staff in Augsburg conducting the KORA studies. The KORA-Study Group consists of A. Peters (speaker), L. Schwettmann, R. Leidl, M. Heier, B. Linkohr, H. Grallert, C. Gieger, J. Linseisen and their coworkers, who are responsible for the design and conduct of the KORA studies. We are grateful to Julia Scarpa and Katharina Faschinger from the Metabolomics Platform of the Genome Analysis Center for performing metabolomic measurements. For the mouse study, we thank the staff of the Institute of Diabetes and Regeneration Research (Anett Seelig, Jürgen Schultheiß), Institute of Experimental Genetics (Moya Wu, Gerhard Przemec), and the animal caretaker staff of the German Mouse Clinic for excellent technical assistance.

Conflicts of Interest: M.F.S. was employed at Helmholtz Center Munich during his Ph.D. thesis and is currently employed in the CardioRenal Medical Department of Bayer AG, however, the company was not involved in work related to data and manuscript generation.

References

- Alicic, R.Z.; Neumiller, J.J.; Johnson, E.J.; Dieter, B.; Tuttle, K.R. Sodium-Glucose Cotransporter 2 Inhibition and Diabetic Kidney Disease. *Diabetes* **2019**, *68*, 248–257. [[CrossRef](#)] [[PubMed](#)]
- GBD Chronic Kidney Disease Collaboration; Bikbov, B.; Purcell, C.; Levey, A.S.; Smith, M.; Abdoli, A.; Abebe, M.; Adebayo, O.M.; Afarideh, M.; Agarwal, S.K.; et al. Global, regional, and national burden of chronic kidney disease, 1990–2017: A systematic analysis for the Global Burden of Disease Study 2017. *Lancet* **2020**, *395*, 709–733. [[CrossRef](#)]
- Manns, B.; Hemmelgarn, B.; Tonelli, M.; Au, F.; Chiasson, T.C.; Dong, J.; Klarenbach, S.; Alberta Kidney Disease, N. Population based screening for chronic kidney disease: Cost effectiveness study. *BMJ* **2010**, *341*, c5869. [[CrossRef](#)] [[PubMed](#)]
- Dunkler, D.; Gao, P.; Lee, S.F.; Heinze, G.; Clase, C.M.; Tobe, S.; Teo, K.K.; Gerstein, H.; Mann, J.F.; Oberbauer, R.; et al. Risk Prediction for Early CKD in Type 2 Diabetes. *Clin. J. Am. Soc. Nephrol.* **2015**, *10*, 1371–1379. [[CrossRef](#)] [[PubMed](#)]
- Nicholson, J.K.; Wilson, I.D. Opinion: Understanding ‘global’ systems biology: Metabolomics and the continuum of metabolism. *Nat. Rev. Drug Discov.* **2003**, *2*, 668–676. [[CrossRef](#)] [[PubMed](#)]
- Gieger, C.; Geistlinger, L.; Altmaier, E.; Hrabe de Angelis, M.; Kronenberg, F.; Meitinger, T.; Mewes, H.W.; Wichmann, H.E.; Weinberger, K.M.; Adamski, J.; et al. Genetics meets metabolomics: A genome-wide association study of metabolite profiles in human serum. *PLoS Genet.* **2008**, *4*, e1000282. [[CrossRef](#)]
- Suhre, K.; Shin, S.Y.; Petersen, A.K.; Mohny, R.P.; Meredith, D.; Wagele, B.; Altmaier, E.; CardioGram; Deloukas, P.; Erdmann, J.; et al. Human metabolic individuality in biomedical and pharmaceutical research. *Nature* **2011**, *477*, 54–60. [[CrossRef](#)] [[PubMed](#)]
- Wang-Sattler, R.; Yu, Z.; Herder, C.; Messias, A.C.; Floegel, A.; He, Y.; Heim, K.; Campillos, M.; Holzapfel, C.; Thorand, B.; et al. Novel biomarkers for pre-diabetes identified by metabolomics. *Mol. Syst. Biol.* **2012**, *8*, 615. [[CrossRef](#)]
- Huang, J.; Huth, C.; Covic, M.; Troll, M.; Adam, J.; Zukunft, S.; Prehn, C.; Wang, L.; Nano, J.; Scheerer, M.F.; et al. Machine Learning Approaches Reveal Metabolic Signatures of Incident Chronic Kidney Disease in Individuals with Prediabetes and Type 2 Diabetes. *Diabetes* **2020**, *69*, 2756–2765. [[CrossRef](#)]
- Fornoni, A.; Merscher, S.; Kopp, J.B. Lipid biology of the podocyte—new perspectives offer new opportunities. *Nat. Rev. Nephrol.* **2014**, *10*, 379–388. [[CrossRef](#)]
- Russo, S.B.; Ross, J.S.; Cowart, L.A. Sphingolipids in obesity, type 2 diabetes, and metabolic disease. *Handb. Exp. Pharmacol.* **2013**, *373–401*. [[CrossRef](#)]
- Lisowska-Myjak, B. Uremic toxins and their effects on multiple organ systems. *Nephron Clin. Pract.* **2014**, *128*, 303–311. [[CrossRef](#)] [[PubMed](#)]
- Sharma, K.; McCue, P.; Dunn, S.R. Diabetic kidney disease in the db/db mouse. *Am. J. Physiol. Renal Physiol.* **2003**, *284*, F1138–F1144. [[CrossRef](#)] [[PubMed](#)]
- Kim, N.H.; Hyeon, J.S.; Kim, N.H.; Cho, A.; Lee, G.; Jang, S.Y.; Kim, M.K.; Lee, E.Y.; Chung, C.H.; Ha, H.; et al. Metabolic changes in urine and serum during progression of diabetic kidney disease in a mouse model. *Arch. Biochem. Biophys.* **2018**, *646*, 90–97. [[CrossRef](#)] [[PubMed](#)]
- Yamamoto, Y.; Maeshima, Y.; Kitayama, H.; Kitamura, S.; Takazawa, Y.; Sugiyama, H.; Yamasaki, Y.; Makino, H. Tumstatin peptide, an inhibitor of angiogenesis, prevents glomerular hypertrophy in the early stage of diabetic nephropathy. *Diabetes* **2004**, *53*, 1831–1840. [[CrossRef](#)] [[PubMed](#)]

16. Cingel-Ristić, V.; Schrijvers, B.F.; van Vliet, A.K.; Rasch, R.; Han, V.K.; Drop, S.L.; Flyvbjerg, A. Kidney growth in normal and diabetic mice is not affected by human insulin-like growth factor binding protein-1 administration. *Exp. Biol. Med. (Maywood)* **2005**, *230*, 135–143. [[CrossRef](#)]
17. Cohen, M.P.; Lautenslager, G.T.; Shearman, C.W. Increased urinary type IV collagen marks the development of glomerular pathology in diabetic d/db mice. *Metabolism* **2001**, *50*, 1435–1440. [[CrossRef](#)] [[PubMed](#)]
18. Trak-Smayra, V.; Paradis, V.; Massart, J.; Nasser, S.; Jebara, V.; Fromenty, B. Pathology of the liver in obese and diabetic ob/ob and db/db mice fed a standard or high-calorie diet. *Int. J. Exp. Pathol.* **2011**, *92*, 413–421. [[CrossRef](#)]
19. Hofmann, A.; Peitzsch, M.; Brunssen, C.; Mittag, J.; Jannasch, A.; Frenzel, A.; Brown, N.; Weldon, S.M.; Eisenhofer, G.; Bornstein, S.R.; et al. Elevated Steroid Hormone Production in the db/db Mouse Model of Obesity and Type 2 Diabetes. *Horm. Metab. Res.* **2017**, *49*, 43–49. [[CrossRef](#)]
20. Chocian, G.; Chabowski, A.; Zendzian-Piotrowska, M.; Harasim, E.; Łukaszuk, B.; Górski, J. High fat diet induces ceramide and sphingomyelin formation in rat's liver nuclei. *Mol. Cell Biochem.* **2010**, *340*, 125–131. [[CrossRef](#)]
21. Tonneijck, L.; Muskiet, M.H.; Smits, M.M.; van Bommel, E.J.; Heerspink, H.J.; van Raalte, D.H.; Joles, J.A. Glomerular Hyperfiltration in Diabetes: Mechanisms, Clinical Significance, and Treatment. *J. Am. Soc. Nephrol.* **2017**, *28*, 1023–1039. [[CrossRef](#)] [[PubMed](#)]
22. Sigrüener, A.; Kleber, M.E.; Heimerl, S.; Liebisch, G.; Schmitz, G.; Maerz, W. Glycerophospholipid and sphingolipid species and mortality: The Ludwigshafen Risk and Cardiovascular Health (LURIC) study. *PLoS ONE* **2014**, *9*, e85724. [[CrossRef](#)] [[PubMed](#)]
23. Tofte, N.; Suvitaival, T.; Trost, K.; Mattila, I.M.; Theilade, S.; Winther, S.A.; Ahluwalia, T.S.; Fridmodt-Møller, M.; Legido-Quigley, C.; Rossing, P. Metabolomic Assessment Reveals Alteration in Polyols and Branched Chain Amino Acids Associated With Present and Future Renal Impairment in a Discovery Cohort of 637 Persons with Type 1 Diabetes. *Front. Endocrinol.* **2019**, *10*, 818. [[CrossRef](#)] [[PubMed](#)]
24. Razquin, C.; Toledo, E.; Clish, C.B.; Ruiz-Canela, M.; Dennis, C.; Corella, D.; Papandreou, C.; Ros, E.; Estruch, R.; Guasch-Ferre, M.; et al. Plasma Lipidomic Profiling and Risk of Type 2 Diabetes in the PREDIMED Trial. *Diabetes Care* **2018**, *41*, 2617–2624. [[CrossRef](#)] [[PubMed](#)]
25. Floegel, A.; Kuhn, T.; Sookthai, D.; Johnson, T.; Prehn, C.; Rolle-Kampczyk, U.; Otto, W.; Weikert, C.; Illig, T.; von Bergen, M.; et al. Serum metabolites and risk of myocardial infarction and ischemic stroke: A targeted metabolomic approach in two German prospective cohorts. *Eur. J. Epidemiol.* **2018**, *33*, 55–66. [[CrossRef](#)] [[PubMed](#)]
26. Chagnac, A.; Zingerman, B.; Rozen-Zvi, B.; Herman-Edelstein, M. Consequences of Glomerular Hyperfiltration: The Role of Physical Forces in the Pathogenesis of Chronic Kidney Disease in Diabetes and Obesity. *Nephron* **2019**, *143*, 38–42. [[CrossRef](#)] [[PubMed](#)]
27. Gartner, K. Glomerular hyperfiltration during the onset of diabetes mellitus in two strains of diabetic mice (c57bl/6j db/db and c57bl/ksj db/db). *Diabetologia* **1978**, *15*, 59–63. [[CrossRef](#)] [[PubMed](#)]
28. Champion, C.G.; Sanchez-Ferraz, O.; Batchu, S.N. Potential Role of Serum and Urinary Biomarkers in Diagnosis and Prognosis of Diabetic Nephropathy. *Can. J. Kidney Health Dis.* **2017**, *4*, 2054358117705371. [[CrossRef](#)]
29. Ostler, J.E.; Maurya, S.K.; Dials, J.; Roof, S.R.; Devor, S.T.; Ziolo, M.T.; Periasamy, M. Effects of insulin resistance on skeletal muscle growth and exercise capacity in type 2 diabetic mouse models. *Am. J. Physiol. Endocrinol. Metab.* **2014**, *306*, E592–E605. [[CrossRef](#)]
30. Kashima, S.; Inoue, K.; Matsumoto, M.; Akimoto, K. Low serum creatinine is a type 2 diabetes risk factor in men and women: The Yuport Health Checkup Center cohort study. *Diabetes Metab.* **2017**, *43*, 460–464. [[CrossRef](#)]
31. Harita, N.; Hayashi, T.; Sato, K.K.; Nakamura, Y.; Yoneda, T.; Endo, G.; Kambe, H. Lower serum creatinine is a new risk factor of type 2 diabetes: The Kansai healthcare study. *Diabetes Care* **2009**, *32*, 424–426. [[CrossRef](#)] [[PubMed](#)]
32. Hallman, M.; Spragg, R.; Harrell, J.H.; Moser, K.M.; Gluck, L. Evidence of lung surfactant abnormality in respiratory failure. Study of bronchoalveolar lavage phospholipids, surface activity, phospholipase activity, and plasma myoinositol. *J. Clin. Invest.* **1982**, *70*, 673–683. [[CrossRef](#)] [[PubMed](#)]
33. Papinska, A.M.; Soto, M.; Meeke, C.J.; Rodgers, K.E. Long-term administration of angiotensin (1-7) prevents heart and lung dysfunction in a mouse model of type 2 diabetes (db/db) by reducing oxidative stress, inflammation and pathological remodeling. *Pharmacol. Res.* **2016**, *107*, 372–380. [[CrossRef](#)] [[PubMed](#)]
34. Lu, F.L.; Johnston, R.A.; Flynt, L.; Theman, T.A.; Terry, R.D.; Schwartzman, I.N.; Lee, A.; Shore, S.A. Increased pulmonary responses to acute ozone exposure in obese db/db mice. *Am. J. Physiol. Lung Cell Mol. Physiol.* **2006**, *290*, L856–L865. [[CrossRef](#)] [[PubMed](#)]
35. Gowda, S.; Yeang, C.; Wadgaonkar, S.; Anjum, F.; Grinkina, N.; Cutaia, M.; Jiang, X.C.; Wadgaonkar, R. Sphingomyelin synthase 2 (SMS2) deficiency attenuates LPS-induced lung injury. *Am. J. Physiol. Lung Cell Mol. Physiol.* **2011**, *300*, L430–L440. [[CrossRef](#)]
36. Mukai, H.; Ming, P.; Lindholm, B.; Heimbürger, O.; Barany, P.; Stenvinkel, P.; Qureshi, A.R. Lung Dysfunction and Mortality in Patients with Chronic Kidney Disease. *Kidney Blood Press Res.* **2018**, *43*, 522–535. [[CrossRef](#)]
37. Kolahian, S.; Leiss, V.; Nürnberg, B. Diabetic lung disease: Fact or fiction? *Rev. Endocr. Metab. Disord.* **2019**, *20*, 303–319. [[CrossRef](#)]
38. Giesbertz, P.; Padberg, I.; Rein, D.; Ecker, J.; Höfle, A.S.; Spanier, B.; Daniel, H. Metabolite profiling in plasma and tissues of ob/ob and db/db mice identifies novel markers of obesity and type 2 diabetes. *Diabetologia* **2015**, *58*, 2133–2143. [[CrossRef](#)]
39. Dahik, V.D.; Frisdal, E.; Le Goff, W. Rewiring of Lipid Metabolism in Adipose Tissue Macrophages in Obesity: Impact on Insulin Resistance and Type 2 Diabetes. *Int. J. Mol. Sci.* **2020**, *21*, 5505. [[CrossRef](#)]

40. Kobayashi, A.; Takanezawa, Y.; Hirata, T.; Shimizu, Y.; Misasa, K.; Kioka, N.; Arai, H.; Ueda, K.; Matsuo, M. Efflux of sphingomyelin, cholesterol, and phosphatidylcholine by ABCG1. *J. Lipid Res.* **2006**, *47*, 1791–1802. [[CrossRef](#)]
41. Edgel, K.A.; McMillen, T.S.; Wei, H.; Pamir, N.; Houston, B.A.; Caldwell, M.T.; Mai, P.O.; Oram, J.F.; Tang, C.; Leboeuf, R.C. Obesity and weight loss result in increased adipose tissue ABCG1 expression in db/db mice. *Biochim. Biophys. Acta* **2012**, *1821*, 425–434. [[CrossRef](#)] [[PubMed](#)]
42. Li, Y.; Dong, J.; Ding, T.; Kuo, M.S.; Cao, G.; Jiang, X.C.; Li, Z. Sphingomyelin synthase 2 activity and liver steatosis: An effect of ceramide-mediated peroxisome proliferator-activated receptor gamma2 suppression. *Arterioscler. Thromb. Vasc. Biol.* **2013**, *33*, 1513–1520. [[CrossRef](#)] [[PubMed](#)]
43. Liu, J.; Zhang, H.; Li, Z.; Hailemariam, T.K.; Chakraborty, M.; Jiang, K.; Qiu, D.; Bui, H.H.; Peake, D.A.; Kuo, M.S.; et al. Sphingomyelin synthase 2 is one of the determinants for plasma and liver sphingomyelin levels in mice. *Arterioscler. Thromb. Vasc. Biol.* **2009**, *29*, 850–856. [[CrossRef](#)] [[PubMed](#)]
44. Mitsutake, S.; Zama, K.; Yokota, H.; Yoshida, T.; Tanaka, M.; Mitsui, M.; Ikawa, M.; Okabe, M.; Tanaka, Y.; Yamashita, T.; et al. Dynamic modification of sphingomyelin in lipid microdomains controls development of obesity, fatty liver, and type 2 diabetes. *J. Biol. Chem.* **2011**, *286*, 28544–28555. [[CrossRef](#)] [[PubMed](#)]
45. Li, Z.; Zhang, H.; Liu, J.; Liang, C.P.; Li, Y.; Li, Y.; Teitelman, G.; Beyers, T.; Bui, H.H.; Peake, D.A.; et al. Reducing plasma membrane sphingomyelin increases insulin sensitivity. *Mol. Cell Biol.* **2011**, *31*, 4205–4218. [[CrossRef](#)]
46. Igal, R.A.; Mandon, E.C.; de Gómez Dumm, I.N. Abnormal metabolism of polyunsaturated fatty acids in adrenal glands of diabetic rats. *Mol. Cell Endocrinol.* **1991**, *77*, 217–227. [[CrossRef](#)]
47. Gross, I.; Ballard, P.L.; Ballard, R.A.; Jones, C.T.; Wilson, C.M. Corticosteroid stimulation of phosphatidylcholine synthesis in cultured fetal rabbit lung: Evidence for de novo protein synthesis mediated by glucocorticoid receptors. *Endocrinology* **1983**, *112*, 829–837. [[CrossRef](#)]
48. Declèves, A.E.; Zolkipli, Z.; Satriano, J.; Wang, L.; Nakayama, T.; Rogac, M.; Le, T.P.; Nortier, J.L.; Farquhar, M.G.; Naviaux, R.K.; et al. Regulation of lipid accumulation by AMP-activated kinase [corrected] in high fat diet-induced kidney injury. *Kidney Int.* **2014**, *85*, 611–623. [[CrossRef](#)]
49. Miyamoto, S.; Hsu, C.C.; Hamm, G.; Darshi, M.; Diamond-Stanic, M.; Declèves, A.E.; Slater, L.; Pennathur, S.; Stauber, J.; Dorrestein, P.C.; et al. Mass Spectrometry Imaging Reveals Elevated Glomerular ATP/AMP in Diabetes/obesity and Identifies Sphingomyelin as a Possible Mediator. *EBioMedicine* **2016**, *7*, 121–134. [[CrossRef](#)]
50. Soler, M.J.; Riera, M.; Battle, D. New experimental models of diabetic nephropathy in mice models of type 2 diabetes: Efforts to replicate human nephropathy. *Exp. Diabetes Res.* **2012**, *2012*, 616313. [[CrossRef](#)]
51. Becker, K.A.; Riethmuller, J.; Seitz, A.P.; Gardner, A.; Boudreau, R.; Kamler, M.; Kleuser, B.; Schuchman, E.; Caldwell, C.C.; Edwards, M.J.; et al. Sphingolipids as targets for inhalation treatment of cystic fibrosis. *Adv. Drug Deliv. Rev.* **2018**, *133*, 66–75. [[CrossRef](#)] [[PubMed](#)]
52. Inker, L.A.; Schmid, C.H.; Tighiouart, H.; Eckfeldt, J.H.; Feldman, H.I.; Greene, T.; Kusek, J.W.; Manzi, J.; Van Lente, F.; Zhang, Y.L.; et al. Estimating glomerular filtration rate from serum creatinine and cystatin C. *N. Engl. J. Med.* **2012**, *367*, 20–29. [[CrossRef](#)] [[PubMed](#)]
53. Stevens, P.E.; Levin, A.; Kidney Disease: Improving Global Outcomes Chronic Kidney Disease Guideline Development Work Group, M. Evaluation and management of chronic kidney disease: Synopsis of the kidney disease: Improving global outcomes 2012 clinical practice guideline. *Ann. Intern. Med.* **2013**, *158*, 825–830. [[CrossRef](#)] [[PubMed](#)]
54. Neschen, S.; Scheerer, M.; Seelig, A.; Huypens, P.; Schultheiss, J.; Wu, M.; Wurst, W.; Rathkolb, B.; Suhre, K.; Wolf, E.; et al. Metformin supports the antidiabetic effect of a sodium glucose cotransporter 2 inhibitor by suppressing endogenous glucose production in diabetic mice. *Diabetes* **2015**, *64*, 284–290. [[CrossRef](#)] [[PubMed](#)]
55. Zukunft, S.; Prehn, C.; Röhring, C.; Möller, G.; Hrabě de Angelis, M.; Adamski, J.; Tokarz, J. High-throughput extraction and quantification method for targeted metabolomics in murine tissues. *Metabolomics* **2018**, *14*, 18. [[CrossRef](#)]
56. Naimi, A.I.; Moodie, E.E.; Auger, N.; Kaufman, J.S. Constructing inverse probability weights for continuous exposures: A comparison of methods. *Epidemiology* **2014**, *25*, 292–299. [[CrossRef](#)]
57. Robins, J.M.; Hernán, M.A.; Brumback, B. Marginal structural models and causal inference in epidemiology. *Epidemiology* **2000**, *11*, 550–560. [[CrossRef](#)]

Apendix A: Paper III

Title: Multi-omics landscape of chronic kidney disease in individuals with prediabetes or type 2 diabetes: from associations towards precision medicine.

Authors: Jialing Huang, Marcela Covic, Gisela Fobo, Corinna Montrone, Zhi Zhao, Arthur Gilly, N William Rayner, Cornelia Huth, Barbara Thorand, Margit Heier, Sonja Kunze, Melanie Waldenberger, Harald Grallert, Gabi Kastenmüller, Jerzy Adamski, Martina Müller-Nurasyid, Konstantin Strauch, Thomas Meitinger, Wolfgang Koenig, Christian Herder, Wolfgang Rathmann, Michael Roden, Johannes Graumann, Freimut Schliess, Christian Gieger, Andreas Ruepp, Eleftheria Zeggini, Karsten Suhre, Annette Peters*, Rui Wang-Sattler*

Status: Manuscript

Multi-omics landscape of chronic kidney disease in individuals with prediabetes or type 2 diabetes: from associations towards precision medicine

Jialing Huang^{1,2}, Marcela Covic¹, Gisela Fobo³, Corinna Montrone³, Zhi Zhao⁴, Arthur Gilly², N William Rayner², Cornelia Huth⁵, Barbara Thorand^{5,6}, Margit Heier^{5,7}, Sonja Kunze¹, Melanie Waldenberger¹, Harald Grallert¹, Gabi Kastenmüller⁸, Jerzy Adamski^{3,9}, Martina Müller-Nurasyid^{10,11}, Konstantin Strauch^{10,11}, Thomas Meitinger¹², Wolfgang Koenig¹³, Christian Herder^{6,14}, Wolfgang Rathmann^{6,15}, Michael Roden^{6,14}, Johannes Graumann¹⁶, Freimut Schliess¹⁷, Christian Gieger¹, Andreas Ruepp³, Eleftheria Zeggini^{2,18}, Karsten Suhre¹⁹, Annette Peters^{5,11,20,21*}, Rui Wang-Sattler^{1,2,6,21*}

¹ Research Unit of Molecular Epidemiology, Institute of Epidemiology, Helmholtz Zentrum München, German Research Center for Environmental Health (HMGU), Neuherberg, Germany

² Institute of Translational Genomics, HMGU, Neuherberg, Germany

³ Institute of Experimental Genetics, HMGU, Neuherberg, Germany

⁴ Institute for Cancer Research, Department of Cancer Genetics, Oslo University Hospital, Oslo, Norway; Centre for Biostatistics and Epidemiology (OCBE), Faculty of Medicine, University of Oslo, Oslo, Norway

⁵ Institute of Epidemiology, HMGU, Neuherberg, Germany

⁶ German Center for Diabetes Research (DZD), München-Neuherberg, Germany.

⁷ KORA Study Centre, University Hospital of Augsburg, Augsburg, Germany

⁸ Institute of Computational Biology, HMGU, Neuherberg, Germany

⁹ Department of Biochemistry, Yong Loo Lin School of Medicine, National University of Singapore, Singapore; Institute of Biochemistry, Faculty of Medicine, University of Ljubljana, Ljubljana, Slovenia.

¹⁰ Institute of Genetic Epidemiology, HMGU, Neuherberg, Germany; Institute of Medical Biostatistics, Epidemiology and Informatics, University Medical Center, Johannes Gutenberg University, Mainz, Germany

¹¹ Institute for Medical Information Processing, Biometry and Epidemiology, Faculty of Medicine, Ludwig-Maximilians-University (LMU), Munich, Germany

¹² Institute of Human Genetics, Klinikum rechts der Isar, Technical University of Munich (TUM), Munich, Germany.

¹³ Deutsches Herzzentrum München, TUM, Munich, Germany, German Centre for Cardiovascular Research (DZHK), partner site Munich Heart Alliance, Munich, Germany and Institute of Epidemiology and Medical Biometry, University of Ulm, Ulm, Germany

¹⁴ Institute for Clinical Diabetology, German Diabetes Center, Leibniz Center for Diabetes Research at Heinrich Heine University Düsseldorf, Düsseldorf, Germany; Department of Endocrinology and Diabetology, Medical Faculty and University Hospital Düsseldorf, Heinrich Heine University, Düsseldorf, Düsseldorf, Germany

¹⁵ Institute for Biometrics and Epidemiology, German Diabetes Center, Leibniz Center for Diabetes Research at Heinrich Heine University, Düsseldorf, Germany.

¹⁶ Institute of Translational Proteomics, Department of Medicine, Philipps-Universität Marburg, Marburg, Germany

¹⁷ Profil Institut für Stoffwechselforschung GmbH, Hellersbergstraße 9, Neuss, Germany

¹⁸ Klinikum Rechts der Isar, TUM, TUM School of Medicine, Munich, Germany

¹⁹ Department of Physiology and Biophysics, Weill Cornell Medicine-Qatar, Doha, Qatar

²⁰ Department of Environmental Health, Harvard School of Public Health, Boston, USA.

²¹ These authors contributed equally

*Correspondence and requests for materials should be addressed to A.P. & R.W.-S. (E-mails: peters@helmholtz-muenchen.de; ruj.wang-sattler@helmholtz-muenchen.de)

Abstract

Precision medicine relies on molecular signatures informing the assessment of individual disease risks, the identification of sub-clinical diseases, and the initiation of personalized prevention and treatment measures. Multi-omics signatures enable a detailed molecular and physiological profiling of an individual's health and disease. Chronic kidney disease (CKD) is a multifactorial condition involving complex pathogenetic processes. We used the longitudinal population-based KORA cohort for a five-level multi-omics (genotyping, DNA methylation, transcriptomics, proteomics, and metabolomics) and clinical assessment of risk signatures prognosticating CKD, thereby covering a 13-year follow-up of individuals. Multi-omics analysis identified 120 candidate biomarkers of CKD in hyperglycemia, of which 64 were replicated and 11 were potentially novel. Our constructed genome-wide polygenic score (GPS) of the estimated glomerular filtration rate (eGFR) showed a strong association with eGFR in the KORA and UK biobank cohorts. Integrating evidence from the association of various omics signatures with eGFR and urinary albumin to creatinine ratio (UACR) phenotypes, genetic analyses (Mendelian Randomization and GPS), and hypothesized pathogenetic traits underlying diabetes-related CKD, we classified 64 replicated candidates into subgroups and connected them to kidney traits to provide insight into their possible roles in personalized management of hyperglycemia-related CKD.

By investigating the interplay between multi-omics markers in hyperglycemia, e.g. by causal mediation analysis, we unraveled novel regulatory interactions between molecular pathways and kidney pathogenetic traits. Moreover, GPS, candidate proteins, and metabolites can improve the prognosis of future CKD in individuals with hyperglycemia. We identified three potentially novel

proteins that classify CKD patients with hyperglycemia into three subgroups more effectively than eGFR and UACR, confirming that distinct pathogenetic traits are predominant in different subgroups of CKD patients, which opens the possibility for personalized prevention and treatment measures targeting distinct molecular pathways towards clinically overt CKD. Altogether, our study presents a systematic multi-omics landscape of CKD in hyperglycemia and demonstrates how to integrate multi-omics profiles for applications to precision medicine.

Keywords

Multi-omics; chronic kidney disease; diabetic kidney disease; prediabetes, type 2 diabetes; causality; Mendelian Randomization; genome-wide polygenic score; precision medicine; prediction.

Introduction

Multi-omics and computational methods show a high potential to improve precision medicine. By combining multi-omics profiling and clinical assessment of a large longitudinal cohort, one can assess individuals' health status comprehensively, identify deviations from baseline and follow the progression of illness, reveal differences between disease cases and healthy controls, and explore the underlying pathophysiological mechanism and pathway, all of which may improve the precision of disease detection and treatment. Despite this promise, few studies have used emerging technologies such as multi-omics profiling in prospective population-based cohorts to identify prognostic disease markers and improve disease management. Commonly, a multi-omics approach is claimed when using up to two levels of omics analysis ¹. While a longitudinal follow-up study reported it used deep multi-omics profiling, the employed sample size (109 individuals) remained limited ².

Chronic kidney disease (CKD) affects approximately 9.1% of the global population ³. Diabetes accounts for 30–50% of all CKD cases ⁴, and undiagnosed diabetes and prediabetes have been associated with a high prevalence of CKD in various populations ^{5,6}. We have explored targeted metabolite profiles of CKD in people with pre-diabetes and type 2 diabetes (T2D) and identified two candidate metabolite biomarkers of incident CKD and a set of predictors ^{7,8}. Early detection of sub-clinical CKD would contribute to improving CKD prevention, care and management, thus reducing morbidity, mortality, and healthcare costs.

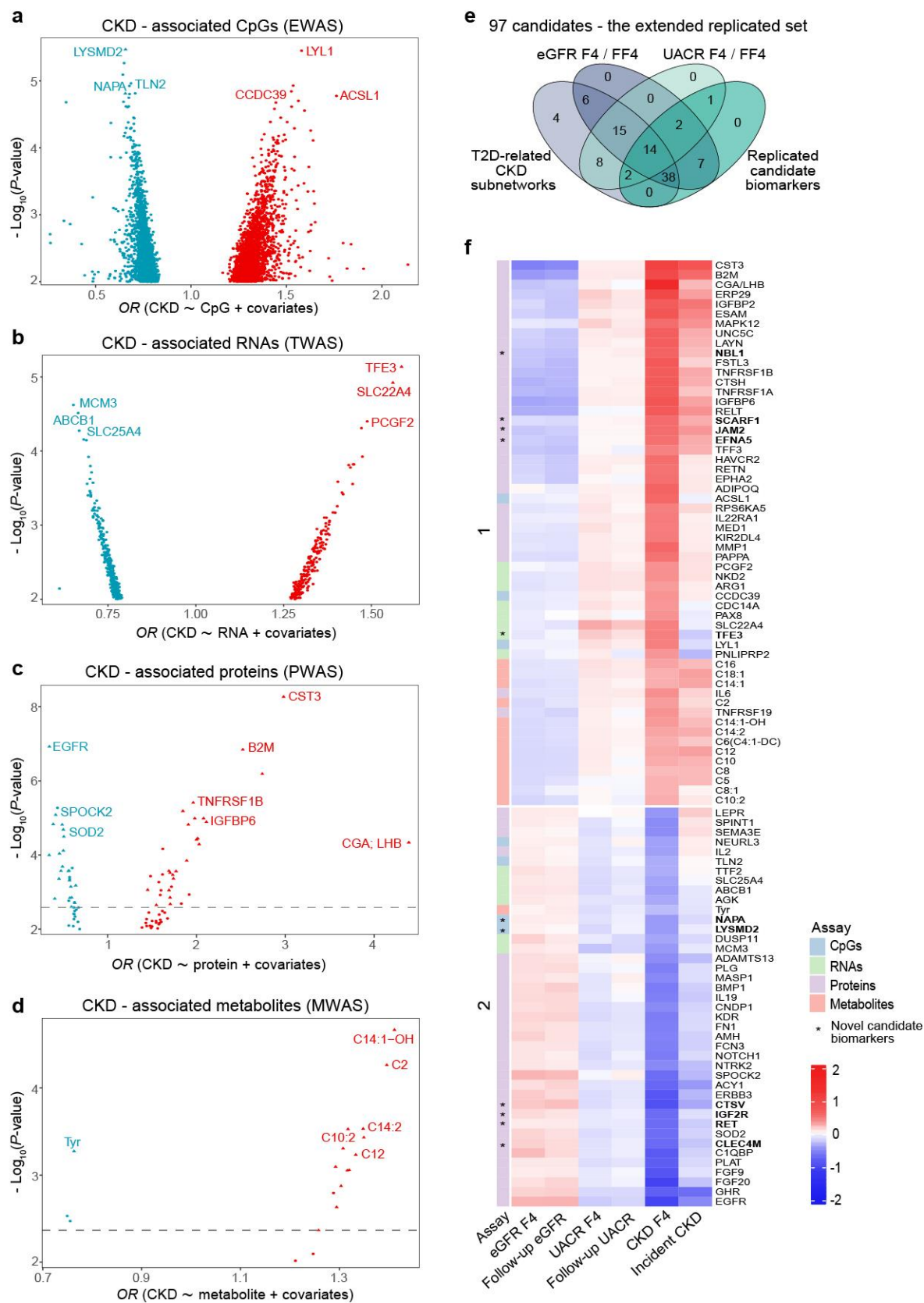
CKD is a multifactorial condition driven by diverse and highly networked pathological processes. It is therefore critical to investigate the specific roles of molecular hallmarks of diabetes-related CKD by means of multi-omics analyses. Due to the complex pathogenetic traits of CKD, identifying sensitive and specific biomarkers that reflect its pathogenetic diversity can improve understanding of the disease and possibly prevent or treat it more precisely at earlier stages. A number of studies have identified omics signatures at a single omics level, and few have examined the underlying interactions between these omics signatures at multiple levels. Exploring the correlations between multi-level omics signatures is necessary to better understand the diversity of individual pathogenetic traits underlying the complex molecular regulation of CKD.

Currently, most proposed biomarkers are based on observational data. To determine the "true" relationship and directionality between such omics profiles and clinical traits, two-sample Mendelian Randomization (2SMR) is a valid approach. The genome-wide polygenic score (GPS) can identify individuals at high genetic risk and signatures at other omics levels that reflect the translation of genetic information into phenotypes. Out of a large number of omics molecules, those that show dominance in the prediction of early CKD when added to currently proposed predictors remain unknown. Also, it is essential to investigate ways to maximize the utility of multi-omics molecular profiles to improve CKD early detection. Moreover, the ability of omics molecules to subtype hyperglycemia-related CKD and the unique patterns in each subgroup need to be explored to benefit for targeted prevention and therapy.

In the present study, individuals from the population-based adult KORA (Cooperative Health Research in Augsburg) cohort have been longitudinally profiled using clinical laboratory tests and multi-omics assessments⁹. The study had three objectives (Extended Data Fig.1). We first sought to identify subgroups of omics signatures we identified and replicated for hyperglycemia-related CKD based on various evidence that included omics signatures-associated phenotypes (i.e., eGFR and urinary albumin to creatinine ratio (UACR)), genetic evidence (i.e., MR and GPS), and knowledge on potential pathophysiologies of diabetes-related CKD. We further suggest potentially novel candidate biomarkers of CKD in hyperglycemia. Second, we examined the potential interplay among multi-omics molecules (i.e., candidates and established biomarkers) of CKD in hyperglycemia to explore the directionality of nephrogenic effects in the connected molecular pathways, potential new causal links, and relevant molecular traits. Third, we explored the prediction of incident CKD and subtyping CKD patients in hyperglycemia using multi-omics profiles. For the prediction part, we proposed cut-off omics levels, the dominant predictive molecules on top of current suggested predictors and highlighted the GPS we built and replicated.

Along with shedding new light on the mechanisms of CKD, our study presents a complex multi-omics landscape for the disease in hyperglycemia and provides deep insight into the effective integration of multi-omics profiles for personalized disease management.

Fig. 1



Results

Identification and replication of multi-omics signatures of CKD associated with kidney traits in hyperglycemia

In a total of 1,401 individuals with prediabetes and T2D, the KORA F4 study contains 166, 206, 59, and 282 CKD cases, for which quality control (QC)-passed epigenomic, transcriptomic, proteomic, and metabolomic-data are available, respectively. Compared with non-CKD individuals, CKD cases were significantly older and displayed higher values of BMI, HbA_{1c}, FG, UACR (current F4 and follow-up FF4), as well as lower eGFR values (Supplementary Table 1). They also self-reported significantly higher anti-hypertensive and anti-diabetic medication.

From these hyperglycemic subcohorts, we identified 120 CKD-associated candidates (20 CpG sites, 20 RNAs, 63 proteins and 17 metabolites) using epigenome-, transcriptome-, proteome-, and metabolome-wide association studies (EWAS, TWAS, PWAS, MWAS), respectively (Figs. 1a-1d, Supplementary Tables 2-5). These associations were independent of age, sex, body mass index (BMI), systolic blood pressure (BP), smoking status, triglycerides, total cholesterol, high-density lipoprotein (HDL) cholesterol, fasting glucose (FG), use of lipid-lowering, antihypertensive and anti-diabetic medication (defined as full model). The strongest significant CKD-associated CpG site was cg22872478 (*LYSMD2*), while the top two significant RNAs were gene expression *TFE3* (ILMN_1764826) and *SLC22A4* (ILMN_1685057). In the proteomic data, CST3 and EGFR were the most significant positive and negative molecules associated with CKD, respectively. Of the identified 17 metabolites, 14 were acylcarnitines, with Tyr being the most significant negative metabolite.

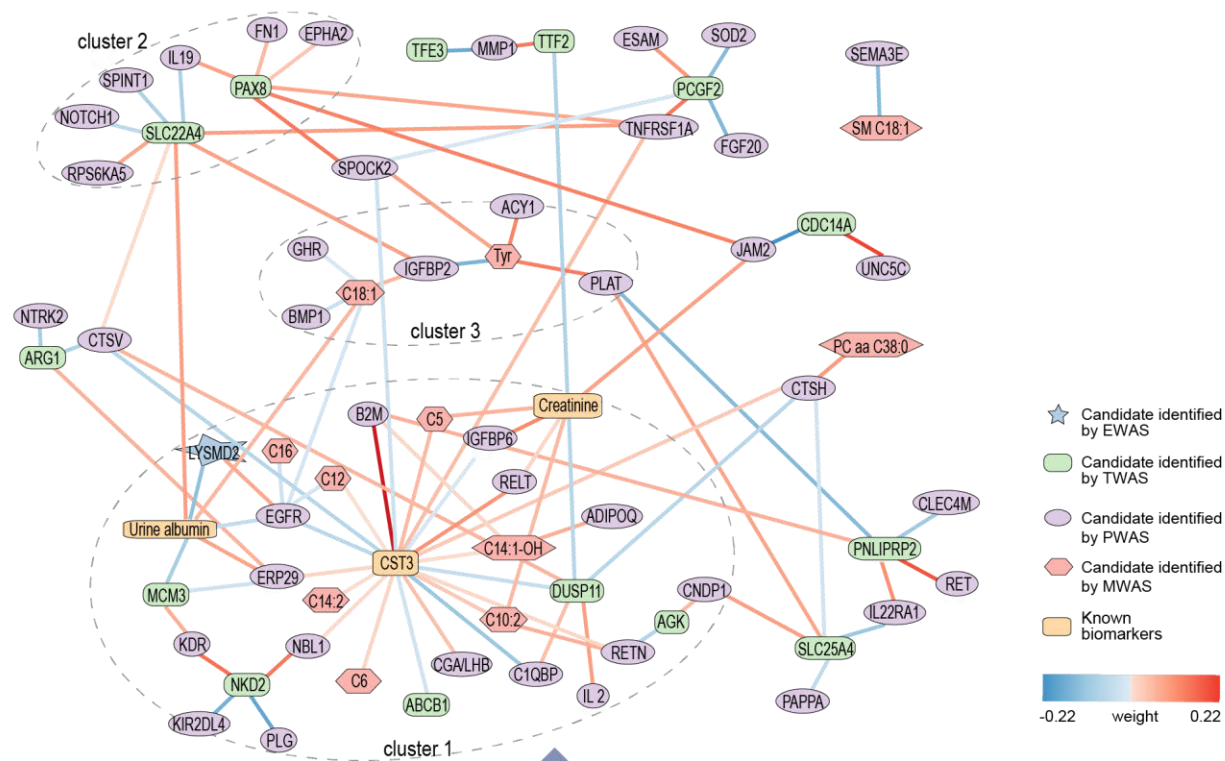
Of the 120 candidate biomarkers, 114 molecules interacted with hyperglycemia, while two metabolites (C14:1-OH and C16) and four proteins (CST3, FSTL3, CTSH and RELT) were also significantly associated (FDR < 0.05) with CKD in individuals with normal glucose tolerance (NGT) of KORA F4 (Supplementary Table 6). To explore potential networks underpinning these 120 candidate biomarkers, we subjected them to CIDeR-based multifactorial interaction network analyses¹⁰. We further found that 87 of 120 candidates or their corresponding genes/proteins were functionally involved in eight T2D-related CKD (T2DCKD) subnetworks: Tyr in diabetic kidney disease (DKD) (T2DCKDtyr), mitochondrial dysfunction (T2DCKDmito), innate immune response in DKD (T2DCKDinna), adipokine influence on DKD (T2DCKDadipo), renin-angiotensin system (RAS) dysfunction in DKD (T2DCKDras), extracellular matrix deposition and renal fibrosis (T2DCKDfibri), advanced glycation end-products (T2DCKDage) and angiogenesis (T2DCKDangi) (Extended Data Fig. 2, Supplementary Figs. 1-7, Supplementary Tables 7-14).

Aiming to replicate our findings in additional studies exhibiting omics-data with CKD, we achieved replication for two CpGs, two RNAs in the KORA F3 study, 46 proteins in the Qatar Biobank (QBB)¹¹ or the Qatar Metabolomics Study on Diabetes (QMDiab) studies, as well as 14 metabolites in the KORA F3 or FF4 studies (Supplementary Tables 2-5). Taken together, 64 candidates were replicated.

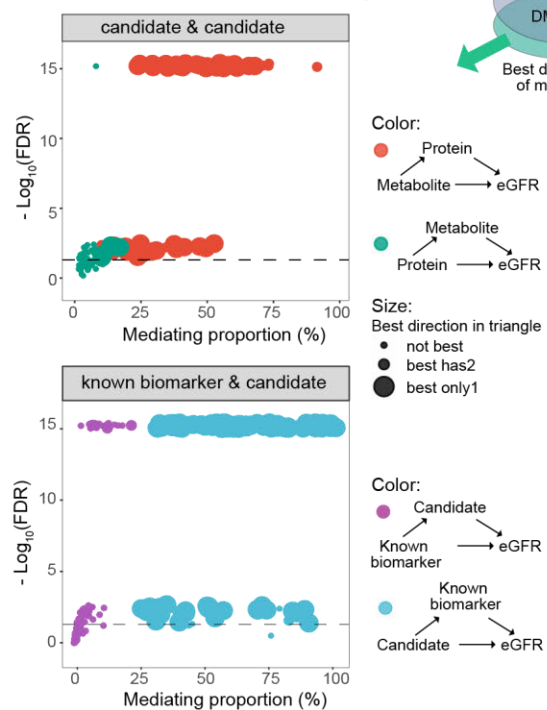
Merging the 64 replicated candidates and 87 molecules involved in eight T2DCKD subnetworks resulted in a set of 97 (i.e. 7 CpGs, 14 RNAs, 62 proteins and 14 metabolites, Fig. 1e, Supplementary Table 15) that were considered as the extended replicated set. It comprises two groups: group 1 with 56 candidates overall negatively associated with eGFR, positively associated with UACR and CKD in hyperglycemia, and group 2 with 41 candidates inversely associated (Fig. 1f). For instance, proteins CST3 and EGFR were the top candidates and representative omics molecules in group 1 and 2, respectively. Protein CST3 showed the strongest negative associations with eGFR values F4 and FF4, while protein EGFR achieved the largest positive regression coefficients. Notably, only protein EGFR was associated with F4 and FF4 eGFR and UACR in hyperglycemia after FDR correction (Extended Data Fig. 3a). Moreover, four proteins (GHR, EGFR, CST3 and B2M) and three metabolites (C12, C14:1 and C18:1) associated with incident CKD in hyperglycemia when using the fully adjusted model and accounting for multiple testing (Extended Data Fig. 3b, Supplementary Table 15).

Fig. 2

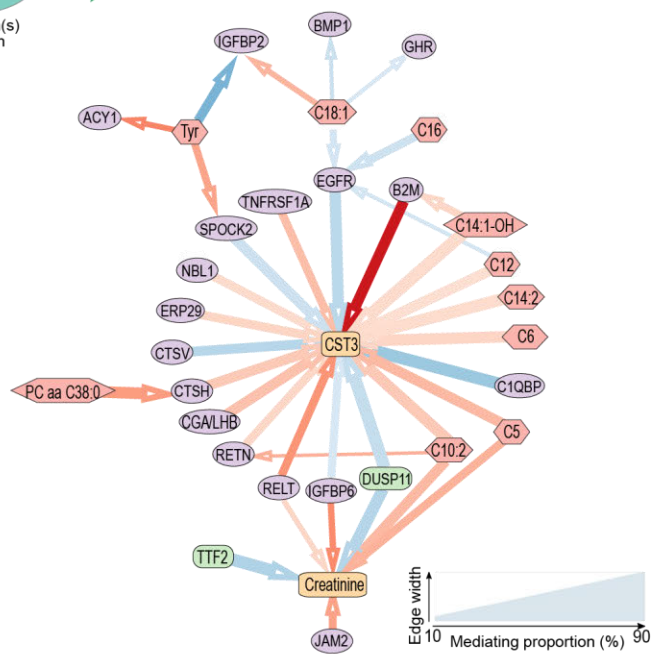
a Different levels of multi-omics integration network (DMOIN)



b Best direction(s) of mediation, e.g.



c Directed mediating multi-omics integration network (DMMOIN), e.g. omics1 → omics2 → eGFR



Integration of four-level omics molecules in hyperglycemia to explore potential interplay across distinct omics levels

Multi-omics integration network (MOIN). Generating an optimal Gaussian Graphical Modeling (GGM) with 101 molecules from four omics levels revealed a potential crosstalk beyond analyte classes (Supplementary Table 16). Intra-omics were found to be more highly associated than inter-omics connections (Extended Data Fig. 4). To investigate inter-omics associations, the edges of the integrated network from different analyte classes were used to construct different levels of MOIN (DMOIN), from which ten sub-clusters emerged using the Markov Cluster Algorithm (MCL) (Fig. 2a), with the largest cluster (cluster 1, 31 nodes) primarily representing subnetworks related to T2DCKD_{intra} and -_{mito}. Cluster 1 included three well-known biomarkers as cluster hubs, with protein B2M displaying the strongest positive correlation with CST3. Furthermore, six (C10:2, C12, C5, C14:2, C14:1-OH and C6) of the eight acylcarnitines preserved in the network exhibited positive linkages to CST3 or creatinine, while C16 and C12 had negative linkages to protein EGFR, which itself was negatively related to urine albumin and CST3. The second largest cluster (cluster 2) had eight nodes. One of the cores, *SLC22A4*, functioning as a transporter for acylcarnitines¹² and ergothioneine¹³, was negatively associated with IL19, SPINT1 and NOTCH1, and positively associated with urine albumin, IGFBP2, and TNFRSF1A. Notably, the T2DCKD_{mito} subnetwork included *SLC22A4* and its four associated omics candidates (IL19, RPS6KA5, NOTCH1, and IGFBP2). Subnetwork T2DCKD_{tyr} regulation was placed into the third largest cluster (cluster 3), including five of the network's seven nodes. Tyr correlated positively with PLAT and ACY1, and negatively with IGFBP2. Tyr's role in the DMOIN network appears distinct from the majority of acylcarnitines, which agreed that they belonged to two distinct clusters based on associations with eGFR and UACR values in hyperglycemia (Fig. 1f).

Candidate proteins and three known biomarkers identified as main mediators connecting omics signatures and kidney traits in hyperglycemia. To identify mediators among different levels of molecules and three time-point (S4 / F4 / FF4) kidney traits (CKD, eGFR and UACR), as well as reveal the optimal mediation directions, we performed causal mediation analysis in three parts (Supplementary Fig. 8). When analyzing part 1 (candidate & candidate & kidney trait, see “Online method”), 640 out of 994 tested mediating triangles were eligible mediating results when kidney trait was used as independent variable (X) or outcome (Y) (Fig. 2b, Extended Data Fig. 5a). Of these 640, 82 were found to be the only best direction (best only1) for the triangles they derived from, and 30 were observed with two possible best directions (best has2) for the corresponding triangles. We further found that 77 of 82 (94%) candidate proteins acted as mediators between candidates (particularly metabolites) and kidney traits (e.g., metabolite → protein → kidney trait, Fig. 2b, Extended Data Fig. 5a, Supplementary Table 17).

For the part 2 (candidate & known biomarkers & kidney trait) analysis, 165 FDR significant molecule pairs between the three known biomarkers and 96 candidates were found, with 72 candidates linked to CST3, 58 to creatinine, and 35 to urine albumin. Of 2,354 tested mediating triangles, 1,534 eligible mediating results were found when the kidney trait was used as X or Y, 191 and 148 of which were found as the best only1 and best has2 for the triangles they derived from, respectively. When one of three known biomarkers acted as a mediator (candidate → known

biomarkers → kidney trait, and kidney trait → known biomarkers → candidate), a majority (187 of 191) represented best directions (Fig. 2b, Extended Data Fig. 5b, Supplementary Table 18). Additionally, in the part 3 (2-mets & kidney traits) analysis, SM C18:1 → creatinine → follow-up eGFRcr (eGFR was calculated from serum creatinine FF4) values and PC aa C38:0 → CTSH → follow-up eGFRcr were found as the best direction in the corresponding triangles (Supplementary Table 19).

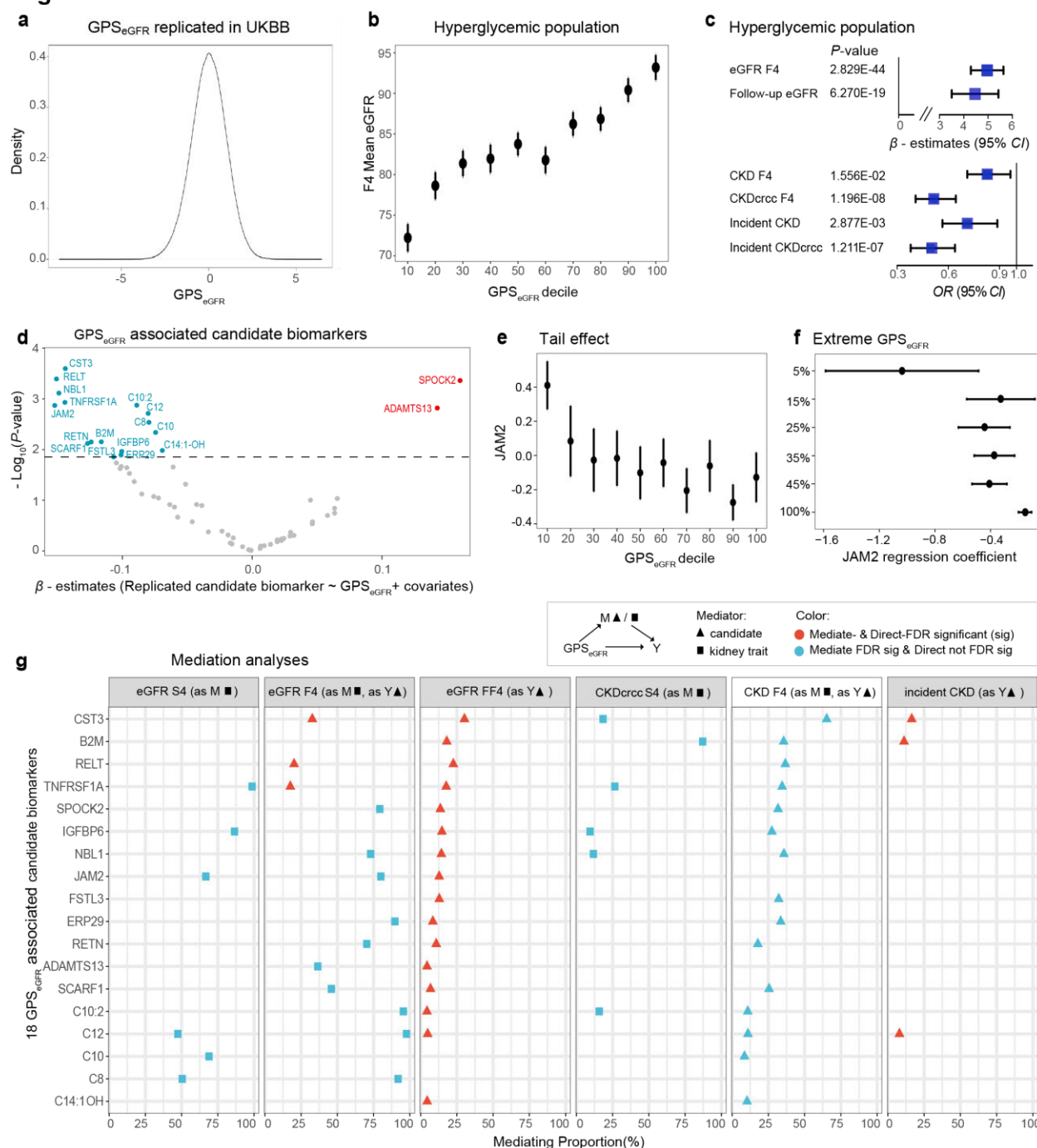
Moreover, for candidate → kidney trait → candidate, only the kidney trait eGFR were kept after structural equation modeling (SEM)¹⁴ and contained best mediation directions (Extended Data Fig. 5c). The best directions were found for known biomarkers → CKD → candidate, as well as candidate → eGFR / UACR → known biomarkers, respectively (Extended Data Fig. 5d).

Taken together, the causal mediation analysis identified 565 best mediation directions, pointing to a complex omics network of regulatory interactions between different levels of molecules and kidney traits. When the kidney trait was served as an X or Y in mediating triangles, the results showed that our candidate proteins and three known biomarkers were major mediators in connecting other omics candidates to kidney traits in both directions.

Directed mediating multi-omics networks reveal potential causal links and relevant molecular pathways. To increase the possibility of identifying potential causal links and relevant molecular pathways, we mapped our DMOIN with the best mediation directions' results from the causal mediation analyses to generate a directed mediating MOIN (DMMOINs) (Fig. 2c, Extended Data Fig. 6, Supplementary Table 20). When CKD was identified as potentially causal X in the mediating triangles, the directed network had 25 nodes and 30 edges with CST3 as the center, followed by creatinine. CST3 served as a mediator to connect 13 molecules and CKD. Interestingly, CST3-B2M, CST3-C1QBP, CST3-CTSH and CST3-NBL1 presented both directions (Extended Data Fig. 6a). When CKD was identified as outcome Y in the mediating triangles, CST3 also represented as the center of the directed network (22 nodes and 22 edges) and served as a mediator to connect 10 molecules and CKD, such as EGFR → CST3 → CKD. We further found that there were 27 and 39 edges in the directed networks when eGFR was served as X or Y in the mediating triangles, respectively (Fig. 2c, Extended Data Fig. 6b). We observed unique mediation directions such as eGFR → EGFR → C16 (Extended Data Fig. 6b), C16 → EGFR → eGFR and PC aa C38:0 → CTSH → eGFR (Fig. 2c). Moreover, connections between C10:2 or C5 and CKD or eGFR were linked by CST3 and creatinine (Extended Data Figs. 6a, 6b). Interestingly, three proteins (EGFR, GHR and IGFBP2) mediated effects of UACR (as X) to metabolite C18:1, while urine albumin was the key hub connecting five molecules and UACR (as Y). DMMOINs were also generated when eGFR or UACR were served as mediators, but not for CKD (Extended Data Fig. 6).

Overall, the directed networks revealed potential causality (see “discussion”) in connections between molecule pairs and their associated kidney traits.

Fig. 3



Identifying the high genetic risk population for CKD and elucidating the role of omics signatures using GPS_{eGFR}

We built GPS for eGFR (GPS_{eGFR}) using reported effect size of SNPs from the CKDGen study with 567,460 European individuals (after first eliminating KORA F4 effects to avoid overfitting) in 2,757 KORA F4 individuals using 162,818 uncorrelated SNPs (LD $r^2 < 0.1$). We found that the GPS_{eGFR} strongly positively associated with eGFR values ($P = 2.233E-81$, Extended Data Fig. 7a)

in F4, and this association was successfully replicated in the UK biobank (UKBB) ($\beta = 2.541$, $P < 2E-16$, Fig. 3a) and testing samples of KORA S4 (non-overlapping individuals, $P = 3.969E-40$, Extended Data Fig. 7b). The GPS_{eGFR} showed normal distribution in F4 population and S4 testing samples, excepted for the tail part of GPS_{eGFR} , there was a trend toward an increase in eGFR values following an increase in GPS_{eGFR} values in the general (Extended Data Fig. 7a) and hyperglycemic population (Fig. 3b) of F4, and this trend was validated in S4 testing samples (Extended Data Fig. 7b).

We next analysed the associations between GPS_{eGFR} and eGFR values (current F4 and follow-up FF4), both prevalent and incident CKD_{crcc} (eGFR-based CKD) and CKD (eGFR- and UACR-based CKD) adjusted for the full model in hyperglycemia, respectively. We found that GPS_{eGFR} showed highly significant increase in eGFR values (P -value = $2.829E-44$) and its follow-up ($P = 6.270E-19$), with an SD increase in GPS_{eGFR} associated with 4.96 and 4.47 increased values, respectively (Fig. 3c). GPS_{eGFR} showed highly significant negative association with CKD_{crcc} ($P = 1.196E-08$) and incident CKD_{crcc} ($P = 1.211E-07$), and the effects were consistent for both prevalent and incident CKD (Fig. 3c).

Of 64 replicated candidates of EWAS, TWAS, PWAS and MWAS, 13 proteins and five metabolites were significantly associated with GPS_{eGFR} in hyperglycemic individuals after adjustment for multiple testing (Fig. 3d, Supplementary Table 21). All 18 GPS_{eGFR} associated candidates were significantly associated with both current and follow-up eGFR values (Supplementary Table 15). The eGFR-candidate associations and the GPS_{eGFR} -candidate associations were all directionally concordant. Protein CST3 had the strongest significance with eGFR ($P = 3.888E-80$ for current, and $P = 1.985E-49$ for its follow-up) as well as GPS_{eGFR} ($P = 2.533E-04$). Moreover, of 18 GPS_{eGFR} associated candidates, proteins CST3 and B2M and metabolite C12 demonstrated significant associations with incident CKD in hyperglycemia adjusted for the full model (Extended Data Fig. 3b, Supplementary Table 15).

Interestingly, the relationship between GPS_{eGFR} and eGFR was not linear. Indeed, the effect was estimated to be much stronger at the distribution's extremes, which was replicated in the test samples of S4 (Extended Data Fig. 7b) and consistent with the previous report¹⁵. The tail effect occurs when the ratio of the effect of the tails to the effect of the overall distribution is greater than one. Both in general and hyperglycemic population, individuals in the first decile of the GPS_{eGFR} distribution exhibited much lower eGFR values than those in other deciles (Fig. 3b, Extended Data Fig. 7), indicating that they were a potential high genetic predisposition subpopulation of developing reduced eGFR values.

To assess this tail effect for the 18 GPS_{eGFR} associated candidates, we stratified the hyperglycemic KORA F4 population according to GPS_{eGFR} deciles. We found a steeper slope for 15 candidate measures at the lower and/or upper extremes of the distribution (Fig. 3e, Supplementary Fig. 9). Additionally, GPS_{eGFR} had a greater than 5-fold effect on 12 candidates (TNFRSF1A, FSTL3, ADAMTS13, RETN, B2M, ERP29, JAM2, NBL1, SPOCK2, C8, C10 and C12) in the 5% tail of the population compared to the full data (Fig. 3f, Supplementary Fig. 10, Supplementary Table

23). Therefore, we observed 11 candidates (TNFRSF1A, FSTL3, ADAMTS13, C8, RETN, B2M, ERP29, JAM2, C10, SPOCK2 and C12) exhibiting strong tail effects with GPS_{eGFR} , not only by presenting a steeper slope regarding eGFR at the extremes of the distribution of GPS_{eGFR} , but also by showing strong tail effects for the associations with GPS_{eGFR} . It demonstrated that extreme GPS_{eGFR} may strongly influence these 11 candidates' levels in hyperglycemia (Figs. 3e-f, Supplementary Figs. 9-10).

With the generated GPS_{eGFR} as potentially causal X, we performed mediation analyses to examine potential mediation effect of kidney traits with 18 identified GPS_{eGFR} -associated candidates. Using eGFR and CKD from three time points (S4 / F4 / FF4), the mediation results indicated that 11 candidates (protein TNFRSF1A, SPOCK2, IGFBP6, NBL1, JAM2, ERP29, RETN, ADAMTS13, SCARF1, metabolite C10:2 and C12) showed both directions for eGFR (e.g., $GPS_{eGFR} \rightarrow eGFR$ S4 \rightarrow TNFRSF1A and $GPS_{eGFR} \rightarrow TNFRSF1A \rightarrow eGFR$ F4/FF4). The value of eGFR S4 mediated 98.57% effect between GPS_{eGFR} and TNFRSF1A. Five candidates (CST3, B2M, RELT, FSTL3 and C14:1-OH) were identified as mediators for eGFR F4 / FF4. Two metabolites (C10 and C8) were found as outcomes for eGFR S4 / F4. Regarding CKD, six candidates (CST3, B2M, TNFRSF1A, IGFBP6, NBL1 and C10:2) presented both directions, while nine candidates (RELT, SPOCK2, FSTL3, ERP29, SCARF1, C12, C10, C8 and C14:1-OH) were identified as mediators for CKD F4/FF4. Strikingly, none of the 18 candidates had significant mediation effects when CKD F4 was used as a mediator, whereas 10 candidates significantly mediated by eGFR F4 (Fig. 3g, Supplementary Table 22).

Potential causal associations between circulating proteins / metabolites and kidney traits

Elucidating causal disease pathways can contribute to develop reliable treatment strategies. We performed a bidirectional 2SMR analysis¹⁶ to identify proteins and metabolites that may play a causal role in the development of kidney traits and reverse, respectively (Fig. 4, Supplementary Tables 24-26).

Of 46 proteins and 14 metabolites that were successfully validated in QBB / QMDiab and in KORA F3 / FF4 study, respectively, we identified suitable genetic instruments for 44 proteins and 13 metabolites (Supplementary Tables 24, 26). Our robust adjusted profile score (RAPS) analysis revealed significant (FDR < 0.05) associations of three candidates (protein SOD2 and metabolites Tyr and C8:1) to CKD, nine candidates to eGFR, and six metabolites to UACR (Fig. 4). Among the candidates with significant MR estimates, eight (IGFBP6, ESAM, EPHA2, Tyr, C8:1, C5, C18:1, and C14:2) for eGFR and five (C5, C2, C18:1, C14:2, and C12) for UACR showed significant evidence of heterogeneity and/or horizontal pleiotropy. We further used outliers-corrected MR analyses to control heterogeneity and horizontal pleiotropy in these MR estimates. Accordingly, four (Tyr, C8:1, C5 and C14:2) out of eight for eGFR values, two (C5 and C14:2) of five for UACR values consistently reached FDR significance with outliers-corrected IVW/Wald ratio or MR_PRESSO outliers-corrected using the SNPs after removing outliers, respectively.

Additionally, ERBB3-to-UACR and C10:2-to-eGFR reached FDR significance with outlier-corrected Wald ratio.

In the case of protein to kidney trait, a second set of genetic instruments summarized by Zheng *et al*¹⁷ was available and 23 of 46 proteins had available MR estimates for either CKD, eGFR, or UACR (Supplementary Table 25). We found that five of 23 proteins (CGA;LHB, PLAT, ADAMTS13, SCARF1 and IGF2R) were nominally significant using the first set, their causal estimates were all directionally consistent using the second set. With the second set of instruments, seven proteins (ESAM, CGA;LHB, CTSH, PLAT, HAVCR2, PLG and B2M) were associated ($P < 0.05$) with at least one kidney trait, all except ESAM were estimated consistently with the first set. Moreover, CGA;LHB and PLAT were significant in the first set. Additionally, the second set revealed that proteins B2M and PLG had FDR associations (B2M-to-CKD, B2M-to-eGFR, B2M-to-UACR, and PLG-to-eGFR). The first set had no available instruments for B2M but yielded a consistent causal estimate that was not significant for PLG-to-eGFR.

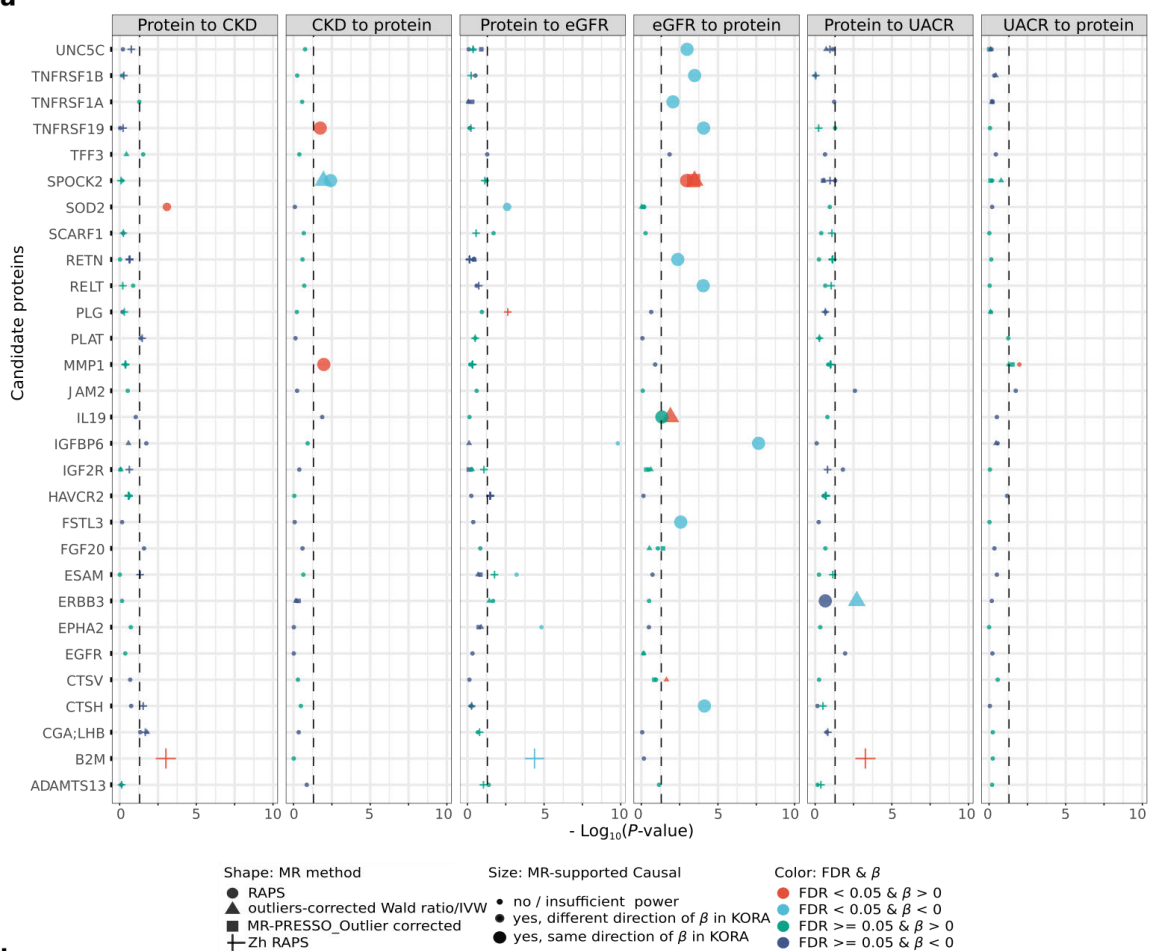
In summary, the associations of four candidates (SOD2, B2M, Tyr, and C8:1)-to-CKD, seven candidates (SOD2, B2M, Tyr, C8:1, C5, C14:2, and C10:2)-to-eGFR, and five candidates (B2M, ERBB3, C8:1, C5, and C14:2)-to-UACR were suggested to be affected by genetic predisposition.

We next investigated the reverse direction, i.e., whether a genetic predisposition to kidney traits affects blood protein and/or metabolite levels. We identified suitable genetic instruments of kidney traits on 46 proteins and 11 metabolites. The 2SMR analyses indicated a significant (RAPS, FDR < 0.05) effect of CKD on three proteins (TNFRSF1A, SPOCK2 and MMP1); of eGFR on 14 candidates (10 proteins and four metabolites); of UACR on protein MMP1, respectively (Fig. 4, Supplementary Table 24, 26). Of which, CKD/eGFR-to-SPOCK2, UACR-to-MMP1 showed significant evidence of heterogeneity or horizontal pleiotropy of the genetic instruments. The corresponding outliers-corrected MR analyses indicated that CKD-to-SPOCK2 and eGFR-to-SPOCK2 consistently reached FDR significance. Additionally, IL19-to-eGFR reached FDR significance with outlier-corrected IVW. In summary, three proteins (TNFRSF1A, SPOCK2 and MMP1) were identified as being influenced by genetic predisposition from CKD, 15 candidates including 11 proteins (UNC5C, TNFRSF1B, TNFRSF1A, TNFRSF119, SPOCK2, RETN, RELT, IGFBP6, FSTL3, CTSH and IL19) and four metabolites (C8:1, C2, C14:2 and C10:2) were from eGFR.

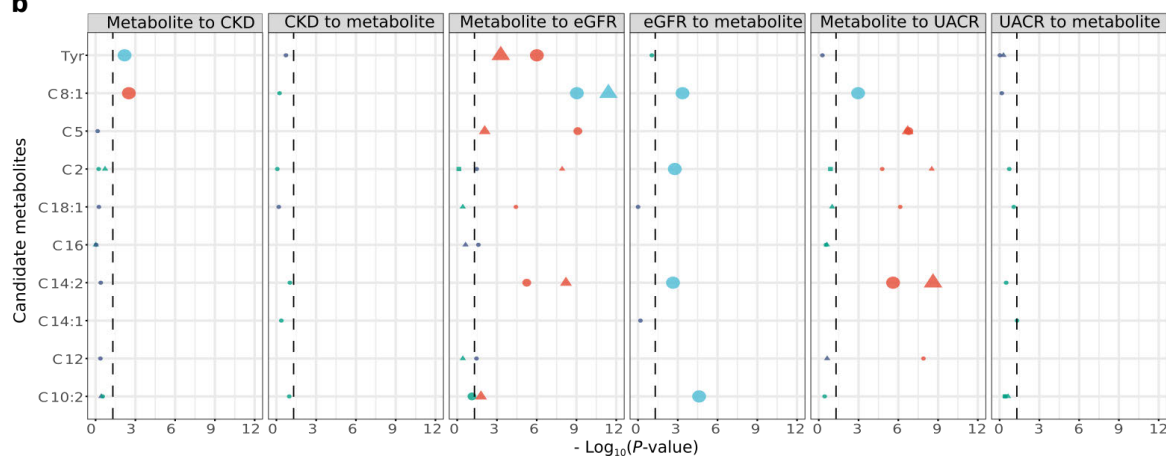
We further compared 2SMR (RAPS and outliers-corrected analyses when required) and observational estimates from KORA for all proteins and metabolites that were indicated as presenting genetic predisposition on kidney traits in either direction. Our causal estimates for all three CKD-to-protein, 15 eGFR-to-protein/metabolite were directionally consistent with corresponding observational estimates for prevalent CKD and current eGFR values, respectively, supporting that these candidates' levels may be altered downstream of the kidney trait or its heritability (Fig. 4, Supplementary Table 24, 26).

Fig. 4

a



b



For three (B2M, Tyr, and C8:1) of the four candidates to CKD causal estimates, the same was true as for the observed estimates of incident CKD. Consistent estimates between causal and follow-up estimates were also found for three (B2M, Tyr, and C8:1) of seven candidates to eGFR, and four (B2M, ERBB3, C8:1 and C14:2) of five candidates to UACR, respectively. However, the follow-up estimates for SOD2-to-CKD/eGFR, C14:2-to-eGFR and C10:2-to-eGFR were inconsistent with their causal estimates and instead all directionally consistent with their

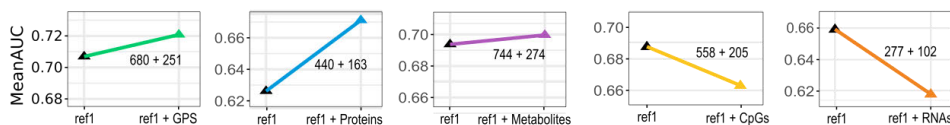
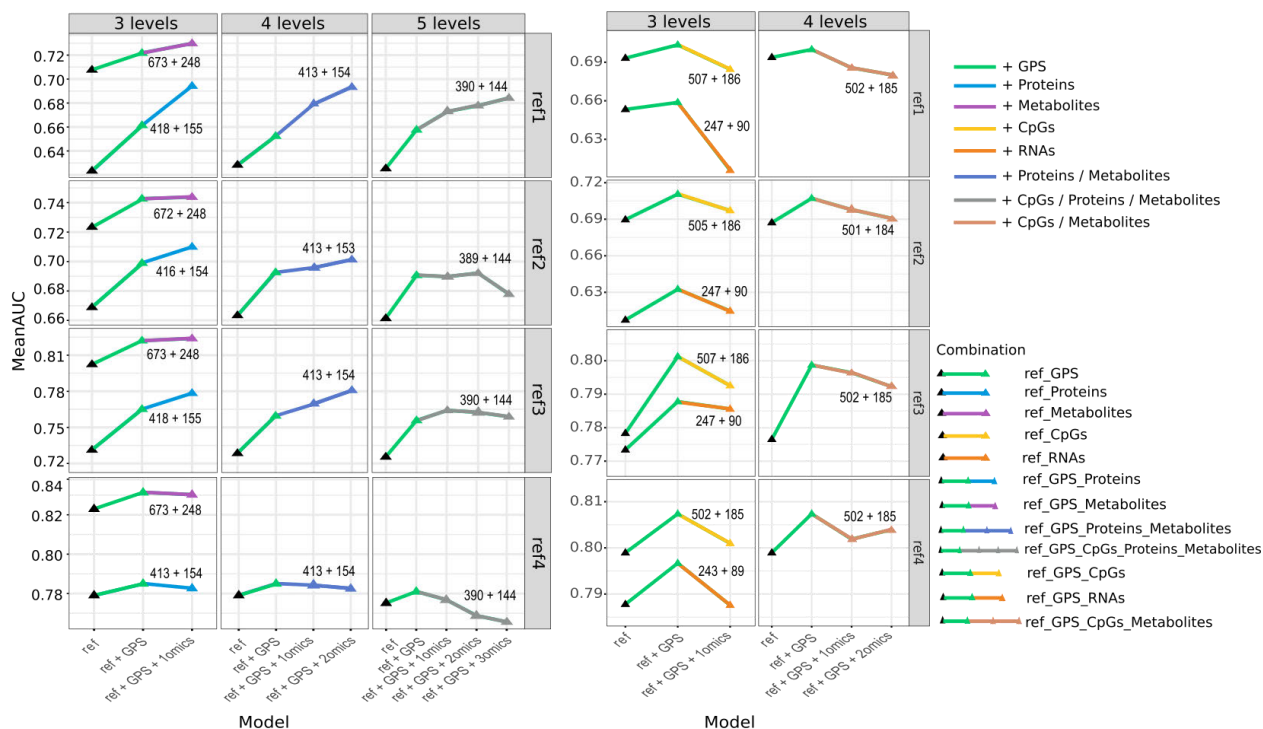
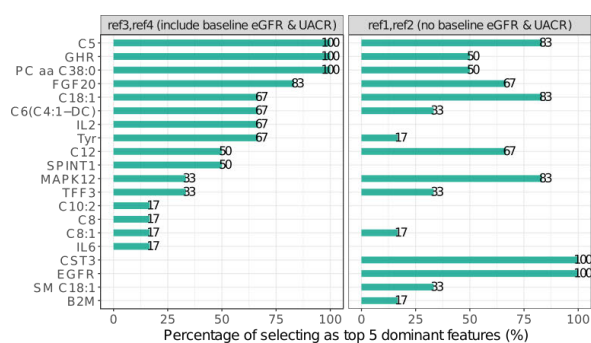
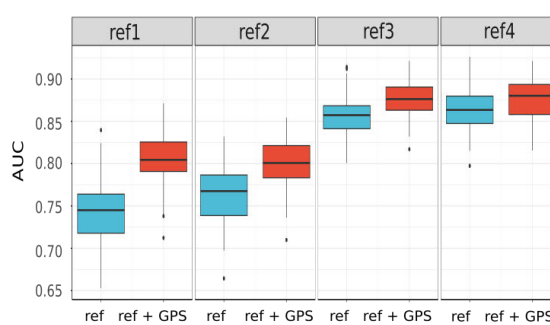
CKD/eGFR to candidate causal estimates (Fig. 4, Supplementary Tables 24-26), two of which (eGFR-to-C14:2 and eGFR-to-C10:2) were statistically significant (FDR < 0.05).

Taken together, after these steps to reduce false-positive findings, we discovered that three candidate biomarkers (B2M, Tyr and C8:1) were potentially causal for developing CKD, while CKD may have a causal effect on three proteins (TNFRSF1A, SPOCK2, and MMP1). The three candidates (B2M, Tyr and C8:1) were potentially causal on eGFR values, while a reverse direction was observed on 15 candidate biomarkers (11 proteins: UNC5C, TNFRSF1B, TNFRSF1A, TNFRSF119, SPOCK2, RETN, RELT, IGFBP6, FSTL3, CTSH, IL19 and four metabolites: C8:1, C2, C14:2, and C10:2), with C8:1 presenting in both directions (C8:1-to-eGFR and eGFR-to-C8:1). Two proteins (B2M and ERBB3) and two metabolites (C8:1 and C14:2) may have a potentially causal role on UACR values.

Five-level multi-omics prediction in hyperglycemia to reveal the optimal cut-off omics levels and dominant molecules

We next investigated the prediction of incident CKD in 751 hyperglycemic individuals of KORA F4 using multi-omics (e.g., GPS_{eGFR} , 62 proteins, 14 metabolites, 7 CpGs and 14 RNAs) to explore cut-off omics levels, and propose the dominant predictive molecules on top of current suggested predictors (i.e., four distinct sets of reference predictors)^{7,18}.

Overall, we found that GPS_{eGFR} , candidate proteins and metabolites improved predictive performance with increasing mean area under the receiver operating characteristic curve (AUC) values in testing data compared to ref sets (i.e., ref₁, ref₂ and ref₃, Fig. 5, Supplementary Table 27). The mean AUC value increased when adding more omics levels except for candidate CpGs and RNAs. For example, in the four levels (combination of ref_ GPS_{eGFR} _Proteins_ Metabolites) analysis for ref₃ (i.e., sex, age, eGFR and UACR), adding GPS_{eGFR} , 1omics and 2omics to ref₃ increased the mean AUC value from 0.729 to 0.760, 0.769 and 0.781, respectively. In the five levels analysis (i.e., combination of ref_ GPS_{eGFR} _CpGs_ Proteins_ Metabolites), mean AUC value of five levels' omics compared to four levels' omics, a slight improvement was observed for ref₁, but decrease were detected for ref₂, ref₃ and ref₄, respectively (Fig. 5b).

Fig. 5**a** Prediction of incident CKD in hyperglycemia of ref1 (age, sex) with addition of either GPS or one omics**b** Prediction of incident CKD in hyperglycemia with multiple levels of omics**c** Dominant predictive features**d** Prediction of incident CKD_{crcc} in hyperglycemia with GPS

Additionally, we observed that sample size was a strong influence factor for the predictive performance (Fig. 5, Supplementary Table 27). One of the potential reasons could be the built predictive models may have become less stable with a smaller sample size. For example, in the combination of ref₃_GPS_{eGFR}_Proteins / Metabolites analyses, mean AUC values were 0.731, 0.765, 0.778 for ref₃, ref₃ + GPS_{eGFR} and ref₃ + GPS_{eGFR} + Proteins in the mean sample size of 418

as training and 155 as testing samples, whereas mean AUC values were 0.802, 0.822, 0.824 for ref₃, ref₃ + GPS_{eGFR} and ref₃ + GPS_{eGFR} + Metabolites in the mean sample size of 680 (training sample) and 251 (testing samples).

Moreover, the top five selected predictors using the priority-Lasso for each combination from two to five omics levels and each reference set (from ref₁ to ref₄, Supplementary Table 28) were presented. For both ref₁ and ref₂, proteins CST3 and EGFR were 100% selected as the top five features in the defined combinations (see “Online Method”) and identified as the dominant molecules for prediction (Fig. 5c). For both ref₃ and ref₄ by including baseline eGFR and UACR values in the reference sets, CST3 and EGFR were no longer the most frequently selected features as eGFR and UACR values represent their main information. In this case, protein GHR, metabolite C5 and PC aa C38:0 were consistently selected as the top five features (Fig. 5c). Compared to our DMMOINs results (Fig. 2), the effects of GHR / PC aa C38:0 on incident CKD may not be directly mediated by CST3, creatinine, or urine albumin, which further supported their predictive effects for incident CKD were independent of baseline eGFR and UACR values.

Additionally, our built GPS_{eGFR} improved predictive performance for incident CKD in hyperglycemia on top of all four reference sets. The improvement was most noticeable for incident CKD_{crcc} (Fig. 5d, Supplementary Table 29), e.g., the median AUC increased by 5.9%, 3.4%, 1.9% and 1.7% when GPS_{eGFR} was added to the four sets of references, respectively. This further proved our GPS_{eGFR} contained a large amount of eGFR information.

Subgroup of CKD patients in hyperglycemia using three potential novel biomarkers

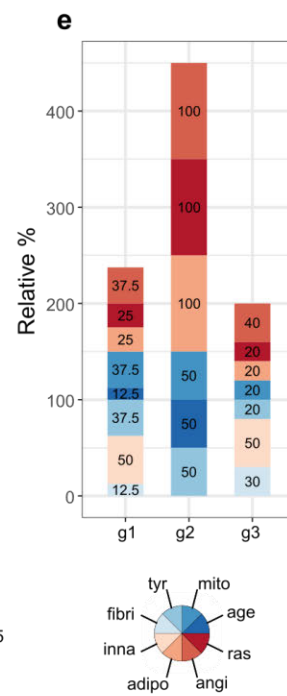
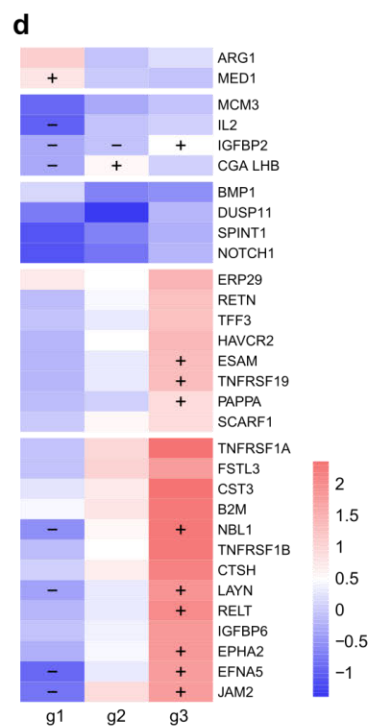
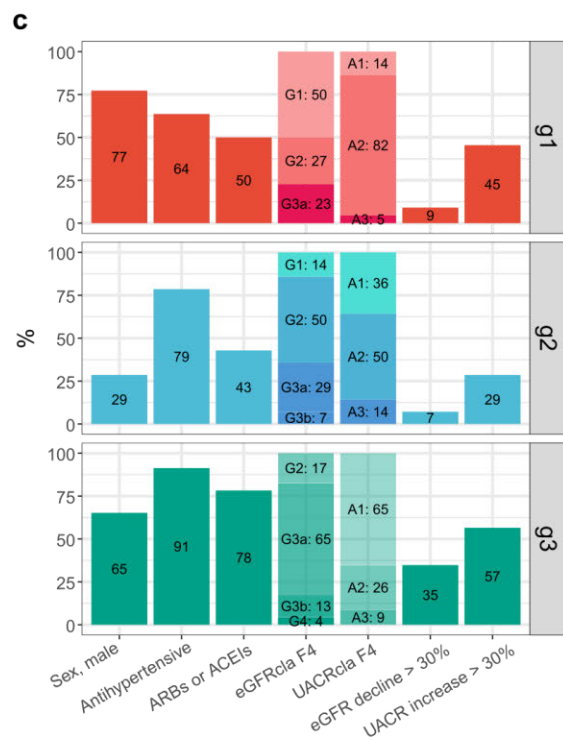
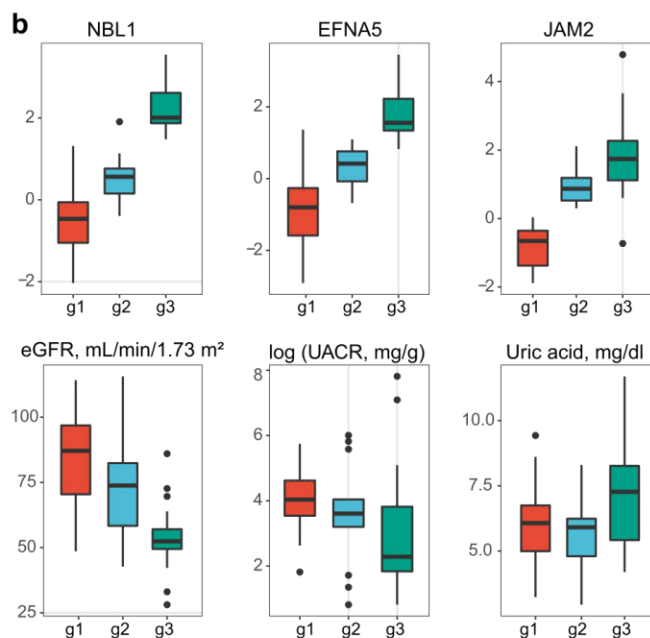
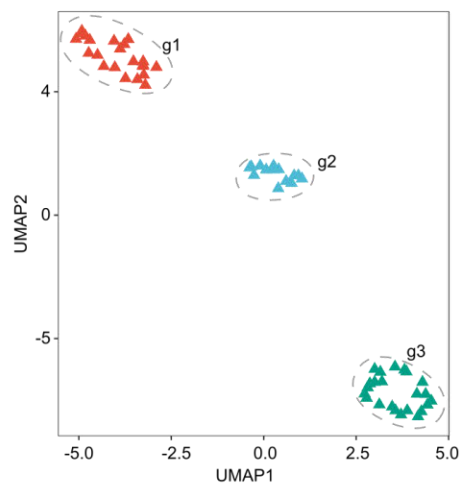
We classified CKD patients with hyperglycemia using various combinations of biomarkers and candidates (Supplementary Fig.11, Supplementary Table 30) and identified three distinct groups of CKD patients by using three potential novel proteins (i.e., NBL1, EFNA5, and JAM2) (Fig. 6a). From group 1 (g1) to g3, median levels for all three proteins consistently got higher, while eGFR and natural log-transformed UACR median levels got lower, whereas g3 CKD patients had higher median uric acid levels than g1 and g2 (Fig. 6b).

Additionally, the levels of other four clinical variables and 28 candidate biomarkers varied significantly among the three groups (Supplementary Fig.12, Supplementary Table 31). From g1 to g3, the percentage of CKD defined by eGFR and the use of antihypertensive therapy got higher, while the percentage of CKD defined by UACR got lower (Fig. 6c, Supplementary Table 32). Eight, two, and ten candidates were identified as dominant molecules for g1, g2, and g3 (Fig. 6d), respectively, with T2DCKD_{inna} being the top likely involved pathological process for g1 and g3, and T2DCKD_{dras}, -angi, and -adipo being the top likely involved pathological processes for g2 (Fig. 6e). One of the key processes for g2's dominant candidates was T2DCKD_{dras}, which may explain why the percentage of g2's patients taking angiotensin receptor blockers (ARBs) or angiotensin-converting enzyme inhibitors (ACEIs) was lowest among three groups, but the percentage of eGFR decline > 30% and UACR increase > 30% were also lowest in g2, implying

that g2 CKD patients could be more sensitive to anti-RAS treatment. The reasons for the highest percentage of eGFR declines > 30% and UACR increases > 30%, and the lowest baseline UACR levels in g3 CKD patients may include the following: 1) the lowest average baseline eGFR values; 2) these patients followed the classical developing model of DKD, with mild proteinuria at the onset and then increasing proteinuria and progression of GFR decline; and 3) the predominant pathological processes in these patients were not RAS, resulting in severe CKD progression despite a high rate of anti-RAS treatment. The current mainstay of CKD therapy is RAS blockade with ARBs and/or ACEIs, which decreases glomerular hyperfiltration and albuminuria and retards the decline in kidney function ¹⁹. However, not all patients with CKD or DKD respond to RAS blockade ¹⁹. The distinct dominant pathological processes observed in three subgroups of CKD patients corroborated this phenomenon and suggested that therapeutic targets focusing on T2DCKDinna, -angi, -mito, and -tyr processes in g1 patients, -ras, -angi, and -adipo processes in g2 patients, and -inna, -angi, and -fibri processes in g3 patients, may have beneficial effects. Our findings shed new light on the subtyping of hyperglycemia-related CKD using omics molecules and demonstrated the distinct characteristics of these subgroups. Furthermore, the three potentially novel proteins have the potential to subgroup CKD patients even more effectively than eGFR and UACR.

Fig. 6

a Subgroup of patients with 3 identified candidates



Discussion

Our study identified 120 multi-omics candidate biomarkers prognosticating CKD in hyperglycemia, 87 were found to be involved in T2D-related CKD networks and 64 have been replicated. All 64 were associated with eGFR or UACR values (current or follow-up), with 57 of them predicting follow-up eGFR or UACR values in hyperglycemia significantly. Previously, 53 of these 64 candidates were reported to be associated with CKD or related kidney traits. However, published studies may report effect size estimates for candidates in a different direction compared with those in KORA and our replication studies. For instance, IL19 was found to be decreased in KORA and two independent studies' CKD patients while it was reported to be increased in DKD patients²⁰. Additionally, 11 of 64 may represent novel omics markers prognosticating CKD in pre- or T2D individuals, with the protein JAM2, NBL1, and SCARF1 being associated with our GPS_{eGFR}. As a result, our data not only confirmed previously established associations, but also revealed novel candidates.

Eight maps of T2DCKD depicting the pathological mechanism. Although many studies have identified potential CKD biomarkers, their roles in underlying pathological processes of T2DCKD have not been thoroughly studied. Our eight T2DCKD subnetworks, which included 87 identified candidate biomarkers of CKD, illustrated the complex interwoven network of pathways involved in hyperglycemia-related CKD. Each process in DKD pathogenesis can affect multiple phenotypes and/or other processes, and many candidate genes/proteins are represented in multiple subnetworks.

The T2DCKD_{tyr} subnetwork presented how Tyr and its metabolism were involved in DKD development/progression and extracellular matrix (ECM) deposition. DKD is characterized by dysregulation of ECM proteins²¹. Tyr may increase Triiodothyronine, which inhibits ECM deposition. We observed that CKD patients had lower concentration of Tyr compared to non-CKD individuals in hyperglycemia, and lower levels of Triiodothyronine could be expected and consequently, lead to deposition of ECM in CKD patients. Moreover, lower levels of Tyr could yield in lower Dopamine levels, which could result in lower glomerular filtration, higher albuminuria, and higher risk of DKD among others (Extended Data Fig. 2).

The subnetwork T2DCKD_{mito} involved 35 candidate biomarkers. Anomalies in serum lipids and ectopic lipid accumulation in the kidney due to mitochondrial dysfunction are associated with the development of kidney diseases²². Incomplete fatty acid beta-oxidation results in acylcarnitine accumulation in CKD patients, indicating mitochondrial dysfunction²³. We found 13 replicated acylcarnitines all showed increased levels in CKD patients, confirming this observation. T2DCKD_{mito} involved C16 and C12 due to the possibility that incomplete fatty acid beta-oxidation could increase their levels, with C16 possibly increasing *PTGS2* gene expression. *PTGS2* may boost the inflammatory response (Supplementary Fig. 1).

The T2DCKD_{adipo} (Supplementary Fig. 3) included three adipokines (ADIPOQ, RETN, and FSTL3) and one leptin receptor (LEPR) from our candidate proteins. Adipose tissue and

adipokines have been linked to kidney disease more than other biological components²⁴. Circulatory adiponectin levels can slow CKD progression in CKD patients²⁴. Serum levels of protein RETN are increased in CKD patients²⁴, and FSTL3 is involved in dyslipidemia and the inflammatory response²⁵. These studies support our findings that CKD patients had significantly higher levels of all three adipokines than non-CKD individuals.

T2DCKDage used seven candidates (C2, CGA;LHB, FN1, B2M, AMH, MMP1, and HVCR2). Evidence supports that inhibiting advanced glycation can slow the progression of experimental DKD²⁶. T2DCKDras had 22 candidates. The intrarenal RAS is implicated in regulating glomerular hemodynamics, and glomerular hypertrophy and sclerosis. Angiotensin II type 1 receptor antagonists and angiotensin converting enzyme inhibitors have been shown to slow DKD progression in patients with type 1 diabetes or T2D²⁶.

T2DCKDfibri's subnetwork contained 29 candidates. Hyperglycemia accelerates the deposition of ECM proteins in DKD²¹. Deposition of ECM thickens glomerular and tubular basement membranes, whereas increased mesangial matrix causes glomerular sclerosis and tubulointerstitial fibrosis²⁷. The largest subnetwork, T2DCKDinna, included 40 identified candidate biomarkers. Activation of innate immunity contributes to kidney inflammation in DKD. Several studies suggest an association between the progression of DKD and pro-inflammatory pathways, including the NLRP3 inflammasome, TLR signaling, and the complement system²⁸. T2DCKDangi had 32 candidates. Abnormal angiogenesis is a well-defined complication of DKD²⁹. Angiogenesis is primarily induced by hypoxia and oxidative stress in the kidney via upregulation of VEGFA to counteract hypoxia³⁰.

Ascertain the function of 11 potential novel candidates. The eight T2DCKD networks show potential to infer the relevant DKD pathways for the potential novel candidates of CKD (Extended Data Fig. 8). Nine of 11 (*LYSM2*, *NAPA*, *TFE3*, *NBL1*, *CTSV*, *CLEC4M*, *IGF2R*, *RET*, *JAM2*, *SCARF1*, and *EFNA5*) are included in the T2DCKD networks. For example, T2DCKDmito (Supplementary Fig. 1) involved three candidates (*EFNA5*, *IGF2R*, and *NAPA*). Silencing *EFNA5* may increase *BCL2* expression³¹, which has been shown to inhibit apoptosis³². Our data showed elevated *EFNA5* levels in CKD patients. *IGF2R* regulates CD36 activity³³, facilitating long-chain fatty acid transport and tubular toxicity²². We observed CpG site (cg23314866) that was negatively associated with CKD, annotating to gene *NAPA*. The function of *NAPA* was reported to reduce AMPK activity and affect mitochondrion organization³⁴. Dysregulated AMPK was observed in the kidney of DKD patients³⁵. That may explain why our study observed a negative link between *NAPA* (cg23314866) methylation and CKD in hyperglycemia.

Genetic drivers. It is important to note that our studies used GPS_{eGFR} and 2SMR as genetic drivers to elucidate the role of CKD-associated omics molecules to kidney traits (CKD, eGFR, and UACR) to extend observational associations to causality.

GPS. With the effect sizes of SNPs for eGFR values from the largest consortium of GWAS studies of European ancestors, we built a GPS for eGFR and validated it externally in the UKBB and

internally in the KORA S4 testing samples. All three studies observed a strong correlation between GPS_{eGFR} and eGFR, indicating that our findings are most likely true positives. In hyperglycemic population, our GPS_{eGFR} showed strong associations with eGFR and its follow-up, CKD and incident CKD, and 18 of our candidate biomarkers of CKD. The GPS_{eGFR} -associated omics molecules contained CST3, a protein with a well-established association with eGFR and CKD, and various other CKD-related proteins such as B2M. Eleven of the 18 candidates showed an augmented effect for individuals at population's tail, with several being critical in the development/progression of T2DCKD. For instance, the proteins TNFRSF1A, RETN, FSTL3, and B2M play essential pathogenetic/physiological roles in T2DCKD innate immunity (Supplementary Fig. 2), primarily by increasing the activity of the NF-kappaB complex ^{24,36} and macrophage activation ²⁵, enhancing HLA-G interaction ³⁷, and participating in the MHC class I complex ³⁸. Extreme GPS_{eGFR} identified 11 candidate biomarkers of CKD in addition to high genetic predisposition individuals, but not any of the other 53 replicated candidates. The 11 candidates formed a set that suggests that the genetic factors of eGFR have a pronounced effect on their circulatory levels. Thus, it may help explain why some individuals develop CKD at an early age, given that the driving factors for CKD can be genetic, behavioral, and environmental, with genetics possibly being the most important for those individuals. Using our GPS_{eGFR} to identify individuals with a high genetic risk of developing CKD may help improve personalized management of CKD in hyperglycemia. We found that these 18 candidates had distinct characteristics because they showed different mediation directions with GPS_{eGFR} and eGFR/CKD, implying their distinct roles (mediator, outcome, or both) in the pathway by which genetic drivers of eGFR ultimately reach GFR and CKD.

2SMR. 2SMR suggested 19 of 60 replicated proteins and metabolites to be causal for kidney traits (CKD/eGFR/UACR) in one or both directions. All 19 candidates associated with CKD or related traits according to literature. Our 2SMR results not only confirm previous findings, but also extend observational associations to causality and shed new light on genetic evidence-based directions. Since the current definition of CKD is predominately based on eGFR and/or UACR values, our 2SMR results attribute the observational signals of CKD to various kidney traits (CKD, eGFR and UACR). For example, 2SMR results suggested that B2M, Tyr, and C8:1 are causal to CKD and eGFR, while B2M and C8:1 are also causal to UACR. T2DCKDinna and -age processes may involve B2M. Because MR causality does not imply a specific molecular mechanism, we also displayed the mediation results for the candidates of MR supported causality from our data to further investigate the potential mechanism. Mediation results for candidate \rightarrow kidney trait (Extended Data Fig. 9c) and kidney trait \rightarrow candidate (Extended Data Fig.9d) were presented. For example, the proteins IGFBP2, ACY1, and SPOCK2 may act as mediators between Tyr and follow-up eGFR values. Our mediation results may shed light on how these 2SMR-supported causal molecules reach phenotypes. Taken together, our 2SMR is the first to our knowledge that systematically investigates the causal relationships between candidate proteins and metabolites and various kidney traits in bi-directions, particularly in the field of targeted metabolomics, and the evidence with mediation results is further provided.

GPS&2SMR. Statistical power and reverse causality are two of the limitations for all MR studies¹². Some candidates with a 2SMR supported direction of CKD/eGFR-to-candidate may also have a GPS_{eGFR} supported direction of candidate-to-CKD/eGFR. Eight (B2M, TNFRSF1A, SPOCK2, IGFBP6, RETN, RELT, FSTL3, and C10:2) of the 18 GPS_{eGFR} associated candidates (Figs. 3g, 4) may be causally linked to kidney traits suggested by 2SMR. Interestingly, all eight candidates were potentially causal for eGFR by 2SMR. Another example, the results of 2SMR and GPS_{eGFR}'s mediation suggested B2M-to-CKD and CKD-to-TNFRSF1A, moreover, GPS_{eGFR}'s mediation results implied the opposite direction as well. Although GPS_{eGFR}'s mediation evidence isn't as strong as that from 2SMR, it not only agreed with the 2SMR results but also suggested possible causal directions that the 2SMR didn't reveal.

Classifying multi-omics signatures into subgroups. eGFR and UACR are not etiological markers for CKD and do not reflect its underlying pathophysiology, particularly in the early stages of disease³⁹. Even when their values remained normal, there may be pathological molecular changes in the kidneys of individuals at risk of CKD⁴⁰. Current treatments for CKD focus on delaying the progression of the disease rather than reversing the underlying pathogenetic process⁴¹. A published simulation study combining clinical trials of patients with T2D demonstrated that intervention in the earliest stages of disease was most effective at delaying the onset of End-Stage Renal Disease (ESRD)⁴². These findings suggest that the most effective preventative treatment would be to intervene early, prior to organ damage manifested by albuminuria and/or decreased eGFR⁴⁰. Therefore, novel diagnostic methodologies are required to determine which individuals would benefit most from early treatment. Identifying high-risk individuals whose eGFR and albuminuria remain normal but who display molecular pathogenetic traits is critical but challenging. As a result, it is essential to identify biomarkers capable of identifying early pathogenetic changes, prognosticating eGFR and/or UACR deterioration, and elucidating the underlying pathogenetic processes. Lesson learned from clinical trials in which drugs targeting a single biomarker, such as transforming growth factor β 1 blockade, failed and drugs targeting a molecular node like RAS succeeded because multiple actions of the RAS promote kidney cell injury, inflammation, and fibrosis⁴³. A panel of multiple protein biomarkers covering the numerous pathogenetic processes underlying DKD may be most appropriate to reliably and accurately predict progression of kidney disease⁴⁴. Therefore, of the concurrent contributions of several pathogenetic processes, a holistic and initially agnostic approach integrating multiple omics levels and clinical outcome assessment for the identification of prognostic signatures is one of the most promising strategies for preventing and treating CKD⁴³.

In our study, we classified our replicated candidates based on their potential directions with eGFR and UACR with and without genetic evidence support (Extended Data Fig.8a, Supplementary Table 33), and further provided their potential involvement in (several) T2DCKD pathological processes to elucidate biological pathways (Extended Data Fig.8b). Thus, a subgroup of molecular profiles indicating specific changes of kidney traits may represent a subgroup of susceptible high-risk individuals for CKD development. For instance, the key omic candidate biomarkers in the group of eGFR→candi→eGFR with genetic evidence support were TNFRSF1A and FSTL3, and the relevant processes in this group included T2DCKD_{inna}, -mito, -fibri, -angi, -adipo, and -tyr.

Targeting molecular candidates in this group may have an effect on these six pathological processes and eGFR values. Moreover, our subgrouping of omic candidates is in line with a truly translatable biomarker discovery methodology, which should prioritize not only clinically evident stages of disease, but also on very early stages of disease when therapeutic interventions can still slow or stop disease progression.

Reveal new underlying links from interplay. Our MOIN can shed light on how the candidate biomarkers were related to kidney traits. For instance, cg22872478 (*LYSMD2*) linked to urine albumin and protein EGFR, and protein NBL1 connected to CST3 in our network. These connections could be the potential paths linking these two of 11 potential novel candidates to CKD. Furthermore, our results agreed with previous reports in which 13 replicated acylcarnitines were increased in patients with CKD, DKD, or ESRD (Supplementary Table 5). But how acylcarnitines contribute to CKD and its complications remains uncertain. Our MOIN retained all 13 acylcarnitines (Extended Data Fig.4), eight of which were associated with CKD biomarkers CST3, creatinine, urine albumin, or EGFR. It suggested that these four biomarkers could act as mediators between the eight acylcarnitines and their associated kidney traits. Our DMMION (Fig.2c, Extended Data Fig.6) confirmed this suggestion by categorizing the eight acylcarnitines into several groups based on their mediators. Additionally, a randomized clinical trial found that carnitine can lower serum CST3 levels⁴⁵. C2, C3, C16, C18, and C18:1 positively correlate with serum CST3⁴⁶. Another example given, CTSH was included in four T2DCKD subnetworks, namely T2DCKDinna, -ras, -tyr, and -angi. CTSH can stimulate angiogenesis⁴⁷, the toll-like receptor 3 signaling pathway⁴⁸, and renin⁴⁹. In our previous study, PC aa C38:0 predicted incident CKD in hyperglycemia⁷. Notably, CTSH was not only strongly associated with PC aa C38:0 in our MOIN, but also acted as a mediator between PC aa C38:0 and follow-up eGFRcr values in our DMMOIN, suggesting that CTSH may be a component of the pathway by which PC aa C38:0 exerts its nephrogenic effects.

Deep mechanism exploration of potential causal links. Our DMMOIN could deduce potential causal links from multi-omics pairs. We conducted mechanism exploration on several pairs of the network to show this capability. For instance, out of six mediating tests, two directions were suggested as best for the mediating triangle of protein IL19, RNA *SLC22A4*, and CKD (Extended Data Fig.9a). RNA *SLC22A4* mediated 54.1% effect of protein IL19-to-CKD and 55.2% effect of CKD-to-protein IL19. The underlying mechanism of IL19→*SLC22A4*→CKD could be that low levels of IL19 (found in CKD patients in our data) could increase IL1B levels, which could increase *SLC22A4* expression (consistent with our findings)⁵⁰. Increased *SLC22A4* gene expression may also be a result of metabolic acidosis, a common phenotype in CKD⁵¹. CKD may also increase *SLC22A4* expression. However, *SLC22A4* activity is decreased in CKD patients and at acidic pH^{52,53}. *SLC22A4* is a transporter for ergothioneine. High expression but low activity of *SLC22A4* may result in low ergothioneine levels, which are associated with increased proteinuria, high BUN levels, low GFR, and expanded mesangial matrix⁵⁴. Each is a CKD phenotype or its progression. Additionally, CKD may also cause ergothioneine deficiency⁵⁵. Interestingly, urine albumin mediated the effect of RNA *SLC22A4* on UACR (Extended Data Fig.6), but only in the

direction of UACR as outcome in our data. This evidence supported the hypothesis that IL19→IL1B→*SLC22A4*→ergothioneine→increased risk of proteinuria/ higher blood urea nitrogen levels/ decreased GFR values. For the direction of CKD→*SLC22A4*→IL19, it may be explained by the possibility that CKD could increase *SLC22A4* expression, which would affect T2D activity and, in turn, IL19 levels (Extended Data Fig. 9b, Supplementary Table 34).

Another example is Tyr, which was potentially causal to eGFR by 2SMR (Fig.4b). We also discovered that proteins IGFBP2, ACY1, and SPOCK2 mediated Tyr's effects on follow-up eGFR values in our data (Extended Data Fig. 9c). The possible mechanism regarding IGFBP2 mediating Tyr and eGFR could be explained as followed (Extended Data Fig.9e). A: It has been reported that higher levels of Tyr increase L-DOPA levels⁵⁶, which can result in decreased IGFBP2 levels⁵⁷. In analogy, this suggests that in a reverse situation, i.e., low levels of Tyr can induce high levels of IGFBP2, resulting in a decline in GFR values⁵⁸. B: CKD causes low Tyr levels⁵⁹ and a disturbed protein metabolism is observed in patients with CKD⁶⁰. Low Tyr levels may result in a lower protein synthesis rate, comparable to a protein restriction state, causing elevated IGFBP2 levels resulting in lower GFR values^{60,61}. Both pathways support our findings that IGFBP2 mediated between Tyr and follow-up eGFR values, as well as the reverse associations between Tyr and IGFBP2, IGFBP2 and follow-up eGFR values, respectively.

Cut-off omics levels and dominant candidate markers of multi-omics prediction. Our multi-omics prediction results indicated that adding GPS, candidate proteins, and metabolites to the reference predictors improved predictive performance for future CKD in hyperglycemia. In contrast, this improvement was consistent for GPS but limited for candidate proteins or metabolites when they were added to ref₄ (i.e., seven predictors), which indicated the superior discriminatory ability of this predictor set that we previously suggested⁷ for future CKD in hyperglycemia and followed the concept of a best combination of predictors. Instead of trying to find the best combination of multi-omics predictors, here, we summarized the dominant omics molecules based on whether they exhibited extra predictive values of future CKD in the extended hyperglycemic population in addition to various reference predictors, e.g., C5, GHR and PC aa C38:0 were the dominant predictive markers on top of reference predictors including baseline eGFR and UACR.

Moreover, we discovered that GPS_{eGFR} improved predictive performance on future CKD in hyperglycemia on top of all four reference sets, notably CKD_{crcc}, and that this improvement was consistent and independent of baseline eGFR and UACR values, suggesting that it may contribute to more personalized prediction of future CKD in hyperglycemia.

Limitation. While our study provides a wealth of molecular data, it has several limitations that necessitate further investigation. First, the extensive analyses of multi-omics molecules in hyperglycemia relied on candidate biomarkers identified from cross-sectional association studies (EWAS, TWAS, PWAS, and MWAS). Because our discovery study only included 1401 individuals with prediabetes and T2D and the incomplete profiling of multi-omics data, it is possible that some omics molecules with true signals were missed. Similarly, limited data of 751 hyperglycemic patients were used for the prediction part, additional longitudinal studies with

larger sample sizes and more complete measurements of multi-omics profiles are required to corroborate our conclusions. Second, in all replication studies for candidate biomarkers, except one (KORA FF4 for replicating metabolites), the replication analyses of candidate biomarkers and CKD were conducted on the general population, with CKD defined solely by eGFR values. Candidates specific to UACR signals and hyperglycemia may not be replicated. So, we combined both published and replicated candidates in some sections of our analyses. Third, because there were multiple omics techniques for profiling omic molecules, each type of analyte class had platform-specific errors. Furthermore, statistical power is one common limitation for MR studies¹⁶. We used both sets of genetic instruments as well as three kidney traits, and consistently observed that protein CST3 was associated with CKD and negatively associated with eGFR values. The insufficient power (only one genetic instrument was available in the two sets) and the fact that the eGFR values were derived from creatinine, which did not include information from cystatin C measurements, may be the causes of the borderline significance of MR results of CST3. The number of putative causal relationships of eGFR-to-candidate was much larger than the one of candidate-to-eGFR from our 2SMR results, which may be because the sample size for the study of genetic instruments for eGFR was over half a million, whereas the sample size for the studies of genetic instruments for proteins or metabolites was only a few thousand individuals. We used stringent criteria to select MR instruments and a recent advanced MR approach that was robust to pleiotropy, conducted outlier-corrected analyses in cases of potential assumption violation, and reported associations of FDR significance and consistency with observational estimates. However, inference of causality should still be explained cautiously due to several limitations of MR validity^{16,62}. Finally, our KORA study was observational with a baseline and two follow-ups, so there was approximately 6.5-year gap between visits, indicating that unknown confounding factors might have influenced the findings of omics molecules and kidney traits at different time points, despite adjusted for 12 confounding variables covering various aspects (e.g., physiological factor, lifestyle, clinical measurements, and medication usage).

Conclusion. Our findings demonstrate a complex omic landscape in the development and progression of CKD in individuals with prediabetes or T2D. Additionally, we show how omic molecules associated with CKD exhibit distinct properties in relation to the complex processes of hyperglycemia-related CKD. These deep multi-omics measurements allow us to investigate the early and specific signs of CKD development in hyperglycemia, enabling more effective prevention and treatment of CKD in the context of integrated personalized diabetes management.

References

1. Misra, B.B., Langefeld, C.D., Olivier, M. & Cox, L.A. Integrated Omics: Tools, Advances, and Future Approaches. *J Mol Endocrinol* (2018).
2. Schussler-Fiorenza Rose, S.M., *et al.* A longitudinal big data approach for precision health. *Nat Med* **25**, 792-804 (2019).
3. Bikbov, B., *et al.* Global, regional, and national burden of chronic kidney disease, 1990-2017: a systematic analysis for the Global Burden of Disease Study 2017. *Lancet (London, England)* **395**, 709-733 (2020).
4. Webster, A.C., Nagler, E.V., Morton, R.L. & Masson, P. Chronic Kidney Disease. *Lancet (London, England)* **389**, 1238-1252 (2017).
5. Plantinga, L.C., *et al.* Prevalence of chronic kidney disease in US adults with undiagnosed diabetes or prediabetes. *Clinical journal of the American Society of Nephrology : CJASN* **5**, 673-682 (2010).
6. Melsom, T., *et al.* Prediabetes and Risk of Glomerular Hyperfiltration and Albuminuria in the General Nondiabetic Population: A Prospective Cohort Study. *American journal of kidney diseases : the official journal of the National Kidney Foundation* **67**, 841-850 (2016).
7. Huang, J., *et al.* Machine Learning Approaches Reveal Metabolic Signatures of Incident Chronic Kidney Disease in Individuals With Prediabetes and Type 2 Diabetes. *Diabetes* **69**, 2756-2765 (2020).
8. Huang, J., *et al.* Validation of Candidate Phospholipid Biomarkers of Chronic Kidney Disease in Hyperglycemic Individuals and Their Organ-Specific Exploration in Leptin Receptor-Deficient db/db Mouse. *Metabolites* **11**, 89 (2021).
9. Herder, C., *et al.* Proinflammatory Cytokines Predict the Incidence and Progression of Distal Sensorimotor Polyneuropathy: KORA F4/FF4 Study. *Diabetes care* **40**, 569-576 (2017).
10. Lechner, M., *et al.* CDeR: multifactorial interaction networks in human diseases. *Genome Biology* **13**, R62 (2012).
11. Al Thani, A., *et al.* Qatar Biobank Cohort Study: Study Design and First Results. *Am J Epidemiol* **188**, 1420-1433 (2019).
12. Ringseis, R., Wen, G. & Eder, K. Regulation of Genes Involved in Carnitine Homeostasis by PPAR α across Different Species (Rat, Mouse, Pig, Cattle, Chicken, and Human). *PPAR Res* **2012**, 868317 (2012).
13. Ben Said, M., *et al.* A mutation in SLC22A4 encoding an organic cation transporter expressed in the cochlear stria vascularis causes human recessive non-syndromic hearing loss DFNB60. *Hum Genet* **135**, 513-524 (2016).
14. Fox, J. Structural equation modeling with the sem package in R. *Structural Equation Modeling* **13**, 465-486 (2006).
15. Khera, A.V., *et al.* Genome-wide polygenic scores for common diseases identify individuals with risk equivalent to monogenic mutations. *Nat Genet* **50**, 1219-1224 (2018).
16. Davey Smith, G. & Hemani, G. Mendelian randomization: genetic anchors for causal inference in epidemiological studies. *Hum Mol Genet* **23**, R89-98 (2014).
17. Zheng, J., *et al.* Phenome-wide Mendelian randomization mapping the influence of the plasma proteome on complex diseases. *Nat Genet* **52**, 1122-1131 (2020).
18. Tangri, N., *et al.* A predictive model for progression of chronic kidney disease to kidney failure. *Jama* **305**, 1553-1559 (2011).
19. Perico, N., Benigni, A. & Remuzzi, G. Present and future drug treatments for chronic kidney diseases: evolving targets in renoprotection. *Nat Rev Drug Discov* **7**, 936-953 (2008).
20. Li, L., *et al.* The association between interleukin-19 concentration and diabetic nephropathy. *BMC Nephrol* **18**, 65 (2017).

21. Mason, R.M. & Wahab, N.A. Extracellular matrix metabolism in diabetic nephropathy. *J Am Soc Nephrol* **14**, 1358-1373 (2003).
22. Opazo-Ríos, L., *et al.* Lipotoxicity and Diabetic Nephropathy: Novel Mechanistic Insights and Therapeutic Opportunities. *Int J Mol Sci* **21**(2020).
23. Devarshi, P.P., McNabney, S.M. & Henagan, T.M. Skeletal Muscle Nucleo-Mitochondrial Crosstalk in Obesity and Type 2 Diabetes. *Int J Mol Sci* **18**(2017).
24. Vahdat, S. The complex effects of adipokines in the patients with kidney disease. *J Res Med Sci* **23**, 60 (2018).
25. Runhua, M., Qiang, J., Yunqing, S., Wenjun, D. & Chunsheng, W. FSTL3 Induces Lipid Accumulation and Inflammatory Response in Macrophages and Associates With Atherosclerosis. *J Cardiovasc Pharmacol* **74**, 566-573 (2019).
26. Fukami, K., *et al.* AGEs activate mesangial TGF-beta-Smad signaling via an angiotensin II type I receptor interaction. *Kidney Int* **66**, 2137-2147 (2004).
27. Hu, C., *et al.* Insights into the Mechanisms Involved in the Expression and Regulation of Extracellular Matrix Proteins in Diabetic Nephropathy. *Curr Med Chem* **22**, 2858-2870 (2015).
28. Tang, S.C.W. & Yiu, W.H. Innate immunity in diabetic kidney disease. *Nat Rev Nephrol* **16**, 206-222 (2020).
29. Nakagawa, T., Sato, W., Kosugi, T. & Johnson, R.J. Uncoupling of VEGF with endothelial NO as a potential mechanism for abnormal angiogenesis in the diabetic nephropathy. *J Diabetes Res* **2013**, 184539 (2013).
30. Honda, T., Hirakawa, Y. & Nangaku, M. The role of oxidative stress and hypoxia in renal disease. *Kidney Res Clin Pract* **38**, 414-426 (2019).
31. Worku, T., *et al.* Regulatory roles of ephrinA5 and its novel signaling pathway in mouse primary granulosa cell apoptosis and proliferation. *Cell Cycle* **17**, 892-902 (2018).
32. Kennedy, A., *et al.* Antiobesity mechanisms of action of conjugated linoleic acid. *J Nutr Biochem* **21**, 171-179 (2010).
33. Qiao, X.R., Wang, L., Liu, M., Tian, Y. & Chen, T. MiR-210-3p attenuates lipid accumulation and inflammation in atherosclerosis by repressing IGF2. *Biosci Biotechnol Biochem* **84**, 321-329 (2020).
34. Wang, L. & Brautigan, D.L. α -SNAP inhibits AMPK signaling to reduce mitochondrial biogenesis and dephosphorylates Thr172 in AMPK α in vitro. *Nat Commun* **4**, 1559 (2013).
35. Juszczak, F., Caron, N., Mathew, A.V. & Declèves, A.E. Critical Role for AMPK in Metabolic Disease-Induced Chronic Kidney Disease. *Int J Mol Sci* **21**(2020).
36. Waschke, K.A., *et al.* Tumor necrosis factor receptor gene polymorphisms in Crohn's disease: association with clinical phenotypes. *Am J Gastroenterol* **100**, 1126-1133 (2005).
37. HoWangYin, K.Y., *et al.* Multimeric structures of HLA-G isoforms function through differential binding to LILRB receptors. *Cell Mol Life Sci* **69**, 4041-4049 (2012).
38. Saigi, M., Albuquerque-Bejar, J.J. & Sanchez-Cespedes, M. Determinants of immunological evasion and immuncheckpoint inhibition response in non-small cell lung cancer: the genetic front. *Oncogene* **38**, 5921-5932 (2019).
39. Eddy, S., Mariani, L.H. & Kretzler, M. Integrated multi-omics approaches to improve classification of chronic kidney disease. *Nat Rev Nephrol* **16**, 657-668 (2020).
40. Pena, M.J., Mischak, H. & Heerspink, H.J. Proteomics for prediction of disease progression and response to therapy in diabetic kidney disease. *Diabetologia* **59**, 1819-1831 (2016).
41. Sanz, A.B., *et al.* Advances in understanding the role of angiotensin-regulated proteins in kidney diseases. *Expert Rev Proteomics* **16**, 77-92 (2019).
42. Schievink, B., *et al.* Early renin-angiotensin system intervention is more beneficial than late intervention in delaying end-stage renal disease in patients with type 2 diabetes. *Diabetes Obes Metab* **18**, 64-71 (2016).

43. Ruiz-Ortega, M., Rayego-Mateos, S., Lamas, S., Ortiz, A. & Rodrigues-Diez, R.R. Targeting the progression of chronic kidney disease. *Nat Rev Nephrol* **16**, 269-288 (2020).
44. Mischak, H., Delles, C., Vlahou, A. & Vanholder, R. Proteomic biomarkers in kidney disease: issues in development and implementation. *Nat Rev Nephrol* **11**, 221-232 (2015).
45. Yaghubi, E., *et al.* Effects of l-carnitine supplementation on cardiovascular and bone turnover markers in patients with pemphigus vulgaris under corticosteroids treatment: A randomized, double-blind, controlled trial. *Dermatol Ther* **32**, e13049 (2019).
46. Hirschel, J., *et al.* Relation of Whole Blood Amino Acid and Acylcarnitine Metabolome to Age, Sex, BMI, Puberty, and Metabolic Markers in Children and Adolescents. *Metabolites* **10**(2020).
47. Gocheva, V., Chen, X., Peters, C., Reinheckel, T. & Joyce, J.A. Deletion of cathepsin H perturbs angiogenic switching, vascularization and growth of tumors in a mouse model of pancreatic islet cell cancer. *Biol Chem* **391**, 937-945 (2010).
48. Okada, R., Zhang, X., Harada, Y., Wu, Z. & Nakanishi, H. Cathepsin H deficiency in mice induces excess Th1 cell activation and early-onset of EAE though impairment of toll-like receptor 3 cascade. *Inflamm Res* **67**, 371-374 (2018).
49. Luetscher, J.A., Bialek, J.W. & Grislis, G. Human kidney cathepsins B and H activate and lower the molecular weight of human inactive renin. *Clin Exp Hypertens A* **4**, 2149-2158 (1982).
50. Maeda, T., Hirayama, M., Kobayashi, D., Miyazawa, K. & Tamai, I. Mechanism of the regulation of organic cation/carnitine transporter 1 (SLC22A4) by rheumatoid arthritis-associated transcriptional factor RUNX1 and inflammatory cytokines. *Drug Metab Dispos* **35**, 394-401 (2007).
51. Gottier Nwafor, J., Nowik, M., Anzai, N., Endou, H. & Wagner, C.A. Metabolic Acidosis Alters Expression of Slc22 Transporters in Mouse Kidney. *Kidney Blood Press Res* **45**, 263-274 (2020).
52. Tamai, I., *et al.* Cloning and characterization of a novel human pH-dependent organic cation transporter, OCTN1. *FEBS Lett* **419**, 107-111 (1997).
53. Wu, X., *et al.* Structural and functional characteristics and tissue distribution pattern of rat OCTN1, an organic cation transporter, cloned from placenta. *Biochim Biophys Acta* **1466**, 315-327 (2000).
54. Dare, A., Channa, M.L. & Nadar, A. L-ergothioneine and its combination with metformin attenuates renal dysfunction in type-2 diabetic rat model by activating Nrf2 antioxidant pathway. *Biomed Pharmacother* **141**, 111921 (2021).
55. Shinozaki, Y., *et al.* Impairment of the carnitine/organic cation transporter 1-ergothioneine axis is mediated by intestinal transporter dysfunction in chronic kidney disease. *Kidney Int* **92**, 1356-1369 (2017).
56. Taveira-da-Silva, R., da Silva Sampaio, L., Vieyra, A. & Einicker-Lamas, M. L-Tyr-Induced Phosphorylation of Tyrosine Hydroxylase at Ser40: An Alternative Route for Dopamine Synthesis and Modulation of Na⁺/K⁺-ATPase in Kidney Cells. *Kidney Blood Press Res* **44**, 1-11 (2019).
57. Charbonnier-Beaupel, F., *et al.* Gene expression analyses identify Narp contribution in the development of L-DOPA-induced dyskinesia. *J Neurosci* **35**, 96-111 (2015).
58. Tönshoff, B., Blum, W.F., Wingen, A.M. & Mehls, O. Serum insulin-like growth factors (IGFs) and IGF binding proteins 1, 2, and 3 in children with chronic renal failure: relationship to height and glomerular filtration rate. The European Study Group for Nutritional Treatment of Chronic Renal Failure in Childhood. *J Clin Endocrinol Metab* **80**, 2684-2691 (1995).
59. Kopple, J.D. Phenylalanine and tyrosine metabolism in chronic kidney failure. *J Nutr* **137**, 1586S-1590S; discussion 1597S-1598S (2007).
60. Garibotto, G., *et al.* Amino acid and protein metabolism in the human kidney and in patients with chronic kidney disease. *Clin Nutr* **29**, 424-433 (2010).
61. Smith, W.J., Underwood, L.E. & Clemmons, D.R. Effects of caloric or protein restriction on insulin-like growth factor-I (IGF-I) and IGF-binding proteins in children and adults. *J Clin Endocrinol Metab* **80**, 443-449 (1995).

62. Holmes, M.V., Ala-Korpela, M. & Smith, G.D. Mendelian randomization in cardiometabolic disease: challenges in evaluating causality. *Nat Rev Cardiol* **14**, 577-590 (2017).

Acknowledgements

We express our appreciation to all KORA study participants for donating their blood and time. We thank the field staff in Augsburg conducting the KORA studies. We are grateful to the staff (J. Scarpa, K. Faschinger, N. Lindemann) from the Institute of Epidemiology and the Genome Analysis Center Metabolomics Platform at the Helmholtz Zentrum München, who helped in the sample logistics, data and straw collection, and metabolomic measurements. Additionally, we thank the staff (e.g. A. Ludolph, S. Jelic and B. Langer) from the Institute of Genetic Epidemiology at the Helmholtz Zentrum München, and the platform KORA-PASST, for their help with KORA data logistics.

Author contributions

J.H., A.P. & R.W.-S. conceived the study; J.H. analyzed the data; A.G., W.R. & K.S. performed replication analyses; J.H., G.F., C.M. & A.R. generated networks and conducted pathway analysis; M.C., Z.Z., C.H., B.T., M.H., S.K., M.W., H.G., G.K., J.A., M.M.-N., K.S., T.M., W.K., C.H., W.R., M.R., J.G., F.S., C.G., E.Z., K.S., A.P. & R.W.-S. contributed to omics data generation and interpretation; J.H. & R.W.-S. wrote the manuscript. All authors revised the manuscript critically for important intellectual content and final approved of the version to be submitted.

Funding

The KORA study was initiated and financed by the Helmholtz Zentrum München – German Research Center for Environmental Health, which is funded by the German Federal Ministry of Education and Research (BMBF) and by the State of Bavaria. Data collection in the KORA study is done in cooperation with the University Hospital of Augsburg. Furthermore, KORA research was supported within the Munich Center of Health Sciences (MC-Health), Ludwig-Maximilians-Universität, as part of LMUinnovativ.

The German Diabetes Center is funded by the German Federal Ministry of Health (Berlin, Germany) and the Ministry of Culture and Science of the State of North Rhine-Westphalia (Dusseldorf, Germany). This study was supported in part by a grant from the German Federal Ministry of Education and Research to the German Center for Diabetes Research (DZD). The diabetes part of the KORA F4 study was funded by a grant from the German Research Foundation (DFG; RA 459/3-1).

Part of this study was supported by the funding from the European Union's Horizon 2020/ Horizon Europe research and innovation programmes: The DeTect2D & 210997-iPDM-GO EIT Health Innovation Project were supported by EIT Health which is co-funded by the European Union; The Innovative Medicines Initiative 2 (IMI2), project CARDIATEAM funded under the Grant Agreement No. 821508. Part of this research has been conducted using data from the UK Biobank, a major biomedical database (www.ukbiobank.ac.uk) with the project ID No. 10205.

K.S. is supported by Biomedical Research Program funds at Weill Cornell Medical College in Qatar, a program funded by the Qatar Foundation.

Online methods

Study participants and design

Study design. We investigated the longitudinal cohort KORA survey 4 (S4) and its two follow-ups, conducted in the area of Augsburg, Southern Germany. Baseline S4 study involved 4,261 individuals (aged 25–74 years) examined between 1999 and 2001. The first follow-up (F4) consisted of 3,080 individuals (aged 32–81 years) examined between 2006 and 2008. In the second follow-up (FF4), 2,269 participants were examined from 2013 to 2014⁹. All study participants gave written informed consent. The KORA study was approved by the ethics committee of the Bavarian Medical Association, Munich, Germany.

Because multi-omics profiles (i.e. epigenetics, transcriptomics, proteomics, and metabolomics) were measured with blood samples collected in the F4 survey, we identified candidate multi-omics biomarkers for CKD in hyperglycemic F4 participants and constructed GPS of eGFR values in the whole F4 population. The identified omics candidates of CKD were replicated in the KORA F3, KORA FF4, QBB, and QMDiab studies, and the constructed GPS of eGFR values was replicated in the UKBB and KORA S4 (non-overlapping individuals compared to those used for constructing GPS) studies, respectively. External replication was used in the KORA F3, QBB, QMDiab, and UKBB studies, whereas internal validation was used in the KORA S4 and FF4 studies.

Study participants. Exclusion criteria for KORA F4 participants used to identify candidate biomarkers of CKD in hyperglycemia included the following: 1) withdrawal of participation agreement (n = 3); 2) missing eGFR or UACR values (n = 36); 3) diagnosis of type 1 diabetes (n = 8), unclear type of diabetes mellitus (n = 75), or drug-induced diabetes (n = 1); 4) individuals with NGT (n = 1,556). The remaining dataset included 1,401 hyperglycemic participants, 968, 677, 518, and 1,378 of whom had QC-passed measurements of epigenetics, transcriptomics, proteomics, and metabolomics, respectively, and served as a discovery dataset to identify candidate biomarkers of CKD. The NGT participants were used for sensitivity analysis of the identified candidate biomarkers. Unless otherwise specified, the subsequent analyses involving the identified candidate biomarkers in KORA S4/F4/FF4 were conducted in a hyperglycemic setting.

The longitudinal analysis for F4→FF4 was conducted in F4 hyperglycemic individuals who had QC-passed omics profiles and available FF4 kidney traits measurements. In the case of incident CKD, 751 hyperglycemic individuals were available, including 558, 277, 441 and 744 individuals with QC-passed epigenetic, transcriptomic, proteomic, and metabolomic data, respectively. For the S4→F4 analysis, we used the same exclusion criteria as the ones in F4, resulting in 841 hyperglycemic individuals, of whom 448, 488, 209 and 572 individuals had QC-passed measurements of epigenetics, transcriptomics, proteomics, and metabolomics, respectively.

Among 2,916 KORA F4 individuals with genetic data, 159 were excluded due to relatedness or missing eGFR values, leaving 2,757 individuals for use in constructing the GPS of eGFR. Except for the construction and replication of GPS and the analysis of

$eGFR \sim GPS_{eGFR} + age + sex + PC_{1-4}$, where PC_{1-4} is the first four principal components of the genotyping data, all other analyses involving GPS were conducted in hyperglycemic individuals as stated above.

Definition of hyperglycemia and kidney traits

Hyperglycemia. Individuals with hyperglycemia and NGT were classified according to fasting and two-hour post load glucose (2-h glucose) values and HbA_{1C} using the ADA diagnostic criteria⁶³. The hyperglycemic group comprised participants with pre-diabetes and newly diagnosed T2D (i.e., fasting glucose ≥ 100 mg/dl or 2-h-glucose ≥ 140 mg/dl or HbA_{1C} $\geq 5.7\%$), as well as known T2D that was diagnosed by physician validated self-reporting and/or current use of anti-diabetes agents⁹.

Definition of kidney traits. The eGFR was calculated from serum creatinine (mg/dl) and cystatin-C (mg/dl, IDMS and IFCC standardized values) using the Chronic Kidney Disease Epidemiology Collaboration (CKD-EPI) equation⁶⁴. CKD was defined as an eGFR < 60 ml/min/1.73 m² or a UACR ≥ 30 mg/g⁶⁵. Incident cases of CKD consisted of participants that were non-CKD at F4 but had reduced kidney function (eGFR < 60 ml/min/1.73 m²) and/or kidney damage (UACR ≥ 30 mg/g) at FF4.

Other definitions of eGFR and CKD were used in part of the study's analyses and were denoted by symbols, including CKD_{crc} (eGFR-based CKD defined as eGFR < 60 ml/min/1.73 m²)⁶⁵, and eGFR_c (eGFR was calculated from serum creatinine, mg/dL, IDMS standardized values) using the CKD-EPI equation⁶⁴. Therefore, incident cases of CKD_{crc} consisted of participants who were non-CKD_{crc} at F4 but had reduced kidney function (eGFR < 60 ml/min/1.73 m²) at FF4.

Since kidney traits were available from three time points (S4/F4/FF4) in the KORA cohort and multi-omics profiles were measured with blood samples collected at the F4 survey, incident CKD, follow-up eGFR, eGFR_c, UACR values were only defined in the analysis of F4-to-FF4 in this study. The value of the follow-up kidney trait was interchangeable with the value of kidney trait FF4. The time point of the kidney trait was indicated, e.g. eGFR S4 meant eGFR values from S4. If not indicated, it meant the kidney trait was measured in F4.

Omics profiling and data normalization

Genotype. The Affymetrix Axiom Array was used to genotyping KORA S4/F4 individuals, of whom 2,916 had visit in F4. After thorough QC, 541,422 autosomal SNPs were used for imputation. Shapeit v2 was used to infer the haplotypes. The imputation was completed using Minimac3 on the Michigan Imputation Server with the 1000G phase 3 reference panel. Exclusion criteria of SNPs or individuals were: 1) SNPs with minor allele frequency (MAF) < 0.02 or Hardy-Weinberg equilibrium (HWE) $P < 5e-10$ or missing genotype data (geno > 0.01); 2) individuals with high rates of genotype missingness (mind > 0.01) or individuals with high or low heterozygosity rates or individuals with relatedness > 0.125 . Finally, there were 8,170,777 SNPs and 2,770 individuals in KORA F4 that passed QC and were used in building GPS of eGFR.

Epigenetics. The DNA methylation levels were measured with Illumina HumanMethylation450 BeadChip array as previously described⁶⁶. Data preprocessing of methylation data was carried out in accordance with the CPACOR pipeline⁶⁷, and R package minfi⁶⁸ was used for background correction. If the detection P value was ≥ 0.01 or the number of beads was ≤ 3 , probes were set to NA. Samples were excluded if the detection rate was < 0.95 . Quantile normalization (QN) and beta-mixture quantile normalization (BMIQ) pipelines were performed for normalization. The CpG methylation proportion was reported as a β -value, which was a continuous variable ranging from 0 to 1. CpG sites with β -values $\geq \text{mean} \pm 5 \times \text{standard deviation (SD)}$ were identified as outliers and replaced as NA. CpG sites on the sex chromosome or with missing rate $> 10\%$ were excluded. There were 461,767 CpG sites and 1,727 individuals passed QC. The remaining methylation data were further processed to account for technical effects and cell type confounding: beta values of each CpG site were adjusted for 30 principal components from control probes and white blood cell proportion estimates (6 Houseman variables), and the remaining residuals of beta values were used in the subsequent analysis.

Additionally, the CpGs with SNPs in the probe-binding sequence were checked and flagged for the identified candidate CpGs based on CpG-SNP pairs where any of the sources indicated that the SNP had a MAF ≥ 0.05 in Europeans from Illumina⁶⁹, 1000G phase 3⁷⁰, KORA F4 Affymetrix Axiom data (*data not shown*), and Chen *et al.* 2013⁷¹ (based on 1000G). Cross-specific probes were checked and flagged for the identified candidate CpGs as well from two previously published lists: Chen *et al.* 2013⁷¹ and Price *et al.* 2013⁷².

Transcriptomics. Gene expression levels were determined using the Illumina HumanHT-12 v3 Expression BeadChip⁷³. Expression data were log2-transformed and QN using the Bioconductor package lumi. Samples with fewer than 6000 detected genes or with an RNA integrity number (RIN) < 7 or that did not cluster according to their gender were excluded from further analysis. RNAs with QC comments for probe mapping not marked as “Good” provided by the manufacturer (Illumina) were excluded. RNA values $\geq \text{mean} \pm 5 \times \text{SD}$ were identified as outliers and replaced as NA, and 0.05% of NA data points were imputed with the k-nearest neighbors algorithm (KNN). There were 28,962 RNAs and 976 individuals passed QC. The residuals of RNA values after adjusting storage time, RIN values and amplification plate to remove potential technical effects were used in the subsequent analysis.

Proteomics. The proteomics data were measured with SOMAscan Assay. Details of the SOMAscan platform have been described elsewhere^{74,75}. One thousand individuals in KORA F4 had SOMAscan protein measurements for 1,129 protein SOMAmer probes. Thirty-four probes and one individual were identified as unqualified and excluded based on the SOMAscan QC. Probe values $\geq \text{mean} \pm 5 \times \text{SD}$ were identified as outliers and replaced as NA, and 0.3% of NA data points were imputed with KNN. There were 1,095 probes and 999 individuals passed QC.

Metabolomics. The serum samples from participants in the KORA F4 study were measured using AbsoluteIDQ™ p150 kit (BIOCRATES Life Sciences AG, Innsbruck,

Austria)⁷⁶. In total, 3,061 serum samples of the F4 study were quantified for 163 metabolites in 38 randomly distributed kit plates. The QC and adjustment of plate effects of metabolites were described previously⁷. Metabolites values $\geq \text{mean} \pm 5 \times \text{SD}$ were identified as outliers and replaced as NA, and 0.09 % of the data points were imputed with KNN. In particular, non-fasting samples were excluded for the analysis of metabolite data. Briefly, there were 125 metabolites and 3,027 individuals kept.

Furthermore, the values of proteins and metabolites were natural-log transformed. For comparability purpose, the values of CpG sites, RNAs, proteins, and metabolites were scaled to a mean value of 0 and a SD of 1 and were used in analysis if not indicated otherwise.

Identification of multi-omics signatures of CKD in hyperglycemia, their replication, and associations with other kidney traits

Preprocessing of clinical variables. The full model included the following covariates: age, sex, BMI, systolic BP, smoking status, triglycerides, total cholesterol, HDL cholesterol, FG, use of lipid-lowering, antihypertensive and anti-diabetic medication. One individual at KORA F4 had a measured UACR value as 9066.038 mg/g, which was deemed to be an extreme value and was replaced with the second maximum value using the winsorizing procedure. The values of UACR, FG, HbA_{1C}, triglycerides, creatinine, CST3, and urine albumin were natural log-transformed prior to analysis due to their right-skewed distribution. All numeric clinical variables were scaled to have a mean value of 0 and a SD of 1 and were used in the subsequent analysis unless otherwise specified.

Discovery. The discovery CKD - EWAS, TWAS, PWAS, and MWAS was performed, respectively, using the following logistic regression models: $\text{CKD} \sim (\beta \text{ value}) \text{CpG} / \text{RNA} / \text{protein} / \text{metabolite} + \text{full model}$. The top 20 significant CpG sites, top 20 RNAs, FDR significant proteins and metabolites consisted of the candidates' set.

We also investigated the associations of our identified candidate biomarkers with CKD in individuals with NGT of KORA F4 using logistic regression with the fully adjusted model except for anti-diabetic medication. Additionally, we conducted exhaustive literature research to cluster corresponding genes/proteins of candidates identified by EWAS, TWAS and PWAS, as well as candidate metabolites into distinct pathophysiology of T2D-related CKD.

Replication. We replicated our identified candidate biomarkers in additional studies. In the KORA F3 study, we replicated CpG sites and RNAs; in the QBB and QMDiab studies, we replicated proteins; and in the KORA F3 and KORA FF4 studies, we replicated metabolites.

Replication in KORA F3. The top 20 CpG sites, top 20 RNAs and FDR significant metabolites of CKD in hyperglycemia were replicated in KORA F3. In KORA F3, 481, 376, and 375 individuals had epigenetic, transcriptomic, and metabolomic measurements, respectively.

The DNA methylation levels were measured with Illumina HumanMethylation450 BeadChip, and the background correction was done with R package minfi⁶⁸. If the detection P value was ≥ 0.01 or the number of beads was ≤ 3 , probes were set to NA. Samples were excluded if the detection rate was < 0.95 . DNA methylation levels were normalized with QN + BMIQ pipeline. The effects of control probes and white blood cells at the CpG site were adjusted in the same way as described previously in KORA F4, and the white blood cell proportion estimates here were derived from Horvath variables. The transcriptomics data were measured using Illumina HumanWG-6 v2 expression BeadChip, and the expression data were log₂-transformed and loess normalized. The AbsoluteIDQ p150 kit was used to measure the targeted metabolites of serum samples. CpG sites with beta values and RNA values $\geq \text{mean} \pm 5 \times \text{SD}$ were identified as outliers and replaced as NA, which was then imputed with KNN, respectively. The plate effect of metabolites was addressed by including plate number as a covariate in the regression models, which are listed below, and metabolite concentrations were natural log transformed.

HbA_{1c} and triglycerides values were natural log transformed. The values of CpG sites, RNAs, proteins, and metabolites and all numeric clinical variables were scaled to a mean value of 0 and a SD of 1. The eGFR was calculated from serum creatinine (mg/dl) (IDMS standardized values) using the CKD-EPI equation⁶⁴. CKD was defined as an eGFR < 60 ml/min/1.73 m²⁶⁵.

The set of covariates defined as full model₂ included all of those in the full model except for FG that was replaced by HbA_{1c}. Since only 13 CKD cases of 481 individuals had methylation measurements, the association between CpG candidates and CKD was estimated using nearest-neighbor propensity score matching in a case-control study design. Propensity scores were generated using a classification tree with CKD as the outcome and covariates from the full model₂ except for BMI and smoking status (13 CKD cases contained NA for these two variables). After 1:4 propensity score matching, we used conditional logistic regression to investigate the association of candidate CpG sites with CKD. For candidate RNAs and metabolites, the following logistic regression models were used, respectively: $\text{CKD} \sim \text{RNA} + \text{full model}_2$, and $\text{CKD} \sim \text{metabolite} + \text{full model}_2 + \text{plate number}$.

Replication in KORA FF4. The identified candidate metabolites of CKD were replicated in hyperglycemic participants of FF4 as well. Individuals with hyperglycemia and NGT were classified according to the same ADA diagnostic criteria as in F4. Among 2,218 individuals who had metabolite measurements in FF4, after excluding non-fasting samples ($n = 15$), samples contained missing eGFR, UACR, or covariate values ($n = 51$), individuals with other or unclear types of diabetes ($n = 64$), and individuals with NGT ($n = 940$). The remaining dataset comprised of 1,148 hyperglycemic participants and was used in the replication analysis.

The clinical variables were preprocessed in the same way as in the F4, except that no UACR values were treated as extreme values and replaced. Serum samples from participants in the FF4 study were measured with the AbsoluteIDQTM p180 Kit. The plate effect adjustment, outlier detection and processing, NA imputation, scaling of metabolite

concentrations, and definition of CKD were identical to those described previously in the F4 study. The following logistic regression models were used: $\text{CKD} \sim \text{metabolite} + \text{full model}$.

Replication in QBB and QMDiab. The QBB is a prospective, population-based cohort study that was established in 2012¹¹. The QMDiab is a cross-sectional case-control study that was conducted in 2012 at Hamad Medical Corporation's Dermatology Department. The SOMAScan platform was used to quantify protein measurements in both QBB and QMDiab studies. The CKD was defined as an $\text{eGFR} < 60 \text{ ml/min/1.73 m}^2$ ⁶⁵. The eGFR in QBB and QMDiab was calculated from serum creatinine (mg/dL) using the CKD-EPI equation⁶⁴. Additionally, there were clinical biochemistry eGFR values in the QMDiab study reported from the medical results. The CKD in QMDiab was defined as $\text{eGFR} < 60 \text{ ml/min/1.73 m}^2$ that was calculated from serum creatinine or reported from clinical biochemistry. There were ten CKD cases in the QBB study while 2,915 individuals were non-CKD. In QMDiab, there were 19 CKD cases and 350 non-CKD individuals. The replication of candidate proteins in QBB and QMDiab used the following logistic regressions: $\text{CKD} \sim \text{protein} + \text{age} + \text{sex} + \text{BMI} + \text{study-specific covariates}$. The study-specific covariates in QMDiab consisted of diabetes status, the first three principal components (PCs) of the genotyping data (genoPC1, genoPC2, and genoPC3) and the first three PCs of the proteomics data (somaPC1, somaPC2, and somaPC3). The protein values in QBB were inverse normal scaled and in QMDiab were natural-log and Z score transformed.

Definition of extended replicated set. Candidate biomarkers of CKD identified by EWAS, TWAS, PWAS and MWAS were considered as replicated if they yielded $P < 0.05$ in replication studies and had the same direction of regression coefficients in replications as in the discovery. If two replication studies were conducted on one candidate, candidates which met this criterion in either study were considered replicated.

The union of replicated candidates and candidate biomarkers that were involved in eight T2DCKD subnetworks comprised of the extended replicated set. Notably, the replicated set and the extended replicated set had distinct purposes, with the former aiming to provide strengthened evidence such as causal support for candidates to become biomarkers and conclude on the potential novel ones based on our discovery, whereas the latter was primarily used to investigate the interplay of omic molecules and improve the understanding of the underlying mechanism. Therefore, the replicated set was used in the GPS and 2SMR analyses, while the extended replicated set was used in the multi-omics integration and prediction investigations.

Associations between candidate biomarkers and other kidney traits. To ascertain the source of the signals from the candidates of CKD in hyperglycemia, we examined the associations between the extended replicated set with UACR and eGFR values, respectively. The following linear regression models were used: $\text{UACR} / \text{eGFR} (\text{F4/FF4}) \sim (\beta \text{ value}) \text{ CpG} / \text{RNA} / \text{protein} / \text{metabolite} + \text{full model}$.

Among 751 hyperglycemic individuals who were included in the analysis while the outcome was incident CKD (F4-to-FF4), the following logistic regression models were

used for the candidates from the extended replicated set: incident CKD ~ (β value) methylation / RNA / protein / metabolite + full model.

Integration and causal mediation analysis of four-level omics signatures in hyperglycemia

Multi-omics integration network (MOIN). To reveal potential novel connections among omics molecules and explore the potential underlying pathway, we performed a data driven approach with GGM to build a network with the extended replicated set (except for SOMAmer probe CST3), and three known biomarkers for CKD (CST3, creatinine and urine albumin), as well as two candidate metabolite biomarkers of incident CKD in hyperglycemia (SM C18:1 and PC aa C38:0) ⁷. Using these 101 molecules, a network was built with an optimal GGM by minimizing the (extended) Bayesian information criterion (EBIC) of unregularized GGM models ⁷⁷ using “qgraph” R package with hyperglycemic individuals of KORA F4. Selecting unregularized GGMs according to EBIC has been shown to converge to the true model ⁷⁸. Briefly, the algorithm starts to run glasso to obtain 100 models, then refit all models without regularization and choose the best one according to EBIC. Each node in the network represents one omics molecule and each edge between two nodes reflected their partial relationship with considering the effects of all the other molecules in the network. The residuals of the omics molecules after removing the effects of full model were used to build the GGM network.

To further investigate the underlying relationship of molecules from different analyte classes, we filtered the network with edges that only connected nodes from different omics groups. CpGs, RNAs, proteins, metabolites, three known biomarkers were defined as distinct groups separately. MCL-cluster was further performed to the DMOIN to present different sub-clusters.

Causal mediation analysis of multi-omics with three time points of kidney traits. To determine whether certain molecules are involved in the pathway by which other omics molecules exert their nephropathic effects, or in other directions, we conducted causal mediation analyses to determine the optimal direction in each mediating triangle (Supplementary Fig. 8).

The mediation analyses consisted of three parts: 1) candidate & candidate & kidney traits: using 97 candidates from the extended replicated set; 2) candidate & known biomarkers & kidney traits: using 96 candidates (excluded SOMAmer probes CST3 from the extended replicated set) and three known biomarkers; 3) 2-mets & molecules & kidney traits: using two metabolites (SM C18:1 and PC aa C38:0) and other molecules (i.e., three known biomarkers and the extended replicated set except for metabolites). All three parts mediation analyses were conducted separated with three time points of kidney traits (CKD, eGFR and UACR) (Supplementary Fig. 8). Note, here we only conducted the mediation’s exploration for omics molecules’ pairs that belonged to different omics groups in each part. Three known biomarkers were defined as one group. Three time points kidney traits included eGFR values S4 / F4 / FF4, UACR values F4 / FF4, CKDcrcc S4, CKD F4, and incident CKD (F4-to-FF4). In the part of 2-mets analysis, kidney traits also included eGFRcr values S4 / F4 / FF4 ⁸.

Following the outline of Baron and Kenny⁷⁹, the pairwise relationship of the compounds (independent variable X, mediator M and outcome Y) consisting one possible mediating triangle was firstly examined and eligibility criteria of one mediating triangle is that if X, M and Y pairwise associated with each other. In detail, the spearman correlation coefficients were calculated for each pair of two omics molecules from different levels in each part using the values of residuals after removing the effects of the full model. The relationship between each of 102 molecules (i.e., 97 from extended replicated set, three known biomarkers and two metabolites) and each of eight kidney traits was examined, respectively. These included CKD (i.e., CKD F4 / incident CKD) ~ molecule + full model using logistic regression for F4/FF4, UACR / eGFR (i.e., eGFR / eGFRcr) ~ molecule + full model using linear regression for F4/FF4, and molecule ~ CKDcrcc / eGFR (i.e., eGFR or eGFRcr) + full model using linear regression for S4. The FDR was calculated per omics level per outcome within each part. Clinical variables CST3 and creatinine were not included in the investigation between UACR values and molecules, and urine albumin was excluded from the analysis between eGFR values and molecules, respectively. The significantly connected molecule pairs (FDR < 0.05) and their associated kidney trait (FDR < 0.05) were included into the mediation analyses to consist as one mediating triangle. In the case of CKD F4, those 97 candidates were regarded to be associated with CKD F4 as they were discovered from the relationships with CKD F4.

After eligible mediating triangles were resulted, the mediating effect was evaluated with the non-parametric casual mediation analysis adjusted for the full model. The mediation analysis was used a nonparametric causal mediation analysis using the R mediation package⁸⁰. The mediation analysis decomposes the total effect of exposure on the outcome into the 1) indirect effect through the mediator of interest and 2) direct effect or through a mediator other than the one in the study. The effect estimates of each association between X and Y in individuals with mediators were compared. The proportion of mediation effect was calculated as mediate effect dividing total effect (sum of direct effect and mediate effect) of the exposure. The *P*-value of mediation effect was calculated by bootstrapping with 1,000 resamples.

In each mediating triangle, to test all possible directions to figure out its best potential direction, the bi-mediation analyses were conducted for kidney trait in the KORA S4 (only used as X, e.g., kidney trait → omics₁ → omics₂) or FF4 (only used as Y, e.g., omics₁ → omics₂ → kidney trait) which was the longitudinal setting, while six mediation tests were performed for kidney trait in the KORA F4 which was cross-sectional setting (Supplementary Fig. 8).

In the cross-sectional analysis (the kidney trait in F4), we further conducted the SEM to reveal the suitable position of the kidney trait in the mediating triangle since it contained six possibilities. We tested the same six models defined in mediation analyses for kidney trait in F4 (Supplementary Fig. 8). In short, for each possible causal system, the SEM method creates a hypothetical covariance structure of the model and compares this with the empirical covariance structure, and rejects the model if a lack of fit is found. In determining whether the model is an acceptable fit, we used the criteria, namely: (1) Goodness of fit test $P \geq 0.05$; (2) $0.9 < \text{Goodness of Fit Index} \leq 1$; (3) Root Mean Square

Error Approximation ≤ 0.1 . If multiple models fitted the data, a given model was regarded as "best fit" if its Akaike Information Criterion (AIC) was at least one unit smaller than the next smallest AIC, otherwise all fitted models were reported and participated in the next selection. All SEM analyses are run in R using the "sem" package. We ran the analysis for each triangle separately. The residuals after removing the effects of the full model of each omics molecule were used to run the SEM.

To get the eligible mediation results, (1) the mediation results with mediating proportions outside the range of 0-100% were excluded; (2) in the case of kidney trait in KORA F4, the results were further filtered based on the results of SEM. The eligible mediation results were involved in the selection of the best direction (s). In each mediating triangle, we used the same criteria to select its best direction, namely: (1) the lowest mediating P value and its FDR < 0.05 ; (2) $10\% \leq$ mediating proportion $\leq 100\%$. If multiple directions fulfilled the criteria, the direction was deemed "best mediation direction" if its mediating proportion was at least 20% larger than the next largest mediating proportion, otherwise all fitted directions were deemed as "best mediation direction". The best mediation direction(s) in each mediating triangle was reported.

The eligible mediation results were visualized as scatter plots separately from the type of kidney trait and its position in the mediating triangle for candidate & candidate & kidney trait and candidate & known biomarkers & kidney trait to present the overall pattern.

Directed mediating multi-omics integration networks. To inspect the direction of how nephropathic effects potentially go through in each connected edge of our DMOIN built with GGM, we mapped mediation results of the best direction(s) with it to generate the DMMOINs.

Briefly, we mapped the results of best mediation direction(s) with the DMOIN for each time point (i.e., S4, F4 and FF4) and type of kidney trait (i.e., CKD, eGFR and UACR values) separately. If there were multiple mediating connections for the directed connected edges (i.e., for the case of the mediation part of 2-mets when the kidney traits were eGFR and eGFRcr), the result of maximum mediating proportion was selected. Among the overlapped part, if the mediation direction consisted of the results from both kidney trait in F4 (cross-sectional design) and in S4 / FF4 (longitudinal design), those in S4 or FF4 would be selected to present in the network based on the strength of the evidence. The DMMOINs were finally visualized separately based on the position of the kidney trait within the triangle (X, M and Y) and the type of kidney trait (CKD, eGFR and UACR).

Genome-wide polygenic score of eGFR

Quality control of effect size data of SNPs. The effect size estimates for SNPs on eGFR values were derived from the GWAS meta analysis results of 42 European ancestor studies⁸¹ (N = 567,460). The result included effect size estimates of 8,885,712 SNPs for eGFR values. Since KORA F4 was included in this meta analysis, to avoid overfitting, we first excluded its effect from the result of the meta analysis and then recalculated the regression coefficient, standard error and P -value of each SNP for eGFR values. We secondly excluded SNPs with MAF < 0.01 or ambiguous SNPs. There were 6,722,832

SNPs passed quality control and contained corrected effect size estimates for eGFR values.

Construction of GPS_{eGFR} . To ensure independence, the overlapped SNPs from the effect size data and genotyping data of KORA F4 were further dealt with strand flipping, deletion of mismatching SNPs, and LD clumping (SNPs with LD $r^2 < 0.1$ were kept). The GPS was constructed with adjusting age, sex, and the first four principal components (PC_{1-4}) of the genotyping data. There were 2,757 of 2,770 individuals in the KORA F4 study with available eGFR values, who were used to build GPS of eGFR. The GPS was constructed using an additive model with PRSice-2⁸². Finally, our GPS of eGFR values was constructed with the effects of 162,818 SNPs. Then, the GPS_{eGFR} values were scaled to have a mean of 0 and a SD of 1 in the subsequent analysis unless indicated otherwise.

Replication of GPS_{eGFR} . We replicated our GPS_{eGFR} in the UKBB and the KORA S4 testing individuals (individuals who had genotyping and phenotype data from KORA S4 but were not involved in the GPS development). The GPS of eGFR values were calculated using the same 162,818 SNPs.

Replication in UKBB. UK Biobank is a large-scale biomedical database and research resource that contains in-depth genetic and health information from half a million UK participants. Genome-wide genotyping was carried out using the UK Biobank Axiom Array. Around 850,000 variants were measured directly, while over 90 million variants were imputed using the Haplotype Reference Consortium and UK10K + 1000 Genomes reference panels. The eGFR was calculated from serum creatinine (mg/dl) and cystatin-C (mg/dl) using the CKD-EPI equation⁶⁴. In a single visit, black ancestry was defined as any ancestry with an African or Caribbean component (UK Biobank codes 2001, 2002, 4001, 4002, 4003, 4). Since there were three visits in UKBB, the black ancestry used in this replication was defined as samples that consistently answered one of the above categories whenever they reported ancestry. Finally, the GPS_{eGFR} in the UKBB was constructed with 463,814 individuals using the same 162,818 SNPs with the provided effect size.

Replication in KORA S4 testing samples. KORA S4 contained 681 independent individuals with genotyping data and available eGFR values. They were different individuals from the 2,757 KORA F4 participants used to construct the GPS for eGFR, and thus can be used as validation data for our constructed GPS. One of the 681 individuals contained an extreme eGFR value (510.52 ml/min/1.73 m²) and was excluded before the analysis. Subsequently, 680 individuals were used in this replication.

Associations of GPS_{eGFR} with eGFR. The GPS_{eGFR} values in both replication studies were scaled to have a mean of 0 and a SD of 1. In each study, the association between eGFR and GPS_{eGFR} was analyzed using linear regression as follows: $eGFR \sim GPS_{eGFR} + age + sex + PC_{1-4}$. The density distribution of GPS_{eGFR} , the stratification plot, and the regression fitting plot between eGFR and GPS_{eGFR} were plotted, respectively. The eGFR values used in the relationship with GPS were on their original scale to show the direct relationship between GPS and eGFR.

Associations of GPS_{eGFR} with kidney traits in hyperglycemia. To investigate whether the associations between GPS_{eGFR} and different kidney traits were consistent in hyperglycemic individuals, we used cross-sectional (F4) and longitudinal design

(F4→FF4) to analyse the associations between GPS_{eGFR} and kidney traits (eGFR, CKDcrcc and CKD) using linear/logistic regressions adjusted for the full model in KORA F4 hyperglycemic individuals, respectively. The stratification plot between eGFR and GPS in the hyperglycemic participants was plotted.

Associations of GPS_{eGFR} with replicated molecules and GPS's tail effect in hyperglycemia. Additionally, we examined the associations between GPS and replicated candidates using linear regression models as (beta value) methylation / RNA / protein / metabolite $\sim GPS_{eGFR} + \text{full model}$. To investigate whether there was a tail effect of GPS_{eGFR} on its associated candidates, we stratified the hyperglycemic KORA F4 population based on GPS_{eGFR} deciles to plot their relationship. Moreover, to investigate whether their associations exhibited a similar tail effect, the different effect sizes and significance levels at various percentiles of the GPS_{eGFR} distribution for all GPS associated candidates with adjusting full model were compared, including 5th, 15th, 25th, 35th and 45th percentiles and the full data set.

Mediation between GPS_{eGFR} , GPS associated molecules and kidney traits in hyperglycemia. To investigate whether GPS-associated candidates are part of the pathway by which GPS exerts its nephropathic effects, and kidney traits are a component of the pathway through which GPS connects to candidates. We conducted mediation analysis using three time points of kidney traits.

Three time points kidney traits included eGFR values (S4 / F4 / FF4), CKDcrcc S4, CKD F4, incident CKD (F4-to-FF4). GPS_{eGFR} (used only as causal X), each of its associated candidates and their associated kidney trait were constituted as one mediating triangle and then included in the mediation analyses. Each mediating triangle included the following testing direction(s):

- 1) kidney trait in S4: $GPS \rightarrow \text{kidney trait} \rightarrow \text{candidate}$.
- 2) kidney trait in F4: $GPS \rightarrow \text{candidate} \rightarrow \text{kidney trait}$ and $GPS \rightarrow \text{kidney trait} \rightarrow \text{candidate}$.
- 3) kidney trait in FF4: $GPS \rightarrow \text{candidate} \rightarrow \text{kidney trait}$.

We used the same criteria as the one in the section on causal mediation analysis to determine the best direction for each mediating triangle, except that the lower limit of the mediating proportion here was set to 0%.

Causality analysis with bi-directional 2SMR

We performed causal inference using bi-directional 2SMR methods to evaluate the potential causality of replicated proteins/metabolites-to-kidney traits and kidney traits-to-replicated proteins/metabolites. The kidney traits included CKD, eGFR and UACR values.

Genetic instruments and data harmonization. To assess the effect of protein-to-kidney trait, we identified protein instruments (first set) from Sun *et al.* study⁸³ (N = 3,301) and Emilsson *et al.* study⁸⁴ (N = 5,457). To evaluate the effect of metabolite levels on kidney traits, we extracted the corresponding SNP-exposure estimates from Dramisa *et al.* study (N = 7,478)⁸⁵ and Lotta *et al.* study (N = 16,828)⁸⁶, respectively. We extracted the corresponding SNP-outcome estimates from CKDGen meta-analysis^{81,87}. We selected instruments for proteins and metabolites to have $P < 1 \times 10^{-6}$ and clumped them for LD to ensure independence (10,000 kb pairs apart, $r^2 < 0.01$). We further eliminated SNPs

associated with more than one protein or metabolite, respectively. There were available genetic instruments for 44 of 46 replicated proteins, and for 13 of 14 replicated metabolites, respectively.

For the direction of kidney trait-to-protein, we identified CKD, eGFR and UACR instruments in the European population of CKDGen meta-analysis (N = 480,698 for CKD, N = 567,460 for eGFR, and N = 547,361 for UACR)^{81,87} and extracted the corresponding SNP-outcome estimates from the Sun *et al.* study⁸³ and Suhre *et al.* study⁸⁸. To evaluate the effect of kidney trait-to-metabolite, we used SNP-outcome estimates from the Dramisa *et al.* study⁸⁵ and Shin *et al.* study⁸⁹ (N = 7,824). We selected CKD, eGFR and UACR instruments that had genome-wide significance ($P < 5 \times 10^{-8}$) and clumped them for LD (10,000 kb pairs apart, $r^2 < 0.01$), respectively. After clumping, there were 24 CKD, 266 eGFR and 64 UACR instruments available. We further eliminated SNPs with potential horizontal pleiotropy traits (e.g. BP, hypertension, T2D, cholesterol and BMI) in the GWAS catalog⁹⁰ and PhenoScanner⁹¹. Moreover, SNPs associated with UACR related traits were eliminated while exposure was eGFR, and SNPs associated with eGFR related traits were eliminated while exposure was UACR, respectively. We downloaded all variant association results from the GWAS catalog (last access: 2021-06-08) and PhenoScanner (last access: 2021-06-10). After these filtration steps and elimination of potentially horizontal pleiotropy SNPs, 17 CKD, 195 eGFR and 30 UACR instruments were used as genetic instruments.

In the case that a specific instrument was not available in the outcome dataset, we used LD tagging ($r^2 > 0.8$) to locate proxy SNPs via “TwoSampleMR” R-package while outcome studies were available in IEU GWAS database or via LDlink using “LDlinkR” R-package while outcome studies were not available in IEU GWAS database⁹². Before performing the MR analysis, the exposure and outcome data were harmonized by aligning the SNPs on the same effect allele for the exposure and outcome. In the case of palindromic SNPs, allele frequency information was used to infer the forward strand where possible. The ambiguous SNPs were excluded from the MR analysis.

In summary, [8-16] CKD, [63-193] eGFR and [8-29] UACR instruments were used in MR analysis for kidney trait-to-protein. In the case of kidney trait-to-metabolite, [9-12] CKD, [105-162] eGFR and [19-25] UACR instruments were available for MR analysis. For protein/metabolite-to-kidney trait, [1-14] protein instruments and [1-4] metabolite instruments were used, respectively.

MR analyses and definitions of causality supported by MR. Our primary MR analysis method was RAPS because it is robust to systematic and idiosyncratic pleiotropy and provides unbiased estimates when there are many weak instruments⁹³. The heterogeneity of the SNP instruments was determined with Cochran's Q statistic of IVW and MR-Egger, and the horizontal pleiotropic effect of the involved SNPs was tested with the intercept of the MR-Egger and global test of MR-PRESSO⁹⁴. MR-PRESSO is a robust method to detect horizontal pleiotropy and outliers. If there was evidence of potential violations of heterogeneity or horizontal pleiotropy ($P < 0.05$), we conducted additional outliers-corrected MR analyses to address the issues. We utilized IVW-radial⁹⁵ to detect outliers of potential heterogeneity and performed outliers-corrected MR analyses with IVW/Wald

ratio using SNPs after removing outliers or the top significant SNP when IVW-Radial was not applicable. Moreover, we applied MR-PRESSO to identify outliers of potential horizontal pleiotropy and used MR-PRESSO outliers-corrected to conduct MR analyses using SNPs after removing the pleiotropic instruments.

Additionally, for the direction of protein-to-kidney trait, the protein instruments summarized from Zheng *et al.* study¹⁷ were used as a second set of instruments, with 23 of 46 replicated proteins containing suitable genetic instruments. The MR estimates were also analyzed with RAPS.

MR-supported causal was defined as either one:

- 1) RAPS FDR < 0.05, and no evidence of heterogeneity and horizontal pleiotropy; 2) FDR < 0.05 of outliers-corrected analyses when there was indication of heterogeneity and horizontal pleiotropy;
- 3) In the case of protein-to-kidney for the second set of instruments, RAPS FDR < 0.05, and significance of RAPS of the first set of instruments if instruments from the first set were available.

Finally, we compared the MR (RAPS, and outliers-corrected analyses when available) and observational estimates for all proteins and metabolites identified as MR-supported causal in either direction in the MR analysis.

To further investigate how these MR-supported causal proteins and metabolites connect to kidney traits, e.g., whether any potential mediators were revealed from our data, we presented their best direction(s) of mediation results from DMMOINs if available based on candidate → kidney trait and kidney trait → candidate, respectively.

All MR analyses were conducted using R packages: MendelianRandomization⁹⁶, TwoSampleMR⁹⁷, RadialMR⁹⁵, mr.raps⁹³ and LDlinkR⁹⁸.

Pathway analysis

Eight T2DCKD subnetworks.

The pathogenesis of T2DCKD is a rather complex process. To figure out the potential roles of our candidates in different pathological processes of T2DCKD and benefit for personalized medicine, we have clustered the genes/proteins of our candidate CpGs/RNAs/proteins and candidate metabolites into eight subnetworks. The interaction networks were built by manual curation and literature mining using the CIDEr database¹⁰ and the resulting graphs were edited with the yED software (yWorks GmbH, Tübingen, Germany). Nodes in the networks were analysed for physical and regulatory interactions and association with CKD. Information about all interactions between network objects was obtained by reading and manual annotation of experimental findings from relevant publications, primarily peer-reviewed "small-scale experiment" literature. Details of the interactions as well as respective literature references are available in Supplemental Tables 7-14.

Potential relevant molecular pathways from multi-omics. We used the DMMOIN to inspect potential causal links from multi-omics molecules and the potential mediators for MR supported causal candidates. The underlying pathway analysis for these potential

causal links was explored with CIDEr database as well. The example of IL19&SLC22A4&CKD and Tyr&IGFBP2&eGFR were given in discussion.

Prediction of incident CKD in hyperglycemia with multi-omics

Multi-omics prediction. To identify the dominant molecules and optimal cut-off number of omics levels used in the prediction of incident CKD in hyperglycemia, we performed 100 runs by bootstrapping individuals to evaluate predictive performance of various combinations of omics levels using GPS_{eGFR} and 97 candidates of the extended replicated set (62 proteins, 14 metabolites, 7 CpGs and 14 RNAs). Their predictive performance was evaluated using AUC. To assess the robustness of the improvement, we defined four sets of reference predictors, ref_1 included age and sex; ref_2 included variables from the full model; ref_3 included age, sex, eGFR and UACR¹⁸; ref_4 included age, FG, total cholesterol, SM C18:1, PC aa C38:0, eGFR and UACR⁷. We tested the following combinations: 1) two levels (ref + one level of omics: ref_GPS, ref_CpGs, ref_RNAs, ref_Proteins and ref_Metabolites); 2) three levels (ref + two levels of omics: ref_GPS_CpGs, ref_GPS_RNAs, ref_GPS_Proteins and ref_GPS_Metabolites); 3) four levels (ref + three levels of omics: ref_GPS_Proteins_Metabolites and ref_GPS_CpGs_Metabolites); 4) five levels (ref + four levels of omics: ref_GPS_CpGs_Proteins_Metabolites).

In the longitudinal analysis for F4→FF4, among 751 hyperglycemic individuals, there were 558 individuals with methylation data measurement. The missing values of the CpG sites in the extended replicated set of these 558 individuals were imputed with KNN and used in the prediction part.

Due to the incomplete sample size of different omics levels, we used bootstrapping to define training data and testing data. Among 751 individuals, after bootstrapping (replacement selection), the samples randomly selected (in bag) were used as training data, and the samples not selected (out of bag) were used as testing data. The numeric variables in the training data were scaled to a mean value of 0 and SD of 1, and the numeric variables in the testing data were scaled using the mean and SD value of the corresponding variable in the training data to avoid data leakage. We used the priority-Lasso⁹⁹ to select predictors for combinations that included candidates from the extended replicated set. When the reference sets were ref_1 , ref_2 and ref_3 , SM C18:1 and PC aa C38:0 were also included in the predictor selection process.

To determine the optimal number of omics levels for prediction and to account for the influence of available sample size in each combination, we built predictive models with random forest (RF) by increasing the number of omics levels used in each combination. For example, when we selected predictors from the combination of ref_GPS_proteins_metabolites, the non-missing records of training data of these variables were used as corresponding training data, the non-missing records of testing data of these variables were used as corresponding testing data. As for the block order in priority-Lasso, ref + GPS was defined as block 1 and was forced into the model (not penalized), while the order of blocks (2 and 3) of proteins and metabolites was defined by cross-validation. The number of maximal coefficients in each block except block 1 was set to 5. The

penalization parameters λ in each block except block 1 were determined by maximizing AUC estimated in a 10-fold cross-validation. The selected proteins and/or metabolites together with ref + GPS were used to develop prediction models with RF. Under the combination of ref _GPS _proteins _metabolites, the respective RF models for 1) ref, 2) ref + GPS, 3) ref + GPS + selected proteins, 4) ref + GPS + selected metabolites, and 5) ref + GPS + selected proteins + selected metabolites were built. In this way, five prediction models were built using training dataset for this combination. The AUC values of respective models were computed for the testing data only.

RF models were fitted with the “randomForest” R-package, which implements Breiman’s classic algorithm¹⁰⁰. The two RF parameters, nTree (i.e., the number of trees to grow for each forest) and mTry (i.e., the number of input variables randomly chosen at each split), were set to 600 and the default setting (floor of square root of the number of features), respectively.

In total, we performed 100 runs of bootstrapping, i.e., the procedure described above was randomly repeated 100 times. The AUC values of RF models with identical omics numbers (ref, ref + GPS, ref + GPS + 1omics, etc) in each omics combination for each reference set were averaged and presented.

Identification of dominant molecules. To identify the dominant molecules of candidate proteins and metabolites for predicting incident CKD in hyperglycemia on top of various reference predictors, and to determine whether their predictive ability is independent of baseline eGFR and UACR values, we calculated the percentage of each candidate (protein or metabolite) that was selected as one of the top five dominant features from different combinations (i.e., ref_Proteins, ref_Metabolites, ref_GPS_Proteins, and ref_GPS_Metabolites and ref_GPS_Proteins_Metabolites) in all four ref sets. The objective here was different from that of mediation analysis, which sought to identify correlated molecules that were potentially involved in the same pathway to aid in biological understanding. By contrast, the former was searching for uncorrelated molecules but potentially interactive with one another to benefit the prediction of the outcome, which aided in personalized prediction. Additionally, the selected times and mean coefficients of priority-Lasso of the top five selected predictors for each combination for each reference set were presented.

GPS_{eGFR} for incident CKD_{crc}. We investigated the improvement of GPS_{eGFR} on top of reference sets for incident CKD_{crc} in hyperglycemia. Briefly, the model building and AUC values calculation were as above. The boxplots of AUC values of the 100 runs for ref and ref + GPS in each reference set were presented.

Subgroup of CKD patients in hyperglycemia

We classified KORA F4 CKD patients with hyperglycemia using various combinations of variables (biomarkers, candidates and GPS) with uniform manifold approximation and projection (UMAP), and identified three distinct groups of CKD patients with three potential novel proteins. The number of CKD patients used for classification depends on the complete cases of the variables used. After classifying the groups, we explored their distinct patterns.

This study compared three potential novel proteins, numeric variables in the full model, serum LDL cholesterol, diastolic BP, 2-h glucose, HbA_{1C}, uric acid, creatinine, CST3, urine albumin, urine creatinine, eGFR, UACR values and candidates involved in eight T2DCKD processes among the generated classified groups. Variables with normal distribution were tested with the ANOVA and those with skewed distribution (HbA_{1C}, FG, triglyceride, creatinine, CST3, urine albumin, urine creatinine and UACR) were tested with the Kruskal-Wallis test. Pairwise comparison of numeric variables among groups was done by the Tukey's test for variables with normal distribution and the Dunn's test for variables with skewed distribution, respectively. The mean levels (scale values) of candidates in each classified group were visualized with heatmap, and the presented candidates were significant ones among groups from three potential novel proteins and candidates of eight T2DCKD processes.

The categorical variables (gender, prediabetes or T2D, eGFR based CKD, UACR based CKD, eGFR categories, UACR categories, CKD risk, eGFR decline > 30%, UACR increase > 30%, use of anti-hypertensive, ARBs, ACEIs, ARBs or ACEIs, anti-diabetic and lipid-lowering medication) were compared between groups using Pearson's chi-squared test or Fisher's exact test (when any theoretical frequency was less than one). The Cochran–Armitage test for trend was also applied if a variable with two categories and another ordinal variable with k categories, respectively.

Data and resource availability

The project agreement for this study was granted under K027/19g. The informed consent given by KORA study participants does not cover data posting in public databases. However, data are available upon request through the KORA-PASST (Project application self-service tool, www.helmholtz-muenchen.de/kora-gen) by means of a project agreement subject to approval by the KORA Board.

References

7. Huang, J., *et al.* Machine Learning Approaches Reveal Metabolic Signatures of Incident Chronic Kidney Disease in Individuals With Prediabetes and Type 2 Diabetes. *Diabetes* **69**, 2756-2765 (2020).
8. Huang, J., *et al.* Validation of Candidate Phospholipid Biomarkers of Chronic Kidney Disease in Hyperglycemic Individuals and Their Organ-Specific Exploration in Leptin Receptor-Deficient db/db Mouse. *Metabolites* **11**, 89 (2021).
9. Herder, C., *et al.* Proinflammatory Cytokines Predict the Incidence and Progression of Distal Sensorimotor Polyneuropathy: KORA F4/FF4 Study. *Diabetes care* **40**, 569-576 (2017).
10. Lechner, M., *et al.* CDeR: multifactorial interaction networks in human diseases. *Genome Biology* **13**, R62 (2012).
11. Al Thani, A., *et al.* Qatar Biobank Cohort Study: Study Design and First Results. *Am J Epidemiol* **188**, 1420-1433 (2019).
17. Zheng, J., *et al.* Phenome-wide Mendelian randomization mapping the influence of the plasma proteome on complex diseases. *Nat Genet* **52**, 1122-1131 (2020).
18. Tangri, N., *et al.* A predictive model for progression of chronic kidney disease to kidney failure. *Jama* **305**, 1553-1559 (2011).
63. Association, A.D. 2. Classification and Diagnosis of Diabetes: Standards of Medical Care in Diabetes—2021. *Diabetes care* **44**, S15-S33 (2020).
64. Inker, L.A., *et al.* Estimating glomerular filtration rate from serum creatinine and cystatin C. *The New England journal of medicine* **367**, 20-29 (2012).
65. Stevens, P.E., Levin, A. & Kidney Disease: Improving Global Outcomes Chronic Kidney Disease Guideline Development Work Group, M. Evaluation and management of chronic kidney disease: synopsis of the kidney disease: improving global outcomes 2012 clinical practice guideline. *Ann Intern Med* **158**, 825-830 (2013).
66. Zeilinger, S., *et al.* Tobacco smoking leads to extensive genome-wide changes in DNA methylation. *PLoS One* **8**, e63812 (2013).
67. Lehne, B., *et al.* A coherent approach for analysis of the Illumina HumanMethylation450 BeadChip improves data quality and performance in epigenome-wide association studies. *Genome Biol* **16**, 37 (2015).
68. Aryee, M.J., *et al.* Minfi: a flexible and comprehensive Bioconductor package for the analysis of Infinium DNA methylation microarrays. *Bioinformatics* **30**, 1363-1369 (2014).
69. Human methylation450 dbsnp137. (Illumina).
70. Auton, A., *et al.* A global reference for human genetic variation. *Nature* **526**, 68-74 (2015).
71. Chen, Y.A., *et al.* Discovery of cross-reactive probes and polymorphic CpGs in the Illumina Infinium HumanMethylation450 microarray. *Epigenetics* **8**, 203-209 (2013).
72. Price, M.E., *et al.* Additional annotation enhances potential for biologically-relevant analysis of the Illumina Infinium HumanMethylation450 BeadChip array. *Epigenetics Chromatin* **6**, 4 (2013).
73. Schurmann, C., *et al.* Analyzing illumina gene expression microarray data from different tissues: methodological aspects of data analysis in the metaxpress consortium. *PLoS One* **7**, e50938 (2012).
74. Gold, L., *et al.* Aptamer-based multiplexed proteomic technology for biomarker discovery. *PLoS One* **5**, e15004 (2010).
75. Kraemer, S., *et al.* From SOMAmer-based biomarker discovery to diagnostic and clinical applications: a SOMAmer-based, streamlined multiplex proteomic assay. *PLoS One* **6**, e26332 (2011).
76. Römisch-Margl, W., *et al.* Procedure for tissue sample preparation and metabolite extraction for high-throughput targeted metabolomics. *Metabolomics* **8**, 133-142 (2012).

77. Krumsiek, J., Suhre, K., Illig, T., Adamski, J. & Theis, F.J. Gaussian graphical modeling reconstructs pathway reactions from high-throughput metabolomics data. *BMC Syst Biol* **5**, 21 (2011).
78. Foygel, R. & Drton, M. Extended Bayesian Information Criteria for Gaussian Graphical Models. in *NIPS* (2010).
79. Baron, R.M. & Kenny, D.A. The moderator-mediator variable distinction in social psychological research: conceptual, strategic, and statistical considerations. *J Pers Soc Psychol* **51**, 1173-1182 (1986).
80. Tingley, D., et al. Mediation: R Package for Causal Mediation Analysis. *Journal of Statistical Software* **59**(2014).
81. Wuttke, M., et al. A catalog of genetic loci associated with kidney function from analyses of a million individuals. *Nat Genet* **51**, 957-972 (2019).
82. Euesden, J., Lewis, C.M. & O'Reilly, P.F. PRSice: Polygenic Risk Score software. *Bioinformatics* **31**, 1466-1468 (2015).
83. Sun, B.B., et al. Genomic atlas of the human plasma proteome. *Nature* **558**, 73-79 (2018).
84. Emilsson, V., et al. Co-regulatory networks of human serum proteins link genetics to disease. *Science* **361**, 769-773 (2018).
85. Draisma, H.H.M., et al. Genome-wide association study identifies novel genetic variants contributing to variation in blood metabolite levels. *Nat Commun* **6**, 7208 (2015).
86. Lotta, L.A., et al. A cross-platform approach identifies genetic regulators of human metabolism and health. *Nat Genet* **53**, 54-64 (2021).
87. Teumer, A., et al. Genome-wide association meta-analyses and fine-mapping elucidate pathways influencing albuminuria. *Nat Commun* **10**, 4130 (2019).
88. Suhre, K., et al. Connecting genetic risk to disease end points through the human blood plasma proteome. *Nat Commun* **8**, 14357 (2017).
89. Shin, S.Y., et al. An atlas of genetic influences on human blood metabolites. *Nat Genet* **46**, 543-550 (2014).
90. Buniello, A., et al. The NHGRI-EBI GWAS Catalog of published genome-wide association studies, targeted arrays and summary statistics 2019. *Nucleic Acids Research* **47**, D1005-D1012 (2019).
91. Staley, J.R., et al. PhenoScanner: a database of human genotype–phenotype associations. *Bioinformatics* **32**, 3207-3209 (2016).
92. Elsworth, B., et al. *The MRC IEU OpenGWAS data infrastructure*, (2020).
93. Zhao, Q., Wang, J., Bowden, J. & Small, D. Statistical inference in two-sample summary-data Mendelian randomization using robust adjusted profile score. *Annals of Statistics* **48**(2018).
94. Verbanck, M., Chen, C.Y., Neale, B. & Do, R. Detection of widespread horizontal pleiotropy in causal relationships inferred from Mendelian randomization between complex traits and diseases. *Nat Genet* **50**, 693-698 (2018).
95. Bowden, J., et al. Improving the visualization, interpretation and analysis of two-sample summary data Mendelian randomization via the Radial plot and Radial regression. *Int J Epidemiol* **47**, 1264-1278 (2018).
96. Yavorska, O.O. & Burgess, S. MendelianRandomization: an R package for performing Mendelian randomization analyses using summarized data. *Int J Epidemiol* **46**, 1734-1739 (2017).
97. Hemani, G., et al. The MR-Base platform supports systematic causal inference across the human phenome. *Elife* **7**(2018).
98. Myers, T.A., Chanock, S.J. & Machiela, M.J. LDlinkR: An R Package for Rapidly Calculating Linkage Disequilibrium Statistics in Diverse Populations. *Frontiers in Genetics* **11**(2020).
99. Klau, S., Jurinovic, V., Hornung, R., Herold, T. & Boulesteix, A.L. Priority-Lasso: a simple hierarchical approach to the prediction of clinical outcome using multi-omics data. *BMC Bioinformatics* **19**, 322 (2018).

100. Liaw, A. & Wiener, M. Classification and Regression by randomForest. *R News* **2**, 18--22 (2002).

Legends of Figure

Figure 1. Multi-omics signature associations with CKD, eGFR and UACR values in hyperglycemia

a-d, volcano plots of 4-level omics associations ($P < 0.05$) with CKD in hyperglycemic individuals of KORA F4. Odds ratios and P -values were from logistic regression analysis adjusted for full model (incl. age, sex, BMI, systolic BP, smoking status, triglyceride, total cholesterol, HDL cholesterol, fasting glucose, use of lipid lowering drugs, antihypertensive and anti-diabetic medication). The dashed lines represent FDR-corrected significance levels at 5%. Points with triangle shape represent replicated in additional study while those with circle shape represent not replicated.

e, venn plot of candidates used in T2D-related CKD subnetworks, replicated candidates, and FDR significant ($FDR < 0.05$) candidates from extended replicated set with eGFR (F4 or FF4) or UACR (F4 or FF4) values in hyperglycemic individuals of KORA F4. Extended replicated set was the union of candidates used in T2D-related CKD subnetworks and replicated candidates.

f, heatmap of regression coefficients for 97 omics molecules from extended replicated set with eGFR F4, follow-up eGFR, UACR F4, follow-up UACR, CKD F4 and incident CKD in hyperglycemic individuals of KORA F4. Regression coefficients were from linear regression analysis for eGFR and UACR values and from logistic regression analysis for CKD, which were all adjusted for full model.

Abbreviations: CKD, chronic kidney disease; eGFR, estimated glomerular filtration rate; UACR, urinary albumin-to-creatinine ratio; EWAS, TWAS, PWAS and MWAS, epigenome-, transcriptome-, proteome- and metabolome-wide association studies.

Figure 2. Interplay of four-level multi-omics molecules in hyperglycemia

a, DMOIN after clustering by the Markov Cluster Algorithm was presented. MOIN constructed with residuals of 96 candidates (extended replicated set except for SOMAmer probe CST3), three known biomarkers (CST3, creatinine, and urine albumin), and two metabolites (SM C18:1 and PC aa C38:0) using GGM, and then retained the edges connecting omics molecules belonging to different omics groups (i.e., GpGs, RNAs, Proteins, Metabolites, eGFRbiom and UACRbiom) and their corresponding nodes to get DMOIN. The residuals of omics molecules were calculated using linear regression models adjusted for full model (incl. age, sex, BMI, systolic BP, smoking status, triglyceride, total cholesterol, HDL cholesterol, fasting glucose, use of lipid lowering drugs, antihypertensive and anti-diabetic medication).

B, Scatter plots of mediation results of candidates and omic molecules (candidates and three known biomarkers) and eGFR values, in which each point represent the result of one mediation analysis. Each mediation analysis was adjusted for full model. Direction represents the omics type of one candidate to the omics type of another candidate within each triangle of mediation analysis. In the case of known biomarkers were involved, the color of points represents the position of one of three known biomarkers within each mediating triangle. The bigger size of points represents the direction was selected as best direction within the mediating triangle it comes from. The dashed lines represent FDR-corrected significance levels at 5%.

c, DMMOIN of eGFR (as Y), which is an overlapping network of DMOIN (a) and best mediation direction(s) of mediation results (b) and Supplementary Table 19 when eGFR was identified or treated as outcome in mediating triangle. Each edge represents one best mediation direction, e.g., B2M→CST3 represents B2M→CST3→eGFR. The width of the edge represents the mediation proportion in the corresponding mediation analysis.

In a, c, the color of the edge represents the weight of the correlation between two nodes calculated by GGM and the color of the node represents the omics group of the node.

Abbreviations: GGM, Gaussian graphical modeling; MOIN, multi-omics integration network; DMOIN, different levels of multi-omics integration network; DMMOIN, directed mediating multi-omics networks; eGFR, estimated glomerular filtration rate; UACR, urinary albumin-to-creatinine ratio; mito, T2DCKDmito subnetwork; adipo, T2DCKDadipo subnetwork; age, T2DCKDage subnetwork; angi, T2DCKDangi subnetwork; inna, T2DCKDinna subnetwork; ras, T2DCKDras subnetwork; tyr, T2DCKDtyr subnetwork; fibri, T2DCKDfibri subnetwork; EWAS, TWAS, PWAS, MWAS, epigenome-, transcriptome-, proteome-, and metabolome-wide association studies; candi, candidate.

Figure 3. GPS_{eGFR} in UKBB replication and hyperglycemic KORA F4 individuals, and its association and mediation with kidney traits and candidate biomarkers.

a, Density plot of GPS_{eGFR} in UKBB.

b, Stratification plots of GPS_{eGFR} decile and eGFR values in hyperglycemic population of KORA F4.

c, Forest plot of regression coefficients with 95% *CI* and *P*-values of GPS_{eGFR} with eGFR values (current and follow-up), *ORs* with 95% *CI* and *P*-values of GPS_{eGFR} with CKD (prevalent and incident) and eGFR-based CKD (prevalent and incident) in hyperglycemic population of KORA F4 is shown, respectively. Regression coefficients were from linear regression models for eGFR values and *ORs* were from logistic regression models for CKD, which all adjusted for full model (incl. age, sex, BMI, systolic BP, smoking status, triglyceride, total cholesterol, HDL cholesterol, fasting glucose, use of lipid lowering drugs, antihypertensive and anti-diabetic medication).

d, Volcano plot of associations between replicated candidates and GPS_{eGFR} in hyperglycemic individuals of KORA F4 is shown. Regression coefficients and *P*-values were from linear regression models adjusted for full models. The dashed lines represent FDR-corrected significance levels at 5%.

e, Scale values of candidate protein JAM2 in stratification of the KORA F4 hyperglycemic individuals according to GPS_{eGFR} deciles. The centers are the mean scale values of JAM2 and the error bar are the 95% confidence intervals.

f, Regression coefficients with 95% *CI* of GPS_{eGFR} to candidate protein JAM2 in full multivariable linear regression model using different percentile of sample size of hyperglycemic individuals of KORA F4 are shown, respectively. The centers represent the regression coefficients, while the error bars represent the 95% confidence intervals. Extreme GPS_{eGFR} is a strong risk factor for decreasing JAM2 levels in hyperglycemic individuals of KORA F4. The effect from linear regression model of GPS_{eGFR} on JAM2 is over fivefold in the extreme 5% of the sample when compared to the full data.

g, Scatter plots of mediation proportion (%) and sign of mediate & direct FDR significance of mediation results (average mediate effect FDR < 0.05) of each mediating triangle in a full adjusted nonparametric causal mediation analysis are shown, respectively. The triangle was composed of GPS_{eGFR} , GPS_{eGFR} associated candidate and kidney trait (eGFR values or CKD). The shape of the point represents the type of mediator (i.e., kidney trait or candidate) in the corresponding triangle. When kidney traits in KORA F4, candidate and kidney trait were used as potential mediator in each mediation analysis, respectively, and the best mediation result of them was shown.

Abbreviations: GPS_{eGFR} , genome-wide polygenic score of eGFR values; CKD, chronic kidney disease; eGFR, estimated glomerular filtration rate; CKDcrcc, eGFR-based CKD that was defined as $eGFR < 60 \text{ ml/min/1.73 m}^2$; UKBB, UK biobank.

Figure 4. Two-sample MR evidence is suggestive of relationships between kidney traits (i.e., CKD, eGFR, UACR) and candidates (i.e., proteins and metabolites) in both directions.

a,b, Scatter plots of results of bi-directional two sample MR of replicated proteins and metabolites and kidney traits (i.e., CKD, eGFR, UACR), respectively. The dashed lines represent FDR-corrected significance levels at 5%.

Abbreviations: MR, Mendelian randomization; CKD, chronic kidney disease; CKDcrcc, CKD was defined by $eGFR < 60 \text{ ml/min/1.73 m}^2$; eGFR, estimated glomerular filtration rate; UACR, urinary albumin-to-creatinine ratio; IVW, inverse variance weighted; RAPS, robust adjusted profile score; MR-PRESSO, MR pleiotropy residual sum and outlier. Zh, genetic instruments of proteins selected from Zheng et al. ¹⁷.

Figure 5. Multi-omics prediction of incident CKD in hyperglycemic individuals of KORA F4.

a, Mean AUC values of predictive models built by ref_1 and $ref_1 + GPS$ /one omics within each two levels of omics combination for ref_1 over 100 times bootstrapping.

b, Mean AUC values of predictive models built by different levels of omics predictors within each omics combination for each reference set over 100 times bootstrapping.

In a-b, omics predictors (metabolites, proteins, RNAs, or CpGs) were selected by priority lasso in the corresponding omics combination for each reference set in each round in the training data. Within each omics combination, the set of selected and reference predictors were used to develop respective prediction models according to the increment of numbers of levels of omics predictors, e.g., if the omics combination selected predictors from five omics levels, the prediction models using predictors of ref , $ref + GPS$, $ref + GPS + 1omics$, $ref + GPS + 2omics$, $ref + GPS + 3omics$ were built accordingly using training data, respectively. The AUC values were computed for the test data only. The mean AUC values of each predictive model of 100 times bootstrapping for each combination within each reference set were displayed in the plot. The mean values of samples size of training and testing data over 100 times bootstrapping are presented, e.g., 680 + 251 in two levels for ref_1 represent 680 is mean values of training samples size and 251 is mean values of testing samples size.

c, The percentage of proteins and metabolites that were selected as the top five dominant features from combination of ref_Proteins, ref_Metabolites, ref_GPS_Proteins, ref_GPS_Metabolites, and ref_GPS_Proteins_Metabolites in four reference sets. The percentage was calculated as the number of selecting as the top five dominant features dividing the number of participating selection for each candidate.

d, Boxplots of AUC values of predictive models built by ref, and ref + GPS in four reference sets for incident CKDcrcc in hyperglycemia over 100 times bootstrapping, respectively. The AUC values were computed for the test data.

ref₁: baseline age, sex; ref₂: baseline age, sex, BMI, systolic BP, smoking status, triglyceride, total cholesterol, HDL cholesterol, fasting glucose, use of lipid lowering drugs, antihypertensive and anti-diabetic medication; ref₃: baseline age, sex, eGFR and UACR; ref₄ included age, FG, total cholesterol, SM C18:1, PC aa C38:0, eGFR and UACR.

Abbreviations: AUC, area under the receiver operating characteristic curve; GPS, genome wide polygenic score of eGFR values; CKD, chronic kidney disease; eGFR, estimated glomerular filtration rate; UACR, urinary albumin-to-creatinine ratio; CKDcrcc, eGFR-based CKD that was defined as eGFR < 60 ml/min/1.73 m².

Figure 6. Three potential novel biomarkers subgroup CKD patients with hyperglycemia and the unique pattern exploration in each group.

a, Scatter plot showed KORA F4 CKD patients with hyperglycemia were clustered into three groups based on the first and second components of UMAP using three potential novel proteins. g1: N = 22; g2: N = 14; g3: N = 23.

b, Boxplots of values of three potential novel proteins, eGFR, natural log-transformed of UACR and uric acid across three groups of KORA F4 CKD patients with hyperglycemia.

c, Barcharts of percentage(s) of male, taking anti-hypertensive, ARBs or ACEIs medication, eGFR categories, UACR categories, eGFR decline > 30% and UACR increase > 30% in each group, respectively.

d, Heatmap of mean levels (scale value) of candidates in each subgroup was showed, and the presented candidates were the significant ones among three groups, which were from three potential novel proteins and 87 candidates used in eight processes. +, the relative average levels of the candidate in this group over 1.5 times of the relative average levels of this candidate of three groups; -, the relative average levels of this candidate of three groups over 1.5 times of the relative average levels of the candidate in this group. The candidates marked with + / - were indicated as dominant candidates for this group.

e, The relative percentage of involved processes of the dominant candidates for each group. Relative % of one process = the number of dominant candidates involved in the specific process / the number of dominant candidates in this group.

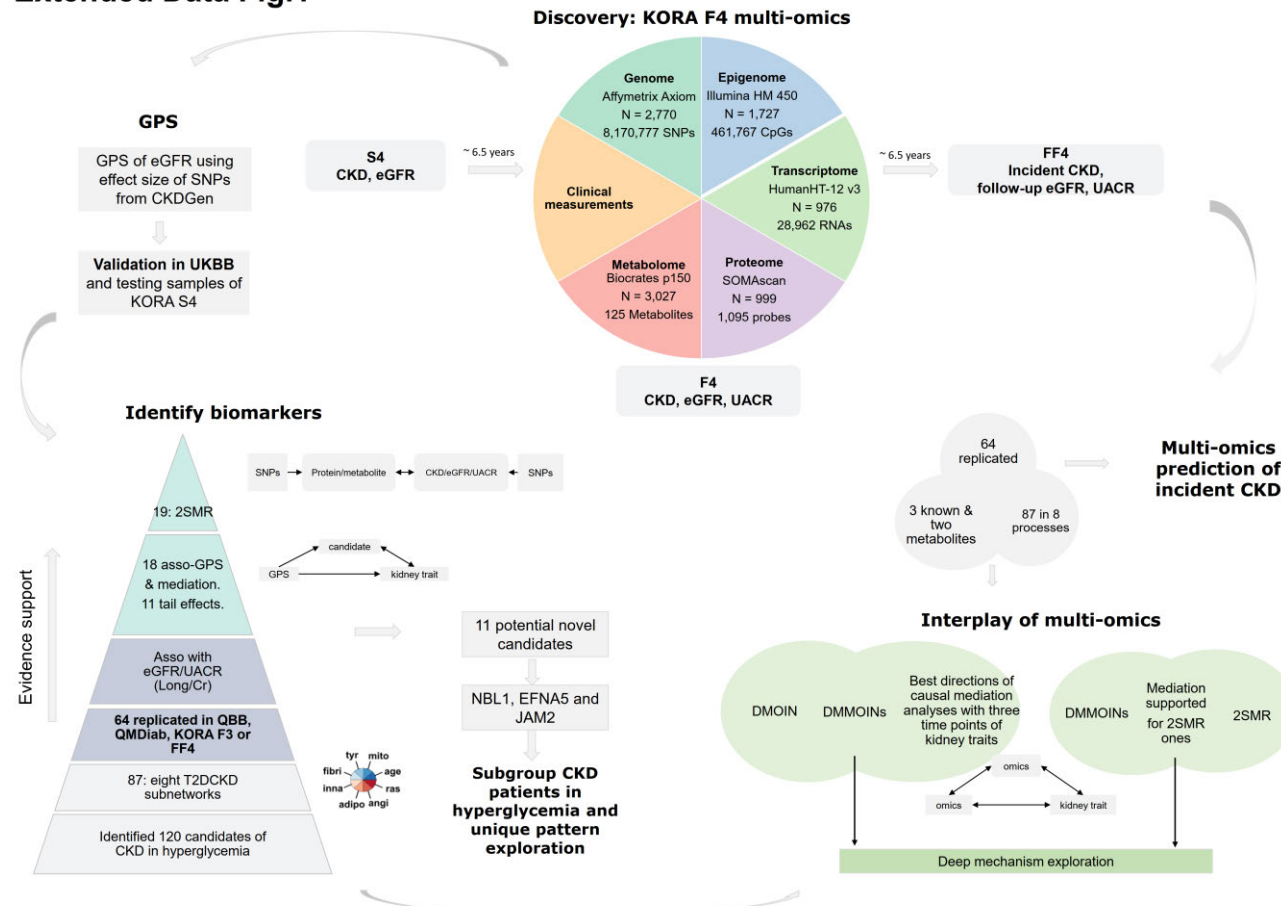
The values of clinical variables here were not scaled and the values of candidates here were scaled.

Abbreviations: ARBs, taking angiotensin 2 receptor blockers; ACEIs, taking angiotensin-converting enzyme inhibitors; eGFRcla, eGFR categories; UACRcla, UACR categories; CKD, chronic kidney disease; eGFR, estimated glomerular filtration rate; UACR, urinary albumin-to-creatinine ratio; mito, T2DCKDmito subnetwork; adipo, T2DCKDadipo subnetwork; age,

T2DCKDage subnetwork; angi, T2DCKDangi subnetwork; inna, T2DCKDinna subnetwork; ras, T2DCKDras subnetwork; tyr, T2DCKDtyr subnetwork; fibri, T2DCKDfibri subnetwork.

Extended Data

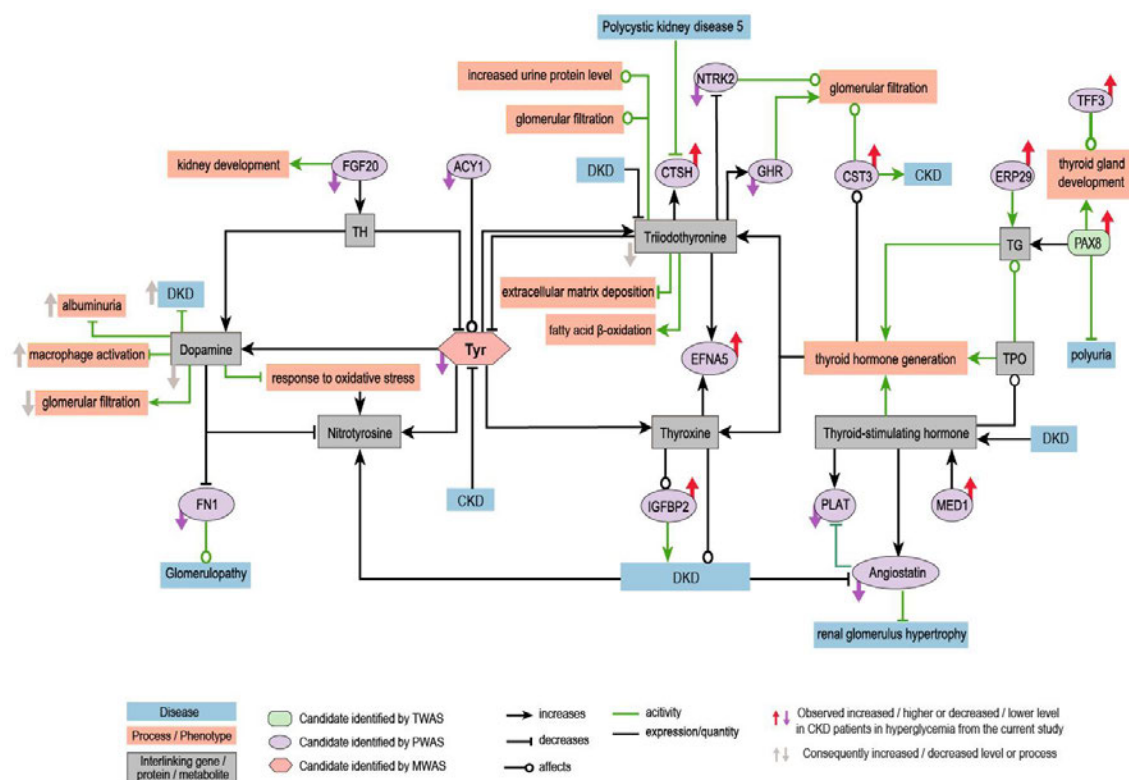
Extended Data Fig.1



Extended Data Fig. 1. Study overview.

Abbreviations: CKD, chronic kidney disease; eGFR, estimated glomerular filtration rate; UACR, urinary albumin-to-creatinine ratio; GPS, genome-wide polygenic score; UKBB, UK biobank; 2SMR, two-sample Mendelian randomization; QBB, Qatar Biobank study; QMDiab, Qatar Metabolomics Study on Diabetes; T2DCKD, T2D related CKD; Cr, cross-sectional association; Long, longitudinal association; mito, T2DCKDmito subnetwork; adipo, T2DCKDadipo subnetwork; age, T2DCKDage subnetwork; angi, T2DCKDangi subnetwork; inna, T2DCKDinna subnetwork; ras, T2DCKDras subnetwork; tyr, T2DCKDtyr subnetwork; fibri, T2DCKDfibri subnetwork; DMOIN, different levels of multi-omics integration network; DMMOIN, directed mediating multi-omics networks.

Extended Data Fig. 2 T2DCKDtyr

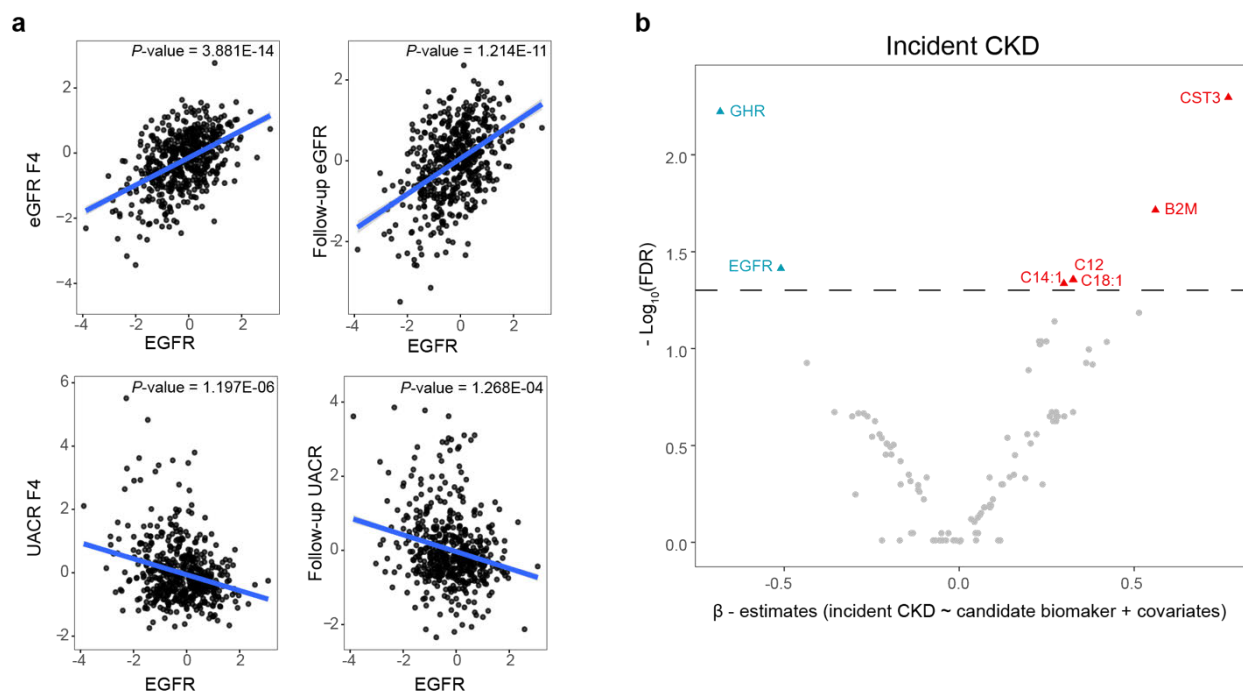


Extended Data Fig. 2. T2DCKDtyr subnetwork

Tyr-related T2DCKD activity network, which was built by literature research.

Abbreviations: T2DCKD, T2D related CKD; CKD, chronic kidney disease.

Extended Data Fig. 3



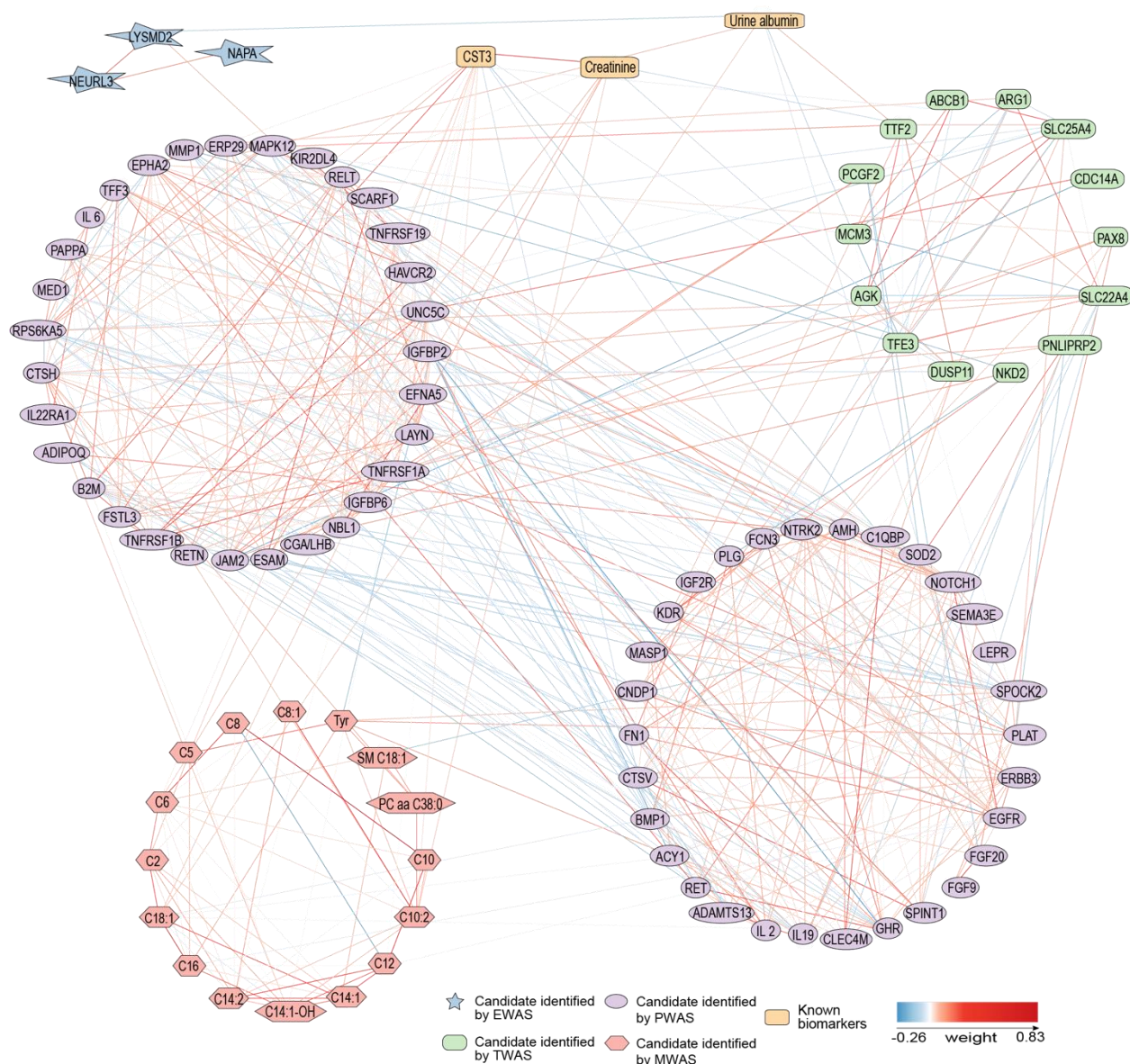
Extended Data Fig. 3. Protein EGFR associated with eGFR and UACR values and incident CKD associated candidates in KORA F4 hyperglycemic individuals.

a, scatter plots of protein EGFR (scale value) with scale values of eGFR F4, follow-up eGFR, UACR F4, follow-up UACR, respectively. The regression fitted lines were shown and the corresponding slopes were calculated with adjusting for the full model (incl. age, sex, BMI, systolic BP, smoking status, triglyceride, total cholesterol, HDL cholesterol, fasting glucose, use of lipid lowering drugs, antihypertensive and anti-diabetic medication).

b, volcano plot of omics molecules from extended replicated set with incident CKD in hyperglycemic individuals of KORA F4. Regression coefficients were from logistic regression analysis for incident CKD, which were adjusted for the full model. The dashed line represents FDR-corrected significance level (5%). FDR of each omics molecule was calculated within each omics level.

Abbreviations: CKD, chronic kidney disease; eGFR, estimated glomerular filtration rate; UACR, urinary albumin-to-creatinine ratio.

Extended Data Fig. 4



Extended Data Fig. 4. Multi-omics integration network

Multi-omics integration network built with residuals of 96 candidates (extended replicated set except for SOMAmer probe CST3), three known biomarkers (CST3, creatinine, and urine albumin), and two metabolites (SM C18:1 and PC aa C38:0) using GGM. The residuals of omics molecules were calculated with linear regression models adjusted for the full model (i.e., age, sex, BMI, systolic BP, smoking status, triglyceride, total cholesterol, HDL cholesterol, fasting glucose, use of lipid-lowering drugs, antihypertensive and anti-diabetic medication). The color of the edge represents the weight of the correlation between two nodes and the color of the node represents the omics group of the node.

Abbreviations: GGM, Gaussian graphical modeling; eGFR, estimated glomerular filtration rate; UACR, urinary albumin-to-creatinine ratio.

Extended Data Fig. 5



Extended Data Fig. 5. Candidate proteins and three known biomarkers identified as main mediators.

a, Scatter plots of mediation results of candidates and candidates and kidney traits (as X or Y). Direction represents the direction of the omics types of the corresponding two candidates in the mediating triangle.

b, Scatter plots of mediation results of candidates and three known biomarkers (CST3, creatinine and urine albumin) and kidney traits (as X or Y). The colors of the points represent the position of the known biomarker in the triangle of mediation analysis.

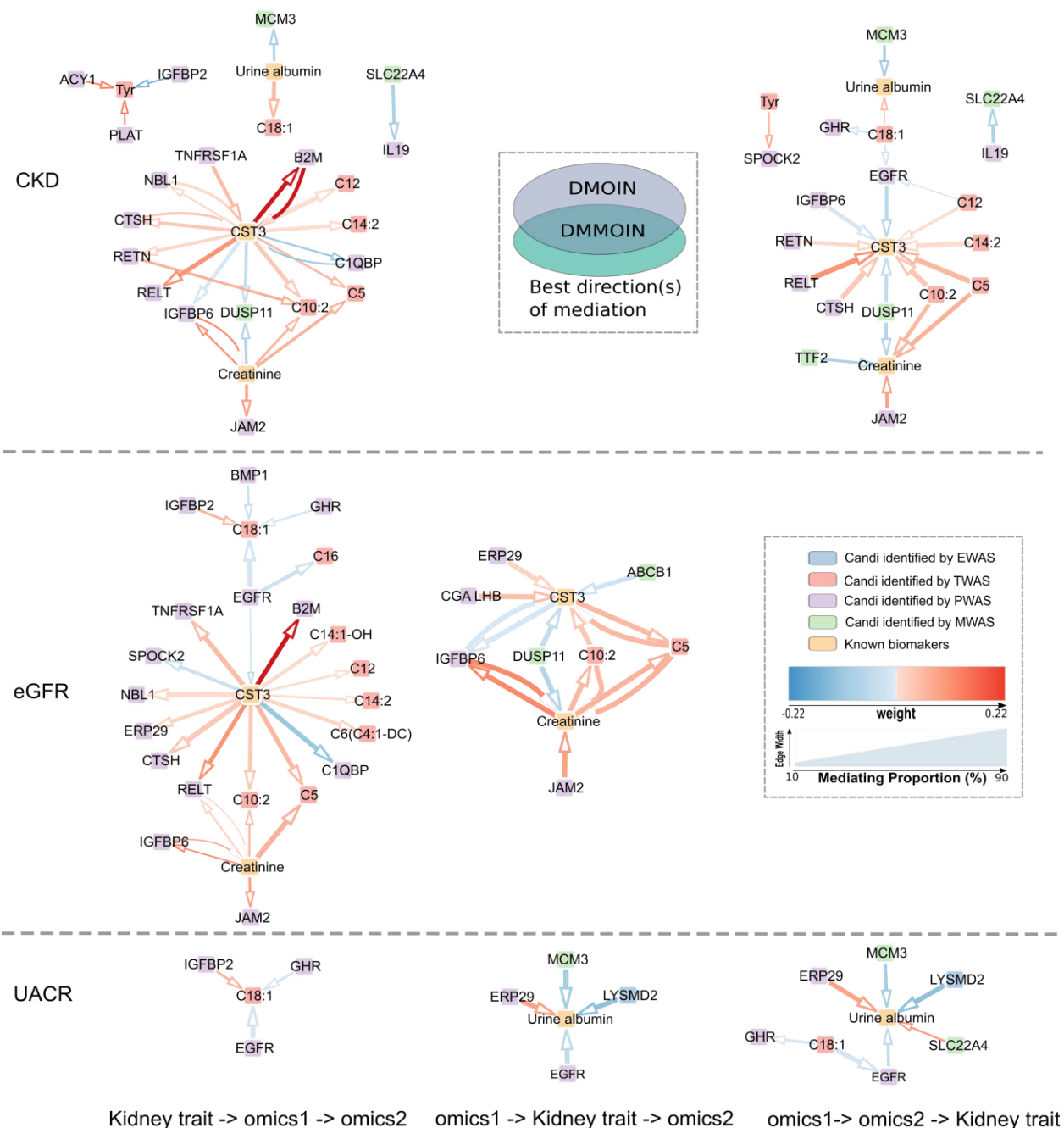
c, Scatter plots of mediation results of candidate → eGFR → candidate. Direction represents the direction of the omics types of the corresponding two candidates in the mediating triangle.

d, Scatter plots of mediation results of candi → kidney trait → known and known → kidney trait → candi. Known biomarkers include CST3, creatinine and urine albumin.

Each point represents the result of one mediation analysis. Each mediation analysis was adjusted full model (i.e., age, sex, BMI, systolic BP, smoking status, triglyceride, total cholesterol, HDL cholesterol, fasting glucose, use of lipid lowering drugs, antihypertensive and anti-diabetic medication). Kidney traits include CKD, eGFR and UACR. The bigger size of points represents the direction was selected as best direction in the mediating triangle it belongs to. X, M, Y represent independent variable, mediator and outcome in the mediating triangle: $X \rightarrow M \rightarrow Y$, respectively. The dashed lines represent FDR-corrected significance levels at 5%.

Abbreviations: CKD, chronic kidney disease; eGFR, estimated glomerular filtration rate; UACR, urinary albumin-to-creatinine ratio; candi, candidate.

Extended Data Fig.6



Extended Data Fig. 6. Directed mediating multi-omics networks

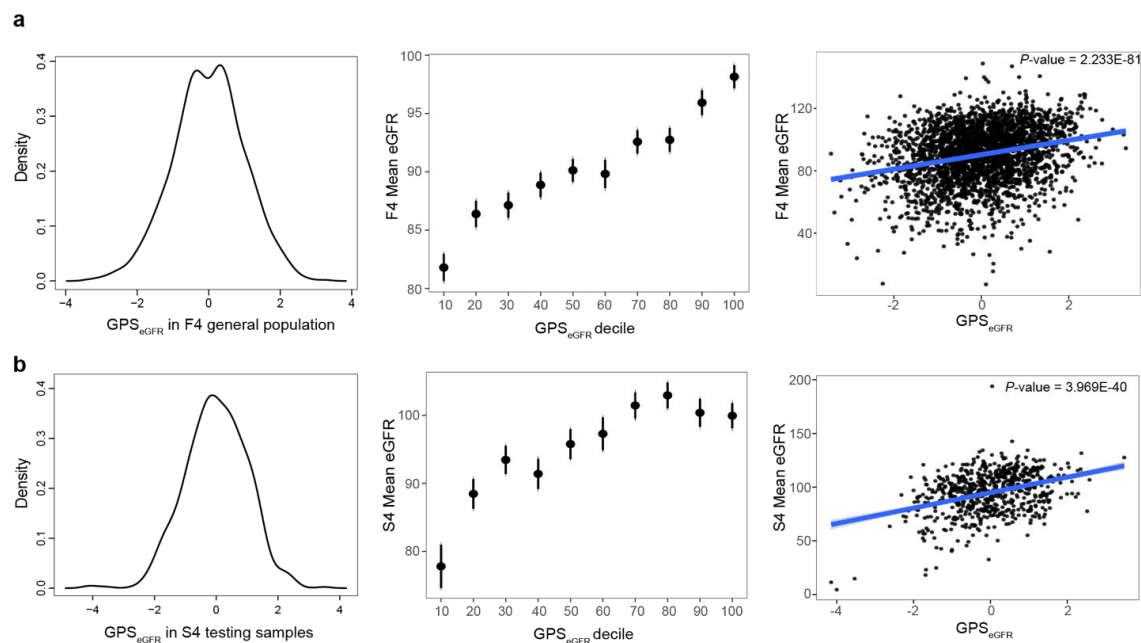
DMMOINs are overlapped networks of DMOIN (Fig. 2a) and best mediation direction(s) of mediation results (Supplementary Tables 17-19) separating for each kidney trait and the position of kidney trait in the mediating triangle. Each edge represents one best mediation direction, e.g., B2M→CST3 when kidney trait was eGFR and the position of kidney trait was X in mediating triangle, it represents eGFR→CST3→B2M.

The width of the edge represents the mediation proportion in each mediation analysis. The color of the edge represents the weight of the correlation between two nodes calculated by GGM and the color of the node represents the omics group of the node.

Abbreviations: GGM, Gaussian graphical modeling; DMMOIN, directed mediating multi-omics integration networks; CKD, chronic kidney disease; eGFR, estimated glomerular filtration rate;

UACR, urinary albumin-to-creatinine ratio; EWAS, TWAS, PWAS and MWAS, epigenome-, transcriptome-, proteome- and metabolome-wide association studies.

Extended Data Fig. 7



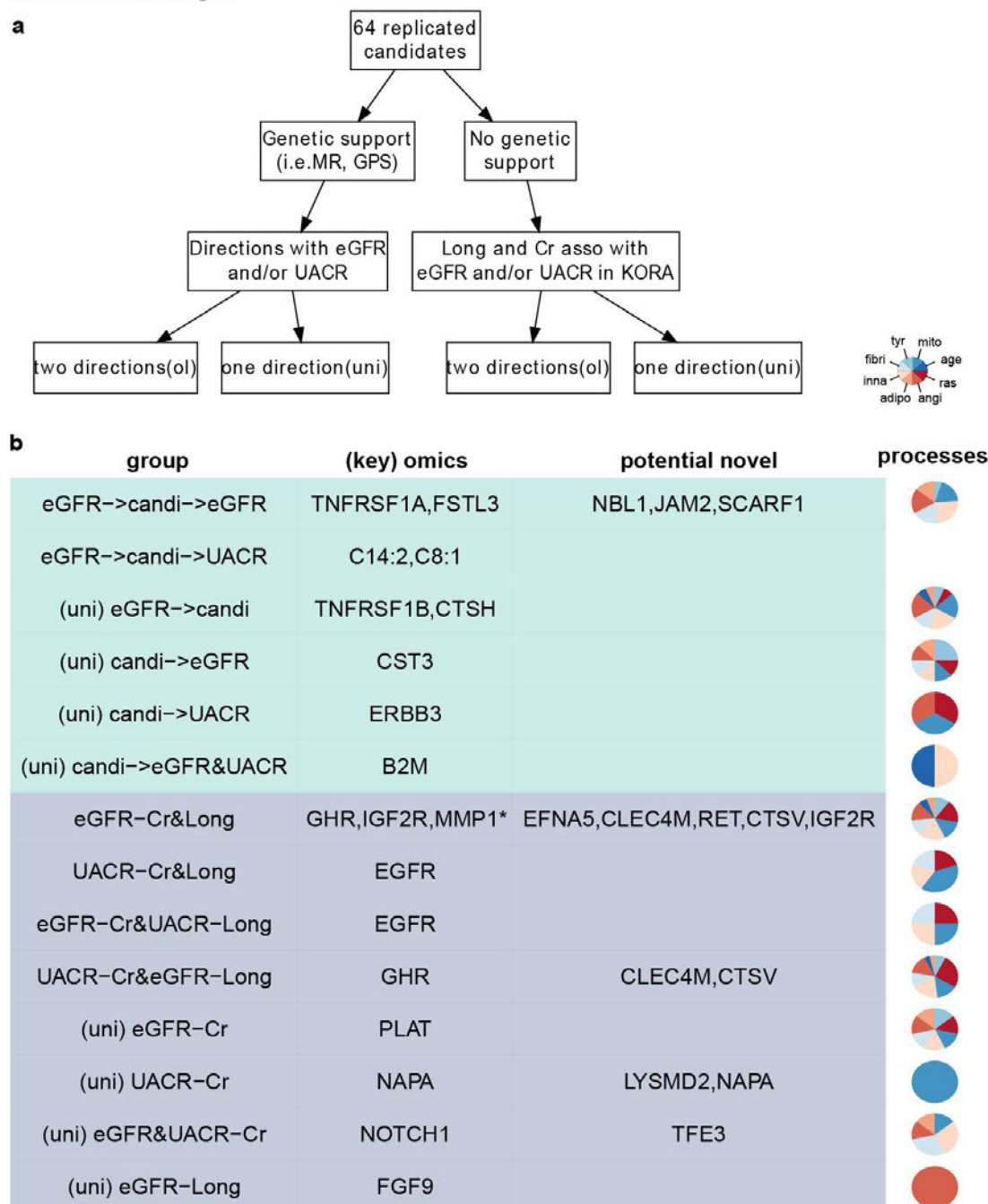
Extended Data Fig. 7. Genome-wide polygenic score of eGFR values in discovery KORA F4 cohort and KORA S4 testing samples.

a, Distribution of GPS_{eGFR} in KORA F4 general population. eGFR values in stratification of the KORA F4 individuals according to GPS_{eGFR} deciles. Scatter plots of GPS_{eGFR} and eGFR values in general population of KORA F4. The slope of regression fitted line was calculated with adjusting for age, sex, and the first four principal components of genetic data.

b, Distribution of GPS_{eGFR} in KORA S4 testing samples. Stratification plot of GPS_{eGFR} decile and eGFR values in KORA S4 testing samples. Scatter plots of GPS_{eGFR} and eGFR values in KORA S4 testing samples. The slope of regression fitted line was calculated with adjusting for age, sex, and the first four principal components of genetic data.

Abbreviations: GPS, genome-wide polygenic score of eGFR values; eGFR, estimated glomerular filtration rate.

Extended Data Fig. 8



Extended Data Fig. 8. Characteristics of replicated multi-omics candidates of CKD with hyperglycemia according to eGFR and/or UACR values-based evidence.

a, Diagram depicting the subdivision of 64 replicated candidates based on different supporting evidence with eGFR and/ or UACR values.

b, The key omics candidates, potential novel candidates identified from our study, and processes involved in eight subnetworks in each group are presented. Green and purple colors denote groups defined by genetic evidence support with eGFR and/or UACR from 2SMR or GPS, and associations (i.e., cross-sectional and longitudinal) with eGFR and/or UACR from the KORA study, respectively. Candidates that were annotated to the most T2DCKD processes were defined

as the key omics candidates in each group. If there were no candidates annotated to eight processes in a group, the omics candidates in this group were shown in the cell of "key omics."

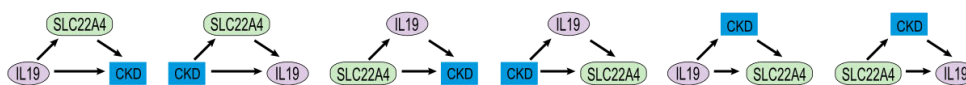
* MMP1: MMP1 was potentially causal with CKD by 2SMR, but no causal relationship was supported for eGFR or UACR.

Abbreviations: 2SMR, two-sample Mendelian randomization; GPS, genome wide polygenic score of eGFR values; CKD, chronic kidney disease; eGFR, estimated glomerular filtration rate; UACR, urinary albumin-to-creatinine ratio; ov: candidates in this group may overlap with other groups in case of two directions; uni: candidates in this group were unique with other groups in case of one direction; Cr, cross-sectional association; Long, longitudinal association; mito, T2DCKDmito process; adipo, T2DCKDadipo process; age, T2DCKDage process; angi, T2DCKDangi process; inna, T2DCKDinna process; ras, T2DCKDras process; tyr, T2DCKDtyr process; fibri, T2DCKDfibri process; T2DCKD, T2D related CKD.

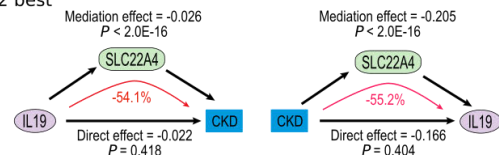
Extended Data Fig. 9

a Mediation analyses

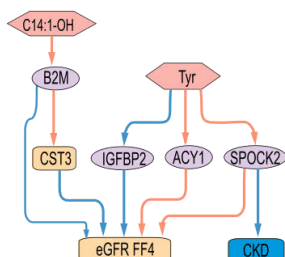
6 tests in triangle



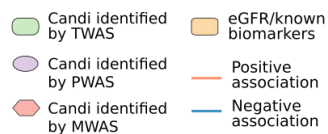
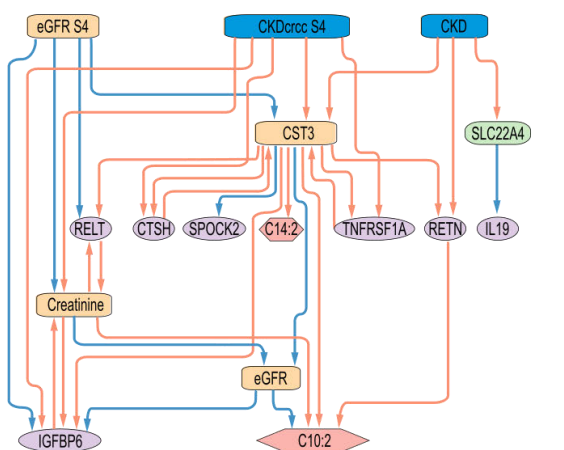
2 best



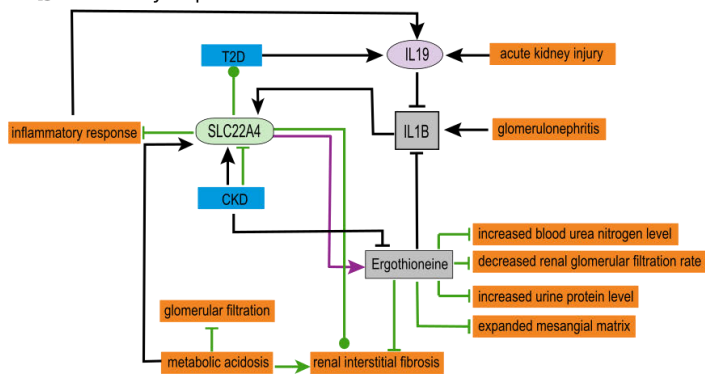
c Overlapped DMMONs and candidates that were MR-supported causal to kidney trait



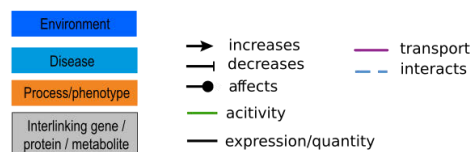
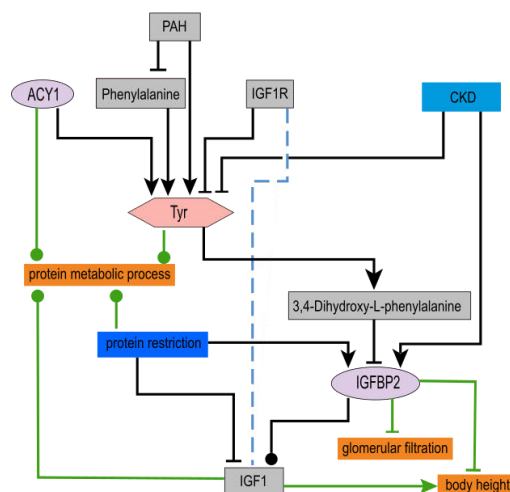
d Overlapped DMMONs and candidates that were MR-supported causal from kidney trait



b Pathway exploration



e



Extended Data Fig. 9. Potential relevant molecular pathways revealed from multi-omics molecules: examples given.

a, Mediation results between *SLC22A4*, IL19 and CKD F4.

b, Pathway exploration of IL19→ *SLC22A4*→CKD and CKD→ *SLC22A4*→ IL19.

c, Hierarchical plot of overlapped DMMOINs and candidates that were MR-supported causal to kidney trait.

d, Hierarchical plot of overlapped DMMOINs and candidates that were suggested MR-supported causal from kidney trait.

In c and d, the edges within each mediating triangle are presented. Only one edge will be presented if there are multiple edges linking two nodes from different mediating triangles. The color of edges represents the direction of KORA observational association between two nodes.

e, Pathway exploration of Tyr→IGFBP2→GFR.

Abbreviations: GGM, Gaussian graphical modeling; DMMOIN, directed mediating multi-omics networks; MR, Mendelian randomization; CKD, chronic kidney disease; CKDcrcc, CKD was defined by eGFR < 60 ml/min/1.73 m²; eGFR, estimated glomerular filtration rate; TWAS, PWAS and MWAS, transcriptome-, proteome- and metabolome-wide association studies.

SUPPLEMENTAL MATERIAL

Full Title: Multi-omics landscape of chronic kidney disease in individuals with prediabetes or type 2 diabetes: from associations towards precision medicine

Supplementary Tables

Supplementary Table 1. Characteristics of the discovery study participants

KORA F4 hyperglycemic participants used for EWAS, TWAS, PWAS and MWAS were classified according to their CKD status, respectively. KORA F4 participants used for building GPS of eGFR are shown. Mean \pm standard deviation or median [25th–75th percentile] is provided for quantitative variables if not indicated otherwise. Unless indicated, *P*-values express the difference between CKD cases and non-CKD controls and were calculated by univariate logistic regression. *P*-values shown in bold represent statistical significance at 0.05 level.

Abbreviations: CKD, chronic kidney disease; HbA_{1c}, glycated hemoglobin; HDL, high-density lipoprotein; LDL, low-density lipoprotein; 2-h glucose, two hour post load glucose; BP, blood pressure; eGFR, estimated glomerular filtration rate; UACR, urinary albumin-to-creatinine ratio; EWAS, TWAS, PWAS, MWAS, epigenome-, transcriptome-, proteome-, and metabolome-wide association studies; GPS, genome-wide polygenic score.

Clinical variables	Hyperglycemic individuals of KORA F4 (N = 1401)												General population of KORA F4
	EWAS			TWAS			PWAS			MWAS			Genotyping
	CKD	Non-CKD	p-value	CKD	Non-CKD	p-value	CKD	Non-CKD	p-value	CKD	Non-CKD	p-value	
Sample Size (n)	166	802		206	471		59	459		282	1096		2757
Age, years	67.95 ± 7.2	62.68 ± 8.37	1.373E-12	73.55 ± 5.33	69.79 ± 4.89	4.718E-16	65.42 ± 7.25	60.91 ± 7.51	3.361E-05	69.71 ± 9.86	60.75 ± 10.95	1.245E-28	56.3 ± 13.22
Sex, male, %	60.24	54.86	2.046E-01	52.43	52.65	9.566E-01	61.02	54.25	3.263E-01	54.26	56.66	4.679E-01	48.1
BMI, kg/m ²	30.85 ± 5.39	29.29 ± 4.72	2.404E-04	30.31 ± 4.94	29.28 ± 4.42	8.016E-03	30.66 ± 5.44	29.08 ± 4.72	2.056E-02	30.31 ± 5.25	29.12 ± 4.73	3.234E-04	27.58 ± 4.82
HbA1c (%)	6.24 ± 1.12	5.81 ± 0.57	9.844E-10	6.14 ± 0.94	5.87 ± 0.64	5.816E-05	6.2 ± 1.21	5.77 ± 0.5	4.654E-05	6.14 ± 0.99	5.79 ± 0.58	2.188E-11	5.55 ± 0.62
Fasting glucose, mg/dl	120.25 ± 33.16	106.76 ± 19.7	3.503E-09	116.78 ± 31.31	108.39 ± 22.1	2.321E-04	118.98 ± 32.1	106.2 ± 17.25	3.075E-05	116.22 ± 31.17	106.38 ± 19.62	3.673E-09	98.34 ± 19.63
2-h glucose, mg/dl	143.7 ± 56.68	134.81 ± 41.72	5.198E-02	145.05 ± 52.09	139.89 ± 42.1	2.400E-01	135.1 ± 50.33	134.08 ± 42.16	8.856E-01	141.11 ± 51.33	132.66 ± 42.55	1.436E-02	112.25 ± 39.19
Systolic BP, mmHg	132.4 ± 24.26	128.29 ± 17.49	1.092E-02	131.04 ± 25.3	129.95 ± 17.47	5.173E-01	130.27 ± 22.56	127.35 ± 17.86	2.533E-01	130.19 ± 23.12	127.58 ± 17.33	3.698E-02	122.21 ± 18.38
Diastolic BP, mmHg	75.43 ± 11.9	76.94 ± 9.9	8.561E-02	72.39 ± 11.42	74.74 ± 9.52	5.939E-03	76.08 ± 11.58	77.42 ± 9.53	3.224E-01	73.58 ± 11.46	76.95 ± 9.91	1.256E-06	75.06 ± 9.91
Triglyceride, mg/dl	146 [99.25 - 204]	122 [89 - 176]	2.169E-01	129.5 [92 - 182.5]	117 [88 - 161]	2.206E-01	135 [96 - 194.5]	120 [87 - 179]	7.512E-01	128.5 [94.25 - 185.5]	121 [87 - 171]	6.986E-01	104 [72 - 150]
Total cholesterol, mg/dl	213.24 ± 43.57	223.08 ± 40.21	4.976E-03	213.53 ± 42.5	221.72 ± 40.53	1.804E-02	210.03 ± 34.62	223.15 ± 40.87	1.904E-02	211.71 ± 42.69	220.86 ± 40.04	8.075E-04	216.02 ± 39.71
HDL cholesterol, mg/dl	50.17 ± 13.07	53.93 ± 13.77	1.399E-03	51.35 ± 12.96	54.58 ± 13.84	4.925E-03	49.63 ± 12.79	54.41 ± 14.3	1.531E-02	50.64 ± 13.1	53.16 ± 13.75	5.951E-03	56.05 ± 14.47
LDL cholesterol, mg/dl	133.42 ± 35.98	142.26 ± 36.18	4.389E-03	133.75 ± 34.56	140.79 ± 35.26	1.695E-02	133.88 ± 29.04	141.68 ± 36.31	1.135E-01	133.24 ± 34.82	141.57 ± 35.55	4.769E-04	135.99 ± 34.9
cGFR, mL/min/1.73 m ²	65.7 ± 21.26	87.06 ± 13.36	2.216E-33	60.77 ± 16.88	80.77 ± 11.57	2.387E-33	69.21 ± 21.17	88.5 ± 13.1	1.210E-14	65.8 ± 20.09	88.41 ± 14.21	2.135E-54	90.36 ± 18.31
Follow-up eGFR, mL/min/1.73 m ²	56.66 ± 21.52	76.32 ± 16.2	1.744E-20 a	52.79 ± 17.82	69.12 ± 14.59	2.008E-14 a	57.13 ± 21.54	77.64 ± 15.43	5.622E-18 a	58.26 ± 21.73	78.82 ± 16.91	1.152E-28 a	83.26 ± 18.39
UACR, mg/g	38.66 [12.44 - 79.27]	6.02 [3.91 - 10.71]	1.163E-29	38.64 [12.71 - 88.43]	7.1 [4.38 - 12.07]	2.831E-25	36.31 [9.57 - 69.35]	5.63 [3.85 - 9.14]	1.872E-14	40.61 [13.91 - 79.89]	6.02 [3.87 - 10.54]	3.265E-49	5.98 [3.67 - 11.84]
Follow-up UACR, mg/g	23.45 [8.52 - 132.35]	5.74 [3.68 - 10.68]	4.800E-31 a	23.54 [9 - 150.46]	6.17 [3.87 - 13.19]	3.477E-18 a	23.51 [8.52 - 113.92]	5.68 [3.62 - 10.64]	6.711E-22 a	25.57 [9.75 - 131.98]	5.45 [3.36 - 9.92]	1.841E-46 a	4.85 [3.14 - 9.37]
Smoking, %			7.111E-01			3.974E-01			8.475E-01			5.717E-01	0.15
Non-smoker	39.16	42.52	Ref.	45.15	50.32	Ref.	38.98	42.7	Ref.	40.43	42.34	Ref.	41.28
Former smoker	48.19	45.01	4.111E-01	48.06	42.89	1.995E-01	47.46	43.79	5.659E-01	46.81	43.89	4.407E-01	40.88
Current smoker	12.65	12.47	7.253E-01	5.83	6.79	8.997E-01	13.56	13.51	8.275E-01	12.06	13.78	6.873E-01	17.7
Medication usage, %													
Lipid-lowering	32.53	18.95	1.044E-04	27.67	25.48	5.041E-01	30.51	15.9	6.630E-03	27.3	17.52	1.947E-04	12.84
Antihypertensive	76.51	44.64	1.172E-12	79.61	56.05	7.460E-09	77.97	39.22	2.171E-07	74.11	41.79	1.055E-20	31.08
Anti-diabetic	28.31	9.85	6.380E-10	22.33	12.74	1.481E-03	25.42	8.06	8.149E-05	23.05	8.58	4.851E-11	5.8

Data are means ± SD for quantitative variables or median [25th-75th percentile] unless otherwise indicated. Hyperglycemic participants of KORA F4 were classified according to their CKD status. P-values were calculated by univariate logistic regression if not indicated otherwise. a. P-values calculated with linear regression as the follow-up clinical variable as outcome and CKD as independent variable.

Supplementary Table 2. CKD - EWAS results in hyperglycemic individuals of KORA: top 20 CpGs and their replication

ORs with 95% CI, P-values of top 20 CpGs with prevalent CKD in discovery study of hyperglycemic individuals of KORA F4 and the replication study of KORA F3 are shown, respectively. In the discovery study, ORs and P-values were from logistic regression analysis adjusted for age, sex, BMI, systolic blood pressure, smoking status, triglyceride, total cholesterol, HDL cholesterol, fasting glucose, use of lipid lowering drugs, antihypertensive and anti-diabetic medication.

Abbreviations: CKD, chronic kidney disease; ORs, odds ratios; T2DCKDmito, T2D-related CKD subnetwork of mitochondrial dysfunction; angi, T2D-related CKD subnetwork of angiogenesis; fibri, T2D-related CKD subnetwork of extracellular matrix deposition and renal fibrosis; inna, T2D-related CKD subnetwork of innate immune response; adipo, T2D-related CKD subnetwork of adipokine influence.

Rank	cg ID	UCSC Ref/Nearest Gene	Note of CpGs with SNPs in the probe-binding sequence And cross-specific probes	Discovery cohort : KORA F4				potential involed processes of T2D-related CKD	Replication cohort : KORA F3 (general population)				Replicated	Reported associations with CKD or related kidney traits for replicated candidates	Extended replicated set
				OR	OR 95% CI (L)	OR 95% CI (U)	p-value		OR	OR 95% CI (L)	OR 95% CI (U)	p-value			
1	cg22872478	LYSDM2		0.66	0.55	0.78	3.386E-06		0.49	0.24	0.99	4.748E-02	yes	no	yes
2	cg12650490	LYL1		1.58	1.30	1.92	3.544E-06	T2DCKDangi	0.8	0.47	1.38	4.291E-01	no	-	yes
3	cg12837173	MEG9		0.65	0.54	0.78	5.413E-06		1.11	0.55	2.24	7.734E-01	no	-	no
4	cg04070692	TUBGCP2		0.64	0.53	0.78	8.060E-06		1.21	0.66	2.22	5.436E-01	no	-	no
5	cg11072723	ERP29		0.69	0.58	0.81	1.085E-05		0.76	0.36	1.62	4.801E-01	no	-	no
6	cg06655560	ZDHH16		1.54	1.27	1.86	1.174E-05		1	0.51	1.97	9.973E-01	no	-	no
7	cg26796069	MAF1		0.68	0.57	0.80	1.189E-05		1.05	0.55	2.01	8.790E-01	no	-	no
8	cg15604682	ALKBH4	with SNPs in the probe-binding seq	1.53	1.26	1.85	1.435E-05		0.74	0.42	1.3	2.928E-01	no	-	no
9	cg02599385	TLN2		0.71	0.60	0.83	1.535E-05	T2DCKDfibri	1	0.54	1.82	9.876E-01	no	-	yes
10	cg23314866	NAPA		0.66	0.54	0.79	1.541E-05	T2DCKDmito	0.12	0.02	0.53	5.782E-03	yes	no	yes
11	cg18524934	NEURL3		0.68	0.57	0.81	1.571E-05	T2DCKDinna	0.88	0.44	1.79	7.297E-01	no	-	yes
12	cg03498175	ACSL1		1.76	1.38	2.31	1.676E-05	T2DCKDadipo,-mito	0.89	0.49	1.6	6.901E-01	no	-	yes
13	cg19719475	UBE2E1		0.67	0.56	0.81	1.782E-05		0.72	0.41	1.27	2.597E-01	no	-	no
14	cg20923676	ALS2CR8	cross specific probe	1.56	1.28	1.93	1.981E-05		0.88	0.52	1.48	6.243E-01	no	-	no
15	cg07546360	LOC400931		0.65	0.53	0.79	2.052E-05		1	0.55	1.81	9.976E-01	no	-	no
16	cg03251287	NR1H2		0.35	0.21	0.55	2.081E-05		1.1	0.5	2.41	8.197E-01	no	-	no
17	cg04766136	CCDC39		1.44	1.22	1.71	2.107E-05	T2DCKDmito	0.95	0.5	1.78	8.623E-01	no	-	yes
18	cg04671476	MGAT1		0.67	0.56	0.81	2.402E-05		1.39	0.6	3.23	4.474E-01	no	-	no
19	cg19497517	PLEC1		0.66	0.54	0.80	2.404E-05		1.38	0.73	2.61	3.205E-01	no	-	no
20	cg04022194	HTRA3		1.53	1.26	1.86	2.427E-05		1.42	0.81	2.49	2.235E-01	no	-	no

Supplementary Table 3. CKD - TWAS results in hyperglycemic individuals of KORA: top 20 RNAs and their replication

ORs with 95% CI, P-values of top 20 RNAs with prevalent CKD in discovery study of hyperglycemic individuals of KORA F4 and the replication study of KORA F3 are shown, respectively. In the discovery study, ORs and P-values were from logistic regression analysis adjusted for age, sex, BMI, systolic blood pressure, smoking status, triglyceride, total cholesterol, HDL cholesterol, fasting glucose, use of lipid lowering drugs, antihypertensive and anti-diabetic medication.

Abbreviations: CKD, chronic kidney disease; ORs, odds ratios; T2DCKDmito, T2D-related CKD subnetwork of mitochondrial dysfunction; T2DCKDadipo, T2D-related CKD subnetwork of adipokine influence; T2DCKDangi, T2D-related CKD subnetwork of angiogenesis; T2DCKDinna, T2D-related CKD subnetwork of innate immune response; T2DCKDras, T2D-related CKD subnetwork of renin-angiotensin system dysfunction; T2DCKDtyr, T2D-related CKD subnetwork of Tyr; T2DCKDfibri, T2D-related CKD subnetwork of extracellular matrix deposition and renal fibrosis.

Rank	name	Matched CHR	Matched Gene	Discovery cohort : KORA F4				potential involved processes of T2DCKD	Replication cohort : KORA F3 (general population)				Replicated	Reported associations with CKD or related kidney traits for KORA F3	Extended replicated set
				OR	OR 95% CI (L)	OR 95% CI (U)	p-value		OR	OR 95% CI (L)	OR 95% CI (U)	p-value			
1	ILMN_1764826	X	TFE3	1.59	1.30	1.95	7.304E-06	T2DCKDadipo,-fibri,-inna	2.14	1.42	3.29	3.349E-04	yes	no	yes
2	ILMN_1685057	5	SLC22A4	1.56	1.28	1.91	1.196E-05	T2DCKDmito	1.41	1.01	1.99	4.190E-02	yes	PMID: 33907247	yes
3	ILMN_1806818	6	MCM3	0.65	0.53	0.79	2.388E-05	T2DCKDinna	0.70	0.48	1.02	6.310E-02	no	-	yes
4	ILMN_1811195	19	ZNF211	0.67	0.55	0.80	3.065E-05		1.42	0.96	2.13	7.828E-02	no	-	no
5	ILMN_1683942	5	PCDHB2	1.49	1.23	1.80	3.980E-05		1.28	0.86	1.90	2.210E-01	no	-	no
6	ILMN_1809859	17	PCGF2	1.47	1.22	1.78	4.899E-05	T2DCKDangi	-	-	-	-	-	-	yes
7	ILMN_1812070	7	ABCB1	0.67	0.55	0.81	5.311E-05	T2DCKDras	1.11	0.76	1.62	5.771E-01	no	-	yes
8	ILMN_1687495	21	SLC37A1	0.68	0.56	0.82	6.996E-05		1.25	0.85	1.85	2.515E-01	no	-	no
9	ILMN_2211780	4	SLC25A4	0.69	0.57	0.83	7.154E-05	T2DCKDmito	-	-	-	-	-	-	yes
10	ILMN_1731206	5	NKD2	1.47	1.21	1.80	1.191E-04	T2DCKDfibri	1.41	0.96	2.08	7.902E-02	no	-	yes
11	ILMN_1740171	2	DUSP11	0.69	0.58	0.83	1.200E-04	T2DCKDinna	1.40	0.95	2.10	9.356E-02	no	-	yes
12	ILMN_1838187	12	SYT1	1.45	1.20	1.76	1.512E-04		1.03	0.71	1.50	8.707E-01	no	-	no
13	ILMN_1656563	2	PAX8	1.45	1.20	1.76	1.513E-04	T2DCKDfibri,-tyr,-angi	0.69	0.43	1.05	1.030E-01	no	-	yes
14	ILMN_2244653	1	CDC14A	1.44	1.19	1.74	1.548E-04	T2DCKDmito	-	-	-	-	-	-	yes
15	ILMN_1772645	7	AGK	0.70	0.58	0.84	1.592E-04	T2DCKDmito,-angi	1.09	0.74	1.62	6.487E-01	no	-	yes
16	ILMN_1712613	10	PNLIPRP2	1.44	1.19	1.75	1.669E-04	T2DCKDadipo	-	-	-	-	-	-	yes
17	ILMN_2205032	X	MAGEE1	0.70	0.58	0.84	1.944E-04		-	-	-	-	-	-	no
18	ILMN_2396292	7	ZNF655	0.70	0.58	0.84	2.383E-04		-	-	-	-	-	-	no
19	ILMN_1812281	6	ARG1	1.40	1.17	1.69	2.598E-04	T2DCKDinna	1.28	0.90	1.80	1.647E-01	no	-	yes
20	ILMN_1810228	1	TFE2	0.71	0.59	0.85	2.679E-04	T2DCKDinna	0.91	0.60	1.36	6.393E-01	no	-	yes

Supplementary Table 4. CKD - PWAS identified 63 proteins in hyperglycemic individuals of KORA and their replication

ORs with 95% CI, P-values and FDR of 63 proteins (FDR < 0.05) with prevalent CKD in discovery study of hyperglycemic individuals of KORA F4, and regression coefficients, standard error and P-values of 63 proteins with prevalent CKD in replication studies of QBB and QMDiab are shown, respectively. In the discovery study, ORs and P-values were from logistic regression analysis adjusted for age, sex, BMI, systolic blood pressure, smoking status, triglyceride, total cholesterol, HDL cholesterol, fasting glucose, use of lipid lowering drugs, antihypertensive and anti-diabetic medication.

Abbreviations: CKD, chronic kidney disease; ORs, odds ratios; T2DCKDmito, T2D-related CKD subnetwork of mitochondrial dysfunction; T2DCKDadipo, T2D-related CKD subnetwork of adipokine influence; T2DCKDage, T2D-related CKD subnetwork of advanced glycation end products; T2DCKDangi, T2D-related CKD subnetwork of angiogenesis; T2DCKDinna, T2D-related CKD subnetwork of innate immune response; T2DCKDras, T2D-related CKD subnetwork of renin-angiotensin system dysfunction; T2DCKDtyr, T2D-related CKD subnetwork of Tyr; T2DCKDfibri, T2D-related CKD subnetwork of extracellular matrix deposition and renal fibrosis.

Rank	Somaid	EntrezGeneSymbol	TargetFullName	Discovery cohort : KORAF4				potential involved processes of T2DCKD	Replication cohort : QBB				Replication cohort : QMDiab				Replicated over 1	Reported associations with CKD or related kidney traits for	Extended replicated set	
				OR	OR 95% CI (L)	OR 95% CI (U)	p-value		FDR	OR	OR 95% CI (L)	OR 95% CI (U)	p-value	OR	OR 95% CI (L)	OR 95% CI (U)				p-value
1	SL001777	CST3	Cystatin-C	2.98	2.09	4.38	5.404E-09	5.917E-04	T2DCKDras,-adipo,-mito,-fibri,-inmu,-tyr,-angi	18.24	5.48	60.75	2.234E-06	8.46	3.00	23.88	5.534E-05	yes	MBD: 31 01049	yes
2	SL002644	EGFR	Epidermal growth factor receptor	0.34	0.23	0.50	1.93E-07	5.237E-05	T2DCKDras,-mito,-fibri,-inmu	0.49	0.24	0.98	4.478E-02	0.70	0.34	1.44	3.32 E-01	yes	PMID: 24705402	yes
3	SL000283	B2M	Beta-2-microglobulin	2.52	1.81	3.61	1.435E-07	5.237E-05	T2DCKDage,-inmu	9.05	3.45	23.77	7.734E-06	4.13	1.70	10.04	1.790E-03	yes	PMID: 31701049	yes
4	SL003522	ERP29	Endoplasmic reticulum resident protein 29	2.74	1.87	4.14	6.477E-07	1.733E-04	T2DCKDtyr	3.79	1.80	7.96	4.456E-04	2.63	1.46	4.75	1.282E-03	yes	PMID: 33888746	yes
5	SL001992	TNFRSF1A	Tumor necrosis factor receptor superfamily member 1A	1.96	1.48	2.64	3.884E-06	8.506E-04	T2DCKDadipo,-fibri,-inmu,-angi	7.18	2.97	17.35	1.167E-05	2.27	1.39	3.71	1.120E-03	yes	PMID: 26200946	yes
6	SL008177	C10BP	Complement component 1 Q subcomponent-binding protein, mitochondrial	0.44	0.30	0.62	5.343E-06	9.750E-04	T2DCKDnitro,-fibri,-inmu	0.70	0.34	1.42	3.236E-01	1.06	0.54	2.08	8.627E-01	no	-	yes
7	SL005156	NBL1	Neuroblastoma suppressor of tumorigenicity 1	1.85	1.42	2.43	6.099E-06	1.018E-03		8.03	3.12	20.65	1.553E-05	8.79	2.90	26.63	1.217E-04	yes	no	yes
8	SL002519	ERBB3	Receptor tyrosine-protein kinase erbB-3	0.42	0.28	0.60	8.286E-06	1.134E-03	T2DCKDras,-mito,-angi	0.32	0.16	0.67	2.367E-03	0.34	0.14	0.83	1.826E-02	yes	PMID: 33888746	yes
9	SL005160	ESAM	Endothelial cell-selective adhesion molecule	2.08	1.52	2.92	1.030E-05	1.135E-03	T2DCKDadipo,-angi	5.57	2.46	12.63	3.937E-05	2.03	0.90	4.58	8.808E-02	yes	PMID: 29804241	yes
10	SL001800	TNFRSF1B	Tumor necrosis factor receptor superfamily member 1B	1.98	1.47	2.71	1.037E-05	1.135E-03	T2DCKDadipo,-fibri,-inmu,-angi	4.31	1.98	9.38	2.252E-04	1.19	0.72	1.95	4.980E-01	yes	PMID: 26200946	yes
11	SL005172	IGFBP6	Insulin-like growth factor-binding protein 6	2.11	1.52	2.98	1.293E-05	1.189E-03	T2DCKDmito,-angi	12.06	4.24	34.33	3.060E-06	7.21	3.19	16.27	1.982E-06	yes	PMID: 212837797	yes
12	SL006910	CTSV	Cathepsin L2	0.39	0.25	0.59	1.476E-05	1.189E-03	T2DCKDras,-fibri,-angi	0.48	0.22	1.02	5.681E-02	0.23	0.07	0.73	1.294E-02	yes	no	yes
13	SL004646	LAYN	Laylin	1.91	1.44	2.59	1.517E-05	1.189E-03	T2DCKDfibri,-inmu	3.40	1.50	7.71	3.475E-03	2.68	1.36	5.30	4.480E-03	yes	PMID: 26410531	yes
14	SL005158	CLEC4M	C-type lectin domain family 4 member M	0.49	0.35	0.67	1.520E-05	1.189E-03	T2DCKDnitro	0.36	0.19	0.71	2.773E-03	0.68	0.37	1.27	2.297E-01	yes	no	yes
15	SL010471	SPOCK2	Testican-2	0.50	0.36	0.68	2.061E-05	1.935E-03	T2DCKDfibri	0.31	0.15	0.65	1.775E-03	0.18	0.06	0.48	6.654E-04	yes	PMID: 33888746	yes
16	SL001815	SOD2	Superoxide dismutase [Mn], mitochondrial	0.51	0.37	0.69	3.208E-05	2.195E-03	T2DCKDras,-adipo,-mito	0.44	0.23	0.86	1.592E-02	0.51	0.23	1.13	9.642E-02	yes	PMID: 34661767	yes
17	SL000346	CTSH	Cathepsin H	2.01	1.45	2.83	3.570E-05	2.299E-03	T2DCKDras,-inmu,-tyr,-angi	3.96	1.81	8.66	5.698E-04	3.96	1.81	8.66	5.698E-04	yes	PMID: 33888746	yes
18	SL005213	RELT	19L	2.00	1.45	2.81	3.832E-05	2.331E-03	T2DCKDnitro	5.12	2.35	11.16	4.013E-05	2.78	1.29	6.03	9.387E-03	yes	PMID: 31101203	yes
19	SL005096	CGA.L1HB	Luteinizing hormone	4.39	2.19	9.14	4.611E-05	2.657E-03	T2DCKDras,-adipo,-age,-angi	3.71	1.16	11.89	2.718E-02	1.27	0.54	2.99	5.906E-01	yes	PMID: 33247564	yes
20	SL009324	FSTL3	Follistatin-related protein 3	2.03	1.46	2.90	5.138E-05	2.813E-03	T2DCKDadipo,-mito,-fibri,-inmu	4.45	1.93	10.27	4.696E-04	66.61	8.82	503.10	4.695E-05	yes	PMID: 28339962	yes
21	SL007806	IL23RA1	Interleukin-22 recep or subunit alpha-1	1.62	1.27	2.06	6.841E-05	3.567E-03	T2DCKDfibri,-inmu,-angi					0.78	0.36	1.73	5.483E-01	no	-	yes
22	SL003679	IGF2R	Cation-independent mannose-6-phosphate receptor	0.50	0.35	0.70	7.657E-05	3.811E-03	T2DCKDras,-mito,-fibri,-inmu,-angi	0.50	0.27	0.93	2.740E-02	1.62	0.82	3.21	1.672E-01	yes	no	yes
23	SL005168	GHR	Growth hormone receptor	0.46	0.31	0.67	9.172E-05	4.367E-03	T2DCKDras,-mito,-inmu,-tyr,-angi	0.41	0.19	0.89	2.442E-02	0.61	0.29	1.26	1.792E-01	yes	PMID: 33125157	yes
24	SL004338	FGF20	Fibroblast growth factor 20	0.34	0.20	0.58	1.012E-04	4.616E-03	T2DCKDtyr	0.17	0.07	0.40	4.976E-05	0.58	0.20	1.66	3.08 E-01	yes	PMID: 34193611	yes
25	SL005230	UNC5C	Netrin receptor UNC5C	1.89	1.37	2.65	1.424E-04	6.237E-03		3.18	1.49	6.80	2.678E-03	8.67	2.32	32.42	1.317E-03	yes	PMID: 33888746	yes
26	SL010378	RET	Proto-oncogene tyrosine-protein kinase receptor	0.49	0.33	0.71	2.045E-04	8.612E-03	T2DCKDras	0.44	0.21	0.93	3.159E-02	0.51	0.24	1.08	7.878E-02	yes	no	yes
27	SL006094	CNDP1	Beta-Ala-His dipeptidase	0.60	0.46	0.79	2.239E-04	9.079E-03	T2DCKDfibri					1.48	0.73	3.00	2.763E-01	no	-	yes
28	SL003201	KDR	Vascular endothelial growth factor receptor 2	0.56	0.41	0.76	2.645E-04	9.400E-03	T2DCKDras,-fibri,-inmu,-angi	0.44	0.20	0.97	4.167E-02	0.56	0.29	1.08	8.55 E-02	yes	PMID: 33282792	yes
29	SL005574	ACY1	Aminoylase-1	0.48	0.31	0.70	2.693E-04	9.400E-03	T2DCKDtyr	0.43	0.21	0.91	2.698E-02	0.38	0.18	0.79	9.613E-03	yes	PMID: 33838163	yes
30	SL002460	RETN	Retin	1.69	1.28	2.25	2.962E-04	9.400E-03	T2DCKDadipo,-mito,-inmu	2.27	1.21	4.26	1.876E-02	1.59	0.93	2.72	9.307E-02	yes	PMID: 33173772	yes
31	SL005703	NOYCH1	Neurogenic locus notch homolog protein 1	0.56	0.40	0.76	2.723E-04	9.400E-03	T2DCKDmito,-fibri,-inmu,-angi	0.72	0.37	1.39	3.230E-01	0.26	0.08	0.88	2.981E-02	yes	PMID: 26419175	yes
32	SL005211	MMP1	Interstitial collagenase	1.77	1.30	2.42	2.474E-04	9.400E-03	T2DCKDras,-adipo,-age,-inmu,-angi	2.13	1.05	4.32	3.558E-02	0.95	0.50	1.80	8.749E-01	yes	PMID: 19506087	yes
33	SL002654	EPHA4	Ephrin type-A receptor 2	1.70	1.28	2.29	3.037E-04	1.008E-02	T2DCKDras,-fibri,-inmu,-angi	4.77	2.05	11.12	2.916E-04	8.81	2.66	29.19	3.677E-04	yes	PMID: 34475336	yes
34	SL012698	KIR2DL4	Killer cell immunoglobulin-like receptor 2DL4	1.62	1.25	2.13	3.354E-04	1.077E-02	T2DCKDnitro	0.72	0.38	1.36	3.130E-01	0.74	0.38	1.44	3.787E-01	no	-	yes
35	SL005193	JAM2	Junctional adhesion molecule B	1.73	1.29	2.36	3.441E-04	1.077E-02	T2DCKDangi	4.04	1.82	9.00	6.273E-04	3.56	1.49	8.48	4.178E-03	yes	no	yes
36	SL000087	IL6	Interleukin-6	1.48	1.19	1.84	3.724E-04	1.133E-02	T2DCKDras,-adipo,-mito,-inmu,-angi	0.75	0.39	1.44	3.870E-01	1.56	0.81	3.00	1.844E-01	no	-	yes
37	SL010348	FNI	Fibronectin Fragment 4	0.57	0.42	0.78	3.945E-04	1.168E-02	T2DCKDras,-adipo,-age,-mito,-fibri,-tyr	0.53	0.27	1.02	5.769E-02	0.52	0.22	1.22	1.309E-01	no	-	yes
38	SL005221	SCARF1	Scavenger receptor class F member 1	1.74	1.29	2.39	4.358E-04	1.227E-02	T2DCKDnitro	1.95	1.06	3.61	3.268E-02	0.89	0.33	2.40	8.159E-01	yes	no	yes
39	SL000053	PLAT	Tissue-type plasminogen activator	0.45	0.29	0.70	4.380E-04	1.227E-02	T2DCKDras,-fibri,-tyr,-angi	0.49	0.25	0.95	3.473E-02	0.51	0.25	1.05	6.832E-02	yes	PMID: 15249548	yes
40	SL002086	FCN3	Ficolin-3	0.57	0.42	0.78	4.814E-04	1.227E-02	T2DCKDfibri,-inmu					0.91	0.45	1.83	7.894E-01	no	-	yes
41	SL002688	PLG	Angiostatin	0.57	0.41	0.78	4.843E-04	1.293E-02	T2DCKDnitro,-fibri,-tyr,-angi	0.43	0.20	0.91	2.636E-02	1.14	0.60	2.19	6.828E-01	yes	PMID: 34548389	yes
42	SL005187	IL3RA	Interleukin-3 receptor subunit alpha	1.58	1.21	2.05	5.389E-04	1.405E-02		0.75	0.37	1.49	4.055E-01	1.23	0.41	3.73	7.099E-01	no	-	yes
43	SL003184	LEPR	Leptin receptor	0.64	0.50	0.83	6.633E-04	1.689E-02	T2DCKDadipo,-mito,-inmu	0.98	0.54	1.77	9.363E-01	0.58	0.35	0.94	2.593E-02	yes	PMID: 25034792	yes
44	SL007281	MAPK12	Mitogen-activated protein kinase 12	1.72	1.26	2.37	7.158E-04	1.744E-02	T2DCKDnitro	1.13	0. 8	2.23	7.141E-01	0.94	0.36	2.44	8.911E-01	no	-	yes
45	SL005201	AMH	Mullerian-inhibiting factor	0.59	0.43	0.79	7.168E-04	1.744E-02	T2DCKDras,-age,-inmu	0.39	0.20	0.75	4.711E-03	1.88	0.76	4.66	1.75 E-01	yes	PMID: 33623676	yes
46	SL004863	TNFRSF19	Tumor necrosis factor receptor superfamily member 19	1.45	1.16	1.81	8.739E-04	2.046E-02	T2DCKDfibri	2.88	1.34	6.20	6.657E-03	1.17	0.69	1.98	5.558E-01	yes	PMID: 31011203	yes
47	SL002755	PAPP4	Pappalysin-1	1.69	1.25	2.32	9.860E-04	2.046E-02	T2DCKDnitro	2.55	1.28	5.06	7.451E-03	1.22	0.62	2.37	5.660E-01	yes	PMID: 27519211	yes
48	SL010328	MED1	Mediator of RNA polymerase II transcription subunit 1																	

Supplementary Table 5. CKD - MWAS identified 17 metabolites in hyperglycemic individuals of KORA and their replication

ORs with 95% CI, *P*-values and FDR of 17 metabolites (FDR < 0.05) with prevalent CKD in discovery study of hyperglycemic individuals of KORA F4 and the replication studies of KORA F3 and of hyperglycemic individuals of KORA FF4 are shown, respectively.

In the discovery study, ORs and *P*-values were from logistic regression analysis adjusted for age, sex, BMI, systolic blood pressure, smoking status, triglyceride, total cholesterol, HDL cholesterol, fasting glucose, use of lipid lowering drugs, antihypertensive and anti-diabetic medication.

Abbreviations: CKD, chronic kidney disease; ORs, odds ratios; T2DCKDmito, T2D-related CKD subnetwork of mitochondrial dysfunction; T2DCKDtyr, T2D-related CKD subnetwork of Tyr.

Rank	Metabolite	Biochemical name	Discovery cohort : KORA F4 hyperglycemic individuals					potential involved processes of T2DCKD	Replication cohort : KORA F3 (general)				Replication cohort : KORA FF4 hyperglycemic				Replicated overall	Reported associations with CKD or related kidney traits for	Extended replicated set
			OR	OR 95% CI (L)	OR 95% CI (U)	<i>p</i> -value	FDR		OR	OR 95% CI (L)	OR 95% CI (U)	<i>p</i> -value	OR	OR 95% CI (L)	OR 95% CI (U)	<i>p</i> -value			
1	C14:1-OH	Hydroxytetradecenoylcarnitine	1.41	1.21	1.66	2.160E-05	2.700E-03		1.66	1.10	2.56	1.783E-02	1.65	1.37	1.98	1.143E-07	yes	PMID 29519950	yes
2	C2	Acetylcarnitine	1.40	1.19	1.64	5.475E-05	3.422E-03	T2DCKDage	1.62	1.10	2.46	1.749E-02	1.42	1.18	1.71	1.902E-04	yes	PMID 33428023	yes
3	C14:2	Tetradecadienylcarnitine	1.35	1.15	1.59	2.943E-04	9.148E-03		1.79	1.14	2.89	1.400E-02	1.60	1.31	1.94	2.771E-06	yes	PMID 30173364	yes
4	C10:2	Decadienylcarnitine	1.32	1.14	1.53	2.971E-04	9.148E-03		1.49	1.01	2.25	4.817E-02					yes	PMID 30173364	yes
5	C16	Hexadecanoylcarnitine, or Palmitoylcarnitine	1.35	1.15	1.59	3.705E-04	9.148E-03	T2DCKDmito	1.15	0.79	1.68	4.730E-01	1.33	1.10	1.60	2.947E-03	yes	PMID 26200946	yes
6	C14:1	Tetradecenoylcarnitine	1.31	1.13	1.52	4.948E-04	9.148E-03		1.29	0.89	1.90	1.908E-01	1.41	1.18	1.69	2.034E-04	yes	PMID 30173364	yes
7	Tyr	Tyrosine	0.76	0.65	0.89	5.324E-04	9.148E-03	T2DCKDtyr	0.64	0.42	0.97	3.436E-02	0.92	0.77	1.10	3.842E-01	yes	PMID 29142974	yes
8	C12	Dodecanoylcarnitine, or	1.33	1.13	1.57	5.855E-04	9.148E-03	T2DCKDmito	1.79	1.18	2.82	8.081E-03	1.69	1.40	2.05	8.961E-08	yes	PMID 16168195	yes
9	C8:1	Octenoylcarnitine	1.29	1.11	1.50	8.036E-04	1.006E-02		1.57	1.07	2.34	2.324E-02					yes	PMID 30173364	yes
10	C10	Decanoylcarnitine	1.32	1.12	1.56	8.764E-04	1.006E-02	T2DCKDmito	1.59	1.08	2.42	2.328E-02	1.48	1.23	1.78	2.649E-05	yes	PMID 29519950	yes
11	C6(C4:1-DC)	Hexanoylcarnitine (Fumaryl carnitine)	1.32	1.12	1.55	8.850E-04	1.006E-02	T2DCKDmito	1.73	1.19	2.66	7.733E-03					yes	PMID 29142974	yes
12	C18:1	Octadecenoylcarnitine	1.30	1.11	1.53	1.336E-03	1.392E-02		1.24	0.83	1.86	2.982E-01	1.20	1.01	1.43	4.172E-02	yes	PMID 16168195	yes
13	C18:2	Octadecadienylcarnitine	1.29	1.10	1.51	1.604E-03	1.543E-02		1.22	0.81	1.87	3.521E-01	1.16	0.97	1.40	1.033E-01	no	-	no
14	C5	Valerylcarnitine	1.29	1.10	1.53	2.331E-03	2.082E-02		1.51	1.05	2.23	2.961E-02	1.47	1.23	1.77	3.138E-05	yes	PMID 29142974	yes
15	SM C24 0	Sphingomyeline C24 0	0.75	0.62	0.91	2.948E-03	2.457E-02		0.78	0.51	1.23	2.737E-01	0.86	0.69	1.08	1.946E-01	no	-	no
16	SM(OH) C22 1	Hydroxysphingomyeline C22 1	0.76	0.63	0.91	3.368E-03	2.631E-02		0.79	0.50	1.29	3.409E-01	0.92	0.74	1.15	4.721E-01	no	-	no
17	C8	Octanoylcarnitine	1.26	1.07	1.47	4.287E-03	3.152E-02	T2DCKDmito	1.62	1.11	2.46	1.867E-02	1.41	1.18	1.68	1.123E-04	yes	PMID 30173364	yes

Supplementary Table 6. Association of identified candidates with CKD in KORA individuals with NGT to investigate whether there were interactions with hyperglycemia.

ORs with 95% CI, *P*-values of 120 candidates with prevalent CKD in KORA F4 individuals with NGT. ORs and *P*-values were from logistic regression analysis adjusted for age, sex, BMI, systolic blood pressure, smoking status, triglyceride, total cholesterol, HDL cholesterol, fasting glucose, use of lipid lowering drugs, antihypertensive medication. FDR was calculated for each omics type.

Abbreviations: CKD, chronic kidney disease; ORs, odds ratios; NGT, normal glucose tolerance.

omics label	omics.type	OR (95% CI)	P-value	FDR
TLN2	CpGs	1.203 (0.855 to 1.824)	3.337E-01	6.673E-01
NR1H2	CpGs	0.917 (0.54 to 1.072)	5.477E-01	7.332E-01
ACSL1	CpGs	0.93 (0.698 to 1.282)	6.365E-01	7.488E-01
HTRA3	CpGs	0.96 (0.719 to 1.286)	7.808E-01	8.239E-01
TUBGCP2	CpGs	0.784 (0.568 to 1.078)	1.355E-01	5.172E-01
MGAT1	CpGs	1.472 (1.067 to 2.056)	2.072E-02	3.480E-01
CCDC39	CpGs	0.653 (0.432 to 0.952)	3.480E-02	3.480E-01
ZDHHC16	CpGs	1.282 (0.951 to 1.725)	1.016E-01	5.079E-01
LOC400931	CpGs	0.869 (0.686 to 1.144)	2.645E-01	6.613E-01
ERP29	CpGs	1.204 (0.855 to 1.755)	3.132E-01	6.673E-01
LYL1	CpGs	0.919 (0.643 to 1.214)	6.042E-01	7.488E-01
MEG9	CpGs	1.104 (0.832 to 1.481)	5.016E-01	7.332E-01
ALKBH4	CpGs	0.987 (0.719 to 1.337)	9.363E-01	9.363E-01
NEURL3	CpGs	0.785 (0.622 to 1.027)	5.303E-02	3.535E-01
PLEC1	CpGs	0.956 (0.692 to 1.314)	7.827E-01	8.239E-01
UBE2E1	CpGs	0.901 (0.656 to 1.239)	5.173E-01	7.332E-01
ALS2CR8	CpGs	1.267 (0.922 to 1.772)	1.551E-01	5.172E-01
LYSMD2	CpGs	1.244 (0.911 to 1.761)	1.967E-01	5.620E-01
NAPA	CpGs	1.102 (0.804 to 1.526)	5.499E-01	7.332E-01
MAF1	CpGs	1.119 (0.794 to 1.605)	5.302E-01	7.332E-01
PAX8	RNAs	0.864 (0.595 to 1.232)	4.311E-01	7.185E-01
PCDHB2	RNAs	1.018 (0.718 to 1.446)	9.178E-01	9.661E-01
SLC22A4	RNAs	1.37 (0.928 to 2.022)	1.115E-01	2.787E-01
SLC37A1	RNAs	0.826 (0.574 to 1.183)	2.976E-01	5.707E-01
PNLIPRP2	RNAs	0.928 (0.65 to 1.319)	6.749E-01	8.602E-01
NKD2	RNAs	1.076 (0.754 to 1.544)	6.882E-01	8.602E-01
DUSP11	RNAs	0.655 (0.45 to 0.943)	2.435E-02	1.492E-01
TFE3	RNAs	1.535 (1.048 to 2.286)	3.027E-02	1.492E-01
AGK	RNAs	0.63 (0.41 to 0.95)	3.020E-02	1.492E-01
MCM3	RNAs	0.673 (0.46 to 0.965)	3.544E-02	1.492E-01
PCGF2	RNAs	1.065 (0.721 to 1.576)	7.503E-01	8.828E-01
TTF2	RNAs	0.807 (0.547 to 1.188)	2.764E-01	5.707E-01
ZNF211	RNAs	0.912 (0.62 to 1.334)	6.378E-01	8.602E-01
ABCB1	RNAs	0.882 (0.597 to 1.294)	5.219E-01	8.030E-01
ARG1	RNAs	1.475 (1.02 to 2.134)	3.729E-02	1.492E-01
SYT1	RNAs	0.956 (0.67 to 1.347)	7.991E-01	8.879E-01
MAGEE1	RNAs	0.679 (0.437 to 1.046)	8.059E-02	2.647E-01
SLC25A4	RNAs	0.8 (0.515 to 1.232)	3.139E-01	5.707E-01
CDC14A	RNAs	1.005 (0.7 to 1.431)	9.781E-01	9.781E-01
ZNF655	RNAs	0.731 (0.502 to 1.044)	9.264E-02	2.647E-01

PLAT	Proteins	0.867 (0.515 to 1.436)	5.840E-01	7.516E-01
IGFBP2	Proteins	2.337 (1.271 to 4.477)	7.879E-03	6.426E-02
CST3	Proteins	2.176 (1.359 to 3.569)	1.471E-03	2.317E-02
EFNA5	Proteins	1.147 (0.725 to 1.84)	5.630E-01	7.516E-01
ERBB3	Proteins	0.599 (0.351 to 1.003)	5.541E-02	1.841E-01
LAYN	Proteins	1.489 (0.986 to 2.219)	5.155E-02	1.841E-01
TNFRSF1A	Proteins	1.933 (1.175 to 3.218)	9.713E-03	6.799E-02
EGFR	Proteins	0.599 (0.368 to 0.945)	3.164E-02	1.525E-01
IGFBP6	Proteins	1.634 (1.033 to 2.54)	3.080E-02	1.525E-01
FGF20	Proteins	0.999 (0.621 to 1.385)	9.962E-01	9.962E-01
FGF9	Proteins	0.682 (0.354 to 1.067)	1.797E-01	3.652E-01
SPINT1	Proteins	0.845 (0.551 to 1.3)	4.390E-01	6.286E-01
NBL1	Proteins	1.473 (1.015 to 2.122)	3.735E-02	1.525E-01
GHR	Proteins	0.604 (0.347 to 1.03)	6.897E-02	1.960E-01
CGA LHB	Proteins	1.118 (0.56 to 2.338)	7.572E-01	8.467E-01
ESAM	Proteins	1.894 (1.212 to 2.994)	5.452E-03	6.426E-02
JAM2	Proteins	1.417 (0.916 to 2.173)	1.120E-01	2.715E-01
CLEC4M	Proteins	0.839 (0.554 to 1.251)	3.958E-01	5.799E-01
IL19	Proteins	0.91 (0.615 to 1.338)	6.326E-01	7.815E-01
RETN	Proteins	1.397 (0.899 to 2.158)	1.327E-01	3.097E-01
IL2	Proteins	0.652 (0.421 to 1.013)	5.552E-02	1.841E-01
TNFRSF1B	Proteins	1.689 (1.041 to 2.813)	3.755E-02	1.525E-01
ADAMTS13	Proteins	0.608 (0.395 to 0.923)	2.076E-02	1.308E-01
RET	Proteins	0.99 (0.592 to 1.583)	9.679E-01	9.835E-01
ACY1	Proteins	0.7 (0.4 to 1.203)	2.050E-01	3.991E-01
BMP1	Proteins	0.704 (0.427 to 1.154)	1.655E-01	3.516E-01
CTSV	Proteins	0.673 (0.408 to 1.071)	1.073E-01	2.704E-01
FN1	Proteins	0.824 (0.542 to 1.24)	3.563E-01	5.501E-01
FSTL3	Proteins	2.669 (1.6 to 4.686)	3.079E-04	6.465E-03
B2M	Proteins	1.923 (1.193 to 3.163)	8.159E-03	6.426E-02
ADIPOQ	Proteins	0.831 (0.461 to 1.489)	5.340E-01	7.476E-01
CNDP1	Proteins	0.769 (0.498 to 1.218)	2.491E-01	4.484E-01
MASP1	Proteins	0.948 (0.592 to 1.487)	8.209E-01	8.917E-01
IL22RA1	Proteins	1.157 (0.773 to 1.544)	3.857E-01	5.785E-01
KDR	Proteins	0.788 (0.516 to 1.212)	2.710E-01	4.548E-01
IGF2R	Proteins	1.469 (0.979 to 2.258)	7.127E-02	1.960E-01
PLG	Proteins	0.928 (0.595 to 1.438)	7.383E-01	8.467E-01
CTSH	Proteins	2.63 (1.702 to 4.143)	1.704E-05	1.074E-03
FCN3	Proteins	0.675 (0.443 to 1.055)	7.298E-02	1.960E-01
RPS6KA5	Proteins	0.664 (0.423 to 1.009)	6.363E-02	1.960E-01

MED1	Proteins	0.589 (0.312 to 0.987)	7.468E-02	1.960E-01
PAPPA	Proteins	1.417 (0.897 to 2.259)	1.377E-01	3.099E-01
IL3RA	Proteins	1.037 (0.664 to 1.474)	8.586E-01	9.168E-01
IL6	Proteins	0.706 (0.351 to 1.216)	2.743E-01	4.548E-01
TFF3	Proteins	1.325 (0.866 to 1.951)	1.674E-01	3.516E-01
EPHA2	Proteins	1.069 (0.686 to 1.666)	7.661E-01	8.467E-01
NTRK2	Proteins	0.983 (0.644 to 1.504)	9.358E-01	9.665E-01
AMH	Proteins	1.091 (0.729 to 1.638)	6.720E-01	8.142E-01
MMP1	Proteins	1.025 (0.693 to 1.497)	8.970E-01	9.419E-01
C1QBP	Proteins	0.891 (0.576 to 1.342)	5.907E-01	7.516E-01
ERP29	Proteins	1.314 (0.864 to 2.037)	2.090E-01	3.991E-01
MAPK12	Proteins	0.887 (0.558 to 1.337)	5.916E-01	7.516E-01
SOD2	Proteins	0.616 (0.385 to 0.972)	3.873E-02	1.525E-01
KIR2DL4	Proteins	0.93 (0.568 to 1.39)	7.557E-01	8.467E-01
NOTCH1	Proteins	0.926 (0.599 to 1.428)	7.289E-01	8.467E-01
RELT	Proteins	2.619 (1.601 to 4.44)	1.927E-04	6.069E-03
SCARF1	Proteins	1.211 (0.806 to 1.836)	3.580E-01	5.501E-01
TNFRSF19	Proteins	1.711 (1.148 to 2.502)	6.264E-03	6.426E-02
HAVCR2	Proteins	0.839 (0.618 to 1.239)	3.105E-01	5.016E-01
UNC5C	Proteins	1.276 (0.829 to 1.874)	2.366E-01	4.385E-01
SEMA3E	Proteins	1.759 (1.058 to 3.003)	3.278E-02	1.525E-01
LEPR	Proteins	1.128 (0.769 to 1.901)	5.965E-01	7.516E-01
SPOCK2	Proteins	0.804 (0.538 to 1.183)	2.741E-01	4.548E-01
C10	Metabolites	1.09 (0.867 to 1.369)	4.580E-01	4.866E-01
C10:2	Metabolites	1.366 (1.076 to 1.735)	1.045E-02	5.924E-02
C12	Metabolites	1.187 (0.938 to 1.501)	1.521E-01	2.350E-01
C14:1	Metabolites	1.261 (0.987 to 1.608)	6.249E-02	1.518E-01
C14:1-OH	Metabolites	1.576 (1.237 to 2.019)	2.703E-04	4.595E-03
C14:2	Metabolites	1.174 (0.923 to 1.495)	1.928E-01	2.521E-01
C16	Metabolites	1.53 (1.188 to 1.977)	1.071E-03	9.105E-03
C18:1	Metabolites	1.31 (1.027 to 1.672)	2.978E-02	1.013E-01
C18:2	Metabolites	1.277 (1.003 to 1.627)	4.782E-02	1.355E-01
C2	Metabolites	1.212 (0.963 to 1.527)	1.013E-01	2.154E-01
C6(C4:1-DC)	Metabolites	1.198 (0.953 to 1.503)	1.204E-01	2.275E-01
C5	Metabolites	1.178 (0.925 to 1.502)	1.851E-01	2.521E-01
C8	Metabolites	1.137 (0.909 to 1.415)	2.540E-01	3.084E-01
C8:1	Metabolites	1.048 (0.834 to 1.316)	6.833E-01	6.833E-01
SM (OH) C22:1	Metabolites	0.811 (0.611 to 1.085)	1.514E-01	2.350E-01
SM C24:0	Metabolites	0.705 (0.525 to 0.946)	1.994E-02	8.474E-02
Tyr	Metabolites	1.123 (0.885 to 1.427)	3.429E-01	3.886E-01

Supplementary Table 7. Interaction of connected edges in T2DCKDtyr subnetwork and the based literatures.

Abbreviations: T2DCKDtyr, T2D-related CKD subnetwork of Tyr.

Subject	Interaction type	Object	Arg_loc	Arg_Mod	PMID	Organism	Disease
TH	decreases_quantity of	Tyrosine			26241318	Mammalia	Metabolic
TH	increases_quantity of	Dopamine			26241318	Mammalia	Metabolic
Tyrosine	increases_quantity of	Dopamine			26241318	Mammalia	Metabolic
IGFBP2	increases_activity of	Nephropathy, diabetic thyroid hormone generation			23781310	Homo sapiens	Nephropathy, diabetic; Diabetes mellitus, type II; Insulin resistance
TG	increases_activity of	Glomerulopathy with fibronectin deposits 2			30599477	Homo sapiens	Thyroid dysmorphogenesis 1
FN1	affects_activity of	kidney development			18268355	Homo sapiens	Cardiovascular disease; Renal
FGF20	increases_activity of	Chronic kidney disease	in T2D patients		22698282	Homo sapiens	Developmental
CST3	increases_activity of	glomerular filtration	in T2D patients		24409655	Homo sapiens	Diabetes mellitus, type II; Chronic kidney disease
CST3	affects_activity of	TH	in neuronal stem cells		24409655	Homo sapiens	Diabetes mellitus, type II; Chronic kidney disease
FGF20	increases_expression of	Tyrosine	in neuronal stem cells		15474354	Mammalia	Neurological
TH	decreases_quantity of	Dopamine	in neuronal stem cells		15474354	Mammalia	Neurological
TH	increases_quantity of	Tyrosine	in plasma		15474354	Mammalia	Neurological
Chronic kidney disease	decreases_quantity of	CTSH			17513431	Mammalia	Chronic kidney disease
Triiodothyronine	increases_expression of	CTSH			21217776	Homo sapiens	Cancer
Triiodothyronine	increases_quantity of	thyroid hormone generation			21217776	Homo sapiens	Cancer
TPO	increases_activity of	TPO			26610751	Mammalia	Metabolic
Thyroid-stimulating hormone	affects_expression of	CTSH	in proximal tubules		26610751	Mammalia	Metabolic
Polycystic kidney disease 5	decreases_activity of	increased urine protein level			8840269	Rattus norvegicus	Polycystic kidney disease 5
Triiodothyronine	affects_activity of			via the catalytic activity of thyroid peroxidase	29660205	Homo sapiens	Nephropathy, diabetic
Tyrosine	increases_quantity of	Triiodothyronine			26610751	Mammalia	Metabolic
Thyroid-stimulating hormone	increases_quantity of	PLAT	in thyroid follicular cells		12065237	Homo sapiens	Metabolic
Thyroid-stimulating hormone	increases_quantity of	Angiostatin	in thyroid follicular cells		12065237	Homo sapiens	Metabolic
Thyroxine	affects_quantity of	IGFBP2	in fetus		7689951	Sus scrofa	Endocrine; Developmental
Thyroxine	increases_quantity of	EFNA5	in the developing hippocampus and hippocampal neurons		29762250	Rattus norvegicus	Neurological; Endocrine
Thyroxine	increases_quantity of	EFNA5	in the developing hippocampus and hippocampal neurons		29762250	Rattus norvegicus	Neurological; Endocrine
Triiodothyronine	increases_quantity of	GHR	in hepatic carcinoma cells		10195688	Homo sapiens	Cancer
Triiodothyronine	increases_expression of	thyroid gland development	in anaplastic thyroid carcinoma cell line 8305C		26458316	Homo sapiens	Endocrine; Thyroid carcinoma
TFF3	affects_activity of	NTRK2	in hyrotropic cells		10978336	Mus musculus	Neurological; Cancer
Triiodothyronine	decreases_expression of	Thyroid-stimulating hormone	in blood		10978336	Mus musculus	Neurological; Cancer
Nephropathy, diabetic	increases_quantity of	Triiodothyronine	in blood		30631416	Homo sapiens	Nephropathy, diabetic
Nephropathy, diabetic	decreases_quantity of	glomerular filtration			30631416	Homo sapiens	Nephropathy, diabetic
Triiodothyronine	affects_activity of	TG			30631416	Homo sapiens	Nephropathy, diabetic
ERP29	increases_activity of				11884402	Rattus norvegicus	Hypothyroidism
MED1	increases_expression of	Thyroid-stimulating hormone		together with Triiodothyronine (T3)	24055033	Mus musculus	Endocrine
PAX8	increases_activity of	thyroid gland development			25350068	Mammalia	Endocrine
PAX8	increases_expression of	TG	in thyroid cells	in cooperation with TTF1 (NKX2-1)	11069301	Rattus norvegicus	Endocrine
NTRK2	affects_activity of	glomerular filtration			25885044	Homo sapiens	Chronic kidney disease
Triiodothyronine	increases_activity of	fatty acid beta-oxidation	in brown adipose tissue		30209975	Mus musculus	Endocrine; Metabolic
Triiodothyronine	decreases_quantity of	Tyrosine	in brown adipose tissue		30209975	Mus musculus	Endocrine; Metabolic

Dopamine	decreases_activity of	Nephropathy, diabetic			23207723	Mammalia	Nephropathy, diabetic
Dopamine	decreases_activity of	albuminuria			23207723	Mammalia	Nephropathy, diabetic
Dopamine	decreases_activity of	response to oxidative stress			22688335	Mammalia	Renal
Dopamine	increases_activity of	glomerular filtration	in kidney		22688335	Mus musculus	Nephropathy, diabetic
Dopamine	decreases_quantity of	FN1	in kidney		22688335	Mus musculus	Nephropathy, diabetic
Dopamine	decreases_activity of	Nephropathy, diabetic			22688335	Mus musculus	Nephropathy, diabetic
response to oxidative stress	increases_quantity of	Nitrotyrosine			17513431	Mammalia	Chronic kidney disease
Tyrosine	increases_quantity of	Nitrotyrosine		on plasma proteins, in the presence of oxygen species	17513431	Mammalia	Chronic kidney disease
CST3	affects_activity of	glomerular filtration			15966508	Homo sapiens	Endocrine; Renal
thyroid hormone generation	affects_quantity of	CST3	in serum		15966508	Homo sapiens	Endocrine Renal
Dopamine	decreases_quantity of	Nitrotyrosine			23207723	Mammalia	Nephropathy, diabetic
TPO	affects_activity of	TG	in the thyroid gland		30886364	Mammalia	
TG	increases_activity of	thyroid hormone generation	in the thyroid gland		30886364	Mammalia	
thyroid hormone generation	increases_quantity of	Triiodothyronine	in the thyroid gland		30886364	Mammalia	
thyroid hormone generation	increases_quantity of	Thyroxine	in the thyroid gland		30886364	Mammalia	
Thyroid-stimulating hormone	increases_activity of	thyroid hormone generation			28153798	Mammalia	Endocrine
Nephropathy, diabetic	increases_quantity of	Nitrotyrosine			10792615	Homo sapiens	Nephropathy, diabetic
Thyroxine	affects_activity of	Nephropathy, diabetic			29196928	Homo sapiens	Nephropathy, diabetic
Nephropathy, diabetic	decreases_quantity of	Angiostatin	in kidney		16394111	Rattus norvegicus	Nephropathy, diabetic
Angiostatin	decreases_activity of	renal glomerulus hypertrophy	in kidney		16394111	Rattus norvegicus	Nephropathy, diabetic
PAX8	decreases_activity of	polyuria			32381599	Mus musculus	Renal
GHR	increases_activity of	glomerular filtration	in kidney		31352157	Mammalia	Nephropathy, diabetic
Triiodothyronine	decreases_activity of	extracellular matrix assembly			21307121	Homo sapiens	Nephropathy, diabetic
ACY1	affects_quantity of	Tyrosine	in kidney		14927637	Sus scrofa	Renal; Metabolic
Dopamine	decreases_activity of	macrophage activation	in adipose tissue		23207723	Mammalia	Nephropathy, diabetic
Tyrosine	increases_quantity of	Thyroxine		via the catalytic activity of thyroid peroxidase	26610751	Mammalia	Metabolic
Angiostatin	decreases_activity of	PLAT	in bovine aortic endothelial cells (BAEC), murine melanoma cells (B16F10) or human ovarian carcinoma cells (OVCA 429)	by binding to tPA (PLAT)	10229661	Mus musculus	Cancer
Angiostatin	decreases_activity of	PLAT			21899046	Homo sapiens	Hematological

Supplementary Table 8. Interaction of connected edges in T2DCKDmito subnetwork and the based literatures.

Abbreviations: T2DCKDmito, T2D-related CKD subnetwork of mitochondrial dysfunction.

Subject	Interaction type	Object	Arg_loc	Arg_Mod	PMID	Organism	Disease
ADIPOQ	increases_activity of	fatty acid beta-oxidation	in muscle		12368907	Mus musculus	Diabetes mellitus, type II; Insulin resistance
FASN	increases_activity of	lipid biosynthetic process	in white adipose tissue		18522830	Mus musculus	Diabetes mellitus, type II; Fatty liver disease, nonalcoholic; Insulin resistance
IL6	decreases_expression of	PPARGC1A	in skeletal muscle	if IL6 is overexpressed in skeletal muscle	18437347	Mus musculus	Diabetes mellitus, type II; Insulin resistance
ADIPOQ	increases_expression of	PPARGC1A	in adipose tissue		17717599	Mus musculus	Diabetes mellitus, type II; Insulin resistance
incomplete fatty acid beta-oxidation	increases_quantity of	Hexanoylcarnitine C6			18945875	Mammalia	Diabetes mellitus, type II; Insulin resistance
incomplete fatty acid beta-oxidation	increases_quantity of	Octanoylcarnitine C8			18945875	Mammalia	Diabetes mellitus, type II; Insulin resistance
incomplete fatty acid beta-oxidation	increases_quantity of	Decanoylcarnitine C10			18945875	Mammalia	Diabetes mellitus, type II; Insulin resistance
incomplete fatty acid beta-oxidation	increases_quantity of	Lauroylcarnitine C12			18945875	Mammalia	Diabetes mellitus, type II; Insulin resistance
incomplete fatty acid beta-oxidation	increases_quantity of	Tetradecanoylcarnitine C14			18945875	Mammalia	Diabetes mellitus, type II; Insulin resistance
incomplete fatty acid beta-oxidation	increases_quantity of	Palmitoylcarnitine C16			18945875	Mammalia	Diabetes mellitus, type II; Insulin resistance
Diabetes mellitus, type II	increases_activity of	incomplete fatty acid beta-oxidation			19369366	Homo sapiens	Diabetes mellitus, type II; Insulin resistance
SREBF1c	increases_activity of	lipid biosynthetic process	in liver		22941588	Mammalia	Metabolic syndrome; Diabetes mellitus, type II; Fatty liver disease, nonalcoholic; Insulin resistance
SLC22A4	is localized in	mitochondrial outer membrane			23150726	Mammalia	Diabetes mellitus, type II; Insulin resistance
MDH2	affects_activity of	tricarboxylic acid cycle			20567778	Mammalia	Diabetes mellitus, type II; Insulin resistance
PPARGC1A	interacts (colocalizes) with	MED1			14636573	Homo sapiens	Diabetes mellitus, type II; Insulin resistance
PPARGC1A	affects_expression of	SOD2			17055439	Mus musculus	Diabetes mellitus, type II; Insulin resistance
PPARGC1A	affects_expression of	SLC25A4			17055439	Mus musculus	Diabetes mellitus, type II; Insulin resistance
BCL2	decreases_activity of	apoptotic process			19954947	Mammalia	Diabetes mellitus, type II; Insulin resistance
PPARA	increases_activity of	fatty acid beta-oxidation	in mitochondria, in peroxisomes		19531645	Mammalia	Diabetes mellitus, type II; Insulin resistance
PTGS2	increases_activity of	inflammatory response			25729473	Mammalia	Diabetes mellitus, type II; Fatty liver disease, nonalcoholic; Insulin resistance
ADIPOQ	decreases_activity of	NADPH oxidase complex	in kidney		28402446	Mammalia	Diabetes mellitus, type II; Nephropathy, diabetic; Insulin resistance
HAVCR2	decreases_quantity of	Reactive oxygen species	in nonalcoholic fatty liver disease		30862474	Mammalia	Nephropathy, diabetic
CCDC39	affects_activity of	cilium assembly			21131972	Homo sapiens	Ciliopathy
ADIPOQ	increases_activity of	ACSL1	in 3T3-L1 adipocytes		20667975	Mus musculus	Diabetes mellitus, type II; Insulin resistance
ACSL1	increases_activity of	AMPK	in 3T3-L1 adipocytes		20667975	Mus musculus	Diabetes mellitus, type II; Insulin resistance
RETN	affects_activity of	CD36	in L6 myoblast cells		16137686	Rattus norvegicus	Diabetes mellitus, type II; Obesity; Insulin resistance
RETN	decreases_activity of	AMPK	in L6 myoblast cells	via decreased phosphorylation	16137686	Rattus norvegicus	Diabetes mellitus, type II; Obesity; Insulin resistance
Reactive oxygen species	increases_quantity of	FN1			26719364	Mammalia	Nephropathy, diabetic
EGFR	increases_expression of	ACSL1			22238402	Homo sapiens	Diabetes mellitus, type II; Insulin resistance
EGFR	increases_expression of	ADIPOQ			22238402	Homo sapiens	Diabetes mellitus, type II; Insulin resistance
ERBB3	decreases_expression of	CD36			22238402	Homo sapiens	Diabetes mellitus, type II; Insulin resistance
EFNA5	affects_expression of	BCL2	in ovarian granulosa cells		29619874	Mus musculus	Infertility
Carnitine	decreases_quantity of	CST3	in serum		31369185	Homo sapiens	Immunological
SLC22A4	increases_transport of	Carnitine			23150726	Mammalia	Diabetes mellitus, type II; Insulin resistance
SLC22A4	increases_transport of	Acylcarnitine			23150726	Mammalia	Diabetes mellitus, type II; Insulin resistance
IGFBP2	decreases_activity of	lipid biosynthetic process	in visceral adipose tissue		25370576	Homo sapiens	Obesity
IGFBP2	decreases_expression of	SREBF1c	in visceral adipose tissue		25370576	Homo sapiens	Obesity
IGFBP2	decreases_expression of	FASN	in visceral adipose tissue		25370576	Homo sapiens	Obesity
IGFBP2	decreases_expression of	PPARG	in visceral adipose tissue		25370576	Homo sapiens	Obesity
IGFBP2	decreases_expression of	ADIPOQ	in visceral adipose tissue		25370576	Homo sapiens	Obesity
Reactive oxygen species	increases_expression of	IGFBP6	in skin fibroblasts		15958393	Homo sapiens	Cardiovascular disease
TFF3	decreases_expression of	PPARGC1A	in hepatocytes		24086476	Mus musculus	Diabetes mellitus, type II; Insulin resistance
TFF3	increases_activity of	cilium assembly	in airway epithelial cells		17008636	Homo sapiens	Lung disease
IL19	increases_expression of	PPARG	in VSMC, but not in EC		27053520	Homo sapiens	Cardiovascular
GHR	increases_quantity of	Reactive oxygen species	in podocytes		21067510	Mammalia	Nephropathy, diabetic
NAPA	decreases_activity of	AMPK	in HEK293T cells		23463002	Homo sapiens	Diabetes mellitus, type II; Insulin resistance
NAPA	affects_activity of	mitochondrion organization			23463002	Homo sapiens	Diabetes mellitus, type II; Insulin resistance
Reactive oxygen species	affects_activity of	RPS6KA5		via p38 MAPK	16531007	Rattus norvegicus	Diabetes mellitus, type II; Insulin resistance
SLC25A4	increases_activity of	mitochondrial ATP transmembrane transport			27693233	Homo sapiens	Cardiomyopathy
SOD2	decreases_quantity of	Reactive oxygen species	in wounds		30362661	Mus musculus	Nephropathy, diabetic
CPT2	decreases_quantity of	Acylcarnitine			33013450	Mammalia	Neuropathy, diabetic
fatty acid beta-oxidation	increases_quantity of	Acetyl-CoA			33013450	Mammalia	Neuropathy, diabetic
Acetyl-CoA	increases_activity of	tricarboxylic acid cycle			33013450	Mammalia	Neuropathy, diabetic
tricarboxylic acid cycle	increases_activity of	oxidative phosphorylation			33013450	Mammalia	Neuropathy, diabetic
oxidative phosphorylation	increases_quantity of	ATP			33013450	Mammalia	Neuropathy, diabetic
PPARGC1A	increases_activity of	mitochondrion organization			33013450	Mammalia	Nephropathy, diabetic
ACSL1	affects_activity of	lipidosis	in kidney		33013450	Mammalia	Nephropathy, diabetic
PPARA	increases_expression of	CD36			33013450	Mammalia	Nephropathy, diabetic
AMPK	increases_activity of	PPARGC1A			33013450	Mammalia	Nephropathy, diabetic
lipidosis	increases_activity of	response to endoplasmic reticulum stress	in kidney		33013450	Mammalia	Nephropathy, diabetic
lipidosis	increases_activity of	abnormal mitochondrial physiology	in kidney		33013450	Mammalia	Nephropathy, diabetic
PPARG	increases_expression of	CD36	in HK-2 cells		31754839	Mammalia	Nephropathy, diabetic
NADPH oxidase complex	increases_quantity of	Reactive oxygen species			31754839	Mammalia	Nephropathy, diabetic
oxidative phosphorylation	increases_quantity of	Reactive oxygen species			31754839	Mammalia	Nephropathy, diabetic
AGK	is_part_of	TIM22 complex	in mitochondrial inner membrane		28867158	Mammalia	Sengers syndrome
TIM22 complex	increases_activity of	protein insertion into mitochondrial inner membrane			28867158	Mammalia	Sengers syndrome
AGK	affects_activity of	lipid biosynthetic process	in mitochondria		28867158	Mammalia	Sengers syndrome
CPT1A	is localized in	mitochondrial outer membrane			32226789	Mammalia	Nephropathy, diabetic
CPT1A	decreases_quantity of	Carnitine			32226789	Mammalia	Nephropathy, diabetic
CPT1A	increases_quantity of	Acylcarnitine			32226789	Mammalia	Nephropathy, diabetic
CPT1A	increases_transport of	Acylcarnitine	across the outer mitochondrial membrane		32226789	Mammalia	Nephropathy, diabetic
CPT2	is localized in	mitochondrial inner membrane			32226789	Mammalia	Nephropathy, diabetic
CPT2	decreases_quantity of	Acylcarnitine	in mitochondrial matrix		32226789	Mammalia	Nephropathy, diabetic
CPT2	increases_quantity of	Acyl-CoA	in mitochondrial matrix		32226789	Mammalia	Nephropathy, diabetic
fatty acid beta-oxidation	decreases_quantity of	Acyl-CoA	in mitochondrial matrix		32226789	Mammalia	Nephropathy, diabetic
fatty acid beta-oxidation	increases_quantity of	Acetyl-CoA	in mitochondrial matrix		32226789	Mammalia	Nephropathy, diabetic
tricarboxylic acid cycle	decreases_quantity of	Acetyl-CoA	in mitochondrial matrix		32226789	Mammalia	Nephropathy, diabetic
PPARGC1A	affects_activity of	fatty acid beta-oxidation			32226789	Mammalia	Nephropathy, diabetic
C1QB	is localized in	mitochondrial matrix	in HeLa cells, in fibroblasts		11083468	Homo sapiens	Cancer

C1QBP	affects activity of	oxidative phosphorylation			28942965	Homo sapiens	Combined oxidative phosphorylation deficiency
ERBB3	interacts (colocalizes) with	EGFR			24520092	Homo sapiens	Cancer
FSTL3	increases expression of	CD36	in macrophages		31815869	Mus musculus	Cardiovascular disease
GHR	increases activity of	fatty acid beta-oxidation			9398741	Homo sapiens	Diabetes mellitus, type II; Insulin resistance
IGF2R	affects activity of	CD36	in THP-1 cells		31680642	Homo sapiens	Cardiovascular disease
LEPR	increases activity of	fatty acid beta-oxidation	in adipose tissue		32733634	Mus musculus	Diabetes mellitus, type II; Insulin resistance
LEPR	increases expression of	PPARGC1A	in adipose tissue		32733634	Mus musculus	Diabetes mellitus, type II; Insulin resistance
LEPR	increases expression of	CD36	in adipose tissue		32733634	Mus musculus	Diabetes mellitus, type II; Insulin resistance
LEPR	affects activity of	JAK2		via phosphorylation	32733634	Mus musculus	Diabetes mellitus, type II; Insulin resistance
JAK2	affects activity of	AMPK		via phosphorylation	32733634	Mus musculus	Diabetes mellitus, type II; Insulin resistance
NOTCH1	decreases expression of	PPARGC1A	in renal tubular epithelial cells		28751525	Mus musculus	Chronic kidney disease
NOTCH1	decreases expression of	CPT1A			28751525	Mus musculus	Chronic kidney disease
NOTCH1	decreases expression of	BCL2			28751525	Mus musculus	Chronic kidney disease
NOTCH1	decreases activity of	fatty acid beta-oxidation			28751525	Mus musculus	Chronic kidney disease
Angiostatin	decreases expression of	BCL2			19465692	Mus musculus	Cancer
Angiostatin	increases expression of	THBS1			19465692	Mus musculus	Cancer
Angiostatin	interacts (colocalizes) with	MDH2	in mitochondria in HUVEC cells, in A2058 tumor cells		19465692	Mus musculus	Cancer
Angiostatin	decreases quantity of	ATP			19465692	Homo sapiens	Cancer
Angiostatin	affects activity of	oxidative phosphorylation	in HUVEC cells		19465692	Homo sapiens	Cancer
IGFBP2	affects expression of	BCL2			21821709	Mus musculus	Cancer
IGFBP6	increases expression of	BCL2	in neurons		28044240	Rattus norvegicus	Cardiovascular disease
Tetradecanoylcarnitine	increases expression of	PTGS2	in RAW 264.7 macrophages		24760988	Mus musculus	Diabetes mellitus, type II; Insulin resistance
Palmitoylcarnitine C16	increases expression of	PTGS2	in RAW 264.7 macrophages		24760988	Mus musculus	Diabetes mellitus, type II; Insulin resistance
Stearoylcarnitine	increases expression of	PTGS2	in RAW 264.7 macrophages		24760988	Mus musculus	Diabetes mellitus, type II; Insulin resistance
Tetradecanoylcarnitine	increases expression of	IL6	in RAW 264.7 macrophages		24760988	Mus musculus	Diabetes mellitus, type II; Insulin resistance
Tetradecanoylcarnitine	increases quantity of	Reactive oxygen species	in RAW 264.7 macrophages		24760988	Mus musculus	Diabetes mellitus, type II; Insulin resistance
Tetradecanoylcarnitine	increases activity of	inflammatory response	in RAW 264.7 macrophages		24760988	Mus musculus	Diabetes mellitus, type II; Insulin resistance
CDC14A	affects activity of	cilium assembly	in hTERT-RPE1 cells		30467237	Homo sapiens	Ciliopathy
PPARA	increases activity of	cilium assembly	in RPE1 cells, in A549 cells, in HK2 cells		29771182	Homo sapiens	Ciliopathy
PPARA	increases activity of	autophagy	in RPE1 cells, in A549 cells, in HK2 cells		29771182	Homo sapiens	Ciliopathy
PPARA	increases activity of	autophagy			29771182	Mus musculus	Ciliopathy
autophagy	increases activity of	cilium assembly			29771182	Mus musculus	Ciliopathy
Palmitic acid	decreases expression of	SOD2	in monocytes		21035442	Homo sapiens	Diabetes mellitus, type II; Insulin resistance
Oleic acid	decreases expression of	SOD2	in monocytes		21035442	Homo sapiens	Diabetes mellitus, type II; Insulin resistance
Carnitine	decreases activity of	NADPH oxidase complex		in L-NAME-treated animals	23223967	Rattus norvegicus	Cardiovascular disease
Angiotensin II	increases expression of	CST3	in aortic smooth muscle cells		31668507	Homo sapiens	Cardiovascular disease
Angiotensin II	increases activity of	EGFR	in glomerular mesangial cells	via phosphorylation	11737589	Mus musculus	Chronic kidney disease
Angiotensin II	increases activity of	NADPH oxidase complex	in kidney		28402446	Mammalia	Diabetes mellitus, type II; Insulin resistance; Nephropathy, diabetic
SREBF1c	increases expression of	FASN	in liver		10940327	Mammalia	Diabetes mellitus, type I; Diabetes mellitus, type II; Hypothyroidism; Insulin resistance
LEP	increases activity of	LEPR	in hypothalamus		8782827	Mus musculus	Diabetes mellitus, type II; Insulin resistance
ACSL1	decreases quantity of	Oleic acid	in kidney, in mitochondria	via increased fatty acid beta-oxidation	33013450	Mammalia	Nephropathy, diabetic
ACSL1	decreases quantity of	Palmitic acid	in kidney, in mitochondria	via increased fatty acid beta-oxidation	33013450	Mammalia	Nephropathy, diabetic

Supplementary Table 9. Interaction of connected edges in T2DCKDinna and the based literatures.

Abbreviations: T2DCKDinna, T2D-related CKD subnetwork of innate immune response.

Subject	Interaction type	Object	Arg_loc	Arg_Mod	PMID	Organism	Disease
TNF	interacts (colocalizes) with	TNFRSF1A			15842589	Homo sapiens	Inflammatory bowel disease
TNF	interacts (colocalizes) with	TNFRSF1B			15842589	Homo sapiens	Inflammatory bowel disease
TNFRSF1A	increases_activity of	NF-kappaB complex		after binding with TNF-alpha	15842589	Homo sapiens	Inflammatory bowel disease
NF-kappaB complex	increases_expression of	IL6		via decreased NF-kappaB activity	31942046	Mammalia	Nephropathy, diabetic
ADIPOQ	decreases_expression of	IL6			30181742	Mammalia	Chronic kidney disease
RETN	increases_activity of	NF-kappaB complex			30181742	Mammalia	Chronic kidney disease
RETN	increases_expression of	IL6			30181742	Mammalia	Chronic kidney disease
AMH	affects_activity of	NF-kappaB complex	in lung cancer		27396341	Mus musculus	Cancer
FCN3	increases_activity of	complement activation, lectin pathway			11907111	Homo sapiens	Hematological; Immunological
HAVCR2	increases_activity of	macrophage activation			30862474	Mus musculus	Nephropathy, diabetic
RELT	increases_activity of	NF-kappaB complex			11313261	Homo sapiens	Hematological
CTSH	increases_activity of	toll-like receptor 3 signaling pathway	in splenocytes		29470604	Mus musculus	Immunological; Multiple sclerosis
AGK	increases_activity of	NF-kappaB complex	in Huh-7 and PLC heptocellular carcinoma cells		25474138	Homo sapiens	Cancer; Hepatocellular carcinoma
B2M	is_part_of	MHC class I complex			31253869	Mammalia	Lung cancer; Immunological
C1QBP	increases_activity of	complement activation			11859136	Mammalia	Inflammation; Immunological
C1QBP	affects_activity of	T cell activation			16177118	Mammalia	Immunological
C1QBP	affects_activity of	toll-like receptor 4 signaling pathway	in macrophages and dendritic cells	via activation of PI3K	16177118	Homo sapiens	Immunological
innate immune response	increases_activity of	complement activation			16177118	Mammalia	Immunological
EFNA5	affects_expression of	TNF	in ovarian granulosa cells		29619874	Mus musculus	Infertility
dendritic cell differentiation	affects_quantity of	CST3			15829557	Homo sapiens	Immunological
CST3	decreases_activity of	CTSH			3202963	Homo sapiens	Metabolic
CLEC4M	increases_activity of	complement activation, lectin pathway			16978536	Mammalia	Immunological
EPHA2	decreases_activity of	NLRP3	in airway epithelial cells	via Tyr phosphorylation	32352641	Mus musculus	Inflammation; Lung disease
EGFR	increases_activity of	toll-like receptor 3 signaling pathway			22810896	Homo sapiens	Immunological
GHR	increases_activity of	NLRP3 inflammasome			26876170	Mus musculus	Immunological
macrophage activation	increases_expression of	IGF2R			30657605	Mus musculus	Immunological
B2M	interacts (colocalizes) with	HLA-G			22802125	Mammalia	Immunological
KIR2DL4	interacts (colocalizes) with	HLA-G			10190900	Homo sapiens	Immunological
MASP1	increases_activity of	complement activation, lectin pathway			24935208	Mammalia	Hematological; Immunological
MED1	increases_expression of	PPARG	in macrophages		28642237	Mus musculus	Atherosclerosis; Cardiovascular
PPARG	affects_activity of	macrophage activation			28642237	Mus musculus	Atherosclerosis; Cardiovascular
toll-like receptor 4 signaling pathway	increases_quantity of	MMP1	in U937 mononuclear cells		21952248	Homo sapiens	Obesity; Immunological
innate immune response	increases_activity of	toll-like receptor 4 signaling pathway			21952248	Homo sapiens	Obesity Immunological
DUSP11	interacts (colocalizes) with	MAP3K7	in macrophages	after stimulation with LPS	32796023	Mus musculus	Immunological
toll-like receptor 4 signaling pathway	increases_activity of	MAP3K7			32796023	Mammalia	Immunological
toll-like receptor 4 signaling pathway	increases_activity of	NOTCH1	in podocytes of IgAN patients	after stimulation with LPS	29230705	Homo sapiens	Renal; Immunological
NOTCH1	increases_activity of	NF-kappaB complex	in podocytes	after stimulation with LPS	29230705	Homo sapiens	Renal; Immunological
SCARF1	increases_activity of	toll-like receptor 4 signaling pathway			25767073	Mammalia	Immunological
SCARF1	increases_activity of	toll-like receptor 3 signaling pathway			25767073	Mammalia	Immunological
toll-like receptor 4 signaling pathway	increases_activity of	NF-kappaB complex			25767073	Mammalia	Immunological
toll-like receptor 3 signaling pathway	increases_activity of	NF-kappaB complex			25767073	Mammalia	Immunological
TNFRSF19	affects_activity of	NF-kappaB complex	in colorectal cancer cell lines		24623448	Homo sapiens	Cancer; Inflammation
NF-kappaB complex	increases_quantity of	IL6			23664135	Mammalia	Immunological
NF-kappaB complex	increases_quantity of	TNF			23664135	Mammalia	Immunological
DUSP11	decreases_activity of	macrophage activation		after stimulation with LPS	32796023	Mus musculus	Immunological
HAVCR2	decreases_quantity of	NLRP3		via downregulation of ROS production, in NASH mice	29735977	Mus musculus	Immunological
NLRP3	increases_activity of	NLRP3 inflammasome			29735977	Mus musculus	Immunological
innate immune response	increases_activity of	macrophage activation			28760771	Mammalia	Nephropathy, diabetic
innate immune response	increases_activity of	NLRP3 inflammasome			28760771	Mammalia	Nephropathy, diabetic
innate immune response	increases_activity of	toll-like receptor 3 signaling pathway			25309543	Mammalia	Immunological
innate immune response	increases_activity of	toll-like receptor 4 signaling pathway			25309543	Mammalia	Immunological

innate immune response	increases_activity of	complement activation, lectin pathway			28760771	Mammalia	Nephropathy, diabetic
MCM3	increases_activity of	NF-kappaB complex			31208444	Homo sapiens	Cancer
complement C1q	interacts (colocalizes) with	C1QBP			11859136	Mammalia	Inflammation; Immunological
TNF	increases_expression of	PAPPA	in mesangial cells		27519211	Homo sapiens	Nephropathy, diabetic
IL2	increases_quantity of	KIR2DL4	on the surface of NK cells		14500636	Homo sapiens	Immunological
KIR2DL4	interacts (colocalizes) with	HLA-G			22934097	Mammalia	Immunological
IL2	increases_activity of	T cell activation	in peripheral blood mononuclear cells		3110074	Homo sapiens	Immunological; Diabetes mellitus
IL19	increases_activity of	dendritic cell differentiation			15827959	Homo sapiens	Immunological
IL22	decreases_activity of	NLRP3 inflammasome			28726774	Mus musculus	Renal; Immunological
toll-like receptor 4 signaling pathway	increases_quantity of	IL22	from dendritic cells		24459235	Mus musculus	Inflammation; Immunological
IL22RA1	interacts (colocalizes) with	IL22			24459235	Mus musculus	Inflammation; Immunological
toll-like receptor 4 signaling pathway	increases_quantity of	TNF			28933050	Mammalia	Nephropathy, diabetic
IL19	increases_quantity of	TNF	in monocytes		12370360	Mus musculus	Inflammation
IL19	increases_quantity of	TNF	in human HepG2cells		23468852	Mammalia	Renal
ADIPOQ	interacts (colocalizes) with	CD93		via binding to C1qRp, the receptor for C1q	10961870	Homo sapiens	Immunological
CD93	interacts (colocalizes) with	complement C1q			10961870	Homo sapiens	Immunological
macrophage activation	increases_activity of	TFE3	in nucleus, in RAW-264 7 cells, in bone marrow-derived macrophages, in microglia		27171064	Mus musculus	Bacterial infection
LEPR	increases_activity of	T cell activation			25917102	Mus musculus	Immunological
HLA-G	affects_activity of	T cell activation		in response to activation via KIR2DL4	22934097	Mammalia	Immunological
IL2	increases_activity of	T cell activation		via activation of STAT5	29619880	Homo sapiens	Immunological; Chronic kidney disease
toll-like receptor 4 signaling pathway	increases_activity of	TFE3	in RAW-264 7 cells		27171064	Mus musculus	Bacterial infection
TFE3	affects_expression of	TNF	in RAW-264 7 cells		27171064	Mus musculus	Bacterial infection
IL6	affects_activity of	T cell activation			28363692	Mammalia	Nephropathy, diabetic
TNFRSF1B	increases_activity of	NF-kappaB complex	in peripheral blood mononuclear cells		30104686	Homo sapiens	Inflammation
TNF	increases_expression of	LAYN	in renal tubular epithelia		26410531	Mus musculus	Chronic kidney disease
TNF	increases_expression of	LAYN	in KMRC-1 cells		26410531	Homo sapiens	Chronic kidney disease
TNF	increases_expression of	NEURL3	in alveolar epithelial type II cells (T7 cells)		15936721	Mus musculus	Lung disease
NEURL3	affects_activity of	Notch signaling pathway	in embryonic lungs		25904058	Mus musculus	Lung disease; Developmental
TTF2	interacts (colocalizes) with	CDC5L	in HeLa cells		12927788	Homo sapiens	Cancer
CDC5L	interacts (colocalizes) with	ATR	in HeLa and HCT-116 cells		1963697	Homo sapiens	Cancer
ATR	increases_activity of	DNA damage checkpoint			15210935	Mammalia	Metabolic
MCM3	increases_activity of	DNA damage checkpoint			15210935	Homo sapiens	Cancer
ATR	affects_activity of	MCM3			15210935	Homo sapiens	Cancer
ATR	increases_activity of	DNA damage checkpoint	in nucleus and mitochondria		32984322	Mammalia	Cancer
ADIPOQ	increases_expression of	ARG1	in the stromal vascular fraction cells of adipose tissue		20028977	Mus musculus	Inflammation
ADIPOQ	affects_activity of	macrophage activation	in the stromal vascular fraction cells of adipose tissue		20028977	Mus musculus	Inflammation
ADIPOQ	increases_quantity of	ARG1	in the stromal vascular fraction cells of adipose tissue		20028977	Mus musculus	Inflammation
macrophage activation	increases_quantity of	ARG1	in renal tissue and serum		32179955	Rattus norvegicus	Renal
ATR	increases_activity of	DNA damage checkpoint	in proximal tubule cells		31589169	Homo sapiens	Inflammation; Renal
FSTL3	increases_activity of	macrophage activation			31815869	Mus musculus	Cardiovascular disease
FCN3	interacts (colocalizes) with	MASPI			11907111	Homo sapiens	Hematological; Immunological
TNF	increases_quantity of	KDR			9705358	Homo sapiens	Anytrophic lateral sclerosis

Supplementary Table 10. Interaction of connected edges in T2DCKDadipo and the based literatures.

Abbreviations: T2DCKDadipo, T2D-related CKD subnetwork of adipokine influence.

Subject	Interaction type	Object	Arg_loc	Arg_Mod	PMID	Organism	Disease
LEP	increases activity of	fatty acid beta-oxidation	in adipose tissue, in liver, in muscle, in pancreas, in pancreatic islet		10940327	Mammalia	Diabetes mellitus, type II; Insulin resistance;
hyperglycemia	decreases expression of	LEPR	in adipose tissue		15536073	Mus musculus	Diabetes mellitus type I Hypothyroidism
LEP	decreases activity of	hyperglycemia			7624776	Mus musculus	Diabetes mellitus type II Insulin resistance
LEP	increases activity of	LEPR	in hypothalamus		8782827	Mus musculus	Diabetes mellitus, type II; Insulin resistance
SOD2	affects activity of	abnormal mitochondrial physiology			22138560	Mammalia	Glaucoma, primary open angle; Diabetes mellitus, type II; Insulin resistance;
hyperglycemia	decreases quantity of	ADIPOQ			24167545	Homo sapiens	Developmental
SOD2	decreases quantity of	Reactive oxygen species			22117616	Mammalia	Diabetes mellitus, type II; Insulin resistance; Cancer
RETN	decreases activity of	AMPK			25841249	Mammalia	Diabetes mellitus, type II; Insulin resistance
TNF	interacts (colocalizes) with	TNFRSF1A			15842589	Homo sapiens	Inflammatory bowel disease
TNF	interacts (colocalizes) with	TNFRSF1B			15842589	Homo sapiens	Inflammatory bowel disease
ACSL1	increases activity of	long-chain fatty-acyl-CoA biosynthetic process			24853887	Mammalia	Diabetes mellitus, type II; Cardiovascular disease; Insulin resistance; Cancer
LEP	increases expression of	IGFBP2			20074524	Mus musculus	Diabetes mellitus, type II; Insulin resistance
IGFBP2	decreases activity of	hyperglycemia			20074524	Mus musculus	Diabetes mellitus type II Insulin resistance
ADIPOQ	increases activity of	AMPK		via ADIPOR1 via ADIPOR1 and AMPK	28402446	Mammalia	Diabetes mellitus, type II; Nephropathy, diabetic; Insulin resistance
ADIPOQ	decreases quantity of	Reactive oxygen species			28402446	Mammalia	Diabetes mellitus, type II; Nephropathy, diabetic; Insulin resistance
ADIPOQ	decreases activity of	abnormal podocyte physiology			28402446	Mammalia	Diabetes mellitus, type II; Nephropathy, diabetic; Insulin resistance
ADIPOQ	decreases activity of	NADPH oxidase complex	in kidney		28402446	Mammalia	Diabetes mellitus, type II; Nephropathy, diabetic; Insulin resistance
ADIPOQ	decreases activity of	NF-kappaB complex	in kidney		28402446	Mammalia	Diabetes mellitus, type II; Nephropathy, diabetic; Insulin resistance
Angiotensin II	increases activity of	NF-kappaB complex	in kidney		28402446	Mammalia	Diabetes mellitus, type II; Nephropathy, diabetic; Insulin resistance
ADIPOQ	decreases expression of	FN1	in kidney		28402446	Mammalia	Diabetes mellitus, type II; Nephropathy, diabetic; Insulin resistance
hyperglycemia	increases activity of	NADPH oxidase complex	in mesangial cells		28402446	Mammalia	Diabetes mellitus, type II; Nephropathy, diabetic; Insulin resistance
ADIPOQ	increases expression of	NOS3			28402446	Mammalia	Diabetes mellitus, type II; Nephropathy, diabetic Insulin resistance
ADIPOQ	affects activity of	lipid metabolic process			28402446	Mammalia	Diabetes mellitus, type II; Nephropathy, diabetic; Insulin resistance
Nephropathy, diabetic	increases quantity of	RETN	in blood serum		32173772	Homo sapiens	Diabetes mellitus, type II; Nephropathy, diabetic; Insulin resistance
ADIPOQ	decreases expression of	TNF		via decreased NF-kappaB activity via decreased NF-kappaB activity	30181742	Mammalia	Chronic kidney disease
ADIPOQ	decreases expression of	IL6			30181742	Mammalia	Chronic kidney disease
LEPR	increases activity of	TGFB1			30181742	Mammalia	Chronic kidney disease
LEPR	increases quantity of	Collagen IV			30181742	Mammalia	Chronic kidney disease
LEPR	increases activity of	Phosphatidylinositol 3-kinase			30181742	Mammalia	Chronic kidney disease
RETN	increases expression of	VCAM1			30181742	Mammalia	Chronic kidney disease
ADIPOQ	decreases expression of	VCAM1			30181742	Mammalia	Chronic kidney disease
RETN	increases activity of	NF-kappaB complex			30181742	Mammalia	Chronic kidney disease
RETN	increases expression of	IL6			30181742	Mammalia	Chronic kidney disease
RETN	increases expression of	TNF			30181742	Mammalia	Chronic kidney disease
MMP1	increases quantity of	VEGFA	in retinal microvascular endothelial cells		27261371	Homo sapiens	Retinopathy, diabetic
hyperglycemia	decreases expression of	SOD2	in mesangial cells		26052839	Homo sapiens	Renal
Angiotensin II	increases expression of	CST3	in aortic smooth muscle cells		31668507	Homo sapiens	Cardiovascular disease
VCAM1	increases activity of	decreased renal glomerular filtration rate			32953797	Homo sapiens	Nephropathy, diabetic
NADPH oxidase complex	increases quantity of	Reactive oxygen species			32098346	Mammalia	Diabetes mellitus, type II; Nephropathy, diabetic; Insulin resistance
Nephropathy, obesity-related	decreases expression of	ACSL1	in kidney		31488013	Homo sapiens	Obesity
ACSL1	affects activity of	lipidosis	in HK-2 cells		31488013	Homo sapiens	Obesity
ADIPOQ	increases activity of	ACSL1	in 3T3-L1 adipocytes		20667975	Mus musculus	Diabetes mellitus, type II; Insulin resistance
ACSL1	increases activity of	AMPK	in 3T3-L1 adipocytes		20667975	Mus musculus	Diabetes mellitus, type II; Insulin resistance
Insulin	increases activity of	ACSL1	in 3T3-L1 adipocytes	via FATP1 and ACSL1 via decreased phosphorylation	20667975	Mus musculus	Diabetes mellitus type II Insulin resistance
RETN	decreases activity of	AMPK	in L6 myoblast cells		16137686	norvegicus	Diabetes mellitus, type II; Obesity; Insulin resistance
ACSL1	increases activity of	fatty acid beta-oxidation			20620995	Mus musculus	Diabetes mellitus, type II; Insulin resistance
hyperglycemia	increases expression of	IGFBP2	in MES-13 cells		18392786	Mus musculus	Nephropathy, diabetic
Angiotensin II	increases expression of	IGFBP2	in MES-13 cells		18392786	Mus musculus	Nephropathy, diabetic
ADIPOQ	affects quantity of	ESAM			29804241	Homo sapiens	Diabetes mellitus, type II; Insulin resistance
hyperglycemia	decreases activity of	ESAM			19323980	Mus musculus	Nephropathy, diabetic
ESAM	affects activity of	abnormal glomerular filtration barrier function			19323980	Mus musculus	Nephropathy diabetic
Nephropathy, diabetic	increases quantity of	Luteinizing hormone			32475064	Homo sapiens	Diabetes mellitus, type II; Nephropathy, diabetic; Insulin resistance
Luteinizing hormone	increases activity of	macroalbuminuria			32475064	Homo sapiens	Diabetes mellitus, type II; Nephropathy, diabetic; Insulin resistance
Luteinizing hormone	affects quantity of	VEGFA	in kidney		32065170	Mammalia	Nephropathy, diabetic
ADIPOQ	decreases quantity of	Luteinizing hormone	in LbetaT2 cells		18006641	Mus musculus	Diabetes mellitus, type II; Insulin resistance
ADIPOQ	increases expression of	MMP1	in dermal fibroblasts		24407161	Homo sapiens	Graft-versus-host disease
CST3	interacts (colocalizes) with	ADIPOQ			28321013	Homo sapiens	Cardiovascular disease

ADIPOQ	increases_expression of	SOD2	in monocytes		21035442	Homo sapiens	Diabetes mellitus, type II; Insulin resistance
TFE3	affects_expression of	ADIPOQ			28483914	Mus musculus	Diabetes mellitus, type II; Insulin resistance
ACE	affects_quantity of	ADIPOQ	in blood plasma in bone marrow-derived macrophages		15711099	Homo sapiens	Diabetes mellitus, type II; Nephropathy, diabetic; Insulin resistance
TFE3	affects_expression of	IL6			27171064	Mus musculus	Bacterial infection
LEPR	interacts (colocalizes) with	LEP			30181742	Mammalia	Chronic kidney disease
FSTL3	increases_activity of	lipidosis	in macrophages		31815869	Mus musculus	Cardiovascular disease
LEP	increases_expression of	PNLIPRP2	in AR4-2J cells		17010228	Rattus norvegicus	Cancer
ACE	increases_quantity of	Angiotensin II			20809236	Mammalia	Retinopathy, diabetic; Diabetes mellitus, type II; Cardiovascular disease; Nephropathy, diabetic; Neuropathy, diabetic; Myocardial infarction; Insulin resistance; Stroke, ischemic
FSTL3	increases_quantity of	TNF	in macrophages		31815869	Mus musculus	Cardiovascular disease

Supplementary Table 11. Interaction of connected edges in T2DCKDras and the based literatures.

Abbreviations: T2DCKDras, T2D-related CKD subnetwork of renin-angiotensin system dysfunction.

Subject	Interaction type	Object	Arg_loc	Arg_Mod	PMID	Organism	Disease
ACE	increases_quantity of	Angiotensin II			20809236	Mammalia	Retinopathy, diabetic; Diabetes mellitus, type II; Cardiovascular disease; Nephropathy, diabetic; Neuropathy, diabetic; Myocardial infarction; Insulin resistance; Stroke, ischemic
Angiotensin (1-7)	decreases_expression of	IL6	in cardiac muscle		19166939	Rattus norvegicus	Diabetes mellitus, type II; Insulin resistance
Angiotensin II	increases_expression of	FN1		via CYBB	16720735	Mus musculus	Diabetes mellitus, type II; Insulin resistance
Aldosterone	increases_expression of	FN1		via CYBB	16720735	Mus musculus	Diabetes mellitus, type II; Insulin resistance
ABCB1	increases_transport of	Aldosterone			21967062	Mammalia	Diabetes mellitus, type II Insulin resistance
IGFBP2	decreases_activity of	hyperglycemia			20074524	Mus musculus	Diabetes mellitus type II Insulin resistance
Angiotensin II	increases_expression of	IGF2R		via AGTR1	24786827	Rattus norvegicus	Cardiovascular disease
Angiotensin II	interacts (colocalizes) with	AGTR2	in HEK293 cells		21542804	Homo sapiens	Cardiovascular disease
REN	increases_activity of	IGF2R			30934934	Mammalia	Diabetes mellitus, type II; Cardiovascular disease; Insulin resistance
IGF2R	increases_transport of	Prorenin	from extracellular space into cell, in cardiomyocytes, in fibroblasts, in vascular smooth muscle cells		30934934	Mammalia	Diabetes mellitus, type II; Cardiovascular disease; Insulin resistance
Angiotensin II	increases_quantity of	PLAT	in extracellular space		12091055	Homo sapiens	Cardiovascular disease
Angiotensin (1-7)	decreases_quantity of	PLAT	in extracellular space		12091055	Homo sapiens	Cardiovascular disease
AGTR1	increases_quantity of	Aldosterone	in adrenal glomerulosa cells		1338730	Rattus norvegicus	Chronic kidney disease
AGTR1	increases_activity of	EGFR			31525726	Mammalia	Obesity, Cancer
hyperglycemia	increases_expression of	KDR			16436494	Bos taurus	Cardiovascular
Angiotensin II	increases_expression of	KDR	in podocytes		26063200	Homo sapiens	Nephropathy, diabetic
hyperglycemia	increases_quantity of	PLAT	mesangial cells		7924884	Homo sapiens	Nephropathy, diabetic
AMH	affects_quantity of	Prorenin		in pregnancy	32853347	Homo sapiens	Preeclampsia
AGTR1	affects_expression of	FN1	in mesangial cells		15569303	Rattus norvegicus	Nephropathy diabetic
ABCB1	affects_activity of	REN	in blood plasma		17372036	Homo sapiens	Cardiovascular disease
CTSH	increases_activity of	REN			6756687	Homo sapiens	Cardiovascular disease
Angiotensin II	increases_expression of	CTSV	in aortic smooth muscle cells		31668507	Homo sapiens	Cardiovascular disease
Angiotensin II	increases_expression of	CST3	in aortic smooth muscle cells		31668507	Homo sapiens	Cardiovascular disease
Angiotensin II	increases_expression of	FN1	in glomerular mesangial cells		11737589	Mus musculus	Chronic kidney disease
EGFR	affects_expression of	FN1	in glomerular mesangial cells		11737589	Mus musculus	Chronic kidney disease
Angiotensin II	increases_activity of	EGFR	in glomerular mesangial cells	via phosphorylation	11737589	Mus musculus	Chronic kidney disease
ERBB3	interacts (colocalizes) with	AGTR2			10710290	Homo sapiens	Cardiovascular disease
Angiotensin (1-7)	decreases_activity of	EGFR	in aortic smooth muscle cells	via MAS1	26536590	Rattus norvegicus	Diabetes mellitus, type II; Insulin resistance
Angiotensin (1-7)	decreases_activity of	ERBB3	in aortic smooth muscle cells		26536590	Rattus norvegicus	Diabetes mellitus, type II Insulin resistance
hyperglycemia	increases_activity of	ERBB3	in aortic smooth muscle cells		26536590	Rattus norvegicus	Diabetes mellitus type II Insulin resistance
hyperglycemia	increases_quantity of	FN1	in MES-13 cells		18392786	Mus musculus	Nephropathy, diabetic
Angiotensin II	increases_expression of	IGFBP2	in MES-13 cells		18392786	Mus musculus	Nephropathy, diabetic
ACE	affects_expression of	EPHA2			18463147	Rattus norvegicus	Cardiovascular disease
Luteinizing hormone	increases_quantity of	Aldosterone			24297486	Homo sapiens	Cardiovascular disease
GHR	affects_quantity of	Angiotensin (1-7)	in heart in kidney		22947377	Mus musculus	Cardiovascular disease
GHR	affects_quantity of	MAS1	in heart, in kidney		22947377	Mus musculus	Cardiovascular disease
GHR	affects_quantity of	ACE2	in heart, in kidney		22947377	Mus musculus	Cardiovascular disease
GHR	affects_quantity of	AGTR1	in heart, in kidney		22947377	Mus musculus	Cardiovascular disease
Angiotensin II	decreases_expression of	MMP1	in cardiac fibroblasts in cardiac myocytes		18296491	Homo sapiens	Cardiovascular disease
Angiotensin II	increases_expression of	MMP1	in cardiac myocytes		18296491	Homo sapiens	Cardiovascular disease
Angiotensin II	increases_activity of	NTRK2			28549782	Rattus norvegicus	Cardiovascular disease
Angiotensin II	increases_activity of	RET			19961928	Mus musculus	Developmental
ACE	affects_activity of	RPS6KA5	in kidney		21377515	Rattus norvegicus	Cardiovascular disease
AGTR1	affects_activity of	RPS6KA5	in kidney		21377515	Rattus norvegicus	Cardiovascular disease
Angiotensin (1-7)	increases_expression of	SOD2	in cardiomyocytes		28411231	Rattus norvegicus	Cardiovascular disease
ACE	affects_quantity of	ADIPOQ	in blood plasma		15711099	Homo sapiens	Diabetes mellitus, type II; Nephropathy, diabetic; Insulin resistance
ERBB3	interacts (colocalizes) with	EGFR			24520092	Homo sapiens	Cancer
Angiotensin II	increases_activity of	AGTR1			25003613	Mammalia	Nephropathy, diabetic
ACE2	decreases_quantity of	Angiotensin II			30978131	Mammalia	Cardiovascular disease
ACE	decreases_quantity of	Angiotensin I	in kidney		19065132	Mammalia	Nephropathy, diabetic
Renin	increases_quantity of	Angiotensin I			10585461	Mammalia	Nephropathy, diabetic
Prorenin	increases_quantity of	Renin			12684512	Homo sapiens	Nephropathy, diabetic
hyperglycemia	decreases_expression of	SOD2	in mesangial cells		26052839	Homo sapiens	Renal
hyperglycemia	increases_activity of	EGFR		via phosphorylation	16105029	Homo sapiens	Nephropathy diabetic
Angiotensin (1-7)	increases_activity of	MAS1	in HEK293 cells		27217404	Homo sapiens	Cardiovascular disease
ACE2	increases_quantity of	Angiotensin (1-7)	in kidney	at neutral to basic pH	23392115	Mus musculus	Endocrine

Supplementary Table 12. Interaction of connected edges in T2DCKDfibri and the based literatures.

Abbreviations: T2DCKDfibri, T2D-related CKD subnetwork of extracellular matrix deposition and renal fibrosis.

Subject	Interaction type	Object	Arg. loc	Arg. Mod	PMID	Organism	Disease
TNFRSF1A	affects_expression of	VEGFA			18413601	Mus musculus	Amyotrophic lateral sclerosis
TNF	interacts (colocalizes) with	TNFRSF1A			15842589	Homo sapiens	Inflammatory bowel disease
TNF	interacts (colocalizes) with	TNFRSF1B			15842589	Homo sapiens	Inflammatory bowel disease
TNFRSF1B	affects_activity of	TNFRSF1A		by mediating the binding of TNF to TNFRSF1A	15842589	Homo sapiens	Inflammatory bowel disease
ACY1	affects_activity of	TGFB1			28454420	Homo sapiens	Colorectal cancer
Thrombin	decreases_quantity of	Fibrinogen			32348783	Mammalia	COVID-19; Cardiovascular disease
Thrombin	increases_quantity of	Fibrin			32348783	Mammalia	COVID-19; Cardiovascular disease
Fibrinogen	increases_quantity of	Fibrin		via proteolytic activity of thrombin	32348783	Mammalia	COVID-19; Cardiovascular disease
Plasminogen	increases_quantity of	Plasmin		via proteolytic activity of PLAT and PLAU	32348783	Mammalia	COVID-19; Cardiovascular disease
PLAT	increases_quantity of	Plasmin		together with PLAU	32348783	Mammalia	COVID-19; Cardiovascular disease
PLAT	decreases_quantity of	Plasminogen		together with PLAU	32348783	Mammalia	COVID-19; Cardiovascular disease
SPOCK2	decreases_expression of	MMP2	in HEC-1A cells, in Ishikawa cells		30832559	Homo sapiens	Cancer
ADIPOQ	decreases_expression of	FN1	in kidney		28402446	Mammalia	Nephropathy, diabetic; Insulin resistance; Diabetes mellitus type II
KDR	interacts (colocalizes) with	VEGFA	in CMT-3 cells		1417831	Canis lupus familiaris	Cardiovascular
hyperglycemia	increases_expression of	KDR			16436494	Bos taurus	Cardiovascular
Thrombin	increases_expression of	KDR	in aortic endothelial cells		11807828	Bos taurus	Cardiovascular
Thrombin	increases_expression of	KDR	in umbilical vein endothelial cells		10446165	Homo sapiens	Cardiovascular
PLAT	decreases_quantity of	Plasmin			7924884	Mammalia	Nephropathy, diabetic
ADAMTS13	decreases_quantity of	Fibrinogen	in plasma		28495930	Mus musculus	Nephropathy, diabetic
ADAMTS13	decreases_quantity of	FN1	in the glomerular compartment		28495930	Mus musculus	Nephropathy, diabetic
Thrombin	increases_quantity of	FN1	in mesenchymal stem cells		24636778	Homo sapiens	Hematological
TGFB	increases_expression of	NOTCH1	in cultured marine tubular epithelial cells.		26119175	Mammalia	Nephropathy, diabetic
IGF2R	interacts (colocalizes) with	Plasminogen			22613725	Mammalia	Hematological
IGF2R	increases_quantity of	Plasmin			22613725	Mammalia	Hematological
FSTL3	decreases_quantity of	FN1	in mesangial cells	under high-glucose condition	26629006	Rattus norvegicus	Nephropathy, diabetic
FCN3	interacts (colocalizes) with	MASP1			11907111	Homo sapiens	Hematological; Immunological
Carnosine	decreases_quantity of	FN1	in podocytes		16046297	Homo sapiens	Nephropathy, diabetic; Diabetes mellitus, type II; Diabetes mellitus, type I
MMP1	decreases_quantity of	Collagen			10703682	Mammalia	Nephropathy, diabetic
hyperglycemia	increases_expression of	FN1	in mesangial cells		10703682	Mammalia	Nephropathy, diabetic
TNFRSF1A	affects_quantity of	Fibrin	in hepatocytes		26052839	Homo sapiens	Renal
Laminin	increases_activity of	extracellular matrix assembly			20218879	Mus musculus	Hematological
LAMC1	is_part_of	Laminin			11801598	Mammalia	Renal
TFE3	increases_expression of	LAMC1	in mesangial cells	together with SMAD3	11801598	Rattus norvegicus	Renal
Collagen	increases_activity of	extracellular matrix assembly			10703682	Mammalia	Nephropathy, diabetic
Fibrin	increases_activity of	extracellular matrix assembly			25867016	Mammalia	Hematological
FCN3	increases_activity of	MASP1			11907111	Homo sapiens	Hematological; Immunological
IGF2R	interacts (colocalizes) with	Plasminogen	in monocytes		10092105	Homo sapiens	Inflammation
CTS3	decreases_activity of	CTS3	in cardiac fibroblasts		20489058	Rattus norvegicus	Cardiovascular disease
CTS3	decreases_quantity of	FN1	in cardiac fibroblasts		20489058	Rattus norvegicus	Cardiovascular disease
FN1	increases_activity of	extracellular matrix assembly	in fibroblasts		20489058	Mammalia	Cardiovascular disease
CTS3	decreases_quantity of	Plasminogen	in cornea		18163891	Homo sapiens	Cardiovascular disease
CTS3	decreases_quantity of	ELN	in monocyte-derived macrophages		15192101	Homo sapiens	Atherosclerosis; Cardiovascular disease
Plasmin	decreases_quantity of	Fibrin			32348783	Mammalia	COVID-19; Cardiovascular disease
CIQBP	decreases_quantity of	Fibrin			10075865	Homo sapiens	Hematological
ELN	increases_activity of	extracellular matrix assembly			24680817	Mammalia	Cancer; Cardiovascular disease
extracellular matrix assembly	increases_activity of	fibrosis			29482391	Mammalia	Liver disease, chronic
CNDP1	decreases_quantity of	Carnosine	in blood serum		16046297	Homo sapiens	Nephropathy, diabetic; Diabetes mellitus, type II; Diabetes mellitus, type I
TGFB1	increases_expression of	FN1	in diabetic kidney		8603776	Mus musculus	Nephropathy, diabetic
BMP1	increases_quantity of	Collagen			29482391	Mammalia	Liver disease, chronic
MASP1	increases_quantity of	Fibrin	in normal citrated plasma		22536427	Homo sapiens	Hematological; Immunological
EGFR	affects_expression of	FN1	in glomerular mesangial cells		11737589	Mus musculus	Chronic kidney disease
Angiostatin	decreases_quantity of	Plasmin		through proteolytic activity of PLAT	19916923	Homo sapiens	Hematological
Plasminogen	increases_quantity of	Plasmin			28837538	Mammalia	Cancer
Plasminogen	increases_quantity of	Angiostatin			28837538	Mammalia	Cancer
Angiostatin	decreases_activity of	PLAT	in bovine aortic endothelial cells (BAEC), murine melanoma cells (B16F10) or human ovariancarcinoma cells (OVCA 429)	by binding to tPA (PLAT)	10229661	Mus musculus	Cancer
PLAT	increases_quantity of	Plasmin			28837538	Mammalia	Cancer
Angiostatin	decreases_activity of	PLAT			21899046	Homo sapiens	Hematological
MASP1	increases_quantity of	Fibrin			24935208	Mammalia	Hematological; Immunological
EPHA2	increases_quantity of	Laminin	in HK-2 cells		27228995	Homo sapiens	Chronic kidney disease
TGFB1	decreases_expression of	PAX8	in FRTL-5 cells		11145590	Rattus norvegicus	
IL22	decreases_quantity of	FN1	in renal glomerular mesangial cells		28726774	Mus musculus	Immunological; Renal
IL22RA1	interacts (colocalizes) with	IL22			24459235	Mus musculus	Inflammation; Immunological
hyperglycemia	increases_quantity of	FN1	in renal glomerular mesangial cells		28726774	Mus musculus	Immunological; Renal
TNFRSF19	interacts (colocalizes) with	TGFB1	in HEK293T cells		29735548	Homo sapiens	Cancer
TNF	increases_expression of	LAYN	in renal tubular epithelia		26410531	Mus musculus	Chronic kidney disease
TGFB	interacts (colocalizes) with	TGFB1			29735548	Homo sapiens	Cancer
NOTCH1	increases_expression of	FN1			28751525	Mus musculus	Chronic kidney disease
Angiostatin	decreases_quantity of	TGFB1	in kidney		16394111	Rattus norvegicus	Nephropathy, diabetic
TGFB1	increases_quantity of	FN1			16394111	Homo sapiens	Renal
Angiostatin	decreases_activity of	TGFB1			16394111	Homo sapiens	Renal
TGFA	interacts (colocalizes) with	EGFR		by accelerating TGFalpha processing and cell-surface delivery	15064403	Mammalia	Cancer
NKD2	increases_activity of	TGFA			15064403	Canis lupus familiaris	Renal
SPINT1	decreases_activity of	HGFAC	in serum-free cultured conditioned medium of a human gastric carcinoma cell line MKN 45		10219059	Mammalia	Cancer

HGFAC	increases activity of	HGF		during kidney development	11032833	Mus musculus	Developmental; Renal
TLN2	increases activity of	extracellular matrix assembly	in NIH3T3 cells		22306379	Mus musculus	Metabolic
TLN2	interacts (colocalizes) with	LAYN			29723415	Homo sapiens	Cancer; Metabolic
HGF	decreases quantity of	Collagen	in glomeruli		15882257	Homo sapiens	Renal
NOTCH1	increases quantity of	Collagen			28751525	Mus musculus	Chronic kidney disease
hyperglycemia	decreases expression of	FSTL3	in mesangial cells		26629006	Rattus norvegicus	Nephropathy, diabetic
hyperglycemia	decreases quantity of	FSTL3	in mesangial cells		26629006	Rattus norvegicus	Nephropathy, diabetic
TGFβ1	increases quantity of	CST3	in profibrogenic hepatic stellate cells		16521186	Rattus norvegicus	Inflammation
TGFβ1	increases quantity of	CST3	in smooth muscle cells		10545518	Homo sapiens	Cardiovascular

Supplementary Table 13. Interaction of connected edges in T2DCKDage and the based literatures.

Abbreviations: T2DCKDage, T2D-related CKD subnetwork of advanced glycation end products.

Subject	Interaction type	Object	Arg_loc	Arg_Mod	PMID	Organism	Disease
Reactive oxygen species	increases quantity of	Advanced glycation end-product			10783895	Bos taurus	Insulin resistance; Diabetes mellitus, type II
hyperglycemia	increases quantity of	Advanced glycation end-product			10082470	Mammalia	Insulin resistance; Diabetes mellitus, type II
hyperglycemia	increases quantity of	Glycated hemoglobin			10082470	Mammalia	Insulin resistance; Diabetes mellitus, type II
AGER	increases activity of	NF-kappaB complex			10082470	Mammalia	Insulin resistance; Diabetes mellitus, type II
Acetylcarnitine	increases quantity of	Glycated hemoglobin			19369366	Homo sapiens	Insulin resistance; Diabetes mellitus, type II; Obesity
Advanced glycation end-product	increases activity of	Nephropathy, diabetic			26900135	Mammalia	Insulin resistance; Diabetes mellitus, type II; Obesity
AGER	increases quantity of	Reactive oxygen species			22582044	Mammalia	Insulin resistance; Diabetes mellitus, type II
Advanced glycation end-product	interacts (colocalizes) with	AGER			31861217	Mammalia	Insulin resistance; Diabetes mellitus, type II
hyperglycemia	increases quantity of	Advanced glycation end-product		in T1D and in T2D	31861217	Mammalia	Insulin resistance; Diabetes mellitus, type II
Advanced glycation end-product	affects quantity of	AMH		in women habituated to high AGE consumption	31861217	Mammalia	Insulin resistance; Diabetes mellitus, type II
AMH	affects activity of	NF-kappaB complex	in lung cancer		27396341	Mus musculus	Cancer
Advanced glycation end-product	increases quantity of	Angiotensin II			15569303	Rattus norvegicus	Nephropathy, diabetic
Advanced glycation end-product	increases expression of	FN1	in mesangial cells		15569303	Rattus norvegicus	Nephropathy, diabetic
HAVCR2	decreases quantity of	Reactive oxygen species	in nonalcoholic fatty liver disease		30862474	Mammalia	Nephropathy, diabetic
HAVCR2	decreases activity of	NLRP3 inflammasome	in nonalcoholic fatty liver disease		30862474	Mammalia	Nephropathy, diabetic
HAVCR2	affects activity of	NF-kappaB complex	in macrophages		30862474	Mammalia	Nephropathy, diabetic
Nephropathy, diabetic	increases quantity of	HAVCR2	in renal macrophages		30862474	Mus musculus	Nephropathy, diabetic
Advanced glycation end-product	increases quantity of	HAVCR2	in peritoneal macrophages and bone marrow cells		30862474	Mus musculus	Nephropathy, diabetic
protein glycation	increases quantity of	B2M-AGE			11792765	Homo sapiens	Insulin resistance; Nephropathy, diabetic; Diabetes mellitus, type II
B2MAGE	increases activity of	extracellular matrix disassembly			11792765	Homo sapiens	Insulin resistance; Nephropathy, diabetic; Diabetes mellitus, type II
B2MAGE	increases expression of	TNF			8113390	Homo sapiens	Chronic kidney disease
B2MAGE	increases expression of	IL1B			8113390	Homo sapiens	Chronic kidney disease
B2MAGE	increases activity of	monocyte chemotaxis			8113390	Homo sapiens	Chronic kidney disease
B2MAGE	increases expression of	MMP1	in synovial fibroblasts		8113390	Homo sapiens	Chronic kidney disease
B2MAGE	increases expression of	TGFβ1	in macrophages		10652049	Homo sapiens	Chronic kidney disease
B2MAGE	increases expression of	TNF	in macrophages		10652049	Homo sapiens	Chronic kidney disease
protein glycation	increases quantity of	Advanced glycation end-product			22117616	Mammalia	Insulin resistance; Cancer; Diabetes mellitus, type II
Advanced glycation end-product	increases quantity of	Collagen IV			32098346	Mammalia	Insulin resistance; Nephropathy, diabetic; Diabetes mellitus, type II
Glycated hemoglobin	increases quantity of	Advanced glycation end-product			10082470	Mammalia	Insulin resistance; Diabetes mellitus, type II
Nephropathy, diabetic	increases expression of	AGER	in kidney		24371263	Homo sapiens	Nephropathy, diabetic
Advanced glycation end-product	affects activity of	Luteinizing hormone	in KGN cells		28914097	Homo sapiens	Polycystic ovary syndrome 1
Luteinizing hormone	increases activity of	ERK1 and ERK2 cascade	in KGN cells		28914097	Homo sapiens	Polycystic ovary syndrome 1
Advanced glycation end-product	decreases activity of	ERK1 and ERK2 cascade	in KGN cells		28914097	Homo sapiens	Polycystic ovary syndrome 1
Advanced glycation end-product	increases activity of	NLRP3 inflammasome			28760771	Mammalia	Nephropathy, diabetic

Supplementary Table 14. Interaction of connected edges in T2DCKDangi and the based literatures. Abbreviations: T2DCKDangi, T2D-related CKD subnetwork of angiogenesis.

Subject	Interaction type	Object	Arg_loc	Arg_Mod	PMID	Organism	Disease
TNFRSF1A	affects expression of	VEGFA			18413601	Mus musculus	Amyotrophic lateral sclerosis
TNF	increases quantity of	KDR			9705358	Homo sapiens	Amyotrophic lateral sclerosis Cancer; Metabolic syndrome; Diabetes mellitus, type II; Insulin resistance
IL6	increases activity of	angiogenesis			21912508	Mammalia	Inflammatory bowel disease
TNF	interacts (colocalizes) with	TNFRSF1A			15842589	Homo sapiens	Inflammatory bowel disease
TNF	interacts (colocalizes) with	TNFRSF1B			15842589	Homo sapiens	Inflammatory bowel disease
KDR	interacts (colocalizes) with	VEGFA	in CMT-3 cells		1417831	Canis lupus familiaris	Cardiovascular
KDR	increases activity of	angiogenesis	in CMT-3 cells		1417831	Canis lupus familiaris	Cardiovascular
hyperglycemia	increases expression of	KDR			16436494	Bos taurus	Cardiovascular
MMP1	increases quantity of	VEGFA	in retinal microvascular endothelial cells		27261371	Homo sapiens	Retinopathy diabetic
CTSV	decreases quantity of	Plasminogen	in cornea		18163891	Homo sapiens	Cardiovascular disease
CTSV	decreases activity of	angiogenesis	in cornea		18163891	Homo sapiens	Cardiovascular disease
CTSH	increases activity of	angiogenesis	in pancreatic islet cell cancer		20731543	Mus musculus	Cancer
NF-kappaB complex	increases expression of	VEGFA			25474138	Mammalia	Cancer; Hepatocellular carcinoma
AGK	increases activity of	angiogenesis	in Huh-7 and PLC heptocellular carcinoma cells		25474138	Homo sapiens	Cancer; Hepatocellular carcinoma
AGK	increases activity of	NF-kappaB complex	in Huh-7 and PLC heptocellular carcinoma cells		25474138	Homo sapiens	Cancer; Hepatocellular carcinoma
NF-kappaB complex	increases quantity of	VEGFA	in Huh-7 and PLC heptocellular carcinoma cells		25474138	Homo sapiens	Cancer; Hepatocellular carcinoma
SEMA3E	interacts (colocalizes) with	PLXND1			19940264	Mammalia	Hematological
SEMA3E	decreases activity of	VEGFA	in HUVECs		19940264	Homo sapiens	Hematological
SEMA3E	decreases expression of	DLL4	in retinal vasculature		21724832	Mus musculus	Ophthalmological
DLL4	increases activity of	NOTCH1			17259973	Mus musculus	Ophthalmological
NOTCH1	affects activity of	angiogenesis		together with DLL4	17259973	Mus musculus	Ophthalmological
VEGFA	increases expression of	DLL4	in angiogenic sprouts		17296940	Mus musculus	Ophthalmological
NOTCH1	affects expression of	KDR	in the subcutaneous site and femoral defect site after 6 weeks of surgery		29674611	Rattus norvegicus	Bone
VEGFA	increases expression of	DLL4	in HUVECs		21724832	Homo sapiens	Ophthalmological
SEMA3E	decreases expression of	DLL4	in HUVECs		21724832	Homo sapiens	Ophthalmological
VEGFA	increases expression of	PLXND1	in angiogenic blood vessels		21724832	Mus musculus	Ophthalmological
JAM2	increases activity of	VEGFA	in HUVECs		25911611	Homo sapiens	Hematological
ADIPOQ	affects activity of	VEGFA	in coronary artery endothelial cells (HCAECs)		18267956	Homo sapiens	Cardiovascular
ADAMTS13	increases expression of	VEGFA	in HUVECs		24950743	Homo sapiens	Hematological
ADAMTS13	increases activity of	KDR	in HUVECs		24950743	Homo sapiens	Hematological Nephropathy, diabetic; Diabetes mellitus, type II;
Reactive oxygen species	increases activity of	NF-kappaB complex			32098346	Mammalia	Insulin resistance
Angiostatin	decreases activity of	angiogenesis			21899046	Mammalia	Cardiovascular
Angiostatin	decreases activity of	angiogenesis			19916923	Homo sapiens	Hematological
Plasminogen	increases quantity of	Angiostatin			28837538	Mammalia	Cancer
Angiostatin	decreases activity of	PLAT	in bovine aortic endothelial cells (BAEC), murine melanoma cells (B16F10) or human ovariancarcinoma cells (OVCA 429)	by binding to tPA (PLAT)	10229661	Mus musculus	Cancer
IGFBP6	decreases activity of	angiogenesis	in vascular endothelial cells		21618524	Homo sapiens	Cancer
IGFBP6	decreases activity of	angiogenesis			30117676	Mammalia	Inflammation
IL19	increases activity of	angiogenesis		during inflammation	20966397	Homo sapiens	Cardiovascular
IL19	increases activity of	angiogenesis	in isolated aortic rings	also in the absence of hypoxia	27053520	Mus musculus	Cardiovascular
EPHA2	decreases activity of	angiogenesis			16400034	Bos taurus	Retinopathy, diabetic; Diabetes mellitus, type II;
LXL1	increases expression of	ANGPT2	in HUVECs		22792348	Homo sapiens	Insulin resistance
LXL1	increases activity of	angiogenesis	in HUVECs		22792348	Homo sapiens	Hematological
ESAM	increases activity of	angiogenesis			12819200	Mus musculus	Cancer
HIF1A	increases expression of	VEGFA	in breast cancer cells		21602890	Homo sapiens	Breast cancer
PCGF2	interacts (colocalizes) with	HIF1A	in breast cancer cells		21602890	Homo sapiens	Breast cancer
PAX8	decreases activity of	angiogenesis	in gastric cancer cell lines		30021604	Homo sapiens	Gastric cancer
Luteinizing hormone	affects quantity of	VEGFA	in kidney	via lowering the level of HIF1-alpha result in down-regulation of VEGF transcription	32065170	Mammalia	Nephropathy, diabetic
PCGF2	decreases activity of	angiogenesis	in breast cancer cells		21602890	Homo sapiens	Breast cancer
CST3	decreases quantity of	VEGFA			28569795	Rattus norvegicus	Neurological; Parkinson disease
NTRK2	affects expression of	VEGFA	in osteoblasts		28098876	Rattus norvegicus	Bone
HIF1A	increases expression of	NTRK2	in Kelly cells		17374610	Homo sapiens	Cancer
ERBB3	increases quantity of	VEGFA	in HUVECs		31934129	Homo sapiens	Cancer
FGF9	increases expression of	KDR	in ovarian cancer cell lines PA1, SKOV3 and IOSE		29904943	Homo sapiens	Cancer
FGF9	increases expression of	VEGFA	in ovarian cancer cell lines PA1, SKOV3 and IOSE		29904943	Homo sapiens	Cancer
BMP1	affects activity of	GHI	in HEK293 cells		17548836	Homo sapiens	Endocrine
GHR	increases activity of	angiogenesis	in renal cell carcinoma cells		30229899	Homo sapiens	Cancer; Renal
GHR	interacts (colocalizes) with	GHI			30229899	Mammalia	Cancer; Renal
SOD2	decreases quantity of	Reactive oxygen species	in wounds		30362661	Mus musculus	Nephropathy diabetic
HIF1A	increases quantity of	IGFBP2	in FM-516 and WM-35 melanoma cells		23233738	Homo sapiens	Cancer
IGFBP2	increases activity of	angiogenesis	in HUVECs		23233738	Homo sapiens	Cancer
HIF1A	increases expression of	IGFBP6	in vascular endothelial cells		21618524	Homo sapiens	Cancer
hypoxia	increases activity of	HIF1A	in vascular endothelial cells		21618524	Homo sapiens	Cancer
IGF2R	interacts (colocalizes) with	Plasminogen	in serum		21273553	Homo sapiens	Cardiovascular
Plasminogen	increases activity of	angiogenesis	in thoracic aortas		11557572	Mus musculus	Cardiovascular
PLAT	increases activity of	angiogenesis	in thoracic aortas		11557572	Mus musculus	Cardiovascular
Angiostatin	decreases activity of	angiogenesis			20687922	Mammalia	Nephropathy, diabetic
IGF2R	affects activity of	angiogenesis	in HUVECs		21273553	Homo sapiens	Cardiovascular
ANGPT2	increases activity of	angiogenesis	in HUVECs		22792348	Homo sapiens	Hematological
BMP1	affects activity of	angiogenesis	in HUVECs	via production of PRL-fragments	17548836	Homo sapiens	Endocrine
TNFRSF1B	affects expression of	VEGFA	in adenocarcinoma SW1116 cells		26693061	Homo sapiens	Cancer
PLAT	increases activity of	Plasminogen		via conversion of inactive plasminogen to active plasmin	28837538	Mammalia	Cancer
IL22RA1	increases activity of	angiogenesis	in muscle		30236983	Mus musculus	Cardiovascular disease
HIF1A	decreases expression of	SOD2	in kidney cell line		23611775	Homo sapiens	Cancer; Renal
EPHA2	decreases activity of	KDR			16400034	Bos taurus	Retinopathy, diabetic; Diabetes mellitus, type II; Insulin resistance

Supplementary Table 15. Associations of identified candidates from extended replicated set with eGFR, UACR values and incident CKD in hyperglycemia.

Regression coefficients with 95% CI, P-values and FDR of candidates in extended replicated set with eGFR values (current and follow-up), UACR values (current and follow-up) and incident CKD in hyperglycemic individuals of KORA F4 are shown, respectively. ORs with 95% CI were additionally shown when outcome was incident CKD. Regression coefficients were from linear regression analysis for eGFR and UACR values and from logistic regression analysis for CKD, which all adjusted for age, sex, BMI, systolic blood pressure, smoking status, triglyceride, total cholesterol, HDL cholesterol, fasting glucose, use of lipid lowering drugs, antihypertensive and anti-diabetic medication. FDR was calculated within each omics type and kidney trait.

Abbreviations: CKD, chronic kidney disease; eGFR, estimated glomerular filtration rate; UACR, urinary albumin-to-creatinine ratio. OR, odds ratio.

omics.label	omics.type	eGFR F4.Estimate (95% CI)	eGFR F4.p-value	eGFR F4.FDR (95% CI)	Follow-up eGFR.Estimate (95% CI)	Follow-up eGFR.p-value	Follow-up eGFR.FDR	UACR F4.Estimate (95% CI)	UACR F4.p-value	UACR F4.FDR	Follow-up UACR.Estimate (95% CI)	Follow-up UACR.p-value	Follow-up UACR.FDR	incident CKD.Estimate (95% CI)	incident CKD.OR (95% CI)	incident CKD.p-value	incident CKD.FDR	
C10	Metabolites	-0.174 (-0.214 to -0.135)	1.585E-17	1.109E-16	-0.147 (-0.2 to -0.093)	8.312E-08	1.164E-06	0.062 (0.003 to 0.121)	3.875E-02	3.875E-02	7.749E-02	-0.004 (-0.072 to 0.064)	9.142E-01	9.142E-01	0.249 (0.019 to 0.48)	1.283 (1.019 to 1.615)	3.373E-02	9.183E-02
C10:2	Metabolites	-0.178 (-0.215 to -0.141)	1.691E-20	2.367E-19	-0.117 (-0.168 to -0.066)	6.984E-06	1.956E-05	0.009 (-0.046 to 0.065)	7.383E-01	8.257E-01	-0.025 (-0.089 to 0.039)	4.425E-01	7.965E-01	0.087 (-0.13 to 0.302)	1.091 (0.879 to 1.353)	4.296E-01	4.626E-01	
C12	Metabolites	-0.175 (-0.215 to -0.135)	3.042E-17	1.420E-16	-0.143 (-0.196 to -0.089)	2.232E-07	1.243E-06	0.071 (0.011 to 0.13)	1.962E-02	5.493E-02	0.012 (-0.056 to 0.08)	7.249E-01	8.821E-01	0.327 (0.098 to 0.559)	1.386 (1.103 to 1.749)	5.401E-03	4.414E-02	
C14:1	Metabolites	-0.117 (-0.155 to -0.079)	1.678E-09	2.136E-09	-0.102 (-0.155 to -0.049)	1.816E-04	3.178E-04	0.081 (0.026 to 0.136)	4.066E-03	1.423E-02	0.029 (-0.037 to 0.095)	3.834E-01	7.965E-01	0.299 (0.075 to 0.53)	1.349 (1.077 to 1.698)	9.877E-03	4.609E-02	
C14:1-OH	Metabolites	-0.165 (-0.204 to -0.127)	9.408E-17	3.293E-16	-0.123 (-0.175 to -0.07)	4.789E-06	1.676E-05	0.045 (-0.012 to 0.102)	1.230E-01	1.565E-01	0.013 (-0.053 to 0.079)	7.064E-01	8.821E-01	0.228 (0.005 to 0.454)	1.256 (1.005 to 1.574)	4.592E-02	9.183E-02	
C14:2	Metabolites	-0.166 (-0.205 to -0.127)	2.691E-16	7.536E-16	-0.112 (-0.165 to -0.059)	3.972E-05	7.944E-05	0.052 (-0.006 to 0.11)	7.622E-02	1.186E-01	0.073 (-0.042 to 0.093)	4.551E-01	7.965E-01	0.272 (0.043 to 0.506)	1.313 (1.044 to 1.658)	2.067E-02	7.235E-02	
C16	Metabolites	-0.09 (-0.131 to -0.049)	1.858E-05	2.168E-05	-0.07 (-0.126 to -0.015)	1.334E-02	1.436E-02	0.118 (0.059 to 0.177)	1.023E-04	7.164E-04	0.073 (0.003 to 0.142)	4.083E-02	2.858E-01	0.23 (-0.006 to 0.471)	1.259 (0.994 to 1.602)	5.825E-02	9.481E-02	
C18:1	Metabolites	-0.081 (-0.121 to -0.04)	9.275E-05	9.989E-05	-0.081 (-0.135 to -0.027)	3.345E-03	4.683E-03	0.107 (0.048 to 0.165)	3.502E-04	1.634E-03	0.083 (0.015 to 0.151)	1.632E-02	2.285E-01	0.325 (0.094 to 0.561)	1.384 (1.098 to 1.752)	6.305E-03	4.414E-02	
C2	Metabolites	-0.149 (-0.189 to -0.109)	3.483E-13	5.419E-13	-0.079 (-0.134 to -0.025)	4.140E-03	5.269E-03	0.067 (0.009 to 0.126)	2.466E-02	5.754E-02	0.036 (-0.032 to 0.104)	3.019E-01	7.965E-01	0.138 (-0.086 to 0.362)	1.148 (0.918 to 1.437)	2.268E-01	2.887E-01	
C6(C4:1-DC)	Metabolites	-0.167 (-0.207 to -0.127)	6.269E-16	1.254E-15	-0.12 (-0.175 to -0.065)	2.184E-05	5.096E-05	0.059 (-0.001 to 0.118)	5.210E-02	9.117E-02	0.028 (-0.042 to 0.098)	4.325E-01	7.965E-01	0.198 (-0.033 to 0.43)	1.219 (0.968 to 1.537)	9.231E-02	1.292E-01	
C5	Metabolites	-0.16 (-0.201 to -0.119)	4.603E-14	8.055E-14	-0.103 (-0.158 to -0.047)	2.980E-04	4.635E-04	-0.007 (-0.067 to 0.054)	8.257E-01	8.257E-01	-0.008 (-0.079 to 0.062)	8.191E-01	8.821E-01	0.232 (-0.01 to 0.477)	1.261 (0.99 to 1.611)	6.095E-02	9.481E-02	
C8	Metabolites	-0.163 (-0.202 to -0.124)	5.665E-16	1.254E-15	-0.139 (-0.192 to -0.087)	2.663E-07	1.243E-06	0.048 (-0.009 to 0.106)	1.013E-01	1.418E-01	0.01 (-0.057 to 0.077)	7.780E-01	8.821E-01	0.234 (0.011 to 0.458)	1.264 (1.011 to 1.58)	3.944E-02	9.183E-02	
C8:1	Metabolites	-0.122 (-0.16 to -0.084)	3.964E-10	5.549E-10	-0.022 (-0.073 to 0.03)	4.105E-01	4.105E-01	0.008 (-0.048 to 0.064)	7.795E-01	8.257E-01	-0.014 (-0.079 to 0.051)	6.741E-01	8.821E-01	0.034 (-0.184 to 0.252)	1.035 (0.832 to 1.287)	7.584E-01	7.584E-01	
TLN2	CpGs	0.054 (0.009 to 0.098)	1.838E-02	5.945E-02	0.024 (-0.034 to 0.081)	4.182E-01	4.879E-01	-0.106 (-0.167 to -0.046)	6.107E-04	1.425E-03	-0.011 (-0.082 to 0.06)	7.567E-01	7.567E-01	0.002 (-0.248 to 0.271)	1.002 (0.781 to 1.311)	9.891E-01	9.891E-01	
ACSL1	CpGs	-0.043 (-0.089 to 0.002)	5.927E-02	1.037E-01	-0.024 (-0.028 to 0.033)	4.135E-01	4.879E-01	0.066 (0.004 to 0.127)	3.586E-02	3.586E-02	0.029 (-0.041 to 0.099)	4.123E-01	6.081E-01	-0.031 (-0.233 to 0.178)	0.97 (0.792 to 1.195)	7.686E-01	8.966E-01	
CDC39	CpGs	-0.053 (-0.1 to -0.007)	2.548E-02	5.945E-02	-0.048 (-0.107 to 0.01)	1.053E-01	3.686E-01	0.075 (0.012 to 0.139)	2.002E-02	2.336E-02	0.029 (-0.042 to 0.1)	4.197E-01	6.081E-01	0.054 (-0.207 to 0.301)	1.055 (0.813 to 1.351)	6.770E-01	8.966E-01	
LYL1	CpGs	-0.024 (-0.073 to 0.025)	3.352E-01	3.352E-01	-0.026 (-0.086 to 0.035)	4.044E-01	4.879E-01	0.122 (0.055 to 0.188)	3.282E-04	1.149E-03	0.053 (-0.042 to 0.126)	1.554E-01	6.081E-01	-0.132 (-0.4 to 0.125)	0.876 (0.67 to 1.133)	3.236E-01	8.966E-01	
NEURL3	CpGs	0.04 (-0.007 to 0.088)	9.833E-02	1.147E-01	0.042 (-0.021 to 0.104)	1.912E-01	4.460E-01	-0.078 (-0.142 to -0.013)	1.877E-02	2.336E-02	0.025 (-0.052 to 0.102)	5.122E-01	6.081E-01	0.047 (-0.204 to 0.304)	1.048 (0.816 to 1.355)	7.175E-01	8.966E-01	
LY5MD2	CpGs	0.04 (-0.007 to 0.087)	9.833E-02	1.147E-01	0.005 (-0.057 to 0.066)	8.822E-01	8.822E-01	-0.163 (-0.226 to -0.099)	6.788E-07	4.751E-06	-0.025 (-0.1 to 0.034)	5.041E-01	6.081E-01	-0.051 (-0.291 to 0.196)	0.95 (0.748 to 1.216)	6.807E-01	8.966E-01	
NAPA	CpGs	0.054 (0.008 to 0.101)	2.173E-02	5.945E-02	0.051 (-0.009 to 0.111)	9.391E-02	3.686E-01	-0.101 (-0.164 to -0.038)	1.743E-03	3.050E-03	-0.039 (-0.113 to 0.036)	2.945E-01	6.081E-01	-0.137 (-0.367 to 0.087)	0.872 (0.693 to 1.091)	2.352E-01	8.966E-01	
PAX8	RNAs	-0.048 (-0.107 to 0.012)	1.151E-01	1.239E-01	-0.001 (-0.087 to 0.085)	9.885E-01	9.885E-01	0.055 (-0.032 to 0.142)	2.141E-01	2.286E-01	-0.004 (-0.12 to 0.112)	9.434E-01	9.434E-01	-0.048 (-0.36 to 0.261)	0.953 (0.698 to 1.298)	7.590E-01	9.774E-01	
SLC22A4	RNAs	-0.05 (-0.11 to 0.01)	1.004E-01	1.172E-01	-0.085 (-0.169 to 0.001)	4.763E-02	1.461E-01	0.282 (0.196 to 0.367)	1.949E-10	2.729E-09	0.204 (0.092 to 0.316)	4.041E-04	5.657E-03	-0.038 (-0.344 to 0.271)	0.963 (0.709 to 1.311)	8.095E-01	9.774E-01	
PNLIPRP2	RNAs	-0.055 (-0.113 to 0.002)	6.071E-02	7.727E-02	-0.015 (-0.09 to -0.061)	7.044E-01	7.696E-01	0.063 (-0.022 to 0.147)	1.477E-01	1.723E-01	-0.052 (-0.153 to 0.05)	3.181E-01	4.048E-01	-0.296 (-0.586 to -0.016)	0.744 (0.557 to 0.984)	4.042E-02	5.659E-01	
NKD2	RNAs	-0.086 (-0.145 to -0.027)	4.311E-03	7.544E-03	-0.057 (-0.135 to 0.022)	1.579E-01	2.710E-01	0.117 (0.031 to 0.204)	7.855E-03	1.290E-02	0.108 (0.003 to 0.213)	4.292E-02	1.394E-01	0.117 (-0.161 to 0.4)	1.125 (0.875 to 1.492)	4.101E-01	9.774E-01	
DUSP11	RNAs	0.164 (0.107 to 0.222)	2.649E-08	3.709E-07	0.092 (0.009 to 0.175)	2.933E-02	1.461E-01	-0.053 (-0.139 to 0.033)	2.286E-01	2.286E-01	-0.175 (-0.286 to -0.065)	2.019E-03	9.672E-03	-0.17 (-0.496 to 0.152)	0.844 (0.609 to 1.164)	3.021E-01	9.774E-01	
TFE3	RNAs	-0.066 (-0.126 to -0.007)	2.969E-02	4.618E-02	-0.016 (-0.101 to 0.07)	7.147E-01	7.696E-01	0.192 (0.105 to 0.279)	1.682E-05	7.847E-05	0.115 (0.023 to 0.231)	4.979E-02	1.394E-01	-0.221 (-0.553 to 0.104)	0.802 (0.575 to 1.11)	1.868E-01	9.774E-01	
AGK	RNAs	0.09 (0.035 to 0.146)	1.537E-03	3.713E-03	0.053 (-0.022 to 0.129)	1.667E-01	2.710E-01	0.356E-02	8.089E-02	8.089E-02	-0.091 (-0.193 to 0.011)	7.946E-02	1.827E-01	-0.074 (-0.355 to 0.207)	0.928 (0.701 to 1.229)	6.023E-01	9.774E-01	
MCM3	RNAs	0.094 (0.034 to 0.155)	2.168E-03	4.338E-03	0.059 (-0.026 to 0.143)	1.742E-01	2.710E-01	-0.248 (-0.335 to -0.161)	3.205E-08	2.244E-07	-0.178 (-0.291 to -0.065)	2.073E-03	a	-0.056 (-0.366 to 0.259)	0.945 (0.693 to 1.295)	7.240E-01	9.774E-01	
PCGF2	RNAs	-0.011 (-0.068 to 0.046)	7.068E-01	7.068E-01	-0.041 (-0.118 to 0.037)	3.058E-01	4.281E-01	0.117 (0.034 to 0.2)	5.747E-03	1.149E-02	0.058 (-0.047 to 0.164)	2.774E-01	4.048E-01	0.111 (-0.174 to 0.399)	1.118 (0.84 to 1.491)	4.443E-01	9.774E-01	
TTF2	RNAs	0.116 (0.059 to 0.173)	7.464E-05	5.225E-04	0.081 (0.0 to 0.162)	4.985E-02	1.461E-01	-0.117 (-0.222 to -0.052)	1.591E-03	3.712E-03	-0.058 (-0.168 to 0.052)	3.037E-01	4.048E-01	0.004 (-0.305 to 0.319)	1.004 (0.737 to 1.375)	9.774E-01	9.774E-01	
ABCB1	RNAs	0.098 (0.024 to 0.156)	9.705E-04	3.397E-03	0.094 (0.012 to 0.176)	2.396E-02	1.461E-01	-0.155 (-0.24 to -0.07)	3.512E-04	1.229E-03	-0.05 (-0.16 to 0.059)	6.363E-01	4.273E-01	-0.069 (-0.376 to 0.234)	0.934 (0.687 to 1.264)	6.577E-01	9.774E-01	
ARG1	RNAs	-0.098 (-0.156 to -0.04)	9.505E-04	3.397E-03	-0.068 (-0.157 to 0.021)	1.334E-01	2.710E-01	0.113 (0.027 to 0.198)	1.009E-02	1.413E-02	0.103 (-0.017 to 0.222)	9.136E-02	1.827E-01	0.048 (-0.278 to 0.371)	1.049 (0.758 to 1.449)	7.692E-01	9.774E-01	
SLC25A4	RNAs	0.09 (0.034 to 0.146)	1.591E-03	3.713E-03	0.076 (-0.001 to 0.152)	5.217E-02	1.461E-01	-0.141 (-0.223 to -0.059)	7.936E-04	2.222E-03	-0.076 (0.119 to 0.027)	1.479E-01	2.588E-01	-0.009 (-0.287 to 0.269)	0.991 (0.715 to 1.308)	9.472E-01	9.774E-01	
CDC14A	RNAs	-0.058 (-0.117 to 0)	5.116E-02	7.163E-02	-0.04 (-0.123 to 0.044)	5.491E-01	4.443E-01	0.117 (0.03 to 0.204)	8.291E-03	1.290E-02	0.046 (-0.066 to 0.158)	4.216E-01	4.540E-01	-0.017 (-0.338 to 0.303)	0.983 (0.713 to 1.353)	9.178E-01	9.774E-01	
Tyr	Metabolites	-0.167 (-0.24 to -0.094)	2.289E-01	2.289E-01	0.073 (0.021 to 0.125)	6.799E-03	6.799E-03	-0.117 (-0.173 to -0.061)	4.502E-05	6.303E-04	-0.05 (-0.16 to 0.016)	1.379E-01	6.434E-01	-0.093 (-0.317 to 0.131)	0.911 (0.728 to 1.14)	4.146E-01	4.626E-01	
PLAT	Proteins	0.089 (0.011 to 0.167)	2.506E-02	2.878E-02	0.089 (0.002 to 0.176)	4.411E-02	5.065E-02	-0.124 (-0.227 to -0.02)	1.940E-02	5.729E-02	-0.088 (-0.194 to 0.19)	1.068E-01	5.032E-01	-0.167 (-0.548 to 0.201)	0.846 (0.578 to 1.223)	5.804E-01	5.023E-01	
HGFBP2	Proteins	-0.167 (-0.24 to -0.094)	8.720E-06	1.638E-05	-0.239 (-0.32 to 0.156)	7.685E-09	2.117E-08	0.114 (0.042 to 0.239)	5.445E-03	2.597E-02	0.094 (-0.008 to 0.117)	7.505E-02	4.002E-01	0.514 (0.158 to 0.882)	1.672 (1.171 to 2.417)	5.269E-03	6	

IGFBP6	Proteins	-0.368 (-0.428 to -0.308)	1.691E-29	2.621E-28	-0.354 (-0.422 to -0.285)	6.692E-22	8.298E-21	0.063 (-0.027 to 0.154)	1.712E-01	2.527E-01	0.047 (-0.046 to 0.141)	3.214E-01	6.392E-01	0.3 (-0.03 to 0.626)	1.35 (0.971 to 1.87)	7.166E-02	5.239E-01
FGF20	Proteins	0.121 (0.063 to 0.178)	4.049E-05	6.277E-05	0.154 (0.091 to 0.217)	1.991E-02	4.749E-06	-0.064 (-0.141 to 0.014)	1.070E-01	1.928E-01	-0.021 (-0.101 to 0.059)	6.070E-01	7.840E-01	-0.249 (-0.63 to 0.021)	0.78 (0.533 to 1.022)	1.334E-01	2.851E-01
FGF9	Proteins	0.058 (-0.004 to 0.121)	6.637E-02	6.974E-02	0.079 (-0.009 to 0.148)	2.713E-02	3.235E-02	-0.063 (-0.147 to 0.02)	1.365E-01	2.082E-01	-0.012 (-0.097 to 0.073)	7.795E-01	9.294E-01	-0.101 (-0.433 to 0.171)	0.904 (0.648 to 1.186)	5.046E-01	5.966E-01
SPINT1	Proteins	0.082 (0.02 to 0.143)	9.404E-03	1.143E-02	0.039 (-0.03 to 0.108)	2.654E-01	2.789E-01	-0.102 (-0.184 to -0.02)	1.478E-02	4.581E-02	-0.005 (-0.089 to 0.079)	9.087E-01	9.541E-01	0.096 (-0.187 to 0.39)	1.101 (0.83 to 1.478)	5.126E-01	5.966E-01
NBL1	Proteins	-0.241 (-0.298 to -0.184)	7.486E-16	4.641E-15	-0.258 (-0.321 to -0.194)	1.359E-14	9.360E-14	0.034 (-0.047 to 0.115)	4.069E-01	5.256E-01	0.045 (-0.038 to 0.128)	2.834E-01	6.392E-01	0.221 (-0.061 to 0.497)	1.247 (0.941 to 1.644)	1.183E-01	2.768E-01
GHR	Proteins	0.157 (0.085 to 0.228)	2.036E-05	3.506E-05	0.178 (0.098 to 0.257)	1.444E-05	3.087E-05	-0.167 (-0.263 to -0.071)	7.015E-04	7.249E-03	-0.152 (-0.251 to -0.053)	2.670E-03	8.278E-02	-0.683 (-1.052 to -0.332)	0.505 (0.349 to 0.718)	1.930E-04	5.982E-03
CGA LHB	Proteins	-0.249 (-0.357 to -0.141)	7.420E-06	1.438E-05	-0.225 (-0.345 to -0.104)	2.919E-04	4.763E-04	0.046 (-0.101 to 0.193)	5.371E-01	6.403E-01	-0.002 (-0.152 to 0.148)	9.819E-01	9.819E-01	0.238 (-0.284 to 0.783)	1.269 (0.753 to 2.189)	3.812E-01	5.023E-01
ESAM	Proteins	-0.204 (-0.263 to -0.145)	2.965E-11	1.021E-10	-0.236 (-0.301 to -0.171)	3.557E-12	1.696E-11	0.093 (0.011 to 0.174)	2.621E-02	7.066E-02	0.049 (-0.036 to 0.134)	2.576E-01	6.392E-01	0.422 (0.109 to 0.743)	1.525 (1.115 to 2.103)	8.934E-03	9.232E-02
JAM2	Proteins	-0.238 (-0.291 to -0.184)	2.243E-17	1.545E-16	-0.216 (-0.277 to -0.156)	8.221E-12	3.186E-11	0.02 (-0.056 to 0.096)	6.080E-01	6.966E-01	0.018 (-0.061 to 0.097)	6.512E-01	8.240E-01	0.363 (0.073 to 0.67)	1.437 (1.076 to 1.955)	1.721E-02	1.185E-01
CLEC4M	Proteins	0.169 (0.111 to 0.227)	2.079E-08	5.155E-08	0.133 (0.066 to 0.199)	1.046E-04	1.908E-04	-0.103 (-0.183 to -0.023)	1.146E-02	4.180E-02	-0.045 (-0.127 to 0.037)	2.779E-01	6.392E-01	-0.24 (-0.527 to 0.04)	0.786 (0.59 to 1.041)	9.558E-02	2.370E-01
IL19	Proteins	0.138 (0.079 to 0.197)	5.103E-06	1.055E-05	0.143 (0.077 to 0.21)	2.452E-05	4.905E-05	-0.072 (-0.152 to 0.007)	7.561E-02	1.465E-01	-0.006 (-0.088 to 0.076)	8.900E-01	9.541E-01	-0.228 (-0.523 to 0.059)	0.796 (0.593 to 1.061)	1.238E-01	2.768E-01
RETN	Proteins	-0.181 (-0.238 to -0.125)	5.914E-10	1.833E-09	-0.226 (-0.289 to -0.163)	5.657E-12	2.465E-11	0.059 (-0.019 to 0.137)	1.376E-01	2.082E-01	0.017 (-0.064 to 0.098)	6.797E-01	8.428E-01	0.071 (-0.212 to 0.35)	1.074 (0.809 to 1.419)	6.179E-01	6.605E-01
IL2	Proteins	0.061 (0.002 to 0.12)	4.367E-02	4.834E-02	0.021 (-0.046 to 0.088)	5.331E-01	5.418E-01	-0.09 (-0.169 to -0.012)	2.471E-02	6.965E-02	-0.042 (-0.123 to 0.04)	3.168E-01	6.392E-01	0.063 (-0.22 to 0.362)	1.065 (0.802 to 1.436)	6.722E-01	7.064E-01
TNFRSF1B	Proteins	-0.277 (-0.332 to -0.222)	3.356E-21	2.973E-20	-0.302 (-0.363 to -0.241)	2.211E-20	2.284E-19	0.031 (-0.049 to 0.111)	4.456E-01	5.594E-01	0.03 (-0.053 to 0.114)	4.798E-01	7.104E-01	0.282 (-0.02 to 0.588)	1.325 (0.98 to 1.8)	6.852E-02	2.239E-01
ADAMTS13	Proteins	0.126 (0.068 to 0.183)	1.886E-05	3.341E-05	0.111 (0.047 to 0.176)	6.823E-04	1.058E-03	-0.018 (-0.095 to 0.06)	6.554E-01	7.128E-01	0.025 (-0.055 to 0.104)	5.411E-01	7.293E-01	-0.273 (-0.551 to 0.002)	0.761 (0.576 to 1.002)	5.273E-02	2.160E-01
RET	Proteins	0.064 (0.002 to 0.126)	4.469E-02	4.861E-02	0.085 (0.015 to 0.154)	1.685E-02	2.090E-02	-0.068 (-0.152 to 0.015)	1.088E-01	1.928E-01	-0.055 (-0.14 to 0.03)	2.059E-01	6.383E-01	-0.221 (-0.525 to 0.064)	0.802 (0.592 to 1.066)	1.402E-01	2.897E-01
ACY1	Proteins	0.123 (0.052 to 0.194)	6.810E-04	9.179E-04	0.157 (0.077 to 0.237)	1.315E-04	2.329E-04	-0.092 (-0.187 to 0.004)	5.967E-02	1.276E-01	-0.069 (-0.166 to 0.029)	1.673E-01	5.849E-01	-0.435 (-0.797 to -0.087)	0.647 (0.451 to 0.916)	1.580E-02	1.185E-01
BMP1	Proteins	0.132 (0.063 to 0.201)	1.811E-04	2.612E-04	0.178 (0.102 to 0.254)	5.497E-06	1.217E-05	-0.079 (-0.172 to 0.014)	9.651E-02	1.813E-01	0.005 (-0.091 to 0.102)	9.114E-01	9.541E-01	-0.21 (-0.543 to 0.115)	0.811 (0.581 to 1.122)	2.105E-01	3.527E-01
CTS5	Proteins	0.197 (0.13 to 0.264)	1.660E-08	4.677E-08	0.213 (0.138 to 0.289)	5.057E-08	1.306E-07	-0.126 (-0.218 to -0.034)	7.520E-03	3.108E-02	-0.06 (-0.155 to 0.035)	2.173E-01	6.392E-01	-0.356 (-0.71 to -0.018)	0.77 (0.492 to 0.983)	4.345E-02	1.238E-01
FN1	Proteins	0.133 (0.074 to 0.192)	1.248E-05	2.275E-05	0.11 (0.044 to 0.177)	1.156E-03	1.748E-03	-0.102 (-0.182 to -0.022)	1.236E-02	4.258E-02	-0.08 (-0.162 to 0.02)	5.464E-02	3.764E-01	-0.144 (-0.415 to 0.127)	0.866 (0.66 to 1.135)	2.959E-01	4.475E-01
FSTL3	Proteins	-0.244 (-0.302 to -0.186)	1.871E-15	1.055E-14	-0.287 (-0.351 to -0.223)	2.672E-17	2.070E-16	0.032 (-0.051 to 0.115)	4.511E-01	5.594E-01	0.027 (-0.058 to 0.112)	5.325E-01	7.293E-01	0.156 (-0.135 to 0.45)	1.169 (0.874 to 1.569)	2.930E-01	4.475E-01
B2M	Proteins	-0.43 (-0.48 to -0.379)	4.438E-50	1.376E-48	-0.384 (-0.446 to -0.323)	1.594E-30	4.943E-29	0.076 (-0.008 to 0.16)	7.506E-02	1.465E-01	0.08 (-0.008 to 0.167)	7.452E-02	4.200E-01	0.561 (0.234 to 0.9)	1.752 (1.264 to 2.46)	9.322E-04	1.927E-02
ADIPPOQ	Proteins	0.009 (-0.067 to 0.084)	8.222E-01	8.222E-01	-0.046 (-0.131 to 0.038)	2.826E-01	2.921E-01	0.044 (-0.057 to 0.145)	3.904E-01	5.074E-01	0.027 (-0.066 to 0.14)	4.821E-01	7.104E-01	0.088 (-0.258 to 0.43)	1.092 (0.774 to 1.537)	6.146E-01	6.605E-01
CNDP1	Proteins	0.124 (0.067 to 0.182)	2.713E-05	4.427E-05	0.141 (0.076 to 0.205)	5.240E-05	4.630E-05	-0.127 (-0.205 to -0.05)	1.357E-03	1.202E-02	-0.086 (-0.167 to -0.004)	3.872E-02	3.691E-01	-0.187 (-0.457 to 0.083)	0.829 (0.633 to 1.086)	4.077E-01	3.137E-01
MASP1	Proteins	0.119 (0.062 to 0.177)	4.669E-05	7.060E-05	0.091 (0.027 to 0.155)	5.181E-03	6.693E-03	-0.085 (-0.162 to -0.008)	3.100E-02	7.392E-02	0.042 (-0.037 to 0.121)	2.965E-01	6.392E-01	-0.117 (-0.407 to 0.142)	0.889 (0.666 to 1.153)	4.702E-01	5.070E-01
IL23RA1	Proteins	-0.046 (-0.108 to 0.016)	1.428E-01	1.476E-01	-0.045 (-0.114 to 0.023)	1.942E-01	2.076E-01	0.083 (0.001 to 0.165)	4.830E-02	1.070E-01	0.049 (-0.035 to 0.134)	2.509E-01	6.392E-01	0.044 (-0.305 to 0.332)	1.045 (0.737 to 1.394)	7.841E-01	7.841E-01
KDR	Proteins	0.153 (0.094 to 0.213)	4.635E-07	1.064E-06	0.163 (0.096 to 0.23)	2.182E-06	5.010E-06	-0.141 (-0.221 to -0.061)	5.484E-04	6.800E-03	-0.091 (-0.173 to -0.009)	3.058E-02	3.691E-01	-0.168 (-0.45 to 0.111)	0.846 (0.638 to 1.118)	2.399E-01	3.813E-01
IGF2R	Proteins	0.138 (0.075 to 0.201)	2.099E-05	3.517E-05	0.108 (0.037 to 0.179)	2.941E-03	4.052E-03	-0.068 (-0.154 to 0.017)	1.156E-01	1.937E-01	-0.039 (-0.126 to 0.049)	3.821E-01	6.769E-01	-0.113 (-0.411 to 0.181)	0.893 (0.663 to 1.198)	4.514E-01	5.488E-01
PLG	Proteins	0.128 (0.068 to 0.189)	3.753E-05	5.966E-05	0.132 (0.063 to 0.2)	1.799E-04	3.098E-04	-0.033 (-0.112 to 0.053)	4.795E-01	5.830E-01	-0.008 (-0.093 to 0.076)	8.512E-01	9.498E-01	-0.117 (-0.413 to 0.174)	0.899 (0.662 to 1.19)	4.318E-01	5.354E-01
CTS5	Proteins	-0.317 (-0.376 to -0.258)	1.036E-23	1.071E-22	-0.301 (-0.369 to -0.234)	2.573E-17	2.070E-16	-0.022 (-0.065 to 0.109)	6.179E-01	6.966E-01	0.042 (-0.047 to 0.132)	3.505E-01	6.392E-01	0.269 (-0.044 to 0.586)	1.308 (0.957 to 1.798)	9.421E-02	2.370E-01
FCN3	Proteins	0.105 (0.04 to 0.169)	1.598E-03	2.064E-03	0.104 (0.032 to 0.177)	4.880E-03	6.437E-03	-0.127 (-0.214 to -0.041)	4.012E-03	2.487E-02	-0.07 (-0.16 to 0.019)	1.217E-01	5.032E-01	-0.207 (-0.499 to 0.087)	0.813 (0.607 to 1.091)	1.652E-01	3.103E-01
RPS6K5	Proteins	-0.08 (-0.138 to -0.022)	7.333E-03	9.093E-03	-0.063 (-0.128 to 0.003)	6.130E-02	6.910E-02	0.105 (0.027 to 0.183)	8.281E-03	3.209E-02	0.007 (-0.073 to 0.088)	8.579E-01	9.498E-01	0.144 (-0.14 to 0.421)	1.155 (0.87 to 1.524)	3.117E-01	4.602E-01
MED1	Proteins	-0.064 (-0.125 to -0.002)	4.308E-02	4.834E-02	-0.079 (-0.148 to -0.01)	2.856E-02	3.118E-02	0.114 (0.032 to 0.196)	6.638E-03	2.940E-02	0.027 (-0.058 to 0.111)	5.341E-01	7.293E-01	0.059 (-0.26 to 0.345)	1.061 (0.771 to 1.412)	6.993E-01	7.226E-01
PAPPA	Proteins	-0.117 (-0.175 to -0.06)	7.240E-05	1.069E-04	-0.134 (-0.198 to -0.07)	4.851E-05	9.314E-05	0.079 (0.001 to 0.157)	4.603E-02	1.057E-01	0.033 (-0.048 to 0.113)	4.242E-01	6.921E-01	0.121 (-0.15 to 0.401)	1.128 (0.861 to 1.493)	3.888E-01	5.023E-01
IL6	Proteins	-0.101 (-0.156 to -0.046)	3.534E-04	4.980E-04	-0.097 (-0.158 to -0.035)	2.116E-03	3.005E-03	0.082 (0.008 to 0.156)	2.976E-02	7.392E-02	0.076 (0.001 to 0.152)	4.763E-01	3.691E-01	0.159 (-0.113 to 0.404)	1.173 (0.893 to 1.497)	2.175E-01	3.548E-01
TFF3	Proteins	-0.237 (-0.297 to -0.176)	6.389E-14	2.829E-13	-0.255 (-0.322 to -0.188)	3.473E-13	2.153E-12	0.02 (-0.065 to 0.105)	6.410E-01	7.097E-01	-0.03 (-0.117 to 0.056)	4.927E-01	7.104E-01	0.265 (0.011 to 0.518)	1.303 (1.011 to 1.679)	3.845E-02	2.128E-01
EPHA2	Proteins	-0.17 (-0.229 to -0.112)	1.800E-08	4.853E-08	-0.227 (-0.291 to -0.163)	1.296E-11	4.464E-11	0.006 (-0.074 to 0.087)	8.828E-01	9.122E-01	-0.012 (-0.094 to 0.071)	7.791E-01	9.294E-01	0.088 (-0.208 to 0.381)	1.092 (0.812 to 1.463)	5.574E-01	6.400E-01
NTRK2	Proteins	0.104 (0.046 to 0.162)	4.388E-04	6.045E-04	0.069 (0.004 to 0.134)	3.799E-02	4.444E-02	-0.11 (-0.188 to -0.033)	5.345E-03	2.597E-02	-0.058 (-0.137 to 0.022)	1.538E-01	5.849E-01	-0.262 (-0.558 to 0.029)	0.769 (0.572 to 1.029)	7.943E-02	2.399E-01
AMH	Proteins	0.171 (0.112 to 0.231)	2.012E-08	5.155E-08	0.112 (0.044 to 0.179)	1.293E-03	1.908E-03	-0.101 (-0.182 to -0.02)	1.420E-02	4.581E-02	-0.067 (-0.151 to 0.017)	1.178E-01	5.032E-01	-0.207 (-0.498 to 0.081)	0.813 (0.608 to 1.084)	1.594E-01	3.089E-01
MMP1	Proteins	-0.077 (-0.138 to -0.017)	1.188E-02	1.416E-02	-0.098 (-0.165 to -0.032)	4.002E-03	5.395E-03	0.073 (-0.007 to 0.154)	7.401E-02	1.465E-01	0.043 (-0.04 to 0.126)	3.058E-01	6.392E-01	0.072 (-0.208 to 0.345)	1.075 (0.812 to 1.412)	6.091E-01	6.605E-01
CIQBPA	Proteins	0.231 (0.174 to 0.288)	1.113E-14	5.750E-14	0.14 (0.074 to 0.206)	3.746E-05	7.257E-05	-0.088 (-0.169 to -0.008)	3.092E-02	7.392E-02	-0.042 (-0.125 to 0.04)	3.143E-01	6.392E-01	-0.197 (-0.491 to 0.087)	0.822 (0.612 to 1.091)	1.819E-01	3.222E-01
ERP29	Proteins	-0.22 (-0.284 to -0.157)	2.348E-11	8.563E-11	-0.232 (-0.303 to -0.161)	3.085											

source.omics1.	target.omics2.1					
label	abel	source.to.target	omics1.type	omics2.type	omics.asso.type	weight
IGFBP2	GHR	IGFBP2 to GHR	Proteins	Proteins	sametype	-0.255
B2M	CST3	B2M to CST3	Proteins	eGFRbiom	diftype	0.219
C12	C8	C12 to C8	Metabolites	Metabolites	sametype	-0.213
IGFBP2	ACY1	IGFBP2 to ACY1	Proteins	Proteins	sametype	-0.201
CDC14A	UNC5C	CDC14A to UNC5C	RNAs	Proteins	diftype	0.209
SLC22A4	MCM3	SLC22A4 to MCM3	RNAs	RNAs	sametype	-0.175
TFE3	MCM3	TFE3 to MCM3	RNAs	RNAs	sametype	-0.168
PNLIPRP2	RET	PNLIPRP2 to RET	RNAs	Proteins	diftype	0.185
NKD2	KDR	NKD2 to KDR	RNAs	Proteins	diftype	0.15
MCM3	ARG1	MCM3 to ARG1	RNAs	RNAs	sametype	-0.153
PCGF2	TNFRSF1A	PCGF2 to TNFRSF1A	RNAs	Proteins	diftype	0.142
RET	ADIPOQ	RET to ADIPOQ	Proteins	Proteins	sametype	-0.146
NKD2	NBL1	NKD2 to NBL1	RNAs	Proteins	diftype	0.142
TTF2	MMP1	TTF2 to MMP1	RNAs	Proteins	diftype	0.139
PAX8	SPOCK2	PAX8 to SPOCK2	RNAs	Proteins	diftype	0.138
Tyr	PLAT	Tyr to PLAT	Metabolites	Proteins	diftype	0.134
NBL1	SPOCK2	NBL1 to SPOCK2	Proteins	Proteins	sametype	-0.134
CTSH	RPS6KA5	CTSH to RPS6KA5	Proteins	Proteins	sametype	-0.132
IL6	SOD2	IL6 to SOD2	Proteins	Proteins	sametype	-0.129
PLAT	ESAM	PLAT to ESAM	Proteins	Proteins	sametype	-0.129
TFE3	SLC25A4	TFE3 to SLC25A4	RNAs	RNAs	sametype	-0.128
EGFR	B2M	EGFR to B2M	Proteins	Proteins	sametype	-0.126
PAX8	JAM2	PAX8 to JAM2	RNAs	Proteins	diftype	0.128
PLAT	IGFBP2	PLAT to IGFBP2	Proteins	Proteins	sametype	-0.123
SLC22A4	AGK	SLC22A4 to AGK	RNAs	RNAs	sametype	-0.119
CTSH	MAPK12	CTSH to MAPK12	Proteins	Proteins	sametype	-0.117
ESAM	SPOCK2	ESAM to SPOCK2	Proteins	Proteins	sametype	-0.112
MED1	EPHA2	MED1 to EPHA2	Proteins	Proteins	sametype	-0.112
Tyr	ACY1	Tyr to ACY1	Metabolites	Proteins	diftype	0.126
IGFBP6	Creatinine	IGFBP6 to Creatinine	Proteins	eGFRbiom	diftype	0.117
ADAMTS13	ERP29	ADAMTS13 to ERP29	Proteins	Proteins	sametype	-0.107
IGFBP2	RET	IGFBP2 to RET	Proteins	Proteins	sametype	-0.107
PNLIPRP2	IL22RA1	PNLIPRP2 to IL22RA1	RNAs	Proteins	diftype	0.109
TNFRSF1A	BMP1	TNFRSF1A to BMP1	Proteins	Proteins	sametype	-0.104
ERP29	SPOCK2	ERP29 to SPOCK2	Proteins	Proteins	sametype	-0.102
IGF2R	RPS6KA5	IGF2R to RPS6KA5	Proteins	Proteins	sametype	-0.102
PLAT	MAPK12	PLAT to MAPK12	Proteins	Proteins	sametype	-0.102
NTRK2	MMP1	NTRK2 to MMP1	Proteins	Proteins	sametype	-0.102
IL2	IL22RA1	IL2 to IL22RA1	Proteins	Proteins	sametype	-0.101
RETN	BMP1	RETN to BMP1	Proteins	Proteins	sametype	-0.098
RELT	CST3	RELT to CST3	Proteins	eGFRbiom	diftype	0.104
IL19	PAPPA	IL19 to PAPPA	Proteins	Proteins	sametype	-0.097
GHR	ADIPOQ	GHR to ADIPOQ	Proteins	Proteins	sametype	-0.094

RPS6KA5	EPHA2	RPS6KA5 to EPHA2	Proteins	Proteins	sametype	-0.094
PCGF2	ESAM	PCGF2 to ESAM	RNAs	Proteins	diftype	0.101
IGFBP2	BMP1	IGFBP2 to BMP1	Proteins	Proteins	sametype	-0.093
TFE3	AGK	TFE3 to AGK	RNAs	RNAs	sametype	-0.092
B2M	IGF2R	B2M to IGF2R	Proteins	Proteins	sametype	-0.09
SPINT1	MMP1	SPINT1 to MMP1	Proteins	Proteins	sametype	-0.087
RPS6KA5	SPOCK2	RPS6KA5 to SPOCK2	Proteins	Proteins	sametype	-0.087
CTSH	PC aa C38:0	CTSH to PC aa C38:0	Proteins	Metabolites	diftype	0.093
CGA LHB	CTSV	CGA LHB to CTSV	Proteins	Proteins	sametype	-0.085
MASP1	SCARF1	MASP1 to SCARF1	Proteins	Proteins	sametype	-0.083
JAM2	Creatinine	JAM2 to Creatinine	Proteins	eGFRbiom	diftype	0.086
SLC22A4	TNFRSF1A	SLC22A4 to TNFRSF1A	RNAs	Proteins	diftype	0.09
RPS6KA5	UNC5C	RPS6KA5 to UNC5C	Proteins	Proteins	sametype	-0.079
DUSP11	IL2	DUSP11 to IL2	RNAs	Proteins	diftype	0.09
ADAMTS13	MMP1	ADAMTS13 to MMP1	Proteins	Proteins	sametype	-0.078
LAYN	MAPK12	LAYN to MAPK12	Proteins	Proteins	sametype	-0.078
TNFRSF1B	SPOCK2	TNFRSF1B to SPOCK2	Proteins	Proteins	sametype	-0.078
LAYN	BMP1	LAYN to BMP1	Proteins	Proteins	sametype	-0.077
RPS6KA5	NTRK2	RPS6KA5 to NTRK2	Proteins	Proteins	sametype	-0.077
FN1	B2M	FN1 to B2M	Proteins	Proteins	sametype	-0.076
IGFBP6	PLG	IGFBP6 to PLG	Proteins	Proteins	sametype	-0.076
IL19	RPS6KA5	IL19 to RPS6KA5	Proteins	Proteins	sametype	-0.075
JAM2	SPOCK2	JAM2 to SPOCK2	Proteins	Proteins	sametype	-0.075
RPS6KA5	AMH	RPS6KA5 to AMH	Proteins	Proteins	sametype	-0.075
ESAM	IL19	ESAM to IL19	Proteins	Proteins	sametype	-0.072
GHR	CGA LHB	GHR to CGA LHB	Proteins	Proteins	sametype	-0.072
SLC25A4	CNDP1	SLC25A4 to CNDP1	RNAs	Proteins	diftype	0.088
C5	Creatinine	C5 to Creatinine	Metabolites	eGFRbiom	diftype	0.063
ARG1	SLC25A4	ARG1 to SLC25A4	RNAs	RNAs	sametype	-0.069
GHR	MED1	GHR to MED1	Proteins	Proteins	sametype	-0.069
PLG	SCARF1	PLG to SCARF1	Proteins	Proteins	sametype	-0.068
KDR	MAPK12	KDR to MAPK12	Proteins	Proteins	sametype	-0.067
SLC22A4	IGFBP2	SLC22A4 to IGFBP2	RNAs	Proteins	diftype	0.085
B2M	SPOCK2	B2M to SPOCK2	Proteins	Proteins	sametype	-0.064
PAX8	IL19	PAX8 to IL19	RNAs	Proteins	diftype	0.083
IGF2R	MMP1	IGF2R to MMP1	Proteins	Proteins	sametype	-0.062
ESAM	FN1	ESAM to FN1	Proteins	Proteins	sametype	-0.061
MED1	C1QBP	MED1 to C1QBP	Proteins	Proteins	sametype	-0.061
C10:2	Creatinine	C10:2 to Creatinine	Metabolites	eGFRbiom	diftype	0.053
EGFR	KIR2DL4	EGFR to KIR2DL4	Proteins	Proteins	sametype	-0.059
ERP29	SOD2	ERP29 to SOD2	Proteins	Proteins	sametype	-0.058
TFE3	ABCB1	TFE3 to ABCB1	RNAs	RNAs	sametype	-0.056
DUSP11	TFE3	DUSP11 to TFE3	RNAs	RNAs	sametype	-0.055
ESAM	ACY1	ESAM to ACY1	Proteins	Proteins	sametype	-0.055
Tyr	SPOCK2	Tyr to SPOCK2	Metabolites	Proteins	diftype	0.082

CNDP1	IL6	CNDP1 to IL6	Proteins	Proteins	sametype	-0.054
MASP1	MED1	MASP1 to MED1	Proteins	Proteins	sametype	-0.053
SLC25A4	PLAT	SLC25A4 to PLAT	RNAs	Proteins	diftype	0.08
ADAMTS13	SCARF1	ADAMTS13 to SCARF1	Proteins	Proteins	sametype	-0.052
RPS6KA5	SEMA3E	RPS6KA5 to SEMA3E	Proteins	Proteins	sametype	-0.052
ERBB3	RPS6KA5	ERBB3 to RPS6KA5	Proteins	Proteins	sametype	-0.048
AMH	SCARF1	AMH to SCARF1	Proteins	Proteins	sametype	-0.048
CTSV	RPS6KA5	CTSV to RPS6KA5	Proteins	Proteins	sametype	-0.046
PAX8	TNFRSF1A	PAX8 to TNFRSF1A	RNAs	Proteins	diftype	0.08
SLC22A4	RPS6KA5	SLC22A4 to RPS6KA5	RNAs	Proteins	diftype	0.078
FSTL3	RPS6KA5	FSTL3 to RPS6KA5	Proteins	Proteins	sametype	-0.044
IL6	NOTCH1	IL6 to NOTCH1	Proteins	Proteins	sametype	-0.042
RET	MAPK12	RET to MAPK12	Proteins	Proteins	sametype	-0.039
GHR	PAPPA	GHR to PAPPA	Proteins	Proteins	sametype	-0.038
FN1	MMP1	FN1 to MMP1	Proteins	Proteins	sametype	-0.036
MMP1	NOTCH1	MMP1 to NOTCH1	Proteins	Proteins	sametype	-0.036
C14:1-OH	C18:1	C14:1-OH to C18:1	Metabolites	Metabolites	sametype	-0.036
CTSV	B2M	CTSV to B2M	Proteins	Proteins	sametype	-0.034
PAPPA	SPOCK2	PAPPA to SPOCK2	Proteins	Proteins	sametype	-0.033
TNFRSF1A	RELT	TNFRSF1A to RELT	Proteins	Proteins	sametype	-0.033
LYSMD2	EGFR	LYSMD2 to EGFR	CpGs	Proteins	diftype	0.076
JAM2	BMP1	JAM2 to BMP1	Proteins	Proteins	sametype	-0.032
RET	RPS6KA5	RET to RPS6KA5	Proteins	Proteins	sametype	-0.032
EFNA5	MED1	EFNA5 to MED1	Proteins	Proteins	sametype	-0.031
GHR	MAPK12	GHR to MAPK12	Proteins	Proteins	sametype	-0.031
IL6	C1QBP	IL6 to C1QBP	Proteins	Proteins	sametype	-0.029
C14:1-OH	ADIPOQ	C14:1-OH to ADIPOQ	Metabolites	Proteins	diftype	0.069
ERBB3	IL6	ERBB3 to IL6	Proteins	Proteins	sametype	-0.028
SOD2	SCARF1	SOD2 to SCARF1	Proteins	Proteins	sametype	-0.028
MCM3	KDR	MCM3 to KDR	RNAs	Proteins	diftype	0.068
EGFR	SCARF1	EGFR to SCARF1	Proteins	Proteins	sametype	-0.027
C10:2	RETN	C10:2 to RETN	Metabolites	Proteins	diftype	0.066
ESAM	TNFRSF1B	ESAM to TNFRSF1B	Proteins	Proteins	sametype	-0.025
C14:2	C18:1	C14:2 to C18:1	Metabolites	Metabolites	sametype	-0.025
PNLIPRP2	B2M	PNLIPRP2 to B2M	RNAs	Proteins	diftype	0.064
C5	CST3	C5 to CST3	Metabolites	eGFRbiom	diftype	0.053
BMP1	SPOCK2	BMP1 to SPOCK2	Proteins	Proteins	sametype	-0.023
EGFR	IL19	EGFR to IL19	Proteins	Proteins	sametype	-0.023
MASP1	MAPK12	MASP1 to MAPK12	Proteins	Proteins	sametype	-0.023
BMP1	PAPPA	BMP1 to PAPPA	Proteins	Proteins	sametype	-0.022
TNFRSF1B	TNFRSF19	TNFRSF1B to TNFRSF19	Proteins	Proteins	sametype	-0.022
MED1	NOTCH1	MED1 to NOTCH1	Proteins	Proteins	sametype	-0.021
EGFR	MMP1	EGFR to MMP1	Proteins	Proteins	sametype	-0.02
AMH	MAPK12	AMH to MAPK12	Proteins	Proteins	sametype	-0.02
C10:2	C8	C10:2 to C8	Metabolites	Metabolites	sametype	-0.017

ARG1	ERP29	ARG1 to ERP29	RNAs	Proteins	diftype	0.062
TFE3	TTF2	TFE3 to TTF2	RNAs	RNAs	sametype	-0.016
DUSP11	CTSV	DUSP11 to CTSV	RNAs	Proteins	diftype	0.059
C18:1	IGFBP2	C18:1 to IGFBP2	Metabolites	Proteins	diftype	0.059
CTSH	UNC5C	CTSH to UNC5C	Proteins	Proteins	sametype	-0.014
CLEC4M	IL6	CLEC4M to IL6	Proteins	Proteins	sametype	-0.014
IGFBP6	JAM2	IGFBP6 to JAM2	Proteins	Proteins	sametype	-0.014
CTSV	SOD2	CTSV to SOD2	Proteins	Proteins	sametype	-0.013
EFNA5	TFF3	EFNA5 to TFF3	Proteins	Proteins	sametype	-0.012
ESAM	CLEC4M	ESAM to CLEC4M	Proteins	Proteins	sametype	-0.012
FN1	IL6	FN1 to IL6	Proteins	Proteins	sametype	-0.012
RELT	HAVCR2	RELT to HAVCR2	Proteins	Proteins	sametype	-0.012
FN1	SCARF1	FN1 to SCARF1	Proteins	Proteins	sametype	-0.011
IGFBP2	TNFRSF1B	IGFBP2 to TNFRSF1B	Proteins	Proteins	sametype	-0.011
AGK	CNDP1	AGK to CNDP1	RNAs	Proteins	diftype	0.055
TNFRSF1A	B2M	TNFRSF1A to B2M	Proteins	Proteins	sametype	-0.011
C10	C14:2	C10 to C14:2	Metabolites	Metabolites	sametype	-0.011
CTSV	C1QBP	CTSV to C1QBP	Proteins	Proteins	sametype	-0.01
LAYN	NBL1	LAYN to NBL1	Proteins	Proteins	sametype	-0.01
LAYN	RELT	LAYN to RELT	Proteins	Proteins	sametype	-0.01
TNFRSF1A	CST3	TNFRSF1A to CST3	Proteins	eGFRbiom	diftype	0.047
EPHA2	UNC5C	EPHA2 to UNC5C	Proteins	Proteins	sametype	-0.009
B2M	PAPPA	B2M to PAPPA	Proteins	Proteins	sametype	-0.008
CNDP1	SPOCK2	CNDP1 to SPOCK2	Proteins	Proteins	sametype	-0.007
RPS6KA5	C1QBP	RPS6KA5 to C1QBP	Proteins	Proteins	sametype	-0.005
TNFRSF1B	TFF3	TNFRSF1B to TFF3	Proteins	Proteins	sametype	-0.005
B2M	ERP29	B2M to ERP29	Proteins	Proteins	sametype	-0.004
EFNA5	TNFRSF19	EFNA5 to TNFRSF19	Proteins	Proteins	sametype	-0.004
EGFR	ERP29	EGFR to ERP29	Proteins	Proteins	sametype	-0.004
EGFR	IL6	EGFR to IL6	Proteins	Proteins	sametype	-0.003
ESAM	BMP1	ESAM to BMP1	Proteins	Proteins	sametype	-0.002
GHR	C1QBP	GHR to C1QBP	Proteins	Proteins	sametype	-0.002
CLEC4M	MASP1	CLEC4M to MASP1	Proteins	Proteins	sametype	-0.001
LAYN	CTSH	LAYN to CTSH	Proteins	Proteins	sametype	-0.001
GHR	ADAMTS13	GHR to ADAMTS13	Proteins	Proteins	sametype	0
AGK	MCM3	AGK to MCM3	RNAs	RNAs	sametype	0.001
PAX8	FN1	PAX8 to FN1	RNAs	Proteins	diftype	0.054
NBL1	FSTL3	NBL1 to FSTL3	Proteins	Proteins	sametype	0.002
C14:1-OH	C6(C4:1-DC)	C14:1-OH to C6(C4:1-DC)	Metabolites	Metabolites	sametype	0.002
IGFBP2	IGFBP6	IGFBP2 to IGFBP6	Proteins	Proteins	sametype	0.003
IGFBP2	FSTL3	IGFBP2 to FSTL3	Proteins	Proteins	sametype	0.004
TNFRSF1A	PAPPA	TNFRSF1A to PAPPA	Proteins	Proteins	sametype	0.004
FN1	CNDP1	FN1 to CNDP1	Proteins	Proteins	sametype	0.005
CGA LHB	CST3	CGA LHB to CST3	Proteins	eGFRbiom	diftype	0.043
CTSH	CST3	CTSH to CST3	Proteins	eGFRbiom	diftype	0.031

C10:2	CST3	C10:2 to CST3	Metabolites	eGFRbiom	diftype	0.031
ERBB3	AMH	ERBB3 to AMH	Proteins	Proteins	sametype	0.006
DUSP11	C1QBP	DUSP11 to C1QBP	RNAs	Proteins	diftype	0.046
C14:2	C8	C14:2 to C8	Metabolites	Metabolites	sametype	0.006
C12	C16	C12 to C16	Metabolites	Metabolites	sametype	0.006
EGFR	FCN3	EGFR to FCN3	Proteins	Proteins	sametype	0.007
IGFBP2	NBL1	IGFBP2 to NBL1	Proteins	Proteins	sametype	0.007
KDR	C1QBP	KDR to C1QBP	Proteins	Proteins	sametype	0.008
C1QBP	NOTCH1	C1QBP to NOTCH1	Proteins	Proteins	sametype	0.009
CTSV	NTRK2	CTSV to NTRK2	Proteins	Proteins	sametype	0.01
C6(C4:1-DC)	C8:1	C6(C4:1-DC) to C8:1	Metabolites	Metabolites	sametype	0.01
ESAM	ERP29	ESAM to ERP29	Proteins	Proteins	sametype	0.011
RETN	TNFRSF1B	RETN to TNFRSF1B	Proteins	Proteins	sametype	0.011
PLAT	AMH	PLAT to AMH	Proteins	Proteins	sametype	0.011
C16	C6(C4:1-DC)	C16 to C6(C4:1-DC)	Metabolites	Metabolites	sametype	0.011
ADAMTS13	CTSV	ADAMTS13 to CTSV	Proteins	Proteins	sametype	0.012
ERP29	CST3	ERP29 to CST3	Proteins	eGFRbiom	diftype	0.015
PAX8	EPHA2	PAX8 to EPHA2	RNAs	Proteins	diftype	0.034
C6(C4:1-DC)	CST3	C6(C4:1-DC) to CST3	Metabolites	eGFRbiom	diftype	0.015
SLC22A4	SLC25A4	SLC22A4 to SLC25A4	RNAs	RNAs	sametype	0.014
IGFBP2	ESAM	IGFBP2 to ESAM	Proteins	Proteins	sametype	0.014
IGFBP2	UNC5C	IGFBP2 to UNC5C	Proteins	Proteins	sametype	0.014
IL19	CNDP1	IL19 to CNDP1	Proteins	Proteins	sametype	0.014
RPS6KA5	NOTCH1	RPS6KA5 to NOTCH1	Proteins	Proteins	sametype	0.014
ACY1	SPOCK2	ACY1 to SPOCK2	Proteins	Proteins	sametype	0.015
RELT	Creatinine	RELT to Creatinine	Proteins	eGFRbiom	diftype	0.013
TNFRSF1A	ERP29	TNFRSF1A to ERP29	Proteins	Proteins	sametype	0.015
TNFRSF1B	BMP1	TNFRSF1B to BMP1	Proteins	Proteins	sametype	0.015
C14:1	C6(C4:1-DC)	C14:1 to C6(C4:1-DC)	Metabolites	Metabolites	sametype	0.015
RETN	CST3	RETN to CST3	Proteins	eGFRbiom	diftype	0.012
EGFR	AMH	EGFR to AMH	Proteins	Proteins	sametype	0.016
FSTL3	PAPPA	FSTL3 to PAPPA	Proteins	Proteins	sametype	0.016
LAYN	RETN	LAYN to RETN	Proteins	Proteins	sametype	0.016
MASP1	RPS6KA5	MASP1 to RPS6KA5	Proteins	Proteins	sametype	0.017
TNFRSF1A	TNFRSF19	TNFRSF1A to TNFRSF19	Proteins	Proteins	sametype	0.018
C2	C8:1	C2 to C8:1	Metabolites	Metabolites	sametype	0.018
CTSH	TNFRSF19	CTSH to TNFRSF19	Proteins	Proteins	sametype	0.019
IGFBP6	PAPPA	IGFBP6 to PAPPA	Proteins	Proteins	sametype	0.019
TFF3	RELT	TFF3 to RELT	Proteins	Proteins	sametype	0.019
PLAT	CLEC4M	PLAT to CLEC4M	Proteins	Proteins	sametype	0.019
IGFBP2	B2M	IGFBP2 to B2M	Proteins	Proteins	sametype	0.02
ERBB3	NOTCH1	ERBB3 to NOTCH1	Proteins	Proteins	sametype	0.021
TNFRSF1A	HAVCR2	TNFRSF1A to HAVCR2	Proteins	Proteins	sametype	0.021
MAPK12	NOTCH1	MAPK12 to NOTCH1	Proteins	Proteins	sametype	0.023
LAYN	PAPPA	LAYN to PAPPA	Proteins	Proteins	sametype	0.024

C14:2	C6(C4:1-DC)	C14:2 to C6(C4:1-DC)	Metabolites	Metabolites	sametype	0.024
CTSV	NOTCH1	CTSV to NOTCH1	Proteins	Proteins	sametype	0.025
ERBB3	IL2	ERBB3 to IL2	Proteins	Proteins	sametype	0.025
JAM2	TNFRSF19	JAM2 to TNFRSF19	Proteins	Proteins	sametype	0.025
NBL1	B2M	NBL1 to B2M	Proteins	Proteins	sametype	0.026
SPINT1	NTRK2	SPINT1 to NTRK2	Proteins	Proteins	sametype	0.026
GHR	AMH	GHR to AMH	Proteins	Proteins	sametype	0.027
IGFBP6	RETN	IGFBP6 to RETN	Proteins	Proteins	sametype	0.028
TNFRSF1B	EPHA2	TNFRSF1B to EPHA2	Proteins	Proteins	sametype	0.028
MASP1	NOTCH1	MASP1 to NOTCH1	Proteins	Proteins	sametype	0.029
ADAMTS13	MASP1	ADAMTS13 to MASP1	Proteins	Proteins	sametype	0.03
EPHA2	RELT	EPHA2 to RELT	Proteins	Proteins	sametype	0.03
NBL1	CST3	NBL1 to CST3	Proteins	eGFRbiom	diftype	0.006
IL2	CNDP1	IL2 to CNDP1	Proteins	Proteins	sametype	0.031
C14:1-OH	CST3	C14:1-OH to CST3	Metabolites	eGFRbiom	diftype	0.006
C16	C2	C16 to C2	Metabolites	Metabolites	sametype	0.031
C14:1	C16	C14:1 to C16	Metabolites	Metabolites	sametype	0.031
EFNA5	FSTL3	EFNA5 to FSTL3	Proteins	Proteins	sametype	0.032
TNFRSF19	HAVCR2	TNFRSF19 to HAVCR2	Proteins	Proteins	sametype	0.032
NTRK2	SPOCK2	NTRK2 to SPOCK2	Proteins	Proteins	sametype	0.032
NBL1	CTSH	NBL1 to CTSH	Proteins	Proteins	sametype	0.033
JAM2	EPHA2	JAM2 to EPHA2	Proteins	Proteins	sametype	0.033
C14:2	CST3	C14:2 to CST3	Metabolites	eGFRbiom	diftype	0.005
CLEC4M	IGF2R	CLEC4M to IGF2R	Proteins	Proteins	sametype	0.034
EPHA2	NOTCH1	EPHA2 to NOTCH1	Proteins	Proteins	sametype	0.034
TNFRSF1A	CTSH	TNFRSF1A to CTSH	Proteins	Proteins	sametype	0.034
RETN	CTSH	RETN to CTSH	Proteins	Proteins	sametype	0.035
C10	C6(C4:1-DC)	C10 to C6(C4:1-DC)	Metabolites	Metabolites	sametype	0.035
CTSH	PAPPA	CTSH to PAPPA	Proteins	Proteins	sametype	0.036
LAYN	TNFRSF19	LAYN to TNFRSF19	Proteins	Proteins	sametype	0.036
LAYN	TFF3	LAYN to TFF3	Proteins	Proteins	sametype	0.036
CTSV	MASP1	CTSV to MASP1	Proteins	Proteins	sametype	0.037
IL19	IGF2R	IL19 to IGF2R	Proteins	Proteins	sametype	0.037
PLAT	ACY1	PLAT to ACY1	Proteins	Proteins	sametype	0.037
TFF3	UNC5C	TFF3 to UNC5C	Proteins	Proteins	sametype	0.038
SPINT1	NOTCH1	SPINT1 to NOTCH1	Proteins	Proteins	sametype	0.039
IGFBP6	B2M	IGFBP6 to B2M	Proteins	Proteins	sametype	0.039
C10:2	C6(C4:1-DC)	C10:2 to C6(C4:1-DC)	Metabolites	Metabolites	sametype	0.039
EPHA2	TNFRSF19	EPHA2 to TNFRSF19	Proteins	Proteins	sametype	0.04
EGFR	FGF20	EGFR to FGF20	Proteins	Proteins	sametype	0.04
GHR	KDR	GHR to KDR	Proteins	Proteins	sametype	0.04
LAYN	HAVCR2	LAYN to HAVCR2	Proteins	Proteins	sametype	0.04
ERBB3	RET	ERBB3 to RET	Proteins	Proteins	sametype	0.041
LAYN	EPHA2	LAYN to EPHA2	Proteins	Proteins	sametype	0.041
TNFRSF1A	ESAM	TNFRSF1A to ESAM	Proteins	Proteins	sametype	0.041

EFNA5	NTRK2	EFNA5 to NTRK2	Proteins	Proteins	sametype	0.042
PLAT	GHR	PLAT to GHR	Proteins	Proteins	sametype	0.042
EFNA5	CTSH	EFNA5 to CTSH	Proteins	Proteins	sametype	0.043
C14:1-OH	B2M	C14:1-OH to B2M	Metabolites	Proteins	diftype	0.012
EFNA5	UNC5C	EFNA5 to UNC5C	Proteins	Proteins	sametype	0.044
FSTL3	CTSH	FSTL3 to CTSH	Proteins	Proteins	sametype	0.044
IL2	ADAMTS13	IL2 to ADAMTS13	Proteins	Proteins	sametype	0.044
BMP1	CTSV	BMP1 to CTSV	Proteins	Proteins	sametype	0.045
IGFBP2	RETN	IGFBP2 to RETN	Proteins	Proteins	sametype	0.045
SLC22A4	CTSV	SLC22A4 to CTSV	RNAs	Proteins	diftype	0.006
TNFRSF1A	TFF3	TNFRSF1A to TFF3	Proteins	Proteins	sametype	0.046
TNFRSF1B	PAPPA	TNFRSF1B to PAPPA	Proteins	Proteins	sametype	0.046
AMH	SOD2	AMH to SOD2	Proteins	Proteins	sametype	0.047
SOD2	NOTCH1	SOD2 to NOTCH1	Proteins	Proteins	sametype	0.047
C12	CST3	C12 to CST3	Metabolites	eGFRbiom	diftype	0.001
C6(C4:1-DC)	SM C18:1	C6(C4:1-DC) to SM C18:1	Metabolites	Metabolites	sametype	0.047
IGFBP2	EFNA5	IGFBP2 to EFNA5	Proteins	Proteins	sametype	0.048
TFE3	ARG1	TFE3 to ARG1	RNAs	RNAs	sametype	0.049
ADAMTS13	RET	ADAMTS13 to RET	Proteins	Proteins	sametype	0.049
CLEC4M	SOD2	CLEC4M to SOD2	Proteins	Proteins	sametype	0.049
ERBB3	CNDP1	ERBB3 to CNDP1	Proteins	Proteins	sametype	0.049
FN1	NOTCH1	FN1 to NOTCH1	Proteins	Proteins	sametype	0.049
C6(C4:1-DC)	C5	C6(C4:1-DC) to C5	Metabolites	Metabolites	sametype	0.049
NBL1	TNFRSF19	NBL1 to TNFRSF19	Proteins	Proteins	sametype	0.05
EGFR	NTRK2	EGFR to NTRK2	Proteins	Proteins	sametype	0.05
IL19	SPOCK2	IL19 to SPOCK2	Proteins	Proteins	sametype	0.05
IL19	MASP1	IL19 to MASP1	Proteins	Proteins	sametype	0.051
MASP1	IGF2R	MASP1 to IGF2R	Proteins	Proteins	sametype	0.051
MMP1	SCARF1	MMP1 to SCARF1	Proteins	Proteins	sametype	0.051
NTRK2	SEMA3E	NTRK2 to SEMA3E	Proteins	Proteins	sametype	0.051
PLAT	FCN3	PLAT to FCN3	Proteins	Proteins	sametype	0.053
IGFBP6	CST3	IGFBP6 to CST3	Proteins	eGFRbiom	diftype	-0.011
ABCB1	CST3	ABCB1 to CST3	RNAs	eGFRbiom	diftype	-0.024
SPOCK2	CST3	SPOCK2 to CST3	Proteins	eGFRbiom	diftype	-0.029
BMP1	SOD2	BMP1 to SOD2	Proteins	Proteins	sametype	0.054
FGF20	CTSV	FGF20 to CTSV	Proteins	Proteins	sametype	0.054
TNFRSF1A	RETN	TNFRSF1A to RETN	Proteins	Proteins	sametype	0.054
PLAT	C1QBP	PLAT to C1QBP	Proteins	Proteins	sametype	0.054
C18:1	GHR	C18:1 to GHR	Metabolites	Proteins	diftype	-0.01
NBL1	UNC5C	NBL1 to UNC5C	Proteins	Proteins	sametype	0.055
CLEC4M	ACY1	CLEC4M to ACY1	Proteins	Proteins	sametype	0.055
DUSP11	CST3	DUSP11 to CST3	RNAs	eGFRbiom	diftype	-0.044
ADAMTS13	NOTCH1	ADAMTS13 to NOTCH1	Proteins	Proteins	sametype	0.056
ERBB3	ADAMTS13	ERBB3 to ADAMTS13	Proteins	Proteins	sametype	0.056
C14:1	C2	C14:1 to C2	Metabolites	Metabolites	sametype	0.056

FSTL3	TFF3	FSTL3 to TFF3	Proteins	Proteins	sametype	0.057
TNFRSF1A	NBL1	TNFRSF1A to NBL1	Proteins	Proteins	sametype	0.057
ERP29	HAVCR2	ERP29 to HAVCR2	Proteins	Proteins	sametype	0.058
IGFBP2	PAPPA	IGFBP2 to PAPPA	Proteins	Proteins	sametype	0.058
PCGF2	SPOCK2	PCGF2 to SPOCK2	RNAs	Proteins	diftype	-0.014
C12	EGFR	C12 to EGFR	Metabolites	Proteins	diftype	-0.015
ADAMTS13	NTRK2	ADAMTS13 to NTRK2	Proteins	Proteins	sametype	0.06
FGF20	NTRK2	FGF20 to NTRK2	Proteins	Proteins	sametype	0.061
C10:2	C14:2	C10:2 to C14:2	Metabolites	Metabolites	sametype	0.061
C18:1	EGFR	C18:1 to EGFR	Metabolites	Proteins	diftype	-0.017
NBL1	ESAM	NBL1 to ESAM	Proteins	Proteins	sametype	0.062
IL2	RET	IL2 to RET	Proteins	Proteins	sametype	0.062
RETN	TNFRSF19	RETN to TNFRSF19	Proteins	Proteins	sametype	0.062
EGFR	IGF2R	EGFR to IGF2R	Proteins	Proteins	sametype	0.063
ERBB3	SOD2	ERBB3 to SOD2	Proteins	Proteins	sametype	0.063
PAPPA	TFF3	PAPPA to TFF3	Proteins	Proteins	sametype	0.063
EGFR	CST3	EGFR to CST3	Proteins	eGFRbiom	diftype	-0.06
SLC25A4	CTSH	SLC25A4 to CTSH	RNAs	Proteins	diftype	-0.024
FSTL3	UNC5C	FSTL3 to UNC5C	Proteins	Proteins	sametype	0.064
IL2	AMH	IL2 to AMH	Proteins	Proteins	sametype	0.064
MASP1	NTRK2	MASP1 to NTRK2	Proteins	Proteins	sametype	0.064
SPINT1	EPHA2	SPINT1 to EPHA2	Proteins	Proteins	sametype	0.065
C10:2	C14:1-OH	C10:2 to C14:1-OH	Metabolites	Metabolites	sametype	0.065
CTSH	RELT	CTSH to RELT	Proteins	Proteins	sametype	0.066
SPINT1	SEMA3E	SPINT1 to SEMA3E	Proteins	Proteins	sametype	0.066
MCM3	ERP29	MCM3 to ERP29	RNAs	Proteins	diftype	-0.026
EGFR	PLG	EGFR to PLG	Proteins	Proteins	sametype	0.067
EGFR	CLEC4M	EGFR to CLEC4M	Proteins	Proteins	sametype	0.067
FGF20	FCN3	FGF20 to FCN3	Proteins	Proteins	sametype	0.067
CGA LHB	B2M	CGA LHB to B2M	Proteins	Proteins	sametype	0.067
RET	ACY1	RET to ACY1	Proteins	Proteins	sametype	0.067
C16	EGFR	C16 to EGFR	Metabolites	Proteins	diftype	-0.028
CTSH	TFF3	CTSH to TFF3	Proteins	Proteins	sametype	0.068
FSTL3	EPHA2	FSTL3 to EPHA2	Proteins	Proteins	sametype	0.068
EGFR	SOD2	EGFR to SOD2	Proteins	Proteins	sametype	0.069
PAPPA	UNC5C	PAPPA to UNC5C	Proteins	Proteins	sametype	0.069
CTSV	CST3	CTSV to CST3	Proteins	eGFRbiom	diftype	-0.066
C16	C5	C16 to C5	Metabolites	Metabolites	sametype	0.069
KDR	IGF2R	KDR to IGF2R	Proteins	Proteins	sametype	0.07
C10:2	Tyr	C10:2 to Tyr	Metabolites	Metabolites	sametype	0.07
TTF2	SLC25A4	TTF2 to SLC25A4	RNAs	RNAs	sametype	0.071
IGFBP6	TNFRSF19	IGFBP6 to TNFRSF19	Proteins	Proteins	sametype	0.071
ADAMTS13	BMP1	ADAMTS13 to BMP1	Proteins	Proteins	sametype	0.072
JAM2	ERP29	JAM2 to ERP29	Proteins	Proteins	sametype	0.072
LAYN	TNFRSF1B	LAYN to TNFRSF1B	Proteins	Proteins	sametype	0.072

TNFRSF1A	UNC5C	TNFRSF1A to UNC5C	Proteins	Proteins	sametype	0.072
BMP1	FCN3	BMP1 to FCN3	Proteins	Proteins	sametype	0.073
CTSV	SPOCK2	CTSV to SPOCK2	Proteins	Proteins	sametype	0.073
ESAM	PAPPA	ESAM to PAPPA	Proteins	Proteins	sametype	0.073
IL19	CTSV	IL19 to CTSV	Proteins	Proteins	sametype	0.073
C2	C5	C2 to C5	Metabolites	Metabolites	sametype	0.073
RET	NTRK2	RET to NTRK2	Proteins	Proteins	sametype	0.074
C10	C10:2	C10 to C10:2	Metabolites	Metabolites	sametype	0.074
DUSP11	SLC25A4	DUSP11 to SLC25A4	RNAs	RNAs	sametype	0.075
ERBB3	BMP1	ERBB3 to BMP1	Proteins	Proteins	sametype	0.075
ERBB3	FGF9	ERBB3 to FGF9	Proteins	Proteins	sametype	0.075
C18:1	BMP1	C18:1 to BMP1	Metabolites	Proteins	diftype	-0.033
GHR	BMP1	GHR to BMP1	Proteins	Proteins	sametype	0.076
IGFBP2	CTSH	IGFBP2 to CTSH	Proteins	Proteins	sametype	0.076
NOTCH1	RELT	NOTCH1 to RELT	Proteins	Proteins	sametype	0.076
CNDP1	AMH	CNDP1 to AMH	Proteins	Proteins	sametype	0.077
ERBB3	CTSV	ERBB3 to CTSV	Proteins	Proteins	sametype	0.077
ESAM	JAM2	ESAM to JAM2	Proteins	Proteins	sametype	0.077
RPS6KA5	KIR2DL4	RPS6KA5 to KIR2DL4	Proteins	Proteins	sametype	0.077
DUSP11	Creatinine	DUSP11 to Creatinine	RNAs	eGFRbiom	diftype	-0.069
KDR	AMH	KDR to AMH	Proteins	Proteins	sametype	0.078
C14:1	SM C18:1	C14:1 to SM C18:1	Metabolites	Metabolites	sametype	0.078
IGFBP6	ERP29	IGFBP6 to ERP29	Proteins	Proteins	sametype	0.079
TTF2	Creatinine	TTF2 to Creatinine	RNAs	eGFRbiom	diftype	-0.078
DUSP11	AGK	DUSP11 to AGK	RNAs	RNAs	sametype	0.08
SLC25A4	PAPPA	SLC25A4 to PAPPA	RNAs	Proteins	diftype	-0.052
LAYN	UNC5C	LAYN to UNC5C	Proteins	Proteins	sametype	0.08
IGFBP2	LAYN	IGFBP2 to LAYN	Proteins	Proteins	sametype	0.081
SLC22A4	NOTCH1	SLC22A4 to NOTCH1	RNAs	Proteins	diftype	-0.054
C1QBP	CST3	C1QBP to CST3	Proteins	eGFRbiom	diftype	-0.111
DUSP11	CTSH	DUSP11 to CTSH	RNAs	Proteins	diftype	-0.063
ESAM	MMP1	ESAM to MMP1	Proteins	Proteins	sametype	0.083
SPINT1	SOD2	SPINT1 to SOD2	Proteins	Proteins	sametype	0.083
IGFBP6	FSTL3	IGFBP6 to FSTL3	Proteins	Proteins	sametype	0.083
IGFBP6	RELT	IGFBP6 to RELT	Proteins	Proteins	sametype	0.083
MED1	MAPK12	MED1 to MAPK12	Proteins	Proteins	sametype	0.083
C14:1-OH	C14:2	C14:1-OH to C14:2	Metabolites	Metabolites	sametype	0.083
IL19	NTRK2	IL19 to NTRK2	Proteins	Proteins	sametype	0.084
MASP1	SPOCK2	MASP1 to SPOCK2	Proteins	Proteins	sametype	0.084
Creatinine	CST3	Creatinine to CST3	eGFRbiom	eGFRbiom	sametype	0.431
JAM2	RELT	JAM2 to RELT	Proteins	Proteins	sametype	0.085
SLC22A4	Urine albumin	SLC22A4 to Urine albumin	RNAs	UACRbiom	diftype	0.09
AGK	RETN	AGK to RETN	RNAs	Proteins	diftype	-0.071
GHR	ACY1	GHR to ACY1	Proteins	Proteins	sametype	0.088
ERP29	Urine albumin	ERP29 to Urine albumin	Proteins	UACRbiom	diftype	0.082

ARG1	CTSV	ARG1 to CTSV	RNAs	Proteins	diftype	-0.079
SLC22A4	SPINT1	SLC22A4 to SPINT1	RNAs	Proteins	diftype	-0.08
PLAT	SPOCK2	PLAT to SPOCK2	Proteins	Proteins	sametype	0.09
SPINT1	MASP1	SPINT1 to MASP1	Proteins	Proteins	sametype	0.091
ERBB3	GHR	ERBB3 to GHR	Proteins	Proteins	sametype	0.092
SLC22A4	IL19	SLC22A4 to IL19	RNAs	Proteins	diftype	-0.086
IGFBP6	NBL1	IGFBP6 to NBL1	Proteins	Proteins	sametype	0.093
MAPK12	KIR2DL4	MAPK12 to KIR2DL4	Proteins	Proteins	sametype	0.093
ACY1	MASP1	ACY1 to MASP1	Proteins	Proteins	sametype	0.094
IL19	ACY1	IL19 to ACY1	Proteins	Proteins	sametype	0.094
LAYN	NOTCH1	LAYN to NOTCH1	Proteins	Proteins	sametype	0.094
MCM3	TTF2	MCM3 to TTF2	RNAs	RNAs	sametype	0.095
C16	Tyr	C16 to Tyr	Metabolites	Metabolites	sametype	0.095
IGFBP2	ADIPOQ	IGFBP2 to ADIPOQ	Proteins	Proteins	sametype	0.096
NOTCH1	SPOCK2	NOTCH1 to SPOCK2	Proteins	Proteins	sametype	0.096
C14:1-OH	C2	C14:1-OH to C2	Metabolites	Metabolites	sametype	0.096
IGFBP2	NOTCH1	IGFBP2 to NOTCH1	Proteins	Proteins	sametype	0.097
IL2	FN1	IL2 to FN1	Proteins	Proteins	sametype	0.097
JAM2	HAVCR2	JAM2 to HAVCR2	Proteins	Proteins	sametype	0.097
RETN	PAPPA	RETN to PAPPA	Proteins	Proteins	sametype	0.098
PLG	AMH	PLG to AMH	Proteins	Proteins	sametype	0.099
NBL1	EPHA2	NBL1 to EPHA2	Proteins	Proteins	sametype	0.099
NBL1	SCARF1	NBL1 to SCARF1	Proteins	Proteins	sametype	0.099
IGFBP6	ESAM	IGFBP6 to ESAM	Proteins	Proteins	sametype	0.099
C14:2	C2	C14:2 to C2	Metabolites	Metabolites	sametype	0.1
C18:1	Urine albumin	C18:1 to Urine albumin	Metabolites	UACRbiom	diftype	0.055
IGFBP6	CTSH	IGFBP6 to CTSH	Proteins	Proteins	sametype	0.101
RPS6KA5	IL6	RPS6KA5 to IL6	Proteins	Proteins	sametype	0.101
PLAT	FGF9	PLAT to FGF9	Proteins	Proteins	sametype	0.101
IL19	NOTCH1	IL19 to NOTCH1	Proteins	Proteins	sametype	0.103
IGFBP2	TFF3	IGFBP2 to TFF3	Proteins	Proteins	sametype	0.104
ARG1	NTRK2	ARG1 to NTRK2	RNAs	Proteins	diftype	-0.097
TNFRSF1A	EPHA2	TNFRSF1A to EPHA2	Proteins	Proteins	sametype	0.104
NOTCH1	SEMA3E	NOTCH1 to SEMA3E	Proteins	Proteins	sametype	0.106
TNFRSF1A	FSTL3	TNFRSF1A to FSTL3	Proteins	Proteins	sametype	0.107
B2M	RELT	B2M to RELT	Proteins	Proteins	sametype	0.108
PNLIPRP2	CLEC4M	PNLIPRP2 to CLEC4M	RNAs	Proteins	diftype	-0.106
MASP1	FCN3	MASP1 to FCN3	Proteins	Proteins	sametype	0.11
EFNA5	NOTCH1	EFNA5 to NOTCH1	Proteins	Proteins	sametype	0.111
IL2	BMP1	IL2 to BMP1	Proteins	Proteins	sametype	0.111
TNFRSF1A	IGFBP6	TNFRSF1A to IGFBP6	Proteins	Proteins	sametype	0.111
C14:2	C8:1	C14:2 to C8:1	Metabolites	Metabolites	sametype	0.112
ERP29	MAPK12	ERP29 to MAPK12	Proteins	Proteins	sametype	0.113
GHR	NTRK2	GHR to NTRK2	Proteins	Proteins	sametype	0.115
SLC25A4	IL22RA1	SLC25A4 to IL22RA1	RNAs	Proteins	diftype	-0.111

TNFRSF1B	CTSH	TNFRSF1B to CTSH	Proteins	Proteins	sametype	0.117
NTRK2	TNFRSF19	NTRK2 to TNFRSF19	Proteins	Proteins	sametype	0.117
Tyr	PC aa C38:0	Tyr to PC aa C38:0	Metabolites	Metabolites	sametype	0.118
IL2	PLG	IL2 to PLG	Proteins	Proteins	sametype	0.121
RETN	RELT	RETN to RELT	Proteins	Proteins	sametype	0.123
IL22RA1	CTSH	IL22RA1 to CTSH	Proteins	Proteins	sametype	0.124
ERBB3	KDR	ERBB3 to KDR	Proteins	Proteins	sametype	0.125
TFF3	AMH	TFF3 to AMH	Proteins	Proteins	sametype	0.126
EGFR	Urine albumin	EGFR to Urine albumin	Proteins	UACRbiom	diftype	-0.046
MCM3	Urine albumin	MCM3 to Urine albumin	RNAs	UACRbiom	diftype	-0.093
MASP1	EPHA2	MASP1 to EPHA2	Proteins	Proteins	sametype	0.128
SM C18:1	PC aa C38:0	SM C18:1 to PC aa C38:0	Metabolites	Metabolites	sametype	0.129
NTRK2	NOTCH1	NTRK2 to NOTCH1	Proteins	Proteins	sametype	0.13
EPHA2	ERP29	EPHA2 to ERP29	Proteins	Proteins	sametype	0.134
SEMA3E	SM C18:1	SEMA3E to SM C18:1	Proteins	Metabolites	diftype	-0.135
AMH	NOTCH1	AMH to NOTCH1	Proteins	Proteins	sametype	0.137
PCGF2	SOD2	PCGF2 to SOD2	RNAs	Proteins	diftype	-0.136
PNLIPRP2	PLAT	PNLIPRP2 to PLAT	RNAs	Proteins	diftype	-0.138
GHR	CNDP1	GHR to CNDP1	Proteins	Proteins	sametype	0.139
RPS6KA5	MED1	RPS6KA5 to MED1	Proteins	Proteins	sametype	0.139
EFNA5	EPHA2	EFNA5 to EPHA2	Proteins	Proteins	sametype	0.141
LAYN	FSTL3	LAYN to FSTL3	Proteins	Proteins	sametype	0.141
MCM3	SLC25A4	MCM3 to SLC25A4	RNAs	RNAs	sametype	0.142
PCGF2	FGF20	PCGF2 to FGF20	RNAs	Proteins	diftype	-0.143
Tyr	IGFBP2	Tyr to IGFBP2	Metabolites	Proteins	diftype	-0.152
MAPK12	SCARF1	MAPK12 to SCARF1	Proteins	Proteins	sametype	0.142
RELT	TNFRSF19	RELT to TNFRSF19	Proteins	Proteins	sametype	0.143
TNFRSF1B	FSTL3	TNFRSF1B to FSTL3	Proteins	Proteins	sametype	0.143
ERBB3	PLG	ERBB3 to PLG	Proteins	Proteins	sametype	0.145
C10:2	PC aa C38:0	C10:2 to PC aa C38:0	Metabolites	Metabolites	sametype	0.145
ADIPOQ	EPHA2	ADIPOQ to EPHA2	Proteins	Proteins	sametype	0.147
RPS6KA5	ERP29	RPS6KA5 to ERP29	Proteins	Proteins	sametype	0.149
MCM3	ABCB1	MCM3 to ABCB1	RNAs	RNAs	sametype	0.15
NKD2	KIR2DL4	NKD2 to KIR2DL4	RNAs	Proteins	diftype	-0.158
NEURL3	NAPA	NEURL3 to NAPA	CpGs	CpGs	sametype	0.151
FGF20	SPOCK2	FGF20 to SPOCK2	Proteins	Proteins	sametype	0.151
ESAM	UNC5C	ESAM to UNC5C	Proteins	Proteins	sametype	0.152
DUSP11	TTF2	DUSP11 to TTF2	RNAs	RNAs	sametype	0.153
RPS6KA5	MAPK12	RPS6KA5 to MAPK12	Proteins	Proteins	sametype	0.155
ERBB3	EGFR	ERBB3 to EGFR	Proteins	Proteins	sametype	0.158
EFNA5	JAM2	EFNA5 to JAM2	Proteins	Proteins	sametype	0.161
EFNA5	LAYN	EFNA5 to LAYN	Proteins	Proteins	sametype	0.161
CLEC4M	AMH	CLEC4M to AMH	Proteins	Proteins	sametype	0.163
NOTCH1	UNC5C	NOTCH1 to UNC5C	Proteins	Proteins	sametype	0.163
EGFR	KDR	EGFR to KDR	Proteins	Proteins	sametype	0.164

LAYN	JAM2	LAYN to JAM2	Proteins	Proteins	sametype	0.167
FN1	SOD2	FN1 to SOD2	Proteins	Proteins	sametype	0.168
IGFBP2	FN1	IGFBP2 to FN1	Proteins	Proteins	sametype	0.17
SLC22A4	TFE3	SLC22A4 to TFE3	RNAs	RNAs	sametype	0.171
FN1	IGF2R	FN1 to IGF2R	Proteins	Proteins	sametype	0.172
B2M	CTSH	B2M to CTSH	Proteins	Proteins	sametype	0.174
BMP1	PLG	BMP1 to PLG	Proteins	Proteins	sametype	0.175
FSTL3	RELT	FSTL3 to RELT	Proteins	Proteins	sametype	0.176
C2	C6(C4:1-DC)	C2 to C6(C4:1-DC)	Metabolites	Metabolites	sametype	0.177
B2M	TFF3	B2M to TFF3	Proteins	Proteins	sametype	0.178
GHR	FCN3	GHR to FCN3	Proteins	Proteins	sametype	0.179
EGFR	FN1	EGFR to FN1	Proteins	Proteins	sametype	0.181
ADIPOQ	NTRK2	ADIPOQ to NTRK2	Proteins	Proteins	sametype	0.183
EFNA5	SPINT1	EFNA5 to SPINT1	Proteins	Proteins	sametype	0.184
TFE3	MMP1	TFE3 to MMP1	RNAs	Proteins	difftype	-0.168
EFNA5	IL2	EFNA5 to IL2	Proteins	Proteins	sametype	0.187
EFNA5	RELT	EFNA5 to RELT	Proteins	Proteins	sametype	0.187
C14:1	C14:1-OH	C14:1 to C14:1-OH	Metabolites	Metabolites	sametype	0.193
AGK	TTF2	AGK to TTF2	RNAs	RNAs	sametype	0.195
EGFR	CNDP1	EGFR to CNDP1	Proteins	Proteins	sametype	0.196
SLC22A4	ARG1	SLC22A4 to ARG1	RNAs	RNAs	sametype	0.197
C14:1-OH	C16	C14:1-OH to C16	Metabolites	Metabolites	sametype	0.198
PLAT	TNFRSF1A	PLAT to TNFRSF1A	Proteins	Proteins	sametype	0.2
IL22RA1	IL6	IL22RA1 to IL6	Proteins	Proteins	sametype	0.202
C12	C14:1-OH	C12 to C14:1-OH	Metabolites	Metabolites	sametype	0.205
NEURL3	LYSMD2	NEURL3 to LYSMD2	CpGs	CpGs	sametype	0.206
RET	TFF3	RET to TFF3	Proteins	Proteins	sametype	0.208
KDR	FCN3	KDR to FCN3	Proteins	Proteins	sametype	0.208
NKD2	PLG	NKD2 to PLG	RNAs	Proteins	difftype	-0.178
TNFRSF1B	B2M	TNFRSF1B to B2M	Proteins	Proteins	sametype	0.209
EPHA2	HAVCR2	EPHA2 to HAVCR2	Proteins	Proteins	sametype	0.211
C5	Tyr	C5 to Tyr	Metabolites	Metabolites	sametype	0.212
CDC14A	JAM2	CDC14A to JAM2	RNAs	Proteins	difftype	-0.218
IL19	ADAMTS13	IL19 to ADAMTS13	Proteins	Proteins	sametype	0.219
KIR2DL4	TNFRSF19	KIR2DL4 to TNFRSF19	Proteins	Proteins	sametype	0.225
ABCB1	SLC25A4	ABCB1 to SLC25A4	RNAs	RNAs	sametype	0.234
AGK	SLC25A4	AGK to SLC25A4	RNAs	RNAs	sametype	0.235
C12	C14:1	C12 to C14:1	Metabolites	Metabolites	sametype	0.235
C14:1	C18:1	C14:1 to C18:1	Metabolites	Metabolites	sametype	0.239
AGK	ABCB1	AGK to ABCB1	RNAs	RNAs	sametype	0.24
C18:1	C2	C18:1 to C2	Metabolites	Metabolites	sametype	0.243
GHR	RET	GHR to RET	Proteins	Proteins	sametype	0.254
SPINT1	CTSV	SPINT1 to CTSV	Proteins	Proteins	sametype	0.265
TNFRSF1B	HAVCR2	TNFRSF1B to HAVCR2	Proteins	Proteins	sametype	0.267
C12	C14:2	C12 to C14:2	Metabolites	Metabolites	sametype	0.268

EFNA5	NBL1	EFNA5 to NBL1	Proteins	Proteins	sametype	0.273
TNFRSF1B	UNC5C	TNFRSF1B to UNC5C	Proteins	Proteins	sametype	0.273
FGF20	FGF9	FGF20 to FGF9	Proteins	Proteins	sametype	0.281
EGFR	NOTCH1	EGFR to NOTCH1	Proteins	Proteins	sametype	0.283
AMH	C1QBP	AMH to C1QBP	Proteins	Proteins	sametype	0.287
TNFRSF1A	TNFRSF1B	TNFRSF1A to TNFRSF1B	Proteins	Proteins	sametype	0.287
ESAM	SCARF1	ESAM to SCARF1	Proteins	Proteins	sametype	0.302
CLEC4M	FN1	CLEC4M to FN1	Proteins	Proteins	sametype	0.319
C6(C4:1-DC)	C8	C6(C4:1-DC) to C8	Metabolites	Metabolites	sametype	0.323
C10:2	C8:1	C10:2 to C8:1	Metabolites	Metabolites	sametype	0.331
CLEC4M	C1QBP	CLEC4M to C1QBP	Proteins	Proteins	sametype	0.364
C14:1	C14:2	C14:1 to C14:2	Metabolites	Metabolites	sametype	0.372
LYSMD2	Urine albumin	LYSMD2 to Urine albumin	CpGs	UACRbiom	diftype	-0.125
C10	C12	C10 to C12	Metabolites	Metabolites	sametype	0.436
C16	C18:1	C16 to C18:1	Metabolites	Metabolites	sametype	0.544
C10	C8	C10 to C8	Metabolites	Metabolites	sametype	0.827

Supplementary Table 17. Best mediation directions of causal mediation analysis of omics candidates & candidates & three times points of kidney traits.

Within each identified best mediation direction, spearman correlation coefficients, *P*-values and FDR of each pair (FDR < 0.05) of residuals of omics candidates, and regression coefficients and *P*-values of omics candidates with kidney traits in hyperglycemic individuals of KORA F4 are shown, respectively. Residuals of omics candidates were calculated with linear regression analysis for full model (incl. age, sex, BMI, systolic blood pressure, smoking status, triglyceride, total cholesterol, HDL cholesterol, fasting glucose, use of lipid lowering drugs, antihypertensive and anti-diabetic medication).

The mediation proportion (%), average mediating effect with 95% *CI*, *P*-values and FDR, average direct effect with 95% *CI*, *P*-values and FDR of the identified best direction(s) of mediating triangles in a nonparametric causal mediation analysis are shown, respectively. Each mediation analysis was adjusted for the full model. FDR of mediating effect and direct effect were calculated for each kidney trait.

Abbreviations: CKD, chronic kidney disease; eGFR, estimated glomerular filtration rate; UACR, urinary albumin-to-creatinine ratio; CKDcrcc, eGFR-based CKD that was defined as eGFR < 60 ml/min/1.73 m².

triangle	omics1.1 label	omics2.1 label	omics1.type	omics2.type	omics.a.sso.type	spearcor	p-value	FDR	kidney.tra it	kidney.t rait_posi tion	Mediation.direction	omics.direction	time.point.k idney.tra it	Proportion.m edia(%)	Avg.media (95% CI)	Avg.media. p-value	Avg.media. FDR	Avg.direct (95% CI)	Avg.direct. p-value	Avg.direct. FDR	Estimate.omi cs1.kidney.tr ait	p-value.omics1. kidney.tra it	Estimate.omics2. kidney.tra it	p-value.omics2. kidney.tra it
2	C10	CNDP1	Metabolites	Proteins	diftype	-0.143	1.201E-03	4.661E-02	CKD F4	Y	C10 to CNDP1 to CKD F4	Metabolite to Protein	kidney trait in F4	36.57	0.006 (0.001 to 0.013)	8.0E-03	2.766E-02	0.011 (-0.019 to 0.045)	5.08E-01	5.990E-01	0.278	8.764E-04	-0.507	2.239E-04
7	C10	B2M	Metabolites	Proteins	diftype	0.187	2.113E-05	3.609E-03	eGFR F4	M	C10 to eGFR F4 to B2M	Metabolite to Protein	kidney trait in F4	79.61	0.135 (0.073 to 0.2)	0.0E+00	0.000E+00	0.034 (-0.045 to 0.111)	3.92E-01	4.136E-01	-0.174	1.585E-17	-0.43	4.438E-50
9	CNDP1	C10	Proteins	Metabolites	diftype	-0.143	1.201E-03	4.661E-02	eGFR F4	M	CNDP1 to eGFR F4 to C10	Protein to Metabolite	kidney trait in F4	30.39	-0.033 (-0.061 to -0.013)	2.0E-03	5.231E-03	-0.075 (-0.159 to -0.003)	4.40E-02	5.803E-02	0.124	2.713E-05	-0.174	1.585E-17
9									eGFR F4	M	C10 to eGFR F4 to CNDP1	Metabolite to Protein	kidney trait in F4	29.51	-0.041 (-0.075 to -0.013)	2.0E-03	5.231E-03	-0.098 (-0.204 to -0.004)	4.40E-02	5.803E-02				
10	B2M	C10	Proteins	Metabolites	diftype	0.187	2.113E-05	3.609E-03	CKD F4	X	CKD F4 to B2M to C10	Protein to Metabolite	kidney trait in F4	92.74	0.139 (0.052 to 0.24)	0.0E+00	0.000E+00	0.011 (-0.278 to 0.311)	9.18E-01	9.381E-01	0.925	1.435E-07	0.278	8.764E-04
10									CKD F4	Y	C10 to B2M to CKD F4	Metabolite to Protein	kidney trait in F4	88.85	0.013 (0.005 to 0.024)	0.0E+00	0.000E+00	0.002 (-0.031 to 0.041)	8.54E-01	8.980E-01				
11	C10	CST3	Metabolites	Proteins	diftype	0.192	1.287E-05	2.783E-03	eGFR F4	M	C10 to eGFR F4 to CST3	Metabolite to Protein	kidney trait in F4	87.33	0.151 (0.084 to 0.213)	0.0E+00	0.000E+00	0.022 (-0.039 to 0.082)	4.60E-01	4.723E-01	-0.174	1.585E-17	-0.551	3.888E-80
13	C10 2	TNFRSF1A	Metabolites	Proteins	diftype	0.145	1.015E-03	4.141E-02	CKD F4	Y	C10 2 to TNFRSF1A to CKD F4	Metabolite to Protein	kidney trait in F4	32.18	0.006 (0.001 to 0.013)	6.0E-03	2.166E-02	0.013 (-0.014 to 0.04)	3.42E-01	4.241E-01	0.276	2.971E-04	0.675	3.884E-06
16	C10 2	TNFRSF1A	Metabolites	Proteins	diftype	0.145	1.015E-03	4.141E-02	eGFR F4	M	C10 2 to eGFR F4 to TNFRSF1A	Metabolite to Protein	kidney trait in F4	72.63	0.083 (0.039 to 0.129)	0.0E+00	0.000E+00	0.031 (-0.041 to 0.108)	4.28E-01	4.476E-01	-0.178	1.691E-20	-0.303	1.193E-25
17	RELT	C10 2	Proteins	Metabolites	diftype	0.177	5.828E-05	7.693E-03	CKD F4	X	CKD F4 to RELT to C10 2	Protein to Metabolite	kidney trait in F4	56.02	0.112 (0.043 to 0.209)	2.0E-03	9.169E-03	0.088 (-0.207 to 0.365)	5.60E-01	6.528E-01	0.694	3.832E-05	0.276	2.971E-04
17									CKD F4	Y	C10 2 to RELT to CKD F4	Metabolite to Protein	kidney trait in F4	53.9	0.009 (0.003 to 0.018)	2.0E-03	9.169E-03	0.008 (-0.019 to 0.036)	5.44E-01	6.378E-01				
19	C10 2	CST3	Metabolites	Proteins	diftype	0.191	1.412E-05	2.783E-03	eGFR F4	Y	C10 2 to CST3 to eGFR F4	Metabolite to Protein	kidney trait in F4	73.44	-0.094 (-0.136 to -0.05)	0.0E+00	0.000E+00	-0.034 (-0.075 to 0.009)	1.34E-01	1.614E-01	-0.178	1.691E-20	-0.551	3.888E-80
19									eGFR F4	M	C10 2 to eGFR F4 to CST3	Metabolite to Protein	kidney trait in F4	67.64	0.118 (0.055 to 0.178)	0.0E+00	0.000E+00	0.056 (0.004 to 0.107)	3.40E-02	4.645E-02				
21	C10 2	B2M	Metabolites	Proteins	diftype	0.153	5.546E-04	3.107E-02	CKD F4	Y	C10 2 to B2M to CKD F4	Metabolite to Protein	kidney trait in F4	79.92	0.012 (0.005 to 0.021)	2.0E-03	9.169E-03	0.003 (-0.022 to 0.029)	7.72E-01	8.333E-01	0.276	2.971E-04	0.925	1.435E-07
25	RETN	C10 2	Proteins	Metabolites	diftype	0.165	1.841E-04	1.474E-02	CKD F4	X	CKD F4 to RETN to C10 2	Protein to Metabolite	kidney trait in F4	46.27	0.092 (0.028 to 0.178)	0.0E+00	0.000E+00	0.107 (-0.172 to 0.395)	4.94E-01	5.876E-01	0.525	2.696E-04	0.276	2.971E-04
27	TNFRSF19	C10 2	Proteins	Metabolites	diftype	0.15	6.887E-04	3.460E-02	eGFR F4	M	TNFRSF19 to eGFR F4 to C10 2	Protein to Metabolite	kidney trait in F4	30.28	0.031 (0.009 to 0.067)	0.0E+00	0.000E+00	0.072 (-0.009 to 0.147)	6.40E-02	7.961E-02	-0.132	2.994E-06	-0.178	1.691E-20
29	C10 2	B2M	Metabolites	Proteins	diftype	0.153	5.546E-04	3.107E-02	eGFR F4	M	C10 2 to eGFR F4 to B2M	Metabolite to Protein	kidney trait in F4	67.51	0.105 (0.05 to 0.162)	0.0E+00	0.000E+00	0.051 (-0.019 to 0.123)	1.48E-01	1.742E-01	-0.178	1.691E-20	-0.43	4.438E-50
32	UNC5C	C10 2	Proteins	Metabolites	diftype	0.15	6.728E-04	3.447E-02	CKD F4	X	CKD F4 to UNC5C to C10 2	Protein to Metabolite	kidney trait in F4	38.02	0.076 (0.018 to 0.16)	0.0E+00	0.000E+00	0.124 (-0.183 to 0.427)	4.42E-01	5.351E-01	0.637	1.424E-04	0.276	2.971E-04
32									CKD F4	Y	C10 2 to UNC5C to CKD F4	Metabolite to Protein	kidney trait in F4	30.72	0.007 (0.002 to 0.014)	0.0E+00	0.000E+00	0.015 (-0.012 to 0.042)	3.06E-01	3.853E-01				

35	C12	CST3	Metabolites	Proteins	diffype	0.201	4.975E-06	1.416E-03	eGFR F4	M	C12 to eGFR F4 to CST3	Metabolite to Protein	kidney trait in F4	78.84	0.137 (0.074 to 0.2)	0.0E+00	0.000E+00	0.037 (-0.023 to 0.099)	2.40E-01	2.680E-01	-0.175	3.042E-17	-0.551	3.888E-80		
39	C12	B2M	Metabolites	Proteins	diffype	0.184	3.094E-05	4.663E-03	eGFR F4	M	C12 to eGFR F4 to B2M	Metabolite to Protein	kidney trait in F4	69.03	0.122 (0.064 to 0.186)	0.0E+00	0.000E+00	0.055 (-0.029 to 0.128)	1.74E-01	2.002E-01	-0.175	3.042E-17	-0.43	4.438E-50		
ADAM	43	TS13	C12	Proteins	Metabolites	diffype	-0.15	7.029E-04	3.463E-02	eGFR F4	M	ADAMTS13 to eGFR F4 to C12	Protein to Metabolite	kidney trait in F4	28.76	-0.031 (-0.057 to -0.011)	0.0E+00	0.000E+00	-0.077 (-0.159 to 0)	4.80E-02	6.171E-02	0.126	1.886E-05	-0.175	3.042E-17	
43																										
45	C12	C1QBP	Metabolites	Proteins	diffype	-0.152	6.018E-04	3.212E-02	eGFR F4	M	C12 to eGFR F4 to C1QBP	Metabolite to Protein	kidney trait in F4	55.37	-0.071 (-0.115 to -0.033)	0.0E+00	0.000E+00	-0.057 (-0.151 to 0.05)	2.82E-01	3.017E-01	-0.175	3.042E-17	0.231	1.113E-14		
45																										
50	C14 1	B2M	Metabolites	Proteins	diffype	0.184	3.089E-05	4.663E-03	eGFR F4	Y	C14 1 to B2M to eGFR F4	Metabolite to Protein	kidney trait in F4	65.59	-0.071 (-0.11 to -0.032)	0.0E+00	0.000E+00	-0.037 (-0.093 to 0.017)	1.70E-01	1.970E-01	-0.117	1.678E-09	-0.43	4.438E-50		
62	C14 1	CST3	Metabolites	Proteins	diffype	0.171	1.082E-04	1.155E-02	eGFR F4	Y	C14 1 to CST3 to eGFR F4	Metabolite to Protein	kidney trait in F4	73.1	-0.079 (-0.122 to -0.035)	0.0E+00	0.000E+00	-0.029 (-0.081 to 0.02)	2.44E-01	2.705E-01	-0.117	1.678E-09	-0.551	3.888E-80		
62																										
96	C14 2	ADIPO Q	Metabolites	Proteins	diffype	0.147	8.623E-04	3.809E-02	CKD F4	Y	C14 2 to ADIPOQ to CKD F4	Metabolite to Protein	kidney trait in F4	87.89	0.007 (0.002 to 0.014)	6.0E-03	2.166E-02	0.001 (-0.03 to 0.036)	8.72E-01	9.099E-01	0.299	2.943E-04	0.604	2.047E-03		
98	C14 2	B2M	Metabolites	Proteins	diffype	0.188	1.873E-05	3.428E-03	eGFR F4	M	C14 2 to eGFR F4 to B2M	Metabolite to Protein	kidney trait in F4	60.28	0.113 (0.058 to 0.171)	0.0E+00	0.000E+00	0.007 (-0.075 to 0.15)	6.20E-02	7.840E-02	-0.166	2.691E-16	-0.43	4.438E-50		
102	C14 2	CST3	Metabolites	Proteins	diffype	0.192	1.319E-05	2.783E-03	eGFR F4	M	C14 2 to eGFR F4 to CST3	Metabolite to Protein	kidney trait in F4	74.57	0.128 (0.068 to 0.192)	0.0E+00	0.000E+00	0.044 (-0.011 to 0.101)	1.38E-01	1.650E-01	-0.166	2.691E-16	-0.551	3.888E-80		
106	C16	KDR	Metabolites	Proteins	diffype	-0.149	7.444E-04	3.476E-02	eGFR F4	Y	C16 to KDR to eGFR F4	Metabolite to Protein	kidney trait in F4	30.55	-0.024 (-0.043 to -0.008)	4.0E-03	9.344E-03	-0.055 (-0.122 to 0.012)	9.60E-02	1.166E-01	-0.09	1.858E-05	0.153	4.635E-07		
107	C16	KDR	Metabolites	Proteins	diffype	-0.149	7.444E-04	3.476E-02	UACR F4	Y	C16 to KDR to UACR F4	Metabolite to Protein	kidney trait in F4	75.01	0.022 (0.006 to 0.045)	4.0E-03	3.600E-02	0.007 (-0.082 to 0.099)	8.74E-01	8.740E-01	0.118	1.023E-04	-0.141	5.484E-04		
107																										
108	C16	EGFR	Metabolites	Proteins	diffype	-0.213	1.241E-06	7.951E-04	eGFR F4	Y	C16 to EGFR to eGFR F4	Metabolite to Protein	kidney trait in F4	70.91	-0.056 (-0.084 to -0.029)	0.0E+00	0.000E+00	0.007 (-0.08 to 0.095)	8.74E-01	8.740E-01						
108																										
112	BMP1	C16	Proteins	Metabolites	diffype	-0.145	1.050E-03	4.141E-02	eGFR F4	X	eGFR F4 to BMP1 to C16	Protein to Metabolite	kidney trait in F4	22.23	-0.029 (-0.058 to -0.006)	6.0E-03	1.249E-02	-0.023 (-0.086 to 0.039)	6.40E-02	7.961E-02	0.132	1.811E-04	-0.09	1.858E-05		
117	C16	C1QBP	Metabolites	Proteins	diffype	-0.146	9.642E-04	4.141E-02	eGFR F4	Y	C16 to C1QBP to eGFR F4	Metabolite to Protein	kidney trait in F4	46.13	-0.036 (-0.064 to -0.012)	0.0E+00	0.000E+00	-0.042 (-0.108 to 0.023)	1.94E-01	2.215E-01	-0.09	1.858E-05	0.231	1.113E-14		
119	C18 1	IGFBP2	Metabolites	Proteins	diffype	0.175	7.070E-05	8.234E-03	eGFR F4	Y	C18 1 to IGFBP2 to eGFR F4	Metabolite to Protein	kidney trait in F4	43.95	-0.027 (-0.046 to -0.011)	0.0E+00	0.000E+00	-0.034 (-0.097 to 0.029)	2.82E-01	3.017E-01	-0.081	9.275E-05	-0.167	8.720E-06		

119									eGFR F4	X	eGFR F4 to IGFBP2 to C18 1	Protein to Metabolite	kidney trait in F4	43.85	-0.048 (-0.084 to -0.017)	0.0E+00	0.000E+00	-0.061 (-0.168 to 0.054)	2.82E-01	3.017E-01				
120	C18 1	CNDP1	Metabolites	Proteins	diftype	-0.149 04	7.380E-04	3.476E-02	eGFR F4	Y	C18 1 to CNDP1 to eGFR F4	Metabolite to Protein	kidney trait in F4	34.35	-0.021 (-0.04 to -0.007)	2.0E-03	5.231E-03	-0.04 (-0.103 to 0.02)	2.14E-01	2.425E-01	-0.081	9.275E-05	0.124	2.713E-05
120									eGFR F4	X	eGFR F4 to CNDP1 to C18 1	Protein to Metabolite	kidney trait in F4	33.71	-0.037 (-0.07 to -0.013)	2.0E-03	5.231E-03	-0.072 (-0.183 to 0.037)	2.14E-01	2.425E-01				
121	C18 1	EGFR	Metabolites	Proteins	diftype	-0.209 06	1.914E-06	9.808E-04	eGFR F4	Y	C18 1 to EGFR to eGFR F4	Metabolite to Protein	kidney trait in F4	91.6	-0.056 (-0.086 to -0.029)	0.0E+00	0.000E+00	-0.005 (-0.067 to 0.052)	8.16E-01	8.268E-01	-0.081	9.275E-05	0.254	3.881E-14
121									eGFR F4	X	eGFR F4 to EGFR to C18 1	Protein to Metabolite	kidney trait in F4	91.01	-0.1 (-0.152 to -0.054)	0.0E+00	0.000E+00	-0.01 (-0.131 to 0.099)	8.16E-01	8.268E-01				
122	GHR	C18 1	Proteins	Metabolites	diftype	-0.148 04	7.800E-04	3.569E-02	UACR F4	X	UACR F4 to GHR to C18 1	Protein to Metabolite	kidney trait in F4	47.99	0.027 (0.008 to 0.052)	6.0E-03	3.600E-02	0.029 (-0.073 to 0.121)	5.50E-01	6.050E-01	-0.167	7.015E-04	0.107	3.502E-04
122									UACR F4	Y	C18 1 to GHR to UACR F4	Metabolite to Protein	kidney trait in F4	47.39	0.027 (0.007 to 0.053)	6.0E-03	3.600E-02	0.03 (-0.072 to 0.121)	5.50E-01	6.050E-01				
123	EGFR	C18 1	Proteins	Metabolites	diftype	-0.209 06	1.914E-06	9.808E-04	UACR F4	X	UACR F4 to EGFR to C18 1	Protein to Metabolite	kidney trait in F4	82.8	0.047 (0.02 to 0.077)	0.0E+00	0.000E+00	0.01 (-0.09 to 0.103)	7.98E-01	8.229E-01	-0.221	1.197E-06	0.107	3.502E-04
123									UACR F4	Y	C18 1 to EGFR to UACR F4	Metabolite to Protein	kidney trait in F4	82.68	0.046 (0.019 to 0.079)	0.0E+00	0.000E+00	0.01 (-0.091 to 0.102)	7.98E-01	8.229E-01				
129	C18 1	CNDP1	Metabolites	Proteins	diftype	-0.149 04	7.380E-04	3.476E-02	CKD F4	Y	C18 1 to CNDP1 to CKD F4	Metabolite to Protein	kidney trait in F4	87.75	0.008 (0.002 to 0.016)	2.0E-03	9.169E-03	0.001 (-0.028 to 0.031)	9.22E-01	9.381E-01	0.265	1.336E-03	-0.507	2.239E-04
132	CNDP1	C18 1	Proteins	Metabolites	diftype	-0.149 04	7.380E-04	3.476E-02	UACR F4	X	UACR F4 to CNDP1 to C18 1	Protein to Metabolite	kidney trait in F4	39.83	0.023 (0.003 to 0.048)	1.4E-02	4.400E-02	0.034 (-0.066 to 0.123)	4.56E-01	5.374E-01	-0.127	1.357E-03	0.107	3.502E-04
133	IGFBP2	C18 1	Proteins	Metabolites	diftype	0.175 05	7.070E-05	8.234E-03	UACR F4	X	UACR F4 to IGFBP2 to C18 1	Protein to Metabolite	kidney trait in F4	42.9	0.024 (0.004 to 0.049)	1.4E-02	4.400E-02	0.032 (-0.071 to 0.126)	4.98E-01	5.667E-01	0.14	5.445E-03	0.107	3.502E-04
135	BMP1	C18 1	Proteins	Metabolites	diftype	-0.176 05	6.822E-05	8.234E-03	eGFR F4	X	eGFR F4 to BMP1 to C18 1	Protein to Metabolite	kidney trait in F4	37.83	-0.041 (-0.077 to -0.012)	2.0E-03	5.231E-03	-0.068 (-0.177 to 0.045)	2.34E-01	2.633E-01	0.132	1.811E-04	-0.081	9.275E-05
135									eGFR F4	Y	C18 1 to BMP1 to eGFR F4	Metabolite to Protein	kidney trait in F4	36.9	-0.023 (-0.042 to -0.006)	2.0E-03	5.231E-03	-0.039 (-0.102 to 0.026)	2.34E-01	2.633E-01				
137	C18 1	GHR	Metabolites	Proteins	diftype	-0.148 04	7.800E-04	3.569E-02	eGFR F4	Y	C18 1 to GHR to eGFR F4	Metabolite to Protein	kidney trait in F4	40.84	-0.025 (-0.047 to -0.009)	0.0E+00	0.000E+00	-0.036 (-0.098 to 0.024)	2.66E-01	2.886E-01	-0.081	9.275E-05	0.157	2.036E-05
137									eGFR F4	X	eGFR F4 to GHR to C18 1	Protein to Metabolite	kidney trait in F4	40.7	-0.044 (-0.083 to -0.015)	0.0E+00	0.000E+00	-0.065 (-0.172 to 0.042)	2.66E-01	2.886E-01				
162	C8	B2M	Metabolites	Proteins	diftype	0.181 05	4.091E-05	5.823E-03	eGFR F4	M	C8 to eGFR F4 to B2M	Metabolite to Protein	kidney trait in F4	75.69	0.12 (0.055 to 0.182)	0.0E+00	0.000E+00	0.038 (-0.043 to 0.114)	3.68E-01	3.910E-01	-0.163	5.665E-16	-0.43	4.438E-50
164	C8	CST3	Metabolites	Proteins	diftype	0.169 04	1.222E-04	1.182E-02	eGFR F4	M	C8 to eGFR F4 to CST3	Metabolite to Protein	kidney trait in F4	91.04	0.135 (0.067 to 0.202)	0.0E+00	0.000E+00	0.013 (-0.044 to 0.072)	6.34E-01	6.467E-01	-0.163	5.665E-16	-0.551	3.888E-80
166	C8	UNC5C	Metabolites	Proteins	diftype	0.145 03	1.025E-03	4.141E-02	CKD F4	Y	C8 to UNC5C to CKD F4	Metabolite to Protein	kidney trait in F4	89.14	0.007 (0.002 to 0.014)	2.0E-03	9.169E-03	0.001 (-0.032 to 0.036)	9.14E-01	9.381E-01	0.23	4.287E-03	0.637	1.424E-04
167	C8	UNC5C	Metabolites	Proteins	diftype	0.145 03	1.025E-03	4.141E-02	eGFR F4	M	C8 to eGFR F4 to UNC5C	Metabolite to Protein	kidney trait in F4	38.34	0.052 (0.021 to 0.089)	0.0E+00	0.000E+00	0.084 (-0.003 to 0.174)	6.00E-02	7.650E-02	-0.163	5.665E-16	-0.198	5.437E-10

208	PLAT	Tyr	Proteins	Metabolites	ditype	0.24	4.146E-08	3.541E-05	CKD F4	X	CKD F4 to PLAT to Tyr	Protein to Metabolite	kidney trait in F4	26.95	-0.12 (-0.211 to -0.045)	0.0E+00	0.000E+00	-0.326 (-0.599 to -0.046)	1.40E-02	2.231E-02	-0.791	4.380E-04	-0.27	5.324E-04
215	IGFBP2	Tyr	Proteins	Metabolites	ditype	-0.283	8.465E-11	1.084E-07	CKD F4	X	CKD F4 to IGFBP2 to Tyr	Protein to Metabolite	kidney trait in F4	28.36	-0.127 (-0.234 to -0.047)	0.0E+00	0.000E+00	-0.32 (-0.617 to -0.037)	2.40E-02	3.510E-02	0.652	1.167E-03	-0.27	5.324E-04
217	ACY1	Tyr	Proteins	Metabolites	ditype	0.286	4.680E-11	1.084E-07	CKD F4	X	CKD F4 to ACY1 to Tyr	Protein to Metabolite	kidney trait in F4	27.71	-0.124 (-0.21 to -0.057)	0.0E+00	0.000E+00	-0.323 (-0.611 to -0.048)	2.20E-02	3.264E-02	-0.744	2.693E-04	-0.27	5.324E-04
218	Tyr	SPOCK2	Metabolites	Proteins	ditype	0.177	6.005E-05	7.693E-03	CKD F4	Y	Tyr to SPOCK2 to CKD F4	Metabolite to Protein	kidney trait in F4	25.15	-0.009 (-0.017 to -0.002)	0.0E+00	0.000E+00	-0.026 (-0.049 to -0.001)	4.20E-02	5.929E-02	-0.27	5.324E-04	-0.689	2.061E-05
292	SLC22A4	IL19	RNAs	Proteins	ditype	-0.242	3.796E-04	2.431E-02	CKD F4	X	CKD F4 to SLC22A4 to IL19	RNA to Protein	kidney trait in F4	55.22	-0.205 (-0.364 to -0.07)	0.0E+00	0.000E+00	-0.166 (-0.57 to 0.248)	4.04E-01	4.980E-01	0.445	1.196E-05	-0.555	1.445E-03
292									CKD F4	Y	IL19 to SLC22A4 to CKD F4	Protein to RNA	kidney trait in F4	54.1	-0.026 (-0.048 to -0.008)	0.0E+00	0.000E+00	-0.022 (-0.066 to 0.037)	4.18E-01	5.106E-01				
380	NTRK2	NAPA	Proteins	CpGs	ditype	0.149	1.047E-03	4.141E-02	CKD F4	X	CKD F4 to NTRK2 to NAPA	Protein to CpG	kidney trait in F4	23.52	-0.059 (-0.124 to -0.011)	6.0E-03	2.166E-02	-0.191 (-0.492 to 0.079)	1.94E-01	2.595E-01	-0.518	1.411E-03	-0.422	1.541E-05
381	NTRK2	NAPA	Proteins	CpGs	ditype	0.149	1.047E-03	4.141E-02	UACR F4	X	UACR F4 to NTRK2 to NAPA	Protein to CpG	kidney trait in F4	20.54	-0.017 (-0.038 to -0.003)	8.0E-03	4.062E-02	-0.066 (-0.15 to 0.028)	1.68E-01	2.218E-01	-0.11	5.345E-03	-0.101	1.743E-03
552	CST3	C10 2	Proteins	Metabolites	ditype	0.191	1.412E-05	2.783E-03	CKDerc S4	X	CKDerc S4 to CST3 to C10 2	Protein to Metabolite	kidney trait in S4 (as X)	98.45	0.461 (0 to 0.793)	4.0E-03	4.800E-02	0.007 (-1.371 to 1.5)	9.32E-01	9.320E-01	1.962	2.259E-04	0.792	1.423E-04
718	C14 1	IGFBP2	Metabolites	Proteins	ditype	0.145	1.007E-03	4.141E-02	eGFR FF4	Y	C14 1 to IGFBP2 to Follow-up eGFR	Metabolite to Protein	kidney trait in FF4 (as Y)	24.59	-0.032 (-0.054 to -0.013)	0.0E+00	0.000E+00	-0.097 (-0.174 to -0.018)	1.60E-02	2.109E-02	-0.102	1.816E-04	-0.239	7.855E-09
719	C18 1	IGFBP2	Metabolites	Proteins	ditype	0.175	7.070E-05	8.234E-03	eGFR FF4	Y	C18 1 to IGFBP2 to Follow-up eGFR	Metabolite to Protein	kidney trait in FF4 (as Y)	40.91	-0.04 (-0.068 to -0.018)	0.0E+00	0.000E+00	-0.058 (-0.132 to 0.016)	1.30E-01	1.409E-01	-0.081	3.345E-03	-0.239	7.855E-09
720	Tyr	IGFBP2	Metabolites	Proteins	ditype	-0.283	8.465E-11	1.084E-07	eGFR FF4	Y	Tyr to IGFBP2 to Follow-up eGFR	Metabolite to Protein	kidney trait in FF4 (as Y)	68.13	0.052 (0.025 to 0.086)	0.0E+00	0.000E+00	0.024 (-0.046 to 0.088)	5.06E-01	5.060E-01	0.073	5.828E-03	-0.239	7.855E-09
721	C14 1-OH	IGFBP2	Metabolites	Proteins	ditype	0.152	5.995E-04	3.212E-02	eGFR FF4	Y	C14 1-OH to IGFBP2 to Follow-up eGFR	Metabolite to Protein	kidney trait in FF4 (as Y)	19.16	-0.027 (-0.047 to -0.01)	2.0E-03	5.273E-03	-0.113 (-0.191 to -0.032)	4.00E-03	6.187E-03	-0.123	4.789E-06	-0.239	7.855E-09
722	C12	CST3	Metabolites	Proteins	ditype	0.201	4.975E-06	1.416E-03	CKD FF4	Y	C12 to CST3 to incident CKD	Metabolite to Protein	kidney trait in FF4 (as Y)	25.46	0.012 (0.003 to 0.024)	4.0E-03	1.800E-02	0.034 (-0.006 to 0.083)	1.08E-01	1.606E-01	0.327	5.401E-03	0.769	8.144E-05
723	C14 1	CST3	Metabolites	Proteins	ditype	0.171	1.082E-04	1.155E-02	CKD FF4	Y	C14 1 to CST3 to incident CKD	Metabolite to Protein	kidney trait in FF4 (as Y)	29.44	0.011 (0.003 to 0.022)	4.0E-03	1.800E-02	0.027 (-0.013 to 0.08)	1.82E-01	2.047E-01	0.299	9.877E-03	0.769	8.144E-05
724	C14 1	CST3	Metabolites	Proteins	ditype	0.171	1.082E-04	1.155E-02	eGFR FF4	Y	C14 1 to CST3 to Follow-up eGFR	Metabolite to Protein	kidney trait in FF4 (as Y)	56.27	-0.072 (-0.115 to -0.035)	0.0E+00	0.000E+00	-0.056 (-0.12 to 0.007)	1.00E-01	1.137E-01	-0.102	1.816E-04	-0.511	1.985E-49
725	C6(C4 1-DC)	CST3	Metabolites	Proteins	ditype	0.149	7.462E-04	3.476E-02	eGFR FF4	Y	C6(C4 1-DC) to CST3 to Follow-up eGFR	Metabolite to Protein	kidney trait in FF4 (as Y)	46.97	-0.061 (-0.106 to -0.021)	2.0E-03	5.273E-03	-0.069 (-0.123 to -0.009)	2.20E-02	2.836E-02	-0.12	2.184E-05	-0.511	1.985E-49
726	C8	CST3	Metabolites	Proteins	ditype	0.169	1.222E-04	1.182E-02	eGFR FF4	Y	C8 to CST3 to Follow-up eGFR	Metabolite to Protein	kidney trait in FF4 (as Y)	49.28	-0.072 (-0.117 to -0.028)	2.0E-03	5.273E-03	-0.074 (-0.131 to -0.014)	1.60E-02	2.109E-02	-0.139	2.663E-07	-0.511	1.985E-49
727	C12	CST3	Metabolites	Proteins	ditype	0.201	4.975E-06	1.416E-03	eGFR FF4	Y	C12 to CST3 to Follow-up eGFR	Metabolite to Protein	kidney trait in FF4 (as Y)	52.41	-0.082 (-0.125 to -0.041)	2.0E-03	5.273E-03	-0.074 (-0.13 to -0.013)	2.40E-02	3.059E-02	-0.143	2.223E-07	-0.511	1.985E-49
728	C14 2	CST3	Metabolites	Proteins	ditype	0.192	1.319E-05	2.783E-03	eGFR FF4	Y	C14 2 to CST3 to Follow-up eGFR	Metabolite to Protein	kidney trait in FF4 (as Y)	58.05	-0.082 (-0.125 to -0.038)	0.0E+00	0.000E+00	-0.059 (-0.122 to 0.001)	5.20E-02	6.349E-02	-0.112	3.972E-05	-0.511	1.985E-49

729	C10	CST3	Metabolites	Proteins	ditype	0.192	1.287E-05	2.783E-03	eGFR FF4	Y	C10 to CST3 to Follow-up eGFR	Metabolite to Protein	kidney trait in FF4 (as Y)	53.38	-0.084 (-0.127 to -0.04)	0.0E+00	0.000E+00	-0.073 (-0.129 to -0.013)	1.80E-02	2.346E-02	-0.147	8.312E-08	-0.511	1.985E-49
730	C14 1-OH	CST3	Metabolites	Proteins	ditype	0.207	2.596E-06	1.068E-03	eGFR FF4	Y	C14 1-OH to CST3 to Follow-up eGFR	Metabolite to Protein	kidney trait in FF4 (as Y)	61.16	-0.086 (-0.129 to -0.045)	0.0E+00	0.000E+00	-0.055 (-0.115 to 0.008)	8.20E-02	9.418E-02	-0.123	4.789E-06	-0.511	1.985E-49
731	C10 2	CST3	Metabolites	Proteins	ditype	0.191	1.412E-05	2.783E-03	eGFR FF4	Y	C10 2 to CST3 to Follow-up eGFR	Metabolite to Protein	kidney trait in FF4 (as Y)	60.09	-0.091 (-0.134 to -0.05)	0.0E+00	0.000E+00	-0.06 (-0.124 to 0.004)	7.00E-02	8.202E-02	-0.117	6.984E-06	-0.511	1.985E-49
732	C10 2	TNFRSF1A	Metabolites	Proteins	ditype	0.145	1.015E-03	4.141E-02	eGFR FF4	Y	C10 2 to TNFRSF1A to Follow-up eGFR	Metabolite to Protein	kidney trait in FF4 (as Y)	23.9	-0.036 (-0.067 to -0.008)	2.0E-02	2.795E-02	-0.115 (-0.178 to -0.045)	0.00E+00	0.000E+00	-0.117	6.984E-06	-0.311	6.192E-22
734	C12	EGFR	Metabolites	Proteins	ditype	-0.196	8.028E-06	2.057E-03	CKD FF4	Y	C12 to EGFR to incident CKD	Metabolite to Protein	kidney trait in FF4 (as Y)	19.04	0.009 (0.002 to 0.019)	6.0E-03	2.160E-02	0.039 (-0.001 to 0.089)	6.20E-02	1.047E-01	0.327	5.401E-03	-0.509	2.488E-03
735	C18 1	EGFR	Metabolites	Proteins	ditype	-0.209	1.914E-06	9.808E-04	CKD FF4	Y	C18 1 to EGFR to incident CKD	Metabolite to Protein	kidney trait in FF4 (as Y)	27.29	0.01 (0.002 to 0.023)	4.0E-03	1.800E-02	0.027 (-0.013 to 0.079)	2.10E-01	2.224E-01	0.325	6.305E-03	-0.509	2.488E-03
736	C18 1	EGFR	Metabolites	Proteins	ditype	-0.209	1.914E-06	9.808E-04	eGFR FF4	Y	C18 1 to EGFR to Follow-up eGFR	Metabolite to Protein	kidney trait in FF4 (as Y)	49.8	-0.049 (-0.077 to -0.023)	0.0E+00	0.000E+00	-0.049 (-0.118 to 0.023)	1.68E-01	1.788E-01	-0.081	3.345E-03	0.259	1.214E-11
737	C6(C4 1-DC)	EGFR	Metabolites	Proteins	ditype	-0.156	4.077E-04	2.547E-02	eGFR FF4	Y	C6(C4 1-DC) to EGFR to Follow-up eGFR	Metabolite to Protein	kidney trait in FF4 (as Y)	24.95	-0.033 (-0.058 to -0.009)	2.0E-03	5.273E-03	-0.098 (-0.165 to -0.027)	1.00E-02	1.381E-02	-0.12	2.184E-05	0.259	1.214E-11
738	C12	EGFR	Metabolites	Proteins	ditype	-0.196	8.028E-06	2.057E-03	eGFR FF4	Y	C12 to EGFR to Follow-up eGFR	Metabolite to Protein	kidney trait in FF4 (as Y)	28.7	-0.045 (-0.069 to -0.024)	0.0E+00	0.000E+00	-0.111 (-0.187 to -0.038)	8.00E-03	1.146E-02	-0.143	2.223E-07	0.259	1.214E-11
739	C14 1-OH	EGFR	Metabolites	Proteins	ditype	-0.206	2.917E-06	1.068E-03	eGFR FF4	Y	C14 1-OH to EGFR to Follow-up eGFR	Metabolite to Protein	kidney trait in FF4 (as Y)	29.7	-0.042 (-0.066 to -0.019)	0.0E+00	0.000E+00	-0.099 (-0.174 to -0.024)	1.40E-02	1.888E-02	-0.123	4.789E-06	0.259	1.214E-11
740	C16	EGFR	Metabolites	Proteins	ditype	-0.213	1.241E-06	7.951E-04	eGFR FF4	Y	C16 to EGFR to Follow-up eGFR	Metabolite to Protein	kidney trait in FF4 (as Y)	60.35	-0.051 (-0.081 to -0.024)	0.0E+00	0.000E+00	-0.034 (-0.106 to 0.048)	3.62E-01	3.651E-01	-0.07	1.334E-02	0.259	1.214E-11
741	C14 1	EGFR	Metabolites	Proteins	ditype	-0.169	1.250E-04	1.182E-02	eGFR FF4	Y	C14 1 to EGFR to Follow-up eGFR	Metabolite to Protein	kidney trait in FF4 (as Y)	23.59	-0.03 (-0.059 to -0.006)	1.2E-02	1.933E-02	-0.098 (-0.165 to -0.023)	1.20E-02	1.638E-02	-0.102	1.816E-04	0.259	1.214E-11
742	Tyr	FGF20	Metabolites	Proteins	ditype	0.173	8.966E-05	9.987E-03	eGFR FF4	Y	Tyr to FGF20 to Follow-up eGFR	Metabolite to Protein	kidney trait in FF4 (as Y)	35.06	0.027 (0.012 to 0.051)	0.0E+00	0.000E+00	0.049 (-0.019 to 0.108)	1.62E-01	1.740E-01	0.073	5.828E-03	0.154	1.991E-06
743	C18 1	GHR	Metabolites	Proteins	ditype	-0.148	7.800E-04	3.569E-02	CKD FF4	Y	C18 1 to GHR to incident CKD	Metabolite to Protein	kidney trait in FF4 (as Y)	35.18	0.013 (0.003 to 0.027)	2.0E-03	1.800E-02	0.024 (-0.016 to 0.074)	2.42E-01	2.420E-01	0.325	6.305E-03	-0.683	1.930E-04
744	C18 1	GHR	Metabolites	Proteins	ditype	-0.148	7.800E-04	3.569E-02	eGFR FF4	Y	C18 1 to GHR to Follow-up eGFR	Metabolite to Protein	kidney trait in FF4 (as Y)	29.49	-0.029 (-0.052 to -0.01)	0.0E+00	0.000E+00	-0.069 (-0.143 to 0.007)	7.60E-02	8.816E-02	-0.081	3.345E-03	0.178	1.444E-05
745	Tyr	GHR	Metabolites	Proteins	ditype	0.169	1.274E-04	1.182E-02	eGFR FF4	Y	Tyr to GHR to Follow-up eGFR	Metabolite to Protein	kidney trait in FF4 (as Y)	34.36	0.026 (0.01 to 0.046)	0.0E+00	0.000E+00	0.05 (-0.013 to 0.11)	1.20E-01	1.313E-01	0.073	5.828E-03	0.178	1.444E-05
746	Tyr	ESAM	Metabolites	Proteins	ditype	-0.147	8.540E-04	3.809E-02	eGFR FF4	Y	Tyr to ESAM to Follow-up eGFR	Metabolite to Protein	kidney trait in FF4 (as Y)	41.21	0.031 (0.008 to 0.058)	4.0E-03	9.098E-03	0.045 (-0.017 to 0.101)	1.80E-01	1.898E-01	0.073	5.828E-03	-0.236	3.557E-12
747	C10 2	RETN	Metabolites	Proteins	ditype	0.165	1.841E-04	1.474E-02	eGFR FF4	Y	C10 2 to RETN to Follow-up eGFR	Metabolite to Protein	kidney trait in FF4 (as Y)	23.96	-0.036 (-0.06 to -0.016)	0.0E+00	0.000E+00	-0.115 (-0.18 to -0.043)	0.00E+00	0.000E+00	-0.117	6.984E-06	-0.226	5.657E-12
748	TS13	C12	Proteins	Metabolites	ditype	-0.15	7.029E-04	3.463E-02	eGFR FF4	Y	ADAMTS13 to C12 to Follow-up eGFR	Protein to Metabolite	kidney trait in FF4 (as Y)	13.48	0.016 (0.004 to 0.032)	2.0E-03	5.273E-03	0.1 (0.045 to 0.161)	0.00E+00	0.000E+00	0.111	6.823E-04	-0.143	2.223E-07
749	ADAM TS13	C10 2	Proteins	Metabolites	ditype	-0.154	5.058E-04	3.014E-02	eGFR FF4	Y	ADAMTS13 to C10 2 to Follow-up eGFR	Protein to Metabolite	kidney trait in FF4 (as Y)	15.87	0.018 (0.005 to 0.036)	2.0E-03	5.273E-03	0.097 (0.042 to 0.156)	0.00E+00	0.000E+00	0.111	6.823E-04	-0.117	6.984E-06

750	C14 1-OH	ADAMTS13	Metabolites	Proteins	diftype	-0.151	6.443E-04	3.369E-02	eGFR FF4	Y	C14 1-OH to ADAMTS13 to Follow-up eGFR	Metabolite to Protein	kidney trait in FF4 (as Y)	10.33	-0.014 (-0.029 to -0.004)	8.0E-03	1.473E-02	-0.126 (-0.203 to -0.05)	2.00E-03	3.412E-03	-0.123	4.789E-06	0.111	6.823E-04
751	Tyr	ACY1	Metabolites	Proteins	diftype	0.286	4.680E-11	1.084E-07	eGFR FF4	Y	Tyr to ACY1 to Follow-up eGFR	Metabolite to Protein	kidney trait in FF4 (as Y)	41.93	0.032 (0.013 to 0.057)	0.0E+00	0.000E+00	0.044 (-0.021 to 0.106)	2.28E-01	2.383E-01	0.073	5.828E-03	0.157	1.315E-04
752	C18 1	BMP1	Metabolites	Proteins	diftype	-0.176	6.822E-05	8.234E-03	eGFR FF4	Y	C18 1 to BMP1 to Follow-up eGFR	Metabolite to Protein	kidney trait in FF4 (as Y)	29.04	-0.028 (-0.053 to -0.008)	6.0E-03	1.160E-02	-0.07 (-0.144 to 0.009)	7.00E-02	8.202E-02	-0.081	3.345E-03	0.178	5.497E-06
753	BMP1	C14 1-OH	Proteins	Metabolites	diftype	-0.162	2.522E-04	1.874E-02	eGFR FF4	Y	BMP1 to C14 1-OH to Follow-up eGFR	Protein to Metabolite	kidney trait in FF4 (as Y)	10.67	0.018 (0.004 to 0.038)	1.6E-02	2.379E-02	0.154 (0.055 to 0.237)	8.00E-03	1.146E-02	0.178	5.497E-06	-0.123	4.789E-06
754	C16	BMP1	Metabolites	Proteins	diftype	-0.145	1.050E-03	4.141E-02	eGFR FF4	Y	C16 to BMP1 to Follow-up eGFR	Metabolite to Protein	kidney trait in FF4 (as Y)	25.96	-0.022 (-0.045 to -0.004)	1.0E-02	1.681E-02	-0.063 (-0.141 to 0.013)	1.14E-01	1.259E-01	-0.07	1.334E-02	0.178	5.497E-06
755	FN1	C14 1-OH	Proteins	Metabolites	diftype	-0.155	4.480E-04	2.732E-02	eGFR FF4	Y	FN1 to C14 1-OH to Follow-up eGFR	Protein to Metabolite	kidney trait in FF4 (as Y)	13.84	0.016 (0.004 to 0.034)	2.0E-03	5.273E-03	0.099 (0.033 to 0.161)	2.00E-03	3.412E-03	0.11	1.156E-03	-0.123	4.789E-06
755									eGFR FF4	Y	C14 1-OH to FN1 to Follow-up eGFR	Metabolite to Protein	kidney trait in FF4 (as Y)	10.13	-0.014 (-0.03 to -0.003)	2.0E-03	5.273E-03	-0.126 (-0.203 to -0.049)	2.00E-03	3.412E-03				
756	C12	B2M	Metabolites	Proteins	diftype	0.184	3.094E-05	4.663E-03	CKD FF4	Y	C12 to B2M to incident CKD	Metabolite to Protein	kidney trait in FF4 (as Y)	18.29	0.009 (0.001 to 0.019)	8.0E-03	2.400E-02	0.038 (-0.002 to 0.091)	6.40E-02	1.047E-01	0.327	5.401E-03	0.561	9.322E-04
757	C14 1	B2M	Metabolites	Proteins	diftype	0.184	3.089E-05	4.663E-03	CKD FF4	Y	C14 1 to B2M to incident CKD	Metabolite to Protein	kidney trait in FF4 (as Y)	25.92	0.01 (0.002 to 0.021)	1.2E-02	2.700E-02	0.029 (-0.011 to 0.083)	1.58E-01	2.031E-01	0.299	9.877E-03	0.561	9.322E-04
758	C18 1	B2M	Metabolites	Proteins	diftype	0.152	5.578E-04	3.107E-02	CKD FF4	Y	C18 1 to B2M to incident CKD	Metabolite to Protein	kidney trait in FF4 (as Y)	27.2	0.011 (0.002 to 0.023)	1.0E-02	2.571E-02	0.029 (-0.015 to 0.082)	1.78E-01	2.047E-01	0.325	6.305E-03	0.561	9.322E-04
759	C6(C4 1-DC)	B2M	Metabolites	Proteins	diftype	0.159	3.112E-04	2.044E-02	eGFR FF4	Y	C6(C4 1-DC) to B2M to Follow-up eGFR	Metabolite to Protein	kidney trait in FF4 (as Y)	40.89	-0.053 (-0.094 to -0.018)	0.0E+00	0.000E+00	-0.077 (-0.14 to -0.015)	1.00E-02	1.381E-02	-0.12	2.184E-05	-0.384	1.594E-30
760	C18 1	B2M	Metabolites	Proteins	diftype	0.152	5.578E-04	3.107E-02	eGFR FF4	Y	C18 1 to B2M to Follow-up eGFR	Metabolite to Protein	kidney trait in FF4 (as Y)	59.84	-0.059 (-0.101 to -0.019)	0.0E+00	0.000E+00	-0.039 (-0.105 to 0.027)	2.62E-01	2.690E-01	-0.081	3.345E-03	-0.384	1.594E-30
761	C12	B2M	Metabolites	Proteins	diftype	0.184	3.094E-05	4.663E-03	eGFR FF4	Y	C12 to B2M to Follow-up eGFR	Metabolite to Protein	kidney trait in FF4 (as Y)	39.14	-0.061 (-0.1 to -0.025)	0.0E+00	0.000E+00	-0.095 (-0.16 to -0.028)	8.00E-03	1.146E-02	-0.143	2.223E-07	-0.384	1.594E-30
762	C14 1-OH	B2M	Metabolites	Proteins	diftype	0.204	3.408E-06	1.091E-03	eGFR FF4	Y	C14 1-OH to B2M to Follow-up eGFR	Metabolite to Protein	kidney trait in FF4 (as Y)	54.55	-0.077 (-0.115 to -0.043)	0.0E+00	0.000E+00	-0.064 (-0.133 to 0.004)	6.40E-02	7.733E-02	-0.123	4.789E-06	-0.384	1.594E-30
763	C10 2	B2M	Metabolites	Proteins	diftype	0.153	5.546E-04	3.107E-02	eGFR FF4	Y	C10 2 to B2M to Follow-up eGFR	Metabolite to Protein	kidney trait in FF4 (as Y)	38.31	-0.058 (-0.092 to -0.023)	0.0E+00	0.000E+00	-0.093 (-0.153 to -0.029)	4.00E-03	6.187E-03	-0.117	6.984E-06	-0.384	1.594E-30
764	C14 1	B2M	Metabolites	Proteins	diftype	0.184	3.089E-05	4.663E-03	eGFR FF4	Y	C14 1 to B2M to Follow-up eGFR	Metabolite to Protein	kidney trait in FF4 (as Y)	49.43	-0.063 (-0.108 to -0.027)	0.0E+00	0.000E+00	-0.065 (-0.131 to 0.006)	6.60E-02	7.893E-02	-0.102	1.816E-04	-0.384	1.594E-30
765	C14 2	B2M	Metabolites	Proteins	diftype	0.188	1.873E-05	3.428E-03	eGFR FF4	Y	C14 2 to B2M to Follow-up eGFR	Metabolite to Protein	kidney trait in FF4 (as Y)	47.41	-0.067 (-0.106 to -0.033)	0.0E+00	0.000E+00	-0.075 (-0.143 to -0.007)	2.60E-02	3.278E-02	-0.112	3.972E-05	-0.384	1.594E-30
766	C10	B2M	Metabolites	Proteins	diftype	0.187	2.113E-05	3.609E-03	eGFR FF4	Y	C10 to B2M to Follow-up eGFR	Metabolite to Protein	kidney trait in FF4 (as Y)	37.4	-0.059 (-0.097 to -0.021)	2.0E-03	5.273E-03	-0.098 (-0.164 to 0.033)	2.00E-03	3.412E-03	-0.147	8.312E-08	-0.384	1.594E-30
767	C8	B2M	Metabolites	Proteins	diftype	0.181	4.091E-05	5.823E-03	eGFR FF4	Y	C8 to B2M to Follow-up eGFR	Metabolite to Protein	kidney trait in FF4 (as Y)	38.15	-0.055 (-0.095 to -0.017)	6.0E-03	1.160E-02	-0.09 (-0.155 to -0.02)	1.00E-02	1.381E-02	-0.139	2.663E-07	-0.384	1.594E-30
769	C18 1	CNDP1	Metabolites	Proteins	diftype	-0.149	7.380E-04	3.476E-02	eGFR FF4	Y	C18 1 to CNDP1 to Follow-up eGFR	Metabolite to Protein	kidney trait in FF4 (as Y)	19.93	-0.02 (-0.038 to -0.004)	6.0E-03	1.160E-02	-0.078 (-0.151 to 0)	5.00E-02	6.170E-02	-0.081	3.345E-03	0.141	2.240E-05

771	Tyr	MASP1	Metabolites	Proteins	diftype	0.153	5.525E-04	3.107E-02	eGFR FF4	Y	Tyr to MASP1 to Follow-up eGFR	Metabolite to Protein	kidney trait in FF4 (as Y)	13.86	0.011 (0.001 to 0.026)	1.0E-02	1.681E-02	0.065 (0.001 to 0.127)	5.00E-02	6.170E-02	0.073	5.828E-03	0.091	5.181E-03
772	C14 1-OH	KDR	Metabolites	Proteins	diftype	-0.169	1.323E-04	1.182E-02	eGFR FF4	Y	C14 1-OH to KDR to Follow-up eGFR	Metabolite to Protein	kidney trait in FF4 (as Y)	14.98	-0.021 (-0.037 to -0.007)	2.0E-03	5.273E-03	-0.119 (-0.195 to -0.048)	4.00E-03	6.187E-03	-0.123	4.789E-06	0.163	2.182E-06
773	C16	KDR	Metabolites	Proteins	diftype	-0.149	7.444E-04	3.476E-02	eGFR FF4	Y	C16 to KDR to Follow-up eGFR	Metabolite to Protein	kidney trait in FF4 (as Y)	25.22	-0.021 (-0.041 to -0.005)	1.0E-02	1.681E-02	-0.063 (-0.141 to 0.014)	1.06E-01	1.194E-01	-0.07	1.334E-02	0.163	2.182E-06
776	Tyr	TFF3	Metabolites	Proteins	diftype	-0.16	2.805E-04	1.936E-02	eGFR FF4	Y	Tyr to TFF3 to Follow-up eGFR	Metabolite to Protein	kidney trait in FF4 (as Y)	49.7	0.038 (0.017 to 0.063)	0.0E+00	0.000E+00	0.038 (-0.029 to 0.096)	2.58E-01	2.672E-01	0.073	5.828E-03	-0.255	3.473E-13
777	AMH	C14 1-OH	Proteins	Metabolites	diftype	-0.142	1.285E-03	4.886E-02	eGFR FF4	Y	AMH to C14 1-OH to Follow-up eGFR	Protein to Metabolite	kidney trait in FF4 (as Y)	16.86	0.019 (0.005 to 0.039)	4.0E-03	9.098E-03	0.094 (0.017 to 0.166)	8.00E-03	1.146E-02	0.112	1.293E-03	-0.123	4.789E-06
778	C14 1-OH	C1QBP	Metabolites	Proteins	diftype	-0.16	2.817E-04	1.936E-02	eGFR FF4	Y	C14 1-OH to C1QBP to Follow-up eGFR	Metabolite to Protein	kidney trait in FF4 (as Y)	12.39	-0.017 (-0.037 to -0.004)	4.0E-03	9.098E-03	-0.123 (-0.2 to -0.045)	2.00E-03	3.412E-03	-0.123	4.789E-06	0.14	3.746E-05
779	C1QBP	C12	Proteins	Metabolites	diftype	-0.152	6.018E-04	3.212E-02	eGFR FF4	Y	C1QBP to C12 to Follow-up eGFR	Protein to Metabolite	kidney trait in FF4 (as Y)	10.16	0.014 (0.001 to 0.032)	2.4E-02	3.164E-02	0.125 (0.059 to 0.192)	0.00E+00	0.000E+00	0.14	3.746E-05	-0.143	2.223E-07
780	C16	C1QBP	Metabolites	Proteins	diftype	-0.146	9.642E-04	4.141E-02	eGFR FF4	Y	C16 to C1QBP to Follow-up eGFR	Metabolite to Protein	kidney trait in FF4 (as Y)	25.15	-0.021 (-0.041 to -0.006)	4.0E-03	9.098E-03	-0.063 (-0.141 to 0.014)	1.10E-01	1.227E-01	-0.07	1.334E-02	0.14	3.746E-05
781	C10 2	RELT	Metabolites	Proteins	diftype	0.177	5.828E-05	7.693E-03	eGFR FF4	Y	C10 2 to RELT to Follow-up eGFR	Metabolite to Protein	kidney trait in FF4 (as Y)	35.95	-0.054 (-0.084 to -0.025)	0.0E+00	0.000E+00	-0.097 (-0.162 to -0.026)	2.00E-03	3.412E-03	-0.117	6.984E-06	-0.343	1.967E-24
782	C10 2	TNFRSF19	Metabolites	Proteins	diftype	0.15	6.887E-04	3.460E-02	eGFR FF4	Y	C10 2 to TNFRSF19 to Follow-up eGFR	Metabolite to Protein	kidney trait in FF4 (as Y)	14.19	-0.021 (-0.043 to -0.006)	6.0E-03	1.160E-02	-0.13 (-0.194 to -0.057)	0.00E+00	0.000E+00	-0.117	6.984E-06	-0.185	2.628E-09
783	C8	UNC5C	Metabolites	Proteins	diftype	0.145	1.025E-03	4.141E-02	eGFR FF4	Y	C8 to UNC5C to Follow-up eGFR	Metabolite to Protein	kidney trait in FF4 (as Y)	22.84	-0.033 (-0.061 to -0.012)	4.0E-03	9.098E-03	-0.112 (-0.184 to -0.04)	2.00E-03	3.412E-03	-0.139	2.663E-07	-0.239	2.111E-11
784	C10 2	UNC5C	Metabolites	Proteins	diftype	0.15	6.728E-04	3.447E-02	eGFR FF4	Y	C10 2 to UNC5C to Follow-up eGFR	Metabolite to Protein	kidney trait in FF4 (as Y)	20.12	-0.03 (-0.052 to -0.01)	2.0E-03	5.273E-03	-0.121 (-0.185 to -0.051)	0.00E+00	0.000E+00	-0.117	6.984E-06	-0.239	2.111E-11
785	Tyr	SPOCK2	Metabolites	Proteins	diftype	0.177	6.005E-05	7.693E-03	eGFR FF4	Y	Tyr to SPOCK2 to Follow-up eGFR	Metabolite to Protein	kidney trait in FF4 (as Y)	52.45	0.04 (0.015 to 0.067)	2.0E-03	5.273E-03	0.036 (-0.027 to 0.1)	2.92E-01	2.971E-01	0.073	5.828E-03	0.23	1.421E-12

Supplementary Table 18. Best mediation directions of causal mediation analysis of omics candidates & known biomarkers & three time points of kidney traits.

Within each identified best mediation direction, spearman correlation coefficients, *P*-values and FDR of each pair (FDR < 0.05) of residuals of omics candidates and three known biomarkers (CST3, creatinine, urine albumin), and regression coefficients and *P*-values of omics molecules with kidney traits in hyperglycemic individuals of KORA F4 are shown, respectively. Residuals of omics molecules were calculated with linear regression analysis for full model (incl. age, sex, BMI, systolic blood pressure, smoking status, triglyceride, total cholesterol, HDL cholesterol, fasting glucose, use of lipid lowering drugs, antihypertensive and anti-diabetic medication).

The mediation proportion (%), average mediating effect with 95% *CI*, *P*-values and FDR, average direct effect with 95% *CI*, *P*-values and FDR of the identified best direction(s) of mediating triangles in a nonparametric causal mediation analysis are shown, respectively. Each mediation analysis was adjusted for the full model. FDR of mediating effect and direct effect were calculated per kidney trait.

Abbreviations: CKD, chronic kidney disease; eGFR, estimated glomerular filtration rate; UACR, urinary albumin-to-creatinine ratio; CKDcrcc, eGFR-based CKD that was defined as eGFR < 60 ml/min/1.73 m².

triangle	omics1.1		omics2.1		omics.asso.				kidney. trait	sitio	Mediation direction	time.point.ki dney. trait	Proportion. media(%)	Avg.media (95% CI)	Avg.media .p-value	Avg.media.F DR	Avg.direct (95% CI)	Avg.direct. p-value	Avg.direct. FDR	P- Estimate.o value.omic		P- Estimate.o value.omic	
	abel	abel	omics1.type	omics2.type	type	spearcor	p-value	FDR												omics1.kidn ey. trait	s1.kidney. trait	omics2.kidn ey. trait	s2.kidney. trait
1	Urine albumin	C10	UACRbiom	Metabolites	diftype	0.072	7.459E-03	1.568E-02	CKD F4	M	Urine albumin to CKD F4 to C10	kidney trait in F4	50.12	0.048 (0.012 to 0.086)	4.0E-03	9.406E-03	0.048 (-0.015 to 0.111)	1.48E-01	1.641E-01	1.585	4.296E-43	0.278	8.764E-04
3	C10	CST3	Metabolites	eGFRbiom	diftype	0.218	3.764E-16	6.377E-15	eGFR F4	M	C10 to eGFR F4 to CST3	kidney trait in F4	92.87	0.172 (0.134 to 0.21)	0.0E+00	0.000E+00	0.013 (-0.008 to 0.037)	2.66E-01	3.463E-01	-0.174	1.585E-17	-0.78	0.000E+00
4	C10	CST3	Metabolites	eGFRbiom	diftype	0.218	3.764E-16	6.377E-15	CKD F4	Y	C10 to CST3 to CKD F4	kidney trait in F4	81.48	0.034 (0.024 to 0.043)	0.0E+00	0.000E+00	0.008 (-0.015 to 0.028)	4.76E-01	4.888E-01	0.278	8.764E-04	1.437	1.040E-29
4									CKD F4	X	CKD F4 to CST3 to C10	kidney trait in F4	79.13	0.203 (0.147 to 0.264)	0.0E+00	0.000E+00	0.054 (-0.077 to 0.188)	4.04E-01	4.184E-01				
8	C10	Creatinine	Metabolites	eGFRbiom	diftype	0.184	6.433E-12	6.617E-11	CKD F4	Y	C10 to Creatinine to CKD F4	kidney trait in F4	62.88	0.025 (0.016 to 0.034)	0.0E+00	0.000E+00	0.015 (-0.005 to 0.035)	1.46E-01	1.624E-01	0.278	8.764E-04	1.153	1.412E-24
8									CKD F4	X	CKD F4 to Creatinine to C10	kidney trait in F4	57.89	0.148 (0.096 to 0.204)	0.0E+00	0.000E+00	0.108 (-0.018 to 0.235)	9.00E-02	1.071E-01				
18	C10:2	Creatinine	Metabolites	eGFRbiom	diftype	0.206	1.449E-14	1.897E-13	CKD F4	Y	C10:2 to Creatinine to CKD F4	kidney trait in F4	71.72	0.027 (0.018 to 0.036)	0.0E+00	0.000E+00	0.011 (-0.01 to 0.028)	3.26E-01	3.422E-01	0.276	2.971E-04	1.153	1.412E-24
18									CKD F4	X	CKD F4 to Creatinine to C10:2	kidney trait in F4	65.55	0.187 (0.127 to 0.254)	0.0E+00	0.000E+00	0.098 (-0.049 to 0.237)	1.92E-01	2.082E-01				
20	C10:2	CST3	Metabolites	eGFRbiom	diftype	0.241	1.527E-19	4.398E-18	CKD F4	Y	C10:2 to CST3 to CKD F4	kidney trait in F4	94.82	0.034 (0.024 to 0.044)	0.0E+00	0.000E+00	0.002 (-0.017 to 0.021)	8.64E-01	8.675E-01	0.276	2.971E-04	1.437	1.040E-29
20									CKD F4	X	CKD F4 to CST3 to C10:2	kidney trait in F4	82.2	0.235 (0.167 to 0.304)	0.0E+00	0.000E+00	0.051 (-0.088 to 0.191)	5.46E-01	5.596E-01				
23	C10:2	CST3	Metabolites	eGFRbiom	diftype	0.241	1.527E-19	4.398E-18	eGFR F4	M	C10:2 to eGFR F4 to CST3	kidney trait in F4	93.33	0.175 (0.138 to 0.216)	0.0E+00	0.000E+00	0.013 (-0.008 to 0.033)	2.50E-01	3.288E-01	-0.178	1.691E-20	-0.78	0.000E+00
24	C10:2	Creatinine	Metabolites	eGFRbiom	diftype	0.206	1.449E-14	1.897E-13	eGFR F4	M	C10:2 to eGFR F4 to Creatinine	kidney trait in F4	97.8	0.174 (0.137 to 0.215)	0.0E+00	0.000E+00	0.004 (-0.02 to 0.03)	7.78E-01	8.185E-01	-0.178	1.691E-20	-0.726	0.000E+00
24									eGFR F4	M	Creatinine to eGFR F4 to C10:2	kidney trait in F4	92.45	0.243 (0.136 to 0.347)	0.0E+00	0.000E+00	0.02 (-0.104 to 0.147)	7.78E-01	8.185E-01				
37	C12	CST3	Metabolites	eGFRbiom	diftype	0.248	1.196E-20	4.304E-19	CKD F4	Y	C12 to CST3 to CKD F4	kidney trait in F4	84.87	0.037 (0.027 to 0.048)	0.0E+00	0.000E+00	0.007 (-0.014 to 0.028)	5.90E-01	6.034E-01	0.288	5.855E-04	1.437	1.040E-29
37									CKD F4	X	CKD F4 to CST3 to C12	kidney trait in F4	83.85	0.222 (0.164 to 0.29)	0.0E+00	0.000E+00	0.043 (-0.084 to 0.172)	5.30E-01	5.437E-01				
42	C12	CST3	Metabolites	eGFRbiom	diftype	0.248	1.196E-20	4.304E-19	eGFR F4	Y	C12 to CST3 to eGFR F4	kidney trait in F4	94.01	-0.165 (-0.201 to -0.13)	0.0E+00	0.000E+00	-0.01 (-0.031 to 0.011)	3.24E-01	4.039E-01	-0.175	3.042E-17	-0.78	0.000E+00

47	Urine albumin	C12	UACRbiom	Metabolites	diotype	0 072 7 402E-03	1 567E-02	CKD F4	M	Urine albumin to CKD F4 to C12	kidney trait in F4	54 72	0 052 (0 016 to 0 09)	4 0E-03	9 406E-03	0 043 (-0 014 to 0 101)	1 32E-01	1 500E-01	1 585 4 296E-43	0 288 5 855E-04
52	C14:1	CST3	Metabolites	eGFRbiom	diotype	0 191 9 890E-13	1 055E-11	CKD F4	Y	C14:1 to CST3 to CKD F4	kidney trait in F4	67 62	0 027 (0 018 to 0 035)	0 0E+00	0 000E+00	0 013 (-0 008 to 0 036)	2 46E-01	2 619E-01	0 268 4 948E-04	1 437 1 040E-29
52								CKD F4	X	CKD F4 to CST3 to C14:1	kidney trait in F4	55 09	0 171 (0 114 to 0 236)	0 0E+00	0 000E+00	0 139 (-0 016 to 0 289)	7 60E-02	9 187E-02		
95	C14:2	CST3	Metabolites	eGFRbiom	diotype	0 244 5 241E-20	1 677E-18	CKD F4	Y	C14:2 to CST3 to CKD F4	kidney trait in F4	84 4	0 035 (0 025 to 0 045)	0 0E+00	0 000E+00	0 006 (-0 016 to 0 03)	6 26E-01	6 350E-01	0 299 2 943E-04	1 437 1 040E-29
95								CKD F4	X	CKD F4 to CST3 to C14:2	kidney trait in F4	74 47	0 215 (0 157 to 0 281)	0 0E+00	0 000E+00	0 074 (-0 068 to 0 214)	3 38E-01	3 545E-01		
99	C14:2	CST3	Metabolites	eGFRbiom	diotype	0 244 5 241E-20	1 677E-18	eGFR F4	Y	C14:2 to CST3 to eGFR F4	kidney trait in F4	93 57	-0 155 (-0 19 to -0 122)	0 0E+00	0 000E+00	-0 011 (-0 031 to 0 01)	2 60E-01	3 396E-01	-0 166 2 691E-16	-0 78 0 000E+00
113	C16	Urine albumin	Metabolites	UACRbiom	diotype	0 133 8 435E-07	3 626E-06	CKD F4	Y	C16 to Urine albumin to CKD F4	kidney trait in F4	63 79	0 026 (0 016 to 0 038)	0 0E+00	0 000E+00	0 015 (-0 007 to 0 04)	1 80E-01	1 960E-01	0 3 3 705E-04	1 585 4 296E-43
113								CKD F4	X	CKD F4 to Urine albumin to C16	kidney trait in F4	51 38	0 147 (0 074 to 0 228)	0 0E+00	0 000E+00	0 139 (-0 011 to 0 302)	7 20E-02	8 778E-02		
118	C18:1	Urine albumin	Metabolites	UACRbiom	diotype	0 127 2 547E-06	1 019E-05	CKD F4	Y	C18:1 to Urine albumin to CKD F4	kidney trait in F4	75 63	0 026 (0 017 to 0 038)	0 0E+00	0 000E+00	0 008 (-0 011 to 0 03)	4 30E-01	4 444E-01	0 265 1 336E-03	1 585 4 296E-43
118								CKD F4	X	CKD F4 to Urine albumin to C18:1	kidney trait in F4	68 37	0 166 (0 099 to 0 248)	0 0E+00	0 000E+00	0 077 (-0 071 to 0 229)	3 26E-01	3 422E-01		
131	C18:1	CST3	Metabolites	eGFRbiom	diotype	0 14 1 998E-07	9 280E-07	CKD F4	Y	C18:1 to CST3 to CKD F4	kidney trait in F4	52 7	0 02 (0 011 to 0 029)	0 0E+00	0 000E+00	0 018 (-0 005 to 0 044)	1 26E-01	1 440E-01	0 265 1 336E-03	1 437 1 040E-29
131								CKD F4	X	CKD F4 to CST3 to C18:1	kidney trait in F4	43 69	0 105 (0 048 to 0 169)	0 0E+00	0 000E+00	0 135 (-0 012 to 0 281)	6 80E-02	8 311E-02		
138	Urine albumin	C2	UACRbiom	Metabolites	diotype	0 077 4 233E-03	9 754E-03	CKD F4	M	Urine albumin to CKD F4 to C2	kidney trait in F4	57 81	0 057 (0 019 to 0 098)	2 0E-03	5 252E-03	0 042 (-0 013 to 0 098)	1 40E-01	1 568E-01	1 585 4 296E-43	0 334 5 475E-05
140	C2	CST3	Metabolites	eGFRbiom	diotype	0 205 2 225E-14	2 670E-13	eGFR F4	Y	C2 to CST3 to eGFR F4	kidney trait in F4	96 81	-0 144 (-0 186 to -0 11)	0 0E+00	0 000E+00	-0 005 (-0 025 to 0 016)	6 28E-01	6 930E-01	-0 149 3 483E-13	-0 78 0 000E+00
141	CST3	C2	eGFRbiom	Metabolites	diotype	0 205 2 225E-14	2 670E-13	CKD F4	X	CKD F4 to CST3 to C2	kidney trait in F4	68 08	0 192 (0 136 to 0 259)	0 0E+00	0 000E+00	0 09 (-0 045 to 0 226)	1 96E-01	2 123E-01	1 437 1 040E-29	0 334 5 475E-05
141								CKD F4	Y	C2 to CST3 to CKD F4	kidney trait in F4	68 06	0 032 (0 022 to 0 043)	0 0E+00	0 000E+00	0 015 (-0 007 to 0 038)	1 82E-01	1 978E-01		

154	C5	Creatinine	Metabolites	eGFRbiom	diftype	0 182	1 204E-11	1 119E-10	eGFR F4	M	C5 to eGFR F4 to Creatinine	kidney trait in F4	97 77	0 156 (0 116 to 0 2)	0 0E+00	0 000E+00	0 004 (-0 022 to 0 029)	8 10E-01	8 429E-01	-0 16	4 603E-14	-0 726	0 000E+00
154									eGFR F4	M	Creatinine to eGFR F4 to C5	kidney trait in F4	92 2	0 181 (0 093 to 0 282)	0 0E+00	0 000E+00	0 015 (-0 096 to 0 129)	8 10E-01	8 429E-01				
155	C5	Creatinine	Metabolites	eGFRbiom	diftype	0 182	1 204E-11	1 119E-10	CKD F4	Y	C5 to Creatinine to CKD F4	kidney trait in F4	74 28	0 024 (0 016 to 0 034)	0 0E+00	0 000E+00	0 008 (-0 013 to 0 031)	4 60E-01	4 734E-01	0 258	2 331E-03	1 153	1 412E-24
155									CKD F4	X	CKD F4 to Creatinine to C5	kidney trait in F4	64 95	0 139 (0 088 to 0 202)	0 0E+00	0 000E+00	0 075 (-0 06 to 0 214)	2 60E-01	2 762E-01				
156	C5	CST3	Metabolites	eGFRbiom	diftype	0 182	1 247E-11	1 122E-10	eGFR F4	M	C5 to eGFR F4 to CST3	kidney trait in F4	97 96	0 157 (0 117 to 0 203)	0 0E+00	0 000E+00	0 003 (-0 02 to 0 025)	7 78E-01	8 185E-01	-0 16	4 603E-14	-0 78	0 000E+00
156									eGFR F4	M	CST3 to eGFR F4 to C5	kidney trait in F4	90 46	0 192 (0 068 to 0 312)	0 0E+00	0 000E+00	0 02 (-0 121 to 0 155)	7 78E-01	8 185E-01				
157	C5	CST3	Metabolites	eGFRbiom	diftype	0 182	1 247E-11	1 122E-10	CKD F4	Y	C5 to CST3 to CKD F4	kidney trait in F4	89 08	0 029 (0 019 to 0 04)	0 0E+00	0 000E+00	0 004 (-0 019 to 0 025)	7 32E-01	7 380E-01	0 258	2 331E-03	1 437	1 040E-29
157									CKD F4	X	CKD F4 to CST3 to C5	kidney trait in F4	77 03	0 165 (0 106 to 0 229)	0 0E+00	0 000E+00	0 049 (-0 085 to 0 185)	4 68E-01	4 811E-01				
160	C8	Urine albumin	Metabolites	UACRbiom	diftype	0 079	3 532E-03	8 270E-03	CKD F4	Y	C8 to Urine albumin to CKD F4	kidney trait in F4	52 78	0 015 (0 005 to 0 025)	0 0E+00	0 000E+00	0 013 (-0 007 to 0 036)	2 16E-01	2 334E-01	0 23	4 287E-03	1 585	4 296E-43
161	C8	CST3	Metabolites	eGFRbiom	diftype	0 213	1 922E-15	3 076E-14	eGFR F4	M	C8 to eGFR F4 to CST3	kidney trait in F4	92 2	0 122 (0 122 to 0 2)	0 0E+00	0 000E+00	0 014 (-0 007 to 0 035)	2 24E-01	3 018E-01	-0 163	5 665E-16	-0 78	0 000E+00
165	C8	Creatinine	Metabolites	eGFRbiom	diftype	0 179	2 374E-11	2 072E-10	CKD F4	Y	C8 to Creatinine to CKD F4	kidney trait in F4	71 69	0 023 (0 015 to 0 032)	0 0E+00	0 000E+00	0 009 (-0 009 to 0 03)	3 50E-01	3 667E-01	0 23	4 287E-03	1 153	1 412E-24
165									CKD F4	X	CKD F4 to Creatinine to C8	kidney trait in F4	61 5	0 144 (0 088 to 0 202)	0 0E+00	0 000E+00	0 09 (-0 043 to 0 224)	1 74E-01	1 897E-01				
168	C8	CST3	Metabolites	eGFRbiom	diftype	0 213	1 922E-15	3 076E-14	CKD F4	Y	C8 to CST3 to CKD F4	kidney trait in F4	89 86	0 032 (0 022 to 0 041)	0 0E+00	0 000E+00	0 004 (-0 016 to 0 023)	7 28E-01	7 347E-01	0 23	4 287E-03	1 437	1 040E-29
168									CKD F4	X	CKD F4 to CST3 to C8	kidney trait in F4	85 29	0 2 (0 145 to 0 265)	0 0E+00	0 000E+00	0 035 (-0 103 to 0 17)	5 94E-01	6 069E-01				
169	C8:1	CST3	Metabolites	eGFRbiom	diftype	0 166	6 150E-10	4 428E-09	eGFR F4	Y	C8:1 to CST3 to eGFR F4	kidney trait in F4	90 16	-0 11 (-0 144 to -0 074)	0 0E+00	0 000E+00	-0 012 (-0 028 to 0 007)	2 36E-01	3 147E-01	-0 122	3 964E-10	-0 78	0 000E+00
169									eGFR F4	M	C8:1 to eGFR F4 to CST3	kidney trait in F4	87 49	0 12 (0 08 to 0 159)	0 0E+00	0 000E+00	0 017 (-0 002 to 0 038)	8 80E-02	1 325E-01				

170	C8:1	Creatinine	Metabolites	eGFRbiom	diotype	0.141	1.648E-07	7.910E-07	eGFR F4	M	C8:1 to eGFR F4 to Creatinine	kidney trait in F4	96.28	0.119 (0.08 to 0.158)	0.0E+00	0.000E+00	0.005 (-0.019 to 0.029)	7.46E-01	7.979E-01	-0.122	3.964E-10	-0.726	0.000E+00
171	C8:1	CST3	Metabolites	eGFRbiom	diotype	0.166	6.150E-10	4.428E-09	CKD F4	Y	C8:1 to CST3 to CKD F4	kidney trait in F4	68.57	0.025 (0.015 to 0.034)	0.0E+00	0.000E+00	0.011 (-0.008 to 0.031)	2.42E-01	2.582E-01	0.257	8.036E-04	1.437	1.040E-29
171									CKD F4	X	CKD F4 to CST3 to C8:1	kidney trait in F4	59.04	0.158 (0.093 to 0.223)	0.0E+00	0.000E+00	0.011 (-0.041 to 0.25)	1.52E-01	1.683E-01				
172	C8:1	Creatinine	Metabolites	eGFRbiom	diotype	0.141	1.648E-07	7.910E-07	CKD F4	Y	C8:1 to Creatinine to CKD F4	kidney trait in F4	56.38	0.019 (0.011 to 0.026)	0.0E+00	0.000E+00	0.014 (-0.005 to 0.034)	1.48E-01	1.641E-01	0.257	8.036E-04	1.153	1.412E-24
172									CKD F4	X	CKD F4 to Creatinine to C8:1	kidney trait in F4	44.24	0.119 (0.064 to 0.179)	0.0E+00	0.000E+00	0.15 (0.013 to 0.294)	4.00E-02	5.197E-02				
175	CST3	PNLIPRP2	eGFRbiom	RNAs	diotype	0.09	1.987E-02	3.692E-02	CKD F4	M	CST3 to CKD F4 to PNLIPRP2	kidney trait in F4	71.52	0.098 (0.03 to 0.171)	0.0E+00	0.000E+00	0.039 (-0.048 to 0.13)	3.92E-01	4.072E-01	1.437	1.040E-29	0.365	1.669E-04
176	Urine albumin	NKD2	UACRbiom	RNAs	diotype	0.139	3.386E-04	1.016E-03	CKD F4	M	Urine albumin to CKD F4 to NKD2	kidney trait in F4	56.62	0.077 (0.027 to 0.131)	2.0E-03	5.252E-03	0.059 (-0.027 to 0.142)	1.70E-01	1.856E-01	1.585	4.296E-43	0.388	1.191E-04
177	Creatinine	NKD2	eGFRbiom	RNAs	diotype	0.11	4.437E-03	1.014E-02	CKD F4	M	Creatinine to CKD F4 to NKD2	kidney trait in F4	56.1	0.081 (0.029 to 0.139)	2.0E-03	5.252E-03	0.064 (-0.017 to 0.148)	1.22E-01	1.396E-01	1.153	1.412E-24	0.388	1.191E-04
178	Urine albumin	NKD2	RNAs	UACRbiom	diotype	0.139	3.386E-04	1.016E-03	UACR F4	Y	Urine albumin to UACR F4	kidney trait in F4	97.49	0.114 (0.039 to 0.197)	2.0E-03	7.459E-03	0.003 (-0.039 to 0.047)	8.82E-01	9.221E-01	0.117	7.855E-03	0.925	0.000E+00
179	NKD2	Creatinine	RNAs	eGFRbiom	diotype	0.11	4.437E-03	1.014E-02	eGFR F4	M	NKD2 to eGFR F4 to Creatinine	kidney trait in F4	86.81	0.09 (0.037 to 0.147)	0.0E+00	0.000E+00	0.014 (-0.02 to 0.046)	4.38E-01	5.175E-01	-0.086	4.311E-03	-0.726	0.000E+00
180	DUSP11	Creatinine	RNAs	eGFRbiom	diotype	-0.134	5.571E-04	1.604E-03	CKD F4	Y	DUSP11 to Creatinine to CKD F4	kidney trait in F4	56.17	-0.038 (-0.058 to -0.018)	0.0E+00	0.000E+00	-0.03 (-0.059 to -0.004)	2.40E-02	3.291E-02	-0.364	1.200E-04	1.153	1.412E-24
180									CKD F4	X	CKD F4 to Creatinine to DUSP11	kidney trait in F4	47.94	-0.177 (-0.299 to -0.071)	0.0E+00	0.000E+00	-0.192 (-0.404 to -0.006)	4.40E-02	5.635E-02				
181	DUSP11	CST3	RNAs	eGFRbiom	diotype	-0.18	2.999E-06	1.183E-05	eGFR F4	Y	DUSP11 to CST3 to eGFR F4	kidney trait in F4	91.76	0.151 (0.084 to 0.223)	0.0E+00	0.000E+00	0.014 (-0.012 to 0.042)	3.42E-01	4.236E-01	0.164	2.649E-08	-0.78	0.000E+00
181									eGFR F4	M	DUSP11 to eGFR F4 to CST3	kidney trait in F4	88.78	-0.182 (-0.268 to -0.103)	0.0E+00	0.000E+00	-0.023 (-0.057 to 0.012)	1.94E-01	2.651E-01				
182	DUSP11	Creatinine	RNAs	eGFRbiom	diotype	-0.134	5.571E-04	1.604E-03	eGFR F4	M	DUSP11 to eGFR F4 to Creatinine	kidney trait in F4	86.31	-0.17 (-0.253 to -0.097)	0.0E+00	0.000E+00	-0.027 (-0.068 to 0.017)	2.56E-01	3.355E-01	0.164	2.649E-08	-0.726	0.000E+00
182									eGFR F4	Y	DUSP11 to Creatinine to eGFR F4	kidney trait in F4	85.34	0.14 (0.072 to 0.206)	0.0E+00	0.000E+00	0.024 (-0.006 to 0.056)	1.14E-01	1.677E-01				
183	DUSP11	CST3	RNAs	eGFRbiom	diotype	-0.18	2.999E-06	1.183E-05	CKD F4	Y	DUSP11 to CST3 to CKD F4	kidney trait in F4	63.68	-0.044 (-0.067 to -0.023)	0.0E+00	0.000E+00	-0.025 (-0.055 to 0.002)	7.60E-02	9.187E-02	-0.364	1.200E-04	1.437	1.040E-29

183							CKD F4	X	CKD F4 to CST3 to DUSP11	kidney trait in F4	52 71	-0 195 (-0 32 to -0 085)	0 0E+00	0 000E+00	-0 175 (-0 393 to 0 036)	8 80E-02	1 050E-01					
184	TFE3	Urine albumin RNAs	UACRbiom	diftype	0 141	2 815E-04	8 533E-04	UACR F4	M	TFE3 to UACR F4 to Urine albumin	kidney trait in F4	96 83	0 147 (0 079 to 0 221)	0 0E+00	0 000E+00	0 005 (-0 034 to 0 045)	8 06E-01	8 747E-01	0 192	1 682E-05	0 925	0 000E+00
186	AGK	CST3 RNAs	eGFRbiom	diftype	-0 099	1 094E-02	2 218E-02	eGFR F4	M	AGK to eGFR F4 to CST3	kidney trait in F4	90 97	-0 101 (-0 172 to -0 033)	0 0E+00	0 000E+00	-0 01 (-0 038 to 0 02)	5 70E-01	6 381E-01	0 09	1 537E-03	-0 78	0 000E+00
186							eGFR F4	Y	AGK to CST3 to eGFR F4	kidney trait in F4	90 18	0 082 (0 025 to 0 136)	0 0E+00	0 000E+00	0 009 (-0 015 to 0 032)	4 68E-01	5 446E-01					
187	AGK	Creatinine RNAs	eGFRbiom	diftype	-0 097	1 251E-02	2 485E-02	eGFR F4	M	AGK to eGFR F4 to Creatinine	kidney trait in F4	85	-0 094 (-0 162 to -0 032)	0 0E+00	0 000E+00	-0 017 (-0 052 to 0 019)	3 68E-01	4 515E-01	0 09	1 537E-03	-0 726	0 000E+00
188	CST3	AGK eGFRbiom RNAs		diftype	-0 099	1 094E-02	2 218E-02	CKD F4	M	CST3 to CKD F4 to AGK	kidney trait in F4	54 06	-0 093 (-0 159 to -0 033)	4 0E-03	9 406E-03	-0 079 (-0 17 to 0 024)	1 40E-01	1 568E-01	1 437	1 040E-29	-0 357	1 592E-04
190	CST3	MCM3 eGFRbiom RNAs		diftype	-0 088	2 343E-02	4 191E-02	CKD F4	M	CST3 to CKD F4 to MCM3	kidney trait in F4	63 93	-0 103 (-0 177 to -0 041)	0 0E+00	0 000E+00	-0 058 (-0 142 to 0 04)	2 22E-01	2 381E-01	1 437	1 040E-29	-0 428	2 388E-05
191	MCM3	Urine albumin RNAs	UACRbiom	diftype	-0 17	1 030E-05	3 802E-05	UACR F4	M	MCM3 to UACR F4 to Urine albumin	kidney trait in F4	96 67	-0 19 (-0 268 to -0 117)	0 0E+00	0 000E+00	-0 007 (-0 052 to 0 04)	7 58E-01	8 717E-01	-0 248	3 205E-08	0 925	0 000E+00
192	MCM3	Urine albumin RNAs	UACRbiom	diftype	-0 17	1 030E-05	3 802E-05	CKD F4	Y	MCM3 to Urine albumin to CKD F4	kidney trait in F4	47 35	-0 035 (-0 05 to -0 021)	0 0E+00	0 000E+00	-0 039 (-0 07 to -0 007)	2 00E-02	2 801E-02	-0 428	2 388E-05	1 585	4 296E-43
192							CKD F4	X	CKD F4 to Urine albumin to MCM3	kidney trait in F4	41 78	-0 16 (-0 269 to -0 067)	0 0E+00	0 000E+00	-0 223 (-0 432 to -0 018)	3 20E-02	4 230E-02					
193	Creatinine	MCM3 eGFRbiom RNAs		diftype	-0 091	1 848E-02	3 502E-02	CKD F4	M	Creatinine to CKD F4 to MCM3	kidney trait in F4	56 5	-0 088 (-0 146 to -0 032)	0 0E+00	0 000E+00	-0 067 (-0 155 to 0 025)	1 40E-01	1 568E-01	1 153	1 412E-24	-0 428	2 388E-05
194	MCM3	CST3 RNAs	eGFRbiom	diftype	-0 088	2 343E-02	4 191E-02	eGFR F4	M	MCM3 to eGFR F4 to CST3	kidney trait in F4	92 01	-0 105 (-0 19 to -0 037)	2 0E-03	4 401E-03	-0 009 (-0 038 to 0 021)	5 46E-01	6 221E-01	0 094	2 169E-03	-0 78	0 000E+00
195	MCM3	Creatinine RNAs	eGFRbiom	diftype	-0 091	1 848E-02	3 502E-02	eGFR F4	Y	MCM3 to Creatinine to eGFR F4	kidney trait in F4	87 55	0 083 (0 029 to 0 147)	2 0E-03	4 401E-03	0 012 (-0 019 to 0 041)	4 54E-01	5 299E-01	0 094	2 169E-03	-0 726	0 000E+00
195							eGFR F4	M	MCM3 to eGFR F4 to Creatinine	kidney trait in F4	85 03	-0 098 (-0 175 to -0 033)	2 0E-03	4 401E-03	-0 017 (-0 055 to 0 016)	3 24E-01	4 039E-01					
196	TTF2	Creatinine RNAs	eGFRbiom	diftype	-0 104	7 237E-03	1 555E-02	eGFR F4	Y	TTF2 to Creatinine to eGFR F4	kidney trait in F4	97 81	0 113 (0 048 to 0 18)	0 0E+00	0 000E+00	0 003 (-0 026 to 0 03)	8 38E-01	8 697E-01	0 116	7 464E-05	-0 726	0 000E+00
197	Urine albumin	TTF2 UACRbiom RNAs		diftype	-0 092	1 745E-02	3 328E-02	CKD F4	M	Urine albumin to CKD F4 to TTF2	kidney trait in F4	54 64	-0 073 (-0 128 to -0 018)	1 6E-02	2 854E-02	-0 061 (-0 147 to 0 016)	1 14E-01	1 315E-01	1 585	4 296E-43	-0 346	2 679E-04

198	TTF2	Urine albumin	RNAs	UACRbiom	diotype	-0.092	1.745E-02	3.328E-02	UACR F4	M	TTF2 to UACR F4 to Urine albumin	kidney trait in F4	93.39	-0.105 (-0.171 to -0.045)	0.0E+00	0.000E+00	-0.007 (-0.047 to 0.033)	7.10E-01	8.447E-01	-0.137	1.591E-03	0.925	0.000E+00
199	TTF2	Creatinine	RNAs	eGFRbiom	diotype	-0.104	7.237E-03	1.555E-02	CKD F4	Y	TTF2 to Creatinine to CKD F4	kidney trait in F4	48.16	-0.031 (-0.05 to -0.012)	0.0E+00	0.000E+00	-0.033 (-0.063 to -0.004)	2.20E-02	3.038E-02	-0.346	2.679E-04	1.153	1.412E-24
200	ABCB1	CST3	RNAs	eGFRbiom	diotype	-0.119	2.139E-03	5.601E-03	eGFR F4	M	ABCB1 to eGFR F4 to CST3	kidney trait in F4	80.14	-0.108 (-0.171 to -0.048)	0.0E+00	0.000E+00	-0.027 (-0.052 to -0.001)	4.20E-02	6.892E-02	0.098	9.705E-04	-0.78	0.000E+00
203	ARG1	Creatinine	RNAs	eGFRbiom	diotype	0.102	8.454E-03	1.752E-02	eGFR F4	M	ARG1 to eGFR F4 to Creatinine	kidney trait in F4	86.8	0.102 (0.039 to 0.175)	0.0E+00	0.000E+00	0.016 (-0.023 to 0.053)	4.10E-01	4.905E-01	-0.098	9.503E-04	-0.726	0.000E+00
204	ARG1	CST3	RNAs	eGFRbiom	diotype	0.089	2.207E-02	3.973E-02	eGFR F4	M	ARG1 to eGFR F4 to CST3	kidney trait in F4	95.12	0.109 (0.044 to 0.186)	0.0E+00	0.000E+00	0.006 (-0.025 to 0.033)	7.84E-01	8.226E-01	-0.098	9.503E-04	-0.78	0.000E+00
205	CST3	ARG1	eGFRbiom	RNAs	diotype	0.089	2.207E-02	3.973E-02	CKD F4	M	CST3 to CKD F4 to ARG1	kidney trait in F4	54.69	0.091 (0.027 to 0.167)	8.0E-03	1.664E-02	0.075 (-0.014 to 0.157)	1.04E-01	1.214E-01	1.437	1.040E-29	0.34	2.598E-04
206	SLC25A4	CST3	RNAs	eGFRbiom	diotype	-0.121	1.724E-03	4.555E-03	eGFR F4	M	SLC25A4 to eGFR F4 to CST3	kidney trait in F4	79.66	-0.1 (-0.173 to -0.035)	0.0E+00	0.000E+00	-0.026 (-0.055 to 0.002)	7.60E-02	1.167E-01	0.09	1.591E-03	-0.78	0.000E+00
222	IGFBP2	CST3	Proteins	eGFRbiom	diotype	0.222	3.600E-07	1.620E-06	CKD F4	Y	IGFBP2 to CST3 to CKD F4	kidney trait in F4	54.22	0.029 (0.014 to 0.051)	0.0E+00	0.000E+00	0.025 (-0.017 to 0.079)	2.46E-01	2.619E-01	0.652	1.167E-03	1.437	1.040E-29
222									CKD F4	X	CKD F4 to CST3 to IGFBP2	kidney trait in F4	46.18	0.19 (0.082 to 0.317)	0.0E+00	0.000E+00	0.222 (-0.035 to 0.472)	6.80E-02	8.311E-02				
225	EFNA5	CST3	Proteins	eGFRbiom	diotype	0.287	3.780E-11	3.202E-10	eGFR F4	M	EFNA5 to eGFR F4 to CST3	kidney trait in F4	88.32	0.195 (0.133 to 0.259)	0.0E+00	0.000E+00	0.026 (-0.011 to 0.063)	1.36E-01	1.949E-01	-0.213	3.653E-12	-0.78	0.000E+00
228	EFNA5	CST3	Proteins	eGFRbiom	diotype	0.287	3.780E-11	3.202E-10	CKD F4	Y	EFNA5 to CST3 to CKD F4	kidney trait in F4	92.18	0.029 (0.014 to 0.048)	0.0E+00	0.000E+00	0.002 (-0.029 to 0.044)	9.12E-01	9.148E-01	0.533	1.406E-03	1.437	1.040E-29
231	Urine albumin	ERBB3	UACRbiom	Proteins	diotype	-0.102	2.064E-02	3.770E-02	CKD F4	M	Urine albumin to CKD F4 to ERBB3	kidney trait in F4	67.36	-0.082 (-0.161 to -0.033)	0.0E+00	0.000E+00	-0.04 (-0.135 to 0.066)	4.48E-01	4.615E-01	1.585	4.296E-43	-0.877	8.286E-06
234	ERBB3	CST3	Proteins	eGFRbiom	diotype	-0.258	2.829E-09	1.771E-08	eGFR F4	M	ERBB3 to eGFR F4 to CST3	kidney trait in F4	87.42	-0.177 (-0.245 to -0.115)	0.0E+00	0.000E+00	-0.026 (-0.054 to 0.007)	9.80E-02	1.453E-01	0.193	6.628E-09	-0.78	0.000E+00
234									eGFR F4	Y	ERBB3 to CST3 to eGFR F4	kidney trait in F4	87.14	0.168 (0.11 to 0.223)	0.0E+00	0.000E+00	0.025 (-0.005 to 0.056)	9.40E-02	1.405E-01				
235	LAYN	CST3	Proteins	eGFRbiom	diotype	0.295	8.726E-12	8.666E-11	eGFR F4	M	LAYN to eGFR F4 to CST3	kidney trait in F4	88.23	0.196 (0.131 to 0.264)	0.0E+00	0.000E+00	0.026 (-0.01 to 0.064)	1.78E-01	2.468E-01	-0.215	8.370E-13	-0.78	0.000E+00
244	EGFR	Urine albumin	Proteins	UACRbiom	diotype	-0.155	4.251E-04	1.237E-03	UACR F4	M	EGFR to UACR F4 to Urine albumin	kidney trait in F4	86.19	-0.174 (-0.26 to -0.1)	0.0E+00	0.000E+00	-0.028 (-0.082 to 0.022)	2.92E-01	3.951E-01	-0.221	1.197E-06	0.925	0.000E+00

244									UACR F4	Y	EGFR to Urine albumin to UACR F4	kidney trait in F4		-0.173 (-0.27 to -0.085)	0.0E+00	0.000E+00	-0.048 (-0.099 to 0.005)	7.20E-02	1.419E-01				
250	IGFBP6	CST3	Proteins	eGFRbiom	diotype	0.437	2.789E-25	2.008E-23	eGFR F4	M	IGFBP6 to eGFR F4 to CST3	kidney trait in F4		97.17 (0.263 to 0.413)	0.0E+00	0.000E+00	0.01 (-0.034 to 0.058)	6.68E-01	7.246E-01	-0.368	1.691E-29	-0.78	0.000E+00
250									eGFR F4	M	CST3 to eGFR F4 to IGFBP6	kidney trait in F4		90.19 (0.263 to 0.661)	0.0E+00	0.000E+00	0.052 (-0.178 to 0.322)	6.68E-01	7.246E-01				
251		Creatinine	Proteins	eGFRbiom	diotype	0.403	1.655E-21	6.807E-20	eGFR F4	M	IGFBP6 to eGFR F4 to Creatinine	kidney trait in F4		96.68 (0.264 to 0.417)	0.0E+00	0.000E+00	0.012 (-0.045 to 0.068)	6.68E-01	7.246E-01	-0.368	1.691E-29	-0.726	0.000E+00
251									eGFR F4	M	Creatinine to eGFR F4 to IGFBP6	kidney trait in F4		91.72 (0.289 to 0.598)	0.0E+00	0.000E+00	0.039 (-0.154 to 0.211)	6.68E-01	7.246E-01				
253	IGFBP6	CST3	Proteins	eGFRbiom	diotype	0.437	2.789E-25	2.008E-23	CKD F4	Y	IGFBP6 to CKD F4	kidney trait in F4		72.35 (0.023 to 0.07)	0.0E+00	0.000E+00	0.017 (-0.025 to 0.057)	4.34E-01	4.480E-01	0.748	1.293E-05	1.437	1.040E-29
253									CKD F4	X	CKD F4 to CST3 to IGFBP6	kidney trait in F4		66.16 (0.409 to 0.61)	0.0E+00	0.000E+00	0.209 (-0.049 to 0.46)	9.40E-02	1.112E-01				
254	Creatinine	FGF20	eGFRbiom	Proteins	diotype	-0.147	8.276E-04	2.337E-03	CKD F4	M	Creatinine to CKD F4 to FGF20	kidney trait in F4		45.18 (-0.068 (-0.14 to -0.024))	0.0E+00	0.000E+00	-0.082 (-0.182 to 0.027)	1.38E-01	1.558E-01	1.153	1.412E-24	-1.071	1.012E-04
256	FGF20	CST3	Proteins	eGFRbiom	diotype	-0.273	3.105E-10	2.293E-09	eGFR F4	Y	FGF20 to CST3 to eGFR F4	kidney trait in F4		95.96 (0.055 to 0.245)	0.0E+00	0.000E+00	0.005 (-0.016 to 0.035)	6.18E-01	6.879E-01	0.121	4.049E-05	-0.78	0.000E+00
256									eGFR F4	M	FGF20 to eGFR F4 to CST3	kidney trait in F4		80.11 (-0.111 (-0.251 to -0.048))	0.0E+00	0.000E+00	-0.028 (-0.064 to -0.01)	4.00E-03	7.529E-03				
259	Urine albumin	SPINT1	UACRbiom	Proteins	diotype	-0.099	2.483E-02	4.414E-02	CKD F4	M	Urine albumin to CKD F4 to SPINT1	kidney trait in F4		37.29 (-0.051 (-0.12 to -0.003))	3.2E-02	4.778E-02	-0.086 (-0.19 to 0.017)	9.40E-02	1.112E-01	1.585	4.296E-43	-0.478	2.608E-03
260	SPINT1	Urine albumin	Proteins	UACRbiom	diotype	-0.099	2.483E-02	4.414E-02	UACR F4	M	SPINT1 to UACR F4 to Urine albumin	kidney trait in F4		75.63 (-0.081 (-0.146 to -0.02))	6.0E-03	1.762E-02	-0.026 (-0.075 to 0.021)	2.80E-01	3.864E-01	-0.102	1.478E-02	0.925	0.000E+00
261	SPINT1	CST3	Proteins	eGFRbiom	diotype	-0.134	2.412E-03	6.202E-03	eGFR F4	M	SPINT1 to eGFR F4 to CST3	kidney trait in F4		86.8 (-0.075 (-0.137 to -0.019))	1.4E-02	2.572E-02	-0.011 (-0.039 to 0.017)	4.28E-01	5.073E-01	0.082	9.404E-03	-0.78	0.000E+00
262	CST3	SPINT1	eGFRbiom	Proteins	diotype	-0.134	2.412E-03	6.202E-03	CKD F4	M	CST3 to CKD F4 to SPINT1	kidney trait in F4		36.19 (-0.062 (-0.138 to -0.008))	1.8E-02	3.137E-02	-0.109 (-0.249 to 0.021)	9.80E-02	1.151E-01	1.437	1.040E-29	-0.478	2.608E-03
266	NBL1	CST3	Proteins	eGFRbiom	diotype	0.373	2.378E-18	5.708E-17	eGFR F4	Y	NBL1 to CST3 to eGFR F4	kidney trait in F4		91.18 (-0.22 (-0.288 to -0.154))	0.0E+00	0.000E+00	-0.021 (-0.054 to 0.012)	2.34E-01	3.131E-01	-0.241	7.486E-16	-0.78	0.000E+00
268	Urine albumin	GHR	UACRbiom	Proteins	diotype	-0.102	2.068E-02	3.770E-02	CKD F4	M	Urine albumin to CKD F4 to GHR	kidney trait in F4		54.33 (-0.068 (-0.138 to -0.024))	0.0E+00	0.000E+00	-0.057 (-0.154 to 0.038)	2.20E-01	2.370E-01	1.585	4.296E-43	-0.781	9.172E-05

269	GHR	Urine albumin	Proteins	UACRbiom	diotype	-0.102	2.068E-02	3.770E-02	UACR F4	M	GHR to UACR F4 to Urine albumin	kidney trait in F4	99.08	-0.132 (-0.22 to -0.048)	2.0E-03	7.459E-03	-0.001 (-0.06 to 0.056)	9.70E-01	9.700E-01	-0.167	7.015E-04	0.925	0.000E+00
272	GHR	CST3	Proteins	eGFRbiom	diotype	-0.207	2.243E-06	9.156E-06	eGFR F4	Y	GHR to CST3 to eGFR F4	kidney trait in F4	94.99	0.091 to 0.207	0.0E+00	0.000E+00	0.008 (-0.033 to 0.046)	7.68E-01	8.147E-01	0.157	2.036E-05	-0.78	0.000E+00
272									eGFR F4	M	GHR to eGFR F4 to CST3	kidney trait in F4	80.86	-0.144 (-0.212 to -0.074)	0.0E+00	0.000E+00	-0.034 (-0.073 to 0.003)	6.60E-02	1.034E-01				
273	Creatinine	GHR	eGFRbiom	Proteins	diotype	-0.124	5.049E-03	1.136E-02	CKD F4	M	Creatinine to CKD F4 to GHR	kidney trait in F4	44.42	-0.061 (-0.119 to -0.022)	0.0E+00	0.000E+00	-0.076 (-0.18 to 0.027)	1.56E-01	1.722E-01	1.153	1.412E-24	-0.781	9.172E-05
276	CGA LHB	CST3	Proteins	eGFRbiom	diotype	0.234	8.101E-08	4.242E-07	eGFR F4	M	CGA LHB to eGFR F4 to CST3	kidney trait in F4	89.94	0.137 to 0.34	0.0E+00	0.000E+00	0.026 (-0.033 to 0.086)	3.68E-01	4.515E-01	-0.249	7.420E-06	-0.78	0.000E+00
276									eGFR F4	Y	CGA LHB to CST3 to eGFR F4	kidney trait in F4	85.39	-0.213 (-0.323 to -0.123)	0.0E+00	0.000E+00	-0.036 (-0.089 to 0.02)	1.96E-01	2.669E-01				
279	ESAM	CST3	Proteins	eGFRbiom	diotype	0.276	1.940E-10	1.510E-09	eGFR F4	Y	ESAM to CST3 to eGFR F4	kidney trait in F4	88.05	-0.179 (-0.235 to -0.123)	0.0E+00	0.000E+00	-0.024 (-0.057 to 0.007)	1.56E-01	2.202E-01	-0.204	2.965E-11	-0.78	0.000E+00
279									eGFR F4	M	ESAM to eGFR F4 to CST3	kidney trait in F4	85.95	0.186 to 0.251	0.0E+00	0.000E+00	0.03 (-0.004 to 0.063)	8.60E-02	1.300E-01				
283	JAM2	Creatinine	Proteins	eGFRbiom	diotype	0.331	1.313E-14	1.801E-13	CKD F4	Y	JAM2 to Creatinine to CKD F4	kidney trait in F4	56.32	0.024 to 0.039	0.0E+00	0.000E+00	0.019 (-0.012 to 0.056)	2.56E-01	2.722E-01	0.55	3.441E-04	1.153	1.412E-24
283									CKD F4	X	CKD F4 to Creatinine to JAM2	kidney trait in F4	51.14	0.302 to 0.477	0.0E+00	0.000E+00	0.289 (-0.043 to 0.638)	1.04E-01	1.214E-01				
285	JAM2	CST3	Proteins	eGFRbiom	diotype	0.341	2.148E-15	3.257E-14	CKD F4	Y	JAM2 to CST3 to CKD F4	kidney trait in F4	75.15	0.027 to 0.043	0.0E+00	0.000E+00	0.009 (-0.019 to 0.048)	5.72E-01	5.856E-01	0.55	3.441E-04	1.437	1.040E-29
285									CKD F4	X	CKD F4 to CST3 to JAM2	kidney trait in F4	59.63	0.353 to 0.56	0.0E+00	0.000E+00	0.239 (-0.115 to 0.595)	2.22E-01	2.381E-01				
286	JAM2	Creatinine	Proteins	eGFRbiom	diotype	0.331	1.313E-14	1.801E-13	eGFR F4	M	JAM2 to eGFR F4 to Creatinine	kidney trait in F4	88.21	0.215 to 0.278	0.0E+00	0.000E+00	0.029 (-0.012 to 0.066)	1.70E-01	2.382E-01	-0.238	2.243E-17	-0.726	0.000E+00
290	M	CLEC4	Proteins	eGFRbiom	diotype	-0.207	2.257E-06	9.156E-06	eGFR F4	Y	CLEC4 to CST3 to eGFR F4	kidney trait in F4	87.68	0.148 to 0.201	0.0E+00	0.000E+00	0.021 (-0.009 to 0.048)	1.72E-01	2.402E-01	0.169	2.079E-08	-0.78	0.000E+00
290									eGFR F4	M	CLEC4 to eGFR F4 to CST3	kidney trait in F4	86.98	-0.155 (-0.215 to -0.093)	0.0E+00	0.000E+00	-0.023 (-0.052 to 0.006)	1.20E-01	1.739E-01				
293	IL19	CST3	Proteins	eGFRbiom	diotype	-0.182	3.397E-05	1.179E-04	CKD F4	Y	IL19 to CST3 to CKD F4	kidney trait in F4	38.25	-0.012 (-0.022 to -0.005)	0.0E+00	0.000E+00	-0.02 (-0.04 to 0.004)	1.06E-01	1.235E-01	-0.555	1.445E-03	1.437	1.040E-29
294	IL19	CST3	Proteins	eGFRbiom	diotype	-0.182	3.397E-05	1.179E-04	eGFR F4	M	IL19 to eGFR F4 to CST3	kidney trait in F4	94.98	-0.128 (-0.189 to -0.066)	0.0E+00	0.000E+00	-0.007 (-0.033 to 0.025)	6.36E-01	6.998E-01	0.138	5.103E-06	-0.78	0.000E+00

294								eGFR F4	Y	IL19 to CST3 to eGFR F4	kidney trait in F4	80.89	0.112 (0.052 to 0.163)	0.0E+00	0.000E+00	0.026 (-0.002 to 0.055)	5.60E-02	8.886E-02						
296	RETN	CST3	Proteins	eGFRbiom	diftype	0.283	6.818E-11	5.455E-10	CKD F4	Y	RETN to CST3 to CKD F4	kidney trait in F4	64	0.026 (0.014 to 0.042)	0.0E+00	0.000E+00	0.015 (-0.018 to 0.054)	3.94E-01	4.084E-01	0.525	2.696E-04	1.437	1.040E-29	
296								CKD F4	X	CKD F4 to CST3 to RETN	kidney trait in F4	54.55	0.324 (0.18 to 0.507)	0.0E+00	0.000E+00	0.27 (-0.102 to 0.667)	1.60E-01	1.762E-01						
299	RETN	CST3	Proteins	eGFRbiom	diftype	0.283	6.818E-11	5.455E-10	eGFR F4	Y	RETN to CST3 to eGFR F4	kidney trait in F4	97.69	-0.177 (-0.23 to -0.119)	0.0E+00	0.000E+00	-0.004 (-0.035 to 0.027)	7.76E-01	8.185E-01	-0.181	5.914E-10	-0.78	0.000E+00	
300	Creatinine	IL2	eGFRbiom	Proteins	diftype	-0.11	1.300E-02	2.536E-02	CKD F4	M	Creatinine to CKD F4 to IL2	kidney trait in F4	43.73	-0.062 (-0.145 to -0.009)	2.2E-02	3.588E-02	-0.079 (-0.195 to 0.038)	2.36E-01	2.520E-01	1.153	1.412E-24	-0.396	2.609E-03	
301	IL2	Creatinine	Proteins	eGFRbiom	diftype	-0.11	1.300E-02	2.536E-02	eGFR F4	Y	IL2 to Creatinine to eGFR F4	kidney trait in F4	89.55	0.055 (0.008 to 0.099)	2.6E-02	4.549E-02	0.006 (-0.026 to 0.04)	7.00E-01	7.551E-01	0.061	4.367E-02	-0.726	0.000E+00	
304	TNFRSF1B	CST3	Proteins	eGFRbiom	diftype	0.415	9.521E-23	4.570E-21	CKD F4	Y	TNFRSF1B to CST3 to CKD F4	kidney trait in F4	80.14	0.04 (0.017 to 0.066)	0.0E+00	0.000E+00	0.01 (-0.028 to 0.053)	6.20E-01	6.295E-01	0.684	1.037E-05	1.437	1.040E-29	
304								CKD F4	X	CKD F4 to CST3 to TNFRSF1B	kidney trait in F4	69.38	0.504 (0.282 to 0.772)	0.0E+00	0.000E+00	-0.223 (-0.134 to 0.59)	2.22E-01	2.381E-01						
307	ADAMTS13	CST3	Proteins	eGFRbiom	diftype	-0.161	2.551E-04	7.900E-04	CKD F4	Y	ADAMTS13 to CST3 to CKD F4	kidney trait in F4	43.8	-0.011 (-0.021 to -0.005)	0.0E+00	0.000E+00	-0.014 (-0.036 to 0.016)	3.14E-01	3.304E-01	-0.461	1.977E-03	1.437	1.040E-29	
307								CKD F4	X	ADAMTS13 to CKD F4 to ADAMTS13	kidney trait in F4	38.2	-0.165 (-0.313 to -0.051)	0.0E+00	0.000E+00	-0.267 (-0.704 to 0.115)	2.18E-01	2.354E-01						
309	ADAMTS13	Creatinine	Proteins	eGFRbiom	diftype	-0.144	1.064E-03	2.891E-03	CKD F4	Y	ADAMTS13 to Creatinine to CKD F4	kidney trait in F4	30.76	-0.009 (-0.016 to -0.003)	2.0E-03	5.252E-03	-0.02 (-0.037 to 0.005)	9.40E-02	1.112E-01	-0.461	1.977E-03	1.153	1.412E-24	
310	ACY1	CST3	Proteins	eGFRbiom	diftype	-0.111	1.212E-02	2.431E-02	eGFR F4	M	ACY1 to eGFR F4 to CST3	kidney trait in F4	99.34	-0.114 (-0.184 to -0.048)	0.0E+00	0.000E+00	-0.001 (-0.035 to 0.034)	9.44E-01	9.565E-01	0.123	6.810E-04	-0.78	0.000E+00	
312	ACY1	Creatinine	Proteins	eGFRbiom	diftype	-0.115	9.386E-03	1.931E-02	eGFR F4	M	ACY1 to eGFR F4 to Creatinine	kidney trait in F4	99.27	-0.114 (-0.183 to -0.048)	0.0E+00	0.000E+00	-0.001 (-0.041 to 0.041)	9.80E-01	9.826E-01	0.123	6.810E-04	-0.726	0.000E+00	
314	Creatinine	BMP1	eGFRbiom	Proteins	diftype	-0.117	8.040E-03	1.678E-02	CKD F4	M	Creatinine to CKD F4 to BMP1	kidney trait in F4	39.97	-0.052 (-0.113 to -0.009)	1.4E-02	2.586E-02	-0.078 (-0.193 to 0.026)	1.62E-01	1.776E-01	1.153	1.412E-24	-0.574	1.717E-03	
315	BMP1	CST3	Proteins	eGFRbiom	diftype	-0.169	1.165E-04	3.686E-04	eGFR F4	Y	BMP1 to CST3 to eGFR F4	kidney trait in F4	90.03	0.119 (0.052 to 0.186)	0.0E+00	0.000E+00	0.013 (-0.022 to 0.05)	5.30E-01	6.093E-01	0.132	1.811E-04	-0.78	0.000E+00	
315								eGFR F4	M	BMP1 to eGFR F4 to CST3	kidney trait in F4	85.55	-0.122 (-0.187 to -0.052)	0.0E+00	0.000E+00	-0.021 (-0.06 to 0.019)	3.32E-01	4.126E-01						
319	CTSV	CST3	Proteins	eGFRbiom	diftype	-0.248	1.199E-08	7.047E-08	eGFR F4	Y	CTSV to CST3 to eGFR F4	kidney trait in F4	94.78	0.187 (0.132 to 0.244)	0.0E+00	0.000E+00	0.01 (-0.021 to 0.041)	5.34E-01	6.103E-01	0.197	1.660E-08	-0.78	0.000E+00	

322	Urine albumin	FN1	UACRbiom	Proteins	diotype	-0.102	2.051E-02	3.770E-02	CKD F4	M	Urine albumin to CKD F4 to FN1	kidney trait in F4	46.06	-0.072 (-0.144 to 0.02)	8.0E-03	1.664E-02	-0.084 (-0.188 to 0.017)	1.12E-01	1.298E-01	1.585	4.296E-43	-0.559	3.945E-04
323	FN1	CST3	Proteins	eGFRbiom	diotype	-0.193	1.020E-05	3.802E-05	eGFR F4	Y	FN1 to CST3 to eGFR F4	kidney trait in F4	97.05	0.074 to 0.185)	0.0E+00	0.000E+00	0.004 (-0.022 to 0.032)	8.10E-01	8.429E-01	0.133	1.248E-05	-0.78	0.000E+00
325	FN1	Urine albumin	Proteins	UACRbiom	diotype	-0.102	2.051E-02	3.770E-02	UACR F4	Y	Urine albumin to UACR F4	kidney trait in F4	96.69	-0.099 (-0.164 to 0.036)	2.0E-03	7.459E-03	-0.003 (-0.051 to 0.04)	9.26E-01	9.396E-01	-0.102	1.236E-02	0.925	0.000E+00
327	Creatinine	FN1	eGFRbiom	Proteins	diotype	-0.133	2.624E-03	6.629E-03	CKD F4	M	Creatinine to CKD F4 to FN1	kidney trait in F4	41.85	-0.067 (-0.135 to 0.019)	4.0E-03	9.406E-03	-0.093 (-0.208 to 0.02)	1.10E-01	1.278E-01	1.153	1.412E-24	-0.559	3.945E-04
331	FSTL3	CST3	Proteins	eGFRbiom	diotype	0.33	1.775E-14	2.223E-13	eGFR F4	M	FSTL3 to eGFR F4 to CST3	kidney trait in F4	88.28	0.223 (0.166 to 0.278)	0.0E+00	0.000E+00	0.03 (-0.016 to 0.073)	2.00E-01	2.714E-01	-0.244	1.871E-15	-0.78	0.000E+00
335	B2M	CST3	Proteins	eGFRbiom	diotype	0.615	1.036E-54	2.985E-52	eGFR F4	Y	B2M to CST3 to eGFR F4	kidney trait in F4	97.18	-0.417 (-0.467 to 0.37)	0.0E+00	0.000E+00	-0.012 (-0.061 to 0.038)	6.62E-01	7.242E-01	-0.43	4.438E-50	-0.78	0.000E+00
335									eGFR F4	X	eGFR F4 to CST3 to B2M	kidney trait in F4	93.05	-0.778 (-1.024 to 0.533)	0.0E+00	0.000E+00	-0.058 (-0.3 to 0.173)	6.62E-01	7.242E-01				
338	MASP1	Urine albumin	Proteins	UACRbiom	diotype	-0.113	1.015E-02	2.074E-02	CKD F4	Y	MASP1 to Urine albumin to CKD F4	kidney trait in F4	38.12	-0.01 (-0.022 to 0.003)	6.0E-03	1.338E-02	-0.016 (-0.036 to 0.007)	1.40E-01	1.568E-01	-0.522	2.509E-03	1.585	4.296E-43
339	CST3	MASP1	eGFRbiom	Proteins	diotype	-0.157	3.603E-04	1.059E-03	CKD F4	X	CKD F4 to CST3 to MASP1	kidney trait in F4	44.88	-0.183 (-0.328 to 0.063)	0.0E+00	0.000E+00	-0.225 (-0.52 to 0.072)	1.32E-01	1.500E-01	1.437	1.040E-29	-0.522	2.509E-03
339									CKD F4	Y	MASP1 to CST3 to CKD F4	kidney trait in F4	38.96	-0.012 (-0.023 to 0.005)	0.0E+00	0.000E+00	-0.019 (-0.043 to 0.002)	7.40E-02	9.000E-02				
342	MASP1	CST3	Proteins	eGFRbiom	diotype	-0.157	3.603E-04	1.059E-03	eGFR F4	M	MASP1 to eGFR F4 to CST3	kidney trait in F4	89.64	-0.11 (-0.183 to 0.048)	0.0E+00	0.000E+00	-0.013 (-0.039 to 0.02)	4.04E-01	4.863E-01	0.119	4.669E-05	-0.78	0.000E+00
342									eGFR F4	Y	MASP1 to CST3 to eGFR F4	kidney trait in F4	85.84	0.102 (0.046 to 0.165)	0.0E+00	0.000E+00	0.017 (-0.009 to 0.052)	2.72E-01	3.517E-01				
346	KDR	CST3	Proteins	eGFRbiom	diotype	-0.264	1.282E-09	8.789E-09	eGFR F4	Y	KDR to CST3 to eGFR F4	kidney trait in F4	94.19	0.145 (0.089 to 0.201)	0.0E+00	0.000E+00	0.009 (-0.02 to 0.04)	5.56E-01	6.298E-01	0.153	4.635E-07	-0.78	0.000E+00
348	Creatinine	IGF2R	eGFRbiom	Proteins	diotype	-0.098	2.672E-02	4.693E-02	CKD F4	M	Creatinine to CKD F4 to IGF2R	kidney trait in F4	51.67	-0.071 (-0.14 to 0.025)	0.0E+00	0.000E+00	-0.066 (-0.192 to 0.053)	2.92E-01	3.085E-01	1.153	1.412E-24	-0.689	7.657E-05
351	IGF2R	CST3	Proteins	eGFRbiom	diotype	-0.187	1.945E-05	6.830E-05	eGFR F4	Y	IGF2R to CST3 to eGFR F4	kidney trait in F4	99.73	0.137 (0.079 to 0.188)	0.0E+00	0.000E+00	0 (-0.029 to 0.033)	9.68E-01	9.756E-01	0.138	2.099E-05	-0.78	0.000E+00
352	CST3	PLG	eGFRbiom	Proteins	diotype	-0.261	1.881E-09	1.204E-08	CKD F4	X	CKD F4 to PLG	kidney trait in F4	46.32	-0.228 (-0.356 to 0.117)	0.0E+00	0.000E+00	-0.264 (-0.6 to 0.106)	1.70E-01	1.856E-01	1.437	1.040E-29	-0.56	4.843E-04
352									CKD F4	Y	PLG to CST3 to CKD F4	kidney trait in F4	46.02	-0.015 (-0.027 to 0.008)	0.0E+00	0.000E+00	-0.018 (-0.036 to 0.012)	2.06E-01	2.229E-01				

356	CTSH	CST3	Proteins	eGFRbiom	diftype	0.415	8.967E-23	4.570E-21	eGFR F4	Y	CTSH to CST3 to eGFR F4	kidney trait in F4	92.52	-0.293 (-0.346 to -0.237)	0.0E+00	0.000E+00	-0.024 (-0.06 to 0.015)	2.44E-01	3.231E-01	-0.317	1.036E-23	-0.78	0.000E+00
356									eGFR F4	X	eGFR F4 to CST3 to CTSH	kidney trait in F4	73.56	-0.425 (-0.639 to -0.221)	0.0E+00	0.000E+00	-0.153 (-0.372 to 0.094)	2.44E-01	3.231E-01				
357	CTSH	CST3	Proteins	eGFRbiom	diftype	0.415	8.967E-23	4.570E-21	CKD F4	Y	CTSH to CST3 to CKD F4	kidney trait in F4	89.7	0.044 (0.024 to 0.071)	0.0E+00	0.000E+00	0.005 (-0.025 to 0.038)	7.72E-01	7.775E-01	0.7	3.570E-05	1.437	1.040E-29
357									CKD F4	X	CKD F4 to CST3 to CTSH	kidney trait in F4	73.28	0.465 (0.29 to 0.665)	0.0E+00	0.000E+00	0.17 (-0.078 to 0.439)	1.60E-01	1.762E-01				
359	FCN3	CST3	Proteins	eGFRbiom	diftype	-0.132	2.699E-03	6.759E-03	eGFR F4	Y	FCN3 to CST3 to eGFR F4	kidney trait in F4	87.94	0.092 (0.041 to 0.144)	2.0E-03	4.401E-03	0.013 (-0.023 to 0.047)	5.06E-01	5.853E-01	0.105	1.598E-03	-0.78	0.000E+00
362	RPS6K A5	Urine albumin	Proteins	UACRbiom	diftype	0.102	2.130E-02	3.858E-02	UACR F4	M	RPS6KA5 to UACR F4 to Urine albumin	kidney trait in F4	97.53	0.083 (0.021 to 0.146)	4.0E-03	1.314E-02	0.002 (-0.039 to 0.046)	9.02E-01	9.289E-01	0.105	8.281E-03	0.925	0.000E+00
364	MED1	Urine albumin	Proteins	UACRbiom	diftype	0.146	9.329E-04	2.584E-03	UACR F4	Y	MED1 to Urine albumin to UACR F4	kidney trait in F4	90.57	0.103 (0.027 to 0.194)	2.0E-03	7.459E-03	0.011 (-0.04 to 0.057)	6.74E-01	8.207E-01	0.114	6.638E-03	0.925	0.000E+00
365	PAPPA	CST3	Proteins	eGFRbiom	diftype	0.193	1.121E-05	4.036E-05	CKD F4	Y	PAPPA to CST3 to CKD F4	kidney trait in F4	43.85	0.019 (0.009 to 0.032)	0.0E+00	0.000E+00	0.025 (-0.01 to 0.067)	1.38E-01	1.558E-01	0.526	8.906E-04	1.437	1.040E-29
365									CKD F4	X	CKD F4 to CST3 to PAPPA	kidney trait in F4	42.47	0.217 (0.083 to 0.362)	0.0E+00	0.000E+00	0.294 (-0.096 to 0.681)	1.16E-01	1.334E-01				
369	Urine albumin	IL6	UACRbiom	Proteins	diftype	0.133	2.452E-03	6.248E-03	CKD F4	M	Urine albumin to CKD F4 to IL6	kidney trait in F4	86.7	0.089 (0.019 to 0.159)	8.0E-03	1.664E-02	0.014 (-0.082 to 0.128)	7.26E-01	7.334E-01	1.585	4.296E-43	0.395	3.724E-04
370	CST3	TFF3	eGFRbiom	Proteins	diftype	0.376	1.102E-18	2.886E-17	CKD F4	X	CKD F4 to CST3 to TFF3	kidney trait in F4	74.11	0.335 (0.193 to 0.5)	0.0E+00	0.000E+00	0.117 (-0.12 to 0.337)	3.08E-01	3.244E-01	1.437	1.040E-29	0.438	2.250E-03
370									CKD F4	Y	TFF3 to CST3 to CKD F4	kidney trait in F4	72.47	0.032 (0.016 to 0.059)	0.0E+00	0.000E+00	0.012 (-0.013 to 0.044)	3.56E-01	3.726E-01				
371	TFF3	Creatinine	Proteins	eGFRbiom	diftype	0.273	2.976E-10	2.255E-09	CKD F4	Y	TFF3 to Creatinine to CKD F4	kidney trait in F4	53.85	0.021 (0.009 to 0.038)	0.0E+00	0.000E+00	0.018 (-0.004 to 0.048)	1.30E-01	1.484E-01	0.438	2.250E-03	1.153	1.412E-24
371									CKD F4	X	CKD F4 to Creatinine to TFF3	kidney trait in F4	43.48	0.196 (0.095 to 0.307)	0.0E+00	0.000E+00	0.255 (0.017 to 0.479)	3.80E-02	4.970E-02				
373	TFF3	CST3	Proteins	eGFRbiom	diftype	0.376	1.102E-18	2.886E-17	eGFR F4	M	TFF3 to eGFR F4 to CST3	kidney trait in F4	88.47	0.216 (0.137 to 0.326)	0.0E+00	0.000E+00	0.028 (-0.008 to 0.07)	1.34E-01	1.927E-01	-0.237	6.389E-14	-0.78	0.000E+00
375	EPHA2	CST3	Proteins	eGFRbiom	diftype	0.256	3.863E-09	2.318E-08	eGFR F4	Y	EPHA2 to CST3 to eGFR F4	kidney trait in F4	96.9	-0.165 (-0.224 to -0.108)	0.0E+00	0.000E+00	-0.005 (-0.039 to 0.028)	7.62E-01	8.128E-01	-0.17	1.800E-08	-0.78	0.000E+00
379	NTRK2	CST3	Proteins	eGFRbiom	diftype	-0.16	2.641E-04	8.091E-04	eGFR F4	Y	NTRK2 to CST3 to eGFR F4	kidney trait in F4	97.74	0.102 (0.054 to 0.151)	0.0E+00	0.000E+00	0.002 (-0.028 to 0.033)	8.56E-01	8.812E-01	0.104	4.388E-04	-0.78	0.000E+00

383	NTRK2	Urine albumin	Proteins	UACRbiom	diotype	-0.13	3.103E-03	7.447E-03	CKD F4	Y	NTRK2 to Urine albumin to CKD F4	kidney trait in F4	38.8	-0.012 (-0.023 to -0.005)	4.0E-03	9.406E-03	-0.018 (-0.037 to 0.002)	7.40E-02	9.000E-02	-0.518	1.411E-03	1.585	4.296E-43
386	AMH	CST3	Proteins	eGFRbiom	diotype	-0.223	3.500E-07	1.600E-06	eGFR F4	Y	AMH to CST3 to eGFR F4	kidney trait in F4	91.19	0.105 (0.105 to 0.213)	0.0E+00	0.000E+00	0.015 (-0.017 to 0.047)	4.06E-01	4.872E-01	0.171	2.012E-08	-0.78	0.000E+00
386									eGFR F4	M	AMH to eGFR F4 to CST3	kidney trait in F4	83.58	-0.157 (-0.223 to -0.094)	0.0E+00	0.000E+00	-0.031 (-0.064 to -0.001)	4.40E-02	7.159E-02				
387	AMH	CST3	Proteins	eGFRbiom	diotype	-0.223	3.500E-07	1.600E-06	CKD F4	Y	AMH to CST3 to CKD F4	kidney trait in F4	54.63	-0.017 (-0.028 to -0.009)	0.0E+00	0.000E+00	-0.014 (-0.035 to 0.009)	1.82E-01	1.978E-01	-0.533	7.168E-04	1.437	1.040E-29
387									CKD F4	X	CKD F4 to CST3 to AMH	kidney trait in F4	51.65	-0.262 (-0.39 to -0.147)	0.0E+00	0.000E+00	-0.246 (-0.581 to 0.068)	1.32E-01	1.500E-01				
389	Creatinine	MMP1	eGFRbiom	Proteins	diotype	0.131	2.925E-03	7.199E-03	CKD F4	M	Creatinine to CKD F4 to MMP1	kidney trait in F4	37.62	0.059 (0.013 to 0.124)	1.2E-02	2.272E-02	0.097 (-0.025 to 0.229)	1.16E-01	1.334E-01	1.153	1.412E-24	0.571	2.747E-04
390	Creatinine	MMP1	Proteins	eGFRbiom	diotype	0.131	2.925E-03	7.199E-03	eGFR F4	M	MMP1 to eGFR F4 to Creatinine	kidney trait in F4	83.73	0.071 (0.013 to 0.132)	2.0E-02	3.547E-02	0.014 (-0.021 to 0.053)	4.18E-01	4.985E-01	-0.077	1.188E-02	-0.726	0.000E+00
390									eGFR F4	Y	MMP1 to Creatinine to eGFR F4	kidney trait in F4	81.97	-0.063 (-0.12 to -0.009)	2.0E-02	3.547E-02	-0.014 (-0.043 to 0.017)	4.52E-01	5.292E-01				
392	C1QBP	CST3	Proteins	eGFRbiom	diotype	-0.35	3.087E-16	5.556E-15	eGFR F4	Y	C1QBP to CST3 to eGFR F4	kidney trait in F4	88.57	0.205 (0.156 to 0.258)	0.0E+00	0.000E+00	0.026 (-0.005 to 0.058)	9.20E-02	1.380E-01	0.231	1.113E-14	-0.78	0.000E+00
395	ERP29	Urine albumin	Proteins	UACRbiom	diotype	0.141	1.329E-03	3.577E-03	UACR F4	M	ERP29 to UACR F4 to Urine albumin	kidney trait in F4	83.85	0.146 (0.075 to 0.215)	0.0E+00	0.000E+00	0.028 (-0.024 to 0.079)	2.42E-01	3.479E-01	0.185	3.315E-05	0.925	0.000E+00
395									UACR F4	Y	ERP29 to Urine albumin to UACR F4	kidney trait in F4	80.78	0.149 (0.067 to 0.231)	0.0E+00	0.000E+00	0.036 (-0.01 to 0.084)	1.52E-01	2.530E-01				
400	ERP29	CST3	Proteins	eGFRbiom	diotype	0.261	1.840E-09	1.204E-08	eGFR F4	M	ERP29 to eGFR F4 to CST3	kidney trait in F4	89.32	0.202 (0.14 to 0.269)	0.0E+00	0.000E+00	0.024 (-0.011 to 0.061)	1.90E-01	2.606E-01	-0.22	2.348E-11	-0.78	0.000E+00
404	Urine albumin	SOD2	UACRbiom	Proteins	diotype	-0.103	1.965E-02	3.675E-02	CKD F4	M	Urine albumin to CKD F4 to SOD2	kidney trait in F4	49.74	-0.08 (-0.164 to -0.029)	2.0E-03	5.252E-03	-0.081 (-0.174 to 0.012)	8.20E-02	9.816E-02	1.585	4.296E-43	-0.678	3.208E-05
406	SOD2	Urine albumin	Proteins	UACRbiom	diotype	-0.103	1.965E-02	3.675E-02	UACR F4	M	SOD2 to UACR F4 to Urine albumin	kidney trait in F4	83.7	-0.103 (-0.179 to -0.036)	2.0E-03	7.459E-03	-0.02 (-0.058 to 0.023)	3.06E-01	4.060E-01	-0.131	1.732E-03	0.925	0.000E+00
407	CST3	KIR2DL4	eGFRbiom	Proteins	diotype	0.125	4.556E-03	1.033E-02	CKD F4	M	CST3 to CKD F4 to KIR2DL4	kidney trait in F4	50.74	0.095 (0.014 to 0.224)	2.0E-02	3.367E-02	0.092 (-0.024 to 0.218)	1.34E-01	1.520E-01	1.437	1.040E-29	0.481	3.354E-04
408	KIR2DL4	Creatinine	Proteins	eGFRbiom	diotype	0.129	3.486E-03	8.229E-03	eGFR F4	M	KIR2DL4 to eGFR F4 to Creatinine	kidney trait in F4	87.28	0.093 (0.039 to 0.158)	0.0E+00	0.000E+00	0.013 (-0.021 to 0.048)	4.42E-01	5.206E-01	-0.101	9.352E-04	-0.726	0.000E+00

411	NOTCH1	Urine albumin	Proteins	UACRbiom	diftype	-0.173	8.450E-05	2.734E-04	UACR F4	Y	NOTCH1 to Urine albumin to UACR F4	kidney trait in F4	94 85	-0.141 (-0.222 to -0.067)	2.0E-03	7.459E-03	-0.008 (-0.056 to 0.044)	8.12E-01	8.747E-01	-0.148	5 220E-04	0.925	0	0.000E+0
413	NOTCH1	CST3	Proteins	eGFRbiom	diftype	-0.13	3.277E-03	7.801E-03	eGFR F4	M	NOTCH1 to eGFR F4	kidney trait in F4	94 08	-0.091 (-0.159 to -0.028)	6.0E-03	1.194E-02	-0.006 (-0.037 to 0.026)	7.16E-01	7.680E-01	0.098	2 210E-03	-0.78	0	0.000E+0
414	NOTCH1	CST3	eGFRbiom	Proteins	diftype	-0.13	3.277E-03	7.801E-03	CKD F4	M	CKD F4 to NOTCH1	kidney trait in F4	39 92	-0.073 (-0.165 to 0.014)	2.0E-02	3.367E-02	-0.11 (-0.252 to 0.037)	1.44E-01	1.605E-01	1.437	1 040E-29	-0.584	2.723E-04	
418	RELT	CST3	Proteins	eGFRbiom	diftype	0.462	1.615E-28	2.325E-26	CKD F4	Y	RELT to CST3 to CKD F4	kidney trait in F4	95.73	0.046 (0.024 to 0.07)	0.0E+00	0.000E+00	0.002 (-0.04 to 0.048)	9.56E-01	9.560E-01	0.694	3 832E-05	1.437	1.040E-29	
418									CKD F4	X	CKD F4 to RELT	kidney trait in F4	77 33	0.503 (0.305 to 0.744)	0.0E+00	0.000E+00	0.147 (-0.172 to 0.456)	3.88E-01	4 043E-01					
419	SCARF1	CST3	Proteins	eGFRbiom	diftype	0.229	1.554E-07	7.590E-07	CKD F4	Y	SCARF1 to CST3 to CKD F4	kidney trait in F4	55	0.021 (0.01 to 0.034)	0.0E+00	0.000E+00	0.017 (-0.011 to 0.052)	2.36E-01	2 520E-01	0.555	4 358E-04	1.437	1.040E-29	
419									CKD F4	X	CKD F4 to CST3 to SCARF1	kidney trait in F4	47 35	0.266 (0.142 to 0.428)	0.0E+00	0.000E+00	0.295 (0.018 to 0.576)	4.00E-02	5.197E-02					
423	TNFRSF19	CST3	Proteins	eGFRbiom	diftype	0.294	1.165E-11	1.119E-10	eGFR F4	M	TNFRSF19 to eGFR F4 to CST3	kidney trait in F4	98 83	0.122 (0.054 to 0.216)	0.0E+00	0.000E+00	0.001 (-0.04 to 0.039)	8.78E-01	8 987E-01	-0.132	2 994E-06	-0.78	0	0.000E+0
424	TNFRSF19	Creatinine	Proteins	eGFRbiom	diftype	0.238	4.825E-08	2.573E-07	eGFR F4	M	TNFRSF19 to eGFR F4 to Creatinine	kidney trait in F4	86 07	0.121 (0.053 to 0.218)	0.0E+00	0.000E+00	0.02 (-0.016 to 0.059)	2.94E-01	3.726E-01	-0.132	2 994E-06	-0.726	0	0.000E+0
424									eGFR F4	Y	TNFRSF19 to Creatinine	kidney trait in F4	78.76	-0.104 (-0.175 to -0.055)	0.0E+00	0.000E+00	-0.028 (-0.075 to 0.014)	1.70E-01	2 382E-01					
425	HAVCR2	CST3	Proteins	eGFRbiom	diftype	0.22	4.911E-07	2.143E-06	CKD F4	Y	HAVCR2 to CST3 to CKD F4	kidney trait in F4	74 32	0.028 (0.013 to 0.048)	0.0E+00	0.000E+00	0.01 (-0.022 to 0.046)	6.06E-01	6.172E-01	0.534	2.122E-03	1.437	1.040E-29	
425									CKD F4	X	CKD F4 to CST3 to HAVCR2	kidney trait in F4	59.12	0.262 (0.129 to 0.444)	0.0E+00	0.000E+00	0.181 (-0.12 to 0.487)	2.74E-01	2 907E-01					
426	HAVCR2	CST3	Proteins	eGFRbiom	diftype	0.22	4.911E-07	2.143E-06	eGFR F4	Y	HAVCR2 to CST3 to eGFR F4	kidney trait in F4	98.41	-0.185 (-0.262 to -0.118)	0.0E+00	0.000E+00	-0.003 (-0.038 to 0.031)	8.64E-01	8 871E-01	-0.188	2 286E-08	-0.78	0	0.000E+0
430	UNC5C	CST3	Proteins	eGFRbiom	diftype	0.24	3.842E-08	2.128E-07	eGFR F4	Y	UNC5C to CST3 to eGFR F4	kidney trait in F4	90 91	-0.18 (-0.243 to -0.117)	0.0E+00	0.000E+00	-0.018 (-0.053 to 0.014)	3.14E-01	3 953E-01	-0.198	5.437E-10	-0.78	0	0.000E+0
434	LEPR	Creatinine	Proteins	eGFRbiom	diftype	-0.127	3.919E-03	9.103E-03	eGFR F4	Y	LEPR to Creatinine to eGFR F4	kidney trait in F4	83.19	0.06 (0.019 to 0.106)	2.0E-03	4.401E-03	0.012 (-0.047 to 0.06)	6.20E-01	6 881E-01	0.072	2 239E-02	-0.726	0	0.000E+0

435	CST3	LEPR	eGFRbiom	Proteins	diftype	-0.132	2.747E-03	6.820E-03	CKD F4	M	CST3 to CKD F4 to LEPR	kidney trait in F4	66.17	-0.089 (-0.215 to -0.014)	1.2E-02	2.272E-02	-0.045 (-0.135 to 0.045)	6.16E-01	6.261E-01	1.437	1.040E-29	-0.444	6.633E-04
436	Creatinine	LEPR	eGFRbiom	Proteins	diftype	-0.127	3.919E-03	9.103E-03	CKD F4	M	Creatinine to CKD F4 to LEPR	kidney trait in F4	44.42	-0.063 (-0.146 to -0.009)	1.2E-02	2.272E-02	-0.079 (-0.17 to 0.015)	1.14E-01	1.315E-01	1.153	1.412E-24	-0.444	6.633E-04
441	ACSL1	Urine albumin	CpGs	UACRbiom	diftype	0.072	2.522E-02	4.455E-02	CKD F4	M	ACSL1 to CKD F4 to Urine albumin	kidney trait in F4	95.08	0.082 (0.03 to 0.156)	0.0E+00	0.000E+00	0.004 (-0.04 to 0.051)	8.50E-01	8.543E-01	0.567	1.676E-05	1.585	4.296E-43
441									CKD F4	M	Urine albumin to CKD F4 to ACSL1	kidney trait in F4	91.12	0.068 (0.042 to 0.133)	0.0E+00	0.000E+00	0.007 (-0.064 to 0.08)	8.50E-01	8.543E-01				
442	ACSL1	Urine albumin	CpGs	UACRbiom	diftype	0.072	2.522E-02	4.455E-02	UACR F4	M	ACSL1 to UACR F4 to Urine albumin	kidney trait in F4	87.51	0.051 (0.017 to 0.086)	1.0E-02	2.706E-02	0.007 (-0.021 to 0.036)	6.12E-01	7.678E-01	0.066	3.586E-02	0.925	0.000E+00
444	LYL1	Urine albumin	CpGs	UACRbiom	diftype	0.081	1.303E-02	2.536E-02	UACR F4	Y	LYL1 to Urine albumin to UACR F4	kidney trait in F4	95.95	0.117 (0.054 to 0.184)	0.0E+00	0.000E+00	0.005 (-0.034 to 0.04)	8.20E-01	8.747E-01	0.122	3.282E-04	0.925	0.000E+00
445	LYSMD2	Urine albumin	CpGs	UACRbiom	diftype	-0.143	1.099E-05	4.005E-05	UACR F4	M	LYSMD2 to UACR F4 to Urine albumin	kidney trait in F4	83.67	-0.125 (-0.179 to -0.071)	0.0E+00	0.000E+00	-0.024 (-0.059 to 0.013)	1.92E-01	3.011E-01	-0.163	6.788E-07	0.925	0.000E+00
445									UACR F4	Y	LYSMD2 to Urine albumin to UACR F4	kidney trait in F4	83.25	-0.135 (-0.195 to -0.076)	0.0E+00	0.000E+00	-0.027 (-0.065 to 0.01)	1.48E-01	2.530E-01				
447	CST3	UNC5C	eGFRbiom	Proteins	diftype	0.24	3.842E-08	2.128E-07	CKDcrcc S4	X	CKDcrcc S4 to CST3 to UNC5C	kidney trait in S4 (as X)	28.63	0.507 (0 to 0.918)	0.0E+00	0.000E+00	1.264 (0 to 2.613)	2.00E-02	3.024E-02	1.705	5.964E-19	1.772	6.033E-03
447									CKDcrcc S4	X	CKDcrcc S4 to UNC5C to CST3	kidney trait in S4 (as X)	21.07	0.295 (0 to 0.634)	0.0E+00	0.000E+00	1.106 (0 to 1.491)	0.00E+00	0.000E+00				
448	CST3	EFNA5	eGFRbiom	Proteins	diftype	0.287	3.780E-11	3.202E-10	CKDcrcc S4	X	CKDcrcc S4 to CST3 to EFNA5	kidney trait in S4 (as X)	38.21	0.619 (0 to 1.111)	2.0E-03	2.583E-03	1.002 (0 to 1.902)	0.00E+00	0.000E+00	1.705	5.964E-19	1.621	8.552E-03
448									CKDcrcc S4	X	CKDcrcc S4 to EFNA5 to CST3	kidney trait in S4 (as X)	25.74	0.361 (0 to 0.638)	2.0E-03	2.583E-03	1.041 (0 to 1.374)	0.00E+00	0.000E+00				

449	TNFRSF1A	CST3	Proteins	eGFRbiom	diftype	0.442	6.356E-26	6.102E-24	CKDcrcc S4	X	CKDcrcc S4 to TNFRSF1A	kidney trait in S4 (as X)	63.62	0.891 (0 to 1.856)	0.00E+00	0.000E+00	0.51 (-0.557 to 1.097)	2.30E-01	2.502E-01	2.332	3.819E-05	1.705	5.964E-19
450		C8:1	eGFRbiom	Metabolites	diftype	0.166	6.150E-10	4.428E-09	CKDcrcc S4	X	CKDcrcc S4 to CST3 to C8:1	kidney trait in S4 (as X)	39.68	0.388 (0.196 to 0.686)	0.00E+00	0.000E+00	0.59 (0.138 to 1.035)	6.00E-03	1.033E-02	1.705	5.964E-19	0.986	2.594E-06
451	TNFRSF1B		eGFRbiom	Proteins	diftype	0.415	9.521E-23	4.570E-21	CKDcrcc S4	X	CKDcrcc S4 to CST3 to TNFRSF1B	kidney trait in S4 (as X)	61.06	0.963 (0 to 1.315)	0.00E+00	0.000E+00	0.614 (-0.657 to 1.688)	2.80E-01	2.942E-01	1.705	5.964E-19	1.578	7.905E-03
451									CKDcrcc S4	X	CKDcrcc S4 to TNFRSF1B to CST3	kidney trait in S4 (as X)	41.99	0.588 (0 to 1.031)	0.00E+00	0.000E+00	0.813 (0 to 1.304)	4.00E-03	7.515E-03				
452	CST3	C1QBP	eGFRbiom	Proteins	diftype	-0.35	3.087E-16	5.556E-15	CKDcrcc S4	X	CKDcrcc S4 to CST3 to C1QBP	kidney trait in S4 (as X)	32.49	-0.554 (-0.897 to 0)	0.00E+00	0.000E+00	-1.151 (-1.65 to 0)	0.00E+00	0.000E+00	1.705	5.964E-19	-1.706	2.021E-03
452									CKDcrcc S4	X	CKDcrcc S4 to C1QBP to CST3	kidney trait in S4 (as X)	30.41	0.426 (0 to 0.715)	0.00E+00	0.000E+00	0.975 (0 to 1.286)	0.00E+00	0.000E+00				
454	CST3	B2M	eGFRbiom	Proteins	diftype	0.615	1.036E-54	2.985E-52	CKDcrcc S4	X	CKDcrcc S4 to CST3 to B2M	kidney trait in S4 (as X)	74.14	1.254 (0 to 1.67)	0.00E+00	0.000E+00	0.437 (-0.47 to 1.544)	3.48E-01	3.537E-01	1.705	5.964E-19	1.691	2.622E-03
454									CKDcrcc S4	X	CKDcrcc S4 to B2M to CST3	kidney trait in S4 (as X)	65.81	0.922 (0 to 1.537)	0.00E+00	0.000E+00	0.479 (-0.186 to 0.966)	1.22E-01	1.513E-01				
455	CST3	FSTL3	eGFRbiom	Proteins	diftype	0.33	1.775E-14	2.223E-13	CKDcrcc S4	X	CKDcrcc S4 to CST3 to FSTL3	kidney trait in S4 (as X)	50.71	0.893 (0 to 1.379)	0.00E+00	0.000E+00	0.868 (-0.383 to 2.154)	2.12E-01	2.347E-01	1.705	5.964E-19	1.761	4.630E-03
455									CKDcrcc S4	X	CKDcrcc S4 to FSTL3 to CST3	kidney trait in S4 (as X)	39.75	0.557 (0 to 1.031)	0.00E+00	0.000E+00	0.844 (0 to 1.292)	1.20E-02	1.860E-02				
456	NBL1	CST3	Proteins	eGFRbiom	diftype	0.373	2.378E-18	5.708E-17	CKDcrcc S4	X	CKDcrcc S4 to NBL1 to CST3	kidney trait in S4 (as X)	49.05	0.687 (0 to 1.158)	0.00E+00	0.000E+00	0.714 (0 to 1.162)	3.00E-02	4.133E-02	2.544	1.010E-04	1.705	5.964E-19
456									CKDcrcc S4	X	CKDcrcc S4 to CST3 to NBL1	kidney trait in S4 (as X)	32.51	0.827 (0 to 1.278)	0.00E+00	0.000E+00	1.717 (0 to 2.788)	0.00E+00	0.000E+00				
458	CST3	C5	eGFRbiom	Metabolites	diftype	0.182	1.247E-11	1.122E-10	CKDcrcc S4	X	CKDcrcc S4 to CST3 to C5	kidney trait in S4 (as X)	39.87	0.243 (0.08 to 0.452)	0.00E+00	0.000E+00	0.367 (-0.027 to 0.735)	7.40E-02	9.558E-02	1.705	5.964E-19	0.611	1.948E-03
459	CST3	C14:2	eGFRbiom	Metabolites	diftype	0.244	5.241E-20	1.677E-18	CKDcrcc S4	X	CKDcrcc S4 to CST3 to C14:2	kidney trait in S4 (as X)	63.78	0.353 (0.188 to 0.6)	0.00E+00	0.000E+00	0.2 (-0.236 to 0.679)	3.98E-01	3.980E-01	1.705	5.964E-19	0.549	6.537E-03
460	CST3	SOD2	eGFRbiom	Proteins	diftype	-0.198	6.329E-06	2.463E-05	CKDcrcc S4	X	CKDcrcc S4 to CST3 to SOD2	kidney trait in S4 (as X)	26.47	-0.509 (-0.906 to 0)	0.00E+00	0.000E+00	-1.415 (-2.88 to 0.844)	2.00E-01	2.255E-01	1.705	5.964E-19	-1.924	7.211E-04

461	CST3	CTSH	eGFRbiom	Proteins	diftype	0.415	8.967E-23	4.570E-21	CKDcrcc S4	X	CKDcrcc S4 to CST3 to CTSH	kidney trait in S4 (as X)	59.8	1 011 (0 to 1.414)	0.0E+00	0.000E+00	0.68 (-0.287 to 2.127)	2.64E-01	2.822E-01	1.705	5.964E-19	1.691	6.212E-03
461									CKDcrcc S4	X	CKDcrcc S4 to CTSH to CST3	kidney trait in S4 (as X)	43.7	0.612 (0 to 1.156)	0.0E+00	0.000E+00	0.789 (0 to 1.213)	3 00E-02	4.133E-02				
462	CST3	C10:2	eGFRbiom	Metabolites	diftype	0.241	1.527E-19	4.398E-18	CKDcrcc S4	X	CKDcrcc S4 to CST3 to C10:2	kidney trait in S4 (as X)	71.92	0 567 (0 321 to 0 943)	0.0E+00	0.000E+00	0.221 (-0.222 to 0.678)	2 90E-01	2.997E-01	1.705	5.964E-19	0.792	1.423E-04
463	CST3	EFNA5	eGFRbiom	Proteins	diftype	0.287	3.780E-11	3.202E-10	eGFR S4	X	eGFR S4 to CST3 to EFNA5	kidney trait in S4 (as X)	44.28	-0.183 (-0 379 to -0 227 (-0.452 to -0 045)	1.0E-02	1.818E-02	-0.231 (-0.465 to 0.015)	7 80E-02	1.030E-01	-0.681	1.738E-47	-0.414	3.797E-05
464	CST3	LAYN	eGFRbiom	Proteins	diftype	0.295	8.726E-12	8.666E-11	eGFR S4	X	eGFR S4 to CST3 to LAYN	kidney trait in S4 (as X)	70.06	-0 227 (-0.452 to -0 045)	1.0E-02	1.818E-02	-0.097 (-0.374 to 0.211)	5.16E-01	5.622E-01	-0.681	1.738E-47	-0.324	2.058E-03
465	CST3	TNFRSF1B	eGFRbiom	Proteins	diftype	0.415	9.521E-23	4.570E-21	eGFR S4	X	eGFR S4 to CST3 to TNFRSF1B	kidney trait in S4 (as X)	84.15	-0 347 (-0 527 to -0 177 (-0.177 to -0 037)	0.0E+00	0.000E+00	-0.065 (-0.268 to 0.141)	5 20E-01	5.622E-01	-0.681	1.738E-47	-0.413	1.963E-05
466	CST3	C5	eGFRbiom	Metabolites	diftype	0.182	1.247E-11	1.122E-10	eGFR S4	X	eGFR S4 to CST3 to C5	kidney trait in S4 (as X)	79.4	-0 09 (-0.155 to -0 024)	0.0E+00	0.000E+00	-0.029 (-0.137 to 0.078)	5 96E-01	6.274E-01	-0.681	1.738E-47	-0.134	9.562E-03
467	CST3	C8	eGFRbiom	Metabolites	diftype	0.213	1.922E-15	3.076E-14	eGFR S4	X	eGFR S4 to CST3 to C8	kidney trait in S4 (as X)	42.93	-0 09 (-0.155 to -0 024)	8.0E-03	1.647E-02	-0.119 (-0.253 to 0.002)	5 80E-02	7.883E-02	-0.681	1.738E-47	-0.207	4.305E-05
468	CST3	SPOCK2	eGFRbiom	Proteins	diftype	-0.335	6.329E-15	9.114E-14	eGFR S4	X	eGFR S4 to CST3 to SPOCK2	kidney trait in S4 (as X)	59.74	0 27 (0.131 to 0.429)	0.0E+00	0.000E+00	0.182 (-0.033 to 0.379)	1.16E-01	1.437E-01	-0.681	1.738E-47	0.451	1.078E-05
469	CST3	NBL1	eGFRbiom	Proteins	diftype	0.373	2.378E-18	5.708E-17	eGFR S4	X	eGFR S4 to CST3 to NBL1	kidney trait in S4 (as X)	89.47	-0 328 (-0 516 to -0 187 (-0 349 to -0 066)	0.0E+00	0.000E+00	-0.039 (-0.35 to 0.287)	8 32E-01	8.502E-01	-0.681	1.738E-47	-0.366	7.546E-04
470	CST3	TFF3	eGFRbiom	Proteins	diftype	0.376	1.102E-18	2.886E-17	eGFR S4	X	eGFR S4 to CST3 to TFF3	kidney trait in S4 (as X)	52.54	-0.187 (-0 349 to -0 066)	0.0E+00	0.000E+00	-0.169 (-0.345 to 0.021)	8.60E-02	1.095E-01	-0.681	1.738E-47	-0.356	1.477E-04
472	CST3	C8:1	eGFRbiom	Metabolites	diftype	0.166	6.150E-10	4.428E-09	eGFR S4	X	eGFR S4 to CST3 to C8:1	kidney trait in S4 (as X)	42.16	-0.13 (-0 22 to -0 049)	2.0E-03	5.385E-03	-0.178 (-0.32 to 0.05)	1 00E-02	1.538E-02	-0.681	1.738E-47	-0.312	1.227E-08
473	CST3	B2M	eGFRbiom	Proteins	diftype	0.615	1.036E-54	2.985E-52	eGFR S4	X	eGFR S4 to CST3 to B2M	kidney trait in S4 (as X)	78.82	-0.435 (-0.625 to -0 297)	0.0E+00	0.000E+00	-0.117 (-0.28 to 0.064)	2 32E-01	2.753E-01	-0.681	1.738E-47	-0.553	5.763E-10
474	CST3	TNFRSF19	eGFRbiom	Proteins	diftype	0.294	1.165E-11	1.119E-10	eGFR S4	X	eGFR S4 to CST3 to TNFRSF19	kidney trait in S4 (as X)	93.64	-0 218 (-0 389 to -0 084)	2.0E-03	5.385E-03	-0.015 (-0.263 to 0.232)	8.14E-01	8.379E-01	-0.681	1.738E-47	-0.233	1.840E-02
475	CST3	C6(C4:1-DC)	eGFRbiom	Metabolites	diftype	0.224	4.939E-17	9.483E-16	eGFR S4	X	eGFR S4 to CST3 to C6(C4:1-DC)	kidney trait in S4 (as X)	65.48	-0.143 (-0 241 to -0 074)	0.0E+00	0.000E+00	-0.075 (-0.201 to 0.045)	2 36E-01	2.776E-01	-0.681	1.738E-47	-0.219	1.804E-05

476	CST3	HAVCR2	eGFRbiom	Proteins	diftype	0.22	4.911E-07	2.143E-06	eGFR S4	X	eGFR S4 to CST3 to HAVCR2	kidney trait in S4 (as X)	70.52	-0.203 (-0.386 to -0.062)	4.0E-03	9.492E-03	-0.085 (-0.324 to 0.144)	4.48E-01	4.978E-01	-0.681	1.738E-47	-0.288	4.237E-03
477	CST3	CTSH	eGFRbiom	Proteins	diftype	0.415	8.967E-23	4.570E-21	eGFR S4	X	eGFR S4 to CST3 to CTSH	kidney trait in S4 (as X)	97.97	-0.382 (-0.572 to -0.233)	0.0E+00	0.000E+00	-0.008 (-0.21 to 0.224)	9.52E-01	9.658E-01	-0.681	1.738E-47	-0.39	1.142E-04
478	CST3	JAM2	eGFRbiom	Proteins	diftype	0.341	2.148E-15	3.257E-14	eGFR S4	X	eGFR S4 to CST3 to JAM2	kidney trait in S4 (as X)	48.1	-0.202 (-0.414 to 0.036)	1.2E-02	2.074E-02	-0.217 (-0.447 to 0.044)	8.00E-02	1.047E-01	-0.681	1.738E-47	-0.419	6.408E-05
479	CST3	C12	eGFRbiom	Metabolites	diftype	0.248	1.196E-20	4.304E-19	eGFR S4	X	eGFR S4 to CST3 to C12	kidney trait in S4 (as X)	41.7	-0.086 (-0.148 to -0.025)	1.0E-02	1.818E-02	-0.12 (-0.241 to -0.011)	3.40E-02	4.907E-02	-0.681	1.738E-47	-0.203	7.154E-05
481	CST3	RELT	eGFRbiom	Proteins	diftype	0.462	1.615E-28	2.325E-26	eGFR S4	X	eGFR S4 to CST3 to RELT	kidney trait in S4 (as X)	73.6	-0.326 (-0.498 to 0.2)	0.0E+00	0.000E+00	-0.117 (-0.321 to 0.109)	2.90E-01	3.301E-01	-0.681	1.738E-47	-0.443	3.019E-06
482	CST3	C1QBP	eGFRbiom	Proteins	diftype	-0.35	3.087E-16	5.556E-15	eGFR S4	X	eGFR S4 to CST3 to C1QBP	kidney trait in S4 (as X)	82.63	0.214 (0.105 to 0.351)	0.0E+00	0.000E+00	0.045 (-0.142 to 0.221)	6.82E-01	7.073E-01	-0.681	1.738E-47	0.259	4.606E-03
483	CST3	ESAM	eGFRbiom	Proteins	diftype	0.276	1.940E-10	1.510E-09	eGFR S4	X	eGFR S4 to CST3 to ESAM	kidney trait in S4 (as X)	63.02	-0.133 (-0.27 to -0.019)	1.4E-02	2.306E-02	-0.078 (-0.272 to 0.151)	4.84E-01	5.335E-01	-0.681	1.738E-47	-0.211	2.078E-02
484	CST3	C14:2	eGFRbiom	Metabolites	diftype	0.244	5.241E-20	1.677E-18	eGFR S4	X	eGFR S4 to CST3 to C14:2	kidney trait in S4 (as X)	36.81	-0.097 (-0.161 to -0.033)	4.0E-03	9.492E-03	-0.166 (-0.285 to -0.058)	0.00E+00	0.000E+00	-0.681	1.738E-47	-0.259	8.109E-07
486	CST3	TNFRSF1A	eGFRbiom	Proteins	diftype	0.442	6.356E-26	6.102E-24	eGFR S4	X	eGFR S4 to CST3 to TNFRSF1A	kidney trait in S4 (as X)	84.51	-0.333 (-0.485 to -0.221)	0.0E+00	0.000E+00	-0.061 (-0.256 to 0.136)	5.80E-01	6.152E-01	-0.681	1.738E-47	-0.394	2.573E-05
487	CST3	SOD2	eGFRbiom	Proteins	diftype	-0.198	6.329E-06	2.463E-05	eGFR S4	X	eGFR S4 to CST3 to SOD2	kidney trait in S4 (as X)	93.54	0.212 (0.098 to 0.381)	0.0E+00	0.000E+00	0.015 (-0.232 to 0.24)	9.78E-01	9.850E-01	-0.681	1.738E-47	0.226	1.695E-02
488	CST3	SCARF1	eGFRbiom	Proteins	diftype	0.229	1.554E-07	7.590E-07	eGFR S4	X	eGFR S4 to CST3 to SCARF1	kidney trait in S4 (as X)	70.69	-0.166 (-0.29 to -0.058)	4.0E-03	9.492E-03	-0.069 (-0.245 to 0.15)	5.22E-01	5.622E-01	-0.681	1.738E-47	-0.235	1.797E-02
489	CST3	ERP29	eGFRbiom	Proteins	diftype	0.261	1.840E-09	1.204E-08	eGFR S4	X	eGFR S4 to CST3 to ERP29	kidney trait in S4 (as X)	66.63	-0.238 (-0.388 to -0.118)	0.0E+00	0.000E+00	-0.119 (-0.327 to 0.097)	2.78E-01	3.217E-01	-0.681	1.738E-47	-0.356	5.110E-04
490	CST3	C10	eGFRbiom	Metabolites	diftype	0.218	3.764E-16	6.377E-15	eGFR S4	X	eGFR S4 to CST3 to C10	kidney trait in S4 (as X)	46.97	-0.1 (-0.16 to -0.032)	6.0E-03	1.292E-02	-0.113 (-0.242 to -0.002)	5.00E-02	7.000E-02	-0.681	1.738E-47	-0.211	2.443E-05
492	CST3	FSTL3	eGFRbiom	Proteins	diftype	0.33	1.775E-14	2.223E-13	eGFR S4	X	eGFR S4 to CST3 to FSTL3	kidney trait in S4 (as X)	58.06	-0.287 (-0.485 to -0.142)	0.0E+00	0.000E+00	-0.207 (-0.44 to 0.039)	1.02E-01	1.275E-01	-0.681	1.738E-47	-0.495	8.577E-07
493	CST3	C14:1-OH	eGFRbiom	Metabolites	diftype	0.229	9.246E-18	1.902E-16	eGFR S4	X	eGFR S4 to CST3 to C14:1-OH	kidney trait in S4 (as X)	65.48	-0.119 (-0.187 to -0.061)	2.0E-03	5.385E-03	-0.062 (-0.19 to 0.059)	2.88E-01	3.301E-01	-0.681	1.738E-47	-0.18	1.000E-03

494	CST3	C10:2	eGFRbiom	Metabolites	diftype	0.241	1.527E-19	4.398E-18	eGFR S4	X	eGFR S4 to CST3 to C10:2	kidney trait in S4 (as X)	73.02	-0.214 (-0.298 to 0.134)	0.0E+00	0.000E+00	-0.079 (-0.224 to 0.052)	2.70E-01	3.150E-01	-0.681	1.738E-47	-0.295	5.422E-08
495	CST3	EPHA2	eGFRbiom	Proteins	diftype	0.256	3.863E-09	2.318E-08	eGFR S4	X	eGFR S4 to CST3 to EPHA2	kidney trait in S4 (as X)	61.94	-0.187 (-0.332 to 0.059)	0.0E+00	0.000E+00	-0.115 (-0.331 to 0.111)	3.10E-01	3.500E-01	-0.681	1.738E-47	-0.301	1.064E-03
497	CST3	C2	eGFRbiom	Metabolites	diftype	0.205	2.225E-14	2.670E-13	eGFR S4	X	eGFR S4 to CST3 to C2	kidney trait in S4 (as X)	61.41	-0.138 (-0.211 to 0.076)	0.0E+00	0.000E+00	-0.086 (-0.207 to 0.033)	1.60E-01	1.931E-01	-0.681	1.738E-47	-0.223	3.846E-05
498	EGFR	CST3	Proteins	eGFRbiom	diftype	-0.371	3.615E-18	8.009E-17	eGFR S4	X	eGFR S4 to EGFR to CST3	kidney trait in S4 (as X)	16.11	-0.083 (-0.157 to 0.027)	0.0E+00	0.000E+00	-0.43 (-0.533 to -0.321)	0.00E+00	0.000E+00	0.273	2.556E-03	-0.681	1.738E-47
500	TNFRSF1A	Creatinine	Proteins	eGFRbiom	diftype	0.283	6.165E-11	5.073E-10	CKDcrcc S4	X	CKDcrcc S4 to TNFRSF1A to Creatinine	kidney trait in S4 (as X)	59.45	0.645 (0 to 1.397)	0.0E+00	0.000E+00	0.44 (-0.2 to 1.087)	1.40E-01	1.702E-01	2.332	3.819E-05	1.496	1.390E-17
501	Creatinine	C14:2	eGFRbiom	Metabolites	diftype	0.164	1.092E-09	7.667E-09	CKDcrcc S4	X	CKDcrcc S4 to Creatinine to C14:2	kidney trait in S4 (as X)	29.81	0.164 (0.016 to 0.367)	3.4E-02	3.904E-02	0.385 (-0.083 to 0.897)	1.16E-01	1.468E-01	1.496	1.390E-17	0.549	6.537E-03
502	Creatinine	C8:1	eGFRbiom	Metabolites	diftype	0.141	1.648E-07	7.910E-07	CKDcrcc S4	X	CKDcrcc S4 to Creatinine to C8:1	kidney trait in S4 (as X)	31.25	0.308 (0.131 to 0.586)	2.0E-03	2.583E-03	0.678 (0.21 to 1.089)	0.00E+00	0.000E+00	1.496	1.390E-17	0.986	2.594E-06
503	Creatinine	TNFRSF1B	eGFRbiom	Proteins	diftype	0.181	3.809E-05	1.306E-04	CKDcrcc S4	X	CKDcrcc S4 to Creatinine to TNFRSF1B	kidney trait in S4 (as X)	33.73	0.532 (0 to 0.935)	0.0E+00	0.000E+00	1.046 (0 to 2.049)	2.60E-02	3.749E-02	1.496	1.390E-17	1.578	7.905E-03
503									CKDcrcc S4	X	CKDcrcc S4 to TNFRSF1B to Creatinine	kidney trait in S4 (as X)	30.84	0.335 (0 to 0.646)	0.0E+00	0.000E+00	0.75 (0 to 1.209)	0.00E+00	0.000E+00				
504	Creatinine	C5	eGFRbiom	Metabolites	diftype	0.182	1.204E-11	1.119E-10	CKDcrcc S4	X	CKDcrcc S4 to Creatinine to C5	kidney trait in S4 (as X)	52.11	0.318 (0.153 to 0.551)	0.0E+00	0.000E+00	0.292 (-0.114 to 0.69)	1.68E-01	1.929E-01	1.496	1.390E-17	0.611	1.948E-03
505	Creatinine	C10:2	eGFRbiom	Metabolites	diftype	0.206	1.449E-14	1.897E-13	CKDcrcc S4	X	CKDcrcc S4 to Creatinine to C10:2	kidney trait in S4 (as X)	46.07	0.365 (0.157 to 0.662)	0.0E+00	0.000E+00	0.427 (0.014 to 0.85)	4.00E-02	5.391E-02	1.496	1.390E-17	0.792	1.423E-04
506	B2M	Creatinine	Proteins	eGFRbiom	diftype	0.317	1.905E-13	2.110E-12	CKDcrcc S4	X	CKDcrcc S4 to B2M to Creatinine	kidney trait in S4 (as X)	40.22	0.436 (0 to 0.812)	0.0E+00	0.000E+00	0.649 (0 to 1.345)	8.00E-03	1.305E-02	1.691	2.622E-03	1.496	1.390E-17
506									CKDcrcc S4	X	CKDcrcc S4 to Creatinine to B2M	kidney trait in S4 (as X)	34.09	0.577 (0 to 0.959)	0.0E+00	0.000E+00	1.115 (-0.01 to 2.081)	5.40E-02	7.123E-02				

508	Creatinine	UNC5C	eGFRbiom	Proteins	diotype	0.178	5.138E-05	1.721E-04	CKDcrcc S4	X	CKDcrcc S4 to Creatinine to UNC5C	kidney trait in S4 (as X)	25.57	0.453 (0 to 0.854)	0.0E+00	0.000E+00	1.319 (0 to 2.523)	0.00E+00	0.000E+00	1.496	1.390E-17	1.772	6.033E-03
508									CKDcrcc S4	X	CKDcrcc S4 to UNC5C to Creatinine	kidney trait in S4 (as X)	25.02	0.271 (0 to 0.607)	0.0E+00	0.000E+00	0.814 (0 to 1.394)	2.00E-03	4.133E-03				
509	C1QBP	Creatinine	Proteins	eGFRbiom	diotype	-0.229	1.555E-07	7.590E-07	CKDcrcc S4	X	CKDcrcc S4 to C1QBP to Creatinine	kidney trait in S4 (as X)	25.86	0.281 (0 to 0.502)	6.0E-03	7.154E-03	0.805 (0 to 1.329)	0.00E+00	0.000E+00	-1.706	2.021E-03	1.496	1.390E-17
509									CKDcrcc S4	X	CKDcrcc S4 to Creatinine to C1QBP	kidney trait in S4 (as X)	20.79	-0.355 (-0.766 to 0)	6.0E-03	7.154E-03	-1.351 (-1.813 to 0)	0.00E+00	0.000E+00				
510	Creatinine	CTSH	eGFRbiom	Proteins	diotype	0.248	1.232E-08	7.096E-08	CKDcrcc S4	X	CKDcrcc S4 to Creatinine to CTSH	kidney trait in S4 (as X)	29.44	0.498 (0 to 0.836)	2.0E-03	2.583E-03	1.193 (0 to 2.553)	6.00E-03	1.033E-02	1.496	1.390E-17	1.691	6.212E-03
510									CKDcrcc S4	X	CKDcrcc S4 to CTSH to Creatinine	kidney trait in S4 (as X)	28.61	0.31 (0 to 0.634)	2.0E-03	2.583E-03	0.775 (0 to 1.372)	0.00E+00	0.000E+00				
511	Creatinine	EFNA5	eGFRbiom	Proteins	diotype	0.215	9.017E-07	3.819E-06	CKDcrcc S4	X	CKDcrcc S4 to Creatinine to EFNA5	kidney trait in S4 (as X)	25.58	0.415 (0 to 0.775)	2.0E-03	2.583E-03	1.206 (0 to 1.987)	0.00E+00	0.000E+00	1.496	1.390E-17	1.621	8.552E-03
511									CKDcrcc S4	X	CKDcrcc S4 to EFNA5 to Creatinine	kidney trait in S4 (as X)	22.91	0.249 (0 to 0.472)	2.0E-03	2.583E-03	0.836 (0 to 1.365)	0.00E+00	0.000E+00				
512	NBL1	Creatinine	Proteins	eGFRbiom	diotype	0.23	1.345E-07	6.796E-07	CKDcrcc S4	X	CKDcrcc S4 to NBL1 to Creatinine	kidney trait in S4 (as X)	31.01	0.336 (0 to 0.698)	4.0E-03	4.960E-03	0.749 (0 to 1.343)	4.00E-03	7.515E-03	2.544	1.010E-04	1.496	1.390E-17
512									CKDcrcc S4	X	CKDcrcc S4 to Creatinine to NBL1	kidney trait in S4 (as X)	15.46	0.393 (0 to 0.733)	4.0E-03	4.960E-03	2.151 (0 to 3.114)	0.00E+00	0.000E+00				
513	IGFBP6	Creatinine	Proteins	eGFRbiom	diotype	0.403	1.655E-21	6.807E-20	CKDcrcc S4	X	CKDcrcc S4 to IGFBP6 to Creatinine	kidney trait in S4 (as X)	31.63	0.343 (0 to 0.604)	0.0E+00	0.000E+00	0.742 (0 to 1.369)	2.00E-03	4.133E-03	1.466	4.846E-03	1.496	1.390E-17
513									CKDcrcc S4	X	CKDcrcc S4 to Creatinine to IGFBP6	kidney trait in S4 (as X)	30.67	0.45 (0 to 0.793)	0.0E+00	0.000E+00	1.016 (0 to 1.673)	1.00E-02	1.590E-02				

514	FSTL3	Creatinine	Proteins	eGFRbiom	diftype	0.21	1.598E-06	6.668E-06	CKDcrcc S4	X	CKDcrcc S4 to FSTL3 to Creatinine	kidney trait in S4 (as X)	36.88	0.4 (0 to 0.78)	0.0E+00	0.000E+00	0.685 (0 to 1.165)	0.00E+00	0.000E+00	1.761	4.630E-03	1.496	1.390E-17
514									CKDcrcc S4	X	CKDcrcc S4 to Creatinine to FSTL3	kidney trait in S4 (as X)	35.39	0.623 (0 to 1.06)	0.0E+00	0.000E+00	1.138 (0 to 2.313)	6.00E-03	1.033E-02				
515	Creatinine	TNFRSF19	eGFRbiom	Proteins	diftype	0.238	4.825E-08	2.573E-07	eGFR S4	X	eGFR S4 to Creatinine to TNFRSF19	kidney trait in S4 (as X)	76.8	-0.179 (-0.31 to -0.071)	2.0E-03	5.385E-03	-0.054 (-0.274 to 0.158)	5.32E-01	5.685E-01	-0.548	7.972E-36	-0.233	1.840E-02
517	B2M	Creatinine	Proteins	eGFRbiom	diftype	0.317	1.905E-13	2.110E-12	eGFR S4	X	eGFR S4 to B2M to Creatinine	kidney trait in S4 (as X)	26.58	-0.099 (-0.178 to 0.027)	1.0E-02	1.818E-02	-0.274 (-0.398 to 0.163)	0.00E+00	0.000E+00	-0.553	5.763E-10	-0.548	7.972E-36
517									eGFR S4	X	eGFR S4 to Creatinine to B2M	kidney trait in S4 (as X)	24.74	-0.137 (-0.26 to 0.037)	1.0E-02	1.818E-02	-0.416 (-0.63 to -0.215)	0.00E+00	0.000E+00				
519	Creatinine	C8:1	eGFRbiom	Metabolites	diftype	0.141	1.648E-07	7.910E-07	eGFR S4	X	eGFR S4 to Creatinine to C8:1	kidney trait in S4 (as X)	28.17	-0.088 (-0.167 to 0.012)	2.6E-02	3.957E-02	-0.224 (-0.365 to 0.094)	0.00E+00	0.000E+00	-0.548	7.972E-36	-0.312	1.227E-08
521	Creatinine	CTSH	eGFRbiom	Proteins	diftype	0.248	1.232E-08	7.096E-08	eGFR S4	X	eGFR S4 to Creatinine to CTSH	kidney trait in S4 (as X)	36.5	-0.142 (-0.258 to 0.038)	6.0E-03	1.292E-02	-0.248 (-0.461 to 0.037)	2.60E-02	3.832E-02	-0.548	7.972E-36	-0.39	1.142E-04
522	Creatinine	EFNA5	eGFRbiom	Proteins	diftype	0.215	9.017E-07	3.819E-06	eGFR S4	X	eGFR S4 to Creatinine to EFNA5	kidney trait in S4 (as X)	24.64	-0.102 (-0.203 to 0.009)	2.2E-02	3.422E-02	-0.312 (-0.522 to 0.099)	2.00E-03	3.415E-03	-0.548	7.972E-36	-0.414	3.797E-05
522									eGFR S4	X	eGFR S4 to EFNA5 to Creatinine	kidney trait in S4 (as X)	10.98	-0.041 (-0.089 to 0.004)	2.2E-02	3.422E-02	-0.332 (-0.455 to 0.23)	0.00E+00	0.000E+00				
523	Creatinine	TNFRSF1B	eGFRbiom	Proteins	diftype	0.181	3.809E-05	1.306E-04	eGFR S4	X	eGFR S4 to Creatinine to TNFRSF1B	kidney trait in S4 (as X)	36.1	-0.149 (-0.286 to 0.034)	1.2E-02	2.074E-02	-0.264 (-0.48 to -0.047)	1.80E-02	2.710E-02	-0.548	7.972E-36	-0.413	1.963E-05
523									eGFR S4	X	eGFR S4 to TNFRSF1B to Creatinine	kidney trait in S4 (as X)	17.34	-0.065 (-0.123 to 0.016)	1.2E-02	2.074E-02	-0.308 (-0.431 to 0.207)	0.00E+00	0.000E+00				
524	Creatinine	RELT	eGFRbiom	Proteins	diftype	0.327	3.216E-14	3.705E-13	eGFR S4	X	eGFR S4 to Creatinine to RELT	kidney trait in S4 (as X)	33.98	-0.151 (-0.268 to 0.049)	2.0E-03	5.385E-03	-0.293 (-0.502 to 0.085)	6.00E-03	9.438E-03	-0.548	7.972E-36	-0.443	3.019E-06
524									eGFR S4	X	eGFR S4 to RELT to Creatinine	kidney trait in S4 (as X)	19.74	-0.074 (-0.139 to 0.024)	2.0E-03	5.385E-03	-0.299 (-0.408 to 0.196)	0.00E+00	0.000E+00				
526	Creatinine	C5	eGFRbiom	Metabolites	diftype	0.182	1.204E-11	1.119E-10	eGFR S4	X	eGFR S4 to Creatinine to C5	kidney trait in S4 (as X)	99.34	-0.133 (-0.198 to 0.074)	0.0E+00	0.000E+00	-0.001 (-0.105 to 0.102)	9.90E-01	9.900E-01	-0.548	7.972E-36	-0.134	9.562E-03
528	Creatinine	C1QBP	eGFRbiom	Proteins	diftype	-0.229	1.555E-07	7.590E-07	eGFR S4	X	eGFR S4 to Creatinine to C1QBP	kidney trait in S4 (as X)	44.27	0.115 (0.02 to 0.22)	1.4E-02	2.306E-02	0.145 (-0.026 to 0.314)	1.18E-01	1.449E-01	-0.548	7.972E-36	0.259	4.606E-03

529	Creatinine	ERP29	eGFRbiom	Proteins	diftype	0.194	9.748E-06	3.694E-05	eGFR S4	X	eGFR S4 to Creatinine to ERP29	kidney trait in S4 (as X)	43.71	-0.156 (-0.271 to 0.059)	0.0E+00	0.000E+00	-0.201 (-0.399 to 0.002)	5.20E-02	7.137E-02	-0.548	7.972E-36	-0.356	5.110E-04
530	Creatinine	TFF3	eGFRbiom	Proteins	diftype	0.273	2.976E-10	2.255E-09	eGFR S4	X	eGFR S4 to Creatinine to TFF3	kidney trait in S4 (as X)	39.15	-0.139 (-0.275 to 0.03)	1.4E-02	2.306E-02	-0.216 (-0.386 to 0.042)	4.00E-03	6.588E-03	-0.548	7.972E-36	-0.356	1.477E-04
534	Creatinine	IGFBP6	eGFRbiom	Proteins	diftype	0.403	1.655E-21	6.807E-20	eGFR S4	X	eGFR S4 to Creatinine to IGFBP6	kidney trait in S4 (as X)	25.63	-0.11 (-0.19 to 0.042)	2.0E-03	5.385E-03	-0.319 (-0.499 to 0.142)	0.00E+00	0.000E+00	-0.548	7.972E-36	-0.428	3.180E-07
534									eGFR S4	X	eGFR S4 to Creatinine to IGFBP6	kidney trait in S4 (as X)	18.07	-0.067 (-0.122 to 0.024)	2.0E-03	5.385E-03	-0.305 (-0.43 to -0.19)	0.00E+00	0.000E+00				
536	Creatinine	JAM2	eGFRbiom	Proteins	diftype	0.331	1.313E-14	1.801E-13	eGFR S4	X	eGFR S4 to Creatinine to JAM2	kidney trait in S4 (as X)	47.05	-0.197 (-0.362 to 0.056)	2.0E-03	5.385E-03	-0.222 (-0.405 to 0.031)	2.00E-02	2.979E-02	-0.548	7.972E-36	-0.419	6.408E-05
541	Creatinine	FSTL3	eGFRbiom	Proteins	diftype	0.21	1.598E-06	6.668E-06	eGFR S4	X	eGFR S4 to Creatinine to FSTL3	kidney trait in S4 (as X)	34.42	-0.17 (-0.297 to 0.066)	0.0E+00	0.000E+00	-0.324 (-0.548 to 0.113)	4.00E-03	6.588E-03	-0.548	7.972E-36	-0.495	8.577E-07
541									eGFR S4	X	eGFR S4 to FSTL3 to Creatinine	kidney trait in S4 (as X)	22.37	-0.083 (-0.141 to 0.033)	0.0E+00	0.000E+00	-0.289 (-0.401 to 0.195)	0.00E+00	0.000E+00				
542	Creatinine	C10:2	eGFRbiom	Metabolites	diftype	0.206	1.449E-14	1.897E-13	eGFR S4	X	eGFR S4 to Creatinine to C10:2	kidney trait in S4 (as X)	35.98	-0.106 (-0.189 to 0.024)	4.0E-03	9.492E-03	-0.189 (-0.337 to 0.056)	1.20E-02	1.826E-02	-0.548	7.972E-36	-0.295	5.422E-08
545	Creatinine	TNFRSF1A	eGFRbiom	Proteins	diftype	0.283	6.165E-11	5.073E-10	eGFR S4	X	eGFR S4 to Creatinine to TNFRSF1A	kidney trait in S4 (as X)	50.77	-0.2 (-0.322 to 0.091)	0.0E+00	0.000E+00	-0.194 (-0.399 to 0)	5.20E-02	7.137E-02	-0.548	7.972E-36	-0.394	2.573E-05
588	EGFR	CST3	Proteins	eGFRbiom	diftype	-0.371	3.615E-18	8.009E-17	CKD FF4	Y	EGFR to CST3 to incident CKD	kidney trait in FF4 (as Y)	58.56	-0.031 (-0.048 to 0.015)	0.0E+00	0.000E+00	-0.022 (-0.05 to 0.017)	2.44E-01	2.519E-01	-0.509	2.488E-03	1.473	5.486E-11
589	C14:1	CST3	Metabolites	eGFRbiom	diftype	0.191	9.890E-13	1.055E-11	CKD FF4	Y	C14:1 to CST3 to incident CKD	kidney trait in FF4 (as Y)	39.62	0.015 (0.008 to 0.025)	0.0E+00	0.000E+00	0.023 (-0.004 to 0.057)	1.06E-01	1.170E-01	0.299	9.877E-03	1.473	5.486E-11
591	C12	CST3	Metabolites	eGFRbiom	diftype	0.248	1.196E-20	4.304E-19	CKD FF4	Y	C12 to CST3 to incident CKD	kidney trait in FF4 (as Y)	51.87	0.023 (0.013 to 0.034)	0.0E+00	0.000E+00	0.021 (-0.009 to 0.053)	1.70E-01	1.813E-01	0.327	5.401E-03	1.473	5.486E-11
592	C18:1	CST3	Metabolites	eGFRbiom	diftype	0.14	1.998E-07	9.280E-07	CKD FF4	Y	C18:1 to CST3 to incident CKD	kidney trait in FF4 (as Y)	33.38	0.014 (0.006 to 0.024)	0.0E+00	0.000E+00	0.029 (-0.002 to 0.066)	6.00E-02	6.857E-02	0.325	6.305E-03	1.473	5.486E-11
593	GHR	CST3	Proteins	eGFRbiom	diftype	-0.207	2.243E-06	9.156E-06	CKD FF4	Y	GHR to CST3 to incident CKD	kidney trait in FF4 (as Y)	18.7	-0.015 (-0.025 to 0.005)	0.0E+00	0.000E+00	-0.064 (-0.095 to 0.024)	0.00E+00	0.000E+00	-0.683	1.930E-04	1.473	5.486E-11

594	MASP1	CST3	Proteins	eGFRbiom	diftype	-0.157	3.603E-04	1.059E-03	eGFR FF4	Y	MASP1 to CST3 to Follow-up eGFR	kidney trait in FF4 (as Y)	89.52	0.082 (0.035 to 0.132)	0.0E+00	0.000E+00	0.01 (-0.031 to 0.049)	6.86E-01	7.054E-01	0.091	5.181E-03	-0.642	5.894E-98
595	ADAMT S13	CST3	Proteins	eGFRbiom	diftype	-0.161	2.551E-04	7.900E-04	eGFR FF4	Y	ADAMTS13 to CST3 to Follow-up eGFR	kidney trait in FF4 (as Y)	69.82	0.078 (0.039 to 0.121)	2.0E-03	3.406E-03	0.034 (-0.013 to 0.081)	1.34E-01	1.546E-01	0.111	6.823E-04	-0.642	5.894E-98
596	C12	CST3	Metabolites	eGFRbiom	diftype	0.248	1.196E-20	4.304E-19	eGFR FF4	Y	C12 to CST3 to Follow-up eGFR	kidney trait in FF4 (as Y)	75.89	-0.108 (-0.144 to -0.073)	0.0E+00	0.000E+00	-0.034 (-0.079 to 0.01)	1.06E-01	1.242E-01	-0.143	2.223E-07	-0.642	5.894E-98
597	BMP1	CST3	Proteins	eGFRbiom	diftype	-0.169	1.165E-04	3.686E-04	eGFR FF4	Y	BMP1 to CST3 to Follow-up eGFR	kidney trait in FF4 (as Y)	52.76	0.094 (0.042 to 0.147)	0.0E+00	0.000E+00	0.084 (0 to 0.162)	5.00E-02	6.337E-02	0.178	5.497E-06	-0.642	5.894E-98
598	HAVCR 2	CST3	Proteins	eGFRbiom	diftype	0.22	4.911E-07	2.143E-06	eGFR FF4	Y	HAVCR2 to CST3 to Follow-up eGFR	kidney trait in FF4 (as Y)	62.6	-0.142 (-0.204 to -0.086)	0.0E+00	0.000E+00	-0.085 (-0.152 to -0.016)	1.80E-02	2.452E-02	-0.227	1.144E-09	-0.642	5.894E-98
599	RELT	CST3	Proteins	eGFRbiom	diftype	0.462	1.615E-28	2.325E-26	eGFR FF4	Y	RELT to CST3 to Follow-up eGFR	kidney trait in FF4 (as Y)	59.83	-0.205 (-0.262 to -0.158)	0.0E+00	0.000E+00	-0.138 (-0.204 to -0.073)	0.00E+00	0.000E+00	-0.343	1.967E-24	-0.642	5.894E-98
600	TNFRSF 19	CST3	Proteins	eGFRbiom	diftype	0.294	1.165E-11	1.119E-10	eGFR FF4	Y	TNFRSF19 to CST3 to Follow-up eGFR	kidney trait in FF4 (as Y)	41.38	-0.077 (-0.158 to -0.02)	1.0E-02	1.473E-02	-0.109 (-0.162 to -0.059)	0.00E+00	0.000E+00	-0.185	2.628E-09	-0.642	5.894E-98
601	TNFRSF 1B	CST3	Proteins	eGFRbiom	diftype	0.415	9.521E-23	4.570E-21	eGFR FF4	Y	TNFRSF1B to CST3 to Follow-up eGFR	kidney trait in FF4 (as Y)	65.8	-0.199 (-0.261 to -0.145)	0.0E+00	0.000E+00	-0.103 (-0.177 to -0.028)	6.00E-03	8.605E-03	-0.302	2.211E-20	-0.642	5.894E-98
602	PAPPA	CST3	Proteins	eGFRbiom	diftype	0.193	1.121E-05	4.036E-05	eGFR FF4	Y	PAPPA to CST3 to Follow-up eGFR	kidney trait in FF4 (as Y)	74.94	-0.1 (-0.149 to -0.058)	0.0E+00	0.000E+00	-0.034 (-0.088 to 0.023)	2.66E-01	2.974E-01	-0.134	4.851E-05	-0.642	5.894E-98
603	CTSV	CST3	Proteins	eGFRbiom	diftype	-0.248	1.199E-08	7.047E-08	eGFR FF4	Y	CTSV to CST3 to Follow-up eGFR	kidney trait in FF4 (as Y)	69.65	0.149 (0.101 to 0.196)	0.0E+00	0.000E+00	0.065 (0.004 to 0.125)	3.40E-02	4.438E-02	0.213	5.057E-08	-0.642	5.894E-98
604	EGFR	CST3	Proteins	eGFRbiom	diftype	-0.371	3.615E-18	8.009E-17	eGFR FF4	Y	EGFR to CST3 to Follow-up eGFR	kidney trait in FF4 (as Y)	81.7	0.211 (0.162 to 0.263)	0.0E+00	0.000E+00	0.047 (-0.014 to 0.11)	1.60E-01	1.836E-01	0.259	1.214E-11	-0.642	5.894E-98
605	FN1	CST3	Proteins	eGFRbiom	diftype	-0.193	1.020E-05	3.802E-05	eGFR FF4	Y	FN1 to CST3 to Follow-up eGFR	kidney trait in FF4 (as Y)	91.77	0.101 (0.056 to 0.149)	0.0E+00	0.000E+00	0.009 (-0.039 to 0.054)	7.70E-01	7.881E-01	0.11	1.156E-03	-0.642	5.894E-98

606	LAYN	CST3	Proteins	eGFRbiom	diotype	0.295	8.726E-12	8.666E-11	eGFR FF4	Y	LAYN to CST3 to Follow-up eGFR	kidney trait in FF4 (as Y)	56.49	-0.135 (-0.194 to -0.085)	0.0E+00	0.000E+00	-0.104 (-0.173 to -0.035)	0.00E+00	0.000E+00	-0.24	5.264E-13	-0.642	5.894E-98
607	KDR	CST3	Proteins	eGFRbiom	diotype	-0.264	1.282E-09	8.789E-09	eGFR FF4	Y	KDR to CST3 to Follow-up eGFR	kidney trait in FF4 (as Y)	72.23	0.118 (0.071 to 0.169)	0.0E+00	0.000E+00	0.045 (-0.012 to 0.103)	1.08E-01	1.259E-01	0.163	2.182E-06	-0.642	5.894E-98
608	RETN	CST3	Proteins	eGFRbiom	diotype	0.283	6.818E-11	5.455E-10	eGFR FF4	Y	RETN to CST3 to Follow-up eGFR	kidney trait in FF4 (as Y)	60.61	-0.137 (-0.183 to -0.096)	0.0E+00	0.000E+00	-0.089 (-0.147 to -0.034)	4.00E-03	5.775E-03	-0.226	5.657E-12	-0.642	5.894E-98
609	KIR2DL4	CST3	Proteins	eGFRbiom	diotype	0.125	4.556E-03	1.033E-02	eGFR FF4	Y	KIR2DL4 to CST3 to Follow-up eGFR	kidney trait in FF4 (as Y)	57.01	-0.058 (-0.102 to -0.015)	4.0E-03	6.229E-03	-0.044 (-0.09 to 0.007)	9.40E-02	1.120E-01	-0.101	2.900E-03	-0.642	5.894E-98
610	C14:2	CST3	Metabolites	eGFRbiom	diotype	0.244	5.241E-20	1.677E-18	eGFR FF4	Y	C14:2 to CST3 to Follow-up eGFR	kidney trait in FF4 (as Y)	87.39	-0.098 (-0.136 to -0.064)	0.0E+00	0.000E+00	-0.014 (-0.057 to 0.027)	4.82E-01	5.126E-01	-0.112	3.972E-05	-0.642	5.894E-98
611	CNDP1	CST3	Proteins	eGFRbiom	diotype	-0.239	4.006E-08	2.177E-07	eGFR FF4	Y	CNDP1 to CST3 to Follow-up eGFR	kidney trait in FF4 (as Y)	80.09	0.113 (0.062 to 0.161)	0.0E+00	0.000E+00	0.028 (-0.039 to 0.086)	4.16E-01	4.467E-01	0.141	2.240E-05	-0.642	5.894E-98
612	NBL1	CST3	Proteins	eGFRbiom	diotype	0.373	2.378E-18	5.708E-17	eGFR FF4	Y	NBL1 to CST3 to Follow-up eGFR	kidney trait in FF4 (as Y)	63.42	-0.163 (-0.227 to -0.113)	0.0E+00	0.000E+00	-0.094 (-0.156 to -0.043)	2.00E-03	2.966E-03	-0.258	1.359E-14	-0.642	5.894E-98
613	ESAM	CST3	Proteins	eGFRbiom	diotype	0.276	1.940E-10	1.510E-09	eGFR FF4	Y	ESAM to CST3 to Follow-up eGFR	kidney trait in FF4 (as Y)	57.76	-0.137 (-0.183 to -0.089)	0.0E+00	0.000E+00	-0.1 (-0.164 to -0.034)	0.00E+00	0.000E+00	-0.236	3.557E-12	-0.642	5.894E-98
614	C14:1	CST3	Metabolites	eGFRbiom	diotype	0.191	9.890E-13	1.055E-11	eGFR FF4	Y	C14:1 to CST3 to Follow-up eGFR	kidney trait in FF4 (as Y)	77.37	-0.079 (-0.114 to -0.047)	0.0E+00	0.000E+00	-0.023 (-0.068 to 0.02)	2.90E-01	3.209E-01	-0.102	1.816E-04	-0.642	5.894E-98
615	IGFBP6	CST3	Proteins	eGFRbiom	diotype	0.437	2.789E-25	2.008E-23	eGFR FF4	Y	IGFBP6 to CST3 to Follow-up eGFR	kidney trait in FF4 (as Y)	57.21	-0.202 (-0.261 to -0.143)	0.0E+00	0.000E+00	-0.151 (-0.215 to -0.086)	0.00E+00	0.000E+00	-0.354	6.692E-22	-0.642	5.894E-98
616	IL19	CST3	Proteins	eGFRbiom	diotype	-0.182	3.397E-05	1.179E-04	eGFR FF4	Y	IL19 to CST3 to Follow-up eGFR	kidney trait in FF4 (as Y)	63	0.09 (0.044 to 0.136)	0.0E+00	0.000E+00	0.053 (0.004 to 0.101)	4.00E-02	5.099E-02	0.143	2.452E-05	-0.642	5.894E-98
618	ERP29	CST3	Proteins	eGFRbiom	diotype	0.261	1.840E-09	1.204E-08	eGFR FF4	Y	ERP29 to CST3 to Follow-up eGFR	kidney trait in FF4 (as Y)	62.86	-0.146 (-0.2 to -0.099)	0.0E+00	0.000E+00	-0.086 (-0.153 to -0.023)	8.00E-03	1.132E-02	-0.232	3.085E-10	-0.642	5.894E-98

620	IL6	CST3	Proteins	eGFRbiom	diftype	0.103	1.937E-02	3.646E-02	eGFR FF4	Y	IL6 to CST3 to Follow-up eGFR	kidney trait in FF4 (as Y)	90.84	-0.088 (-0.137 to -0.037)	0.0E+00	0.000E+00	-0.009 (-0.051 to 0.029)	6.36E-01	6.571E-01	-0.097	2.116E-03	-0.642	5.894E-98
621	C14:1-OH	CST3	Metabolites	eGFRbiom	diftype	0.229	9.246E-18	1.902E-16	eGFR FF4	Y	C14:1-OH to CST3 to Follow-up eGFR	kidney trait in FF4 (as Y)	89.91	-0.11 (-0.148 to -0.077)	0.0E+00	0.000E+00	-0.012 (-0.057 to 0.03)	5.68E-01	5.982E-01	-0.123	4.789E-06	-0.642	5.894E-98
622	FGF20	CST3	Proteins	eGFRbiom	diftype	-0.273	3.105E-10	2.293E-09	eGFR FF4	Y	FGF20 to CST3 to Follow-up eGFR	kidney trait in FF4 (as Y)	57.68	0.089 (0.045 to 0.193)	0.0E+00	0.000E+00	0.065 (0.028 to 0.13)	0.00E+00	0.000E+00	0.154	1.991E-06	-0.642	5.894E-98
623	C8	CST3	Metabolites	eGFRbiom	diftype	0.213	1.922E-15	3.076E-14	eGFR FF4	Y	C8 to CST3 to Follow-up eGFR	kidney trait in FF4 (as Y)	65.94	-0.092 (-0.124 to -0.062)	0.0E+00	0.000E+00	-0.047 (-0.085 to -0.007)	2.80E-02	3.677E-02	-0.139	2.663E-07	-0.642	5.894E-98
624	UNC5C	CST3	Proteins	eGFRbiom	diftype	0.24	3.842E-08	2.128E-07	eGFR FF4	Y	UNC5C to CST3 to Follow-up eGFR	kidney trait in FF4 (as Y)	57.61	-0.138 (-0.196 to -0.082)	0.0E+00	0.000E+00	-0.101 (-0.168 to -0.034)	4.00E-03	5.775E-03	-0.239	2.111E-11	-0.642	5.894E-98
625	CTSH	CST3	Proteins	eGFRbiom	diftype	0.415	8.967E-23	4.570E-21	eGFR FF4	Y	CTSH to CST3 to Follow-up eGFR	kidney trait in FF4 (as Y)	72.55	-0.219 (-0.272 to -0.168)	0.0E+00	0.000E+00	-0.083 (-0.153 to -0.017)	1.20E-02	1.656E-02	-0.301	2.573E-17	-0.642	5.894E-98
626	EPHA2	CST3	Proteins	eGFRbiom	diftype	0.256	3.863E-09	2.318E-08	eGFR FF4	Y	EPHA2 to CST3 to Follow-up eGFR	kidney trait in FF4 (as Y)	55.83	-0.127 (-0.181 to -0.078)	0.0E+00	0.000E+00	-0.1 (-0.182 to -0.025)	1.20E-02	1.656E-02	-0.227	1.296E-11	-0.642	5.894E-98
628	TNFRSF1A	CST3	Proteins	eGFRbiom	diftype	0.442	6.356E-26	6.102E-24	eGFR FF4	Y	TNFRSF1A to CST3 to Follow-up eGFR	kidney trait in FF4 (as Y)	59.6	-0.185 (-0.24 to -0.133)	0.0E+00	0.000E+00	-0.125 (-0.202 to -0.053)	2.00E-03	2.966E-03	-0.311	6.192E-22	-0.642	5.894E-98
629	CGA LHB	CST3	Proteins	eGFRbiom	diftype	0.234	8.101E-08	4.242E-07	eGFR FF4	Y	CGA LHB to CST3 to Follow-up eGFR	kidney trait in FF4 (as Y)	75.02	-0.168 (-0.262 to -0.093)	0.0E+00	0.000E+00	-0.056 (-0.151 to 0.03)	2.10E-01	2.397E-01	-0.225	2.919E-04	-0.642	5.894E-98
630	GHR	CST3	Proteins	eGFRbiom	diftype	-0.207	2.243E-06	9.156E-06	eGFR FF4	Y	GHR to CST3 to Follow-up eGFR	kidney trait in FF4 (as Y)	67.53	0.12 (0.074 to 0.167)	0.0E+00	0.000E+00	0.058 (-0.009 to 0.122)	9.60E-02	1.137E-01	0.178	1.444E-05	-0.642	5.894E-98
631	IGFBP2	CST3	Proteins	eGFRbiom	diftype	0.222	3.600E-07	1.620E-06	eGFR FF4	Y	IGFBP2 to CST3 to Follow-up eGFR	kidney trait in FF4 (as Y)	54.57	-0.131 (-0.195 to -0.076)	0.0E+00	0.000E+00	-0.109 (-0.178 to -0.038)	2.00E-03	2.966E-03	-0.239	7.855E-09	-0.642	5.894E-98
632	C10	CST3	Metabolites	eGFRbiom	diftype	0.218	3.764E-16	6.377E-15	eGFR FF4	Y	C10 to CST3 to Follow-up eGFR	kidney trait in FF4 (as Y)	67.28	-0.099 (-0.13 to -0.068)	0.0E+00	0.000E+00	-0.048 (-0.087 to -0.007)	2.40E-02	3.190E-02	-0.147	8.312E-08	-0.642	5.894E-98
633	SCARF1	CST3	Proteins	eGFRbiom	diftype	0.229	1.554E-07	7.590E-07	eGFR FF4	Y	SCARF1 to CST3 to Follow-up eGFR	kidney trait in FF4 (as Y)	69.56	-0.108 (-0.151 to -0.07)	0.0E+00	0.000E+00	-0.047 (-0.097 to 0.004)	7.00E-02	8.621E-02	-0.156	1.011E-06	-0.642	5.894E-98

635	C16	CST3	Metabolites	eGFRbiom	diftype	0.141	1.681E-07	7.935E-07	eGFR FF4	Y	C16 to CST3 to Follow-up eGFR	kidney trait in FF4 (as Y)	92.05	-0.065 (-0.102 to 0.031)	0.0E+00	0.000E+00	-0.006 (-0.052 to 0.037)	8.22E-01	8.296E-01	-0.07	1.334E-02	-0.642	5.894E-98
636	FGF9	CST3	Proteins	eGFRbiom	diftype	-0.167	1.394E-04	4.363E-04	eGFR FF4	Y	FGF9 to CST3 to Follow-up eGFR	kidney trait in FF4 (as Y)	84.72	0.067 (0.022 to 0.12)	6.0E-03	9.211E-03	0.012 (-0.038 to 0.062)	6.28E-01	6.550E-01	0.079	2.713E-02	-0.642	5.894E-98
637	EFNA5	CST3	Proteins	eGFRbiom	diftype	0.287	3.780E-11	3.202E-10	eGFR FF4	Y	EFNA5 to CST3 to Follow-up eGFR	kidney trait in FF4 (as Y)	58.8	-0.14 (-0.189 to 0.094)	0.0E+00	0.000E+00	-0.098 (-0.156 to 0.035)	2.00E-03	2.966E-03	-0.237	5.965E-12	-0.642	5.894E-98
639	PLG	CST3	Proteins	eGFRbiom	diftype	-0.261	1.881E-09	1.204E-08	eGFR FF4	Y	PLG to CST3 to Follow-up eGFR	kidney trait in FF4 (as Y)	89.25	0.118 (0.077 to 0.167)	0.0E+00	0.000E+00	0.014 (-0.04 to 0.067)	6.34E-01	6.571E-01	0.132	1.799E-04	-0.642	5.894E-98
640	CLEC4 M	CST3	Proteins	eGFRbiom	diftype	-0.207	2.257E-06	9.156E-06	eGFR FF4	Y	CLEC4M to CST3 to Follow-up eGFR	kidney trait in FF4 (as Y)	91.39	0.121 (0.076 to 0.163)	0.0E+00	0.000E+00	0.011 (-0.042 to 0.066)	7.76E-01	7.905E-01	0.133	1.046E-04	-0.642	5.894E-98
641	C10:2	CST3	Metabolites	eGFRbiom	diftype	0.241	1.527E-19	4.398E-18	eGFR FF4	Y	C10:2 to CST3 to Follow-up eGFR	kidney trait in FF4 (as Y)	81.51	-0.095 (-0.132 to 0.06)	0.0E+00	0.000E+00	-0.022 (-0.071 to 0.022)	3.66E-01	3.950E-01	-0.117	6.984E-06	-0.642	5.894E-98
642	C5	CST3	Metabolites	eGFRbiom	diftype	0.182	1.247E-11	1.122E-10	eGFR FF4	Y	C5 to CST3 to Follow-up eGFR	kidney trait in FF4 (as Y)	74.32	-0.076 (-0.116 to 0.043)	0.0E+00	0.000E+00	-0.026 (-0.068 to 0.017)	2.18E-01	2.462E-01	-0.103	2.980E-04	-0.642	5.894E-98
643	FSTL3	CST3	Proteins	eGFRbiom	diftype	0.33	1.775E-14	2.223E-13	eGFR FF4	Y	FSTL3 to CST3 to Follow-up eGFR	kidney trait in FF4 (as Y)	53.09	-0.152 (-0.208 to 0.1)	0.0E+00	0.000E+00	-0.135 (-0.191 to 0.068)	0.00E+00	0.000E+00	-0.287	2.672E-17	-0.642	5.894E-98
644	ACY1	CST3	Proteins	eGFRbiom	diftype	-0.111	1.212E-02	2.431E-02	eGFR FF4	Y	ACY1 to CST3 to Follow-up eGFR	kidney trait in FF4 (as Y)	51.36	0.081 (0.032 to 0.129)	2.0E-03	3.406E-03	0.076 (0.01 to 0.141)	2.20E-02	2.942E-02	0.157	1.315E-04	-0.642	5.894E-98
646	SPOCK2	CST3	Proteins	eGFRbiom	diftype	-0.335	6.329E-15	9.114E-14	eGFR FF4	Y	SPOCK2 to CST3 to Follow-up eGFR	kidney trait in FF4 (as Y)	74.88	0.172 (0.126 to 0.222)	0.0E+00	0.000E+00	0.058 (-0.008 to 0.124)	8.80E-02	1.060E-01	0.23	1.421E-12	-0.642	5.894E-98
647	C18:1	CST3	Metabolites	eGFRbiom	diftype	0.14	1.998E-07	9.280E-07	eGFR FF4	Y	C18:1 to CST3 to Follow-up eGFR	kidney trait in FF4 (as Y)	73.23	-0.059 (-0.098 to 0.025)	2.0E-03	3.406E-03	-0.022 (-0.067 to 0.024)	3.08E-01	3.374E-01	-0.081	3.345E-03	-0.642	5.894E-98
649	B2M	CST3	Proteins	eGFRbiom	diftype	0.615	1.036E-54	2.985E-52	eGFR FF4	Y	B2M to CST3 to Follow-up eGFR	kidney trait in FF4 (as Y)	77.55	-0.298 (-0.369 to 0.235)	0.0E+00	0.000E+00	-0.086 (-0.176 to 0.007)	8.00E-02	9.689E-02	-0.384	1.594E-30	-0.642	5.894E-98
650	C6(C4:1-DC)	CST3	Metabolites	eGFRbiom	diftype	0.224	4.939E-17	9.483E-16	eGFR FF4	Y	C6(C4:1-DC) to CST3 to Follow-up eGFR	kidney trait in FF4 (as Y)	81.21	-0.097 (-0.131 to 0.063)	0.0E+00	0.000E+00	-0.023 (-0.067 to 0.019)	2.90E-01	3.209E-01	-0.12	2.184E-05	-0.642	5.894E-98

651	FCN3	CST3	Proteins	eGFRbiom	diotype	-0.132	2.699E-03	6.759E-03	eGFR FF4	Y	FCN3 to CST3 to Follow-up eGFR	kidney trait in FF4 (as Y)	71.82	0.075 (0.032 to 0.118)	2.0E-03	3.406E-03	0.029 (-0.023 to 0.084)	3.22E-01	3.492E-01	0.104	4.880E-03	-0.642	5.894E-98
652	TFF3	CST3	Proteins	eGFRbiom	diotype	0.376	1.102E-18	2.886E-17	eGFR FF4	Y	TFF3 to CST3 to Follow-up eGFR	kidney trait in FF4 (as Y)	58.88	-0.15 (-0.234 to -0.092)	0.0E+00	0.000E+00	-0.105 (-0.169 to -0.051)	0.00E+00	0.000E+00	-0.255	3.473E-13	-0.642	5.894E-98
653	JAM2	CST3	Proteins	eGFRbiom	diotype	0.341	2.148E-15	3.257E-14	eGFR FF4	Y	JAM2 to CST3 to Follow-up eGFR	kidney trait in FF4 (as Y)	61.81	-0.134 (-0.182 to -0.086)	0.0E+00	0.000E+00	-0.083 (-0.143 to -0.028)	2.00E-03	2.966E-03	-0.216	8.221E-12	-0.642	5.894E-98
655	C18:1	Urine albumin	Metabolites	UACRbiom	diotype	0.127	2.547E-06	1.019E-05	CKD FF4	Y	C18:1 to Urine albumin to incident CKD	kidney trait in FF4 (as Y)	20.65	0.009 (0.003 to 0.018)	4.0E-03	1.600E-02	0.036 (0.005 to 0.073)	2.60E-02	3.328E-02	0.325	6.305E-03	0.914	2.369E-08
659	MCM3	Urine albumin	RNAs	UACRbiom	diotype	-0.17	1.030E-05	3.802E-05	UACR FF4	Y	MCM3 to Urine albumin to Follow-up UACR	kidney trait in FF4 (as Y)	59.88	-0.107 (-0.181 to -0.042)	0.0E+00	0.000E+00	-0.071 (-0.169 to 0.023)	1.36E-01	1.360E-01	-0.178	2.073E-03	0.573	1.129E-59
660	SLC22A4	Urine albumin	RNAs	UACRbiom	diotype	0.159	3.884E-05	1.316E-04	UACR FF4	Y	SLC22A4 to Urine albumin to Follow-up UACR	kidney trait in FF4 (as Y)	35.46	0.072 (0.011 to 0.141)	1.6E-02	3.000E-02	0.132 (0.03 to 0.223)	4.00E-03	6.000E-03	0.204	4.041E-04	0.573	1.129E-59
661	EGFR	Urine albumin	Proteins	UACRbiom	diotype	-0.155	4.251E-04	1.237E-03	UACR FF4	Y	EGFR to Urine albumin to Follow-up UACR	kidney trait in FF4 (as Y)	51.06	-0.092 (-0.142 to -0.048)	0.0E+00	0.000E+00	-0.088 (-0.181 to 0.009)	7.40E-02	8.880E-02	-0.18	1.268E-04	0.573	1.129E-59
662	Creatinine	C12	eGFRbiom	Metabolites	diotype	0.159	3.494E-09	2.141E-08	CKD FF4	Y	Creatinine to C12 to incident CKD	kidney trait in FF4 (as Y)	11.63	0.007 (0.001 to 0.016)	1.0E-02	3.556E-02	0.054 (-0.002 to 0.114)	5.80E-02	6.857E-02	0.459	6.259E-03	0.327	5.401E-03
667	B2M	Creatinine	Proteins	eGFRbiom	diotype	0.317	1.905E-13	2.110E-12	CKD FF4	Y	B2M to Creatinine to incident CKD	kidney trait in FF4 (as Y)	21.16	0.018 (0.004 to 0.038)	1.2E-02	3.840E-02	0.068 (0.011 to 0.124)	2.00E-02	2.667E-02	0.561	9.322E-04	0.459	6.259E-03
669	TNFRSF1B	Creatinine	Proteins	eGFRbiom	diotype	0.181	3.809E-05	1.306E-04	eGFR FF4	Y	TNFRSF1B to Creatinine to Follow-up eGFR	kidney trait in FF4 (as Y)	30.11	-0.091 (-0.133 to -0.051)	0.0E+00	0.000E+00	-0.211 (-0.282 to -0.142)	0.00E+00	0.000E+00	-0.302	2.211E-20	-0.529	1.462E-67
669									eGFR FF4	Y	Creatinine to TNFRSF1B to Follow-up eGFR	kidney trait in FF4 (as Y)	12.79	-0.07 (-0.103 to -0.036)	0.0E+00	0.000E+00	-0.478 (-0.55 to -0.402)	0.00E+00	0.000E+00				

670	FN1	Creatinine	Proteins	eGFRbiom	diftype	-0.133	6.242E-03	6.629E-03	eGFR FF4	Y	FN1 to Creatinine to Follow-up eGFR	kidney trait in FF4 (as Y)	40.33	0.045 (0.005 to 0.082)	3.0E-02	4.012E-02	0.066 (0.009 to 0.118)	2.20E-02	2.942E-02	0.11	1.156E-03	-0.529	1.462E-67
671	ERBB3	Creatinine	Proteins	eGFRbiom	diftype	-0.176	6.339E-05	2.098E-04	eGFR FF4	Y	ERBB3 to Creatinine to Follow-up eGFR	kidney trait in FF4 (as Y)	57.17	0.08 (0.042 to 0.12)	0.0E+00	0.000E+00	0.06 (-0.007 to 0.132)	8.00E-02	9.689E-02	0.14	2.266E-04	-0.529	1.462E-67
672	HAVCR2	Creatinine	Proteins	eGFRbiom	diftype	0.111	1.216E-02	2.431E-02	eGFR FF4	Y	HAVCR2 to Creatinine to Follow-up eGFR	kidney trait in FF4 (as Y)	32.72	-0.074 (-0.12 to -0.034)	2.0E-03	3.406E-03	-0.153 (-0.226 to -0.086)	0.00E+00	0.000E+00	-0.227	1.144E-09	-0.529	1.462E-67
673	KIR2DL4	Creatinine	Proteins	eGFRbiom	diftype	0.129	3.486E-03	8.229E-03	eGFR FF4	Y	KIR2DL4 to Creatinine to Follow-up eGFR	kidney trait in FF4 (as Y)	63.35	-0.064 (-0.105 to -0.03)	0.0E+00	0.000E+00	-0.037 (-0.095 to 0.029)	2.92E-01	3.215E-01	-0.101	2.900E-03	-0.529	1.462E-67
674	NBL1	Creatinine	Proteins	eGFRbiom	diftype	0.23	1.345E-07	6.796E-07	eGFR FF4	Y	NBL1 to Creatinine to Follow-up eGFR	kidney trait in FF4 (as Y)	37.68	-0.097 (-0.145 to -0.055)	0.0E+00	0.000E+00	-0.161 (-0.232 to -0.102)	0.00E+00	0.000E+00	-0.258	1.359E-14	-0.529	1.462E-67
675	LAYN	Creatinine	Proteins	eGFRbiom	diftype	0.194	9.148E-06	3.513E-05	eGFR FF4	Y	LAYN to Creatinine to Follow-up eGFR	kidney trait in FF4 (as Y)	40.09	-0.096 (-0.142 to -0.054)	0.0E+00	0.000E+00	-0.144 (-0.224 to -0.065)	0.00E+00	0.000E+00	-0.24	5.264E-13	-0.529	1.462E-67
676	TNFRSF1A	Creatinine	Proteins	eGFRbiom	diftype	0.283	6.165E-11	5.073E-10	eGFR FF4	Y	TNFRSF1A to Creatinine to Follow-up eGFR	kidney trait in FF4 (as Y)	36.48	-0.113 (-0.153 to -0.076)	0.0E+00	0.000E+00	-0.197 (-0.279 to -0.12)	0.00E+00	0.000E+00	-0.311	6.192E-22	-0.529	1.462E-67
677	AMH	Creatinine	Proteins	eGFRbiom	diftype	-0.131	3.018E-03	7.336E-03	eGFR FF4	Y	AMH to Creatinine to Follow-up eGFR	kidney trait in FF4 (as Y)	50.87	0.057 (0.016 to 0.098)	2.0E-03	3.406E-03	0.055 (-0.016 to 0.124)	1.22E-01	1.415E-01	0.112	1.293E-03	-0.529	1.462E-67
678	GHR	Creatinine	Proteins	eGFRbiom	diftype	-0.124	5.049E-03	1.136E-02	eGFR FF4	Y	GHR to Creatinine to Follow-up eGFR	kidney trait in FF4 (as Y)	33.18	0.059 (0.012 to 0.108)	1.0E-02	1.473E-02	0.119 (0.046 to 0.193)	2.00E-03	2.966E-03	0.178	1.444E-05	-0.529	1.462E-67
679	IL19	Creatinine	Proteins	eGFRbiom	diftype	-0.12	6.708E-03	1.475E-02	eGFR FF4	Y	IL19 to Creatinine to Follow-up eGFR	kidney trait in FF4 (as Y)	42.58	0.061 (0.025 to 0.099)	4.0E-03	6.229E-03	0.082 (0.028 to 0.132)	4.00E-03	5.775E-03	0.143	2.452E-05	-0.529	1.462E-67
680	CTSV	Creatinine	Proteins	eGFRbiom	diftype	-0.122	5.518E-03	1.222E-02	eGFR FF4	Y	CTSV to Creatinine to Follow-up eGFR	kidney trait in FF4 (as Y)	27.73	0.059 (0.019 to 0.098)	4.0E-03	6.229E-03	0.154 (0.081 to 0.212)	0.00E+00	0.000E+00	0.213	5.057E-08	-0.529	1.462E-67
681	CTSH	Creatinine	Proteins	eGFRbiom	diftype	0.248	1.232E-08	7.096E-08	eGFR FF4	Y	CTSH to Creatinine to Follow-up eGFR	kidney trait in FF4 (as Y)	40.12	-0.121 (-0.163 to -0.082)	0.0E+00	0.000E+00	-0.18 (-0.246 to -0.121)	0.00E+00	0.000E+00	-0.301	2.573E-17	-0.529	1.462E-67

682	C14:1-OH	Creatinine	Metabolites	eGFRbiom	diotype	0.153	1.423E-08	8.037E-08	eGFR FF4	Y	C14:1-OH to Creatinine to Follow-up eGFR	kidney trait in FF4 (as Y)	56.44	-0.069 (-0.099 to -0.101 to -0.039)	0.0E+00	0.000E+00	-0.053 (-0.098 to -0.008)	2.00E-02	2.708E-02	-0.123	4.789E-06	-0.529	1.462E-67
683	C12	Creatinine	Metabolites	eGFRbiom	diotype	0.159	3.494E-09	2.141E-08	eGFR FF4	Y	C12 to Creatinine to Follow-up eGFR	kidney trait in FF4 (as Y)	48.69	-0.069 (-0.101 to -0.039)	0.0E+00	0.000E+00	-0.073 (-0.12 to -0.029)	4.00E-03	5.775E-03	-0.143	2.223E-07	-0.529	1.462E-67
684	UNC5C	Creatinine	Proteins	eGFRbiom	diotype	0.178	5.138E-05	1.721E-04	eGFR FF4	Y	UNC5C to Creatinine to Follow-up eGFR	kidney trait in FF4 (as Y)	37.94	-0.091 (-0.135 to -0.045)	0.0E+00	0.000E+00	-0.148 (-0.218 to -0.075)	0.00E+00	0.000E+00	-0.239	2.111E-11	-0.529	1.462E-67
685	C14:1	Creatinine	Metabolites	eGFRbiom	diotype	0.106	8.567E-05	2.742E-04	eGFR FF4	Y	C14:1 to Creatinine to Follow-up eGFR	kidney trait in FF4 (as Y)	51.17	-0.052 (-0.083 to -0.025)	2.0E-03	3.406E-03	-0.05 (-0.097 to -0.003)	4.00E-02	5.099E-02	-0.102	1.816E-04	-0.529	1.462E-67
686	TFF3	Creatinine	Proteins	eGFRbiom	diotype	0.273	2.976E-10	2.255E-09	eGFR FF4	Y	TFF3 to Creatinine to Follow-up eGFR	kidney trait in FF4 (as Y)	39.75	-0.102 (-0.161 to -0.056)	0.0E+00	0.000E+00	-0.154 (-0.235 to -0.094)	0.00E+00	0.000E+00	-0.255	3.473E-13	-0.529	1.462E-67
688	ADAMT S13	Creatinine	Proteins	eGFRbiom	diotype	-0.144	1.064E-03	2.891E-03	eGFR FF4	Y	ADAMTS13 to Creatinine to Follow-up eGFR	kidney trait in FF4 (as Y)	53.05	0.059 (0.023 to 0.094)	4.0E-03	6.229E-03	0.052 (0.003 to 0.102)	4.00E-02	5.099E-02	0.111	6.823E-04	-0.529	1.462E-67
689	MASP1	Creatinine	Proteins	eGFRbiom	diotype	-0.119	7.177E-03	1.554E-02	eGFR FF4	Y	MASP1 to Creatinine to Follow-up eGFR	kidney trait in FF4 (as Y)	53.66	0.049 (0.009 to 0.093)	1.4E-02	1.982E-02	0.042 (-0.009 to 0.085)	9.20E-02	1.102E-01	0.091	5.181E-03	-0.529	1.462E-67
690	SPOCK2	Creatinine	Proteins	eGFRbiom	diotype	-0.222	3.795E-07	1.682E-06	eGFR FF4	Y	SPOCK2 to Creatinine to Follow-up eGFR	kidney trait in FF4 (as Y)	42.59	0.098 (0.062 to 0.139)	0.0E+00	0.000E+00	0.132 (0.064 to 0.199)	0.00E+00	0.000E+00	0.23	1.421E-12	-0.529	1.462E-67
691	FGF20	Creatinine	Proteins	eGFRbiom	diotype	-0.147	8.276E-04	2.337E-03	eGFR FF4	Y	FGF20 to Creatinine to Follow-up eGFR	kidney trait in FF4 (as Y)	25.94	0.04 (0.009 to 0.113)	4.0E-03	6.229E-03	0.114 (0.067 to 0.214)	0.00E+00	0.000E+00	0.154	1.991E-06	-0.529	1.462E-67
692	C5	Creatinine	Metabolites	eGFRbiom	diotype	0.182	1.204E-11	1.119E-10	eGFR FF4	Y	C5 to Creatinine to Follow-up eGFR	kidney trait in FF4 (as Y)	60.36	-0.062 (-0.096 to -0.03)	0.0E+00	0.000E+00	-0.041 (-0.085 to 0.007)	1.04E-01	1.226E-01	-0.103	2.980E-04	-0.529	1.462E-67
693	JAM2	Creatinine	Proteins	eGFRbiom	diotype	0.331	1.313E-14	1.801E-13	eGFR FF4	Y	JAM2 to Creatinine to Follow-up eGFR	kidney trait in FF4 (as Y)	56.6	-0.122 (-0.167 to -0.079)	0.0E+00	0.000E+00	-0.094 (-0.169 to -0.028)	0.00E+00	0.000E+00	-0.216	8.221E-12	-0.529	1.462E-67
694	EGFR	Creatinine	Proteins	eGFRbiom	diotype	-0.134	2.287E-03	5.935E-03	eGFR FF4	Y	EGFR to Creatinine to Follow-up eGFR	kidney trait in FF4 (as Y)	29.07	0.075 (0.035 to 0.117)	2.0E-03	3.406E-03	0.184 (0.116 to 0.252)	0.00E+00	0.000E+00	0.259	1.214E-11	-0.529	1.462E-67

695	BMP1	Creatinine	Proteins	eGFRbiom	diftype	-0.117	8.040E-03	1.678E-02	eGFR FF4	Y	BMP1 to Creatinine to Follow-up eGFR	kidney trait in FF4 (as Y)	31.48	0.056 (0.011 to 0.103)	1.6E-02	2.250E-02	0.122 (0.022 to 0.215)	8.00E-03	1.132E-02	0.178	5.497E-06	-0.529	1.462E-67
696	ESAM	Creatinine	Proteins	eGFRbiom	diftype	0.188	1.885E-05	6.702E-05	eGFR FF4	Y	ESAM to Creatinine to Follow-up eGFR	kidney trait in FF4 (as Y)	33.1	-0.078 (-0.121 to -0.039)	0.0E+00	0.000E+00	-0.158 (-0.23 to -0.082)	0.00E+00	0.000E+00	-0.236	3.557E-12	-0.529	1.462E-67
697	C1QBP	Creatinine	Proteins	eGFRbiom	diftype	-0.229	1.555E-07	7.590E-07	eGFR FF4	Y	C1QBP to Creatinine to Follow-up eGFR	kidney trait in FF4 (as Y)	62.22	0.087 (0.051 to 0.126)	0.0E+00	0.000E+00	0.053 (-0.002 to 0.106)	6.00E-02	7.432E-02	0.14	3.746E-05	-0.529	1.462E-67
698	B2M	Creatinine	Proteins	eGFRbiom	diftype	0.317	1.905E-13	2.110E-12	eGFR FF4	Y	B2M to Creatinine to Follow-up eGFR	kidney trait in FF4 (as Y)	32.76	-0.126 (-0.17 to -0.085)	0.0E+00	0.000E+00	-0.258 (-0.322 to -0.19)	0.00E+00	0.000E+00	-0.384	1.594E-30	-0.529	1.462E-67
698									eGFR FF4	Y	Creatinine to B2M to Follow-up eGFR	kidney trait in FF4 (as Y)	22.02	-0.121 (-0.167 to -0.08)	0.0E+00	0.000E+00	-0.427 (-0.5 to -0.35)	0.00E+00	0.000E+00				
699	C10:2	Creatinine	Metabolites	eGFRbiom	diftype	0.206	1.449E-14	1.897E-13	eGFR FF4	Y	C10:2 to Creatinine to Follow-up eGFR	kidney trait in FF4 (as Y)	73.6	-0.086 (-0.119 to -0.055)	0.0E+00	0.000E+00	-0.031 (-0.077 to 0.017)	2.18E-01	2.462E-01	-0.117	6.984E-06	-0.529	1.462E-67
700	CLEC4M	Creatinine	Proteins	eGFRbiom	diftype	-0.173	8.408E-05	2.734E-04	eGFR FF4	Y	CLEC4M to Creatinine to Follow-up eGFR	kidney trait in FF4 (as Y)	53.4	0.071 (0.032 to 0.11)	0.0E+00	0.000E+00	0.062 (-0.004 to 0.122)	5.80E-02	7.225E-02	0.133	1.046E-04	-0.529	1.462E-67
701	C6(C4:1-DC)	Creatinine	Metabolites	eGFRbiom	diftype	0.162	1.813E-09	1.204E-08	eGFR FF4	Y	C6(C4:1-DC) to Creatinine to Follow-up eGFR	kidney trait in FF4 (as Y)	59.59	-0.071 (-0.102 to -0.045)	0.0E+00	0.000E+00	-0.048 (-0.097 to 0.001)	5.40E-02	6.805E-02	-0.12	2.184E-05	-0.529	1.462E-67
702	EFNA5	Creatinine	Proteins	eGFRbiom	diftype	0.215	9.017E-07	3.819E-06	eGFR FF4	Y	EFNA5 to Creatinine to Follow-up eGFR	kidney trait in FF4 (as Y)	41.04	-0.097 (-0.143 to -0.057)	0.0E+00	0.000E+00	-0.14 (-0.209 to -0.072)	0.00E+00	0.000E+00	-0.237	5.965E-12	-0.529	1.462E-67
703	C14:2	Creatinine	Metabolites	eGFRbiom	diftype	0.164	1.092E-09	7.667E-09	eGFR FF4	Y	C14:2 to Creatinine to Follow-up eGFR	kidney trait in FF4 (as Y)	61.73	-0.069 (-0.099 to -0.042)	0.0E+00	0.000E+00	-0.043 (-0.089 to 0.003)	7.40E-02	9.063E-02	-0.112	3.972E-05	-0.529	1.462E-67
704	TNFRSF19	Creatinine	Proteins	eGFRbiom	diftype	0.238	4.825E-08	2.573E-07	eGFR FF4	Y	TNFRSF19 to Creatinine to Follow-up eGFR	kidney trait in FF4 (as Y)	39.98	-0.074 (-0.129 to -0.038)	0.0E+00	0.000E+00	-0.111 (-0.179 to -0.06)	0.00E+00	0.000E+00	-0.185	2.628E-09	-0.529	1.462E-67
705	C2	Creatinine	Metabolites	eGFRbiom	diftype	0.143	1.224E-07	6.295E-07	eGFR FF4	Y	C2 to Creatinine to Follow-up eGFR	kidney trait in FF4 (as Y)	69.93	-0.055 (-0.087 to -0.024)	4.0E-03	6.229E-03	-0.024 (-0.074 to 0.027)	3.22E-01	3.492E-01	-0.079	4.140E-03	-0.529	1.462E-67

706	FSTL3	Creatinine	Proteins	eGFRbiom	ditype	0.21	1.598E-06	6.668E-06	eGFR FF4	Y	FSTL3 to Creatinine to Follow-up eGFR	kidney trait in FF4 (as Y)	33.35	-0.096 (-0.135 to 0.058)	0.0E+00	0.000E+00	-0.191 (-0.252 to 0.127)	0.00E+00	0.000E+00	-0.287	2.672E-17	-0.529	1.462E-67
707	KDR	Creatinine	Proteins	eGFRbiom	ditype	-0.131	3.031E-03	7.336E-03	eGFR FF4	Y	KDR to Creatinine to Follow-up eGFR	kidney trait in FF4 (as Y)	35.19	0.057 (0.021 to 0.1)	2.0E-03	3.406E-03	0.106 (0.051 to 0.165)	0.00E+00	0.000E+00	0.163	2.182E-06	-0.529	1.462E-67
708	C8	Creatinine	Metabolites	eGFRbiom	ditype	0.179	2.374E-11	2.072E-10	eGFR FF4	Y	C8 to Creatinine to Follow-up eGFR	kidney trait in FF4 (as Y)	57.33	-0.08 (-0.11 to 0.055)	0.0E+00	0.000E+00	-0.059 (-0.102 to 0.013)	1.00E-02	1.397E-02	-0.139	2.663E-07	-0.529	1.462E-67
709	ACY1	Creatinine	Proteins	eGFRbiom	ditype	-0.115	9.386E-03	1.931E-02	eGFR FF4	Y	ACY1 to Creatinine to Follow-up eGFR	kidney trait in FF4 (as Y)	42.48	0.067 (0.019 to 0.115)	4.0E-03	6.229E-03	0.09 (0.022 to 0.155)	1.00E-02	1.397E-02	0.157	1.315E-04	-0.529	1.462E-67
710	CGA LHB	Creatinine	Proteins	eGFRbiom	ditype	0.145	1.030E-03	2.825E-03	eGFR FF4	Y	CGA LHB to Creatinine to Follow-up eGFR	kidney trait in FF4 (as Y)	50.1	-0.113 (-0.186 to 0.046)	0.0E+00	0.000E+00	-0.112 (-0.22 to -0.014)	2.80E-02	3.677E-02	-0.225	2.919E-04	-0.529	1.462E-67
711	ERP29	Creatinine	Proteins	eGFRbiom	ditype	0.194	9.748E-06	3.694E-05	eGFR FF4	Y	ERP29 to Creatinine to Follow-up eGFR	kidney trait in FF4 (as Y)	37.54	-0.087 (-0.133 to 0.047)	0.0E+00	0.000E+00	-0.145 (-0.211 to 0.086)	0.00E+00	0.000E+00	-0.232	3.085E-10	-0.529	1.462E-67
712	C10	Creatinine	Metabolites	eGFRbiom	ditype	0.184	6.433E-12	6.617E-11	eGFR FF4	Y	C10 to Creatinine to Follow-up eGFR	kidney trait in FF4 (as Y)	60.89	-0.089 (-0.119 to 0.062)	0.0E+00	0.000E+00	-0.057 (-0.101 to 0.012)	1.40E-02	1.919E-02	-0.147	8.312E-08	-0.529	1.462E-67
713	RETN	Creatinine	Proteins	eGFRbiom	ditype	0.157	3.471E-04	1.031E-03	eGFR FF4	Y	RETN to Creatinine to Follow-up eGFR	kidney trait in FF4 (as Y)	32.95	-0.074 (-0.117 to 0.036)	0.0E+00	0.000E+00	-0.152 (-0.211 to 0.087)	0.00E+00	0.000E+00	-0.226	5.657E-12	-0.529	1.462E-67
714	RELT	Creatinine	Proteins	eGFRbiom	ditype	0.327	3.216E-14	3.705E-13	eGFR FF4	Y	RELT to Creatinine to Follow-up eGFR	kidney trait in FF4 (as Y)	39.38	-0.135 (-0.175 to 0.094)	0.0E+00	0.000E+00	-0.208 (-0.278 to 0.144)	0.00E+00	0.000E+00	-0.343	1.967E-24	-0.529	1.462E-67
715	EPHA2	Creatinine	Proteins	eGFRbiom	ditype	0.149	7.322E-04	2.088E-03	eGFR FF4	Y	EPHA2 to Creatinine to Follow-up eGFR	kidney trait in FF4 (as Y)	32.02	-0.073 (-0.118 to 0.032)	0.0E+00	0.000E+00	-0.154 (-0.238 to 0.081)	0.00E+00	0.000E+00	-0.227	1.296E-11	-0.529	1.462E-67
717	IGFBP6	Creatinine	Proteins	eGFRbiom	ditype	0.403	1.655E-21	6.807E-20	eGFR FF4	Y	IGFBP6 to Creatinine to Follow-up eGFR	kidney trait in FF4 (as Y)	45.56	-0.161 (-0.211 to 0.113)	0.0E+00	0.000E+00	-0.193 (-0.264 to 0.126)	0.00E+00	0.000E+00	-0.354	6.692E-22	-0.529	1.462E-67

Supplementary Table 19. Best mediation directions of causal mediation analysis of two metabolites & omics molecules & three times points of kidney traits.

Within each identified best mediation direction, spearman correlation coefficients, *P*-values and FDR of each pair (FDR < 0.05) of residuals of two metabolites and omics molecules, and regression coefficients and *P*-values of omics molecules with kidney traits in hyperglycemic individuals of KORA F4 are shown, respectively. Residuals of omics molecules were calculated with linear regression analysis for full model (incl. age, sex, BMI, systolic blood pressure, smoking status, triglyceride, total cholesterol, HDL cholesterol, fasting glucose, use of lipid lowering drugs, antihypertensive and anti-diabetic medication).

The mediation proportion (%), average mediating effect with 95% *CI*, *P*-values and FDR, average direct effect with 95% *CI*, *P*-values and FDR of the identified best direction(s) of mediating triangles in a nonparametric causal mediation analysis are shown, respectively. Each mediation analysis was adjusted for full model. FDR of mediating effect and direct effect were calculated per kidney trait.

Abbreviations: eGFRcr, estimated glomerular filtration rate was calculated from serum creatinine (mg/dL) (IDMS standardized values).

triangle	omics1.label	omics2.label	omics1.type	omics2.type	omics.asso.type	spearcor	p-value	FDR	kidney.traits	sitio	Mediation direction	time.point.kidney.traits	Proportion media (%)	Avg.media (95% CI)	Avg.media p-value	Avg.media FDR	Avg.direct (95% CI)	Avg.direct p-value	Avg.direct FDR	Estimate.o p-mics1.kidney.traits		Estimate.o p-mics2.kidney.traits		
																				value.omics1.kidney.traits	value.omics2.kidney.traits	value.omics1.kidney.traits	value.omics2.kidney.traits	
668	SM C18:1	Creatinine	Metabolites	eGFRbiom	diotype	0.091	8.104E-04	4.646E-02	eGFRcr	FF4	Y	SM C18:1 to Creatinine to Follow-up eGFRcr in FF4 (as Y)	kidney trait in FF4 (as Y)	70.32	-0.054 (-0.093 to -0.016)	0.0E+00	0.000E+00	-0.023 (-0.072 to 0.028)	3.20E-01	4.267E-01	-0.077	2.097E-02	-0.61	2.626E-81
774	PC aa C38:0	CTSH	Metabolites	Proteins	diotype	0.153	5.430E-04	4.646E-02	eGFRcr	FF4	Y	PC aa C38:0 to CTSH to Follow-up eGFRcr in FF4 (as Y)	kidney trait in FF4 (as Y)	84.35	-0.048 (-0.077 to -0.022)	0.0E+00	0.000E+00	-0.009 (-0.082 to 0.068)	8.42E-01	8.420E-01	-0.095	9.872E-04	-0.31	6.16E-15

Supplementary Table 20. Corresponding edges and nodes of directed mediating multi-omics integration networks.

The edge weight, mediation direction, and mediation proportion (%) of directed mediating multi-omics integration networks, which were generated by overlapping the different levels of multi-omics integration network and omics pairs from best mediation directions of causal mediation analysis, are shown.

Abbreviations: CKD, chronic kidney disease; eGFR, estimated glomerular filtration rate; UACR, urinary albumin-to-creatinine ratio; CKDcrcc, eGFR-based CKD that was defined as eGFR < 60 ml/min/1.73 m²; eGFRcr, estimated glomerular filtration rate was calculated from serum creatinine (mg/dL) (IDMS standardized values).

kidney.trait. position	kidney.trait. type	time.point.kidney.trait	source.omics1. label	target.omics2. label	source.to.target	omics1 type	omics2.type	omics.asso. type	weight	kidney.trait	Mediation.direction	Proportion. media(%)
X	CKD	kidney trait in S4 (as X)	B2M	CST3	B2M to CST3	Proteins	eGFRbiom	ditype	0.219	CKDcrcc S4	CKDcrcc S4 to B2M to CST3	65.81
X	CKD	kidney trait in S4 (as X)	C1QBP	CST3	C1QBP to CST3	Proteins	eGFRbiom	ditype	-0.111	CKDcrcc S4	CKDcrcc S4 to C1QBP to CST3	30.41
X	CKD	kidney trait in S4 (as X)	Creatinine	C10:2	Creatinine to C10:2	Metabolites	eGFRbiom	ditype	0.053	CKDcrcc S4	CKDcrcc S4 to Creatinine to C10:2	46.07
X	CKD	kidney trait in S4 (as X)	Creatinine	C5	Creatinine to C5	Metabolites	eGFRbiom	ditype	0.063	CKDcrcc S4	CKDcrcc S4 to Creatinine to C5	52.11
X	CKD	kidney trait in S4 (as X)	Creatinine	IGFBP6	Creatinine to IGFBP6	Proteins	eGFRbiom	ditype	0.117	CKDcrcc S4	CKDcrcc S4 to Creatinine to IGFBP6	30.67
X	CKD	kidney trait in S4 (as X)	CST3	B2M	CST3 to B2M	Proteins	eGFRbiom	ditype	0.219	CKDcrcc S4	CKDcrcc S4 to CST3 to B2M	74.14
X	CKD	kidney trait in S4 (as X)	CST3	C10:2	CST3 to C10:2	Metabolites	eGFRbiom	ditype	0.031	CKDcrcc S4	CKDcrcc S4 to CST3 to C10:2	71.92
X	CKD	kidney trait in S4 (as X)	CST3	C14:2	CST3 to C14:2	Metabolites	eGFRbiom	ditype	0.005	CKDcrcc S4	CKDcrcc S4 to CST3 to C14:2	63.78
X	CKD	kidney trait in S4 (as X)	CST3	C1QBP	CST3 to C1QBP	Proteins	eGFRbiom	ditype	-0.111	CKDcrcc S4	CKDcrcc S4 to CST3 to C1QBP	32.49
X	CKD	kidney trait in S4 (as X)	CST3	C5	CST3 to C5	Metabolites	eGFRbiom	ditype	0.053	CKDcrcc S4	CKDcrcc S4 to CST3 to C5	39.87
X	CKD	kidney trait in S4 (as X)	CST3	CTSH	CST3 to CTSH	Proteins	eGFRbiom	ditype	0.031	CKDcrcc S4	CKDcrcc S4 to CST3 to CTSH	59.8
X	CKD	kidney trait in S4 (as X)	CST3	NBL1	CST3 to NBL1	Proteins	eGFRbiom	ditype	0.006	CKDcrcc S4	CKDcrcc S4 to CST3 to NBL1	32.51
X	CKD	kidney trait in S4 (as X)	CTSH	CST3	CTSH to CST3	Proteins	eGFRbiom	ditype	0.031	CKDcrcc S4	CKDcrcc S4 to CTSH to CST3	43.7
X	CKD	kidney trait in S4 (as X)	IGFBP6	Creatinine	IGFBP6 to Creatinine	Proteins	eGFRbiom	ditype	0.117	CKDcrcc S4	CKDcrcc S4 to IGFBP6 to Creatinine	31.63
X	CKD	kidney trait in S4 (as X)	NBL1	CST3	NBL1 to CST3	Proteins	eGFRbiom	ditype	0.006	CKDcrcc S4	CKDcrcc S4 to NBL1 to CST3	49.05
X	CKD	kidney trait in S4 (as X)	TNFRSF1A	CST3	TNFRSF1A to CST3	Proteins	eGFRbiom	ditype	0.047	CKDcrcc S4	CKDcrcc S4 to TNFRSF1A to CST3	63.62
X	eGFR	kidney trait in S4 (as X)	Creatinine	C10:2	Creatinine to C10:2	Metabolites	eGFRbiom	ditype	0.053	eGFR S4	eGFR S4 to Creatinine to C10:2	35.98
X	eGFR	kidney trait in S4 (as X)	Creatinine	C5	Creatinine to C5	Metabolites	eGFRbiom	ditype	0.063	eGFR S4	eGFR S4 to Creatinine to C5	99.34
X	eGFR	kidney trait in S4 (as X)	Creatinine	IGFBP6	Creatinine to IGFBP6	Proteins	eGFRbiom	ditype	0.117	eGFR S4	eGFR S4 to Creatinine to IGFBP6	25.63
X	eGFR	kidney trait in S4 (as X)	Creatinine	JAM2	Creatinine to JAM2	Proteins	eGFRbiom	ditype	0.086	eGFR S4	eGFR S4 to Creatinine to JAM2	47.05
X	eGFR	kidney trait in S4 (as X)	Creatinine	RELT	Creatinine to RELT	Proteins	eGFRbiom	ditype	0.013	eGFR S4	eGFR S4 to Creatinine to RELT	33.98
X	eGFR	kidney trait in S4 (as X)	CST3	B2M	CST3 to B2M	Proteins	eGFRbiom	ditype	0.219	eGFR S4	eGFR S4 to CST3 to B2M	78.82
X	eGFR	kidney trait in S4 (as X)	CST3	C10:2	CST3 to C10:2	Metabolites	eGFRbiom	ditype	0.031	eGFR S4	eGFR S4 to CST3 to C10:2	73.02
X	eGFR	kidney trait in S4 (as X)	CST3	C12	CST3 to C12	Metabolites	eGFRbiom	ditype	0.001	eGFR S4	eGFR S4 to CST3 to C12	41.7
X	eGFR	kidney trait in S4 (as X)	CST3	C14:1-OH	CST3 to C14:1-OH	Metabolites	eGFRbiom	ditype	0.006	eGFR S4	eGFR S4 to CST3 to C14:1-OH	65.48
X	eGFR	kidney trait in S4 (as X)	CST3	C14:2	CST3 to C14:2	Metabolites	eGFRbiom	ditype	0.005	eGFR S4	eGFR S4 to CST3 to C14:2	36.81
X	eGFR	kidney trait in S4 (as X)	CST3	C1QBP	CST3 to C1QBP	Proteins	eGFRbiom	ditype	-0.111	eGFR S4	eGFR S4 to CST3 to C1QBP	82.63
X	eGFR	kidney trait in S4 (as X)	CST3	C5	CST3 to C5	Metabolites	eGFRbiom	ditype	0.053	eGFR S4	eGFR S4 to CST3 to C5	79.4

X	eGFR	kidney trait in S4 (as X)	CST3	C6(C4:1-DC)	CST3 to C6(C4:1-DC)	Metabolites	eGFRbiom	ditype	0.015	eGFR S4	eGFR S4 to CST3 to C6(C4:1-DC)	65.48
X	eGFR	kidney trait in S4 (as X)	CST3	CTSH	CST3 to CTSH	Proteins	eGFRbiom	ditype	0.031	eGFR S4	eGFR S4 to CST3 to CTSH	97.97
X	eGFR	kidney trait in S4 (as X)	CST3	ERP29	CST3 to ERP29	Proteins	eGFRbiom	ditype	0.015	eGFR S4	eGFR S4 to CST3 to ERP29	66.63
X	eGFR	kidney trait in S4 (as X)	CST3	NBL1	CST3 to NBL1	Proteins	eGFRbiom	ditype	0.006	eGFR S4	eGFR S4 to CST3 to NBL1	89.47
X	eGFR	kidney trait in S4 (as X)	CST3	RELT	CST3 to RELT	Proteins	eGFRbiom	ditype	0.104	eGFR S4	eGFR S4 to CST3 to RELT	73.6
X	eGFR	kidney trait in S4 (as X)	CST3	SPOCK2	CST3 to SPOCK2	Proteins	eGFRbiom	ditype	-0.029	eGFR S4	eGFR S4 to CST3 to SPOCK2	59.74
X	eGFR	kidney trait in S4 (as X)	CST3	TNFRSF1A	CST3 to TNFRSF1A	Proteins	eGFRbiom	ditype	0.047	eGFR S4	eGFR S4 to CST3 to TNFRSF1A	84.51
X	eGFR	kidney trait in S4 (as X)	EGFR	CST3	EGFR to CST3	Proteins	eGFRbiom	ditype	-0.06	eGFR S4	eGFR S4 to EGFR to CST3	16.11
X	eGFR	kidney trait in S4 (as X)	IGFBP6	Creatinine	IGFBP6 to Creatinine	Proteins	eGFRbiom	ditype	0.117	eGFR S4	eGFR S4 to IGFBP6 to Creatinine	18.07
X	eGFR	kidney trait in S4 (as X)	RELT	Creatinine	RELT to Creatinine	Proteins	eGFRbiom	ditype	0.013	eGFR S4	eGFR S4 to RELT to Creatinine	19.74
M	eGFR	kidney trait in F4	ABCB1	CST3	ABCB1 to CST3	RNAs	eGFRbiom	ditype	-0.024	eGFR F4	ABCB1 to eGFR F4 to CST3	80.14
M	eGFR	kidney trait in F4	C10:2	Creatinine	C10:2 to Creatinine	Metabolites	eGFRbiom	ditype	0.053	eGFR F4	C10:2 to eGFR F4 to Creatinine	97.8
M	eGFR	kidney trait in F4	C10:2	CST3	C10:2 to CST3	Metabolites	eGFRbiom	ditype	0.031	eGFR F4	C10:2 to eGFR F4 to CST3	93.33
M	eGFR	kidney trait in F4	C5	Creatinine	C5 to Creatinine	Metabolites	eGFRbiom	ditype	0.063	eGFR F4	C5 to eGFR F4 to Creatinine	97.77
M	eGFR	kidney trait in F4	C5	CST3	C5 to CST3	Metabolites	eGFRbiom	ditype	0.053	eGFR F4	C5 to eGFR F4 to CST3	97.96
M	eGFR	kidney trait in F4	CGA LHB	CST3	CGA LHB to CST3	Proteins	eGFRbiom	ditype	0.043	eGFR F4	CGA LHB to eGFR F4 to CST3	89.94
M	eGFR	kidney trait in F4	Creatinine	C10:2	Creatinine to C10:2	Metabolites	eGFRbiom	ditype	0.053	eGFR F4	Creatinine to eGFR F4 to C10:2	92.45
M	eGFR	kidney trait in F4	Creatinine	C5	Creatinine to C5	Metabolites	eGFRbiom	ditype	0.063	eGFR F4	Creatinine to eGFR F4 to C5	92.2
M	eGFR	kidney trait in F4	Creatinine	IGFBP6	Creatinine to IGFBP6	Proteins	eGFRbiom	ditype	0.117	eGFR F4	Creatinine to eGFR F4 to IGFBP6	91.72
M	eGFR	kidney trait in F4	CST3	C5	CST3 to C5	Metabolites	eGFRbiom	ditype	0.053	eGFR F4	CST3 to eGFR F4 to C5	90.46
M	eGFR	kidney trait in F4	CST3	IGFBP6	CST3 to IGFBP6	Proteins	eGFRbiom	ditype	-0.011	eGFR F4	CST3 to eGFR F4 to IGFBP6	90.19
M	eGFR	kidney trait in F4	DUSP11	Creatinine	DUSP11 to Creatinine	RNAs	eGFRbiom	ditype	-0.069	eGFR F4	DUSP11 to eGFR F4 to Creatinine	86.31
M	eGFR	kidney trait in F4	DUSP11	CST3	DUSP11 to CST3	RNAs	eGFRbiom	ditype	-0.044	eGFR F4	DUSP11 to eGFR F4 to CST3	88.78
M	eGFR	kidney trait in F4	ERP29	CST3	ERP29 to CST3	Proteins	eGFRbiom	ditype	0.015	eGFR F4	ERP29 to eGFR F4 to CST3	89.32
M	eGFR	kidney trait in F4	IGFBP6	Creatinine	IGFBP6 to Creatinine	Proteins	eGFRbiom	ditype	0.117	eGFR F4	IGFBP6 to eGFR F4 to Creatinine	96.68
M	eGFR	kidney trait in F4	IGFBP6	CST3	IGFBP6 to CST3	Proteins	eGFRbiom	ditype	-0.011	eGFR F4	IGFBP6 to eGFR F4 to CST3	97.17
M	eGFR	kidney trait in F4	JAM2	Creatinine	JAM2 to Creatinine	Proteins	eGFRbiom	ditype	0.086	eGFR F4	JAM2 to eGFR F4 to Creatinine	88.21

M	UACR	kidney trait in F4	EGFR	Urine albumin	EGFR to Urine albumin	Proteins	UACRbiom	ditype	-0.046	UACR F4	EGFR to UACR F4 to Urine albumin	86.19
M	UACR	kidney trait in F4	ERP29	Urine albumin	ERP29 to Urine albumin	Proteins	UACRbiom	ditype	0.082	UACR F4	ERP29 to UACR F4 to Urine albumin	83.85
M	UACR	kidney trait in F4	LYSMD2	Urine albumin	LYSMD2 to Urine albumin	CpGs	UACRbiom	ditype	-0.125	UACR F4	LYSMD2 to UACR F4 to Urine albumin	83.67
M	UACR	kidney trait in F4	MCM3	Urine albumin	MCM3 to Urine albumin	RNAs	UACRbiom	ditype	-0.093	UACR F4	MCM3 to UACR F4 to Urine albumin	96.67
X	CKD	kidney trait in F4	ACY1	Tyr	ACY1 to Tyr	Metabolites	Proteins	ditype	0.126	CKD F4	CKD F4 to ACY1 to Tyr	27.71
X	CKD	kidney trait in F4	Creatinine	DUSP11	Creatinine to DUSP11	RNAs	eGFRbiom	ditype	-0.069	CKD F4	CKD F4 to Creatinine to DUSP11	47.94
X	CKD	kidney trait in F4	Creatinine	JAM2	Creatinine to JAM2	Proteins	eGFRbiom	ditype	0.086	CKD F4	CKD F4 to Creatinine to JAM2	51.14
X	CKD	kidney trait in F4	CST3	C12	CST3 to C12	Metabolites	eGFRbiom	ditype	0.001	CKD F4	CKD F4 to CST3 to C12	83.85
X	CKD	kidney trait in F4	CST3	DUSP11	CST3 to DUSP11	RNAs	eGFRbiom	ditype	-0.044	CKD F4	CKD F4 to CST3 to DUSP11	52.71
X	CKD	kidney trait in F4	CST3	IGFBP6	CST3 to IGFBP6	Proteins	eGFRbiom	ditype	-0.011	CKD F4	CKD F4 to CST3 to IGFBP6	66.16
X	CKD	kidney trait in F4	CST3	RELT	CST3 to RELT	Proteins	eGFRbiom	ditype	0.104	CKD F4	CKD F4 to CST3 to RELT	77.33
X	CKD	kidney trait in F4	CST3	RETN	CST3 to RETN	Proteins	eGFRbiom	ditype	0.012	CKD F4	CKD F4 to CST3 to RETN	54.55
X	CKD	kidney trait in F4	IGFBP2	Tyr	IGFBP2 to Tyr	Metabolites	Proteins	ditype	-0.152	CKD F4	CKD F4 to IGFBP2 to Tyr	28.36
X	CKD	kidney trait in F4	PLAT	Tyr	PLAT to Tyr	Metabolites	Proteins	ditype	0.134	CKD F4	CKD F4 to PLAT to Tyr	26.95
X	CKD	kidney trait in F4	RETN	C10:2	RETN to C10:2	Metabolites	Proteins	ditype	0.066	CKD F4	CKD F4 to RETN to C10:2	46.27
X	CKD	kidney trait in F4	SLC22A4	IL19	SLC22A4 to IL19	RNAs	Proteins	ditype	-0.086	CKD F4	CKD F4 to SLC22A4 to IL19	55.22
X	CKD	kidney trait in F4	Urine albumin	C18:1	Urine albumin to C18:1	Metabolites	UACRbiom	ditype	0.055	CKD F4	CKD F4 to Urine albumin to C18:1	68.37
X	CKD	kidney trait in F4	Urine albumin	MCM3	Urine albumin to MCM3	RNAs	UACRbiom	ditype	-0.093	CKD F4	CKD F4 to Urine albumin to MCM3	41.78
X	eGFR	kidney trait in F4	BMP1	C18:1	BMP1 to C18:1	Metabolites	Proteins	ditype	-0.033	eGFR F4	eGFR F4 to BMP1 to C18:1	37.83
X	eGFR	kidney trait in F4	EGFR	C16	EGFR to C16	Metabolites	Proteins	ditype	-0.028	eGFR F4	eGFR F4 to EGFR to C16	68.79
X	eGFR	kidney trait in F4	EGFR	C18:1	EGFR to C18:1	Metabolites	Proteins	ditype	-0.017	eGFR F4	eGFR F4 to EGFR to C18:1	91.01
X	eGFR	kidney trait in F4	GHR	C18:1	GHR to C18:1	Metabolites	Proteins	ditype	-0.01	eGFR F4	eGFR F4 to GHR to C18:1	40.7
X	eGFR	kidney trait in F4	IGFBP2	C18:1	IGFBP2 to C18:1	Metabolites	Proteins	ditype	0.059	eGFR F4	eGFR F4 to IGFBP2 to C18:1	43.85
X	UACR	kidney trait in F4	EGFR	C18:1	EGFR to C18:1	Metabolites	Proteins	ditype	-0.017	UACR F4	UACR F4 to EGFR to C18:1	82.8
X	UACR	kidney trait in F4	GHR	C18:1	GHR to C18:1	Metabolites	Proteins	ditype	-0.01	UACR F4	UACR F4 to GHR to C18:1	47.99
X	UACR	kidney trait in F4	IGFBP2	C18:1	IGFBP2 to C18:1	Metabolites	Proteins	ditype	0.059	UACR F4	UACR F4 to IGFBP2 to C18:1	42.9
Y	CKD	kidney trait in F4	C10:2	Creatinine	C10:2 to Creatinine	Metabolites	eGFRbiom	ditype	0.053	CKD F4	C10:2 to Creatinine to CKD F4	71.72

Y	CKD	kidney trait in F4	C10:2	CST3	C10:2 to CST3	Metabolites	eGFRbiom	ditype	0.031	CKD F4	C10:2 to CST3 to CKD F4	94.82
Y	CKD	kidney trait in F4	C14:2	CST3	C14:2 to CST3	Metabolites	eGFRbiom	ditype	0.005	CKD F4	C14:2 to CST3 to CKD F4	84.4
Y	CKD	kidney trait in F4	C5	Creatinine	C5 to Creatinine	Metabolites	eGFRbiom	ditype	0.063	CKD F4	C5 to Creatinine to CKD F4	74.28
Y	CKD	kidney trait in F4	C5	CST3	C5 to CST3	Metabolites	eGFRbiom	ditype	0.053	CKD F4	C5 to CST3 to CKD F4	89.08
Y	CKD	kidney trait in F4	CTSH	CST3	CTSH to CST3	Proteins	eGFRbiom	ditype	0.031	CKD F4	CTSH to CST3 to CKD F4	89.7
Y	CKD	kidney trait in F4	DUSP11	Creatinine	DUSP11 to Creatinine	RNAs	eGFRbiom	ditype	-0.069	CKD F4	DUSP11 to Creatinine to CKD F4	56.17
Y	CKD	kidney trait in F4	DUSP11	CST3	DUSP11 to CST3	RNAs	eGFRbiom	ditype	-0.044	CKD F4	DUSP11 to CST3 to CKD F4	63.68
Y	CKD	kidney trait in F4	IGFBP6	CST3	IGFBP6 to CST3	Proteins	eGFRbiom	ditype	-0.011	CKD F4	IGFBP6 to CST3 to CKD F4	72.35
Y	CKD	kidney trait in F4	IL19	SLC22A4	IL19 to SLC22A4	RNAs	Proteins	ditype	-0.086	CKD F4	IL19 to SLC22A4 to CKD F4	54.1
Y	CKD	kidney trait in F4	JAM2	Creatinine	JAM2 to Creatinine	Proteins	eGFRbiom	ditype	0.086	CKD F4	JAM2 to Creatinine to CKD F4	56.32
Y	CKD	kidney trait in F4	MCM3	Urine albumin	MCM3 to Urine albumin	RNAs	UACRbiom	ditype	-0.093	CKD F4	MCM3 to Urine albumin to CKD F4	47.35
Y	CKD	kidney trait in F4	RELT	CST3	RELT to CST3	Proteins	eGFRbiom	ditype	0.104	CKD F4	RELT to CST3 to CKD F4	95.73
Y	CKD	kidney trait in F4	RETN	CST3	RETN to CST3	Proteins	eGFRbiom	ditype	0.012	CKD F4	RETN to CST3 to CKD F4	64
Y	CKD	kidney trait in F4	TTF2	Creatinine	TTF2 to Creatinine	RNAs	eGFRbiom	ditype	-0.078	CKD F4	TTF2 to Creatinine to CKD F4	48.16
Y	CKD	kidney trait in F4	Tyr	SPOCK2	Tyr to SPOCK2	Metabolites	Proteins	ditype	0.082	CKD F4	Tyr to SPOCK2 to CKD F4	25.15
Y	eGFR	kidney trait in F4	C1QBP	CST3	C1QBP to CST3	Proteins	eGFRbiom	ditype	-0.111	eGFR F4	C1QBP to CST3 to eGFR F4	88.57
Y	eGFR	kidney trait in F4	DUSP11	Creatinine	DUSP11 to Creatinine	RNAs	eGFRbiom	ditype	-0.069	eGFR F4	DUSP11 to Creatinine to eGFR F4	85.34
Y	eGFR	kidney trait in F4	DUSP11	CST3	DUSP11 to CST3	RNAs	eGFRbiom	ditype	-0.044	eGFR F4	DUSP11 to CST3 to eGFR F4	91.76
Y	eGFR	kidney trait in F4	TTF2	Creatinine	TTF2 to Creatinine	RNAs	eGFRbiom	ditype	-0.078	eGFR F4	TTF2 to Creatinine to eGFR F4	97.81
Y	UACR	kidney trait in F4	C18:1	EGFR	C18:1 to EGFR	Metabolites	Proteins	ditype	-0.017	UACR F4	C18:1 to EGFR to UACR F4	82.68
Y	UACR	kidney trait in F4	C18:1	GHR	C18:1 to GHR	Metabolites	Proteins	ditype	-0.01	UACR F4	C18:1 to GHR to UACR F4	47.39
Y	UACR	kidney trait in F4	ERP29	Urine albumin	ERP29 to Urine albumin	Proteins	UACRbiom	ditype	0.082	UACR F4	ERP29 to Urine albumin to UACR F4	80.78
Y	UACR	kidney trait in F4	LYSMD2	Urine albumin	LYSMD2 to Urine albumin	CpGs	UACRbiom	ditype	-0.125	UACR F4	LYSMD2 to Urine albumin to UACR F4	83.25
Y	CKD	kidney trait in FF4 (as Y)	C12	CST3	C12 to CST3	Metabolites	eGFRbiom	ditype	0.001	CKD FF4	C12 to CST3 to incident CKD	51.87
Y	CKD	kidney trait in FF4 (as Y)	C12	EGFR	C12 to EGFR	Metabolites	Proteins	ditype	-0.015	CKD FF4	C12 to EGFR to incident CKD	19.04
Y	CKD	kidney trait in FF4 (as Y)	C18:1	EGFR	C18:1 to EGFR	Metabolites	Proteins	ditype	-0.017	CKD FF4	C18:1 to EGFR to incident CKD	27.29
Y	CKD	kidney trait in FF4 (as Y)	C18:1	GHR	C18:1 to GHR	Metabolites	Proteins	ditype	-0.01	CKD FF4	C18:1 to GHR to incident CKD	35.18

Y	CKD	kidney trait in FF4 (as Y)	C18:1	Urine albumin	C18:1 to Urine albumin	Metabolites	UACRbiom	diotype	0.055	CKD FF4	C18:1 to Urine albumin to incident CKD	20.65
Y	CKD	kidney trait in FF4 (as Y)	EGFR	CST3	EGFR to CST3	Proteins	eGFRbiom	diotype	-0.06	CKD FF4	EGFR to CST3 to incident CKD	58.56
Y	eGFR	kidney trait in FF4 (as Y)	B2M	CST3	B2M to CST3	Proteins	eGFRbiom	diotype	0.219	eGFR FF4	B2M to CST3 to Follow-up eGFR	77.55
Y	eGFR	kidney trait in FF4 (as Y)	C10:2	Creatinine	C10:2 to Creatinine	Metabolites	eGFRbiom	diotype	0.053	eGFR FF4	C10:2 to Creatinine to Follow-up eGFR	73.6
Y	eGFR	kidney trait in FF4 (as Y)	C10:2	CST3	C10:2 to CST3	Metabolites	eGFRbiom	diotype	0.031	eGFR FF4	C10:2 to CST3 to Follow-up eGFR	81.51
Y	eGFR	kidney trait in FF4 (as Y)	C10:2	RETN	C10:2 to RETN	Metabolites	Proteins	diotype	0.066	eGFR FF4	C10:2 to RETN to Follow-up eGFR	23.96
Y	eGFR	kidney trait in FF4 (as Y)	C12	CST3	C12 to CST3	Metabolites	eGFRbiom	diotype	0.001	eGFR FF4	C12 to CST3 to Follow-up eGFR	75.89
Y	eGFR	kidney trait in FF4 (as Y)	C12	EGFR	C12 to EGFR	Metabolites	Proteins	diotype	-0.015	eGFR FF4	C12 to EGFR to Follow-up eGFR	28.7
Y	eGFR	kidney trait in FF4 (as Y)	C14:1-OH	B2M	C14:1-OH to B2M	Metabolites	Proteins	diotype	0.012	eGFR FF4	C14:1-OH to B2M to Follow-up eGFR	54.55
Y	eGFR	kidney trait in FF4 (as Y)	C14:1-OH	CST3	C14:1-OH to CST3	Metabolites	eGFRbiom	diotype	0.006	eGFR FF4	C14:1-OH to CST3 to Follow-up eGFR	89.91
Y	eGFR	kidney trait in FF4 (as Y)	C14:2	CST3	C14:2 to CST3	Metabolites	eGFRbiom	diotype	0.005	eGFR FF4	C14:2 to CST3 to Follow-up eGFR	87.39
Y	eGFR	kidney trait in FF4 (as Y)	C16	EGFR	C16 to EGFR	Metabolites	Proteins	diotype	-0.028	eGFR FF4	C16 to EGFR to Follow-up eGFR	60.35
Y	eGFR	kidney trait in FF4 (as Y)	C18:1	BMP1	C18:1 to BMP1	Metabolites	Proteins	diotype	-0.033	eGFR FF4	C18:1 to BMP1 to Follow-up eGFR	29.04
Y	eGFR	kidney trait in FF4 (as Y)	C18:1	EGFR	C18:1 to EGFR	Metabolites	Proteins	diotype	-0.017	eGFR FF4	C18:1 to EGFR to Follow-up eGFR	49.8
Y	eGFR	kidney trait in FF4 (as Y)	C18:1	GHR	C18:1 to GHR	Metabolites	Proteins	diotype	-0.01	eGFR FF4	C18:1 to GHR to Follow-up eGFR	29.49
Y	eGFR	kidney trait in FF4 (as Y)	C18:1	IGFBP2	C18:1 to IGFBP2	Metabolites	Proteins	diotype	0.059	eGFR FF4	C18:1 to IGFBP2 to Follow-up eGFR	40.91
Y	eGFR	kidney trait in FF4 (as Y)	C5	Creatinine	C5 to Creatinine	Metabolites	eGFRbiom	diotype	0.063	eGFR FF4	C5 to Creatinine to Follow-up eGFR	60.36
Y	eGFR	kidney trait in FF4 (as Y)	C5	CST3	C5 to CST3	Metabolites	eGFRbiom	diotype	0.053	eGFR FF4	C5 to CST3 to Follow-up eGFR	74.32
Y	eGFR	kidney trait in FF4 (as Y)	C6(C4:1-DC)	CST3	C6(C4:1-DC) to CST3	Metabolites	eGFRbiom	diotype	0.015	eGFR FF4	C6(C4:1-DC) to CST3 to Follow-up eGFR	81.21
Y	eGFR	kidney trait in FF4 (as Y)	CGA LHB	CST3	CGA LHB to CST3	Proteins	eGFRbiom	diotype	0.043	eGFR FF4	CGA LHB to CST3 to Follow-up eGFR	75.02
Y	eGFR	kidney trait in FF4 (as Y)	CTSH	CST3	CTSH to CST3	Proteins	eGFRbiom	diotype	0.031	eGFR FF4	CTSH to CST3 to Follow-up eGFR	72.55
Y	eGFR	kidney trait in FF4 (as Y)	CTSV	CST3	CTSV to CST3	Proteins	eGFRbiom	diotype	-0.066	eGFR FF4	CTSV to CST3 to Follow-up eGFR	69.65
Y	eGFR	kidney trait in FF4 (as Y)	EGFR	CST3	EGFR to CST3	Proteins	eGFRbiom	diotype	-0.06	eGFR FF4	EGFR to CST3 to Follow-up eGFR	81.7
Y	eGFR	kidney trait in FF4 (as Y)	ERP29	CST3	ERP29 to CST3	Proteins	eGFRbiom	diotype	0.015	eGFR FF4	ERP29 to CST3 to Follow-up eGFR	62.86
Y	eGFR	kidney trait in FF4 (as Y)	IGFBP6	Creatinine	IGFBP6 to Creatinine	Proteins	eGFRbiom	diotype	0.117	eGFR FF4	IGFBP6 to Creatinine to Follow-up eGFR	45.56
Y	eGFR	kidney trait in FF4 (as Y)	IGFBP6	CST3	IGFBP6 to CST3	Proteins	eGFRbiom	diotype	-0.011	eGFR FF4	IGFBP6 to CST3 to Follow-up eGFR	57.21
Y	eGFR	kidney trait in FF4 (as Y)	JAM2	Creatinine	JAM2 to Creatinine	Proteins	eGFRbiom	diotype	0.086	eGFR FF4	JAM2 to Creatinine to Follow-up eGFR	56.6

Y	eGFR	kidney trait in FF4 (as Y)	NBL1	CST3	NBL1 to CST3	Proteins	eGFRbiom	ditype	0.006	eGFR FF4	NBL1 to CST3 to Follow-up eGFR	63.42
Y	eGFR	kidney trait in FF4 (as Y)	PC aa C38:0	CTSH	PC aa C38:0 to CTSH	Proteins	Metabolites	ditype	0.093	eGFRcr FF4	PC aa C38:0 to CTSH to Follow-up eGFRcr	84.35
Y	eGFR	kidney trait in FF4 (as Y)	RELT	Creatinine	RELT to Creatinine	Proteins	eGFRbiom	ditype	0.013	eGFR FF4	RELT to Creatinine to Follow-up eGFR	39.38
Y	eGFR	kidney trait in FF4 (as Y)	RELT	CST3	RELT to CST3	Proteins	eGFRbiom	ditype	0.104	eGFR FF4	RELT to CST3 to Follow-up eGFR	59.83
Y	eGFR	kidney trait in FF4 (as Y)	RETN	CST3	RETN to CST3	Proteins	eGFRbiom	ditype	0.012	eGFR FF4	RETN to CST3 to Follow-up eGFR	60.61
Y	eGFR	kidney trait in FF4 (as Y)	SPOCK2	CST3	SPOCK2 to CST3	Proteins	eGFRbiom	ditype	-0.029	eGFR FF4	SPOCK2 to CST3 to Follow-up eGFR	74.88
Y	eGFR	kidney trait in FF4 (as Y)	TNFRSF1A	CST3	TNFRSF1A to CST3	Proteins	eGFRbiom	ditype	0.047	eGFR FF4	TNFRSF1A to CST3 to Follow-up eGFR	59.6
Y	eGFR	kidney trait in FF4 (as Y)	Tyr	ACY1	Tyr to ACY1	Metabolites	Proteins	ditype	0.126	eGFR FF4	Tyr to ACY1 to Follow-up eGFR	41.93
Y	eGFR	kidney trait in FF4 (as Y)	Tyr	IGFBP2	Tyr to IGFBP2	Metabolites	Proteins	ditype	-0.152	eGFR FF4	Tyr to IGFBP2 to Follow-up eGFR	68.13
Y	eGFR	kidney trait in FF4 (as Y)	Tyr	SPOCK2	Tyr to SPOCK2	Metabolites	Proteins	ditype	0.082	eGFR FF4	Tyr to SPOCK2 to Follow-up eGFR	52.45
Y	UACR	kidney trait in FF4 (as Y)	EGFR	Urine albumin	EGFR to Urine albumin	Proteins	UACRbiom	ditype	-0.046	UACR FF4	EGFR to Urine albumin to Follow-up UACR	51.06
Y	UACR	kidney trait in FF4 (as Y)	MCM3	Urine albumin	MCM3 to Urine albumin	RNAs	UACRbiom	ditype	-0.093	UACR FF4	MCM3 to Urine albumin to Follow-up UACR	59.88
Y	UACR	kidney trait in FF4 (as Y)	SLC22A4	Urine albumin	SLC22A4 to Urine albumin	RNAs	UACRbiom	ditype	0.09	UACR FF4	SLC22A4 to Urine albumin to Follow-up UACR	35.46

Supplementary Table 21. Associations between GPS_{eGFR} and replicated candidates in hyperglycemia.

Regression coefficients with 95% *CI*, *P*-values and FDR of GPS_{eGFR} with 64 replicated omics candidates using multivariable linear regression models in hyperglycemic individuals of KORA F4 are shown, respectively. Regression model was adjusted for age, sex, BMI, systolic blood pressure, smoking status, triglyceride, total cholesterol, HDL cholesterol, fasting glucose, use of lipid lowering drugs, antihypertensive and anti-diabetic medication. FDR shown in bold represents statistical significance at 0.05 level. FDR was calculated for each omics type.

Abbreviations: GPS_{eGFR} , genome-wide polygenic score of eGFR values; eGFR, estimated glomerular filtration rate.

X	omics.label	Estimate (95%)	p-value	FDR
GPS	C10:2	-0.089 (-0.143 to -0.035)	1.337E-03	1.216E-02
GPS	TNFRSF1A	-0.144 (-0.231 to -0.057)	1.176E-03	1.216E-02
GPS	NBL1	-0.149 (-0.235 to -0.062)	7.709E-04	1.216E-02
GPS	C14:1	-0.023 (-0.078 to 0.032)	4.074E-01	6.063E-01
GPS	JAM2	-0.152 (-0.245 to -0.059)	1.350E-03	1.216E-02
GPS	C14:2	-0.061 (-0.113 to -0.009)	2.212E-02	6.599E-02
GPS	C16	0.006 (-0.045 to 0.058)	8.045E-01	8.727E-01
GPS	C18:1	-0.001 (-0.053 to 0.051)	9.741E-01	9.741E-01
GPS	C2	-0.019 (-0.07 to 0.033)	4.835E-01	6.727E-01
GPS	C6(C4:1-DC)	-0.051 (-0.102 to 0)	4.824E-02	1.188E-01
GPS	C5	-0.039 (-0.089 to 0.011)	1.270E-01	2.390E-01
GPS	ADAMTS13	0.143 (0.055 to 0.23)	1.520E-03	1.216E-02
GPS	C8:1	-0.043 (-0.097 to 0.011)	1.211E-01	2.363E-01
GPS	LYSMD2	-0.007 (-0.073 to 0.058)	8.244E-01	8.794E-01
GPS	NAPA	-0.001 (-0.068 to 0.065)	9.660E-01	9.741E-01
GPS	SLC22A4	-0.063 (-0.144 to 0.017)	1.218E-01	2.363E-01
GPS	TFE3	-0.034 (-0.116 to 0.049)	4.209E-01	6.088E-01
GPS	Tyr	0.045 (-0.009 to 0.098)	9.949E-02	2.054E-01
GPS	PLAT	0.009 (-0.058 to 0.077)	7.875E-01	8.689E-01
GPS	C12	-0.08 (-0.131 to -0.03)	1.939E-03	1.379E-02
GPS	EFNA5	-0.095 (-0.18 to -0.009)	2.958E-02	7.888E-02
GPS	ERBB3	0.023 (-0.057 to 0.103)	5.776E-01	7.249E-01
GPS	LAYN	-0.076 (-0.162 to 0.01)	8.443E-02	1.930E-01
GPS	C8	-0.08 (-0.132 to -0.027)	2.911E-03	1.863E-02
GPS	EGFR	-0.003 (-0.08 to 0.075)	9.457E-01	9.741E-01
GPS	C10	-0.074 (-0.126 to -0.023)	4.600E-03	2.676E-02
GPS	FGF20	0.064 (-0.029 to 0.156)	1.793E-01	3.101E-01
GPS	FGF9	0.046 (-0.036 to 0.128)	2.662E-01	4.156E-01
GPS	RETN	-0.124 (-0.214 to -0.034)	7.090E-03	3.464E-02
GPS	GHR	0.03 (-0.044 to 0.103)	4.281E-01	6.088E-01
GPS	CGA LHB	-0.015 (-0.063 to 0.033)	5.519E-01	7.209E-01
GPS	ESAM	-0.101 (-0.187 to -0.015)	2.159E-02	6.599E-02
GPS	B2M	-0.116 (-0.201 to -0.032)	7.033E-03	3.464E-02
GPS	CLEC4M	0.006 (-0.083 to 0.095)	8.920E-01	9.359E-01
GPS	IL19	0.058 (-0.031 to 0.147)	1.992E-01	3.355E-01
GPS	SCARF1	-0.127 (-0.22 to -0.034)	7.578E-03	3.464E-02
GPS	TNFRSF1B	-0.091 (-0.179 to -0.003)	4.289E-02	1.098E-01
GPS	C14:1-OH	-0.069 (-0.122 to -0.016)	1.042E-02	4.357E-02
GPS	RET	-0.017 (-0.101 to 0.068)	6.959E-01	8.098E-01

GPS	ACY1	0.019 (-0.054 to 0.092)	6.050E-01	7.446E-01
GPS	CTSV	0.066 (-0.011 to 0.142)	9.246E-02	1.972E-01
GPS	IGFBP6	-0.1 (-0.178 to -0.023)	1.089E-02	4.357E-02
GPS	ERP29	-0.101 (-0.18 to -0.022)	1.277E-02	4.809E-02
GPS	MASP1	0.032 (-0.06 to 0.125)	4.949E-01	6.739E-01
GPS	KDR	-0.016 (-0.104 to 0.073)	7.301E-01	8.331E-01
GPS	IGF2R	0.024 (-0.059 to 0.107)	5.648E-01	7.229E-01
GPS	PLG	0.046 (-0.04 to 0.133)	2.920E-01	4.449E-01
GPS	CTSH	-0.046 (-0.128 to 0.035)	2.657E-01	4.156E-01
GPS	PAPPA	-0.057 (-0.148 to 0.034)	2.157E-01	3.540E-01
GPS	TFF3	-0.072 (-0.156 to 0.011)	9.046E-02	1.972E-01
GPS	EPHA2	-0.105 (-0.191 to -0.018)	1.829E-02	6.162E-02
GPS	NTRK2	0.023 (-0.068 to 0.113)	6.239E-01	7.534E-01
GPS	AMH	0.029 (-0.057 to 0.115)	5.076E-01	6.768E-01
GPS	MMP1	-0.102 (-0.19 to -0.014)	2.372E-02	6.599E-02
GPS	FSTL3	-0.107 (-0.192 to -0.022)	1.395E-02	4.960E-02
GPS	SOD2	0.063 (-0.022 to 0.149)	1.439E-01	2.558E-01
GPS	NOTCH1	0.014 (-0.07 to 0.098)	7.420E-01	8.331E-01
GPS	CST3	-0.144 (-0.221 to -0.067)	2.533E-04	9.283E-03
GPS	RELT	-0.151 (-0.234 to -0.068)	4.048E-04	9.283E-03
GPS	TNFRSF19	-0.085 (-0.179 to 0.009)	7.531E-02	1.785E-01
GPS	HAVCR2	-0.06 (-0.139 to 0.019)	1.363E-01	2.493E-01
GPS	UNC5C	-0.097 (-0.18 to -0.014)	2.276E-02	6.599E-02
GPS	LEPR	0.019 (-0.066 to 0.105)	6.575E-01	7.793E-01
GPS	SPOCK2	0.16 (0.071 to 0.249)	4.352E-04	9.283E-03

Supplementary Table 22. Mediation results among GPS_{eGFR} and its associated candidates and kidney traits in hyperglycemia.

The mediation proportion (%), average mediating effect with 95% *CI*, *P*-values and FDR, average direct effect with 95% *CI*, *P*-values and FDR of each mediating triangle including GPS_{eGFR} , GPS_{eGFR} associated candidate and kidney trait in a nonparametric causal mediation analysis are shown, respectively. Each mediation analysis was adjusted for age, sex, BMI, systolic blood pressure, smoking status, triglyceride, total cholesterol, HDL cholesterol, fasting glucose, use of lipid lowering drugs, antihypertensive and anti-diabetic medication. FDR of mediating effect and direct effect were calculated for each kidney trait.

Abbreviations: GPS_{eGFR} , genome-wide polygenic score of eGFR values; CKD, chronic kidney disease; eGFR, estimated glomerular filtration rate; CKDcrcc, eGFR-based CKD that was defined as $eGFR < 60 \text{ ml/min/1.73 m}^2$.

X	omics.label	omics.type	kidney.tra it_posit ion	kidney.t rait_posit ion	Mediation.direction.label1	Mediation.direction.label2	time.point.kidney.tra it_posit ion	Propotion. media(%)	Avg.media_95			Avg.direct_95		
									CI	Avg.media.p	Avg.media.fdr	CI	Avg.direct.p	Avg.direct.fdr
GPS	C10	Metabolites	eGFR S4	M	GPS->eGFR S4->Candi	GPS to eGFR S4 to C10	kidney trait in S4 (as M)	68.87	-0.073 (-0.122 to -0.028)	4.00E-03	5.333E-03	-0.033 (-0.122 to 0.05)	4.48E-01	8.896E-01
GPS	C10	Metabolites	eGFR F4	M	eGFR F4 (bidirection)	GPS to eGFR F4 to C10	kidney trait in F4	103.35	-0.077 (-0.101 to -0.055)	0.00E+00	0.000E+00	0.002 (-0.054 to 0.06)	8.84E-01	9.614E-01
				Y	eGFR F4 (bidirection)	GPS to C10 to eGFR F4	kidney trait in F4	4.16	0.011 (0.002 to 0.02)	1.20E-02	1.234E-02	0.255 (0.216 to 0.292)	0.00E+00	0.000E+00
GPS	C10	Metabolites	eGFR FF4	Y	GPS->Candi->Follow-up eGFR	GPS to C10 to Follow-up eGFR	kidney trait in FF4 (as Y)	3.83	0.009 (0 to 0.019)	6.40E-02	6.776E-02	0.226 (0.178 to 0.271)	0.00E+00	0.000E+00
GPS	C10	Metabolites	CKD F4	M	CKD F4 (bidirection)	GPS to CKD F4 to C10	kidney trait in F4	5.36	-0.004 (-0.016 to 0.002)	1.36E-01	2.225E-01	-0.068 (-0.12 to -0.015)	6.00E-03	2.618E-02
				Y	CKD F4 (bidirection)	GPS to C10 to CKD F4	kidney trait in F4	8.52	-0.002 (-0.005 to 0)	1.60E-02	3.840E-02	-0.024 (-0.043 to -0.002)	3.60E-02	6.171E-02
GPS	C10:2	Metabolites	eGFR S4	M	GPS->eGFR S4->Candi	GPS to eGFR S4 to C10:2	kidney trait in S4 (as M)	121.49	-0.118 (-0.181 to -0.059)	0.00E+00	0.000E+00	0.021 (-0.084 to 0.124)	6.90E-01	9.748E-01
GPS	C10:2	Metabolites	eGFR F4	M	eGFR F4 (bidirection)	GPS to eGFR F4 to C10:2	kidney trait in F4	95.54	-0.085 (-0.109 to -0.06)	0.00E+00	0.000E+00	-0.004 (-0.066 to 0.055)	8.46E-01	9.614E-01
				Y	eGFR F4 (bidirection)	GPS to C10:2 to eGFR F4	kidney trait in F4	4.93	0.013 (0.005 to 0.022)	0.00E+00	0.000E+00	0.253 (0.215 to 0.29)	0.00E+00	0.000E+00
GPS	C10:2	Metabolites	eGFR FF4	Y	GPS->Candi->Follow-up eGFR	GPS to C10:2 to Follow-up eGFR	kidney trait in FF4 (as Y)	4.43	0.01 (0.003 to 0.02)	4.00E-03	9.000E-03	0.225 (0.173 to 0.271)	0.00E+00	0.000E+00
GPS	C10:2	Metabolites	CKDcrcc S4	M	GPS->CKDcrcc S4->Candi	GPS to CKDcrcc S4 to C10:2	kidney trait in S4 (as M)	15.77	-0.01 (-0.032 to -0.002)	6.00E-03	2.567E-02	-0.054 (-0.149 to 0.034)	2.08E-01	2.912E-01
GPS	C10:2	Metabolites	CKD F4	M	CKD F4 (bidirection)	GPS to CKD F4 to C10:2	kidney trait in F4	5.1	-0.004 (-0.017 to 0.002)	1.36E-01	2.225E-01	-0.081 (-0.14 to -0.024)	8.00E-03	2.618E-02
				Y	CKD F4 (bidirection)	GPS to C10:2 to CKD F4	kidney trait in F4	10.76	-0.003 (-0.006 to -0.001)	0.00E+00	0.000E+00	-0.023 (-0.043 to -0.002)	3.20E-02	6.063E-02
GPS	C12	Metabolites	eGFR S4	M	GPS->eGFR S4->Candi	GPS to eGFR S4 to C12	kidney trait in S4 (as M)	47.38	-0.066 (-0.115 to -0.02)	6.00E-03	7.385E-03	-0.074 (-0.169 to 0.014)	1.10E-01	4.400E-01
GPS	C12	Metabolites	eGFR F4	M	eGFR F4 (bidirection)	GPS to eGFR F4 to C12	kidney trait in F4	97.67	-0.078 (-0.104 to -0.054)	0.00E+00	0.000E+00	-0.002 (-0.054 to 0.056)	9.38E-01	9.648E-01
				Y	eGFR F4 (bidirection)	GPS to C12 to eGFR F4	kidney trait in F4	4.7	0.013 (0.004 to 0.021)	0.00E+00	0.000E+00	0.254 (0.214 to 0.291)	0.00E+00	0.000E+00
GPS	C12	Metabolites	eGFR FF4	Y	GPS->Candi->Follow-up eGFR	GPS to C12 to Follow-up eGFR	kidney trait in FF4 (as Y)	4.89	0.011 (0.002 to 0.023)	1.00E-02	1.800E-02	0.223 (0.173 to 0.269)	0.00E+00	0.000E+00
GPS	C12	Metabolites	CKD F4	M	CKD F4 (bidirection)	GPS to CKD F4 to C12	kidney trait in F4	5.66	-0.004 (-0.017 to 0.002)	1.36E-01	2.225E-01	-0.072 (-0.121 to -0.02)	8.00E-03	2.618E-02
				Y	CKD F4 (bidirection)	GPS to C12 to CKD F4	kidney trait in F4	10.91	-0.003 (-0.006 to -0.001)	2.00E-03	1.200E-02	-0.023 (-0.042 to -0.001)	3.60E-02	6.171E-02
GPS	C12	Metabolites	CKD FF4	Y	GPS->Candi->incident CKD	GPS to C12 to incident CKD	kidney trait in FF4 (as Y)	7.96	-0.003 (-0.007 to 0)	4.20E-02	4.200E-02	-0.034 (-0.059 to -0.006)	2.00E-02	2.000E-02
GPS	C14:1-OH	Metabolites	eGFR S4	M	GPS->eGFR S4->Candi	GPS to eGFR S4 to C14:1-OH	kidney trait in S4 (as M)	122.27	-0.073 (-0.12 to -0.022)	4.00E-03	5.333E-03	0.013 (-0.088 to 0.099)	7.92E-01	9.748E-01
GPS	C14:1-OH	Metabolites	eGFR F4	M	eGFR F4 (bidirection)	GPS to eGFR F4 to C14:1-OH	kidney trait in F4	112.37	-0.078 (-0.103 to -0.053)	0.00E+00	0.000E+00	0.009 (-0.049 to 0.065)	7.36E-01	9.434E-01
				Y	eGFR F4 (bidirection)	GPS to C14:1-OH to eGFR F4	kidney trait in F4	3.69	0.01 (0.002 to 0.018)	8.00E-03	9.290E-03	0.256 (0.217 to 0.294)	0.00E+00	0.000E+00
GPS	C14:1-OH	Metabolites	eGFR FF4	Y	GPS->Candi->Follow-up eGFR	GPS to C14:1-OH to Follow-up eGFR	kidney trait in FF4 (as Y)	4.54	0.011 (0.002 to 0.022)	1.60E-02	2.057E-02	0.224 (0.175 to 0.27)	0.00E+00	0.000E+00

GPS	C14:1-OH	Metabolites	CKD F4	M	CKD F4 (bidirection)	GPS to CKD F4 to C14:1-OH	kidney trait in F4	7 82	-0 005 (-0 02 to 0 002)	1 36E-01	2 225E-01	-0 06 (-0 114 to -0 009)	2 20E-02	4 950E-02
				Y	CKD F4 (bidirection)	GPS to C14:1-OH to CKD F4	kidney trait in F4	10 31	-0 003 (-0 006 to -0 001)	8 00E-03	2 880E-02	-0 024 (-0 043 to -0 003)	3 20E-02	6 063E-02
GPS	C8	Metabolites	eGFR S4	M	GPS->eGFR S4->Candi	GPS to eGFR S4 to C8	kidney trait in S4 (as M)	50 44	-0 064 (-0 112 to -0 018)	1 20E-02	1 280E-02	-0 063 (-0 15 to 0 024)	1 50E-01	4 800E-01
GPS	C8	Metabolites	eGFR F4	M	eGFR F4 (bidirection)	GPS to eGFR F4 to C8	kidney trait in F4	91 89	-0 073 (-0 098 to -0 051)	0 00E+00	0 000E+00	-0 006 (-0 066 to 0 051)	8 74E-01	9 614E-01
				Y	eGFR F4 (bidirection)	GPS to C8 to eGFR F4	kidney trait in F4	4 08	0 011 (0 003 to 0 02)	1 00E-02	1 091E-02	0 255 (0 217 to 0 294)	0 00E+00	0 000E+00
GPS	C8	Metabolites	eGFR FF4	Y	GPS->Candi->Follow-up eGFR	GPS to C8 to Follow-up eGFR	kidney trait in FF4 (as Y)	3 13	0 007 (-0 002 to 0 018)	1 16E-01	1 160E-01	0 228 (0 18 to 0 273)	0 00E+00	0 000E+00
GPS	C8	Metabolites	CKD F4	M	CKD F4 (bidirection)	GPS to CKD F4 to C8	kidney trait in F4	4 55	-0 003 (-0 015 to 0 001)	1 44E-01	2 254E-01	-0 073 (-0 127 to -0 018)	2 00E-03	1 800E-02
				Y	CKD F4 (bidirection)	GPS to C8 to CKD F4	kidney trait in F4	7 37	-0 002 (-0 005 to 0)	2 60E-02	5 506E-02	-0 024 (-0 043 to -0 002)	3 20E-02	6 063E-02
GPS	CST3	Proteins	eGFR S4	M	GPS->eGFR S4->Candi	GPS to eGFR S4 to CST3	kidney trait in S4 (as M)	175 04	-0 258 (-0 354 to -0 173)	0 00E+00	0 000E+00	0 111 (-0 005 to 0 225)	6 20E-02	4 267E-01
GPS	CST3	Proteins	eGFR F4	M	eGFR F4 (bidirection)	GPS to eGFR F4 to CST3	kidney trait in F4	152	-0 219 (-0 275 to -0 164)	0 00E+00	0 000E+00	0 075 (0 022 to 0 129)	1 00E-02	1 895E-02
				Y	eGFR F4 (bidirection)	GPS to CST3 to eGFR F4	kidney trait in F4	32 69	0 075 (0 039 to 0 111)	0 00E+00	0 000E+00	0 154 (0 11 to 0 197)	0 00E+00	0 000E+00
GPS	CST3	Proteins	eGFR FF4	Y	GPS->Candi->Follow-up eGFR	GPS to CST3 to Follow-up eGFR	kidney trait in FF4 (as Y)	30 24	0 07 (0 035 to 0 108)	0 00E+00	0 000E+00	0 161 (0 114 to 0 21)	0 00E+00	0 000E+00
GPS	CST3	Proteins	CKDerce S4	M	GPS->CKDerce S4->Candi	GPS to CKDerce S4 to CST3	kidney trait in S4 (as M)	18 42	-0 02 (-0 054 to 0)	2 20E-02	2 567E-02	-0 087 (-0 223 to 0 038)	1 88E-01	2 912E-01
GPS	CST3	Proteins	CKD F4	M	CKD F4 (bidirection)	GPS to CKD F4 to CST3	kidney trait in F4	8 49	-0 011 (-0 056 to 0 017)	3 18E-01	3 515E-01	-0 124 (-0 189 to -0 056)	0 00E+00	0 000E+00
				Y	CKD F4 (bidirection)	GPS to CST3 to CKD F4	kidney trait in F4	65 23	-0 011 (-0 018 to -0 005)	0 00E+00	0 000E+00	-0 006 (-0 027 to 0 021)	6 52E-01	6 520E-01
GPS	CST3	Proteins	CKD FF4	Y	GPS->Candi->incident CKD	GPS to CST3 to incident CKD	kidney trait in FF4 (as Y)	16 45	-0 008 (-0 017 to -0 002)	2 00E-03	6 000E-03	-0 043 (-0 072 to -0 011)	1 40E-02	2 000E-02
GPS	TNFRSF1A	Proteins	eGFR S4	M	GPS->eGFR S4->Candi	GPS to eGFR S4 to TNFRSF1A	kidney trait in S4 (as M)	98 57	-0 139 (-0 233 to -0 059)	0 00E+00	0 000E+00	-0 002 (-0 142 to 0 152)	9 80E-01	9 800E-01
GPS	TNFRSF1A	Proteins	eGFR F4	M	eGFR F4 (bidirection)	GPS to eGFR F4 to TNFRSF1A	kidney trait in F4	104 23	-0 15 (-0 197 to -0 106)	0 00E+00	0 000E+00	0 006 (-0 083 to 0 089)	9 08E-01	9 614E-01
				Y	eGFR F4 (bidirection)	GPS to TNFRSF1A to eGFR F4	kidney trait in F4	17 58	0 04 (0 015 to 0 07)	0 00E+00	0 000E+00	0 189 (0 134 to 0 241)	0 00E+00	0 000E+00
GPS	TNFRSF1A	Proteins	eGFR FF4	Y	GPS->Candi->Follow-up eGFR	GPS to TNFRSF1A to Follow-up eGFR	kidney trait in FF4 (as Y)	17 63	0 041 (0 015 to 0 072)	2 00E-03	6 000E-03	0 19 (0 136 to 0 246)	0 00E+00	0 000E+00
GPS	TNFRSF1A	Proteins	CKDerce S4	M	GPS->CKDerce S4->Candi	GPS to CKDerce S4 to TNFRSF1A	kidney trait in S4 (as M)	26 56	-0 024 (-0 073 to 0)	2 20E-02	2 567E-02	-0 067 (-0 201 to 0 065)	3 18E-01	3 710E-01
GPS	TNFRSF1A	Proteins	CKD F4	M	CKD F4 (bidirection)	GPS to CKD F4 to TNFRSF1A	kidney trait in F4	6 94	-0 01 (-0 046 to 0 016)	3 22E-01	3 515E-01	-0 128 (-0 218 to -0 037)	8 00E-03	2 618E-02
				Y	CKD F4 (bidirection)	GPS to TNFRSF1A to CKD F4	kidney trait in F4	34 49	-0 007 (-0 013 to -0 002)	0 00E+00	0 000E+00	-0 013 (-0 034 to 0 014)	3 00E-01	3 554E-01
GPS	IGFBP6	Proteins	eGFR S4	M	GPS->eGFR S4->Candi	GPS to eGFR S4 to IGFBP6	kidney trait in S4 (as M)	86 49	-0 145 (-0 23 to -0 075)	0 00E+00	0 000E+00	-0 023 (-0 159 to 0 104)	7 50E-01	9 748E-01
GPS	IGFBP6	Proteins	eGFR F4	M	eGFR F4 (bidirection)	GPS to eGFR F4 to IGFBP6	kidney trait in F4	144 61	-0 145 (-0 19 to -0 105)	0 00E+00	0 000E+00	0 045 (-0 033 to 0 116)	2 88E-01	4 380E-01

				Y	eGFR F4 (bidirection)	GPS to IGFBP6 to eGFR F4	kidney trait in F4	14 95	0 034 (0 009 to 0 063)	1 20E-02	1 234E-02	0 195 (0 144 to 0 243)	0 00E+00	0 000E+00
GPS	IGFBP6	Proteins	eGFR FF4	Y	GPS->Candi->Follow-up eGFR	GPS to IGFBP6 to Follow-up eGFR	kidney trait in FF4 (as Y)	14 71	0 034 (0 008 to 0 063)	1 40E-02	2 057E-02	0 197 (0 142 to 0 248)	0 00E+00	0 000E+00
GPS	IGFBP6	Proteins	CKDcrcc S4	M	GPS->CKDcrcc S4->Candi	GPS to CKDcrcc S4 to IGFBP6	kidney trait in S4 (as M)	9 48	-0 013 (-0 043 to 0)	2 20E-02	2 567E-02	-0 126 (-0 261 to -0 01)	4 00E-02	1 400E-01
GPS	IGFBP6	Proteins	CKD F4	M	CKD F4 (bidirection)	GPS to CKD F4 to IGFBP6	kidney trait in F4	7 4	-0 007 (-0 036 to 0 011)	3 26E-01	3 515E-01	-0 088 (-0 168 to -0 017)	1 60E-02	4 800E-02
				Y	CKD F4 (bidirection)	GPS to IGFBP6 to CKD F4	kidney trait in F4	27 43	-0 005 (-0 01 to -0 001)	1 20E-02	3 600E-02	-0 013 (-0 033 to 0 013)	3 06E-01	3 554E-01
GPS	NBL1	Proteins	eGFR S4	M	GPS->eGFR S4->Candi	GPS to eGFR S4 to NBL1	kidney trait in S4 (as M)	38 61	-0 097 (-0 213 to 0 008)	7 00E-02	7 000E-02	-0 155 (-0 327 to 0 022)	8 00E-02	4 267E-01
GPS	NBL1	Proteins	eGFR F4	M	eGFR F4 (bidirection)	GPS to eGFR F4 to NBL1	kidney trait in F4	72 95	-0 109 (-0 15 to -0 067)	0 00E+00	0 000E+00	-0 04 (-0 129 to 0 038)	2 92E-01	4 380E-01
				Y	eGFR F4 (bidirection)	GPS to NBL1 to eGFR F4	kidney trait in F4	13 23	0 03 (0 013 to 0 054)	0 00E+00	0 000E+00	0 199 (0 139 to 0 254)	0 00E+00	0 000E+00
GPS	NBL1	Proteins	eGFR FF4	Y	GPS->Candi->Follow-up eGFR	GPS to NBL1 to Follow-up eGFR	kidney trait in FF4 (as Y)	14 32	0 033 (0 014 to 0 06)	0 00E+00	0 000E+00	0 197 (0 145 to 0 253)	0 00E+00	0 000E+00
GPS	NBL1	Proteins	CKDcrcc S4	M	GPS->CKDcrcc S4->Candi	GPS to CKDcrcc S4 to NBL1	kidney trait in S4 (as M)	11 74	-0 024 (-0 065 to 0)	2 00E-02	2 567E-02	-0 179 (-0 33 to -0 025)	1 80E-02	1 260E-01
GPS	NBL1	Proteins	CKD F4	M	CKD F4 (bidirection)	GPS to CKD F4 to NBL1	kidney trait in F4	6 61	-0 009 (-0 047 to 0 015)	3 16E-01	3 515E-01	-0 133 (-0 216 to -0 058)	0 00E+00	0 000E+00
				Y	CKD F4 (bidirection)	GPS to NBL1 to CKD F4	kidney trait in F4	35 74	-0 006 (-0 013 to -0 002)	0 00E+00	0 000E+00	-0 011 (-0 031 to 0 016)	4 20E-01	4 320E-01
GPS	JAM2	Proteins	eGFR S4	M	GPS->eGFR S4->Candi	GPS to eGFR S4 to JAM2	kidney trait in S4 (as M)	66 68	-0 132 (-0 234 to -0 054)	2 00E-03	3 200E-03	-0 066 (-0 254 to 0 129)	5 40E-01	8 896E-01
GPS	JAM2	Proteins	eGFR F4	M	eGFR F4 (bidirection)	GPS to eGFR F4 to JAM2	kidney trait in F4	79 97	-0 122 (-0 173 to -0 075)	0 00E+00	0 000E+00	-0 03 (-0 128 to 0 071)	5 80E-01	7 733E-01
				Y	eGFR F4 (bidirection)	GPS to JAM2 to eGFR F4	kidney trait in F4	13 16	0 03 (0 011 to 0 052)	4 00E-03	5 333E-03	0 199 (0 144 to 0 255)	0 00E+00	0 000E+00
GPS	JAM2	Proteins	eGFR FF4	Y	GPS->Candi->Follow-up eGFR	GPS to JAM2 to Follow-up eGFR	kidney trait in FF4 (as Y)	12 81	0 03 (0 011 to 0 054)	2 00E-03	6 000E-03	0 201 (0 141 to 0 257)	0 00E+00	0 000E+00
GPS	JAM2	Proteins	CKD F4	M	CKD F4 (bidirection)	GPS to CKD F4 to JAM2	kidney trait in F4	4 31	-0 006 (-0 035 to 0 01)	3 18E-01	3 515E-01	-0 141 (-0 227 to -0 045)	4 00E-03	2 057E-02
				Y	CKD F4 (bidirection)	GPS to JAM2 to CKD F4	kidney trait in F4	29 85	-0 005 (-0 011 to 0)	2 60E-02	5 506E-02	-0 012 (-0 033 to 0 016)	3 46E-01	3 664E-01
GPS	RETN	Proteins	eGFR F4	M	eGFR F4 (bidirection)	GPS to eGFR F4 to RETN	kidney trait in F4	70 32	-0 087 (-0 13 to -0 048)	0 00E+00	0 000E+00	-0 037 (-0 137 to 0 055)	4 10E-01	5 904E-01
				Y	eGFR F4 (bidirection)	GPS to RETN to eGFR F4	kidney trait in F4	8 14	0 019 (0 004 to 0 035)	8 00E-03	9 290E-03	0 211 (0 155 to 0 267)	0 00E+00	0 000E+00
GPS	RETN	Proteins	eGFR FF4	Y	GPS->Candi->Follow-up eGFR	GPS to RETN to Follow-up eGFR	kidney trait in FF4 (as Y)	10 78	0 025 (0 007 to 0 047)	4 00E-03	9 000E-03	0 206 (0 148 to 0 263)	0 00E+00	0 000E+00
GPS	RETN	Proteins	CKD F4	M	CKD F4 (bidirection)	GPS to CKD F4 to RETN	kidney trait in F4	4 79	-0 006 (-0 031 to 0 009)	3 44E-01	3 538E-01	-0 114 (-0 203 to -0 025)	2 00E-02	4 950E-02
				Y	CKD F4 (bidirection)	GPS to RETN to CKD F4	kidney trait in F4	17 74	-0 004 (-0 008 to 0)	1 60E-02	3 840E-02	-0 017 (-0 036 to 0 008)	1 60E-01	2 304E-01
GPS	ADAMTS13	Proteins	eGFR F4	M	eGFR F4 (bidirection)	GPS to eGFR F4 to ADAMTS13	kidney trait in F4	36 49	0 052 (0 015 to 0 089)	2 00E-03	2 880E-03	0 091 (-0 003 to 0 191)	5 60E-02	9 600E-02
				Y	eGFR F4 (bidirection)	GPS to ADAMTS13 to eGFR F4	kidney trait in F4	5 87	0 013 (0 003 to 0 026)	4 00E-03	5 333E-03	0 216 (0 16 to 0 273)	0 00E+00	0 000E+00

GPS	ADAMTS13	Proteins	eGFR FF4	Y	GPS->Candi->Follow-up eGFR	GPS to ADAMTS13 to Follow-up eGFR	kidney trait in FF4 (as Y)	4 44	0 01 (0 001 to 0 024)	3 40E-02	3 825E-02	0 22 (0 162 to 0 28)	0 00E+00	0 000E+00
GPS	ADAMTS13	Proteins	CKD F4	M	CKD F4 (bidirection)	GPS to CKD F4 to ADAMTS13	kidney trait in F4	2 47	0 003 (-0 006 to 0 024)	4 18E-01	4 180E-01	0 137 (0 056 to 0 223)	4 00E-03	2 057E-02
				Y	CKD F4 (bidirection)	GPS to ADAMTS13 to CKD F4	kidney trait in F4	17 27	-0 003 (-0 009 to 0)	1 02E-01	2 040E-01	-0 017 (-0 037 to 0 008)	1 80E-01	2 492E-01
GPS	FSTL3	Proteins	eGFR S4	M	GPS->eGFR S4->Candi	GPS to eGFR S4 to FSTL3	kidney trait in S4 (as M)	103 61	-0 177 (-0 271 to -0 094)	0 00E+00	0 000E+00	0 006 (-0 144 to 0 171)	9 38E-01	9 800E-01
GPS	FSTL3	Proteins	eGFR F4	M	eGFR F4 (bidirection)	GPS to eGFR F4 to FSTL3	kidney trait in F4	104 6	-0 112 (-0 154 to -0 07)	0 00E+00	0 000E+00	0 005 (-0 081 to 0 093)	8 72E-01	9 614E-01
				Y	eGFR F4 (bidirection)	GPS to FSTL3 to eGFR F4	kidney trait in F4	10 08	0 023 (0 006 to 0 043)	8 00E-03	9 290E-03	0 206 (0 152 to 0 261)	0 00E+00	0 000E+00
GPS	FSTL3	Proteins	eGFR FF4	Y	GPS->Candi->Follow-up eGFR	GPS to FSTL3 to Follow-up eGFR	kidney trait in FF4 (as Y)	12 86	0 03 (0 006 to 0 057)	1 60E-02	2 057E-02	0 201 (0 146 to 0 257)	0 00E+00	0 000E+00
GPS	FSTL3	Proteins	CKDcrcc S4	M	GPS->CKDcrcc S4->Candi	GPS to CKDcrcc S4 to FSTL3	kidney trait in S4 (as M)	12 22	-0 017 (-0 048 to 0)	5 00E-02	5 000E-02	-0 119 (-0 265 to 0 032)	9 60E-02	2 240E-01
GPS	FSTL3	Proteins	CKD F4	M	CKD F4 (bidirection)	GPS to CKD F4 to FSTL3	kidney trait in F4	8 17	-0 008 (-0 042 to 0 013)	3 20E-01	3 515E-01	-0 092 (-0 17 to -0 006)	4 20E-02	6 574E-02
				Y	CKD F4 (bidirection)	GPS to FSTL3 to CKD F4	kidney trait in F4	32 12	-0 006 (-0 012 to -0 001)	8 00E-03	2 880E-02	-0 012 (-0 031 to 0 013)	3 22E-01	3 578E-01
GPS	B2M	Proteins	eGFR S4	M	GPS->eGFR S4->Candi	GPS to eGFR S4 to B2M	kidney trait in S4 (as M)	384 93	-0 23 (-0 34 to -0 138)	0 00E+00	0 000E+00	0 17 (0 028 to 0 315)	2 20E-02	3 520E-01
GPS	B2M	Proteins	eGFR F4	M	eGFR F4 (bidirection)	GPS to eGFR F4 to B2M	kidney trait in F4	174 59	-0 203 (-0 255 to -0 152)	0 00E+00	0 000E+00	0 087 (0 013 to 0 159)	3 00E-02	5 400E-02
				Y	eGFR F4 (bidirection)	GPS to B2M to eGFR F4	kidney trait in F4	20 24	0 046 (0 012 to 0 083)	1 00E-02	1 091E-02	0 183 (0 135 to 0 226)	0 00E+00	0 000E+00
GPS	B2M	Proteins	eGFR FF4	Y	GPS->Candi->Follow-up eGFR	GPS to B2M to Follow-up eGFR	kidney trait in FF4 (as Y)	18 05	0 042 (0 009 to 0 077)	8 00E-03	1 600E-02	0 189 (0 138 to 0 243)	0 00E+00	0 000E+00
GPS	B2M	Proteins	CKDcrcc S4	M	GPS->CKDcrcc S4->Candi	GPS to CKDcrcc S4 to B2M	kidney trait in S4 (as M)	87 13	-0 019 (-0 058 to 0)	2 20E-02	2 567E-02	-0 003 (-0 164 to 0 145)	9 74E-01	9 740E-01
GPS	B2M	Proteins	CKD F4	M	CKD F4 (bidirection)	GPS to CKD F4 to B2M	kidney trait in F4	10 33	-0 011 (-0 052 to 0 017)	3 32E-01	3 515E-01	-0 097 (-0 187 to -0 015)	2 20E-02	4 950E-02
				Y	CKD F4 (bidirection)	GPS to B2M to CKD F4	kidney trait in F4	35 56	-0 007 (-0 013 to -0 002)	1 00E-02	3 273E-02	-0 013 (-0 033 to 0 011)	2 64E-01	3 277E-01
GPS	B2M	Proteins	CKD FF4	Y	GPS->Candi->incident CKD	GPS to B2M to incident CKD	kidney trait in FF4 (as Y)	11 16	-0 006 (-0 014 to -0 001)	3 20E-02	4 200E-02	-0 046 (-0 074 to -0 017)	4 00E-03	1 200E-02
GPS	ERP29	Proteins	eGFR S4	M	GPS->eGFR S4->Candi	GPS to eGFR S4 to ERP29	kidney trait in S4 (as M)	301 11	-0 144 (-0 228 to -0 072)	0 00E+00	0 000E+00	0 096 (-0 093 to 0 272)	2 90E-01	6 629E-01
GPS	ERP29	Proteins	eGFR F4	M	eGFR F4 (bidirection)	GPS to eGFR F4 to ERP29	kidney trait in F4	89 67	-0 091 (-0 124 to -0 057)	0 00E+00	0 000E+00	-0 01 (-0 093 to 0 074)	7 60E-01	9 434E-01
				Y	eGFR F4 (bidirection)	GPS to ERP29 to eGFR F4	kidney trait in F4	8 86	0 02 (0 004 to 0 039)	1 60E-02	1 600E-02	0 209 (0 153 to 0 263)	0 00E+00	0 000E+00
GPS	ERP29	Proteins	eGFR FF4	Y	GPS->Candi->Follow-up eGFR	GPS to ERP29 to Follow-up eGFR	kidney trait in FF4 (as Y)	8 42	0 019 (0 002 to 0 039)	3 40E-02	3 825E-02	0 211 (0 156 to 0 267)	0 00E+00	0 000E+00
GPS	ERP29	Proteins	CKD F4	M	CKD F4 (bidirection)	GPS to CKD F4 to ERP29	kidney trait in F4	9 52	-0 009 (-0 043 to 0 014)	3 14E-01	3 515E-01	-0 085 (-0 163 to -0 007)	4 00E-02	6 545E-02
				Y	CKD F4 (bidirection)	GPS to ERP29 to CKD F4	kidney trait in F4	33 54	-0 008 (-0 015 to -0 001)	1 60E-02	3 840E-02	-0 015 (-0 032 to 0 009)	2 42E-01	3 111E-01
GPS	RELT	Proteins	eGFR S4	M	GPS->eGFR S4->Candi	GPS to eGFR S4 to RELT	kidney trait in S4 (as M)	133 42	-0 16 (-0 261 to -0 081)	0 00E+00	0 000E+00	0 04 (-0 082 to 0 167)	5 56E-01	8 896E-01

GPS	RELT	Proteins	eGFR F4	M	eGFR F4 (bidirection)	GPS to eGFR F4 to RELT	kidney trait in F4	100.36	-0.151 (-0.202 to -0.108)	0.00E+00	0.000E+00	0.001 (-0.075 to 0.074)	9.94E-01	9.940E-01
				Y	eGFR F4 (bidirection)	GPS to RELT to eGFR F4	kidney trait in F4	20.15	0.046 (0.023 to 0.073)	0.00E+00	0.000E+00	0.183 (0.13 to 0.237)	0.00E+00	0.000E+00
GPS	RELT	Proteins	eGFR FF4	Y	GPS->Candi->Follow-up eGFR	GPS to RELT to Follow-up eGFR	kidney trait in FF4 (as Y)	22.55	0.052 (0.026 to 0.082)	0.00E+00	0.000E+00	0.178 (0.123 to 0.238)	0.00E+00	0.000E+00
GPS	RELT	Proteins	CKD F4	M	CKD F4 (bidirection)	GPS to CKD F4 to RELT	kidney trait in F4	5.16	-0.007 (-0.038 to 0.011)	3.22E-01	3.515E-01	-0.138 (-0.214 to -0.063)	0.00E+00	0.000E+00
				Y	CKD F4 (bidirection)	GPS to RELT to CKD F4	kidney trait in F4	36.69	-0.007 (-0.014 to -0.002)	4.00E-03	1.800E-02	-0.012 (-0.031 to 0.014)	3.28E-01	3.578E-01
GPS	SCARF1	Proteins	eGFR S4	M	GPS->eGFR S4->Candi	GPS to eGFR S4 to SCARF1	kidney trait in S4 (as M)	102.96	-0.087 (-0.167 to -0.02)	8.00E-03	9.143E-03	0.003 (-0.168 to 0.174)	9.08E-01	9.800E-01
GPS	SCARF1	Proteins	eGFR F4	M	eGFR F4 (bidirection)	GPS to eGFR F4 to SCARF1	kidney trait in F4	45.86	-0.058 (-0.092 to -0.023)	0.00E+00	0.000E+00	-0.069 (-0.164 to 0.026)	1.50E-01	2.455E-01
				Y	eGFR F4 (bidirection)	GPS to SCARF1 to eGFR F4	kidney trait in F4	5.22	0.012 (0.003 to 0.025)	6.00E-03	7.714E-03	0.217 (0.161 to 0.273)	0.00E+00	0.000E+00
GPS	SCARF1	Proteins	eGFR FF4	Y	GPS->Candi->Follow-up eGFR	GPS to SCARF1 to Follow-up eGFR	kidney trait in FF4 (as Y)	6.81	0.016 (0.003 to 0.03)	1.20E-02	1.964E-02	0.215 (0.162 to 0.273)	0.00E+00	0.000E+00
GPS	SCARF1	Proteins	CKD F4	M	CKD F4 (bidirection)	GPS to CKD F4 to SCARF1	kidney trait in F4	5.55	-0.007 (-0.034 to 0.01)	3.22E-01	3.515E-01	-0.115 (-0.198 to -0.029)	1.80E-02	4.950E-02
				Y	CKD F4 (bidirection)	GPS to SCARF1 to CKD F4	kidney trait in F4	25.47	-0.005 (-0.01 to -0.001)	4.00E-03	1.800E-02	-0.015 (-0.033 to 0.009)	2.18E-01	2.907E-01
GPS	SPOCK2	Proteins	eGFR S4	M	GPS->eGFR S4->Candi	GPS to eGFR S4 to SPOCK2	kidney trait in S4 (as M)	202.79	0.181 (0.103 to 0.268)	0.00E+00	0.000E+00	-0.092 (-0.262 to 0.067)	2.80E-01	6.629E-01
GPS	SPOCK2	Proteins	eGFR F4	M	eGFR F4 (bidirection)	GPS to eGFR F4 to SPOCK2	kidney trait in F4	79.28	0.127 (0.084 to 0.168)	0.00E+00	0.000E+00	0.033 (-0.054 to 0.126)	4.60E-01	6.369E-01
				Y	eGFR F4 (bidirection)	GPS to SPOCK2 to eGFR F4	kidney trait in F4	15.74	0.036 (0.017 to 0.06)	0.00E+00	0.000E+00	0.193 (0.142 to 0.245)	0.00E+00	0.000E+00
GPS	SPOCK2	Proteins	eGFR FF4	Y	GPS->Candi->Follow-up eGFR	GPS to SPOCK2 to Follow-up eGFR	kidney trait in FF4 (as Y)	13.64	0.031 (0.012 to 0.053)	0.00E+00	0.000E+00	0.199 (0.148 to 0.255)	0.00E+00	0.000E+00
GPS	SPOCK2	Proteins	CKD F4	M	CKD F4 (bidirection)	GPS to CKD F4 to SPOCK2	kidney trait in F4	5.24	0.008 (-0.011 to 0.042)	3.18E-01	3.515E-01	0.146 (0.055 to 0.235)	4.00E-03	2.057E-02
				Y	CKD F4 (bidirection)	GPS to SPOCK2 to CKD F4	kidney trait in F4	31.65	-0.007 (-0.014 to -0.002)	0.00E+00	0.000E+00	-0.016 (-0.033 to 0.008)	1.60E-01	2.304E-01

Supplementary Table 23. Associations of GPS_{eGFR} with eGFR values and GPS_{eGFR} -associated candidates in different percentiles of sample size of hyperglycemic individuals.

Regression coefficients with 95% *CI*, *P*-values of GPS_{eGFR} with eGFR values, and 18 GPS_{eGFR} -associated candidates using multivariable linear regression models in different percentiles of sample size of hyperglycemic individuals of KORA F4 are shown, respectively. Regression model was adjusted for age, sex, BMI, systolic blood pressure, smoking status, triglyceride, total cholesterol, HDL cholesterol, fasting glucose, use of lipid lowering drugs, antihypertensive and anti-diabetic medication.

Abbreviations: GPS_{eGFR} , genome-wide polygenic score of eGFR values; eGFR, estimated glomerular filtration rate.

X	outcome	samplesize	Estimate (95%)	p-value
GPS	F4 Mean eGFR	5%	0.437 (-0.01 to 0.884)	5.506E-02
GPS	F4 Mean eGFR	15%	0.415 (0.207 to 0.622)	1.156E-04
GPS	F4 Mean eGFR	25%	0.426 (0.286 to 0.565)	5.633E-09
GPS	F4 Mean eGFR	35%	0.332 (0.218 to 0.447)	2.364E-08
GPS	F4 Mean eGFR	45%	0.372 (0.277 to 0.466)	4.645E-14
GPS	F4 Mean eGFR	full data	0.273 (0.236 to 0.31)	2.829E-44
GPS	C10	5%	-0.481 (-1.087 to 0.126)	1.176E-01
GPS	C10	15%	-0.195 (-0.49 to 0.1)	1.928E-01
GPS	C10	25%	-0.134 (-0.344 to 0.076)	2.090E-01
GPS	C10	35%	-0.1 (-0.263 to 0.063)	2.305E-01
GPS	C10	45%	-0.133 (-0.263 to -0.003)	4.482E-02
GPS	C10	full data	-0.074 (-0.126 to -0.023)	4.600E-03
GPS	C10:2	5%	0.096 (-0.548 to 0.74)	7.650E-01
GPS	C10:2	15%	-0.045 (-0.341 to 0.251)	7.634E-01
GPS	C10:2	25%	-0.091 (-0.298 to 0.117)	3.907E-01
GPS	C10:2	35%	-0.051 (-0.216 to 0.114)	5.462E-01
GPS	C10:2	45%	-0.102 (-0.237 to 0.033)	1.382E-01
GPS	C10:2	full data	-0.089 (-0.143 to -0.035)	1.337E-03
GPS	C12	5%	-0.435 (-1.039 to 0.17)	1.548E-01
GPS	C12	15%	-0.325 (-0.609 to -0.042)	2.479E-02
GPS	C12	25%	-0.218 (-0.419 to -0.016)	3.434E-02
GPS	C12	35%	-0.153 (-0.311 to 0.006)	5.892E-02
GPS	C12	45%	-0.158 (-0.286 to -0.031)	1.515E-02
GPS	C12	full data	-0.08 (-0.131 to -0.03)	1.939E-03
GPS	C14:1-OH	5%	0.036 (-0.55 to 0.622)	9.027E-01
GPS	C14:1-OH	15%	-0.137 (-0.422 to 0.149)	3.453E-01
GPS	C14:1-OH	25%	-0.075 (-0.272 to 0.122)	4.540E-01
GPS	C14:1-OH	35%	-0.074 (-0.232 to 0.084)	3.581E-01
GPS	C14:1-OH	45%	-0.115 (-0.243 to 0.012)	7.572E-02
GPS	C14:1-OH	full data	-0.069 (-0.122 to -0.016)	1.042E-02
GPS	C8	5%	-0.61 (-1.239 to 0.02)	5.731E-02
GPS	C8	15%	-0.124 (-0.44 to 0.191)	4.385E-01
GPS	C8	25%	-0.104 (-0.323 to 0.115)	3.529E-01
GPS	C8	35%	-0.1 (-0.265 to 0.065)	2.344E-01
GPS	C8	45%	-0.124 (-0.255 to 0.006)	6.156E-02
GPS	C8	full data	-0.08 (-0.132 to -0.027)	2.911E-03
GPS	CST3	5%	0.097 (-1.109 to 1.302)	8.640E-01
GPS	CST3	15%	-0.252 (-0.643 to 0.138)	2.015E-01
GPS	CST3	25%	-0.212 (-0.472 to 0.048)	1.091E-01
GPS	CST3	35%	-0.017 (-0.248 to 0.214)	8.841E-01
GPS	CST3	45%	-0.129 (-0.326 to 0.068)	1.974E-01
GPS	CST3	full data	-0.144 (-0.221 to -0.067)	2.533E-04
GPS	TNFRSF1A	5%	-1.972 (-3.283 to -0.662)	6.579E-03
GPS	TNFRSF1A	15%	-0.538 (-1.069 to -0.006)	4.744E-02

GPS	TNFRSF1A	25%	-0.316 (-0.637 to 0.005)	5.345E-02
GPS	TNFRSF1A	35%	-0.091 (-0.34 to 0.159)	4.753E-01
GPS	TNFRSF1A	45%	-0.165 (-0.384 to 0.055)	1.411E-01
GPS	TNFRSF1A	full data	-0.144 (-0.231 to -0.057)	1.176E-03
GPS	IGFBP6	5%	0.158 (-1.074 to 1.391)	7.845E-01
GPS	IGFBP6	15%	-0.14 (-0.615 to 0.335)	5.576E-01
GPS	IGFBP6	25%	-0.198 (-0.49 to 0.095)	1.829E-01
GPS	IGFBP6	35%	-0.083 (-0.314 to 0.148)	4.786E-01
GPS	IGFBP6	45%	-0.132 (-0.321 to 0.056)	1.685E-01
GPS	IGFBP6	full data	-0.1 (-0.178 to -0.023)	1.089E-02
GPS	NBL1	5%	-0.849 (-2.23 to 0.531)	2.049E-01
GPS	NBL1	15%	-0.095 (-0.578 to 0.388)	6.954E-01
GPS	NBL1	25%	-0.259 (-0.574 to 0.057)	1.073E-01
GPS	NBL1	35%	-0.118 (-0.364 to 0.129)	3.472E-01
GPS	NBL1	45%	-0.218 (-0.425 to -0.011)	3.920E-02
GPS	NBL1	full data	-0.149 (-0.235 to -0.062)	7.709E-04
GPS	JAM2	5%	-1.036 (-2.235 to 0.163)	8.423E-02
GPS	JAM2	15%	-0.326 (-0.816 to 0.164)	1.885E-01
GPS	JAM2	25%	-0.447 (-0.813 to -0.08)	1.753E-02
GPS	JAM2	35%	-0.373 (-0.659 to -0.086)	1.121E-02
GPS	JAM2	45%	-0.408 (-0.656 to -0.16)	1.358E-03
GPS	JAM2	full data	-0.152 (-0.245 to -0.059)	1.350E-03
GPS	RETN	5%	-0.888 (-2.15 to 0.373)	1.509E-01
GPS	RETN	15%	-0.186 (-0.656 to 0.284)	4.325E-01
GPS	RETN	25%	-0.072 (-0.408 to 0.265)	6.739E-01
GPS	RETN	35%	-0.121 (-0.384 to 0.142)	3.648E-01
GPS	RETN	45%	-0.127 (-0.35 to 0.096)	2.620E-01
GPS	RETN	full data	-0.124 (-0.214 to -0.034)	7.090E-03
GPS	ADAMTS13	5%	1.125 (-0.4 to 2.65)	1.340E-01
GPS	ADAMTS13	15%	0.001 (-0.564 to 0.565)	9.983E-01
GPS	ADAMTS13	25%	0.119 (-0.233 to 0.471)	5.034E-01
GPS	ADAMTS13	35%	0.169 (-0.09 to 0.429)	1.991E-01
GPS	ADAMTS13	45%	0.021 (-0.199 to 0.241)	8.492E-01
GPS	ADAMTS13	full data	0.143 (0.055 to 0.23)	1.520E-03
GPS	FSTL3	5%	-1.18 (-2.155 to -0.206)	2.164E-02
GPS	FSTL3	15%	-0.273 (-0.76 to 0.214)	2.666E-01
GPS	FSTL3	25%	-0.337 (-0.653 to -0.022)	3.646E-02
GPS	FSTL3	35%	-0.199 (-0.444 to 0.046)	1.105E-01
GPS	FSTL3	45%	-0.206 (-0.421 to 0.008)	5.960E-02
GPS	FSTL3	full data	-0.107 (-0.192 to -0.022)	1.395E-02
GPS	B2M	5%	-0.798 (-2.04 to 0.443)	1.864E-01
GPS	B2M	15%	-0.246 (-0.706 to 0.214)	2.891E-01
GPS	B2M	25%	-0.148 (-0.448 to 0.152)	3.306E-01
GPS	B2M	35%	0.072 (-0.179 to 0.324)	5.707E-01
GPS	B2M	45%	-0.092 (-0.309 to 0.125)	4.042E-01

GPS	B2M	full data	-0.116 (-0.201 to -0.032)	7.033E-03
GPS	ERP29	5%	-0.689 (-2.255 to 0.877)	3.566E-01
GPS	ERP29	15%	-0.007 (-0.516 to 0.502)	9.776E-01
GPS	ERP29	25%	-0.172 (-0.493 to 0.148)	2.886E-01
GPS	ERP29	35%	-0.15 (-0.388 to 0.088)	2.152E-01
GPS	ERP29	45%	-0.218 (-0.409 to -0.028)	2.484E-02
GPS	ERP29	full data	-0.101 (-0.18 to -0.022)	1.277E-02
GPS	RELT	5%	-0.278 (-1.081 to 0.525)	4.653E-01
GPS	RELT	15%	-0.008 (-0.477 to 0.46)	9.712E-01
GPS	RELT	25%	-0.151 (-0.465 to 0.163)	3.427E-01
GPS	RELT	35%	-0.073 (-0.322 to 0.176)	5.640E-01
GPS	RELT	45%	-0.163 (-0.381 to 0.055)	1.423E-01
GPS	RELT	full data	-0.151 (-0.234 to -0.068)	4.048E-04
GPS	SCARF1	5%	-0.15 (-1.57 to 1.271)	8.223E-01
GPS	SCARF1	15%	-0.109 (-0.557 to 0.338)	6.266E-01
GPS	SCARF1	25%	0.141 (-0.182 to 0.464)	3.894E-01
GPS	SCARF1	35%	-0.08 (-0.327 to 0.168)	5.263E-01
GPS	SCARF1	45%	-0.185 (-0.399 to 0.029)	9.024E-02
GPS	SCARF1	full data	-0.127 (-0.22 to -0.034)	7.578E-03
GPS	SPOCK2	5%	0.887 (-0.507 to 2.28)	1.907E-01
GPS	SPOCK2	15%	0.396 (-0.107 to 0.9)	1.207E-01
GPS	SPOCK2	25%	0.145 (-0.165 to 0.456)	3.553E-01
GPS	SPOCK2	35%	0.132 (-0.121 to 0.385)	3.033E-01
GPS	SPOCK2	45%	0.206 (-0.014 to 0.425)	6.587E-02
GPS	SPOCK2	full data	0.16 (0.071 to 0.249)	4.352E-04

Supplementary Table 24. Two-sample MR evidence is suggestive of relationships between kidney traits (CKD, eGFR and UACR) and replicated proteins in both directions.

Results of bi-directional two-sample MR of 46 replicated proteins and kidney traits (CKD, eGFR and UACR).

Abbreviations: CKD, chronic kidney disease; eGFR, estimated glomerular filtration rate; UACR, urinary albumin-to-creatinine ratio; MR, Mendelian Randomization.

TNFRSF1A	265 -19,1	UACR	Robust adjusted profile score (RAPS) out-liers-corrected In erse variance weighted	Protein To UACR	San 2018	Teuner 2019	7	-0.013	0.007	5.778E-02	237E-01	0 7E-01	137E-01	3.335E-01	0.33		before	no / insufficient power	UACR To Protein	San 2018	Teuner 2019	27	-0.13	0.31	6.79E-01	6.79E-01								fler	no / insufficient power
TNFRSF1A	265 -19,1	UACR	Robust adjusted profile score (RAPS)	Protein To UACR	San 2018	Teuner 2019	7	-0.013	0.007	5.778E-02	237E-01	0 7E-01	137E-01	3.335E-01	0.33		before	no / insufficient power	UACR To Protein	San 2018	Teuner 2019	29	-0.168	0.32	5.990E-01	6.07 E-01	.56E-02	.197E-02	.58E-01	0.0 6	2		efore	no / insufficient power	
EGFR	2677-1,1	CKD	Robust adjusted profile score (RAPS)	Protein To CKD	San 2018	Wanke 2019	2	0.0 7	0.06	.335E-01	8 670E-01	6.092E-02					before	no / insufficient power	CKD To Protein	San 2018	Wanke 2019	16	-0.00	0.1	9.677E-01	9.677E-01	.807E-01	7.23 E-01	6.295E-02	0. 77			efore	no / insufficient power	
EGFR	2677-1,1	eGFR	Robust adjusted profile score (RAPS) out-liers-corrected In erse variance weighted	Protein To eGFR	San 2018	Wanke 2019	2	-0.002	0.002	.688E-01	8 250E-01	1.33 E-01					before	no / insufficient power	eGFR To Protein	San 2018	Wanke 2019	178	0.2 6	0.669	7.132E-01	7.132E-01								fler	no / insufficient power
EGFR	2677-1,1	eGFR	Robust adjusted profile score (RAPS)	Protein To eGFR	San 2018	Wanke 2019	2	-0.002	0.002	.688E-01	8 250E-01	1.33 E-01					before	no / insufficient power	eGFR To Protein	San 2018	Wanke 2019	193	0.2 2	0.671	7.187E-01	9.582E-01	7.805E-03	7.783E-03	3.519E-01	0.013		No signficant outliers	efore	no / insufficient power	
EGFR	2677-1,1	UACR	Robust adjusted profile score (RAPS)	Protein To UACR	San 2018	Teuner 2019	2	-0.032	0.012	1.113E-02	2 288E-01	3.921E-01					before	no / insufficient power	UACR To Protein	San 2018	Teuner 2019	29	-0.166	0.32	6.0 6E-01	9.582E-01	3.755E-01	3.561E-01	. 5 E-01	0.387			efore	no / insufficient power	
IGFBP6	2686-67,2	CKD	Robust adjusted profile score (RAPS) out-liers-corrected Wald ratio	Protein To CKD	San 2018	Wanke 2019	1	-0.076	0.068	2.670E-01	. 95E-01						after	no / insufficient power																	
IGFBP6	2686-67,2	CKD	Robust adjusted profile score (RAPS)	Protein To CKD	San 2018	Wanke 2019	3	-1.012	0. 29	1.823E-02	2 907E-01	2.522E-0	8 550E-02	2.777E-01			before	no / insufficient power	CKD To Protein	San 2018	Wanke 2019	16	0.155	0.1	1.208E-01	1.7 8E-01	5. 38E-01	6.912E-01	1.1 9E-01	0.597			efore	no / insufficient power	
IGFBP6	2686-67,2	eGFR	Robust adjusted profile score (RAPS) out-liers-corrected Wald ratio	Protein To eGFR	San 2018	Wanke 2019	1	-0.001	0.003	7.83 E-01	9 239E-01						after	no / insufficient power																	
IGFBP6	2686-67,2	eGFR	Robust adjusted profile score (RAPS)	Protein To eGFR	San 2018	Wanke 2019	3	-0.03	0.005	1.5 6E-10	6 803E-09	5.358E-19	1 137E-01	1.103E-01			before	no / insufficient power	eGFR To Protein	San 2018	Wanke 2019	193	-3.75	0.671	2.2 2E-08	8.969E-08	5.962E-02	5.39 E-02	9.98 E-01	0.063			efore	yes same drection of beta in KORA	
IGFBP6	2686-67,2	UACR	Robust adjusted profile score (RAPS) out-liers-corrected In erse variance weighted	Protein To UACR	San 2018	Teuner 2019	26	-0.316	0.338	3. 96E-01								no / insufficient power	UACR To Protein	San 2018	Teuner 2019	26	-0.316	0.338	3. 96E-01	3. 96E-01								fler	no / insufficient power
IGFBP6	2686-67,2	UACR	Robust adjusted profile score (RAPS)	Protein To UACR	San 2018	Teuner 2019	3	-0.003	0.011	8.0 3E-01	8 8 8E-01	2.007E-01	5 908E-01	3.369E-01			before	no / insufficient power	UACR To Protein	San 2018	Teuner 2019	29	-0.3 9	0.322	2.799E-01	2.799E-01	5. 50E-02	.06E-02	6.955E-01	0.06			efore	no / insufficient power	
FGF20	2763-66,2	CKD	Robust adjusted profile score (RAPS) MR-PRESSO_Outlier corrected	Protein To CKD	San 2018	Wanke 2019	5	-0.088	0.0	2.588E-02	2 907E-01	6.657E-01	9 029E-01	2.710E-01	0.685		before	no / insufficient power	CKD To Protein	San 2018	Wanke 2019	16	-0.112	0.1	2.603E-01	3. 71E-01	5. 79E-01	5.87 E-01	2. 53E-01	0.559			efore	no / insufficient power	
FGF20	2763-66,2	eGFR	Robust adjusted profile score (RAPS) out-liers-corrected In erse variance weighted	Protein To eGFR	San 2018	Wanke 2019	5										before	no / insufficient power	eGFR To Protein	San 2018	Wanke 2019	192	1.512	0.726	3.86 E-02	5.317E-01				0.001	1		efore	no / insufficient power	
FGF20	2763-66,2	eGFR	Robust adjusted profile score (RAPS)	Protein To eGFR	San 2018	Wanke 2019	5	0.002	0.001	1. 9E-01	250E-01	1.516E-01	1 222E-01	5.387E-01	0.237		before	no / insufficient power	eGFR To Protein	San 2018	Wanke 2019	171	0.706	0.678	2.972E-01	2.972E-01							fler	no / insufficient power	
FGF20	2763-66,2	eGFR	Robust adjusted profile score (RAPS)	Protein To eGFR	San 2018	Wanke 2019	5	0.002	0.001	1. 9E-01	250E-01	1.516E-01	1 222E-01	5.387E-01	0.237		before	no / insufficient power	eGFR To Protein	San 2018	Wanke 2019	193	1.161	0.671	8.375E-02	3.116E-01	1.088E-03	1.185E-03	2.35 E-01	0.001	1		efore	no / insufficient power	
FGF20	2763-66,2	UACR	Robust adjusted profile score (RAPS)	Protein To UACR	San 2018	Teuner 2019	5	0.009	0.008	2.155E-01	613E-01	3. 7 E-01	2. 33E-01	6.809E-01	0. 3		before	no / insufficient power	UACR To Protein	San 2018	Teuner 2019	29	-0.2 3	0.32	. 77E-01	. 77E-01	2.15E-01	.098E-01	3.873E-01	0. 8			efore	no / insufficient power	
FGF9	276 -20,2	CKD	Robust adjusted profile score (RAPS)	Protein To CKD	San 2018	Wanke 2019	3	-0.018	0.055	7. 77E-01	9. 00E-01	2.51 E-01	6.708E-01	3.5 5E-01			before	no / insufficient power	CKD To Protein	San 2018	Wanke 2019	16	-0.019	0.101	8.511E-01	8.511E-01	1.231E-01	1.371E-01	2.963E-01	0.12			efore	no / insufficient power	
FGF9	276 -20,2	eGFR	Robust adjusted profile score (RAPS)	Protein To eGFR	San 2018	Wanke 2019	3	0	0.002	9.801E-01	9 836E-01	5.291E-02	7 838E-02	5.172E-01			before	no / insufficient power	eGFR To Protein	San 2018	Wanke 2019	193	0. 97	0.67	.582E-01	8.511E-01	1.220E-01	1.858E-01	1.387E-02	0.13			efore	no / insufficient power	
FGF9	276 -20,2	UACR	Robust adjusted profile score (RAPS) out-liers-corrected In erse variance weighted	Protein To UACR	San 2018	Teuner 2019	25	-0.306	0.32	3.392E-01								no / insufficient power	UACR To Protein	San 2018	Teuner 2019	25	-0.306	0.32	3.392E-01	3.392E-01								fler	no / insufficient power
FGF9	276 -20,2	UACR	Robust adjusted profile score (RAPS)	Protein To UACR	San 2018	Teuner 2019	2	-0.011	0.013	3.882E-01	6 162E-01	5.2 7E-01					before	no / insufficient power	UACR To Protein	San 2018	Teuner 2019	29	-0.1 9	0.322	6. 31E-01	8.511E-01	1.635E-02	1.37 E-02	5.6 3E-01	0.016		No signficant outliers	efore	no / insufficient power	
NBL1	29 -66,2	CKD	Robust adjusted profile score (RAPS)	Protein To CKD	San 2018	Wanke 2019	2	-0.02	0.05	7.065E-01	9. 00E-01	.315E-01					before	no / insufficient power	CKD To Protein	San 2018	Wanke 2019	16	0.105	0.099	2.925E-01	5.8 9E-01	9.236E-01	9.016E-01	6.26 E-01	0.92			efore	no / insufficient power	
NBL1	29 -66,2	eGFR	Robust adjusted profile score (RAPS)	Protein To eGFR	San 2018	Wanke 2019	2	0	0.002	8.778E-01	9 656E-01	7.562E-01					before	no / insufficient power	eGFR To Protein	San 2018	Wanke 2019	193	-1.072	0.667	1.083E-01	331E-01	9.701E-01	9.680E-01	5.3 5E-01	0.973			efore	no / insufficient power	
NBL1	29 -66,2	UACR	Robust adjusted profile score (RAPS)	Protein To UACR	San 2018	Teuner 2019	2	0.005	0.012	6.81 E-01	8 039E-01	8.392E-02					before	no / insufficient power	UACR To Protein	San 2018	Teuner 2019	29	0.006	0.32	9.8 1E-01	9.8 1E-01	3.1 1E-01	2.951E-01	.591E-01	0.318			efore	no / insufficient power	
GHR	29 8-58,2	CKD	Robust adjusted profile score (RAPS)	Protein To CKD	San 2018	Wanke 2019	5	0.028	0.038	.70 E-01	9 000E-01	3.355E-01	2 830E-01	.97 E-01	0.36		before	no / insufficient power	CKD To Protein	San 2018	Wanke 2019	16	-0.05	0.1	5.922E-01	9.393E-01	3.167E-01	5.362E-01	6.075E-02	0.327			efore	no / insufficient power	
GHR	29 8-58,2	eGFR	Robust adjusted profile score (RAPS)	Protein To eGFR	San 2018	Wanke 2019	5	-0.002	0.001	1.328E-01	173E-01	9. 71E-01	8 839E-01	7.96 E-01	0.938		before	no / insufficient power	eGFR To Protein	San 2018	Wanke 2019	193	-0.215	0.669	7. 79E-01	9.393E-01	.077E-01	3.908E-01	7.065E-01	0. 5			efore	no / insufficient power	
GHR	29 8-58,2	UACR	Robust adjusted profile score (RAPS) out-liers-corrected Wald ratio	Protein To UACR	San 2018	Teuner 2019	5	0.009	0.008	2. 19E-01	627E-01	5.953E-01	8 502E-01	2.538E-01	0.632		before	no / insufficient power	UACR To Protein	San 2018	Teuner 2019	29	0.02	0.318	9.393E-01	9.393E-01	7.656E-01	7.591E-01	3.881E-01	0.8			efore	no / insufficient power	
CGALHB	2953-31,2	CKD	Robust adjusted profile score (RAPS) out-liers-corrected Wald ratio	Protein To CKD	San 2018	Wanke 2019	1	-0.057	0.02	1.668E-02	8 339E-02						after	no / insufficient power																	
CGALHB	2953-31,2	CKD	Robust adjusted profile score (RAPS)	Protein To CKD	San 2018	Wanke 2019	2	-0.0 8	0.02	.572E-02	2 907E-01	1.676E-02					before	no / insufficient power	CKD To Protein	San 2018	Wanke 2019	16	-0.073	0.099	.660E-01	8. 2E-01	8.028E-01	8.18 E-01	3.185E-01	0.821			efore	no / insufficient power	

ADAMT3	3175-51_5	UACR	Robust adjusted profile score (RAPS)	Protein To UACR	Sun 2018	Teuner 2019			0.001	0.003	.05 E-01	8.039E-01	314E-01	3.061E-01	6.266E-01	0.521								before	no / insufficient power	UACR To Protein	Sun 2018	Teuner 2019	29	0.15	0.319 6.387E-01	6.387E-01	5.05E-01	5.091E-01	5.21 E-01	0.559			before	no / insufficient power	
RET	3220_0_2	CKD	Robust adjusted profile score (RAPS)	Protein To CKD	Sun 2018	Wanke 2019	3	0.05	0.033	.787E-01	5.701E-01	5.68E-01	2.720E-01	9.87E-01									before	no / insufficient power	CKD To Protein	Sun 2018	Wanke 2019	16	-0.128	0.101 2.03E-01	6.971E-01	1.331E-01	1.218E-01	.573E-01	0.135			before	no / insufficient power		
RET	3220_0_2	eGFR	Robust adjusted profile score (RAPS)	Protein To eGFR	Sun 2018	Wanke 2019	3	0	0.001	.836E-01	9.836E-01	8.363E-01	5.523E-01	9.575E-01									before	no / insufficient power	eGFR To Protein	Sun 2018	Wanke 2019	193	-0.606	0.668 3.61E-01	6.971E-01	7.86E-01	7.367E-01	5.959E-01	0.755			before	no / insufficient power		
RET	3220_0_2	UACR	Robust adjusted profile score (RAPS)	Protein To UACR	Sun 2018	Teuner 2019	3	0.002	0.007	.275E-01	8.881E-01	8.322E-01	5.56E-01	9.16E-01									before	no / insufficient power	UACR To Protein	Sun 2018	Teuner 2019	29	-0.1	0.32 7.538E-01	7.538E-01	2.296E-01	1.08E-01	3.11E-02	0.226			before	no / insufficient power		
ACY1	33_3-1_	CKD	Robust adjusted profile score (RAPS)	Protein To CKD	Sun 2018	Wanke 2019	3	0	0.001	.836E-01	9.836E-01	8.363E-01	5.523E-01	9.575E-01									before	no / insufficient power	CKD To Protein	Sun 2018	Wanke 2019	16	-0.128	0.101 2.03E-01	6.971E-01	1.331E-01	1.218E-01	.573E-01	0.135			before	no / insufficient power		
ACY1	33_3-1_	eGFR	MR-PRESSO_Outlier corrected	Protein To eGFR	Sun 2018	Wanke 2019	3	0	0.001	.836E-01	9.836E-01	8.363E-01	5.523E-01	9.575E-01									before	no / insufficient power	eGFR To Protein	Sun 2018	Wanke 2019	193	-0.606	0.668 3.61E-01	6.971E-01	7.86E-01	7.367E-01	5.959E-01	0.755			before	no / insufficient power		
ACY1	33_3-1_	eGFR	outliers-corrected In esse variance weighted	Protein To eGFR	Sun 2018	Wanke 2019	3	0	0.001	.836E-01	9.836E-01	8.363E-01	5.523E-01	9.575E-01									after	no / insufficient power	eGFR To Protein	Sun 2018	Wanke 2019	193	-0.606	0.668 3.61E-01	6.971E-01	7.86E-01	7.367E-01	5.959E-01	0.755			before	no / insufficient power		
ACY1	33_3-1_	eGFR	Robust adjusted profile score (RAPS)	Protein To eGFR	Sun 2018	Wanke 2019	3	0	0.001	.836E-01	9.836E-01	8.363E-01	5.523E-01	9.575E-01									before	no / insufficient power	eGFR To Protein	Sun 2018	Wanke 2019	193	-0.606	0.668 3.61E-01	6.971E-01	7.86E-01	7.367E-01	5.959E-01	0.755			before	no / insufficient power		
ACY1	33_3-1_	UACR	Robust adjusted profile score (RAPS)	Protein To UACR	Sun 2018	Teuner 2019	3	0.005	0.008	.556E-01	7.117E-01	5.73E-01	3.58E-01	5.91E-01	0.53									before	no / insufficient power	UACR To Protein	Sun 2018	Teuner 2019	29	0.39	0.319 2.733E-01	5.67E-01	8.20E-01	7.938E-01	6.618E-01	0.836			before	no / insufficient power	
CTSV	336_-76_2	CKD	Robust adjusted profile score (RAPS)	Protein To CKD	Sun 2018	Wanke 2019	3	-0.07	0.037	.073E-01	5.701E-01	9.79E-01	6.652E-01	3.378E-01	0.52								before	no / insufficient power	CKD To Protein	Sun 2018	Wanke 2019	16	0.065	0.15 1.83E-01	6.911E-01	2.23E-01	3.792E-01	5.379E-01	0.27			before	no / insufficient power		
CTSV	336_-76_2	eGFR	MR-PRESSO_Outlier corrected	Protein To eGFR	Sun 2018	Wanke 2019	3	0	0.001	.836E-01	9.836E-01	8.363E-01	5.523E-01	9.575E-01									before	no / insufficient power	eGFR To Protein	Sun 2018	Wanke 2019	192	1.077	0.731 1.2E-01	6.196E-01					-0.001	1			before	no / insufficient power
CTSV	336_-76_2	eGFR	outliers-corrected In esse variance weighted	Protein To eGFR	Sun 2018	Wanke 2019	3	0	0.001	.836E-01	9.836E-01	8.363E-01	5.523E-01	9.575E-01									after	no / insufficient power	eGFR To Protein	Sun 2018	Wanke 2019	176	1.509	0.663 2.282E-02	2.282E-02									after	no / insufficient power
CTSV	336_-76_2	eGFR	Robust adjusted profile score (RAPS)	Protein To eGFR	Sun 2018	Wanke 2019	3	0	0.001	.50 E-01	8.92 E-01	8.379E-01	6.885E-01	7.802E-01	0.878								before	no / insufficient power	eGFR To Protein	Sun 2018	Wanke 2019	193	1.265	0.791 1.096E-01	.38E-01	8.563E-01	7.52 E-01	6.627E-01	-0.001	1			before	no / insufficient power	
CTSV	336_-76_2	UACR	Robust adjusted profile score (RAPS)	Protein To UACR	Sun 2018	Teuner 2019	3	0.005	0.008	.556E-01	7.117E-01	5.73E-01	3.58E-01	5.91E-01	0.53									before	no / insufficient power	UACR To Protein	Sun 2018	Teuner 2019	29	0.39	0.319 2.733E-01	5.67E-01	8.20E-01	7.938E-01	6.618E-01	0.836			before	no / insufficient power	
FSTL3	3_38-10_2	CKD	Robust adjusted profile score (RAPS)	Protein To CKD	Sun 2018	Wanke 2019	3	-0.018	0.06	.008E-01	9.00E-01	2.510E-01	9.96 E-01	3.7E-01									before	no / insufficient power	CKD To Protein	Sun 2018	Wanke 2019	16	-0.019	0.18 8.80E-01	9.380E-01	6.319E-01	5.75 E-01	6.381E-01	0.659			before	no / insufficient power		
FSTL3	3_38-10_2	eGFR	Robust adjusted profile score (RAPS)	Protein To eGFR	Sun 2018	Wanke 2019	3	-0.001	0.002	.163E-01	7.632E-01	.793E-01	2.73E-01	7.19E-01									before	no / insufficient power	eGFR To Protein	Sun 2018	Wanke 2019	193	-2.009	0.669 2.683E-03	1.073E-02	5.55E-01	.28E-01	.958E-01	0.56			before	yes same direction of beta in KORA		
FSTL3	3_38-10_2	UACR	Robust adjusted profile score (RAPS)	Protein To UACR	Sun 2018	Teuner 2019	3	-0.005	0.01	.919E-01	7.235E-01	9.00E-02	9.261E-01	2.72 E-01									before	no / insufficient power	UACR To Protein	Sun 2018	Teuner 2019	29	0.025	0.321 9.380E-01	9.380E-01	3.593E-01	3.195E-01	6.729E-01	0.39			before	no / insufficient power		
B2M	3_85-28_2	CKD	Robust adjusted profile score (RAPS)	Protein To CKD	Sun 2018	Wanke 2019	3	0	0.001	.836E-01	9.836E-01	8.363E-01	5.523E-01	9.575E-01									before	no / insufficient power	CKD To Protein	Sun 2018	Wanke 2019	16	-0.128	0.101 2.03E-01	6.971E-01	1.331E-01	1.218E-01	.573E-01	0.135			before	no / insufficient power		
B2M	3_85-28_2	eGFR	Robust adjusted profile score (RAPS)	Protein To eGFR	Sun 2018	Wanke 2019	3	0	0.001	.836E-01	9.836E-01	8.363E-01	5.523E-01	9.575E-01									before	no / insufficient power	eGFR To Protein	Sun 2018	Wanke 2019	193	-0.803	1.9 1.6793E-01	9.753E-01	8.171E-01	7.929E-01	8.19 E-01	0.828			before	no / insufficient power		
B2M	3_85-28_2	UACR	Robust adjusted profile score (RAPS)	Protein To UACR	Sun 2018	Teuner 2019	3	0.005	0.008	.556E-01	7.117E-01	5.73E-01	3.58E-01	5.91E-01	0.53								before	no / insufficient power	UACR To Protein	Sun 2018	Teuner 2019	29	0.39	0.319 2.733E-01	5.67E-01	8.20E-01	7.938E-01	6.618E-01	0.836			before	no / insufficient power		
MASPI	3605-77_	CKD	Robust adjusted profile score (RAPS)	Protein To CKD	Sun 2018	Wanke 2019	2	-0.061	0.059	.963E-01	6.901E-01	1.853E-02											before	no / insufficient power	CKD To Protein	Sun 2018	Wanke 2019	16	-0.12	0.12 3.25E-01	6.233E-01	.75 E-01	1.35E-01	6.870E-01	0.76			before	no / insufficient power		
MASPI	3605-77_	eGFR	MR-PRESSO_Outlier corrected	Protein To eGFR	Sun 2018	Wanke 2019	2	0	0.001	.836E-01	9.836E-01	8.363E-01	5.523E-01	9.575E-01									before	no / insufficient power	eGFR To Protein	Sun 2018	Wanke 2019	192	0.803	0.71 2.59 E-01	9.621E-01					0.006	1			before	no / insufficient power
MASPI	3605-77_	eGFR	outliers-corrected In esse variance weighted	Protein To eGFR	Sun 2018	Wanke 2019	2	0	0.001	.836E-01	9.836E-01	8.363E-01	5.523E-01	9.575E-01									after	no / insufficient power	eGFR To Protein	Sun 2018	Wanke 2019	177	-0.093	0.672 8.90 E-01	8.90 E-01									after	no / insufficient power
MASPI	3605-77_	eGFR	Robust adjusted profile score (RAPS)	Protein To eGFR	Sun 2018	Wanke 2019	2	0.003	0.002	.170E-02	3.380E-01	6.37E-01												before	no / insufficient power	eGFR To Protein	Sun 2018	Wanke 2019	193	0.508	0.7 7.966E-01	6.233E-01	5.233E-03	.676E-03	6.699E-01	0.006	1			before	no / insufficient power
MASPI	3605-77_	UACR	outliers-corrected In esse variance weighted	Protein To UACR	Sun 2018	Teuner 2019	2	-0.002	0.012	.725E-01	9.10E-01	3.23 E-01											after	no / insufficient power	UACR To Protein	Sun 2018	Teuner 2019	25	0.201	0.32 5.36E-01	8.90 E-01									after	no / insufficient power
MASPI	3605-77_	UACR	Robust adjusted profile score (RAPS)	Protein To UACR	Sun 2018	Teuner 2019	2	-0.002	0.012	.725E-01	9.10E-01	3.23 E-01											before	no / insufficient power	UACR To Protein	Sun 2018	Teuner 2019	29	0.162	0.322 6.12E-01	6.233E-01	1.582E-02	1.698E-02	3.37 E-01	0.019		No significant outliers	before	no / insufficient power		
KDR	3651-50_5	CKD	Robust adjusted profile score (RAPS)	Protein To CKD	Sun 2018	Wanke 2019	8	-0.001	0.01	.283E-01	9.706E-01	1.20E-01	3.572E-01	5.099E-01	0.356								before	no / insufficient power	CKD To Protein	Sun 2018	Wanke 2019	16	0.03	0.1 7.632E-01	9.19 E-01	5.56E-01	3.869E-01	8.028E-01	0.56			before	no / insufficient power		
KDR	3651-50_5	eGFR	outliers-corrected In esse variance weighted	Protein To eGFR	Sun 2018	Wanke 2019	7	0	0.001	.33E-01	9.33E-01												after	no / insufficient power	eGFR To Protein	Sun 2018	Wanke 2019	193	0.872	0.669 1.925E-01	7.700E-01	9.79E-01	9.38E-01	3.719E-01	0.518			before	no / insufficient power		
KDR	3651-50_5	eGFR	Robust adjusted profile score (RAPS)	Protein To eGFR	Sun 2018	Wanke 2019	8	0	0.001	.706E-01	9.836E-01	3.378E-02	2.052E-02	7.806E-01	0.11								before	no / insufficient power	eGFR To Protein	Sun 2018	Wanke 2019	193	0.872	0.669 1.925E-01	7.700E-01	9.79E-01	9.38E-01	3.719E-01	0.518			before	no / insufficient power		

EPHA2	83 -61_2	UACR	Robust adjusted profile score (RAPS)	Protein To UACR	Sun 2018	Teumer 2019											0.006	0.008	662E-01	6.838E-01	5.885E-01	3.879E-01	8.805E-01	0.612					before	no / insufficient power	UACR To Protein	Sun 2018	Teumer 2019	29	0.003	0.32	9.918E-01	9.918E-01	2.0	1E-01	1.707E-01	8.276E-01	0.216			before	no / insufficient power		
NTRK2	866-59_2	CKD	Robust adjusted profile score (RAPS)	Protein To CKD	Sun 2018	Wanke 2019	1	-0.017	0.092	9.96E-01	9.706E-01																			before	no / insufficient power	CKD To Protein	Sun 2018	Wanke 2019	16	-0.177	0.1	7.625E-02	3.050E-01	6.2	E-01	5.802E-01	5.33E-01	0.629			before	no / insufficient power	
NTRK2	866-59_2	eGFR	Robust adjusted profile score (RAPS)	Protein To eGFR	Sun 2018	Wanke 2019	1	-0.002	0.003	1.3E-01	8.381E-01																			before	no / insufficient power	eGFR To Protein	Sun 2018	Wanke 2019	193	0.878	0.67	1.896E-01	3.791E-01	1.35E-01	1.35	E-01	6.07	E-01	0.13			before	no / insufficient power
NTRK2	866-59_2	UACR	Robust adjusted profile score (RAPS)	Protein To UACR	Sun 2018	Teumer 2019	1	-0.016	0.017	5.18E-01	6.161E-01																			before	no / insufficient power	UACR To Protein	Sun 2018	Teumer 2019	29	-0.038	0.321	9.059E-01	9.059E-01	1.230E-01	1.21	E-01	3.726E-01	0.138			before	no / insufficient power	
AMH	923-79_1	CKD	Robust adjusted profile score (RAPS)	Protein To CKD	Sun 2018	Wanke 2019		-0.023	0.03	9.91E-01	9.150E-01	5.33E-01	3.366E-01	9.187E-01	0.559															before	no / insufficient power	CKD To Protein	Sun 2018	Wanke 2019	16	-0.063	0.1	5.25	E-01	7.006E-01	7.380E-01	6.733E-01	8.395E-01	0.735			before	no / insufficient power	
AMH	923-79_1	eGFR	Robust adjusted profile score (RAPS)	Protein To eGFR	Sun 2018	Wanke 2019		-0.001	0.001	2.78E-01	8.381E-01	1.236E-01	1.556E-01	0.5E-01	0.25															before	no / insufficient power	eGFR To Protein	Sun 2018	Wanke 2019	193	-0.566	0.668	3.973E-01	7.006E-01	7.823E-01	7.970E-01	1.69	E-01	0.78			before	no / insufficient power	
AMH	923-79_1	UACR	Robust adjusted profile score (RAPS)	Protein To UACR	Sun 2018	Teumer 2019		-0.006	0.008	0.62E-01	6.162E-01	3.90E-01	5.525E-01	2.8	0E-01	0.35														before	no / insufficient power	UACR To Protein	Sun 2018	Teumer 2019	29	0.2	5	0.32	3.1E-01	7.006E-01	5.065E-01	6.89E-01	5.819E-01	0.505			before	no / insufficient power	
MMP1	92 -32_1	CKD	Robust adjusted profile score (RAPS)	Protein To CKD	Emilsson 2018	Wanke 2019	1	0.01	0.018	2.28E-01	8.670E-01																		before	no / insufficient power	CKD To Protein	Salze 2017	Wanke 2019	8	0.6	1	0.251	1.061E-02	2.122E-02	5.98	E-01	5.095E-01	6.53E-01	0.612			before	yes same direction of beta in KORA	
MMP1	92 -32_1	eGFR	Robust adjusted profile score (RAPS)	Protein To eGFR	Emilsson 2018	Wanke 2019	1	0	0.001	0.76E-01	8.381E-01																		before	no / insufficient power	eGFR To Protein	Salze 2017	Wanke 2019	63	-3.223	2.103	1.25	E-01	1.369E-01	6.179E-01	5.826E-01	9.628E-01	0.61			before	no / insufficient power		
MMP1	92 -32_1	UACR	MIR PRESSO_Outlier corrected																										before	no / insufficient power	UACR To Protein	Salze 2017	Teumer 2019	7	153	1.6	2.970E-02	1.230E-01					0.031	1		before	no / insufficient power		
MMP1	92 -32_1	UACR	outliers-corrected in one variance weighted																										alter	no / insufficient power	UACR To Protein	Salze 2017	Teumer 2019	6	2.9	6	1.508	5.072E-02	5.072E-02							alter	no / insufficient power		
MMP1	92 -32_1	UACR	Robust adjusted profile score (RAPS)	Protein To UACR	Emilsson 2018	Teumer 2019	1	0.006	0.00	3.78E-01	6.13E-01																		before	no / insufficient power	UACR To Protein	Salze 2017	Teumer 2019	8	3.5	7	1.386	1.0	9E-02	2.122E-02	2.358E-02	2.5	6E-02	2.32E-01	0.031	1		before	no / insufficient power
ERP29	983-6_1	CKD	Robust adjusted profile score (RAPS)	Protein To CKD	Sun 2018	Wanke 2019	3	0.006	0.0	7.967E-01	9.706E-01	6.076E-01	3.185E-01	9.759E-01															before	no / insufficient power	CKD To Protein	Sun 2018	Wanke 2019	16	-0.0	0.1	6.912E-01	6.912E-01	5.556E-01	6.737E-01	1.399E-01	0.603			before	no / insufficient power			
ERP29	983-6_1	eGFR	Robust adjusted profile score (RAPS)	Protein To eGFR	Sun 2018	Wanke 2019	3	0.001	0.002	3.26E-01	8.381E-01	1.693E-01	2.706E-01	3.975E-01															before	no / insufficient power	eGFR To Protein	Sun 2018	Wanke 2019	193	0.816	0.669	2.225E-01	6.912E-01	3.078E-01	3.30E-01	6.97E-03	0.332			before	no / insufficient power			
ERP29	983-6_1	UACR	Robust adjusted profile score (RAPS)	Protein To UACR	Sun 2018	Teumer 2019	3	0.013	0.01	9.03E-01	6.13E-01	8.02E-01	9.779E-01	3.9	E-01														before	no / insufficient power	UACR To Protein	Sun 2018	Teumer 2019	29	-0.139	0.317	6.621E-01	6.912E-01	9.831E-01	9.892E-01	2.282E-01	0.965			before	no / insufficient power			
SOD2	5008-51_1	CKD	Robust adjusted profile score (RAPS)	Protein To CKD	Sun 2018	Wanke 2019	3	0.057	0.017	2.99E-01	3.652E-02	7.33E-01	9.5E-01	7.82	E-01														before	yes if direction of beta in KORA	CKD To Protein	Sun 2018	Wanke 2019	16	-0.023	0.101	8.226E-01	8.226E-01	1.26E-01	1.880E-01	1.988E-01	0.1	6			before	no / insufficient power		
SOD2	5008-51_1	eGFR	MIR PRESSO_Outlier corrected																										before	no / insufficient power	eGFR To Protein	Sun 2018	Wanke 2019	191	0.189	0.6	8.7706E-01	8.73	E-01					0.002	2		before	no / insufficient power	
SOD2	5008-51_1	eGFR	outliers-corrected in one variance weighted																										alter	no / insufficient power	eGFR To Protein	Sun 2018	Wanke 2019	180	0.05	0.66	9.01E-01	9.01E-01								alter	no / insufficient power		
SOD2	5008-51_1	eGFR	Robust adjusted profile score (RAPS)	Protein To eGFR	Sun 2018	Wanke 2019	3	-0.002	0.001	5.56E-03	2.812E-02	9.90	E-01	9.29	E-01	9.321E-01													before	yes if direction of beta in KORA	eGFR To Protein	Sun 2018	Wanke 2019	193	0.31	0.669	6.3	E-01	8.226E-01	5.570E-03	9.0	E-03	7.69	E-01	0.002	2		before	no / insufficient power
SOD2	5008-51_1	UACR	Robust adjusted profile score (RAPS)	Protein To UACR	Sun 2018	Teumer 2019	3	0.006	0.00	1.22E-01	6.13E-01	6.666E-01	8.15E-01	5.12E-01															before	no / insufficient power	UACR To Protein	Sun 2018	Teumer 2019	29	-0.15	0.32	6.295E-01	8.226E-01	3.298E-01	3.288E-01	3.39	E-01	0.371			before	no / insufficient power		
NOTCH1	5107-7_2	CKD	Robust adjusted profile score (RAPS)	Protein To CKD	Sun 2018	Wanke 2019	3	0.03	0.039	8.70E-01	8.51	E-01	6.59E-01	6.136E-01	6.17E-01														before	no / insufficient power	CKD To Protein	Sun 2018	Wanke 2019	16	-0.015	0.099	8.799E-01	9.703E-01	8.27E-01	7.951E-01	7.7	9E-01	0.865			before	no / insufficient power		
NOTCH1	5107-7_2	eGFR	Robust adjusted profile score (RAPS)	Protein To eGFR	Sun 2018	Wanke 2019	3	-0.003	0.002	2.17E-02	3.380E-01	1.20E-01	9.039E-01	2.885E-01															before	no / insufficient power	eGFR To Protein	Sun 2018	Wanke 2019	193	0.025	0.67	9.703E-01	9.703E-01	9.809E-02	9.272E-02	5.580E-01	0.1			before	no / insufficient power			
NOTCH1	5107-7_2	UACR	Robust adjusted profile score (RAPS)	Protein To UACR	Sun 2018	Teumer 2019	3	0.008	0.009	6.1E-01	6.161E-01	3.76E-01	5.1	2E-01	3.30E-01														before	no / insufficient power	UACR To Protein	Sun 2018	Teumer 2019	29	-0.307	0.321	3.389E-01	9.703E-01	1.039E-01	9.907E-02	1.65E-01	0.111			before	no / insufficient power			
RELT	5115-31_3	CKD	Robust adjusted profile score (RAPS)	Protein To CKD	Sun 2018	Wanke 2019	3	0.037	0.025	3.29E-01	5.317E-01	1.05E-01	8.863E-02	5.933E-01															before	no / insufficient power	CKD To Protein	Sun 2018	Wanke 2019	16	0.128	0.1	2.010E-01	0.020E-01	2.65E-01	6.6	5E-01	6.30	E-02	0.58			before	no / insufficient power	
RELT	5115-31_3	eGFR	Robust adjusted profile score (RAPS)	Protein To eGFR	Sun 2018	Wanke 2019	3	-0.001	0.001	5.03E-01	6.132E-01	5.672E-01	8.988E-01	8.23E-01															before	no / insufficient power	eGFR To Protein	Sun 2018	Wanke 2019	193	-2.617	0.669	9.1	6E-05	3.658E-01	5.791E-01	5.6	2E-01	6.111E-01	0.581			before	yes same direction of beta in KORA	
RELT	5115-31_3	UACR	Robust adjusted profile score (RAPS)	Protein To UACR	Sun 2018	Teumer 2019	3	0.007	0.005	1.92E-01	6.13E-01	2.78E-01	3.939E-01	3.872E-01															before	no / insufficient power	UACR To Protein	Sun 2018	Teumer 2019	29	0.038	0.319	9.050E-01	9.050E-01	2.528E-01	2.0E-01	3.98	E-01	0.272			before	no / insufficient power		
SCARF1	5129-12_3	CKD	Robust adjusted profile score (RAPS)	Protein To CKD	Emilsson 2018	Wanke 2019	1	-0.011	0.02	9.22E-01	9.00E-01																	before	no / insufficient power	CKD To Protein	Salze 2017	Wanke 2019	8	0.312	0.251	2.136E-01	8.5	E-01	2.567E-01	1.789E-01	8.78	E-01	0.318			before	no / insufficient power		
SCARF1	5129-12_3	eGFR	Robust adjusted profile score (RAPS)	Protein To eGFR	Emilsson 2018	Wanke 2019	1	0.002	0.001	9.89E-02	1.562E-01																		before	no / insufficient power	eGFR To Protein	Salze 2017	Wanke 2019	63	1.326	2.09	5.268E-01	9.602E-01	6.868E-01	6.5	0E-01	9.106E-01	0.68			before	no / insufficient power		
SCARF1	5129-12_3	UACR	Robust adjusted profile score (RAPS)	Protein To																																													

TNFRSF19	5131-15.3	CKD	Robust adjusted profile score (RAPS)	Protein To CKD	Sun 2018	Wanke 2019	2	-0.006	0.068	3.38E-01	9.706E-01	2.77E-01									no / insufficient power	CKD To Protein	Sun 2018	Wanke 2019	16	0.237	0.11816E-02	3.632E-02	6.021E-01	6.32 E-01	2.686E-01	0.611		before	yes same direction of be a n KORA			
TNFRSF19	5131-15.3	cGFR	Robust adjusted profile score (RAPS)	Protein To eGFR	Sun 2018	Wanke 2019	2	-0.001	0.002	897E-01	8.922E-01	8.32 E-01									no / insufficient power	cGFR To Protein	Sun 2018	Wanke 2019	193	-2.628	0.669 8.619E-05	3. 8E-0	2.316E-01	2.236E-01	5.000E-01	0.225		before	yes same direction of be a n KORA			
TNFRSF19	5131-15.3	UACR	Robust adjusted profile score (RAPS)	Protein To UACR	Sun 2018	Teumer 2019	2	0.02	0.012	060E-02	.237E-01	.339E-01									no / insufficient power	UACR To Protein	Sun 2018	Teumer 2019	29	0.05	0.319 8.66 E-01	9.526E-01	7.908E-01	7.513E-01	7.95 E-01	0.778		before	no / insufficient power			
HAWCR2	513 -52.2	CKD	Robust adjusted profile score (RAPS)	Protein To CKD	Sun 2018	Wanke 2019	6	0.02	0.017	.292E-01	5.932E-01	.985E-01	3.636E-01	8.653E-01	0.688							no / insufficient power	CKD To Protein	Sun 2018	Wanke 2019	16	0.013	0.099 8.937E-01	8.937E-01	8.978E-01	8.7 0E-01	5.877E-01	0.89		before	no / insufficient power		
HAWCR2	513 -52.2	cGFR	Robust adjusted profile score (RAPS)	Protein To eGFR	Sun 2018	Wanke 2019	6	0	0.001	.577E-01	8.381E-01	6.700E-01	5.535E-01	7.022E-01	0.769							no / insufficient power	cGFR To Protein	Sun 2018	Wanke 2019	193	-0.236	0.668 7.2 2E-01	8.937E-01	6. 88E-01	6. 7E-01	3.810E-01	0.631		before	no / insufficient power		
HAWCR2	513 -52.2	UACR	Robust adjusted profile score (RAPS)	Protein To UACR	Sun 2018	Teumer 2019	6	-0.006	0.006	.756E-01	5.052E-01	8.53 E-01	8.1 3E-01	5.61 E-01	0.827							no / insufficient power	UACR To Protein	Sun 2018	Teumer 2019	29	-0.589	0.321 6.6 6E-02	2.659E-01	2. 93E-01	2.176E-01	6.589E-01	0.256		before	no / insufficient power		
UNCSC	5139-32.3	CKD	Robust adjusted profile score (RAPS)	Protein To CKD	Sun 2018	Wanke 2019	5	-0.013	0.026	.172E-01	9. 00E-01	3.33 E-01	8.95 E-01	1. 02E-01	0.368							no / insufficient power	CKD To Protein	Sun 2018	Wanke 2019	16	0.135	0.11781E-01	3.561E-01	6.800E-01	7.192E-01	2.5 0E-01	0.696		before	no / insufficient power		
UNCSC	5139-32.3	cGFR	MIR-PRESSO_Outlier corrected	Protein To eGFR	Sun 2018	Wanke 2019	3	-0.001	0.001	2. 6E-01	6.8 3E-01			0.0	2							no / insufficient power	cGFR To Protein	Sun 2018	Wanke 2019	193									before			
UNCSC	5139-32.3	cGFR	Wald corrected	Protein To eGFR	Sun 2018	Wanke 2019	1	0.001	0.001	.153E-01	7.071E-01											no / insufficient power															after	
UNCSC	5139-32.3	cGFR	Robust adjusted profile score (RAPS)	Protein To eGFR	Sun 2018	Wanke 2019	5	0	0.001	.278E-01	9. 0 E-01	1.059E-03	1.217E-01	8. 20E-02	0.0	2						no / insufficient power	cGFR To Protein	Sun 2018	Wanke 2019	193	-2.196	0.669 1.035E-03	.1 1E-03	6. 3E-01	.517E-01	5.396E-01	0. 8		before	yes same direction of be a n KORA		
UNCSC	5139-32.3	UACR	MIR-PRESSO_Outlier corrected	Protein To UACR	Sun 2018	Teumer 2019	5															no / insufficient power	UACR To Protein	Sun 2018	Teumer 2019	28	0.012	0.355 9.726E-01	9.726E-01				0.009	1	before	no / insufficient power		
UNCSC	5139-32.3	UACR	outliers-corrected In eGFR variance weighted	Protein To UACR	Sun 2018	Teumer 2019		-0.007	0.005	.915E-01	3.320E-01											no / insufficient power	UACR To Protein	Sun 2018	Teumer 2019	27	-0.093	0.33 7.800E-01	7.800E-01						after	no / insufficient power		
UNCSC	5139-32.3	UACR	Robust adjusted profile score (RAPS)	Protein To UACR	Sun 2018	Teumer 2019	5	-0.01	0.005	.067E-02	. 2E-01	2.003E-02	2.535E-02	. 87E-01	0.078							no / insufficient power	UACR To Protein	Sun 2018	Teumer 2019	29	-0.126	0.322 4.953E-01	6.953E-01	1.23 E-02	1.117E-02	.751E-01	0.009	1	before	no / insufficient power		
LEPR	5 00-52.3	CKD	Robust adjusted profile score (RAPS)	Protein To CKD	Sun 2018	Wanke 2019	6	-0.013	0.011	.858E-01	5.701E-01	9.632E-01	9.783E-01	5.018E-01	0.85							no / insufficient power	CKD To Protein	Sun 2018	Wanke 2019	16	0.067	0.1 5.01 E-01	6.686E-01	0.17E-01	3.381E-01	7.6 7E-01	0. 33		before	no / insufficient power		
LEPR	5 00-52.3	cGFR	Robust adjusted profile score (RAPS)	Protein To eGFR	Sun 2018	Wanke 2019	6	0	0	.367E-01	8.381E-01	8.781E-02	6.3 9E-02	6.096E-01	0.372							no / insufficient power	cGFR To Protein	Sun 2018	Wanke 2019	193	0.5 9	0.668 .112E-01	6.686E-01	7.172E-01	6.996E-01	9.308E-01	0.757		before	no / insufficient power		
LEPR	5 00-52.3	UACR	Robust adjusted profile score (RAPS)	Protein To UACR	Sun 2018	Teumer 2019	6	0.003	0.002	.039E-01	.613E-01	1.207E-01	8.722E-02	6.156E-01	0.35							no / insufficient power	UACR To Protein	Sun 2018	Teumer 2019	29	-0.015	0.32 9.622E-01	9.622E-01	3.287E-01	3.691E-01	1.923E-01	0.362		before	no / insufficient power		
SPOCK2	5 91-12.3	CKD	outliers-corrected In eGFR variance weighted	Protein To CKD	Sun 2018	Wanke 2019																no / insufficient power	CKD To Protein	Sun 2018	Wanke 2019	1	-0.276	0.109 1.116E-02	1.67 E-02						after	yes same direction of be a n KORA		
SPOCK2	5 91-12.3	CKD	Robust adjusted profile score (RAPS)	Protein To CKD	Sun 2018	Wanke 2019	6	0.01	0.027	.8 5E-01	9. 00E-01	9.909E-01	9.711E-01	9.399E-01	0.995							no / insufficient power	CKD To Protein	Sun 2018	Wanke 2019	16	-0.295	0.102 3.823E-03	7.6 6E-03	1.10 E-02	1.380E-02	3.178E-01	0.012	No significant outliers	before	yes same direction of be a n KORA		
SPOCK2	5 91-12.3	cGFR	MIR-PRESSO_Outlier corrected	Protein To eGFR	Sun 2018	Wanke 2019	6															no / insufficient power	cGFR To Protein	Sun 2018	Wanke 2019	190	2.6 5	0.732 3.873E-0	.358E-03				-0.001	3	before	yes same direction of be a n KORA		
SPOCK2	5 91-12.3	cGFR	outliers-corrected In eGFR variance weighted	Protein To eGFR	Sun 2018	Wanke 2019																no / insufficient power	cGFR To Protein	Sun 2018	Wanke 2019	172	2. 2	0.675 3.3 6E-0	1.00 E-03						after	yes same direction of be a n KORA		
SPOCK2	5 91-12.3	cGFR	Robust adjusted profile score (RAPS)	Protein To eGFR	Sun 2018	Wanke 2019	6	0.002	0.001	.7 6E-02	2.563E-01	2.968E-01	2.106E-01	7.017E-01	0.39							no / insufficient power	cGFR To Protein	Sun 2018	Wanke 2019	193	2.507	0.77 1.122E-03	. 89E-03	1.090E-05	1.967E-05	7.852E-02	-0.001	3	before	yes same direction of be a n KORA		
SPOCK2	5 91-12.3	UACR	MIR-PRESSO_Outlier corrected	Protein To UACR	Sun 2018	Teumer 2019	3	-0.01	0.007	.961E-01	7.8 7E-01				-0.001	3						no / insufficient power	UACR To Protein	Sun 2018	Teumer 2019	28	0.09	0.3 9.7986E-01	7.986E-01				-0.001	1	before	no / insufficient power		
SPOCK2	5 91-12.3	UACR	outliers-corrected In eGFR variance weighted	Protein To UACR	Sun 2018	Teumer 2019	3	-0.01	0.009	.766E-01	3.320E-01											no / insufficient power	UACR To Protein	Sun 2018	Teumer 2019	25	0. 66	0.33 1.62 E-01	1.62 E-01						after	no / insufficient power		
SPOCK2	5 91-12.3	UACR	Robust adjusted profile score (RAPS)	Protein To UACR	Sun 2018	Teumer 2019	6	-0.012	0.006	.926E-02	.237E-01	5.27 E-07	3.619E-07	6.803E-01	<0.001	3						no / insufficient power	UACR To Protein	Sun 2018	Teumer 2019	29	0.156	0.32 6.265E-01	6.265E-01	1.0 8E-03	1.968E-03	1.8 5E-01	<0.001	1	before	no / insufficient power		

Supplementary Table 25. Two-sample MR evidence is suggestive of relationships of replicated proteins to kidney traits (CKD, eGFR and UACR) using genetic instruments summarized from Zheng et al¹.

Results of two sample MR of 23 out of 46 replicated proteins to kidney traits (CKD, eGFR and UACR) using genetic instruments summarized by Zheng et al¹.

Abbreviations: CKD, chronic kidney disease; eGFR, estimated glomerular filtration rate; UACR, urinary albumin-to-creatinine ratio; MR, Mendelian Randomization.

Protein	Protein.SeqId	Kidney.traits	method	study_pro	study_kidney	nsp	b	se	pval	fdr	IVW.Q_pval
ADAMTS13	3175-51_5	eGFR	adjusted profile score (RAPS)	Sun	Wuttke 2019	1	0 001	0 001	8 984E-02	2 583E-01	
ADAMTS13	3175-51_5	UACR	adjusted profile score (RAPS)	Sun	Teumer 2019	1	0 003	0 004	4 245E-01	5 743E-01	
ADAMTS13	3175-51_5	CKD	adjusted profile score (RAPS)	Sun	Wuttke 2019	1	0 006	0 019	7 422E-01	8 129E-01	
AMH	4923-79_1	CKD	adjusted profile score (RAPS)	Sun	Wuttke 2019	1	-0 048	0 047	3 005E-01	5 760E-01	
AMH	4923-79_1	UACR	adjusted profile score (RAPS)	Sun	Teumer 2019	1	0 004	0 01	6 678E-01	6 998E-01	
AMH	4923-79_1	eGFR	adjusted profile score (RAPS)	Sun	Wuttke 2019	1	-0 001	0 002	7 004E-01	7 986E-01	
B2M	3485-28_2	eGFR	adjusted profile score (RAPS)	Yao	Wuttke 2019	1	-0 016	0 004	4 159E-05	9 565E-04	
B2M	3485-28_2	UACR	adjusted profile score (RAPS)	Yao	Teumer 2019	1	0 071	0 021	5 285E-04	1 216E-02	
B2M	3485-28_2	CKD	adjusted profile score (RAPS)	Yao	Wuttke 2019	1	0 311	0 094	9 668E-04	2 224E-02	
CGA:LHB	2953-31_2	CKD	adjusted profile score (RAPS)	Sun	Wuttke 2019	1	-0 057	0 025	2 125E-02	1 969E-01	
CGA:LHB	2953-31_2	UACR	adjusted profile score (RAPS)	Sun	Teumer 2019	1	-0 008	0 006	1 510E-01	3 279E-01	
CGA:LHB	2953-31_2	eGFR	adjusted profile score (RAPS)	Sun	Wuttke 2019	1	0 001	0 001	1 620E-01	3 727E-01	
CST3	2609-59_2	eGFR	adjusted profile score (RAPS)	Yao	Wuttke 2019	1	-0 002	0 001	1 245E-01	3 183E-01	
CST3	2609-59_2	UACR	adjusted profile score (RAPS)	Yao	Teumer 2019	1	-0 008	0 006	2 239E-01	3 432E-01	
CST3	2609-59_2	CKD	adjusted profile score (RAPS)	Yao	Wuttke 2019	1	0 046	0 03	1 340E-01	5 137E-01	
CTSH	3737-6_3	CKD	adjusted profile score (RAPS)	Sun	Wuttke 2019	1	-0 032	0 015	2 931E-02	1 969E-01	
CTSH	3737-6_3	UACR	adjusted profile score (RAPS)	Sun	Teumer 2019	1	0 003	0 003	3 092E-01	4 445E-01	
CTSH	3737-6_3	eGFR	adjusted profile score (RAPS)	Sun	Wuttke 2019	1	0	0 001	5 333E-01	7 552E-01	
ESAM	2981-9_3	eGFR	adjusted profile score (RAPS)	Sun	Wuttke 2019	1	0 004	0 002	1 719E-02	1 318E-01	
ESAM	2981-9_3	CKD	adjusted profile score (RAPS)	Sun	Wuttke 2019	1	-0 088	0 044	4 682E-02	2 154E-01	
ESAM	2981-9_3	UACR	adjusted profile score (RAPS)	Sun	Teumer 2019	1	0 019	0 01	7 095E-02	3 116E-01	

HAVCR2	5134-52_2	eGFR	adjusted profile score (RAPS)	Sun	Wuttke 2019	2	-0.001	0.001	3.285E-02	1.889E-01	1.539E-01
HAVCR2	5134-52_2	UACR	adjusted profile score (RAPS)	Sun	Teumer 2019	2	0.005	0.004	2.015E-01	3.432E-01	6.026E-01
HAVCR2	5134-52_2	CKD	adjusted profile score (RAPS)	Sun	Wuttke 2019	2	0.017	0.015	2.628E-01	5.494E-01	6.961E-01
IGF2R	3676-15_3	eGFR	adjusted profile score (RAPS)	Sun	Wuttke 2019	1	0.001	0.001	8.366E-02	2.583E-01	
IGF2R	3676-15_3	UACR	adjusted profile score (RAPS)	Sun	Teumer 2019	1	-0.005	0.003	1.568E-01	3.279E-01	
IGF2R	3676-15_3	CKD	adjusted profile score (RAPS)	Sun	Wuttke 2019	1	-0.019	0.016	2.325E-01	5.347E-01	
KDR	3651-50_5	UACR	adjusted profile score (RAPS)	Sun	Teumer 2019	1	-0.008	0.005	1.219E-01	3.116E-01	
KDR	3651-50_5	CKD	adjusted profile score (RAPS)	Sun	Wuttke 2019	1	-0.028	0.029	3.290E-01	5.821E-01	
KDR	3651-50_5	eGFR	adjusted profile score (RAPS)	Sun	Wuttke 2019	1	0	0.001	8.986E-01	8.986E-01	
LEPR	5400-52_3	UACR	adjusted profile score (RAPS)	Sun	Teumer 2019	1	0.002	0.002	2.232E-01	3.432E-01	
LEPR	5400-52_3	CKD	adjusted profile score (RAPS)	Sun	Wuttke 2019	1	-0.012	0.009	1.856E-01	5.337E-01	
LEPR	5400-52_3	eGFR	adjusted profile score (RAPS)	Sun	Wuttke 2019	1	0	0.8508E-01	8.894E-01		
MASP1	3605-77_4	eGFR	adjusted profile score (RAPS)	Suhre	Wuttke 2019	1	0.002	0.001	7.027E-02	2.583E-01	
MASP1	3605-77_4	UACR	adjusted profile score (RAPS)	Suhre	Teumer 2019	1	-0.003	0.006	6.694E-01	6.998E-01	
MASP1	3605-77_4	CKD	adjusted profile score (RAPS)	Suhre	Wuttke 2019	1	0.001	0.039	7.69E-01	9.769E-01	
MMP1	4924-32_1	UACR	adjusted profile score (RAPS)	Folkersen	Teumer 2019	2	0.01	0.006	9.965E-02	3.116E-01	9.259E-01
MMP1	4924-32_1	CKD	adjusted profile score (RAPS)	Folkersen	Wuttke 2019	2	0.023	0.028	4.224E-01	6.940E-01	8.714E-01
MMP1	4924-32_1	eGFR	adjusted profile score (RAPS)	Folkersen	Wuttke 2019	2	0.001	0.001	4.665E-01	7.152E-01	5.627E-01
PLAT	2212-69_1	CKD	adjusted profile score (RAPS)	Emilsson	Wuttke 2019	1	-0.118	0.056	3.424E-02	1.969E-01	
PLAT	2212-69_1	eGFR	adjusted profile score (RAPS)	Emilsson	Wuttke 2019	1	0.002	0.002	3.119E-01	5.519E-01	
PLAT	2212-69_1	UACR	adjusted profile score (RAPS)	Emilsson	Teumer 2019	1	0.008	0.012	5.289E-01	6.759E-01	
PLG	3710-49_2	eGFR	adjusted profile score (RAPS)	Suhre	Wuttke 2019	1	0.004	0.001	2.329E-03	2.679E-02	
PLG	3710-49_2	UACR	adjusted profile score (RAPS)	Suhre	Teumer 2019	1	-0.008	0.006	2.170E-01	3.432E-01	
PLG	3710-49_2	CKD	adjusted profile score (RAPS)	Suhre	Wuttke 2019	1	0.021	0.034	9.972E-01	7.623E-01	
RELT	5115-31_3	UACR	adjusted profile score (RAPS)	Sun	Teumer 2019	1	0.01	0.006	9.001E-02	3.116E-01	
RELT	5115-31_3	eGFR	adjusted profile score (RAPS)	Sun	Wuttke 2019	1	-0.001	0.001	1.831E-01	3.829E-01	
RELT	5115-31_3	CKD	adjusted profile score (RAPS)	Sun	Wuttke 2019	1	0.013	0.027	6.326E-01	7.658E-01	

RET	3220-40_2	UACR	adjusted profile score (RAPS)	Sun	Teumer 2019	1	0.005	0.009	6.071E-01	6.982E-01	
RET	3220-40_2	CKD	adjusted profile score (RAPS)	Sun	Wuttke 2019	1	0.017	0.042	6.918E-01	7.956E-01	
RET	3220-40_2	eGFR	adjusted profile score (RAPS)	Sun	Wuttke 2019	1	-0.001	0.002	7.291E-01	7.986E-01	
RETN	3046-31_1	UACR	adjusted profile score (RAPS)	Yao	Teumer 2019	2	0.02	0.011	7.391E-02	3.116E-01	4.018E-01
RETN	3046-31_1	CKD	adjusted profile score (RAPS)	Yao	Wuttke 2019	2	-0.064	0.053	2.263E-01	5.347E-01	1.400E-01
RETN	3046-31_1	eGFR	adjusted profile score (RAPS)	Yao	Wuttke 2019	2	-0.001	0.002	7.216E-01	7.986E-01	1.866E-01
SCARF1	5129-12_3	UACR	adjusted profile score (RAPS)	Suhre	Teumer 2019	1	0.008	0.004	8.115E-02	3.116E-01	
SCARF1	5129-12_3	eGFR	adjusted profile score (RAPS)	Suhre	Wuttke 2019	1	0.001	0.001	2.707E-01	5.188E-01	
SCARF1	5129-12_3	CKD	adjusted profile score (RAPS)	Suhre	Wuttke 2019	1	0.011	0.019	5.736E-01	7.647E-01	
SPOCK2	5491-12_3	eGFR	adjusted profile score (RAPS)	Sun	Wuttke 2019	1	0.003	0.002	7.308E-02	2.583E-01	
SPOCK2	5491-12_3	UACR	adjusted profile score (RAPS)	Sun	Teumer 2019	1	-0.015	0.01	1.069E-01	3.116E-01	
SPOCK2	5491-12_3	CKD	adjusted profile score (RAPS)	Sun	Wuttke 2019	1	0.011	0.043	8.055E-01	8.421E-01	
TNFRSF19	5131-15_3	UACR	adjusted profile score (RAPS)	Emilsson	Teumer 2019	1	0.024	0.045	5.957E-01	6.982E-01	
TNFRSF19	5131-15_3	eGFR	adjusted profile score (RAPS)	Emilsson	Wuttke 2019	1	0.005	0.009	5.910E-01	7.552E-01	
TNFRSF19	5131-15_3	CKD	adjusted profile score (RAPS)	Emilsson	Wuttke 2019	1	-0.102	0.194	5.985E-01	7.647E-01	
TNFRSF1B	3152-57_1	eGFR	adjusted profile score (RAPS)	Sun	Wuttke 2019	1	0.001	0.002	5.740E-01	7.552E-01	
TNFRSF1B	3152-57_1	CKD	adjusted profile score (RAPS)	Sun	Wuttke 2019	1	-0.034	0.056	5.393E-01	7.647E-01	
TNFRSF1B	3152-57_1	UACR	adjusted profile score (RAPS)	Sun	Teumer 2019	1	-0.001	0.011	9.237E-01	9.237E-01	
UNC5C	5139-32_3	UACR	adjusted profile score (RAPS)	Sun	Teumer 2019	1	-0.013	0.008	1.085E-01	3.116E-01	
UNC5C	5139-32_3	CKD	adjusted profile score (RAPS)	Sun	Wuttke 2019	1	-0.053	0.039	1.745E-01	5.337E-01	
UNC5C	5139-32_3	eGFR	adjusted profile score (RAPS)	Sun	Wuttke 2019	1	0.001	0.001	4.286E-01	7.042E-01	

Supplementary Table 26. Two-sample MR evidence is suggestive of relationships between kidney traits (CKD, eGFR and UACR) and replicated metabolites in both directions.

Results of bi-directional two-sample MR of 14 replicated metabolites and kidney traits (CKD, eGFR and UACR). **Abbreviations:** CKD, chronic kidney disease; eGFR, estimated glomerular filtration rate; UACR, urinary albumin-to-creatinine ratio; MR, Mendelian Randomization.

C181	UACR	Robust adjusted profile score (RAPS) ou k ers-corrected In esse variance weigh ed	Me abole: To UACR	Draisma 2015	Teuner 2019	3	0.225	0.0 5 7.280E-07	3.133E-06	6.8 3E-05	1.955E-03	5.000E-01			efore	no / insufficient power	UACR To Metaboli	Draisma 2015	Teuner 2019	25	0.122	0.071 8 503E-02	.31 E-01	8. 88E-01	8. 53E-01	3.899E-01	0.833	before	o / sufficient over		
C2	CKD	Robust adjusted profile score (RAPS) ou k ers-corrected In esse variance weigh ed	Me abole: To CKD	Draisma 2015	Wanke 2019	3	0.203	0.156 1.933E-01	5.5 6E-01						fer	no / insufficient power															
C2	CKD	Robust adjusted profile score (RAPS) MR-PRESSO Ou k ers-corrected	Me abole: To CKD	Draisma 2015	Wanke 2019		0.06	0.112 5.902E-01	8.752E-01	2.917E-02	1.351E-02	7.890E-01	0.17		efore	no / insufficient power	CKD To Metaboli	Draisma 2015	Wanke 2019	12	0.006	0.031 8 516E-01	.516E-01	6. 87E-01	6. 55E-01	3.703E-01	0.671	before	o / sufficient over		
C2	eGFR	Robust adjusted profile score (RAPS) MR-PRESSO Ou k ers-corrected	Me abole: To eGFR	Draisma 2015	Wanke 2019	2	0.003	0.007 7. 5 E-01	8.069E-01				0.006		efore	no / insufficient power	eGFR To Metaboli	Draisma 2015	Wanke 2019	161								before			
C2	eGFR	Robust adjusted profile score (RAPS) MR-PRESSO Ou k ers-corrected Wald ratio	Me abole: To eGFR	Draisma 2015	Wanke 2019	1	0.0	0.007 1.21 E-08	3.6 2E-08						fer	no / insufficient power															
C2	eGFR	Robust adjusted profile score (RAPS) MR-PRESSO Ou k ers-corrected	Me abole: To eGFR	Draisma 2015	Wanke 2019		-0.009	0.00 3.387E-02	5.707E-02	5.821E-08	8.823E-07	5.137E-01	0.006		efore	no / insufficient power	eGFR To Metaboli	Draisma 2015	Wanke 2019	161	-0.615	0.196 1 672E-03	.688E-03	8.559E-02	7.965E-02	6.579E-01	0.089	before	es same direction of eta in KORA o / sufficient over		
C2	UACR	Robust adjusted profile score (RAPS) MR-PRESSO Ou k ers-corrected	Me abole: To UACR	Draisma 2015	Teuner 2019	2	0.1	0.021 1.326E-01	3.051E-01				0.0 2		efore	no / insufficient power	UACR To Metaboli	Draisma 2015	Teuner 2019	25								before			
C2	UACR	Robust adjusted profile score (RAPS) MR-PRESSO Ou k ers-corrected Wald ratio	Me abole: To UACR	Draisma 2015	Teuner 2019	1	0.2 1	0.0 1 3.032E-09	9.095E-09						fer	no / insufficient power															
C2	UACR	Robust adjusted profile score (RAPS) MR-PRESSO Ou k ers-corrected	Me abole: To UACR	Draisma 2015	Teuner 2019		0.111	0.026 1.637E-05	2.56E-05	7.655E-05	1.22E-0	.70 E-01	0.0 2		efore	no / insufficient power	UACR To Metaboli	Draisma 2015	Teuner 2019	25	0.118	0.09 1 87 E-01	.737E-01	6.919E-01	6.369E-01	9.576E-01	0.70	before	o / sufficient over		
C6(C 1-DC)	CKD	Robust adjusted profile score (RAPS) MR-PRESSO Ou k ers-corrected	Me abole: To CKD	Lotta 2021	Wanke 2019	1	-0.8	0.076 2.689E-01	8.752E-01						efore	no / insufficient power	CKD To Metaboli	Shan 201	Wanke 2019	12	0.002	0.016 8 995E-01	.995E-01	5. 03E-01	5.273E-01	3.812E-01	0.538	before	o / sufficient over		
C6(C 1-DC)	eGFR	Robust adjusted profile score (RAPS) MR-PRESSO Ou k ers-corrected	Me abole: To eGFR	Lotta 2021	Wanke 2019	1	0.006	0.003 5.308E-02	7.667E-02						efore	no / insufficient power	eGFR To Metaboli	Shan 201	Wanke 2019	1 2	-0.196	0.103 5 683E-02	.273E-01	1.768E-01	2.196E-01	6.387E-02	0 18	before	o / sufficient over		
C6(C 1-DC)	UACR	Robust adjusted profile score (RAPS) MR-PRESSO Ou k ers-corrected	Me abole: To UACR	Lotta 2021	Teuner 2019	1	-0.02	0.016 1. 05E-01	2.608E-01						efore	no / insufficient power	UACR To Metaboli	Shan 201	Teuner 2019	2	-0.019	0.0 5 6.785E-01	.995E-01	9.551E-02	7.501E-02	8.113E-01	0.108	before	o / sufficient over		
C5	CKD	Robust adjusted profile score (RAPS) MR-PRESSO Ou k ers-corrected	Me abole: To CKD	Lotta 2021	Wanke 2019	3	-0.017	0.0 6.976E-01	8.752E-01	7.3 1E-02	3.195E-01	2.880E-01			efore	no / insufficient power															
C5	eGFR	Robust adjusted profile score (RAPS) MR-PRESSO Ou k ers-corrected	Me abole: To eGFR	Lotta 2021	Wanke 2019	1	0.01	0.00 8. 29E-03	1.517E-02						fer	yes dif d rection of be a n KORA															
C5	eGFR	Robust adjusted profile score (RAPS) MR-PRESSO Ou k ers-corrected Wald ratio	Me abole: To eGFR	Lotta 2021	Wanke 2019	3	0.011	0.002 7.931E-10	6.081E-09	2.078E-06	3.230E-0	.963E-01			fer	yes dif d rection of be a n KORA															
C5	UACR	Robust adjusted profile score (RAPS) MR-PRESSO Ou k ers-corrected	Me abole: To UACR	Lotta 2021	Teuner 2019	1	0.06	0.012 1.972E-07	3.9 3E-07						fer	yes dif d rection of be a n KORA															
C5	UACR	Robust adjusted profile score (RAPS) MR-PRESSO Ou k ers-corrected Wald ratio	Me abole: To UACR	Lotta 2021	Teuner 2019	3	0.05	0.01 1.625E-07	1.056E-06	1.690E-03	1.22 E-02	.9 7E-01			efore	yes dif d rection of be a n KORA															
C8	CKD	Robust adjusted profile score (RAPS) MR-PRESSO Ou k ers-corrected	Me abole: To CKD	Draisma 2015	Wanke 2019	1	-0.071	0.197 7.17 E-01	8.752E-01						efore	no / insufficient power	CKD To Metaboli	Draisma 2015	Wanke 2019	12	0.057	0.0 7 2 212E-01	.25E-01	.307E-01	3.653E-01	6. 22E-01	0. 16	before	o / sufficient over		
C8	eGFR	Robust adjusted profile score (RAPS) MR-PRESSO Ou k ers-corrected	Me abole: To eGFR	Draisma 2015	Wanke 2019	1	0.011	0.008 1. 57E-01	1.6 7E-01						efore	no / insufficient power	eGFR To Metaboli	Draisma 2015	Wanke 2019	152	-0. 87	0.295 9 916E-02	.966E-01	2.976E-01	3.008E-01	2.892E-01	0.302	before	o / sufficient over		
C8	UACR	Robust adjusted profile score (RAPS) MR-PRESSO Ou k ers-corrected In esse variance weigh ed															UACR To Metaboli	Draisma 2015	Teuner 2019	21	0.033	0.139 8 105E-01	.105E-01								
C8	UACR	Robust adjusted profile score (RAPS) MR-PRESSO Ou k ers-corrected	Me abole: To UACR	Draisma 2015	Teuner 2019	1	-0.007	0.0 3 8.7 8E-01	8.786E-01						efore	no / insufficient power	UACR To Metaboli	Draisma 2015	Teuner 2019	25	0.131	0.137 3 382E-01	.509E-01	3.0 3E-02	2.283E-02	8.016E-01	0.033	No significant ou lers	o / sufficient over		
C81	CKD	Robust adjusted profile score (RAPS) MR-PRESSO Ou k ers-corrected	Me abole: To CKD	Draisma 2015	Wanke 2019		0.308	0.10 3.095E-03	.02 E-02	.03 E-01	5.581E-01	3.160E-01	0. 33		efore	yes same direction of beta n KORA	CKD To Metaboli	Draisma 2015	Wanke 2019	12	0.022	0.0 5 809E-01	.8 8 E-01	1.651E-01	1.210E-01	8.252E-01	0.157	before	o / sufficient over		
C81	eGFR	Robust adjusted profile score (RAPS) MR-PRESSO Ou k ers-corrected	Me abole: To eGFR	Draisma 2015	Wanke 2019	1	-0.038	0.005 3.906E-12	3.515E-11						fer	yes same direction of beta n KORA															
C81	eGFR	Robust adjusted profile score (RAPS) MR-PRESSO Ou k ers-corrected	Me abole: To eGFR	Draisma 2015	Wanke 2019		-0.028	0.005 9.355E-10	6.081E-09	1.751E-02	5.065E-02	3.589E-01	0.157		efore	yes same direction of beta n KORA	eGFR To Metaboli	Draisma 2015	Wanke 2019	161	-0.879	0.25 383E-0	.753E-03	2. 2E-01	2.398E-01	3.981E-01	0.26	before	es same direction of eta in KORA o / sufficient over		
C81	UACR	Robust adjusted profile score (RAPS) MR-PRESSO Ou k ers-corrected	Me abole: To UACR	Draisma 2015	Teuner 2019		-0.072	0.022 1.08 E-03	2.3 9E-03	9.129E-01	7.726E-01	9.265E-01	0.927		efore	yes same direction of beta n KORA	UACR To Metaboli	Draisma 2015	Teuner 2019	25	-0.0 6	0.11 6 8 E-01	.8 8 E-01	5.150E-01	8 7E-01	.918E-01	0.552	before	o / sufficient over		
Tyr	CKD	Robust adjusted profile score (RAPS) MR-PRESSO Ou k ers-corrected	Me abole: To CKD	Draisma 2015	Wanke 2019	3	-0.65	0.239 6.502E-03	2.26E-02	1.931E-01	5.297E-01	3.383E-01			efore	yes same direction of beta n KORA	CKD To Metaboli	Draisma 2015	Wanke 2019	12	-0.028	0.021 1.915E-01	.830E-01	3. 37E-01	2.857E-01	6.396E-01	0.331	before	o / sufficient over		
Tyr	eGFR	Robust adjusted profile score (RAPS) MR-PRESSO Ou k ers-corrected	Me abole: To eGFR	Draisma 2015	Wanke 2019	1	0.0 5	0.013 5.162E-0	1.162E-03						fer	yes same direction of beta n KORA															
Tyr	eGFR	Robust adjusted profile score (RAPS) MR-PRESSO Ou k ers-corrected	Me abole: To eGFR	Draisma 2015	Wanke 2019	3	0.052	0.011 9.790E-07	2. 3E-06	1.2 1E-02	5.529E-01	2.112E-01			efore	yes same direction of beta n KORA	eGFR To Metaboli	Draisma 2015	Wanke 2019	162	0.22	0.132 9 01 E-02	.605E-01	7.293E-02	6.776E-02	6.022E-01	0.08	before	o / sufficient over		
Tyr	UACR	Robust adjusted profile score (RAPS) MR-PRESSO Ou k ers-corrected In esse variance weigh ed															UACR To Metaboli	Draisma 2015	Teuner 2019	22	-0.0	0.061 5 110E-01	.110E-01								
Tyr	UACR	Robust adjusted profile score (RAPS) MR-PRESSO Ou k ers-corrected	Me abole: To UACR	Draisma 2015	Teuner 2019	3	-0.031	0.05 5.367E-01	6.977E-01	3.066E-01	1.892E-01	6.515E-01			efore	no / insufficient power	UACR To Metaboli	Draisma 2015	Teuner 2019	25	-0.003	0.061 9 557E-01	.557E-01	1.7 9E-02	1.306E-02	7.529E-01	0.027	No significant ou lers	o / sufficient over		

Supplementary Table 27. Multi-omics prediction of incident CKD in hyperglycemic individuals of KORA F4.

Over 100 times of bootstrapping, the mean (\pm SD) and median AUC (95% CI) of predictive models built by each number of levels of omics predictors for each omics combination in each reference set are shown, respectively. AUC values were calculated with random forest using testing data.

ref₁: baseline age, sex; ref₂: baseline age, sex, BMI, systolic blood pressure, smoking status, triglyceride, total cholesterol, HDL cholesterol, fasting glucose, use of lipid lowering drugs, antihypertensive and anti-diabetic medication; ref₃: baseline age, sex, eGFR and UACR; ref₄: baseline age, eGFR, UACR, total cholesterol, fasting glucose, SM C18:1 and PC aa C38:0.

Abbreviations: AUC, area under the receiver operating characteristic curve; GPS, genome wide polygenic score of eGFR values; CKD, chronic kidney disease; eGFR, estimated glomerular filtration rate; UACR, urinary albumin-to-creatinine ratio.

num.omics.levels.combination	ref	model	combination	mean.SampleSize.train	mean.SampleSize.test	median.95CLAUC.test	mean.SD.AUC.test
two levels	ref1	ref	ref_Metabolites	744	274	0.694(0.639 - 0.75)	0.694 +/- 0.033
two levels	ref1	ref + 1omics	ref_Metabolites	744	274	0.7(0.629 - 0.759)	0.7 +/- 0.035
two levels	ref1	ref	ref_GPS	680	251	0.708(0.647 - 0.764)	0.707 +/- 0.034
two levels	ref1	ref + 1omics	ref_GPS	680	251	0.718(0.666 - 0.774)	0.721 +/- 0.031
three levels	ref1	ref	ref_GPS_Metabolites	673	248	0.709(0.645 - 0.765)	0.708 +/- 0.033
three levels	ref1	ref + GPS	ref_GPS_Metabolites	673	248	0.722(0.658 - 0.773)	0.722 +/- 0.032
three levels	ref1	ref + GPS + 1omics	ref_GPS_Metabolites	673	248	0.732(0.68 - 0.788)	0.73 +/- 0.03
four levels	ref1	ref	ref_GPS_CpGs_Metabolites	502	185	0.697(0.621 - 0.771)	0.694 +/- 0.043
four levels	ref1	ref + GPS	ref_GPS_CpGs_Metabolites	502	185	0.702(0.623 - 0.781)	0.7 +/- 0.041
four levels	ref1	ref + GPS + 1omics	ref_GPS_CpGs_Metabolites	502	185	0.682(0.631 - 0.758)	0.686 +/- 0.035
four levels	ref1	ref + GPS + 2omics	ref_GPS_CpGs_Metabolites	502	185	0.684(0.61 - 0.74)	0.68 +/- 0.032
three levels	ref1	ref	ref_GPS_CpGs	507	186	0.698(0.624 - 0.764)	0.693 +/- 0.04
three levels	ref1	ref + GPS	ref_GPS_CpGs	507	186	0.708(0.631 - 0.776)	0.704 +/- 0.04
three levels	ref1	ref + GPS + 1omics	ref_GPS_CpGs	507	186	0.682(0.622 - 0.747)	0.685 +/- 0.035
five levels	ref1	ref	ref_GPS_CpGs_Proteins_Metabolites	390	144	0.624(0.52 - 0.709)	0.625 +/- 0.052
five levels	ref1	ref + GPS	ref_GPS_CpGs_Proteins_Metabolites	390	144	0.662(0.549 - 0.74)	0.658 +/- 0.053
five levels	ref1	ref + GPS + 1omics	ref_GPS_CpGs_Proteins_Metabolites	390	144	0.673(0.569 - 0.777)	0.673 +/- 0.055
five levels	ref1	ref + GPS + 2omics	ref_GPS_CpGs_Proteins_Metabolites	390	144	0.678(0.583 - 0.771)	0.678 +/- 0.053
five levels	ref1	ref + GPS + 3omics	ref_GPS_CpGs_Proteins_Metabolites	390	144	0.685(0.606 - 0.766)	0.684 +/- 0.047
three levels	ref1	ref	ref_GPS_Proteins	418	155	0.625(0.527 - 0.708)	0.623 +/- 0.052
three levels	ref1	ref + GPS	ref_GPS_Proteins	418	155	0.662(0.565 - 0.745)	0.661 +/- 0.049
three levels	ref1	ref + GPS + 1omics	ref_GPS_Proteins	418	155	0.693(0.608 - 0.79)	0.694 +/- 0.052
four levels	ref1	ref	ref_GPS_Proteins_Metabolites	413	154	0.632(0.518 - 0.711)	0.628 +/- 0.051
four levels	ref1	ref + GPS	ref_GPS_Proteins_Metabolites	413	154	0.657(0.557 - 0.733)	0.652 +/- 0.05
four levels	ref1	ref + GPS + 1omics	ref_GPS_Proteins_Metabolites	413	154	0.681(0.594 - 0.767)	0.679 +/- 0.051
four levels	ref1	ref + GPS + 2omics	ref_GPS_Proteins_Metabolites	413	154	0.694(0.602 - 0.773)	0.693 +/- 0.045
three levels	ref1	ref	ref_GPS_RNAs	247	90	0.655(0.553 - 0.741)	0.653 +/- 0.054
three levels	ref1	ref + GPS	ref_GPS_RNAs	247	90	0.653(0.572 - 0.735)	0.659 +/- 0.045
three levels	ref1	ref + GPS + 1omics	ref_GPS_RNAs	247	90	0.6(0.485 - 0.705)	0.606 +/- 0.053
two levels	ref1	ref	ref_CpGs	558	205	0.691(0.618 - 0.756)	0.687 +/- 0.04
two levels	ref1	ref + 1omics	ref_CpGs	558	205	0.661(0.586 - 0.733)	0.663 +/- 0.038
two levels	ref1	ref	ref_Proteins	440	163	0.629(0.518 - 0.706)	0.626 +/- 0.049
two levels	ref1	ref + 1omics	ref_Proteins	440	163	0.668(0.581 - 0.754)	0.671 +/- 0.05
two levels	ref1	ref	ref_RNAs	277	102	0.657(0.575 - 0.761)	0.659 +/- 0.049
two levels	ref1	ref + 1omics	ref_RNAs	277	102	0.622(0.539 - 0.694)	0.619 +/- 0.046
two levels	ref2	ref	ref_Metabolites	743	274	0.72(0.664 - 0.769)	0.718 +/- 0.028
two levels	ref2	ref + 1omics	ref_Metabolites	743	274	0.725(0.667 - 0.773)	0.724 +/- 0.028
two levels	ref2	ref	ref_GPS	677	250	0.727(0.664 - 0.78)	0.726 +/- 0.03
two levels	ref2	ref + 1omics	ref_GPS	677	250	0.748(0.695 - 0.798)	0.747 +/- 0.027

three levels	ref2	ref	ref_GPS_Metabolites	672	248	0 723(0 661 - 0 779)	0 723 +/- 0 032
three levels	ref2	ref + GPS	ref_GPS_Metabolites	672	248	0 744(0 687 - 0 796)	0 743 +/- 0 028
three levels	ref2	ref + GPS + 1omics	ref_GPS_Metabolites	672	248	0 746(0 682 - 0 797)	0 744 +/- 0 028
four levels	ref2	ref	ref_GPS_CpGs_Metabolites	501	184	0 689(0 614 - 0 747)	0 687 +/- 0 033
four levels	ref2	ref + GPS	ref_GPS_CpGs_Metabolites	501	184	0 709(0 644 - 0 773)	0 707 +/- 0 033
four levels	ref2	ref + GPS + 1omics	ref_GPS_CpGs_Metabolites	501	184	0 7(0 632 - 0 755)	0 698 +/- 0 032
four levels	ref2	ref + GPS + 2omics	ref_GPS_CpGs_Metabolites	501	184	0 689(0 607 - 0 753)	0 691 +/- 0 037
three levels	ref2	ref	ref_GPS_CpGs	505	186	0 692(0 617 - 0 752)	0 69 +/- 0 033
three levels	ref2	ref + GPS	ref_GPS_CpGs	505	186	0 712(0 644 - 0 773)	0 711 +/- 0 031
three levels	ref2	ref + GPS + 1omics	ref_GPS_CpGs	505	186	0 693(0 615 - 0 771)	0 697 +/- 0 037
five levels	ref2	ref	ref_GPS_CpGs_Proteins_Metabolites	389	144	0 661(0 566 - 0 746)	0 661 +/- 0 045
five levels	ref2	ref + GPS	ref_GPS_CpGs_Proteins_Metabolites	389	144	0 692(0 613 - 0 776)	0 691 +/- 0 042
five levels	ref2	ref + GPS + 1omics	ref_GPS_CpGs_Proteins_Metabolites	389	144	0 685(0 606 - 0 784)	0 69 +/- 0 047
five levels	ref2	ref + GPS + 2omics	ref_GPS_CpGs_Proteins_Metabolites	389	144	0 688(0 602 - 0 788)	0 692 +/- 0 048
five levels	ref2	ref + GPS + 3omics	ref_GPS_CpGs_Proteins_Metabolites	389	144	0 673(0 584 - 0 777)	0 678 +/- 0 05
three levels	ref2	ref	ref_GPS_Proteins	416	154	0 668(0 586 - 0 748)	0 669 +/- 0 047
three levels	ref2	ref + GPS	ref_GPS_Proteins	416	154	0 697(0 627 - 0 78)	0 699 +/- 0 04
three levels	ref2	ref + GPS + 1omics	ref_GPS_Proteins	416	154	0 705(0 63 - 0 81)	0 71 +/- 0 048
four levels	ref2	ref	ref_GPS_Proteins_Metabolites	413	153	0 661(0 581 - 0 743)	0 663 +/- 0 047
four levels	ref2	ref + GPS	ref_GPS_Proteins_Metabolites	413	153	0 689(0 619 - 0 769)	0 693 +/- 0 04
four levels	ref2	ref + GPS + 1omics	ref_GPS_Proteins_Metabolites	413	153	0 696(0 601 - 0 789)	0 696 +/- 0 048
four levels	ref2	ref + GPS + 2omics	ref_GPS_Proteins_Metabolites	413	153	0 705(0 606 - 0 777)	0 701 +/- 0 046
three levels	ref2	ref	ref_GPS_RNAs	247	90	0 604(0 545 - 0 686)	0 607 +/- 0 041
three levels	ref2	ref + GPS	ref_GPS_RNAs	247	90	0 632(0 556 - 0 711)	0 633 +/- 0 04
three levels	ref2	ref + GPS + 1omics	ref_GPS_RNAs	247	90	0 615(0 522 - 0 683)	0 615 +/- 0 044
two levels	ref2	ref	ref_CpGs	556	204	0 693(0 626 - 0 766)	0 69 +/- 0 035
two levels	ref2	ref + 1omics	ref_CpGs	556	204	0 672(0 605 - 0 745)	0 674 +/- 0 038
two levels	ref2	ref	ref_Proteins	438	162	0 67(0 586 - 0 747)	0 671 +/- 0 042
two levels	ref2	ref + 1omics	ref_Proteins	438	162	0 689(0 605 - 0 784)	0 688 +/- 0 047
two levels	ref2	ref	ref_RNAs	277	102	0 63(0 561 - 0 695)	0 629 +/- 0 038
two levels	ref2	ref + 1omics	ref_RNAs	277	102	0 622(0 518 - 0 688)	0 615 +/- 0 048
two levels	ref3	ref	ref_Metabolites	744	274	0 79(0 738 - 0 834)	0 788 +/- 0 026
two levels	ref3	ref + 1omics	ref_Metabolites	744	274	0 806(0 756 - 0 857)	0 806 +/- 0 027
two levels	ref3	ref	ref_GPS	680	251	0 802(0 758 - 0 855)	0 801 +/- 0 026
two levels	ref3	ref + 1omics	ref_GPS	680	251	0 82(0 771 - 0 867)	0 82 +/- 0 025
three levels	ref3	ref	ref_GPS_Metabolites	673	248	0 803(0 753 - 0 85)	0 802 +/- 0 027
three levels	ref3	ref + GPS	ref_GPS_Metabolites	673	248	0 822(0 775 - 0 868)	0 822 +/- 0 026
three levels	ref3	ref + GPS + 1omics	ref_GPS_Metabolites	673	248	0 824(0 771 - 0 874)	0 824 +/- 0 027
four levels	ref3	ref	ref_GPS_CpGs_Metabolites	502	185	0 779(0 717 - 0 84)	0 777 +/- 0 033
four levels	ref3	ref + GPS	ref_GPS_CpGs_Metabolites	502	185	0 8(0 728 - 0 855)	0 799 +/- 0 032

four levels	ref3	ref + GPS + 1omics	ref_GPS_CpGs_Metabolites	502	185	0 793(0 742 - 0 848)	0 796 +/- 0 029
four levels	ref3	ref + GPS + 2omics	ref_GPS_CpGs_Metabolites	502	185	0 793(0 742 - 0 844)	0 792 +/- 0 029
three levels	ref3	ref	ref_GPS_CpGs	507	186	0 785(0 72 - 0 84)	0 778 +/- 0 033
three levels	ref3	ref + GPS	ref_GPS_CpGs	507	186	0 804(0 743 - 0 852)	0 801 +/- 0 03
three levels	ref3	ref + GPS + 1omics	ref_GPS_CpGs	507	186	0 796(0 728 - 0 842)	0 793 +/- 0 031
five levels	ref3	ref	ref_GPS_CpGs_Proteins_Metabolites	390	144	0 729(0 648 - 0 798)	0 726 +/- 0 041
five levels	ref3	ref + GPS	ref_GPS_CpGs_Proteins_Metabolites	390	144	0 755(0 667 - 0 817)	0 756 +/- 0 039
five levels	ref3	ref + GPS + 1omics	ref_GPS_CpGs_Proteins_Metabolites	390	144	0 765(0 686 - 0 848)	0 764 +/- 0 042
five levels	ref3	ref + GPS + 2omics	ref_GPS_CpGs_Proteins_Metabolites	390	144	0 768(0 672 - 0 85)	0 762 +/- 0 041
five levels	ref3	ref + GPS + 3omics	ref_GPS_CpGs_Proteins_Metabolites	390	144	0 758(0 683 - 0 817)	0 759 +/- 0 035
three levels	ref3	ref	ref_GPS_Proteins	418	155	0 731(0 65 - 0 793)	0 731 +/- 0 038
three levels	ref3	ref + GPS	ref_GPS_Proteins	418	155	0 764(0 682 - 0 83)	0 765 +/- 0 039
three levels	ref3	ref + GPS + 1omics	ref_GPS_Proteins	418	155	0 782(0 695 - 0 847)	0 778 +/- 0 037
four levels	ref3	ref	ref_GPS_Proteins_Metabolites	413	154	0 731(0 642 - 0 794)	0 729 +/- 0 041
four levels	ref3	ref + GPS	ref_GPS_Proteins_Metabolites	413	154	0 759(0 675 - 0 822)	0 76 +/- 0 04
four levels	ref3	ref + GPS + 1omics	ref_GPS_Proteins_Metabolites	413	154	0 772(0 696 - 0 842)	0 769 +/- 0 038
four levels	ref3	ref + GPS + 2omics	ref_GPS_Proteins_Metabolites	413	154	0 785(0 719 - 0 842)	0 781 +/- 0 034
three levels	ref3	ref	ref_GPS_RNAs	247	90	0 77(0 693 - 0 863)	0 773 +/- 0 042
three levels	ref3	ref + GPS	ref_GPS_RNAs	247	90	0 79(0 714 - 0 859)	0 788 +/- 0 039
three levels	ref3	ref + GPS + 1omics	ref_GPS_RNAs	247	90	0 789(0 711 - 0 853)	0 786 +/- 0 04
two levels	ref3	ref	ref_CpGs	558	205	0 775(0 713 - 0 826)	0 772 +/- 0 031
two levels	ref3	ref + 1omics	ref_CpGs	558	205	0 779(0 716 - 0 834)	0 777 +/- 0 031
two levels	ref3	ref	ref_Proteins	440	163	0 719(0 631 - 0 778)	0 718 +/- 0 039
two levels	ref3	ref + 1omics	ref_Proteins	440	163	0 762(0 69 - 0 827)	0 76 +/- 0 037
two levels	ref3	ref	ref_RNAs	277	102	0 766(0 68 - 0 854)	0 767 +/- 0 041
two levels	ref3	ref + 1omics	ref_RNAs	277	102	0 778(0 699 - 0 866)	0 777 +/- 0 041
two levels	ref4	ref	ref_Metabolites	744	274	0 826(0 775 - 0 856)	0 821 +/- 0 023
two levels	ref4	ref + 1omics	ref_Metabolites	744	274	0 818(0 778 - 0 86)	0 82 +/- 0 024
two levels	ref4	ref	ref_GPS	673	248	0 826(0 779 - 0 864)	0 823 +/- 0 024
two levels	ref4	ref + 1omics	ref_GPS	673	248	0 832(0 784 - 0 878)	0 831 +/- 0 026
three levels	ref4	ref	ref_GPS_Metabolites	673	248	0 826(0 779 - 0 864)	0 823 +/- 0 024
three levels	ref4	ref + GPS	ref_GPS_Metabolites	673	248	0 832(0 784 - 0 878)	0 831 +/- 0 026
three levels	ref4	ref + GPS + 1omics	ref_GPS_Metabolites	673	248	0 833(0 786 - 0 869)	0 83 +/- 0 023
four levels	ref4	ref	ref_GPS_CpGs_Metabolites	502	185	0 8(0 743 - 0 851)	0 799 +/- 0 027
four levels	ref4	ref + GPS	ref_GPS_CpGs_Metabolites	502	185	0 811(0 757 - 0 859)	0 807 +/- 0 027
four levels	ref4	ref + GPS + 1omics	ref_GPS_CpGs_Metabolites	502	185	0 803(0 753 - 0 856)	0 802 +/- 0 029
four levels	ref4	ref + GPS + 2omics	ref_GPS_CpGs_Metabolites	502	185	0 802(0 751 - 0 846)	0 804 +/- 0 026
three levels	ref4	ref	ref_GPS_CpGs	502	185	0 8(0 743 - 0 851)	0 799 +/- 0 027
three levels	ref4	ref + GPS	ref_GPS_CpGs	502	185	0 811(0 757 - 0 859)	0 807 +/- 0 027
three levels	ref4	ref + GPS + 1omics	ref_GPS_CpGs	502	185	0 804(0 742 - 0 862)	0 801 +/- 0 03

five levels	ref4	ref	ref_GPS_CpGs_Proteins_Metabolites	390	144	0.777(0.68 - 0.846)	0.775 +/- 0.039
five levels	ref4	ref + GPS	ref_GPS_CpGs_Proteins_Metabolites	390	144	0.783(0.694 - 0.849)	0.781 +/- 0.04
five levels	ref4	ref + GPS + 1omics	ref_GPS_CpGs_Proteins_Metabolites	390	144	0.779(0.695 - 0.836)	0.777 +/- 0.037
five levels	ref4	ref + GPS + 2omics	ref_GPS_CpGs_Proteins_Metabolites	390	144	0.774(0.673 - 0.83)	0.769 +/- 0.04
five levels	ref4	ref + GPS + 3omics	ref_GPS_CpGs_Proteins_Metabolites	390	144	0.77(0.658 - 0.832)	0.766 +/- 0.048
three levels	ref4	ref	ref_GPS_Proteins	413	154	0.783(0.694 - 0.838)	0.779 +/- 0.039
three levels	ref4	ref + GPS	ref_GPS_Proteins	413	154	0.785(0.696 - 0.853)	0.785 +/- 0.04
three levels	ref4	ref + GPS + 1omics	ref_GPS_Proteins	413	154	0.784(0.702 - 0.852)	0.783 +/- 0.038
four levels	ref4	ref	ref_GPS_Proteins_Metabolites	413	154	0.783(0.694 - 0.838)	0.779 +/- 0.039
four levels	ref4	ref + GPS	ref_GPS_Proteins_Metabolites	413	154	0.785(0.696 - 0.853)	0.785 +/- 0.04
four levels	ref4	ref + GPS + 1omics	ref_GPS_Proteins_Metabolites	413	154	0.787(0.705 - 0.852)	0.784 +/- 0.038
four levels	ref4	ref + GPS + 2omics	ref_GPS_Proteins_Metabolites	413	154	0.782(0.717 - 0.837)	0.783 +/- 0.037
three levels	ref4	ref	ref_GPS_RNAs	243	89	0.787(0.716 - 0.865)	0.788 +/- 0.038
three levels	ref4	ref + GPS	ref_GPS_RNAs	243	89	0.797(0.728 - 0.867)	0.797 +/- 0.037
three levels	ref4	ref + GPS + 1omics	ref_GPS_RNAs	243	89	0.79(0.708 - 0.853)	0.788 +/- 0.041
two levels	ref4	ref	ref_CpGs	553	203	0.805(0.756 - 0.853)	0.801 +/- 0.026
two levels	ref4	ref + 1omics	ref_CpGs	553	203	0.795(0.74 - 0.846)	0.793 +/- 0.028
two levels	ref4	ref	ref_Proteins	436	161	0.781(0.687 - 0.833)	0.775 +/- 0.039
two levels	ref4	ref + 1omics	ref_Proteins	436	161	0.776(0.686 - 0.844)	0.77 +/- 0.041
two levels	ref4	ref	ref_RNAs	274	100	0.786(0.721 - 0.859)	0.789 +/- 0.036
two levels	ref4	ref + 1omics	ref_RNAs	274	100	0.782(0.72 - 0.855)	0.785 +/- 0.036

Supplementary Table 28. The mean value of coefficients and the selected times and frequency of the top five selected candidates for each combination in four reference sets over 100 times of bootstrapping.

Over 100 times of bootstrapping, the mean value of coefficients, the selected times and frequency of the top five selected features using priority lasso for each omics combination in each reference set are presented. ref₁: baseline age, sex; ref₂: baseline age, sex, BMI, systolic blood pressure, smoking status, triglyceride, total cholesterol, HDL cholesterol, fasting glucose, use of lipid lowering drugs, antihypertensive and anti-diabetic medication; ref₃: baseline age, sex, eGFR and UACR; ref₄: baseline age, eGFR, UACR, total cholesterol, fasting glucose, SM C18:1 and PC aa C38:0.

Abbreviations: GPS, genome wide polygenic score of eGFR values; CKD, chronic kidney disease; eGFR, estimated glomerular filtration rate; UACR, urinary albumin-to-creatinine ratio.

num.omics levels.				Selected.	Selected.		
combine	ref	combination	Predictor	mean.coef	Times	rate	rank
two levels	ref1	ref_CpGs	NAPA	-0.113	52	0.52	1
two levels	ref1	ref_CpGs	LYL1	-0.077	40	0.4	2
two levels	ref1	ref_CpGs	NEURL3	0.055	30	0.3	3
two levels	ref1	ref_CpGs	ACSL1	-0.01	28	0.28	4
two levels	ref1	ref_CpGs	CCDC39	0.062	26	0.26	5
two levels	ref1	ref_RNAs	PNLIPRP2	-0.156	55	0.55	1
two levels	ref1	ref_RNAs	NKD2	0.085	25	0.25	2
two levels	ref1	ref_RNAs	ARG1	0.051	20	0.2	3
two levels	ref1	ref_RNAs	TFE3	-0.104	19	0.19	4
two levels	ref1	ref_RNAs	DUSP11	-0.124	16	0.16	5
two levels	ref1	ref_Proteins	CST3	0.211	90	0.9	1
two levels	ref1	ref_Proteins	EGFR	-0.1	44	0.44	2
two levels	ref1	ref_Proteins	TFF3	0.092	34	0.34	3
two levels	ref1	ref_Proteins	B2M	0.096	26	0.26	4
two levels	ref1	ref_Proteins	MAPK12	0.11	21	0.21	5
two levels	ref1	ref_Metabolites	C5	0.148	79	0.79	1
two levels	ref1	ref_Metabolites	C18:1	0.109	60	0.6	2
two levels	ref1	ref_Metabolites	PC aa C38:0	0.106	54	0.54	3
two levels	ref1	ref_Metabolites	C12	0.118	45	0.45	4
two levels	ref1	ref_Metabolites	Tyr	-0.062	26	0.26	5
three levels	ref1	ref_GPS_CpGs	NAPA	-0.097	44	0.44	1
three levels	ref1	ref_GPS_CpGs	ACSL1	-0.083	39	0.39	2
three levels	ref1	ref_GPS_CpGs	LYL1	-0.101	36	0.36	3
three levels	ref1	ref_GPS_CpGs	TLN2	0.07	29	0.29	4
three levels	ref1	ref_GPS_CpGs	NEURL3	0.086	24	0.24	5
three levels	ref1	ref_GPS_RNAs	PNLIPRP2	-0.139	40	0.4	1
three levels	ref1	ref_GPS_RNAs	TFE3	-0.138	27	0.27	2
three levels	ref1	ref_GPS_RNAs	DUSP11	-0.117	23	0.23	3
three levels	ref1	ref_GPS_RNAs	PAX8	-0.098	20	0.2	4
three levels	ref1	ref_GPS_RNAs	ABCB1	-0.098	19	0.19	5
three levels	ref1	ref_GPS_Proteins	CST3	0.171	74	0.74	1
three levels	ref1	ref_GPS_Proteins	EGFR	-0.129	68	0.68	2
three levels	ref1	ref_GPS_Proteins	TFF3	0.102	32	0.32	3
three levels	ref1	ref_GPS_Proteins	FGF20	-0.096	26	0.26	4
three levels	ref1	ref_GPS_Proteins	MAPK12	0.12	25	0.25	5
three levels	ref1	ref_GPS_Metabolites	C5	0.193	90	0.9	1
three levels	ref1	ref_GPS_Metabolites	C18:1	0.13	71	0.71	2
three levels	ref1	ref_GPS_Metabolites	C6(C4:1-DC)	0.104	40	0.4	3
three levels	ref1	ref_GPS_Metabolites	C8:1	0.069	37	0.37	4
three levels	ref1	ref_GPS_Metabolites	C12	0.074	28	0.28	5
four levels	ref1	ref_GPS_Proteins_Me tabolites	CST3	0.167	64	0.64	1
four levels	ref1	ref_GPS_Proteins_Me tabolites	EGFR	-0.148	59	0.59	2
four levels	ref1	ref_GPS_Proteins_Me tabolites	C5	0.146	45	0.45	3

four levels	ref1	ref_GPS_Proteins_Metabolites	C18:1	0.14	43	0.43	4
four levels	ref1	ref_GPS_Proteins_Metabolites	C6(C4:1-DC)	0.155	39	0.39	5
four levels	ref1	ref_GPS_CpGs_Metabolites	C5	0.194	76	0.76	1
four levels	ref1	ref_GPS_CpGs_Metabolites	LYL1	-0.128	44	0.44	2
four levels	ref1	ref_GPS_CpGs_Metabolites	ACSL1	-0.094	38	0.38	3
four levels	ref1	ref_GPS_CpGs_Metabolites	NAPA	-0.103	37	0.37	4
four levels	ref1	ref_GPS_CpGs_Metabolites	TLN2	0.097	30	0.3	5
five levels	ref1	ref_GPS_CpGs_Proteins_Metabolites	CST3	0.167	86	0.86	1
five levels	ref1	ref_GPS_CpGs_Proteins_Metabolites	LYL1	-0.166	64	0.64	2
five levels	ref1	ref_GPS_CpGs_Proteins_Metabolites	EGFR	-0.125	57	0.57	3
five levels	ref1	ref_GPS_CpGs_Proteins_Metabolites	C5	0.155	42	0.42	4
five levels	ref1	ref_GPS_CpGs_Proteins_Metabolites	C6(C4:1-DC)	0.174	39	0.39	5
two levels	ref2	ref_CpGs	NAPA	-0.115	50	0.5	1
two levels	ref2	ref_CpGs	LYL1	-0.103	36	0.36	2
two levels	ref2	ref_CpGs	NEURL3	0.067	30	0.3	3
two levels	ref2	ref_CpGs	LYSMD2	-0.044	30	0.3	4
two levels	ref2	ref_CpGs	TLN2	-0.001	29	0.29	5
two levels	ref2	ref_RNAs	PNLIPRP2	-0.18	53	0.53	1
two levels	ref2	ref_RNAs	TFE3	-0.118	32	0.32	2
two levels	ref2	ref_RNAs	PCGF2	0.084	30	0.3	3
two levels	ref2	ref_RNAs	DUSP11	-0.147	26	0.26	4
two levels	ref2	ref_RNAs	ARG1	0.032	24	0.24	5
two levels	ref2	ref_Proteins	CST3	0.136	66	0.66	1
two levels	ref2	ref_Proteins	GHR	-0.109	44	0.44	2
two levels	ref2	ref_Proteins	EGFR	-0.087	32	0.32	3
two levels	ref2	ref_Proteins	FGF20	-0.118	29	0.29	4
two levels	ref2	ref_Proteins	MAPK12	0.097	22	0.22	5
two levels	ref2	ref_Metabolites	PC aa C38:0	0.162	85	0.85	1
two levels	ref2	ref_Metabolites	C12	0.12	56	0.56	2
two levels	ref2	ref_Metabolites	C18:1	0.105	55	0.55	3
two levels	ref2	ref_Metabolites	C5	0.112	50	0.5	4
two levels	ref2	ref_Metabolites	SMC18:1	0.069	27	0.27	5
three levels	ref2	ref_GPS_CpGs	NAPA	-0.118	40	0.4	1
three levels	ref2	ref_GPS_CpGs	ACSL1	-0.075	33	0.33	2
three levels	ref2	ref_GPS_CpGs	LYL1	-0.116	31	0.31	3
three levels	ref2	ref_GPS_CpGs	TLN2	0.063	26	0.26	4
three levels	ref2	ref_GPS_CpGs	NEURL3	0.096	24	0.24	5
three levels	ref2	ref_GPS_RNAs	PNLIPRP2	-0.141	44	0.44	1

three levels	ref2	ref_GPS_RNAs	DUSP11	-0.143	43	0.43	2
three levels	ref2	ref_GPS_RNAs	TFE3	-0.143	37	0.37	3
three levels	ref2	ref_GPS_RNAs	PCGF2	0.095	23	0.23	4
three levels	ref2	ref_GPS_RNAs	ABCB1	-0.082	19	0.19	5
three levels	ref2	ref_GPS_Proteins	EGFR	-0.127	58	0.58	1
three levels	ref2	ref_GPS_Proteins	CST3	0.117	54	0.54	2
three levels	ref2	ref_GPS_Proteins	GHR	-0.109	54	0.54	3
three levels	ref2	ref_GPS_Proteins	MAPK12	0.11	32	0.32	4
three levels	ref2	ref_GPS_Proteins	FGF20	-0.108	30	0.3	5
three levels	ref2	ref_GPS_Metabolites	C18:1	0.124	64	0.64	1
three levels	ref2	ref_GPS_Metabolites	C5	0.161	64	0.64	2
three levels	ref2	ref_GPS_Metabolites	PC aa C38:0	0.11	45	0.45	3
three levels	ref2	ref_GPS_Metabolites	SM C18:1	0.094	38	0.38	4
three levels	ref2	ref_GPS_Metabolites	C12	0.093	37	0.37	5
four levels	ref2	ref_GPS_Proteins_Metabolites	EGFR	-0.115	56	0.56	1
four levels	ref2	ref_GPS_Proteins_Metabolites	CST3	0.1	47	0.47	2
four levels	ref2	ref_GPS_Proteins_Metabolites	GHR	-0.12	41	0.41	3
four levels	ref2	ref_GPS_Proteins_Metabolites	MAPK12	0.11	35	0.35	4
four levels	ref2	ref_GPS_Proteins_Metabolites	FGF20	-0.118	30	0.3	5
four levels	ref2	ref_GPS_CpGs_Metabolites	C5	0.151	60	0.6	1
four levels	ref2	ref_GPS_CpGs_Metabolites	NAPA	-0.112	40	0.4	2
four levels	ref2	ref_GPS_CpGs_Metabolites	LYL1	-0.128	37	0.37	3
four levels	ref2	ref_GPS_CpGs_Metabolites	ACSL1	-0.075	33	0.33	4
four levels	ref2	ref_GPS_CpGs_Metabolites	C12	0.114	31	0.31	5
five levels	ref2	ref_GPS_CpGs_Proteins_Metabolites	CST3	0.111	54	0.54	1
five levels	ref2	ref_GPS_CpGs_Proteins_Metabolites	LYL1	-0.181	49	0.49	2
five levels	ref2	ref_GPS_CpGs_Proteins_Metabolites	EGFR	-0.127	48	0.48	3
five levels	ref2	ref_GPS_CpGs_Proteins_Metabolites	NAPA	-0.102	32	0.32	4
five levels	ref2	ref_GPS_CpGs_Proteins_Metabolites	GHR	-0.115	32	0.32	5
two levels	ref3	ref_CpGs	LYL1	-0.101	47	0.47	1
two levels	ref3	ref_CpGs	NAPA	-0.091	45	0.45	2
two levels	ref3	ref_CpGs	TLN2	0.082	33	0.33	3
two levels	ref3	ref_CpGs	NEURL3	0.039	30	0.3	4
two levels	ref3	ref_CpGs	ACSL1	0.055	29	0.29	5
two levels	ref3	ref_RNAs	PNLIPRP2	-0.162	36	0.36	1
two levels	ref3	ref_RNAs	TFE3	-0.096	21	0.21	2

two levels	ref3	ref_RNAs	SLC22A4	-0.07	20	0.2	3
two levels	ref3	ref_RNAs	AGK	-0.158	20	0.2	4
two levels	ref3	ref_RNAs	PCGF2	0.099	19	0.19	5
two levels	ref3	ref_Proteins	GHR	-0.135	39	0.39	1
two levels	ref3	ref_Proteins	IL2	0.1	21	0.21	2
two levels	ref3	ref_Proteins	TFF3	0.1	21	0.21	3
two levels	ref3	ref_Proteins	FGF20	-0.062	20	0.2	4
two levels	ref3	ref_Proteins	SPINT1	0.056	16	0.16	5
two levels	ref3	ref_Metabolites	PC aa C38:0	0.147	76	0.76	1
two levels	ref3	ref_Metabolites	Tyr	-0.103	38	0.38	2
two levels	ref3	ref_Metabolites	C12	0.116	37	0.37	3
two levels	ref3	ref_Metabolites	C5	0.111	35	0.35	4
two levels	ref3	ref_Metabolites	C18:1	0.086	27	0.27	5
three levels	ref3	ref_GPS_CpGs	LYL1	-0.103	57	0.57	1
three levels	ref3	ref_GPS_CpGs	TLN2	0.1	43	0.43	2
three levels	ref3	ref_GPS_CpGs	NAPA	-0.091	35	0.35	3
three levels	ref3	ref_GPS_CpGs	NEURL3	0.007	31	0.31	4
three levels	ref3	ref_GPS_CpGs	LYSMD2	0.084	31	0.31	5
three levels	ref3	ref_GPS_RNAs	AGK	-0.16	35	0.35	1
three levels	ref3	ref_GPS_RNAs	DUSP11	-0.126	32	0.32	2
three levels	ref3	ref_GPS_RNAs	PNLIPRP2	-0.132	27	0.27	3
three levels	ref3	ref_GPS_RNAs	PCGF2	0.117	23	0.23	4
three levels	ref3	ref_GPS_RNAs	TFE3	-0.141	22	0.22	5
three levels	ref3	ref_GPS_Proteins	GHR	-0.137	46	0.46	1
three levels	ref3	ref_GPS_Proteins	FGF20	-0.064	27	0.27	2
three levels	ref3	ref_GPS_Proteins	IL2	0.091	23	0.23	3
three levels	ref3	ref_GPS_Proteins	MAPK12	0.093	21	0.21	4
three levels	ref3	ref_GPS_Proteins	TFF3	0.078	19	0.19	5
three levels	ref3	ref_GPS_Metabolites	C5	0.16	46	0.46	1
three levels	ref3	ref_GPS_Metabolites	PC aa C38:0	0.132	43	0.43	2
three levels	ref3	ref_GPS_Metabolites	Tyr	-0.118	39	0.39	3
three levels	ref3	ref_GPS_Metabolites	C18:1	0.115	33	0.33	4
three levels	ref3	ref_GPS_Metabolites	C6(C4:1-DC)	0.096	33	0.33	5
four levels	ref3	ref_GPS_Proteins_Metabolites	GHR	-0.139	41	0.41	1
four levels	ref3	ref_GPS_Proteins_Metabolites	PC aa C38:0	0.156	32	0.32	2
four levels	ref3	ref_GPS_Proteins_Metabolites	C5	0.13	31	0.31	3
four levels	ref3	ref_GPS_Proteins_Metabolites	C6(C4:1-DC)	0.133	25	0.25	4
four levels	ref3	ref_GPS_Proteins_Metabolites	C8:1	0.139	25	0.25	5

four levels	ref3	ref_GPS_CpGs_Metabolites	LYL1	-0.137	57	0.57	1
four levels	ref3	ref_GPS_CpGs_Metabolites	C5	0.152	49	0.49	2
four levels	ref3	ref_GPS_CpGs_Metabolites	Tyr	-0.144	47	0.47	3
four levels	ref3	ref_GPS_CpGs_Metabolites	PC aa C38:0	0.124	44	0.44	4
four levels	ref3	ref_GPS_CpGs_Metabolites	TLN2	0.122	43	0.43	5
five levels	ref3	ref_GPS_CpGs_Proteins_Metabolites	LYL1	-0.191	67	0.67	1
five levels	ref3	ref_GPS_CpGs_Proteins_Metabolites	GHR	-0.143	47	0.47	2
five levels	ref3	ref_GPS_CpGs_Proteins_Metabolites	NAPA	-0.061	38	0.38	3
five levels	ref3	ref_GPS_CpGs_Proteins_Metabolites	LYSMD2	0.112	34	0.34	4
five levels	ref3	ref_GPS_CpGs_Proteins_Metabolites	NEURL3	0.039	31	0.31	5
two levels	ref4	ref_CpGs	LYL1	-0.1	45	0.45	1
two levels	ref4	ref_CpGs	TLN2	0.081	31	0.31	2
two levels	ref4	ref_CpGs	NEURL3	0.02	27	0.27	3
two levels	ref4	ref_CpGs	LYSMD2	0.062	27	0.27	4
two levels	ref4	ref_CpGs	NAPA	-0.072	25	0.25	5
two levels	ref4	ref_RNAs	PNLIPRP2	-0.158	47	0.47	1
two levels	ref4	ref_RNAs	NKD2	0.082	28	0.28	2
two levels	ref4	ref_RNAs	DUSP11	-0.097	26	0.26	3
two levels	ref4	ref_RNAs	PCGF2	0.1	23	0.23	4
two levels	ref4	ref_RNAs	TFE3	-0.108	20	0.2	5
two levels	ref4	ref_Proteins	GHR	-0.132	44	0.44	1
two levels	ref4	ref_Proteins	FGF20	-0.091	39	0.39	2
two levels	ref4	ref_Proteins	SPINT1	0.101	24	0.24	3
two levels	ref4	ref_Proteins	IL2	0.106	19	0.19	4
two levels	ref4	ref_Proteins	MAPK12	0.092	17	0.17	5
two levels	ref4	ref_Metabolites	C12	0.152	53	0.53	1
two levels	ref4	ref_Metabolites	C5	0.11	43	0.43	2
two levels	ref4	ref_Metabolites	C10:2	-0.13	40	0.4	3
two levels	ref4	ref_Metabolites	C18:1	0.092	39	0.39	4
two levels	ref4	ref_Metabolites	Tyr	-0.109	39	0.39	5
three levels	ref4	ref_GPS_CpGs	LYL1	-0.147	46	0.46	1
three levels	ref4	ref_GPS_CpGs	NEURL3	-0.017	30	0.3	2
three levels	ref4	ref_GPS_CpGs	ACSL1	-0.021	28	0.28	3
three levels	ref4	ref_GPS_CpGs	NAPA	-0.073	28	0.28	4
three levels	ref4	ref_GPS_CpGs	TLN2	0.123	24	0.24	5
three levels	ref4	ref_GPS_RNAs	PNLIPRP2	-0.145	37	0.37	1
three levels	ref4	ref_GPS_RNAs	DUSP11	-0.155	37	0.37	2
three levels	ref4	ref_GPS_RNAs	AGK	-0.138	36	0.36	3

three levels	ref4	ref_GPS_RNAs	TFE3	-0.127	24	0.24	4
three levels	ref4	ref_GPS_RNAs	PCGF2	0.13	24	0.24	5
three levels	ref4	ref_GPS_Proteins	GHR	-0.167	43	0.43	1
three levels	ref4	ref_GPS_Proteins	FGF20	-0.108	35	0.35	2
three levels	ref4	ref_GPS_Proteins	SPINT1	0.121	21	0.21	3
three levels	ref4	ref_GPS_Proteins	IL6	0.122	18	0.18	4
three levels	ref4	ref_GPS_Proteins	IL2	0.107	17	0.17	5
three levels	ref4	ref_GPS_Metabolites	C5	0.154	54	0.54	1
three levels	ref4	ref_GPS_Metabolites	Tyr	-0.123	45	0.45	2
three levels	ref4	ref_GPS_Metabolites	C18:1	0.12	37	0.37	3
three levels	ref4	ref_GPS_Metabolites	C6(C4:1-DC)	0.117	32	0.32	4
three levels	ref4	ref_GPS_Metabolites	C12	0.121	31	0.31	5
four levels	ref4	ref_GPS_Proteins_Metabolites	GHR	-0.162	46	0.46	1
four levels	ref4	ref_GPS_Proteins_Metabolites	FGF20	-0.096	41	0.41	2
four levels	ref4	ref_GPS_Proteins_Metabolites	C5	0.18	31	0.31	3
four levels	ref4	ref_GPS_Proteins_Metabolites	C6(C4:1-DC)	0.131	27	0.27	4
four levels	ref4	ref_GPS_Proteins_Metabolites	C8	0.139	25	0.25	5
four levels	ref4	ref_GPS_CpGs_Metabolites	LYL1	-0.133	51	0.51	1
four levels	ref4	ref_GPS_CpGs_Metabolites	C5	0.169	50	0.5	2
four levels	ref4	ref_GPS_CpGs_Metabolites	Tyr	-0.116	49	0.49	3
four levels	ref4	ref_GPS_CpGs_Metabolites	C10:2	-0.122	30	0.3	4
four levels	ref4	ref_GPS_CpGs_Metabolites	C12	0.118	30	0.3	5
five levels	ref4	ref_GPS_CpGs_Proteins_Metabolites	LYL1	-0.168	56	0.56	1
five levels	ref4	ref_GPS_CpGs_Proteins_Metabolites	GHR	-0.156	44	0.44	2
five levels	ref4	ref_GPS_CpGs_Proteins_Metabolites	FGF20	-0.099	39	0.39	3
five levels	ref4	ref_GPS_CpGs_Proteins_Metabolites	C6(C4:1-DC)	0.163	32	0.32	4
five levels	ref4	ref_GPS_CpGs_Proteins_Metabolites	NEURL3	0.015	32	0.32	5

Supplementary Table 29. Predictive improvement of GPS_{eGFR} on top of four reference sets for incident CKD_{crcc} in hyperglycemic individuals of KORA F4.

Over 100 times of bootstrapping, the mean (\pm SD) and median AUC (95% CI) of predictive models built with ref and ref + GPS for incident CKD_{crcc} in hyperglycemic individuals of KORA F4 are shown, respectively. The ref included ref1-4. AUC values were calculated with random forest using testing data.

ref₁: baseline age, sex; ref₂: baseline age, sex, BMI, systolic blood pressure, smoking status, triglyceride, total cholesterol, HDL cholesterol, fasting glucose, use of lipid lowering drugs, antihypertensive and anti-diabetic medication; ref₃: baseline age, sex, eGFR and UACR; ref₄: baseline age, eGFR, UACR, total cholesterol, fasting glucose, SM C18:1 and PC aa C38:0.

Abbreviations: AUC, area under the receiver operating characteristic curve; GPS, genome wide polygenic score of eGFR values; CKD, chronic kidney disease; eGFR, estimated glomerular filtration rate; UACR, urinary albumin-to-creatinine ratio; CKD_{crcc}, eGFR-based CKD that was defined as eGFR < 60 ml/min/1.73 m².

ref	Model	mean.Sample Size.train	mean.Sample Size.test	median.95CI.AUC.test	mean.SD.AUC.test
ref1	ref	680	251	0.745(0.663 - 0.815)	0.742 +/- 0.037
ref1	ref + GPS	680	251	0.804(0.739 - 0.855)	0.805 +/- 0.029
ref2	ref	677	250	0.767(0.703 - 0.824)	0.762 +/- 0.033
ref2	ref + GPS	677	250	0.801(0.746 - 0.839)	0.8 +/- 0.027
ref3	ref	680	251	0.857(0.811 - 0.906)	0.857 +/- 0.023
ref3	ref + GPS	680	251	0.876(0.838 - 0.917)	0.877 +/- 0.021
ref4	ref	673	248	0.863(0.819 - 0.905)	0.864 +/- 0.025
ref4	ref + GPS	673	248	0.88(0.828 - 0.919)	0.876 +/- 0.024

Supplementary Table 30. The various combinations of variables used in exploring subgrouping KORA F4 CKD patients with hyperglycemia.

combination	variables in each combination
combination1	eGFR,UACR
combination2	eGFR,UACR,GPS
combination3	eGFR,UACR,GPS,C10,C10:2,C12,C14:1,C14:1-OH,C14:2,C16,C18:1,C2,C6(C4:1-DC),C5,C8,C8:1,TLN2,ACSL1,CCDC39,LYL1,NEURL3,LYSMD2,NAPA,PAX8,SLC22A4,PNLIPRP2,NKD2,DUSP11,TFE3,AGK,MCM3,PCGF2,TTF2,ABCB1,ARG1,SLC25A4,CDC14A,Tyr,PLAT,IGFBP2,CST3,EFNA5,ERBB3,LAYN,TNFRSF1A,EGFR,IGFBP6,FGF20,FGF9,SPINT1,NBL1,GHR,CGA LHB,ESAM,JAM2,CLEC4M,IL19,RETN,IL2,TNFRSF1B,ADAMTS13,RET,ACY1,BMP1,CTSV,FN1,FSTL3,B2M,ADIPOQ,CNDP1,MASP1,IL22RA1,KDR,IGF2R,PLG,CTSH,FCN3,RPS6KA5,MED1,PAPPA,IL6,TFF3,EPHA2,NTRK2,AMH,MMP1,C1QBP,ERP29,MAPK12,SOD2,KIR2DL4,NOTCH1,RELT,SCARF1,TNFRSF19,HAVCR2,UNC5C,SEMA3E,LEPR,SPOCK2,PC aa C38:0,SM C18:1
combination4	C10,C10:2,C12,C14:1,C14:1-OH,C14:2,C16,C18:1,C2,C6(C4:1-DC),C5,C8,C8:1,Tyr,PLAT,IGFBP2,CST3,EFNA5,ERBB3,LAYN,TNFRSF1A,EGFR,IGFBP6,FGF20,FGF9,SPINT1,NBL1,GHR,CGA LHB,ESAM,JAM2,CLEC4M,IL19,RETN,IL2,TNFRSF1B,ADAMTS13,RET,ACY1,BMP1,CTSV,FN1,FSTL3,B2M,ADIPOQ,CNDP1,MASP1,IL22RA1,KDR,IGF2R,PLG,CTSH,FCN3,RPS6KA5,MED1,PAPPA,IL6,TFF3,EPHA2,NTRK2,AMH,MMP1,C1QBP,ERP29,MAPK12,SOD2,KIR2DL4,NOTCH1,RELT,SCARF1,TNFRSF19,HAVCR2,UNC5C,SEMA3E,LEPR,SPOCK2
combination5	C10,C10:2,C12,C14:1,C14:1-OH,C14:2,C16,C18:1,C2,C6(C4:1-DC),C5,C8,C8:1,Tyr
combination6	C14:1,C16,C18:1,NKD2,DUSP11,TFE3,MCM3,TTF2,ABCB1,ARG1,SLC25A4,Tyr,IGFBP2,ERBB3,EGFR,SPINT1,GHR,CLEC4M,CTSV,FN1,CNDP1,KDR,FCN3,RPS6KA5,MED1,NTRK2,AMH,ERP29,MAPK12,SOD2,NOTCH1
combination7	Tyr,ERBB3
combination8	C14:1,C16,C18:1,NKD2,DUSP11,TFE3,MCM3,TTF2,ABCB1,ARG1,SLC25A4,IGFBP2,EGFR,SPINT1,GHR,CLEC4M,CTSV,FN1,CNDP1,KDR,FCN3,RPS6KA5,MED1,NTRK2,AMH,ERP29,MAPK12,SOD2,NOTCH1
combination9	C10,C10:2,C12,C14:1-OH,C14:2,C2,C6(C4:1-DC),C5,C8,C8:1,AGK,PLAT,CST3,EFNA5,LAYN,TNFRSF1A,IGFBP6,FGF20,FGF9,NBL1,CGA LHB,ESAM,JAM2,IL19,RETN,IL2,TNFRSF1B,ADAMTS13,RET,ACY1,BMP1,FSTL3,B2M,MASP1,IGF2R,PLG,CTSH,PAPPA,IL6,TFF3,EPHA2,MMP1,C1QBP,KIR2DL4,RELT,SCARF1,TNFRSF19,HAVCR2,UNC5C,LEPR,SPOCK2
combination10	C10,C10:2,C12,C14:1-OH,C14:2,C2,C8,C8:1,CST3,TNFRSF1A,IGFBP6,NBL1,JAM2,IL19,RETN,TNFRSF1B,ADAMTS13,FSTL3,B2M,CTSH,MMP1,RELT,SCARF1,TNFRSF19,UNC5C,SPOCK2
combination11	C6(C4:1-DC),C5,AGK,PLAT,EFNA5,LAYN,FGF20,FGF9,CGA LHB,ESAM,IL2,RET,ACY1,BMP1,MASP1,IGF2R,PLG,PAPPA,IL6,TFF3,EPHA2,C1QBP,KIR2DL4,HAVCR2,LEPR
combination12	TLN2,ACSL1,CCDC39,LYL1,NEURL3,LYSMD2,NAPA,SLC22A4,PCGF2,CDC14A,SEMA3E
combination13	GPS,C10,C10:2,C12,C14:1,C14:1-OH,C14:2,C16,C18:1,C2,C6(C4:1-DC),C5,C8,C8:1,TLN2,ACSL1,CCDC39,LYL1,NEURL3,LYSMD2,NAPA,PAX8,SLC22A4,PNLIPRP2,NKD2,DUSP11,TFE3,AGK,MCM3,PCGF2,TTF2,ABCB1,ARG1,SLC25A4,CDC14A,Tyr,PLAT,IGFBP2,CST3,EFNA5,ERBB3,LAYN,TNFRSF1A,EGFR,IGFBP6,FGF20,FGF9,SPINT1,NBL1,GHR,CGA LHB,ESAM,JAM2,CLEC4M,IL19,RETN,IL2,TNFRSF1B,ADAMTS13,RET,ACY1,BMP1,CTSV,FN1,FSTL3,B2M,ADIPOQ,CNDP1,MASP1,IL22RA1,KDR,IGF2R,PLG,CTSH,FCN3,RPS6KA5,MED1,PAPPA,IL6,TFF3,EPHA2,NTRK2,AMH,MMP1,C1QBP,ERP29,MAPK12,SOD2,KIR2DL4,NOTCH1,RELT,SCARF1,TNFRSF19,HAVCR2,UNC5C,SEMA3E,LEPR,SPOCK2,PC aa C38:0,SM C18:1

combination14	C10,C10:2,C12,C14:1,C14:1-OH,C14:2,C16,C18:1,C2,C6(C4:1-DC),C5,C8,C8:1,TLN2,ACSL1,CCDC39,LYL1,NEURL3,LYSMD2,NAPA,PAX8,SLC22A4,PNLIPRP2,NKD2,DUSP11,TFE3,AGK,MCM3,PCGF2,TTF2,ABCB1,ARG1,SLC25A4,CDC14A,Tyr,PLAT,IGFBP2,CST3,EFNA5,ERBB3,LAYN,TNFRSF1A,EGFR,IGFBP6,FGF20,FGF9,SPINT1,NBL1,GHR,CGA LHB,ESAM,JAM2,CLEC4M,IL19,RETN,IL2,TNFRSF1B,ADAMTS13,RET,ACY1,BMP1,CTSV,FN1,FSTL3,B2M,ADIPOQ,CNDP1,MASP1,IL22RA1,KDR,IGF2R,PLG,CTSH,FCN3,RPS6KA5,MED1,PAPPA,IL6,TFF3,EPHA2,NTRK2,AMH,MMP1,C1QBP,ERP29,MAPK12,SOD2,KIR2DL4,NOTCH1,RELT,SCARF1,TNFRSF19,HAVCR2,UNC5C,SEMA3E,LEPR,SPOCK2,GPS
combination15	C10,C10:2,C12,C14:1,C14:1-OH,C14:2,C16,C18:1,C2,C6(C4:1-DC),C5,C8,C8:1,TLN2,ACSL1,CCDC39,LYL1,NEURL3,LYSMD2,NAPA,PAX8,SLC22A4,PNLIPRP2,NKD2,DUSP11,TFE3,AGK,MCM3,PCGF2,TTF2,ABCB1,ARG1,SLC25A4,CDC14A,Tyr,PLAT,IGFBP2,CST3,EFNA5,ERBB3,LAYN,TNFRSF1A,EGFR,IGFBP6,FGF20,FGF9,SPINT1,NBL1,GHR,CGA LHB,ESAM,JAM2,CLEC4M,IL19,RETN,IL2,TNFRSF1B,ADAMTS13,RET,ACY1,BMP1,CTSV,FN1,FSTL3,B2M,ADIPOQ,CNDP1,MASP1,IL22RA1,KDR,IGF2R,PLG,CTSH,FCN3,RPS6KA5,MED1,PAPPA,IL6,TFF3,EPHA2,NTRK2,AMH,MMP1,C1QBP,ERP29,MAPK12,SOD2,KIR2DL4,NOTCH1,RELT,SCARF1,TNFRSF19,HAVCR2,UNC5C,SEMA3E,LEPR,SPOCK2
combination16	C10,C10:2,C12,C14:1,C14:1-OH,C14:2,C16,C18:1,C2,C6(C4:1-DC),C5,C8,C8:1,Tyr,PLAT,IGFBP2,CST3,EFNA5,ERBB3,LAYN,TNFRSF1A,EGFR,IGFBP6,FGF20,FGF9,SPINT1,NBL1,GHR,CGA LHB,ESAM,JAM2,CLEC4M,IL19,RETN,IL2,TNFRSF1B,ADAMTS13,RET,ACY1,BMP1,CTSV,FN1,FSTL3,B2M,ADIPOQ,CNDP1,MASP1,IL22RA1,KDR,IGF2R,PLG,CTSH,FCN3,RPS6KA5,MED1,PAPPA,IL6,TF3,EPHA2,NTRK2,AMH,MMP1,C1QBP,ERP29,MAPK12,SOD2,KIR2DL4,NOTCH1,RELT,SCARF1,TNFRSF19,HAVCR2,UNC5C,SEMA3E,LEPR,SPOCK2
combination17	TLN2,ACSL1,CCDC39,LYL1,NEURL3,LYSMD2,NAPA,PAX8,SLC22A4,PNLIPRP2,NKD2,DUSP11,TFE3,AGK,MCM3,PCGF2,TTF2,ABCB1,ARG1,SLC25A4,CDC14A
combination18	C10,C12,C16,C2,C6(C4:1-DC),C8,TLN2,ACSL1,CCDC39,LYL1,NEURL3,NAPA,PAX8,SLC22A4,PNLIPRP2,NKD2,DUSP11,TFE3,AGK,MCM3,PCGF2,TTF2,ABCB1,ARG1,SLC25A4,CDC14A,Tyr,PLAT,IGFBP2,CST3,EFNA5,ERBB3,LAYN,TNFRSF1A,EGFR,IGFBP6,FGF20,FGF9,SPINT1,GHR,CGA LHB,ESAM,JAM2,CLEC4M,IL19,RETN,IL2,TNFRSF1B,ADAMTS13,RET,ACY1,BMP1,CTSV,FN1,FSTL3,B2M,ADIPOQ,CNDP1,MASP1,IL22RA1,KDR,IGF2R,PLG,CTSH,FCN3,RPS6KA5,MED1,PAPPA,IL6,TFF3,EPHA2,NTRK2,AMH,MMP1,C1QBP,ERP29,MAPK12,SOD2,KIR2DL4,NOTCH1,RELT,SCARF1,TNFRSF19,HAVCR2,SEMA3E,LEPR,SPOCK2,GPS
combination19	C10,C12,C16,C2,C6(C4:1-DC),C8,TLN2,ACSL1,CCDC39,LYL1,NEURL3,NAPA,PAX8,SLC22A4,PNLIPRP2,NKD2,DUSP11,TFE3,AGK,MCM3,PCGF2,TTF2,ABCB1,ARG1,SLC25A4,CDC14A,Tyr,PLAT,IGFBP2,CST3,EFNA5,ERBB3,LAYN,TNFRSF1A,EGFR,IGFBP6,FGF20,FGF9,SPINT1,GHR,CGA LHB,ESAM,JAM2,CLEC4M,IL19,RETN,IL2,TNFRSF1B,ADAMTS13,RET,ACY1,BMP1,CTSV,FN1,FSTL3,B2M,ADIPOQ,CNDP1,MASP1,IL22RA1,KDR,IGF2R,PLG,CTSH,FCN3,RPS6KA5,MED1,PAPPA,IL6,TFF3,EPHA2,NTRK2,AMH,MMP1,C1QBP,ERP29,MAPK12,SOD2,KIR2DL4,NOTCH1,RELT,SCARF1,TNFRSF19,HAVCR2,SEMA3E,LEPR,SPOCK2
combination20	C10,C12,C16,C6(C4:1-DC),C8,ACSL1,CCDC39,NAPA,SLC22A4,AGK,SLC25A4,CDC14A,IGFBP2,CST3,EFNA5,ERBB3,EGFR,IGFBP6,GHR,IL19,RETN,FN1,FSTL3,ADIPOQ,IGF2R,PLG,RPS6KA5,MED1,IL6,TFF3,C1QBP,SOD2,NOTCH1,HAVCR2,LEPR
combination21	C2,CGA LHB,FN1,B2M,AMH,MMP1,HAVCR2
combination22	TLN2,PAX8,NKD2,TFE3,PLAT,CST3,LAYN,TNFRSF1A,EGFR,SPINT1,TNFRSF1B,ADAMTS13,BMP1,CTSV,FN1,FSTL3,ADIPOQ,CNDP1,MASP1,IL22RA1,KDR,IGF2R,PLG,FCN3,EPHA2,C1QBP,NOTCH1,TNFRSF19,SPOCK2

combination23	NEURL3,DUSP11,TFE3,MCM3,TTF2,ARG1,CST3,EFNA5,LAYN,TNFRSF1A,EGFR,GHR,CLEC4M,IL19,RETN,IL2,TNFRSF1B,FSTL3,B2M,ADIPOQ,MASP1,IL22RA1,KDR,IGF2R,CTSH,FCN3,MED1,PAPPA,IL6,EPHA2,AMH,MMP1,C1QBP,MAPK12,KIR2DL4,NOTCH1,REL,SCARF1,HA VCR2,LEPR
combination24	PAX8,Tyr,PLAT,IGFBP2,CST3,EFNA5,FGF20,GHR,ACY1, FN1,PLG,CTSH,MED1,TFF3,NTRK2,ERP29
combination25	LYL1,PAX8,AGK,PCGF2,PLAT,IGFBP2,CST3,ERBB3,TNFRSF1A,IGFBP6,FGF9,GHR,CGA LHB,ESAM,JAM2,IL19,TNFRSF1B,ADAMTS13,BMP1,CTSV,ADIPOQ,IL22RA1,KDR,IGF2R,PLG,CTSH,IL6,EPHA2,NTRK2,MMP1,NOTCH1,SEMA3E
combination26	ABCB1,PLAT,IGFBP2,CST3,ERBB3,EGFR,GHR,CGA LHB,RET,CTSV, FN1,ADIPOQ,KDR,IGF2R,CTSH,RPS6KA5,IL6,EPHA2,NTRK2,AMH,MMP1,SOD2
combination27	ACSL1,PNLIPRP2,TFE3,IGFBP2,CST3,TNFRSF1A,CGA LHB,ESAM,RETN,TNFRSF1B, FN1,FSTL3,ADIPOQ,IL6,MMP1,SOD2,LEPR
combination28	TNFRSF1A,SPOCK2,IGFBP6,NBL1,JAM2,ERP29,RETN,ADAMTS13,SCARF1,C10:2,C12,CST3,B2M,REL, FSTL3,C14:1-OH,C10,C8
combination29	TNFRSF1A,FSTL3,ADAMTS13,C8,RETN,B2M,ERP29,JAM2,C10,SPOCK2,C12
combination30	B2M,TNFRSF1A,SPOCK2,MMP1,UNC5C,TNFRSF1B,TNFRSF19,RETN,REL,IGFBP6,FSTL3,CTSH,IL19,ERBB3,Tyr,C8:1,C2,C14:2,C10:2
combination31	LYSMD2,NAPA,TFE3,CLEC4M,CTSV,EFNA5,IGF2R,JAM2,NBL1,RET,SCARF1
combination32	CLEC4M,CTSV,EFNA5,IGF2R,JAM2,NBL1,RET,SCARF1
combination33	LYSMD2,NAPA,TFE3,CLEC4M,CTSV,EFNA5,IGF2R,JAM2,NBL1,RET,SCARF1,B2M,TNFRSF1A,SPOCK2,MMP1,UNC5C,TNFRSF1B,TNFRSF19,RETN,REL,IGFBP6,FSTL3,CTSH,IL19,ERBB3,Tyr,C8:1,C2,C14:2,C10:2
combination34	CLEC4M,CTSV,EFNA5,IGF2R,JAM2,NBL1,RET,SCARF1,B2M,TNFRSF1A,SPOCK2,MMP1,UNC5C,TNFRSF1B,TNFRSF19,RETN,REL,IGFBP6,FSTL3,CTSH,IL19,ERBB3,Tyr,C8:1,C2,C14:2,C10:2
combination35	B2M,TNFRSF1A,SPOCK2,MMP1,UNC5C,TNFRSF1B,TNFRSF19,RETN,REL,IGFBP6,FSTL3,CTSH,IL19,ERBB3,Tyr,C8:1,C2,C14:2,C10:2,NBL1,EFNA5,JAM2
three identified candidate biomarkers	NBL1,EFNA5,JAM2

Supplementary Table 31. Significant numeric variables among three groups of KORA F4 CKD patients with hyperglycemia.

P-values of significant ($P < 0.05$) numeric variables among three groups of KORA F4 CKD patients with hyperglycemia are shown. *P*-values of pairwise comparison are shown as well. Variables with normal distribution were tested with anova test and those with skewed distribution (HbA1c, FG, triglyceride, creatinine, CST3, urine albumin, urine creatinine and UACR) were tested with Kruskal-Wallis test. Pairwise comparison of numeric variables among groups was done by Tukey HSD test for variables with normal distribution and Dunn's test for variables with skewed distribution, respectively.

Abbreviations: eGFR, estimated glomerular filtration rate; UACR, urinary albumin-to-creatinine ratio; 2-1, g2 vs g1; 3-1, g3 vs g1; 3-2, g3 vs g2.

var	annovaORk				distribution
	ru.p-value	2-1.p-value	3-1.p-value	3-2.p-value	
NBL1	2.418E-18	1.055E-04	7.306E-12	3.803E-09	normal
EFNA5	9.607E-15	1.293E-04	7.325E-12	8.294E-06	normal
JAM2	4.838E-14	3.808E-07	7.356E-12	8.723E-03	normal
Age, years	2.581E-02	9.804E-01	4.951E-02	6.219E-02	normal
eGFR, mL/min/1.73 m ²	1.162E-06	3.030E-01	9.285E-07	1.893E-03	normal
UACR, mg/g	3.118E-02	3.037E-01	2.571E-02	3.033E-01	skewed
Creatinine, mg/dl	5.281E-05	9.916E-01	2.090E-04	7.286E-04	skewed
Cystatin C, mg/l	1.685E-05	5.037E-01	2.553E-05	1.779E-03	skewed
Urine albumin, mg/l	1.403E-03	1.226E-01	8.710E-04	1.543E-01	skewed
Uric acid, mg/dl	2.458E-02	7.039E-01	1.079E-01	3.000E-02	normal
DUSP11	4.518E-02	4.409E-01	3.222E-01	4.161E-02	normal
MCM3	2.951E-02	2.382E-01	2.403E-02	8.336E-01	normal
ARG1	5.235E-03	1.340E-02	1.349E-02	7.864E-01	normal
IGFBP2	1.363E-02	7.608E-01	1.206E-02	1.484E-01	normal
CST3	2.515E-07	4.127E-01	2.677E-07	3.768E-04	normal
LAYN	7.864E-09	1.447E-01	6.001E-09	1.667E-04	normal
TNFRSF1A	8.485E-11	6.251E-03	4.620E-11	2.605E-04	normal
IGFBP6	5.163E-10	3.418E-01	7.610E-10	5.185E-06	normal
SPINT1	5.986E-03	2.588E-01	4.088E-03	3.770E-01	normal
CGA LHB	1.406E-02	1.014E-02	3.040E-01	1.968E-01	normal
ESAM	8.183E-05	4.509E-01	6.451E-05	1.644E-02	normal
RETN	2.075E-04	3.179E-01	1.366E-04	4.957E-02	normal
IL2	4.908E-02	1.636E-01	5.567E-02	9.752E-01	normal
TNFRSF1B	1.266E-09	1.940E-01	1.239E-09	2.712E-05	normal
BMP1	3.612E-02	6.607E-02	7.506E-02	9.366E-01	normal
FSTL3	1.746E-08	1.480E-03	8.757E-09	4.208E-02	normal
B2M	5.937E-06	6.567E-01	7.565E-06	1.319E-03	normal
CTSH	1.812E-08	1.518E-01	1.344E-08	2.866E-04	normal
MED1	1.570E-02	6.064E-02	2.302E-02	9.985E-01	normal
PAPPA	5.557E-03	8.359E-01	5.711E-03	6.854E-02	normal
TFF3	5.875E-08	2.981E-01	5.595E-08	2.357E-04	normal
EPHA2	4.898E-08	1.445E-01	3.385E-08	6.292E-04	normal
ERP29	4.051E-03	7.391E-01	2.321E-02	7.428E-03	normal
NOTCH1	7.522E-03	6.449E-01	6.073E-03	1.416E-01	normal
RELT	4.273E-11	1.752E-01	5.693E-11	2.235E-06	normal
SCARF1	1.136E-02	2.138E-01	8.487E-03	5.753E-01	normal
TNFRSF19	4.420E-03	5.868E-01	3.442E-03	1.215E-01	normal
HAVCR2	2.092E-06	1.050E-01	1.159E-06	1.210E-02	normal

Supplementary Table 32. Difference among three groups of KORA F4 CKD patients with hyperglycemia regarding rate of male, use of anti-hypertensive, ARBs or ACEIs medication, eGFR based CKD, UACR based CKD, eGFR categories, UACR categories, eGFR decline > 30% and UACR increase > 30%.

P-values of difference among three groups calculated using Pearson chi-squared test or fisher exact test (when any theoretical frequency was less than one) are shown. When applicable, the *P*-values calculated using the Cochran–Armitage test of testing trend of both sides, increasing and decreasing side are shown as well, respectively.

Abbreviations: ARBs, taking angiotensin 2 receptor blockers; ACEIs, taking angiotensin-converting enzyme inhibitors; eGFRcla, eGFR categories; UACRcla, UACR categories; CKD, chronic kidney disease; eGFR, estimated glomerular filtration rate; UACR, urinary albumin-to-creatinine ratio; CKDcrcc, eGFR-based CKD that was defined as eGFR < 60 ml/min/1.73 m²; CKDuacr, UACR-based CKD that was defined as UACR ≥ 30 mg/g.

var	trend.both.p-value	trend.dec.p-value	trend.incr.p-value	chisq.OR fisher. p-value
Sex, male, %	4.249E-01	2.124E-01	7.876E-01	1.221E-02 a
Antihypertensive	2.524E-02	9.874E-01	1.262E-02	7.684E-02 b
ARBs or ACEIs	5.182E-02	9.741E-01	2.591E-02	5.547E-02 a
CKDcrcc F4	5.607E-05	1.000E+00	2.803E-05	1.617E-04 a
CKDuacr F4	3.862E-04	1.931E-04	9.998E-01	1.782E-03 a
eGFRcla F4	-	-	-	1.267E-04 b
UACRcla F4	-	-	-	1.559E-03 b
eGFR decline > 30%	2.480E-02	9.876E-01	1.240E-02	5.240E-02 b
UACR increase > 30%	2.205E-01	8.898E-01	1.102E-01	1.061E-01 a

a, p-value calculated using Pearson chi-squared test; b, p-value calculated using fisher exact test.

Supplementary Table 33. Characteristics of replicated multi-omics candidates of CKD in hyperglycemia based on various evidence with eGFR and/or UACR.

Groups of replicated candidates are shown, in which the groups were defined by genetic evidence support with eGFR and/or UACR from 2SMR or GPS, or associations (i.e., cross-sectional and longitudinal) with eGFR and/or UACR from the hyperglycemia individuals of KORA study. The omics candidates, key omics candidates, potential novel candidates identified from our study, and processes involved in eight T2DCKD subnetworks in each group are presented. Candidates that were annotated to the most T2DCKD processes were defined as the key omics candidates in each group. If there were no candidates annotated to eight processes in a group, the omics candidates in this group were shown in the cell of "key omics".

* MMP1: MMP1 was potentially causal with CKD by our 2SMR, but no supported causal relationship for eGFR or UACR by 2SMR.

Abbreviations: 2SMR, two-sample Mendelian randomization; GPS, genome wide polygenic score of eGFR values; CKD, chronic kidney disease; eGFR, estimated glomerular filtration rate; UACR, urinary albumin-to-creatinine ratio; uni, candidates in this group were unique compared to other groups in case of one direction; Cr, cross-sectional association; Long, longitudinal association; mito, T2DCKDmito process; adipo, T2DCKDadipo process; age, T2DCKDage process; angi, T2DCKDangi process; inna, T2DCKDinna process; ras, T2DCKDras process; tyr, T2DCKDtyr process; fibri, T2DCKDfibri process; T2DCKD, T2D related CKD.

group	omics.label	(key) omics	potential novel	T2DCKD processes
eGFR->candi->eGFR	ADAMTS13,C10:2,C12,C8:1,ERP29,FSTL3,IGFBP6,JAM2,NBL1,RELT,RETN,SCARF1,SPOCK2,TNFRSF1A	TNFRSF1A,FSTL3	NBL1,JAM2,SCARF1	inna,mito,fibri,angi,adipo,tyr
eGFR->candi->UACR	C14:2,C8:1	C14:2,C8:1		
(uni) eGFR->candi	C10,C2,C8,CTSH,IL19,TNFRSF19,TNFRSF1B,UNC5C	TNFRSF1B,CTSH		mito,inna,angi,fibri,ras,adipo,AGEs,tyr
(uni) candi->eGFR	C14:1-OH,CST3,Tyr	CST3		tyr,ras,adipo,mito,fibri,inna,angi
(uni) candi->UACR	ERBB3	ERBB3		ras,mito,angi
(uni) candi->eGFR&UACR	B2M	B2M		AGEs,inna
eGFR-Cr&Long	ACY1,AMH,C14:1,C16,C18:1,C5,C6(C4:1-DC),CGA LHB,CLEC4M,CTSV,EFNA5,EGFR,EPHA2,ESAM,FGF20,GHR,HAVCR2,IGF2R,KDR,LAYN,MASP1,MMP1,NTRK2,PAPPA,PLG,RET,SOD2,TFF3	GHR,IGF2R,MMP1	EFNA5,CLEC4M,RET,CTSV,IGF2R	inna,ras,mito,angi,fibri,tyr,adipo,AGEs
UACR-Cr&Long	EGFR,SLC22A4	EGFR		mito,ras,fibri,inna
eGFR-Cr&UACR-Long	EGFR	EGFR		ras,mito,fibri,inna
UACR-Cr&eGFR-Long	AMH,C14:1,C16,C18:1,CLEC4M,CTSV,EGFR,GHR,KDR,NTRK2,SOD2	GHR	CLEC4M,CTSV	ras,inna,mito,angi,fibri,tyr,adipo,AGEs
(uni) eGFR-Cr	LEPR,PLAT	PLAT		ras,adipo,mito,fibri,inna,tyr,angi
(uni) UACR-Cr	LYSMD2,NAPA	NAPA	LYSMD2,NAPA	mito
(uni) eGFR&UACR-Cr	NOTCH1,TFE3	NOTCH1	TFE3	fibri,inna,adipo,mito,angi
(uni) eGFR-Long	FGF9	FGF9		angi

Supplementary Table 34. Interactions of connected edges in T2DCKD-SLC22A4-IL19 and T2DCKD-Tyr-IGFBP2 and the based literatures.

T2DCKD-SLC22A4-IL19									
Subject	Subject type	Interaction type	Object	Object type	Arg_loc	Arg_Mod	PMID	Organism	Disease
Diabetes mellitus, type II	disease	increases_quantity of	IL19	gene/protein	in blood		32585310	Homo sapiens	Insulin resistance; Diabetes mellitus, type II
SLC22A4	gene/protein	increases_transport of	Ergothioneine	compound	into cells		27023905	Homo sapiens	Hearing loss
SLC22A4	gene/protein	increases_transport of	Ergothioneine	compound			20224991	Mus musculus	Inflammatory bowel disease
SLC22A4	gene/protein	increases_transport of	Ergothioneine	compound	in HEK293 cells		15795384	Homo sapiens	Inflammatory bowel disease
inflammatory response	process	increases_quantity of	IL19	gene/protein	in nonimmune cells		32667867	Mammalia	Coronary artery disease; Asthma; Immunological; Inflammation
SLC22A4	gene/protein	affects_activity of	renal interstitial fibrosis	phenotype		in streptozocin-induced diabetes	33907247	Mus musculus	Nephropathy, diabetic
Chronic kidney disease	disease	decreases_activity of	SLC22A4	gene/protein	in intestine		28754554	Mus musculus	Chronic kidney disease
metabolic acidosis	phenotype	increases_expression of	SLC22A4	gene/protein	in kidney		32062662	Mus musculus	Renal
Chronic kidney disease	disease	decreases_quantity of	Ergothioneine	drug/chemical compound	in blood	via decreased activity of intestinal SLC22A4	28754554	Mus musculus	Chronic kidney disease
Chronic kidney disease	disease	decreases_quantity of	Ergothioneine	compound	in blood		28754554	Homo sapiens	Chronic kidney disease
acute kidney injury	phenotype	increases_quantity of	IL19	gene/protein	in AKI mice		23468852	Mus musculus	Renal
IL1B	gene/protein	increases_expression of	SLC22A4	gene/protein		via the NF-kappaB signaling cascade	17142562	Homo sapiens	Rheumatic disease; Inflammation
Ergothioneine	drug/chemical compound	decreases_activity of	increased blood urea nitrogen level	phenotype		in streptozocin-induced diabetes	34346315	Rattus norvegicus	Nephropathy, diabetic
Ergothioneine	drug/chemical compound	decreases_activity of	increased urine protein level	phenotype		in streptozocin-induced diabetes	34346315	Rattus norvegicus	Nephropathy, diabetic
Ergothioneine	drug/chemical compound	decreases_activity of	expanded mesangial matrix	phenotype		in streptozocin-induced diabetes	34346315	Rattus norvegicus	Nephropathy, diabetic
IL19	gene/protein	decreases_quantity of	IL1B	gene/protein			19834971	Mus musculus	Inflammatory bowel disease; Inflammation
Ergothioneine	drug/chemical compound	decreases_quantity of	IL1B	gene/protein	in blood		17603080	Rattus norvegicus	Nephropathy, diabetic
glomerulonephritis	phenotype	increases_quantity of	IL1B	gene/protein	in serum		16889043	Homo sapiens	Renal
IL19	gene/protein	decreases_quantity of	IL1B	gene/protein			26404542	Homo sapiens	Bone; Inflammation
SLC22A4	gene/protein	affects_activity of	Diabetes mellitus, type II	disease			30274012	Homo sapiens	Insulin resistance; Diabetes mellitus, type II
Chronic kidney disease	disease	increases_expression of	SLC22A4	gene/protein	epithelial		28754554	Mus musculus	Chronic kidney disease
SLC22A4	gene/protein	decreases_activity of	inflammatory response	process			28754554	Mus musculus	Chronic kidney disease
Ergothioneine	drug/chemical compound	decreases_activity of	decreased renal glomerular filtration rate	phenotype			28754554	Homo sapiens	Chronic kidney disease
metabolic acidosis	phenotype	decreases_activity of	glomerular filtration	process			31988269	Mammalia	Chronic kidney disease; Renal
metabolic acidosis	phenotype	increases_activity of	renal interstitial fibrosis	phenotype			31988269	Mammalia	Chronic kidney disease; Renal
Ergothioneine	drug/chemical compound	decreases_activity of	renal interstitial fibrosis	phenotype		in streptozocin-induced diabetes	34346315	Rattus norvegicus	Nephropathy, diabetic

T2DCKD-Tyr-IGFBP2									
Subject	Subject type	Interaction type	Object	Object type	Arg_loc	Arg_Mod	PMID	Organism	Disease
Chronic kidney disease	disease	decreases quantity of	Tyrosine	compound	in plasma		17513431	Mammalia	Chronic kidney disease
Phenylalanine	drug/chemical compound	increases_quantity of	Tyrosine	drug/chemical compound		via phenylalanine hydroxylase	17513431	Mammalia	Chronic kidney disease
PAH	gene/protein	increases_quantity of	Tyrosine	drug/chemical compound		via phenylalanine hydroxylase	17513431	Mammalia	Chronic kidney disease
PAH	gene/protein	decreases_quantity of	Phenylalanine	drug/chemical compound		via phenylalanine hydroxylase	17513431	Mammalia	Chronic kidney disease
ACY1	gene/protein	increases_quantity of	Tyrosine	compound	in kidney		14927637	Sus scrofa	Metabolic; Renal
ACY1	gene/protein	affects_activity of	protein metabolic process	process	in kidney		18222180	Mammalia	Renal
Tyrosine	drug/chemical compound	increases_quantity of	3,4-Dihydroxy-L-phenylalanine	drug/chemical compound	in proximal tubule epithelial cells		30808844	Sus scrofa	Renal
IGFBP2	gene/protein	decreases_activity of	glomerular filtration	process			23781310	Homo sapiens	Insulin resistance; Nephropathy, diabetic; Diabetes mellitus, type II
Chronic kidney disease	disease	increases_quantity of	IGFBP2	gene/protein	in plasma		10662705	Homo sapiens	Renal; Chronic kidney disease
IGF1R	gene/protein	decreases_quantity of	Tyrosine	drug/chemical compound	in hind limb muscle	indicating increased protein degradation	27525440	Homo sapiens	Insulin resistance; Muscular
3,4-Dihydroxy-L-phenylalanine	drug/chemical compound	decreases_expression of	IGFBP2	gene/protein	in striatum		25568106	Mus musculus	Parkinson disease; Neurological
IGFBP2	gene/protein	affects_quantity of	IGF1	gene/protein	in muscle		20207454	Mammalia	Renal; Muscular
IGF1	gene/protein	affects_activity of	protein metabolic process	process	in muscle		20207454	Mammalia	Renal; Muscular
IGF1R	gene/protein	interacts (colocalizes) with	IGF1	gene/protein			27525440	Homo sapiens	Insulin resistance; Muscular
Tyrosine	compound	affects_activity of	protein metabolic process	process			20207454	Mammalia	Renal; Muscular
protein restriction	environment	decreases quantity of	IGF1	gene/protein	in serum of adults		7531712	Homo sapiens	Metabolic
protein restriction	environment	increases_quantity of	IGFBP2	gene/protein	in serum of adults and children		7531712	Homo sapiens	Metabolic
Chronic kidney disease	disease	increases_quantity of	IGFBP2	gene/protein	in serum		7545697	Homo sapiens	Chronic kidney disease
IGFBP2	gene/protein	decreases activity of	glomerular filtration	process			7545697	Homo sapiens	Chronic kidney disease
IGF1	gene/protein	increases_activity of	body height	phenotype			7545697	Homo sapiens	Chronic kidney disease
IGFBP2	gene/protein	decreases_activity of	body height	phenotype			7545697	Homo sapiens	Chronic kidney disease
protein restriction	environment	affects_activity of	protein metabolic process	process			7692021	norvegicus	Metabolic

Supplementary Figures

Fig. S1 T2DCKDmito

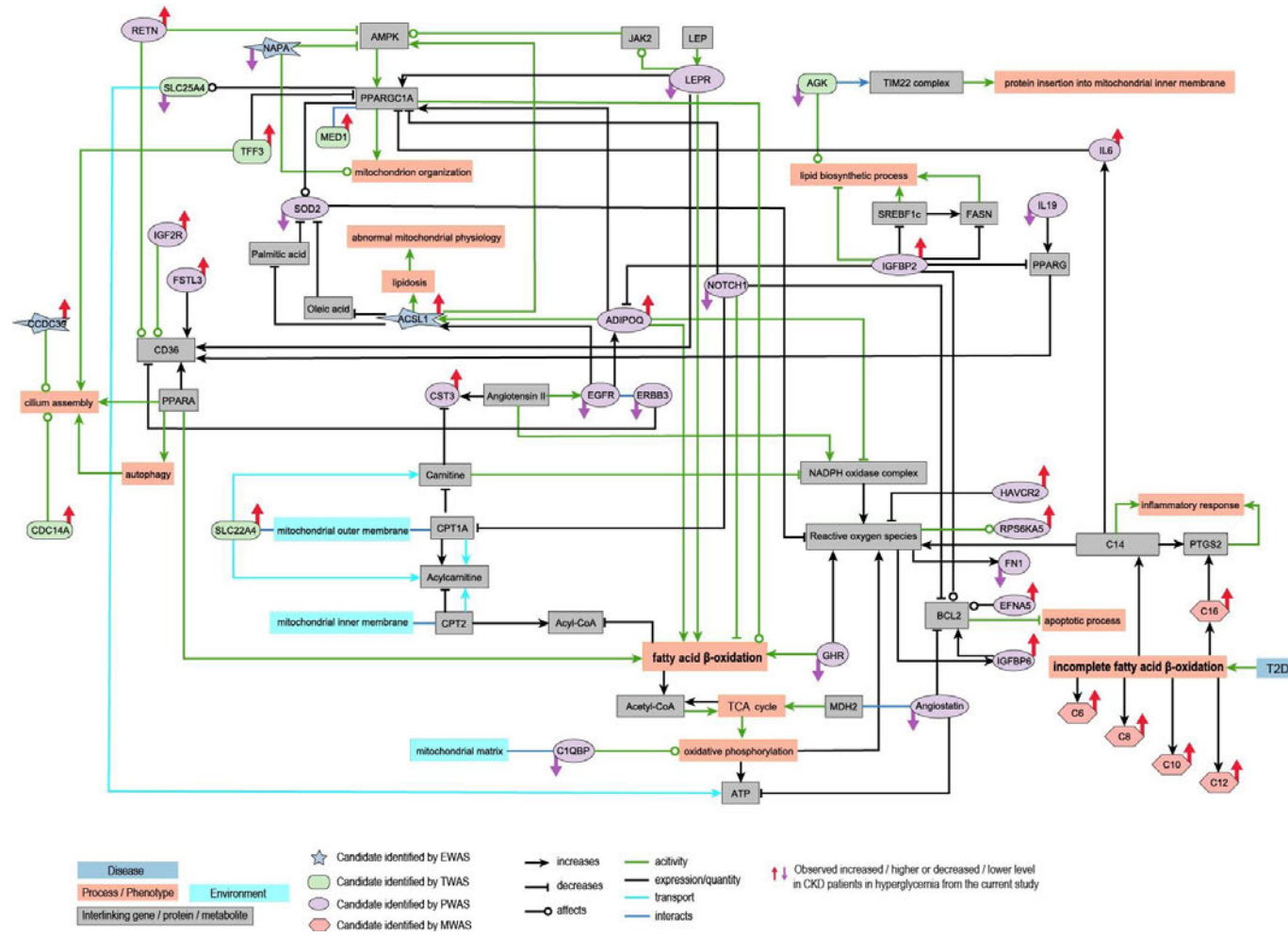
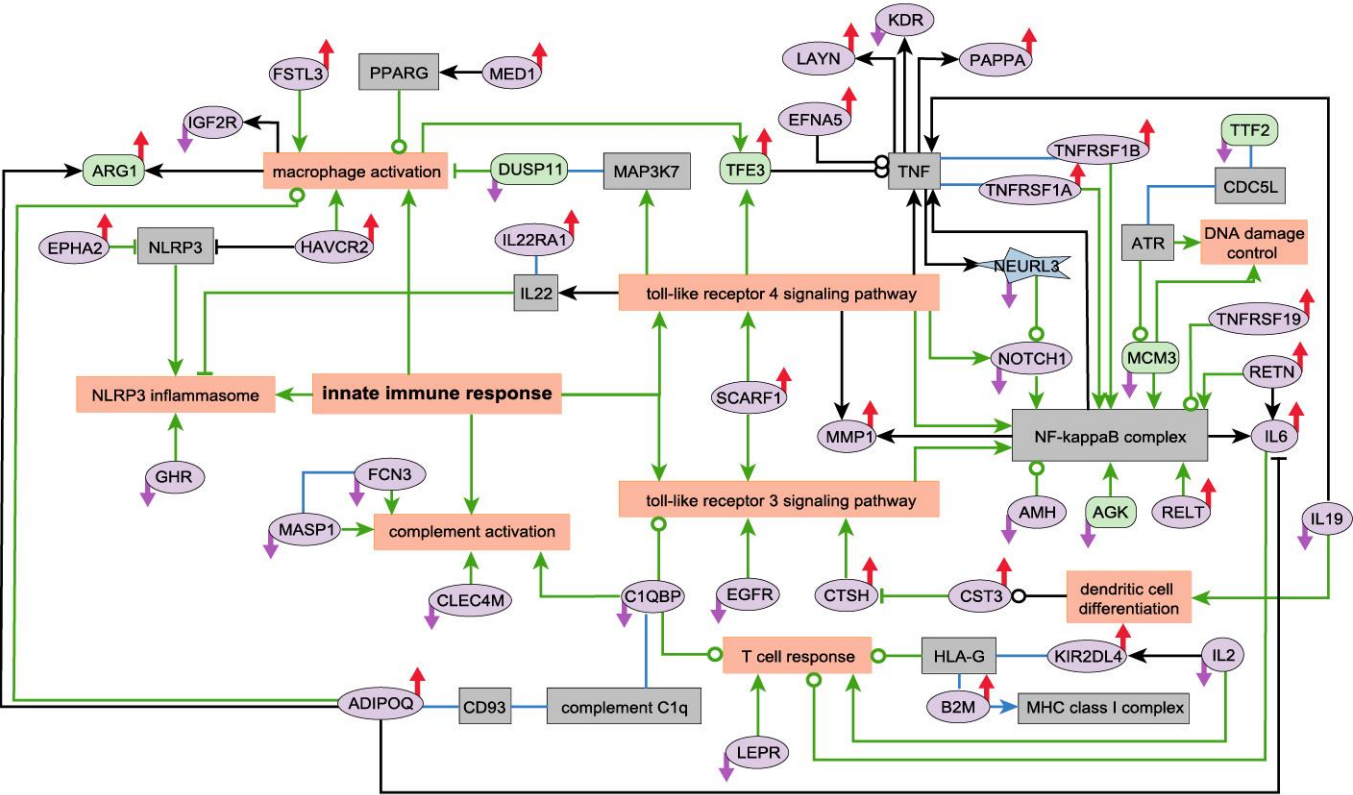


Fig. S2 T2DCKDinna



Process / Phenotype	★ Candidate identified by EWAS	→ increases	— activity	↑↓ Observed increased / higher or decreased / lower level in CKD patients in hyperglycemia from the current study
Interlinking gene / protein / metabolite	○ Candidate identified by TWAS	⇝ decreases	— expression/quantity	
	○ Candidate identified by PWAS	○ affects	— interacts	
	◇ Candidate identified by MWAS			

Fig. S3 T2DCKDadipo

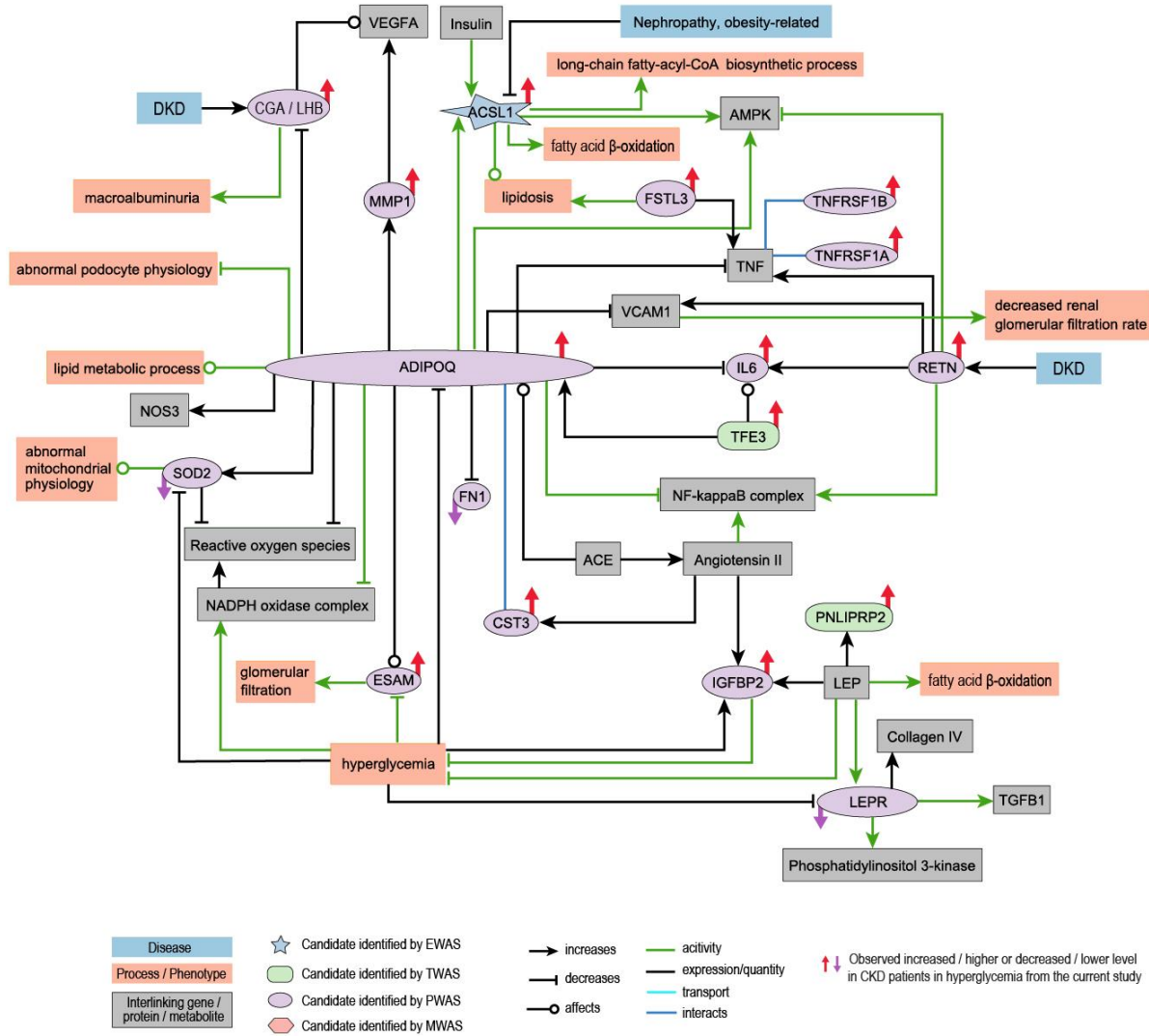


Fig. S4 T2DCKDras

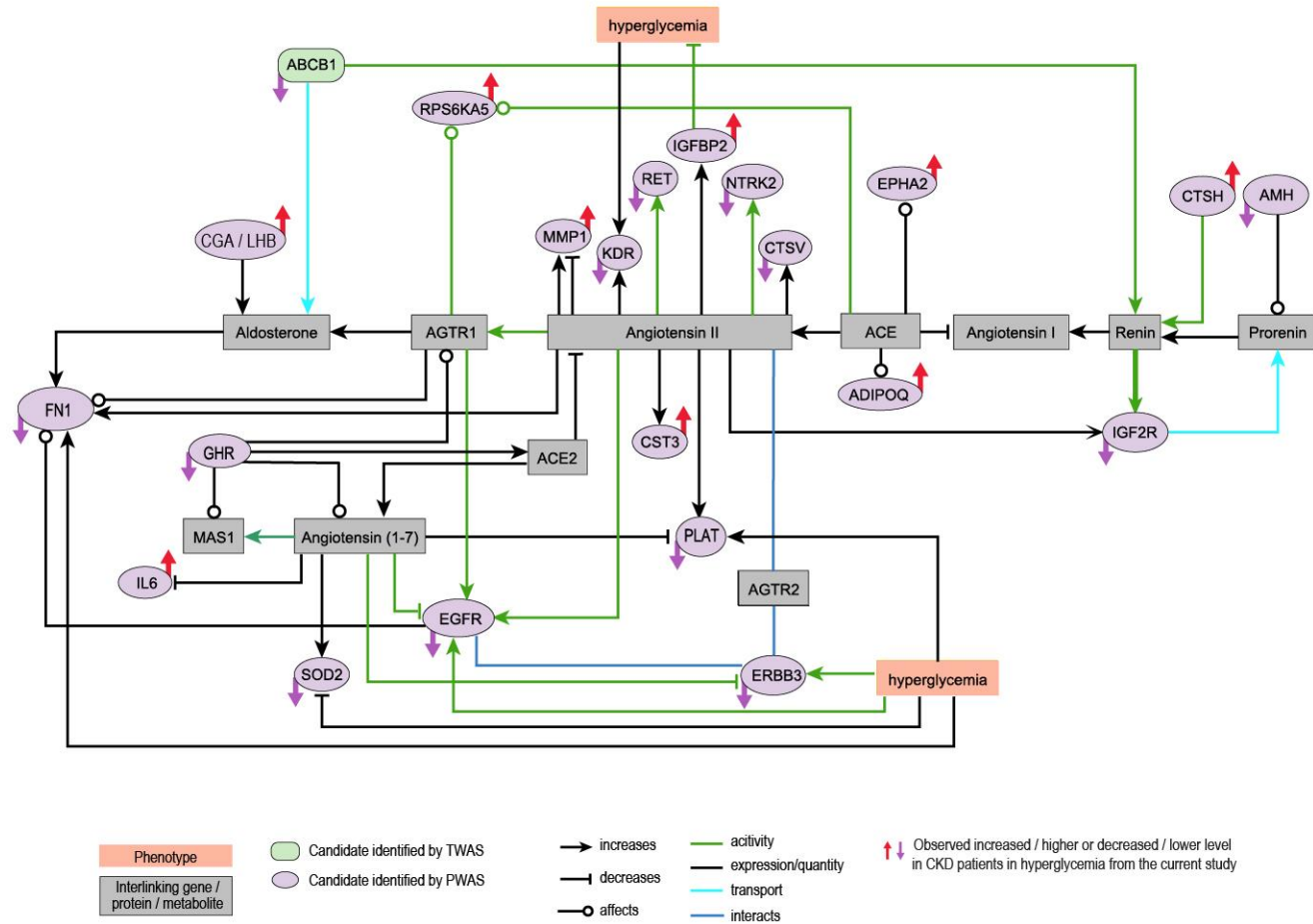


Fig. S5 T2DCKDfibri

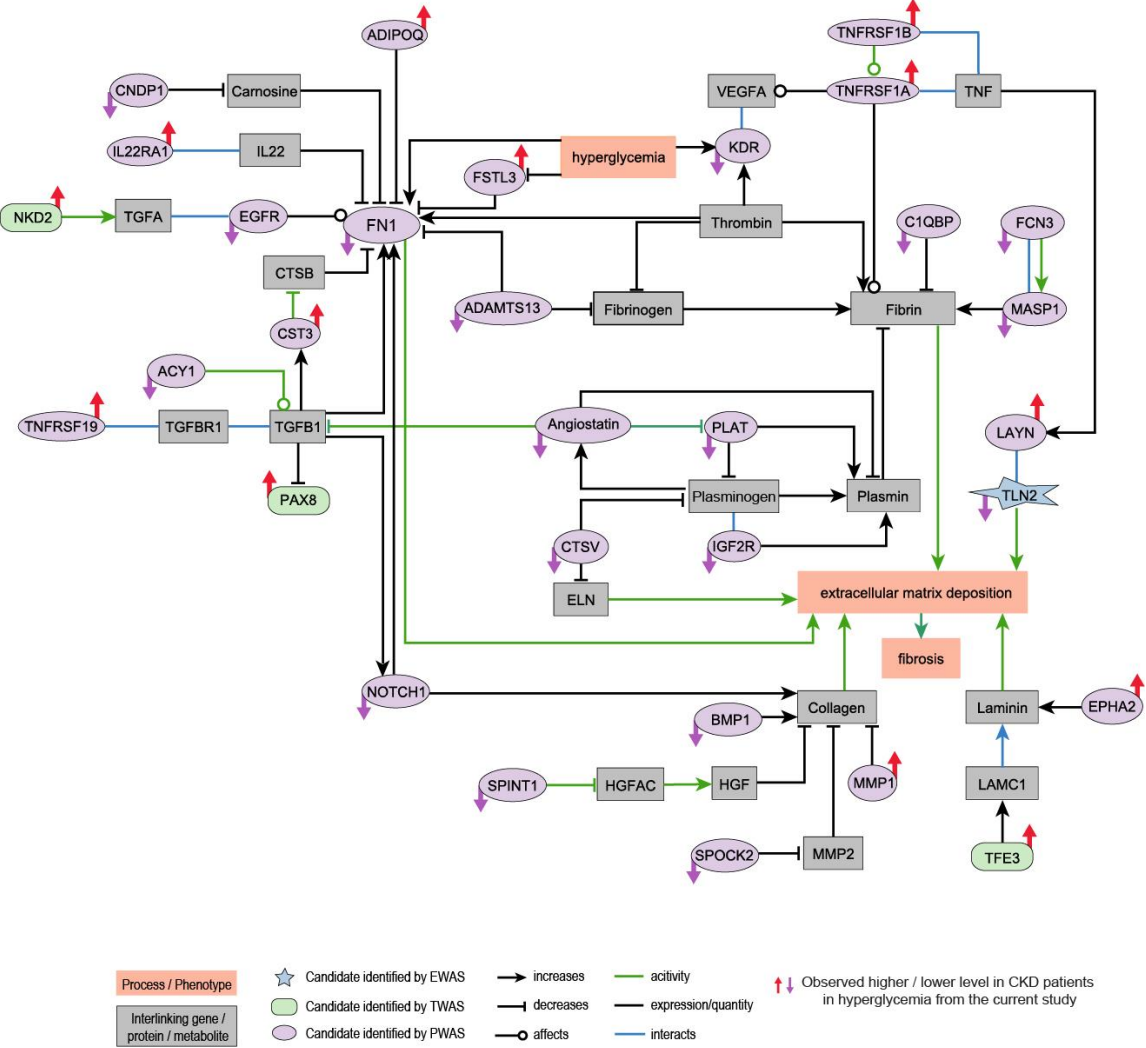


Fig. S6 T2DCKDage

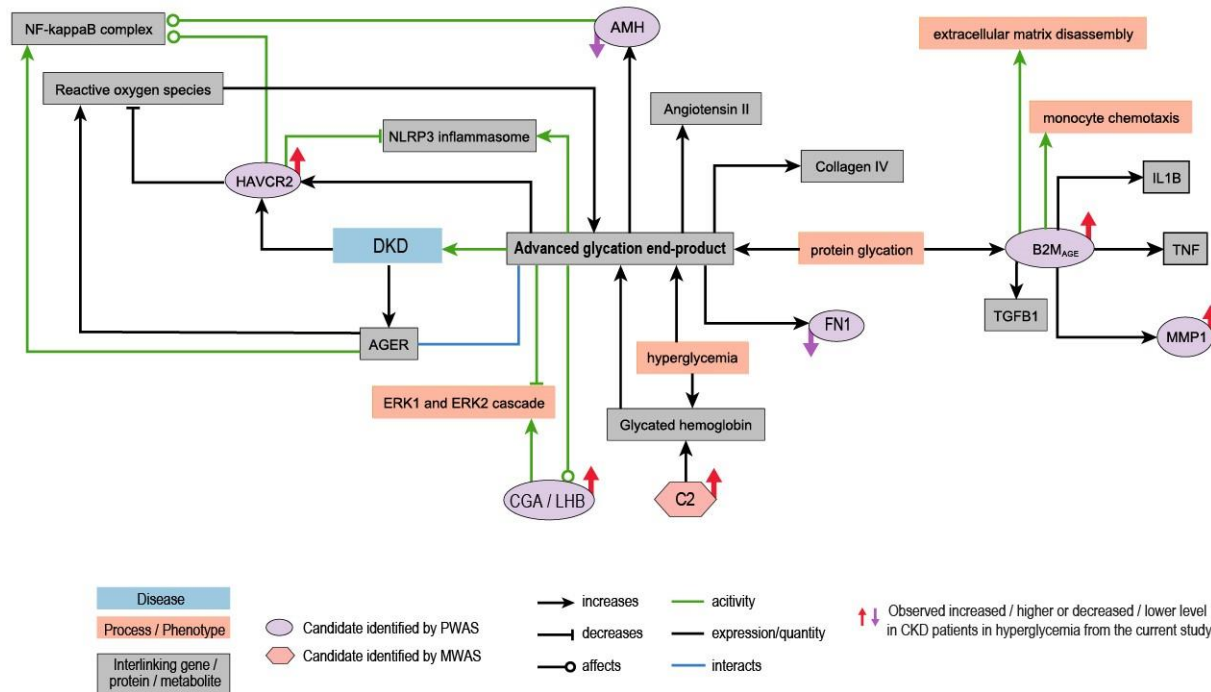
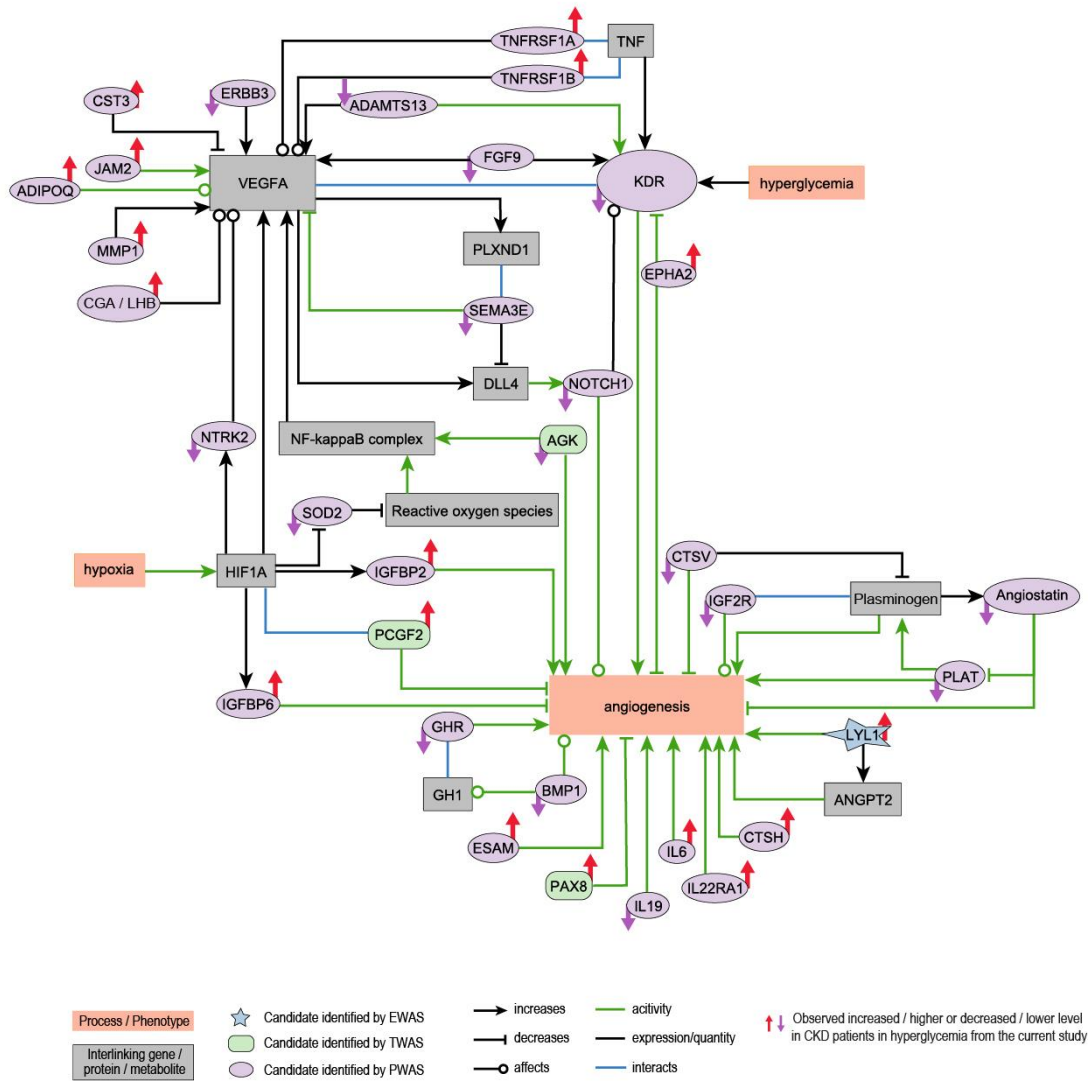
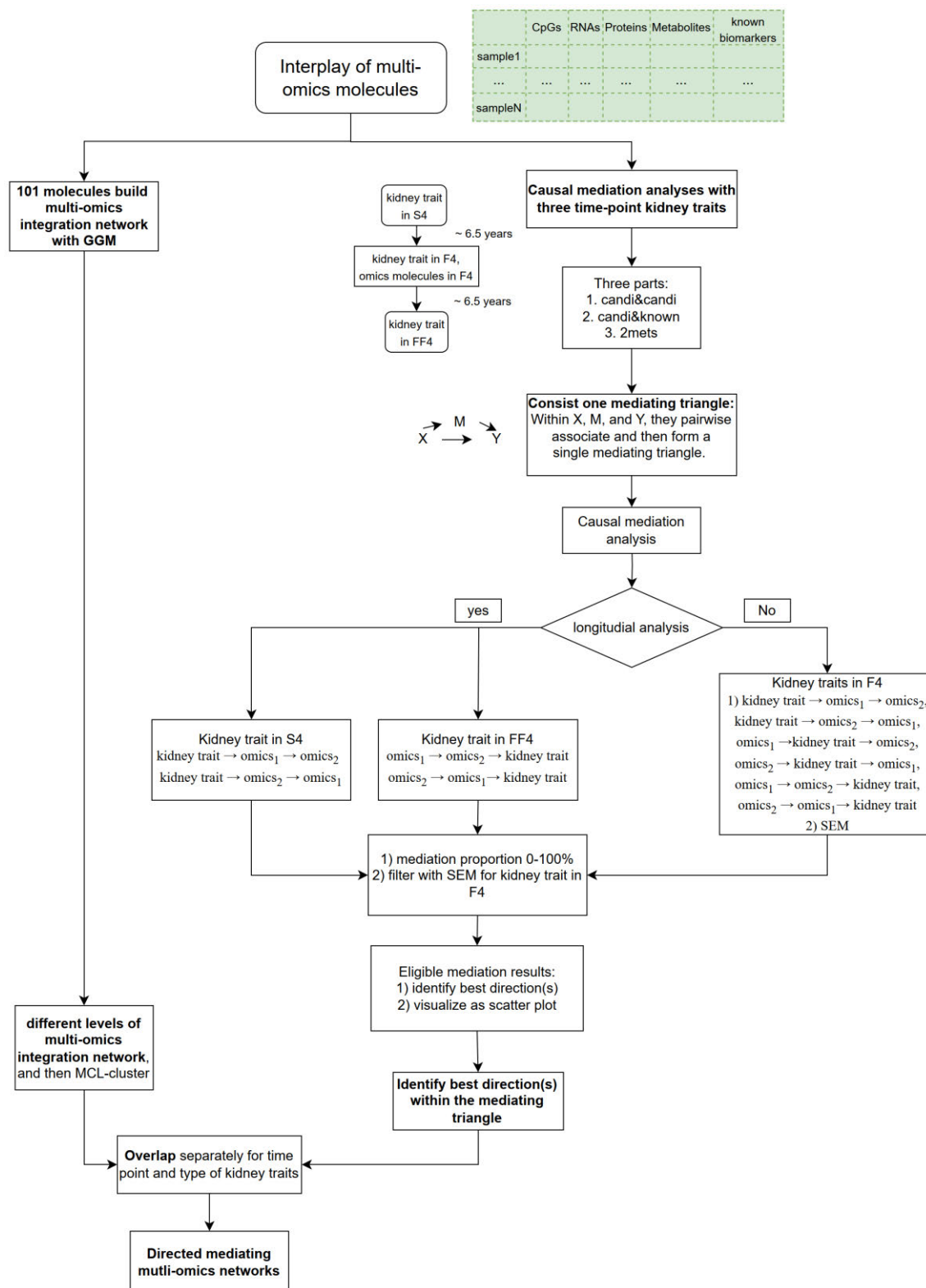


Fig. S7 T2DCKDangi

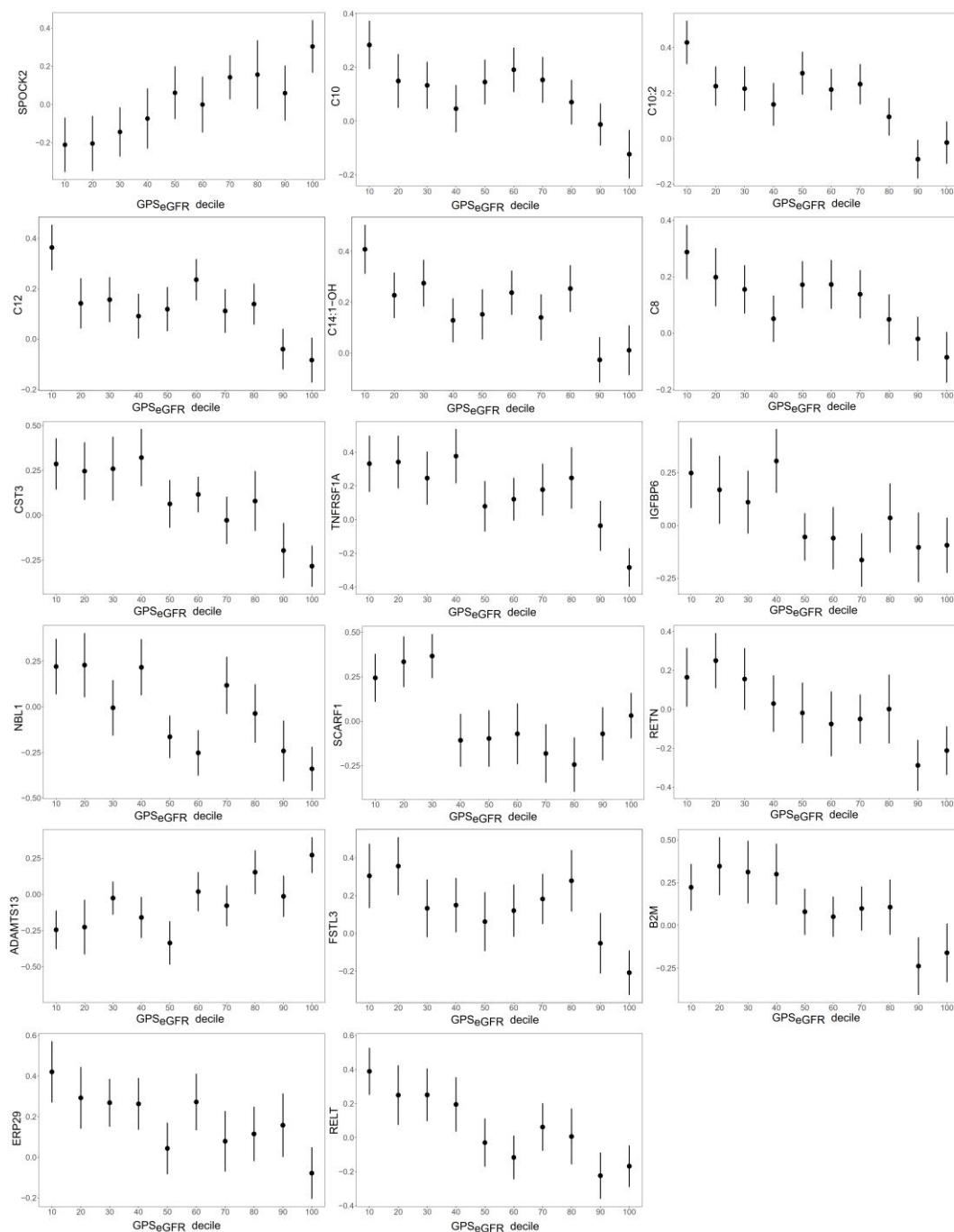


Supplementary Fig. 1-7. Seven T2DCKD subnetworks

Seven T2DCKD subnetworks including 1)T2DCKDmito, T2D-related CKD subnetwork of mitochondrial dysfunction; 2)T2DCKDinna, T2D-related CKD subnetwork of innate immune response; 3)T2DCKDadipo, T2D-related CKD subnetwork of adipokine influence; 4)T2DCKDras, T2D-related CKD subnetwork of renin-angiotensin system dysfunction; 5)T2DCKDfibri, T2D-related CKD subnetwork of extracellular matrix deposition and renal fibrosis; 6)T2DCKDage, T2D-related CKD subnetwork of advanced glycation end products; 7)T2DCKDangi, T2D-related CKD subnetwork of angiogenesis.



Supplementary Fig. 8. Diagram of the procedures of interplaying of multi-omics molecules.



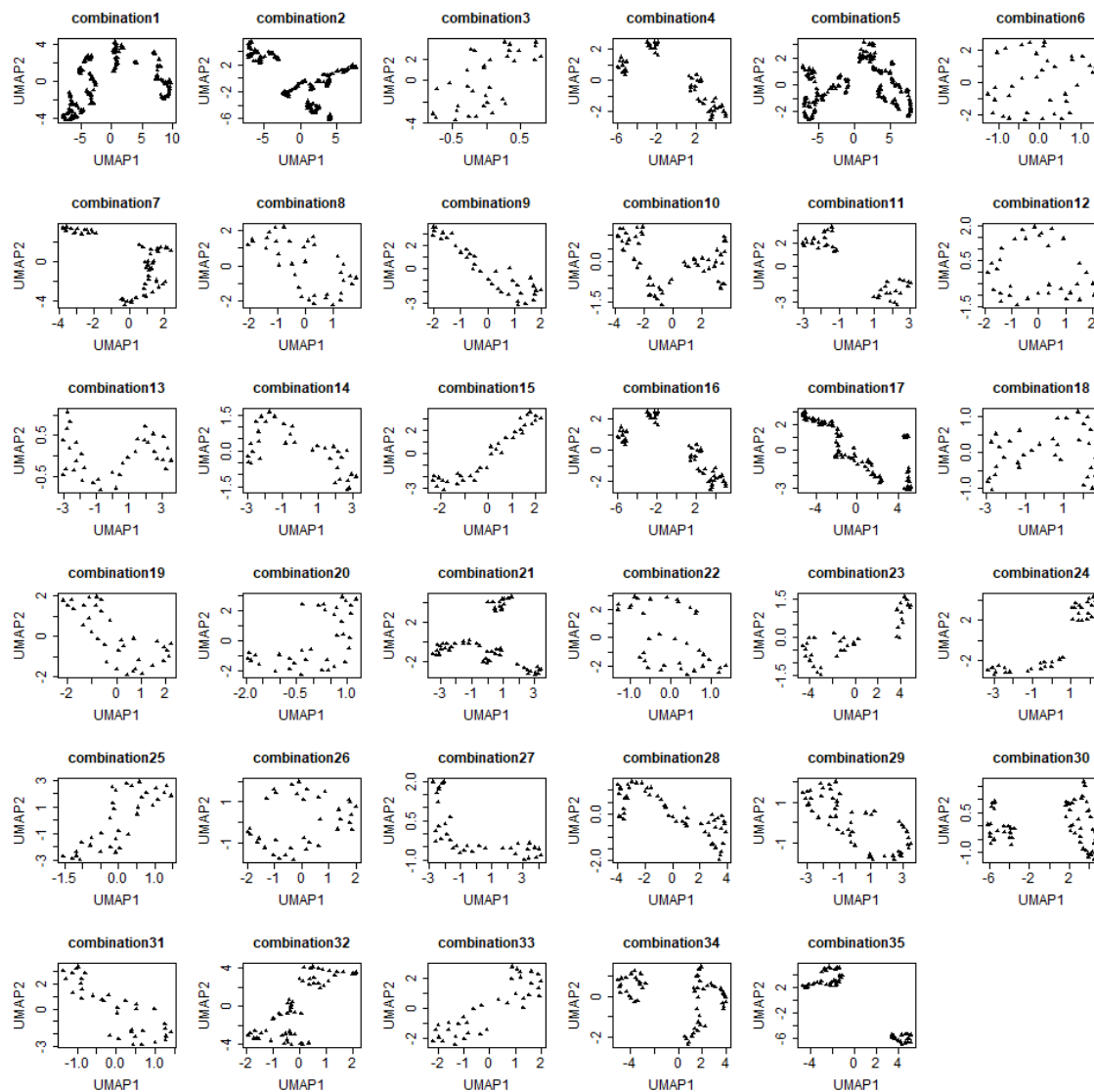
Supplementary Fig. 9. Scaling values of GPS_{eGFR} -associated candidates in stratification of the KORA F4 hyperglycemic individuals according to GPS_{eGFR} deciles

Stratification plots of GPS_{eGFR} deciles and scaling values of GPS_{eGFR} -associated candidates in hyperglycemic individuals of KORA F4. The centers are the mean scaling values of omics candidates and the error bars are the 95% confidence intervals. **Abbreviations:** GPS, genome-wide polygenic score of eGFR values; eGFR, estimated glomerular filtration rate.



Supplementary Fig. 10. Extreme GPS_{eGFR} is a strong risk factor for increasing omics candidate levels and eGFR values in KORA F4 hyperglycemic individuals.

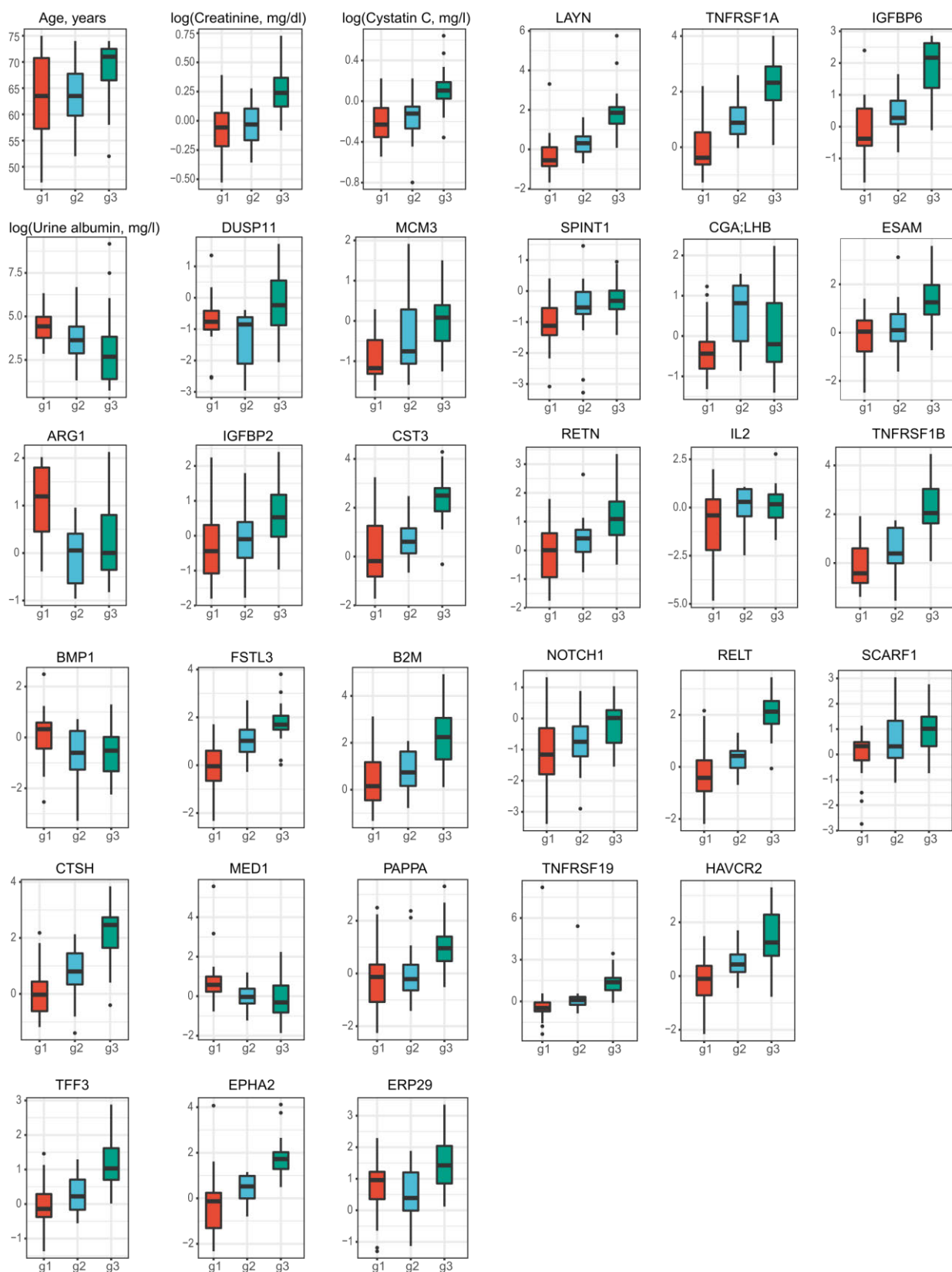
Regression coefficients with 95% *CI* of GPS_{eGFR} to eGFR and 17 omics candidates in different percentiles of sample size of KORA F4 hyperglycemic individuals are shown, respectively. Regression coefficients were from linear regression analysis adjusted for full model (incl. age, sex, BMI, systolic blood pressure, smoking status, triglyceride, total cholesterol, HDL cholesterol, fasting glucose, use of lipid lowering drugs, antihypertensive and anti-diabetic medication). The centers represent the regression coefficients, while the error bars represent the 95% confidence intervals.



Supplementary Fig. 11. Scatter plots of the corresponding first and second components of UMAP with different combinations of variables to cluster CKD patients in hyperglycemia.

Scatter plots of KORA F4 CKD patients with hyperglycemia who were classified based on the first and second components of UMAP calculated with various combinations of biomarkers and omics candidates, respectively. The used biomarkers and/or omics candidates for each combination in the classification are listed in Supplementary Table 30. In each combination, the number of CKD patients used to be classified depended on the complete cases of the used variables.

Fig. S12



Supplementary Fig. 12. Significant clinical variables and omics candidates across three groups of CKD patients classified by three potential novel proteins.

Boxplots of values of significant ($P < 0.05$) clinical variables and omic candidates across three groups of KORA F4 CKD patients with hyperglycemia classified by three potential novel proteins are shown. The examined omic candidates were from 87 candidates used in eight T2DCKD subnetworks. g1: N = 22; g2: N = 14; g3: N = 23. The values of clinical variables here were not scaled and the values of candidates here were scaling values.

References

- 1. Zheng, J., *et al.* Phenome-wide Mendelian randomization mapping the influence of the plasma proteome on complex diseases. *Nat Genet* **52**, 1122-1131 (2020).

Acknowledgements

First, I would like to thank my supervisor, Prof. Dr. Annette Peters, Director of the Institute of Epidemiology at Helmholtz Zentrum München. Throughout my studies, Prof. Dr. Peters provided me with insightful instructions and counsel.

I would like to express my gratitude to my co-supervisor, Dr. Rui Wang-Sattler, for her unwavering support and invaluable suggestions throughout the projects. She exerted a lot of effort in coordinating the projects and in making the data accessible for the studies in the thesis. She has also supported my participation in external courses and international conferences.

I would like to thank all my colleagues. Special thanks go to Dr. Marcela Covic, who assisted me greatly throughout my PhD studies. Many thanks to Dr. Li Wang for her kindness and emotional support. She always answered my questions with patience. I also appreciate the contributions of all the co-authors with whom I've collaborated.

I would like to express my profound gratitude to my family and friends for their love, trust, and encouragement.